Behavioural Study of Stimuli Triggered Biopolymer for Non-invasive Drug Delivery

THESIS

Submitted in partial fulfillment of the requirements for the degree of

DOCTOR OF PHILOSOPHY

by

TAMALIKA BHAKAT
2010PHXF0402P

Under the Supervision of

Dr. Sachin Ulhasrao Belgamwar

Department of Mechanical Engineering
Birla Institute of Technology & Science Pilani, Pilani Campus
Pilani - 333 031 (Rajasthan)

Co- Supervision of

Prof. Niti Nipun Sharma

Department of Mechanical Engineering
School of Automobile, Mechanical & Mechatronics Engineering
Manipal University, Jaipur - 303 007 (Rajasthan)

&

Dr. Ajay Agarwal
Nano Bio Sensors
CSIR-Central Electronics Engineering Research Institute
Pilani - 333 031 (Rajasthan)

BITS Pilani
Pilani | Dubai | Goa | Hyderabad

BIRLA INSTITUTE OF TECHNOLOGY & SCIENCE
PILANI – 333031 (RAJASTHAN) INDIA

2019

BIRLA INSTITUTE OF TECHNOLOGY & SCIENCE
PILANI – 333 031 (RAJASTHAN) INDIA

CERTIFICATE

This is to certify that the thesis entitled **"Behavioural Study of Stimuli Triggered Biopolymer for Non-invasive Drug Delivery"** submitted by **Tamalika Bhakat,** ID.No. **2010PHXF0402P** for award of Ph.D. of the Institute embodies original work done by her under my supervision.

Signature of the Supervisor
Dr. Sachin Ulhasrao Belgamwar
Assistant Professor
Department of Mechanical Engineering
Birla Institute of Technology & Science, Pilani - 333 031 Jaipur (Raj.)
Date: 22/11/2019

Signature of the Co-Supervisor
Prof. Niti Nipun Sharma
Pro-President and Professor & Dean-Faculty of Engineering
Department of Mechanical Engineering
Manipal University, Jaipur - 303 007 (Raj.)
Date: 22/11/2019

Signature of the Co-Supervisor
Dr. Ajay Agarwal
Sr. Principal Scientist, Group Head, Nano Bio Sensors,
CSIR-Central Electronics Engineering Research Institute
Pilani - 333 031 (Raj.)
Date: 22/11/2019

Dedicated to my loving Heavenly Father

"Lord Jesus Christ"

ACKNOWLEDGEMENT

Firstly, I am boundless thankful to my Heavenly Father "Jesus Christ" for His showers of blessings, strength, fortitude and patience to complete my research successfully. I would like to thank my lovable mom-dad, my sister and my in-laws for their everlasting support and care through my life.

I am extremely grateful to my supervisor Dr. Sachin Ulhasrao Belgamwar, (Faculty In-charge, First Degree - Test (AUGSD) BITS-Pilani, Pilani Campus). He is an immensely patient person and helped me beyond measure to finish this thesis. He is good researcher, wonderful teacher great advisor. He was available at any time for discussing any research query and other problem that I faced. His experience helped me a lot to face many ups and downs through the research work.

I also extremely thankful to my co-supervisor(s) Dr. Ajay Agarwal (Sr. Principal Scientist, Group Head, Nano Bio Sensors, CSIR-CEERI, Pilani) and Prof. Niti Nipun Sharma (Pro-President and Dean-Faculty of Engineering, Department of Mechanical Engineering, Manipal University, Jaipur) for their guidance and support throughout the course of this research. Their expertise in presenting the scientific work added scientific value in my thesis. Their advices inspired, motivated and encouraged me to overcome the difficult moments.

I am immensely thankful to Prof. Souvik Bhattacharyya, Vice-Chancellor, BITS-Pilani; Prof. Ashoke Kumar Sarkar, Director, BITS-Pilani, Pilani Campus for allowing me the opportunity to pursue my research work. I am thankful to Prof. S.K. Verma, (Dean, Administration, BITS-Pilani, Pilani Campus) for his king support. I express my gratitude to Prof. Srinivas Krishnaswamy (Dean, Academic Graduate Studies & Research Division); Prof. Ajit Pratap Singh (Dean, Academic-Undergraduate Studies Division (AUGSD)), Prof. Jitendra Panwar (Associate Dean, Academic Graduate Studies & Research Division), BITS-Pilani, Pilani Campus, for their constant and official support and encouragement.

My sincere thanks to Prof. Mani Sankar Dasgupta (Head of the Department, Mechanical Engineering), Dr. Prabhat N. Jha (Head of the Department, Biological Science),

Prof. Atish T. Paul (Head of the Department, Pharmacy), Dr. Saumi Ray (Head of the Department, Chemistry) and Dr. Hare Krishna Mohanta (Head of the Department, Chemical Engineering) for their kind support during completion of the research work. I am grateful to the entire faculty of Mechanical Engineering Department for their kind support and assistance.

I thank Prof. Kuldip Singh Sangwan (Chief, Central Placement Unit); Doctoral Research Committee (DRC); my Doctoral Advisory Committee (DAC) members, Prof. Mani Sankar Dasgupta (Mechanical Engineering Department) and Prof. Anshuman Dalvi (Department of Physics); for their precious suggestions to improve the quality of my PhD thesis. My thanks to Prof. Srikanta Routroy (Associate Dean, Student Welfare Division, BITS-Pilani, Pilani Campus), Prof. B.K. Rout (Associate Professor, Mechanical Engineering, BITS Pilani, Pilani Campus) and Dr. Jitendra Singh Rathore (Faculty In-charge, Registration & Counselling (AUGSD) BITS-Pilani, Pilani Campus) for their great help and support. I am thankful to Prof, Manoj Soni (coordinator of Center for Renewable Energy and Environmental Development (CREED) of BITS, Pilani) for his time to time and patienceful guidance.

I am immensely grateful to Prof. Madhushree Sarkar, Assistant Professor, Prof. Surojit Pande, Associate Professor, Department of Chemistry, BITS-Pilani, Pilani Campus, Prof. Aniruddha Roy, Assistant Professor, Department of Pharmacy, BITS, Pilani; Prof. Suresh Gupta, (Associate Dean, Academic Under Graduate Studies Division & Associate Professor, Department of Chemical Engineering, BITS-Pilani, Pilani Campus) for shearing their knowledge, experience and valuable advice on my thesis work. My deep gratitude to Prof. Surekha Bhanot (Department of Electronics and Electrical/Instrumentation) and Mrs. Neelam Bhatia for their continuous motivations throughout my research period.

I express my gratitude to Dr. Samir V. Kamat (Ex-Director, Defense Metallurgical Research Laboratory, DRDO, Hyderabad), Dr. Partha Ghoshal (Scientist "F" & Head, Defense Metallurgical Research Laboratory, DRDO, Hyderabad) and their team for allowing me to access their characterization facilities, because of which I was able to finish my all experimental works. My boundless vote of thanks to Dr. Debmalya Roy (Head, Directorate of Nanomaterials & Technologies, Defence Materials and Stores Research and Development Establishment, DRDO, Kanpur) and Dr. Dibyendu Sekhar Bag (Head, Polymer Matrix Composites Division & Joint Director, Defence Materials

and Stores Research and Development Establishment, DRDO, Kanpur). I am thankful to Dr. Girish Aren, Macwin India Pvt. Ltd. and his team for their extreme support in times thick and thin. My special vote of thanks to my all time chemistry teacher, Mr. Bhabatosh Kar (M.Sc in Organic Chemistry), Head of Chemistry Department, Kamalpur Netaji High School, Bankura, West Bengal for his intrinsic motivational teaching in chemistry and without his influential instruction I could not take courage to do research in "Polymer Engineering".

I would also like to express my gratitude to all the technical staff, Mechanical Engineering Department, especially to Sh. Rohitash Kumar, Sh. Pawan, Sh Harish Soni and Sh. Dhannaram Saini for providing their immense support. I would like to thanks Sh. Santosh Kumar Saini (Academic Under graduate Studies Division, BITS-Pilani Campus) for his help in assembling of my thesis. Thanks to Sh. Suresh Kumar, Academic Under-graduate Studies Division (AUGSD) for his support.

My endless thanks to my friends: Dr. Vijay Kumar, Dr. Rahul Ramachandran, Dr. Neha Arora, Mrs. Shivani Nain, Mrs. Paridhi Puri, Mr. Ayush, Mr. Ajay, Mr. Rahul Kotesa who endured this long process with me, always offering support and care. My boundless thank to Ms Shraddha Mishra for her help and support.

In particular I must acknowledge my husband Er. Tonmoy Kanti Das (Sci Tech Services), a deepest gratitude for his understanding, endless patience and encouragement for completion of my thesis.

TAMALIKA BHAKAT

ABSTRACT

Non-invasive or minimally invasive drug delivery is painless, easy to use, patient compatible. But due to many challenges during non-invasive delivery hydrogel has been used as drug carrier material to facilitate the drug delivery without any hurdle by utilizing its many good points like stimuli sensitivity (pH, temperature, etc.), controlled the drug release, prevention of the unexpected drug leakage, mucoadhesivity, drug protection from enzymetic degradation etc. In existing research, hydrogel has been utilized in non-invasive delivery with different formulations. This research has been found that some actions by hydrogel during drug delivery are still few milestones away. For instances: enhanced grafting for the synthesis of biohydrogel, acid stability of drug carrier, simultaneous exposure of multi stimuli, etc. To cover those mile stones, this research has proposed some points which have been executed and described in details in respective chapters. From the material selection for gel preparation to the confirmation of being "Biohydrogel", this research is presented the way of execution of proposed in seven chapters which are briefly described in below:

- Chapter 1 discussed the importance and the types of drug delivery in terms of the routes of their administration. Conventionally, invasive routes were applied for drug administration but many difficulties related to drug placing, pharmacist are compelled to introduce the non-invasive drug delivery. With many positive points non-invasive delivery are struggles with some disadvantages which are discussed in the chapter. The introduction of hydrogel as drug carrier, its properties, and its role to recover the challenges of non-invasive delivery are discussed.

- Chapter 2 involves an extensive review on different hydrogel based dosage formulations and their stimuli triggered drug release mechanisms to maintain (i) accurate dose, (ii) protection to the drug, from gastric acid, enzymatic degradation, (iv) easy administration of drugs within body tissues, (v) controlled release mechanism with optimal drug action, (vi) prolonged and sustained medication as per requirements, (vii) usage of desired vehicle for insoluble drugs. The utilization of hydrogel based formulations in the discussed routes from Chapter 1, have been

extensively reviewed in terms of the drug encapsulation and release. This chapter is highlighted the gaps in reported research especially on polymer synthesis, properties and stimuli sensitivities. How the gaps can be resolved, some ideas are proposed at the end section of this chapter.

- Chapter 3 is dedicated for selecting the material to synthesis the positive hydrogel. This research categorised two kind of positive hydro and they are Upper Volume Phase Transition Temperature (UVPTT) based hydrogel and Non Upper Volume Phase Transition Temperature (Non-UVPTT) based hydrogel. UVPTT based hydrogel was composed of β-Cyclodextrin and poly(acrylic acid-co-acrylamide) where as Non-UVPTT contained guar gum and acrylamide. To synthesis the polymers, selection of crosslinker, initiator have been discussed in this chapter.

- Chapter 4 contains the gel synthesis protocol and morphological characterization of polymer to confirm about the gel synthesis. The available synthesis techniques and their know-how are discussed. The thermal assisted free radical bulk polymerization is discussed the polymerization process in detail. The formation of polymer and grafting was confirmed by attenuated total reflectance (ATR) spectroscopy and nuclear magnetic resonance (NMR) spectroscopy. Differential scanning calorimetry (DSC) and thermogravimetric analysis (TGA) are discussed to determine the glass transition temperature and thermal stability of both UVPTT and non UVPTT based polymer. The synthesis of gold nanoparticle reinforced nanocomposites is briefly described to add photo responsive property.

- Chapter 5 discussed the stimuli sensitivity of synthesized UVPTT and non-UVPTT based positive hydrogel. The temperature, pH and visible light were used as stimuli. The stimuli triggered reversible volume switching and polymer network parameters are discussed. Diffusion based swelling kinetics is analyzed. In this research, all stimuli sensitive memory losses with released solvent were observed without help of mechanical shaker. During dual responsive solvent release phenomena temperature and pH both stimuli were applied simultaneously.

- Chapter 6 dedicated for stimuli triggered drug release phenomena by both UVPTT and non-UVPTT based positive hydrogels. Ciprofloxacin hydrochloride (CFXH) has been used as model drug. Temperature and light assisted loading-release of CFXH is

discussed and the data were compared between the gels to evaluate the release efficiency. Temperature and light controlled loading helped the polymer to titrate the dose on-demand. This will help the patient to load and release the drug with required dose according to their need. The light and temperature responsive drug release phenomena can be applied as transdermal delivery. pH sensitive drug release was observed duribg prolonged time to evaluated in-vitro gastroretentive drug delivery. For gastroretentive drug delivery, polymeric drug dispenser should be chemically stable in acidic medium which is discussed in Chapter 4. After prolonged release of CFXH, its bioactivity was confirmed on in-vitro bacteria culture and the released solvent was successfully inhibited the bacterial cell proliferation with increasing amount of drug.

- Chapter 7 described the biocompatibility of polymer to prevent the transportation of toxic agent from carrier to drug to target area. To avoid the cruelty, hazardous act on animals in-vitro findings has been investigated on the viable mouse breast cancer cell line(L929). The antimicrobial property of both polymer were evaluated on gram positive (*Bascillus Subtilis*) and gram negative bacteria (*E. Coli*) by inhibiting their cell proliferation. The successful biocompatibility and antibacterial testing decided the polymer to be biomaterial.

Table of Contents

CONTENTS	Page No.
Acknowledgement	i-iii
Abstract	v-vii
Table of Contents	ix-xii
List of Figures	xiii-xx
List of Tables	xxi-xxii
CHAPTER 1 Introduction	**1-24**
1.1 Drug Delivery and Its Importance	1
1.2 Invasive Drug Delivery	2
1.3 Non-invasive or Minimally Invasive Drug Delivery	5
1.4 Challenges in Non-invasive Delivery	7
1.5 Introduction of Hydrogel	8
1.5.1 Types of Hydrogel	10
1.5.2 Self-assembled Hydrogels	15
1.5.3 Biohydrogels	15
1.6 Role of Hydrogel in Non-invasive Drug Delivery	16
1.7 Conclusion	18
References	20
CHAPTER 2 Literature Review	**25-86**
2.1 Introduction	25
2.2 Different Hydrogels Based Dosage Formulations	26
2.3 Utilization of Dosage Formulations Non-invasively	36
2.4 Gaps in Existing Research	67
2.5 Scope of Research	69
2.6 Methodology	71
References	75
CHAPTER 3 Material Selection	**87-104**
3.1 Introduction	87

CONTENTS Page No.

3.2 Selection of Material 87

3.2.1 Upper Volume Phase Transition Temperature (UVPTT) based Hydrogel 88

3.2.2 Non-Upper Volume Phase Transition Temperature (Non-UVPTT) based Hydrogel 92

3.2.3 Polymerization Assisted Material 93

3.2.4 Hydrogel Nanocomposite 94

3.3 Detailing of Materials 97

3.4 Conclusion 97

References 99

CHAPTER 4 Gel Synthesis and Morphological Characterization 105-150

4.1 Introduction 105

4.2 Bulk Polymerization Synthesis Process 107

4.2.1 Synthesis Protocol for UVPTT based β-CD Modified Positive Hydrogel 110

4.2.2 Synthesis Protocol For Non-UVPTT Based Guar Gum Modified Positive Hydrogel 111

4.2.3 Synthesis Protocol for Hydrogel Nanocomposite 113

4.3 Polymer Synthesis 114

4.3.1 Synthesis of UVPTT based β-Cyclodextrin Modified Positive Hydrogel 114

4.3.2 Synthesis of Non-UVPTT based Guar Gum Modified Positive Hydrogel 117

4.3.3 Preparation of Hydrogel Nanocomposite 125

4.4 Formulation Codes of Synthesized Gels 127

4.5 Morphological Characterization 128

4.6 Morphological Characterization of Gel Nanocomposites 140

4.7 Stability in Acidic Medium 142

4.8 Conclusions 144

References 146

CONTENTS Page No.

CHAPTER 5 Functional Characterization of Polymer 151-230

5.1 Introduction 151

5.2 Experimental Procedure: Effects of Stimuli on Equilibrium Swelling (ES) Studies 152

5.2.1 Effect of Medium pH on ES 153

5.2.2 Effect of Medium Temperature on ES 154

5.2.3 Effect of Visible Light on ES 154

5.3 Results and Discussions: Effects of Stimuli on Equilibrium Swelling (ES) Studies 155

5.4 Theoretical Aspect: Equilibrium Swelling Kinetics 164

5.5 Experimental Aspect: Equilibrium Swelling Kinetics 165

5.6 Theoretical View: Role of Gel Network and Diffusion on Equilibrium Swelling 169

5.7 Experimental Analysis: Role of Gel Network on Equilibrium Swelling Stimuli 174

5.8 Experimental Analysis: Role of Diffusion on Equilibrium Swelling Stimuli 191

5.9 Experimental Procedure: Stimuli Assisted Volume Switching of Polymer 198

5.10 Experimental Analysis: Stimuli Assisted Volume Switching of Polymer 201

5.11 Swelling and De-Swelling: Role of Network Energy on Stimuli 213

5.12 Comparison Between UVPTT and Non-UVPTT on Stimuli Responsiveness 217

5.13 Conclusion 219

References 225

CHAPTER 6 Polymer Application Studies 231-302

6.1 Introduction 231

6.2 Ciprofloxacine Hydrochloride: A model Drug 233

6.3 Experimental procedure: Gel as Drug Dispenser 234

6.3.1 Combination I 236

6.3.2 Combination II 239

6.3.3 Combination III 241

6.3.4 Combination IV 243

CONTENTS		Page No.
6.4	Results and Discussions: Gel as Drug Dispenser	243
6.5	Comparison Study on Drug Release Efficacy of Both UVPTT and Non-UVPTT based Gels Under Different Stimuli Combinations	267
6.6	Drug Entrapment-Release Kinetics: Theoretical Overview	272
6.7	Drug entrapment-Release Kinetics: Investigational Analysis	277
6.8	Confirmation on CFXH release	282
6.9	Conclusion	287
	References	297
CHAPTER 7	**Biocompatibility Analysis, Conclusion and Future Scope**	**303-320**
7.1	Introduction	303
7.2	Cytotoxicity Analysis	304
7.3	Antibacterial Analysis	307
7.4	Overall Conclusions	312
7.5	Future Scope Of Works	313
	References	315
Annexure I		321-336
Annexure II		337-341
Annexure III		342-346
List of Publications		347
Brief biography of the Candidate		349
Brief biography of the Supervisor		351
Brief biography of the Co-Supervisor		353
Brief biography of the Co-Supervisor		355

List of Figures

Figure No.	Title	Page No.
1.1	Steroid injection into spine	2
1.2	Anti-VEGF drug injection into eyes	3
1.3(a)	Transdermal patch with microneedle array	6
1.3(a)	Transdermal patch without microneedle array	6
1.4	Structures of different synthetic hydrogel	9
1.5	Types of Hydrogels according to polymeric composition	10
1.6	pH-dependent ionization of Poly(acrylic acid) (top) and poly(N,N'-diethylaminoethyl methacrylate) (bottom)	12
1.7	Structure of leuco derivative molecule bis(4-(dimethylamino)phenyl) (4-vinylphenyl)methyl leucocyanide	14
1.8	Photoisomerization of hydrogel	14
1.9	Schematic for In-situ formation of hydrogel using chemical or physical crosslinking methods	15
2.1	Sol-gel transition of PEG based *in-situ* polymer	27
2.2	Polymeric nanoparticle	30
2.3	Polymeric liposome	32
2.4	Core-Shell Micelle in nonpolar solvent	33
2.5	optical and TEM image of polymeric nanoparticle reinforced nanogel	35
3.1	Structure of Cyclodextrin	90
3.2	Primary and secondary opening of β-Cyclodextrin	90
3.2(a)	Molecular exclusion of β-CD with Maleic Anhydride	92
3.2(b)	Molecular inclusion of β-CD	92
3.3	Structure of guar gum (GG)	93
4.1	Schematics of bulk polymerization setup	107
4.2	Schematic of Synthesis protocol of β-cyclodextrin modified hybrid UVPTT hydrogel	110

Figure No.	Title	Page No.
4.3	Schematic for gel synthesis protocol	112
4.4	Schematics of AuNP reinforcement into polymer by Dip method	113
4.5	Schematics of AuNP reinforcement into polymer by *In-situ* synthesis method	113
4.6	Reaction schematic for the synthesis of reactive monomer MAH-β-CD	114
4.7	Reaction schematic for the synthesis of Paac-g-β-CD	115
4.8 (a)	Copolymerization method between β-CD-g-Paac and Paam	116
4.8 (b)	Reaction schematic for the synthesis of β-CD-g-(Paac-*co*-Paam)	117
4.9	Grafting method between GG and Paam	119
4.10	Structure of synthesized graft polymer (GG-*g*-Paam)	121
4.11	Percentage of grafting efficiency of TGs	121
4.12(a)	Precipitation during synthesis with ACS with 150 minutes	122
4.12(b)	Gel formation with ACS with 300 minutes	122
4.13	IPN formation by cross linking with GG and GA	124
4.14	Structure of synthesized double crosslinked (DC-GG-PaamGAi) polymer	124
4.15(a)	Monodispersed solution of AuNP	126
4.15(b)	AuNP reinforced polymer composite	126
4.15(c)	Agglomerated nanoparticle without CTAB	127
4.15(d)	MonodispersedAuNP solution using guar gum and /or beta-CD as stabilizer	127
4.15(e)	Precipitation of gold salt in polymer network	127
4.15(f)	MonodispersedAuNP solution using guar gum and/or beta CD as stabilizer	127
4.16(a)	ATR spectra of Polyacrylamide (Paam)	129
4.16(b)	ATR spectra of β-Cyclodextrin (β-CD)	129
4.16(c):	ATR spectra of β-CD-g-(Paac-co-Paam)IPN	129
4.17	Solid state 13C NMR spectra for β-CD-g-(Paac-*co*-Paam) IPN gel	130
4.18	DSC thermogram of β-CD-g-(Paac-co-Paam) IPN	131
4.19	ESEM of β-CD-g-(Paac-co-Paam) IPN	132

Figure No.	Title	Page No.
4.20	ATR spectra of (a) acrylamide (Aam), (b) crude guar gum, (c) graft polymer (GG-*g*-Paam) and (d) double crosslinked polymer (DC-GG-PaamGA4.39)	133
4.21(a)	Solid state 13C NMR spectra for crude guar gum	134
4.21(b)	Solid state 13C NMR spectra for polyacrylamide (Paam)	135
4.21(c)	Solid state 13C NMR spectra for GG-*g*-Paam	135
4.21(d)	Solid state 13C NMR spectra for DC-GG-PaamGA4.39	136
4.21(e)	^{1}H NMR spectra for G-g-Paam	136
4.22	DSC Thermogram of (a) Crude guar gum (GG), (b) Acrylamide (Aam), (c) Graft polymer (GG-*g*-Paam) and (d) Double crosslinked polymer (DC-GG-Paam$_{GA4.39}$)	137
4.23	TGA of (a) Crude guar gum (GG), (b) Acrylamide(Aam), (c) Graft polymer (GG-*g*-Paam) and (d) GA containing double crooslinked polymer (DC-GG-PaamGA$_{4.39}$)	138
4.24(a)	ESEM image of GG-g-Paam	139
4.24(b)	ESEM image of DC-GG-Paam$_{GA0.80}$	139
4.24(c)	ESEM image of DC-GG-Paam$_{GA1.60}$	139
4.24(d)	ESEM image of DC-GG-Paam$_{GA2.20}$	139
4.24(e)	ESEM image of DC-GG-Paam$_{GA4.39}$	140
4.24(f)	ESEM image of DC-GG-Paam$_{GA6.59}$	140
4.25(a)	TEM of β-CD-g-(Paac-*co*-Paam)-1 composite	141
4.25(b)	TEM of β-CD-g-(Paac-*co*-Paam)-3 composite	141
4.26(a)	TEM of DC-GG-PaamGA4.39-1 composite	141
4.26(b)	TEM of DC-GG-PaamGA4.39-3 composite	141
4.26(c)	TEM of DC-GG-PaamGA4.39-5 composite	141
4.26(d)	AuNP size distribution of polymer composite	142
4.26(e)	UV-vis Spectra of β-CD-g-(Paac-*co*-Paam) composites	142
4.26(f):	Fig. UV-vis Spectra of DC-GG-Paam$_{GA4.39}$ composites	142
4.27	ATR spectra of IPN β-CD-g-(Paac-*co*-Paam)	143
4.28(a)	ATR Spectra of acid hydrolyzed GG-g-Paam	143

Figure No.	Title	Page No.
4.28(b)	ATR Spectra of acid hydrolyzed DC-GG-Paam$_{GA4.39}$	144
5.1	Schematic illustration of stimuli triggered ES phenomenon	155
5.2	Equilibrium swelling, ES (wt/wt) % in different medium stimuli	156
5.3	Volumetric equilibrium swelling, ES (v/v) % in different pH stimuli	157
5.4	Equilibrium swelling, ES (wt/wt) % at temperature stimuli	157
5.5	Volumetric equilibrium swelling, ES (v/v) % at different temperature	158
5.6	Equilibrium swelling, ES (wt/wt) % at visible light stimuli	159
5.7	Equilibrium swelling, ES (v/v) % at visible light stimuli	159
5.8(a)	Equilibrium swelling, ES (wt/wt) % in pH4 buffer medium	160
5.8(b)	Equilibrium swelling, ES (wt/wt) % in pH7 buffer medium	160
5.8(c)	Equilibrium swelling, ES (wt/wt) % in pH9.2 buffer medium	161
5.9	Volumetric equilibrium swelling, ES % in acidic, neutral and alkaline stimuli	161
5.10(a)	Equilibrium swelling (wt/wt) % at 10°C	162
5.10(b)	Equilibrium swelling (wt/wt) % at 40°C	162
5.11	Equilibrium swelling, ES (v/v) % at 10°C and 40°C	163
5.12	Equilibrium swelling (wt/wt) % under visible light exposure	164
5.13	Equilibrium swelling (v/v) % under visible light exposure	164
5.14	Dependencies of polymer volume fraction, φ during ES	175
5.15	Dependencies of molecular weight between two cross links, MC during ES	176
5.16	Dependencies of Cross link density, CLD (ρC) during ES	176
5.17	Dependencies of Mesh size, (ζ) during ES	177
5.18	Dependencies of Porosity during ES	177
5.19	Dependencies of Tortuosity during ES	177
5.20	Dependencies of enthalpy and entropy on pH during ES with pH stimuli	178
5.21	Dependencies of enthalpy and entropy during temperature assisted ES	178
5.22	Dependencies of Chain configurational entropy energy on pH and temperature stimulated ES	179

Figure No.	Title	Page No.
5.23	Schematic of temperature and light assisted ES phenomenon	180
5.24(a)	Dependencies of ES % and Cross link density on non-UVPTT network in acidic buffer stimuli	181
5.24(b)	Dependencies of ES % and Cross link density on non-UVPTT network in neutral buffer stimuli	182
5.24(c)	Dependencies of ES % and Cross link density on non-UVPTT network in alkaline buffer stimuli	182
5.25(a)	Effect of mol. wt. between two cross links (MC) and mesh size (ζ) on non-UVPTT network in acidic buffer	183
5.25(b)	Effect of mol. wt. between two cross links (MC) and mesh size (ζ) on non-UVPTT network in neutral buffer	183
5.25(c)	Effect of mol. wt. between two cross links (MC) and mesh size (ζ) on non-UVPTT network in alkaline buffer	184
5.26	Dependencies of polymer volume fraction (ϕ) in different stimuli medium	184
5.27	Stimuli effect on porosity in all gels	185
5.28	Stimuli effect on tortuosity for all samples	185
5.29(a)	Dependencies of ES (v/v)% and CLD on GA into gel network at 10°C ES temperature	186
5.29(b)	Dependencies of ES (v/v)% and CLD on GA into gel network at 40 °C ES temperature	186
5.30(a)	Dependencies of molecular weight between two cross links, MC and Mesh size, ζ on GA into gel network at 10 °C ES temperature	187
5.30(b)	Dependencies of molecular weight between two cross links, MC and Mesh size, ζ on GA into gel network at 40 °C ES temperature	187
5.31	Dependencies of Polymer volume fraction, ϕ on GA into gel network at 10 °C and 40 °C ES temperature	188
5.32	Dependencies of Porosity, P on GA into gel network at 10°C and 40°C ES temperature	188
5.33	Dependencies of Tortuosity, τ on GA into gel network at 10°C and 40°C ES temperature	189
5.34	Schematic illustrations of laser assisted nanoparticle heating	191
5.35(a)	Case I: Effect of pH switching (pH4-pH7-pH4-pH7-pH4)	201
5.35(b)	Case II: Effect of pH switching (pH4-pH9.2-pH4-pH9.2-pH4)	202
5.35(c)	Case III: Effect of pH switching (pH7-ph9.2-pH7-pH9.2-pH7)	202
5.36(a)	Forward Approach (FWA), the effect of temperature on volume	203

Figure No.	Title	Page No.
	alteration	
5.36(b)	Reverse Approach (REVA), the effect of temperature on volume alteration	204
5.37	Responsivity of UVPTT gel on dual stimuli	205
5.38	Visible light switching effect on UVPTT composites	206
5.39(a)	Case I: Effect of pH switching on ES samples	207
5.39(b)	Case II: Effect of pH switching on ES samples	207
5.39(c)	Case III: Effect of pH switching on ES samples	208
5.40(a)	Forward Approach (FWA), the effect of temperature on volume alteration	209
5.40(b)	Reverse Approach (REVA), the effect of temperature on volume alteration	209
5.41(a)	Dual responsivity in Case I	211
5.41(b)	Dual responsivity in Case II	212
5.41(c)	Dual responsivity in Case III	212
5.42	Visible light stimuli effect on volume switching of non-UVPTT composites	213
6.1	Structure of Ciprofloxacine hydrochloride	233
6.2	Flow chart for drug dispensing activities in different combinations	236
6.3	Percentage of CFXH solute entrapment for 0.3 (v/v) % and 0.7 (v/v) % solutions	245
6.4	Percentage of CFXH solute release for 0.3 (v/v) % and 0.7 (v/v) % solutions	245
6.5	CFXH solute retention (mg.cc -1) % for both CFXH solutions	246
6.6	Percentage of CFXH solute entrapment into β-CD modified ExtLS	247
6.7	Release of CFXH solute (wt/wt) % for 0.3 (v/v) % and 0.7 (v/v) % CFXH solutions	248
6.8	CFXH solute retention (mg.cc-1) % for 0.3 (v/v) % and 0.7 (v/v) % CFXH solutions	248
6.9	Release of CFXH solute (wt/wt) % for 0.3 (v/v) % and 0.7 (v/v) % CFXH solution	249
6.10	CFXH solute retention (mg.cc-1) % for 0.3 (v/v) % and 0.7 (v/v) % CFXH solution	249
6.11(a)	CFXH solute entrapment and release profile for 0.3 (v/v) % CFXH solution for β-CD-g-(Paac-co-Paam)-1 composite gel	250
6.11(b)	CFXH solute entrapment and release profile for 0.7 (v/v) % CFXH solution in β-CD-g-(Paac-co-Paam)-1 composite	251

Figure No.	Title	Page No.
6.11(c)	CFXH solute entrapment and release profile for 0.3 (v/v) % CFXH solution in β-CD-g-(Paac-co-Paam)-3 composite	251
6.11(d)	CFXH solute entrapment and release profile for 0.7 (v/v) % CFXH solution in β-CD-g-(Paac-co-Paam)-3 composite	252
6.12	Percentage of CFXH solute retention for 0.7 (v/v) % CFXH solution in β-CD modified UVPTT based composites	252
6.13(a)	Percentage of CFXH solute entrapment for 0.3 (v/v) % CFXH solution	254
6.13(b)	Percentage of CFXH solute entrapment for 0.7 (v/v) % CFXH solution	254
6.14(a)	Percentage of CFXH solute release for 0.3 (v/v) % CFXH solution	254
6.14(b)	Percentage of CFXH solute release for 0.7 (v/v) % CFXH solution	255
6.15	CFXH solute retention (mg.cc -1) % for both CFXH solutions	255
6.16(a)	Percentage of CFXH solute entrapment into GG-g-Paam ExtLS	256
6.16(b)	Percentage of CFXH solute entrapment into DC-GG-PaamGA4.39	257
6.17(a)	Release of CFXH solute (wt/wt) % for 0.3 (v/)\v) % CFXH solution	258
6.17(b)	Release of CFXH solute (wt/wt) % for 0.7 (v/)\v) % CFXH solution	258
6.18(a)	Change of sample weight (%) for 0.3% CFXH solution in pH7	259
6.18(b)	Change of sample weight (%) for 0.7% CFXH solution in pH7	259
6.18(c)	Change of sample weight (%)for 0.3% CFXH solution in pH9.2	260
6.18(d)	Change of sample weight (%)for 0.7% CFXH solution in pH9.2	260
6.19	CFXH solute retention (mg.cc-1) % for 0.3 (v/v) % and 0.7 (v/v) % CFXH	261
6.20(a)	Case I: Release of CFXH solute (wt/wt) % for 0.3 (v/v) % CFXH solution	262
6.20(b)	Case I: Release of CFXH solute (wt/wt) % for 0.7 (v/)\v) % CFXH solution	262
6.20(c)	Case II: Release of CFXH solute (wt/wt) % for 0.3 (v/v) % CFXH solution	263
6.20(d)	Case II: Release of CFXH solute (wt/wt) % for 0.7 (v/)\v) % CFXH solution	263
6.20(e)	Case III: Release of CFXH solute (wt/wt) % for 0.3 (v/v) % CFXH solution	264
6.20(f)	Case III: Release of CFXH solute (wt/wt) % for 0.7 (v/v) % CFXH solution	264
6.21	CFXH solute retention (mg.cc-1) % for 0.3 (v/v) % and 0.7 (v/v) % CFXH solution	265

Figure No.	Title	Page No.
6.22(a)	CFXH solute entrapment and release profile for 0.3 (v/v)% CFXH solution in non-UVPTT based composite gels	266
6.22(b)	CFXH solute entrapment and release profile for 0.7 (v/v) % CFXH solution in non-UVPTT based composite gels	266
6.23	Percentage of CFXH solute retention non-UVPTT based composite gels	267
6.24(a)	UV-Spectra of 0.3% CFX release	282
6.24 (b)	UV-Spectra of 0.7% CFX release	282
6.25	12 Well cell culture plate	284
6.26(a)	Effect of 0.3% CFXH on E. coli proliferation	284
6.26(b)	Effect of 0.7% CFXH on E. coli proliferation	285
6.26(c)	Effect of 0.3% CFXH on Bacillus proliferation	285
6.26(d)	Effect of 0.7% CFXH on Bacillus proliferation	285
7.1	Cell viability of L929 cell with variable concentration of β-CD-g-(Paac-co-Paam)	305
7.2	Cell viability of L929 cell with variable concentration of DC-GG-PaamGA4.39	305
7.3	Cell viability of L929 cell with variable concentration of GG-g-Paam	306
7.4	Cell viability of L929 cell with variable concentration of β-CD-g-(Paac-co-Paam) nanocomposite	307
7.5	Cell viability of L929 cell with variable concentration of GG-g-Paam composites	307
7.6	Bacterial inhibition effect of β-CD-g-(Paac-co-Paam)	309
7.7	Bacterial inhibition effect of GG-g-Paam	309
7.8	Bacterial inhibition effect of DC-GG-PaamGA4.39	310
7.9(a)	Bacterial inhibition effect of β-CD IPN composites on E. Coli	310
7.9(b)	Bacterial inhibition effect of β-CD IPN composites on B. Subtilis	311
7.10(a)	Bacterial inhibition effect of non-UVPTT composites on E. Coli	311
7.10(b)	Bacterial inhibition effect of non-UVPTT composites on Bacillus. Subtilis	311

List of Tables

Table No.	Title	Page No.
2.1	Summarization of reported works on hydrogel based dosage formulation for non-invasive delivery	59
3.1	List of materials	97
4.1.	Composition of all TGs	118
4.2	Percentage of Grafting efficiency for all TGs	120
4.3	Compositions of differently formulated polymer samples	123
4.4	Gel formulation code	127
5.1	Dry/ Initial Sample parameters	153
5.2A	Swelling rate constant for 1st order and 2nd order kinetics at Equilibrium Swelled (ES) state under applied buffer stimuli for UVPTT based polymer	166
5.3A	Swelling rate constant for 1st order and 2nd order kinetics at Equilibrium Swelled (ES) state under applied temperature for UVPTT based polymer	166
5.4A	Swelling rate constant for 1st order and 2nd order kinetics at Equilibrium Swelled (ES) state under applied visible light (laser irradiation) stimuli for UVPTT based polymer	166
5.2B	Swelling rate constant for 1st order and 2nd order kinetics at Equilibrium Swelled (ES) state under applied medium buffer stimuli for non-UVPTT based polymer	167
5.3B	Swelling rate constant for 1st order and 2nd order kinetics at Equilibrium Swelled (ES) conditions under external temperature stimuli for non-UVPTT based polymer	168
5.4B	Swelling rate constant for 1st order and 2nd order kinetics at Equilibrium Swelled (ES) state under applied visible light (laser irradiation) stimuli for non-UVPTT based polymer	168
5.5	Density of water at different temperatures	170
5.6	Measure network parameter of β-CD-g-(Paac-*co*-Paam) composites during light assisted ES	180
5.7	Measure network parameter of non-UVPTT based composites during laser irradiated ES	190

Table No.	Title	Page No.
5.8(a)	Measured values of Diffusion rate constant with Adj.R-square, diffusion co-efficient, diffusion exponent, front velocity and type of diffusion at environmental medium stimuli ES phenomenon	194
5.8(b)	Measured values of Diffusion rate constant with Adj.R-square, diffusion co-efficient, diffusion exponent, front velocity and type of diffusion at temperature stimulated ES phenomenon	196
5.8(c)	Measured values of Diffusion rate constant with Adj.R-square, diffusion co-efficient, diffusion exponent, front velocity and type of diffusion at visible light irradiated ES phenomenon	197
5.9	Dependencies of enthalpy, solvent entropy and the chain configurational entropy energies on pulsatile stimuli	215
5.10A	Effect of solo pH switching on percentage of Memory Loss (ML%) of β-CD modified UVPTT gel	218
5.10B	Effect of solo pH switching on percentage of Memory Loss (ML%) of guar gum modified non-UVPTT gels	218
5.11A	Effect of solo temperature switching on percentage of Memory Loss (ML%) of UVPTT gel	218
5.11B	Effect of solo temperature switching on percentage of Memory Loss (ML%) of non-UVPTT gels	218
5.12	Stimuli responsiveness on equilibrium swelling in current research	223
5.13	Summarization of stimuli responsive swelling on reported hydrogel	224
6.1	Dry/initial sample parameters	244
6.2(a)	The efficiency of UVPTT based gels and composites for 0.3 (v/v) % CFXH release	268
6.2(b)	The efficiency of UVPTT based gels and composites for 0.7 (v/v) % CFXH release	269
6.3(a)	The efficiency of non-UVPTT based gels and composites for 0.3 (v/v) % CFXH release	270
6.3(b)	The efficiency of non-UVPTT based gels and composites for 0.7 (v/v) % CFXH release	271
6.4	Antibacterial effect on *E. Coli.* and *Bacillus Subtilis*	286
6.5	Drug Encapsulation/Release on reported research	291

Chapter 1

Introduction

This chapter contains the demands and limitations of drug delivery. Importance of choosing different routes of drug administrations, their benefits and shortcomings are described here. How material, especially polymer plays the role in different routes of administration is detailed here.

1.1 Drug Delivery and Its Importance

Drug delivery is a process or technique to administer the pharmaceutical agent to achieve a therapeutic effect in mammalian body. Drugs are fast and/or slow acting bio-chemical compounds that are generally dispensed orally or as injectable. In biomedical field drug delivery is very important and critical action. For instances, in tissue engineering, to repair the damaged tissue, regeneration of healthy cells and tissue with fast growth rate can be achieved by drug delivery system [1]. Drug delivery into brain is difficult and perilous action due to complex structure of brain and unhealthy blood brain barrier, which is a semipermeable membrane for separating the circulating blood from brain to central nervous system [2]. The disrupted BBB of brains of patients with Parkinson's disease, Alzheimer's disease and brain tumors obstructs the drug to be diffused into the brain [3]. Good bioavailability is the principal pharmacokinetic properties of drugs, is described as fraction of an administered dose of unchanged drug that reaches the systemic circulation [4]. Administered drug with low bioavailability, drops its blood plasma concentration below an effective level, which leads to re-administration of drug. This can lead to decreased patient compliance and increase the possibility of an overdose [5]. The demand for drug delivery and different limitations are compelled to design optimal medication, dose titration and therapeutic drug monitoring [6] for the diseased like cancer, neural diseases, and other infectious diseases. The drug delivery at predetermined rate, for a determined period is a good alternative to accomplish the above discussed issues during administration. The drug delivery process controls the drug release rate at the targeted place but experienced some side effect as the drug can interact to the healthy cell and tissue which are not targeted place for drug

delivery. The decision making on selecting the pathological routes for drug administration is the first step to maintain the key points of drug delivery. Drug administration routes are categorized as invasive and minimally or non-invasive delivery. Let's discuss about the invasive route of administration.

1.2 Invasive Drug Delivery

"Invasive" is the term of a medical procedure which includes some surgical actions, to deliver the drug inside body[1]. The examples of invasive delivery techniques are:

Pain Management: For treating neck and back pain, invasive technique offers the injection and/or placement of devices into the body. Steroid or analgesic is delivered into joints, ligaments, muscles, or around nerves through injection[2] which provides temporary relief but for permanent solution can only possible to implant external device at painful area.

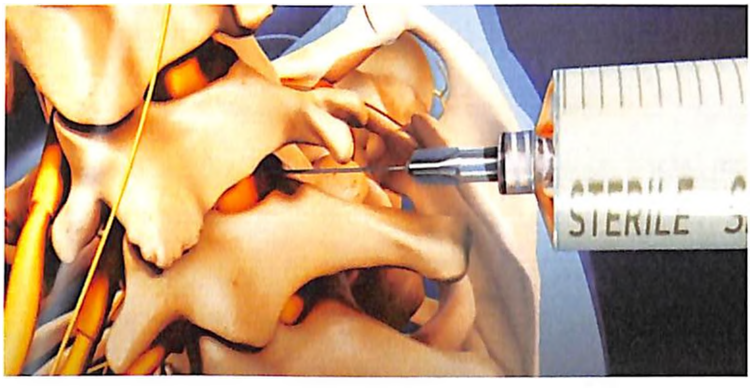

Fig. 1.1: Steroid injection into spine[2]

Another injection approach to treat connective tissue injuries of the musculoskeletal system which cannot be healable by nonsurgical therapies are called sclera-therapy or prolo-therapy [7]. This technique involves injection of an irritant therapeutic agent to stimulate blood circulation at affected site.

Vascular Endothelial Growth Factor (VEGF) Treatment: Different disorders of the blood vessels in the retina like, (i) leakage in blood vessels due to increased permeability than existing, (ii) internal bleeding for growth of new blood vessels, are responsible for facing lack of oxygen (hypoxia) in blood vessels and ocular tissue [8]. During hypoxia they overproduce a protein called vascular endothelial growth factor (VEGF) which

[1] https://www.cancer.gov/publications/dictionaries/cancer-terms/def/invasive-procedure
[2] https://www.spine-health.com/treatment/injections/injections-back-pain-relief

stimulates the growth of new blood vessels after injury and the growth of muscle[3].The elevated expression of VEGF and over growth of blood vessel leads to malignant tumor growth. So anti-VEGF therapy is to inject the medicines to reduce hind the growth of new blood vessel [9].

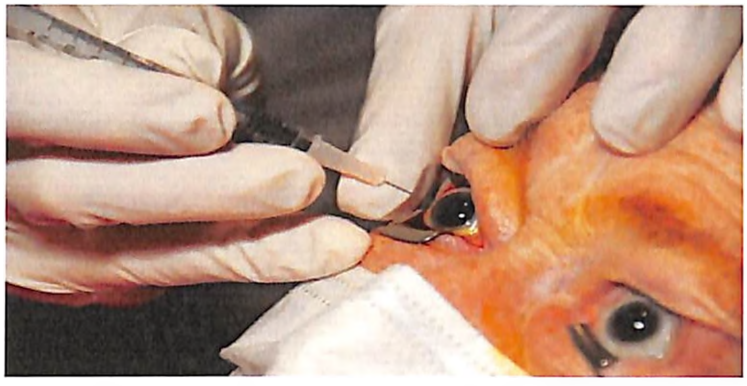

Fig. 1.2: Anti-VEGF drug injection into eyes[3]

Protein Delivery: There is protein drugs, for instance, insulin and vaccine are still be administered by the cumbersome procedure of injection under the skin. If proteins are taken orally, they are digested and cannot reach their target cells.

Rectal Drug Delivery: The rectal route of administration is traditional way of delivery. The rectal mucosa is the rapid absorbing tissue which captures the water and/or saline and enhanced absorption of medications. Although rectal administration is the alternation of oral administration by using gel, ointment, cream and suppository[4] but sometimes it becomes invasive when a special kind of catheter and/or bulb syringe [10] installed for rectal administration of medications and liquids.

Intravenous (IV) and Intramuscular (IM) Administration: IV and IM administrations are called parental administration. These two methods are suitable for delivering drug to the systemic circulation by avoiding first pass metabolism. Through IV administration drug level in the blood stream achieves a constant level and through IM administration drug slowly releases at targeted site with constant rate.

Drug Delivery to Central Nervous System (CNS): The central nervous system is one of the important parts of human body but due to disrupted BBB it is a struggling factor to deliver therapeutic cargo into it. Often genes are involved in neurological diseases.

[3] https://www.news-medical.net/life-sciences/What-is-VEGF.aspx
[4] https://www.macycatheter.com/alternate-routes-medication-administration/

Neurosurgical process allows the direct access of CNS and provides the surgical tool for direct gene delivery to the brain in terms of the penetration depth or treatment volume [11].

Although invasive delivery has widely been used but due to some valid reason invasive procedures are being avoided by medical practitioners such as:

Poor Patient Compliance: The traditional invasive drug delivery process is needle based delivery. The conventional metal needle penetrates the dermis layers where sharp tip of needle damages the dermal nerve tissue and vessels [12]. So the needle insertion delivery is painful to the patients and sometimes it creates inflammation to the infants. Repeated injection of drug for anti-VEGF therapy leads to increase the intraocular pressure as well as eye irritation, redness, retinal detachment. Low permeation of neurological drugs is assigned for repeated administration, leads to overdosing of drug.

Needle Poked Injury and Contamination: Due to skin puncture by sharp edge of needle tip causes needle stick injuries and inflammation. As example, insulin delivery is hazardous by hypodermic syringes which injure the dermal layer of diabetic patient and infected [13]. Anti-VEGF injection and blindness therapy is highly dependent on the sterilization of needle. Injection of life saving vaccines is dangerous by contaminated needles and drug. Small amount of contaminated drug can spread any disease very effectively. For drug or gene delivery into CNS, first important point to be noted that the sterilization of surgical tool.

Discarding Issue: Needle based drug delivery is suffers the problem of needle disposal to prevent transmission of diseases. Blood borne pathogens can be easily transmitted due to disposal problem of needles[5].

Need of Experienced Operator: Needle based delivery requires a trained person to puncture the needle into skin with proper depth with an accurate force. For anti-VEGF treatment it requires clear view of the retina to inject the drug for which a good ophthalmologist is expected [14]. The ocular disorder for repeated injection of ocular drug can only be avoided by an expert eye doctor[6]. Sometimes steroid is being

[5] https://www.tbs-sct.gc.ca/rpp/2007-2008/CCOHS-CCHST/ccohs-cchst-eng.pdf
[6] http://www.uhs.nhs.uk/Media/Controlleddocuments/Patientinformation/Eyes/Anti-VEGF-injection-treatment-patient-information.pdf

administered for instant relief in back pain which gives a temporary effect and influenced for repeated administration. So only an expert orthopedic can decide the proper drug for pain management with proper dose.

Storage Temperature: Many protein drugs especially insulin and some vaccine are stored within specific temperature ranges from (2-8 °C) to maintain potency. For instances, temperature controlled polio vaccine supply is a problem. Poor handling and storage, inadequate infrastructure and poor maintenance are associated with vaccine wastage [15].

When these critical points are affected the drug delivery, medical scholars have been overcome the drug delivery issues with needle free delivery or minimally invasive approach by miniaturized needle [16].

1.3 Non-invasive or Minimally Invasive Drug Delivery

Non-invasive or minimally invasive drug delivery is painless, easy to use, good patient compliance. This process can easily deliver the drug where drug delivery is difficult and need to be delivered invasively. Let's discuss the different noninvasive delivery approaches:

Oral Administration: Oral administration is the convenient way with good patient convenience. Tablet, syrup, capsule are the dosage forms of drug which are being administered by oral cavity. During oral administration, the principal goal is to ensure high bioavailability of the drug[7].

Pulmonary Route: The drug is delivered by inhaling the drug through mouth for treating pulmonary disease, which is chronic, and obstructed the airflow from the lungs[8]. The lungs and its vascular network offer a large surface area and high permeability for drug absorption. Inhalers, aerosol of the drug, jet or ultrasonic nebulizers are the different options for drug release. The drug particle with stable aerodynamic diameter and certain surface properties are pass through the trachea to deposit in pulmonary sac [17].

[7] https://www.americanpharmaceuticalreview.com/Featured-Articles/148747-Major-Advances-in-Oral-Drug-Delivery-over-the-Past-15-Years/
[8] https://www.mayoclinic.org/diseases-conditions/copd/symptoms-causes/syc-20353679

Intranasal Route: By intranasal route, the therapeutic agent experiences relatively high permeability than pulmonary route. Nasal drops or a nasal spray, nasal gel can be used as dosage formulation. The drug has low enzymatic degradation activity than oral route. The clear mucocilliary path can quickly transport the administered dose from the nasal cavity to the stomach [18]. Nasal route is the alternate way of neurosurgical drug delivery to CNS[9].

Ocular Route: This non-invasive route is suitable for the localized delivery of ophthalmic drug like gel, eye drop, suspension, ointment etc. to treat ocular disease.

Transdermal Route: Drug delivery through transdermal route is technically known as transdermal patch. It is the non-invasive way to deliver medications by using largest organ of human body i.e. skin surface. This process is an alternative way of IV, IM and hypodermic injection. Through transdermal route, therapeutic agents are released in sustained manner which reduces daily dosing schedule. The drug with short half-life such as ciprofloxacin, insulin, C-peptide, anesthetics are suitable for the transdermal patch. The drug can be safe from the first-pass metabolism effect by the patch delivery which is a sign of good bioavailability and patient friendly [19].

Fig. 1.3(a): Transdermal patch with microneedle array[10]

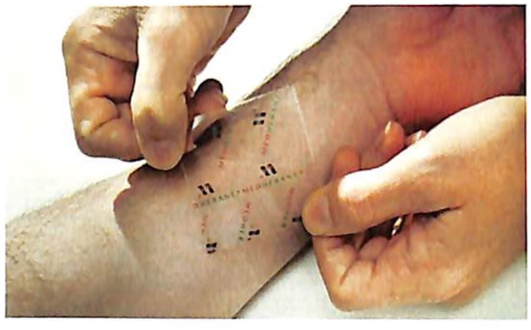

Fig. 1.3(b): Transdermal patch without microneedle array[10]

Drug delivery through transdermal patch is often known as minimally invasive because there is a batch of microneedle placed at the bottom surface of patch which punctures the surface of the skin [Fig. 1.3(a)] to deliver the drug into dermal capillaries and blood stream [20]. The patch without microneedle is called non-invasive patch [Fig. 1.3(b)] because, at bottom surface of the patch, there is a permeable, adhesive polymeric

[9] https://www.ingentaconnect.com/content/ben/cdd/2005/00000002/00000002/art00005
[10] https://archives.drugabuse.gov/news-events/nida-notes/2009/11/naltrexone-skin-patch-proves-effectiveness-new-technology

membrane placed which delivers the drug in a controlled manner by diffusion process[11]. Although non-invasive route of drug delivery is the matter of interest in recent trends but some challenges are hindered the efficiency of delivery and bioactivity of therapeutic agents which are discussed in the next section.

1.4 Challenges in Non-invasive Delivery

Although oral delivery is simpler, provide good patient compliance than traditional injection based administration [21]. But the oral formulation is instable in the variation of pH environment and experiences enzymatic degradation in the oral cavity as well as in the area of absorption of gastrointestinal (GI) tract which are the reason of low bioavailability of drug and poor absorption capability into intestinal membrane [22], [23]. During pulmonary delivery, the inhaled drug particles first deposit on the mucosa into the respiratory system to start the therapeutic effect, which is depends on number of particles, particle size, shape and density and the duration between inspiration and expiration [24]. Non-uniform sizes of drug particles affect the solubility of drug in the mucosal matrix and diffusion process into the epithelial lining. Drug with large size particle is poorly soluble in mucosal matrix, for which the particles are deposited on that and cannot be distributed to epithelial lining fluid where as smaller sized drug particles rapidly distributed, diffused and become available for absorption according to their physicochemical properties[12]. The deposition of large drug particle obstructs the distribution and absorption of drug by epithelial lining for which drug produces lower bioavailability, lack of applied dosage for therapeutic effect as well as toxic effect in mucocilliary body. The main challenge in intranasal drug delivery is the nasal mucociliary clearance (NMC). The NMC system produces the mucus layer which varies patient to patient and this mucus covers the nasal epithelium to protect the respiratory system from damage by inhaled substances [18]. Due to mucocilliary clearance drug particles get cleared from the nose before complete absorption through nasal mucosa[13] for which the drug creates lack of dosage and repeated administration with overdose effect. Another challenging point is that the small area of the nasal epithelium for permeation which limits the administered dose range. For ocular drug delivery ocular

[11] https://newatlas.com/ibuprofen-skin-patch/40812/
[12] http://www.pharmtech.com/four-challenges-pulmonary-drug-delivery
[13] https://www.ncbi.nlm.nih.gov/pmc/articles/PMC4649785/

gel, eye drop are commonly used formulation. Some times after using eye drop by patient him/her self, some quantity of applied drug overflows with blinking of eyes which is a loss of drug and poor bioavailability. For that reason drug fails to provide the therapeutic effect and also require frequent dosing. Eye drop has limited therapeutic effect in eye due to low permeability to cornea [25]. Dose of ocular gel is uncontrollable by patients, can cause overdosing effect. Due to thicken form of eye gel, drug would not reach in the required site of action. The painless transdermal delivery eliminates dangerous needles. This process protects the drug from enzymatic degradation. By this process, peak plasma levels of the drug are reduced which decreased side effects [26]. Patients can deliver the drug by themselves and don't need to go to the medical practitioners. The patch can provide a sustain deliverance of drug for prolonged time. But still the transdermal patch exhibits some challenges during delivery and these are: the patch cannot deliver ionic and large molecule drug due to low permeability of the membrane [27]. The patch cannot be used for pulsatile and on-demand basis of delivery because there is continuous drag transport is occurred from patch to skin. Heat is transdermal delivery enhancer by increasing skin and membrane permeability, drug solubility and diffusion rate of drug through microneedle to skin or membrane to skin[14]. For this reason it has been suggested that no heating element should be present near of transdermal patch.

By observing the limitations of individual non-invasive approach, researchers have been looked for overcome all of the problems by a single material only. They have been applying the polymeric material which has good permeability to handle high molecule drug. They have found the mucoadhesive property of polymer provided gastroretentive drug delivery by shielding the drug from enzymatic degradation. Main strategy was to use that polymer with pulsatile, sustain and/or controlled manner with on-demand basis which was executed successfully because of stimuli sensitivity of polymer. This smart polymer is called "Hydrogel". Let's discuss about hydrogel from next sections.

1.5 Introduction of Hydrogel

Hydrogel is three dimensional, hydrophilic macromolecular polymeric networks, for which the hydrogel is able to hold the solvent and thus swells into aqueous media. Due to

[14] http://www.jarcet.com/articles/Vol2Iss1/Hull.htm

soft tissue-like adequate flexibility of hydrogel it is good candidate for biomedical applications. Hydrogels are biocompatible, tuned biodegradable, porous and mechanically flexible etc. Along with swelling, hydrogels can deswell by environmental stimuli including pH, chemical agents, temperature, light and magnetic fields. Hydrogels are synthesized from monomers by the crosslinking method of Van der Waal interaction or covalent bond or hydrogen bonding creates three dimensional polymer network [29]. In 1960, the first reported hydrogel for drug delivery was a synthetic hydrogel. The synthetic polymers are categorized as polyethers, polyesters and poloxamers.

Polyethers: The synthetic polyether is composed of more than one monomer by containing ether functional group. The commonly known polymer falls in the polyether family is poly(ethylene glycol) (PEG). The structure of PEG is commonly expressed as $H-(O-CH_2-CH_2)_n-OH$. Research has shown that PEG is non-toxic, non-immunogenic, non-antigenic, highly water soluble and good material for the delivery of therapeutic agent.

Polyesters: The monomer with ester group is the main ingredient of polyesters. This polymer has been famous for proteins and peptide vehicles. Common biodegradable and biocompatible polyesters used in drug delivery applications include poly(lactic acid) (PLA), poly(caprolactones) (PCL), poly(glycolide) (PGA), poly(dioxanone) (PDO), poly(butyrolactone) (PBL), poly(valerolactone) (PVL), and poly(lactide-*co*-glycolide) (PLGA). Poly (N-isopropylacrylamide) (PNIPaam) is also a synthetic ester grouped polymer, famous for tissue engineering and controlled drug delivery.

Poloxamers: Poloxamers or pluronics are non-ionic triblock hydrogels. The polymer consists of hydrophobic central part of polypropylene oxide (PPO) and hydrophilic surroundings by polyethylene oxide (PEO).

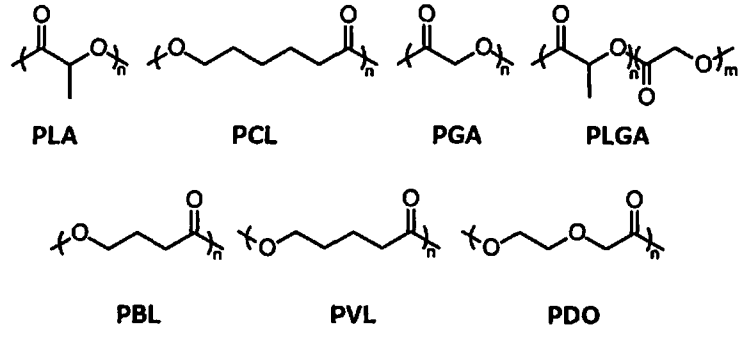

Fig. 1.4: Structures of different synthetic hydrogel

The mentioned synthetic polymers and their derivatives are exhibit stimuli sensitivity. The type of hydrogel according to the composition and arrangement of monomers as well as stimuli sensitivity have been discussed.

1.5.1 Types of Hydrogel

The hydrogels are broadly categories as below

1.5.1.1 Classification Based on Composition

The method of hydrogel preparation directs to classes of hydrogels and can be examplified by the following[15] (Fig. 1.5):

(a) Homopolymeric hydrogels are derived from a single species of monomer. Based on monomer nature and polymerization technique, the homopolymers may have crosslinked.

(b) Copolymeric hydrogels are composed of two or more different species of monomers with minimum one hydrophilic component. The monomers are chemically crosslinked in an alternating or blocked or random configuration.

(c) Multipolymer or Interpenetrating Polymer Network hydrogel (IPN), is made of two independent crosslinked synthetic and/or natural polymer. In semi-IPN hydrogel, one component is a crosslinked polymer and other one is noncrosslinked gel.

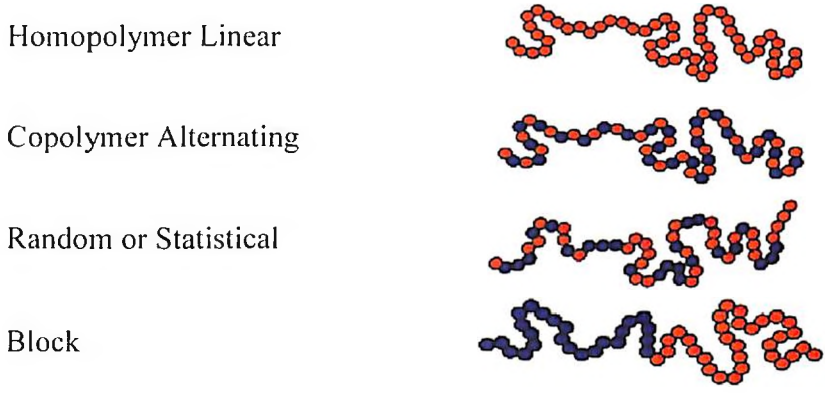

Fig. 1.5: Types of Hydrogels according to polymeric composition

[15] http://shodhganga.inflibnet.ac.in/bitstream/10603/174342/5/05_chapter%201.pdf

1.5.1.2 Classification According to Stimuli Responsiveness

The hydrogels are responsive to many stimuli like temperature, pH, magnetic field etc which are discussed in this section.

(a) Thermo Sensitive Hydrogels

Thermo sensitive hydrogels exhibit a critical solution temperature or volume phase transition temperature and offer temperature responsive phase transition phenomena included either sol-gel transition [30] or swelling- deswelling [31] of polymer respectively at its critical solution temperature. The temperature has a remarkable effect on the hydrophobic interactions between hydrophobic polymer segments and the hydrophilic interactions between hydrophilic polymer segments and water molecules. The contained hydrophobic groups are methyl, ethyl and propyl groups. Poly(N-isopropylacrylamide) (PNIPaam), poly(N,N-diethylacrylamide (PDEaam) are temperature sensitive polymers with critical solution temperature (CST) at 25-32 °C.

Negatively Thermosensitive Hydrogel: Negative hydrogel swells in volume or forms solution below its volume phase transition temperature (VPTT) or critical solution temperature (CST) respectively and contracts or converts into gel above its VPTT or CST respectively. This temperature called lower critical solution temperature (LCST) or lower volume phase transition temperature (LVPTT). The copolymers of poly(ethylene oxide) (PEO) and poly(propylene oxide) (PPO) possesses negative thermo sensitivity. In the work done by Vernon's group [32], they synthesized a temperature-responsive graft copolymer based on PNIPaam and Jeffamine M-1000 acrylamide (Jaam), which showed controlled swelling properties without introducing degradable moieties or increasing the lower critical solution temperature (LCST) above body temperature.

Positively Thermosensitive Hydrogel: Positive hydrogels swells in volume or forms solution above its VPTT or CST and contracts or converts into gel below VPTT or CST. This temperature called upper VPTT (UVPTT) or upper critical solution temperature (UCST). A positive thermo responsive hydrogel composed of poly(acrylic acid) and polyacrylamide (Paam) was synthesized by Yang *et al.* [33]. The swelling indicated that the phase-transition temperature of the IPN hydrogel was approximately 35 °C. The polymer swelled at 36 °C as well as deswelled at 10 °C.

(b) pH Sensitive Hydrogels

pH sensitive hydrogels are a class of polymer that exhibit desirable swelling-deswelling and chemical properties at specific pH ranges. Acidic or basic groups are chemically bonded to the backbone of polymer chains. The acidic groups are protonated at low pH, while the basic groups are deprotonated at high pH. The association, dissociation, and binding of various ions with polymer chains cause the hydrogel swelling-deswelling. The polymers with a large number of ionizable groups are known as polyelectrolytes. Fig. 1.6 shows examples of anionic and cationic polyelectrolytes and their pH-assisted ionization. For instances, Poly(acrylic acid) (Paac) ionized at high pH with higher swelling, whereas poly(N,N'-diethylaminoethyl methacrylate) (PDEAEM) ionized at low pH and swells more.

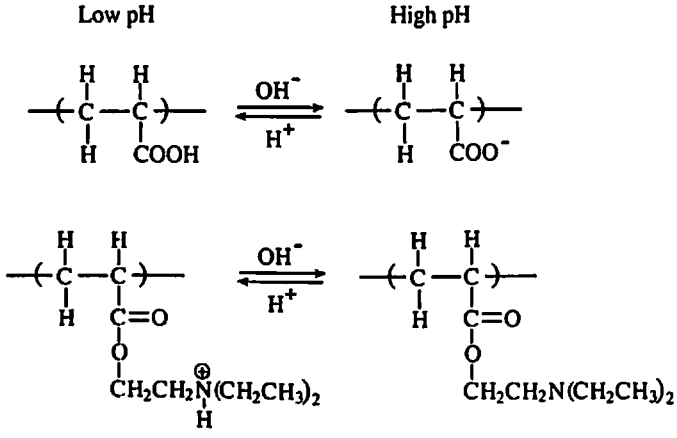

Fig. 1.6: pH-dependent ionization of Poly(acrylic acid) (top) and poly(N,N'-diethylaminoethyl methacrylate) (bottom) [34]

(c) Ion Sensitive Hydrogel

Neutral hydrogel may undergo phase transition in presence of various ions. The binding energy for ions introduces the free energy into the network, which causes for swelling. Ion sensitive hydrogel sensors have been reported for the detection of Na^+, K^+, Pb^{2+}, Ba^{2+} [35], [36]. The deprotonation of metal ions introduced the hydrophobicity of the polymers and thus deswell performed.

(d) Magnetically Responsive Hydrogel

Magnetic micro and/or nano particle reinforced into hydrogel or copolymeric hydrogel, are terms as magnetically responsive polymers. A new type of hydrogel with magnetic

nanoparticles as the crosslinking reagent has been presented [37]. The magnetic nanoparticles can be reinforced with different polymers and correspondingly different functional groups on their surfaces. The polyethylene glycol (PEG), poly(acrylamide) (Paam) and polysaccharide can be used as a base material.. If magnetic nanoparticle is reinforced into temperature responsive polymer then applied magnetic field would heated up the nanoparticle which also increased the local temperature of polymer. Thus the polymer would swell or contract according to its critical solution temperature [38].

(e) Light Responsive Hydrogels

Light sensitive hydrogels have potential applications in ophthalmic drug delivery application [39]. Light sensitive hydrogel may possess some advantages over thermo sensitive and pH sensitive hydrogel as the sensitivity of temperature sensitive hydrogels is rate limited by thermal diffusion, while pH responsive hydrogels can be controlled by hydrogen ion diffusion [40]. Light sensitive hydrogels are categorized as ultra violet (UV) sensitive and visible light sensitive hydrogels. Visible light is safe for mammalian tissue than UV light. The UV responsive polymers are synthesized by adding leuco derivative molecule, bis(4-dimethylamino)phenylmethyl leucocyanide chromophore, into the polymer network which dissociates into ion pairs under ultraviolet irradiation producing triphenylmethyl cations [41]. The chromophore absorbs the UV rays and dissipates the heat by producing cyanide ions which increases local temperature of polymer as well as osmotic pressure within the gel. Then the polymer exhibits the phase transition or volume switching according to its critical solution temperature. As shown in Fig. 1.7, the leuco derivative molecule can be ionized upon ultraviolet irradiation. Photoisomerization is reversible and repeatable process for photoresponsive polymeric system. By this process the photosensitive moiety changes its molecular behaviour in terms of structural change of its functional groups caused by photo excitation. The azobenzene moiety is the known photo reactive compound, which isomerizes from *-trans* form to the hydrophobic *-cis* form with higher polarity by UV irradiation and revert to the *–trans* form by visible light irradiation [42]. The spiropyran group is also widely used to control function of biomaterials by light. The photoresponsive hydrogels were developed by utilizing the property of spiropyrane moiety (Fig. 1.8) [43].

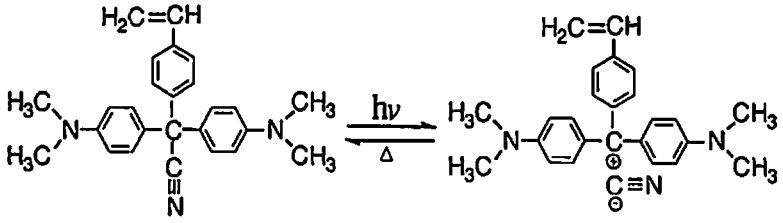

Fig. 1.7: Structure of leuco derivative molecule bis(4-(dimethylamino)phenyl) (4-vinylphenyl)methyl leucocyanide [41]

Visible light-sensitive hydrogels were prepared by introducing a light sensitive chromophore (e.g. trisodium salt of copper chlorophyllin) to poly(N-isopropylacrylamide) hydrogels [44]. The chromophore absorbs the visible rays and dissipates the heat by which increases local temperature of polymer. Then the polymer exhibits the phase transition or volume switching according to its critical solution temperature. The increment of temperature is directly proportional to the light intensity and the chromospheres concentration.

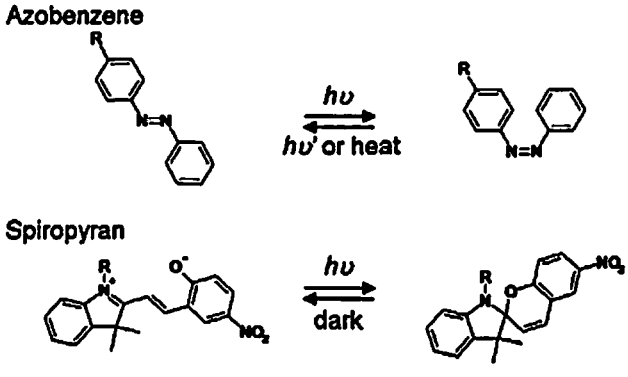

Fig. 1.8: Photoisomerization of hydrogel [43]

In recent years researchers are reinforcing nanomaterial into hydrogel for photoresponse in the absence of the chromophores. Different metal salt like silver nitrate($AgNO_3$), Hydrogen tetrachloroauric acid ($HAuCl_4$) are being used as silver and gold source respectively for nanoparticle formation. The silver nanoparticle reinforced photosynthesized hydrogel applied as antimicrobial material. Gold nanorods, nanoparticles have been reinforced into polymer to actuate it from visible range to near infrared region which can expand the application area as well as range of operating light.

1.5.2 Self-assembled Hydrogels

Self-assembled hydrogels are capable to recover their chemical structures and propertied upon injury, which are extremely attractive in emerging biomedical applications. The self assembled hydrogel offers *in-situ* crosslinking nature and are advantageous over conventional volume switchable. Due to their visible sol-gel phase transition they can be administered via minimally invasive for sustained release at a desired site (Fig. 1.9) [45]. Covalent and noncovalent interactions between moieties, both are responsible to design self-healing hydrogels. Hydrogels, by covalent crosslinking methods can be synthesized using vinyl monomers. Physically crosslinked hydrogels are very interesting for their mild processing conditions like hydrophobic interactions, ionic interactions, hydrogen bond between water and polymer chains, Van der Waals interactions and injectability [46]. Fig. 1.8 is the schematic for in situ injectable hydrogel matrix. *In-situ* hydrogels are prepared, by (A) photo-polymerization or stimuli-sensitive sol-gel transition, and (B) self-assembled. After injection, the polymer solution changed into gel state at 37 °C and/or pH 7.4.

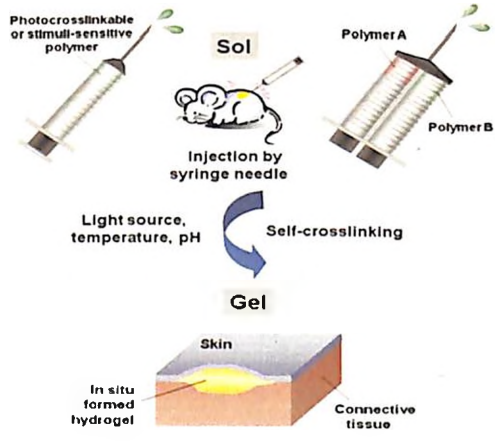

Fig. 1.9: A schematic for *in-situ* formation of hydrogel using chemical or physical crosslinking methods [45]

1.5.3 Biohydrogels

The synthetic hydrogels like, PEG, PVA; are biocompatible polymers for drug delivery but they are unable to interact with biological systems which hinders the interactions between biological object with drug. Some synthetic polymers create toxic effects after enzymatic degradation and polluted the drug. To address this need, polysaccharides have been conjugated to synthetic polymers to impart desired bioactivity [47] or the polymers

made of polysaccharide is termed as biohydrogel. Hyaluronic acid, alginate, gum ghatti, guar gum, xanthan gum, carboxymethylcellose and chitosan are chosen for preparing biocompatible hydrogels. Biohydrogels have the advantages of increased biocompatibility, tunable biodegradability, good mechanical flexibility, porous structure, high capacity of water absorption than synthetic biocompatible polymers [29]. For these plus points, synthetic biohydrogels are replacing by natural saccharide modified biohydrogel. Sodium alginate is an anionic water soluble polysaccharide that is one of the most abundantly available biosynthesized materials, derived from brown seaweed and bacteria, potentially used for tissue engineering. Xanthan gum is a plant polysaccharide, an acidic polymer. Xanthan gum was used to prepare biodegradable polymeric crosslinked hydrogels. Guar gum is a galactomannan applicable in drug delivery. Chitosan and guar gum were employed for synthesizing biohydrogels for controlled, release through transdermal routes [48]. Drug delivery with predetermined rate through transdermal route is advantageous over the first-pass metabolism and reduction of drug concentration.

1.6 Role of Hydrogel in Non-invasive Drug Delivery

Stimuli sensitivity of hydrogels are the matter of interest for oral delivery because, by responding the biochemical stimuli inside the body like, temperature, pH(main stimuli), pH strength; the polymers alter its network structure, swelling-deswelling behavior, and can control drug release [29]. Hydrogel can sense the pH variation inside body and it can tune the drug release by its pH sensitive functional group. Created chemical bonding and ionic interaction between drug and polymer, prevent the unexpected drug leakage. A controlled delivery of drug is the primary objective in oral route due to sustained concentration of a molecule is released from tablet which can effectively achieved by hydrogel [49]. Hydrogel protects the encapsulated therapeutic agent from first pass metabolism. During the gastro retentive delivery, the hydrogel does not migrate from stomach to intestine due to mucoadhesivity and increases bioavailability of drug for prolonged time by interaction between polymer and biological surface [50]. The size of drug particle in pulmonary route is non-uniform for which the created difficulties have been discussed in the section 1.4. To solve the issue of deposition and absorption and clearance of non-uniform drug particle, hydrogel have been employed by researchers. Controlled release property of hydrogel reduces the side effect of excess deposited drug

in respiratory system by eliminating frequent administration. Less amount of drug with constant flow rate and concentration increases the duration of deliverance for prolonged time which is a good patient compliance with chronic disease such as asthma[16]. Liposome, microsphere, nanoparticle are made of hydrogel have been used as controlled dispenser. Liposomes are composed of lipids bi-layer, spherical structured object with a hydrophobic inner layer and a hydrophilic outer layer which are able to encapsulate both hydrophobic and hydrophilic drugs [51]. Diameter of liposome can be easily tuned with uniform shape and dimension can be achieved. Mucoadhesive nature of hydrogel allows the inhaled drug containing dry liposome or microsphere powder to make the direct physical contact with mucocilliary matrix which can increase bioavailability of drug and longer residence time. Long time contact of polymer particulates prevents cilliary clearance and permits a prolonged time for drug penetration and absorption [24]. Poly(ethylene glycol) based enzyme responsive hydrogel microparticles were developed for pulmonary drug delivery [52]. Swelling of polymer avoided clearance by alveolar macrophages in lungs. During pulmonary disease matrix metalloproteinase (MMP) enzyme is become elevated. That's why the PEG microparticle has been used to release the drug by sensing MMP enzyme. After realize the contact of MMP, the mesh size of polymer was increased and preceded for degradation. Same qualities of hydrogel in pulmonary route delivery are being applicable for nasal route drug delivery also because of, drug particle deposition, absorption all are issues are common in delivery through nasal route. The invasive way of drug delivery in CNS is being replaced by noninvasive nasal route delivery. The blood brain barrier hinders the transport of drug through endothelial capillaries to the brain [3] and to overcome this challenge drug encapsulated hydrogel is being administered via nose to brain route for the treatment of neurological disease [53]. *In-situ* gel based hydrogel solution or nasal drop is administered in nose which deposited on the cilliary matrix and converted to gel by sensing body temperature or pH or enzyme etc. The formation of gel broke the chemical bond with drug and drug was released. A thermosensitive polymeric nasal formulation composed of PEG and chitosan has been developed [54]. The nasal spray or drop was administered and sol–gel transition was occurred in the temperature range 32–35 °C at nasal mucus. The physical contact with nasal mucus, gel released the drug for prolonged time with controlled rate.

[16] http://investor.inva.com/news-releases/news-release-details/theravance-reports-fourth-quarter-and-full-year-2012-financial

Stimuli sensitivity of hydrogel is very useful for ophthalmic drug delivery especially temperature and light sensitive hydrogels. Conventional used eye drop have little permeability to the cornea and are thus limited to treatment in the outer segment of the eye [25] which creates poor bioavailability of drug. To solve this problem, sustain delivery of ophthalmic drug is expected. Polymeric ophthalmic drops are being administered in recent years. Sol-gel transition of *in-situ* gelling system can be stimulated by the alterations in pH, temperature and ion concentration [55]. Mucoadhesivity of gel offers the prolonged resident time and enhanced ocular bioavailability[17]. Polymeric micelles, liposome with hydrophobic inner core and hydrophilic corona, can encapsulate the hydrphobic ophthalmic drug. They are stable as solution before administration but after administration, they turned into gel by sensing the temperature or pH and released the drug in sustained manner for prolonged time [56].

Hydrogel has some excellent points to overcome the challenges in transdermal delivery. The silicon based microneedle array has been replaced by swellable hydrogel by Yang *et al.* [57]. The hydrogel microneedle array was mechanically interlocked with tissue through swellable microneedle tips, by utilizing the adhesion capability of hydrogel. Conical shaped dry microneedles were penetrated tissue with minimal insertion force and depth with smooth, significant pull out force because of swelling of needles. Due to good permeability and ion sensitivity of hydrogel can easily encapsulate and deliver the ionic drug. The large molecular weight and highly porous structure of crosslinked hydrogel doesn't have any limitation for large molecule drug loading. The stimuli sensitive functional groups can alter their physio-chemical property on the intensity of applied stimuli for which an on-off action in terms of physical changes of hydrogel can deliver the drug in pulsatile fashion with on-demand basis. This process limits the continuous drug delivery from the conventional patch and reduces the overdosing effect.

1.7 Conclusion

This chapter showed the wide versatility of hydrogels in non-invasive delivery. The properties make it good drug delivery dispenser. The hydrogel acts as sensor, transducer and actuator in single run to deliver the drug which has been a matter of interest for pharmaceutical engineers. The crosslinking method offers on-demand degradability and

[17] https://www.ncbi.nlm.nih.gov/pmc/articles/PMC3482766/

nondegradability to polymer. Hydrogel exhibits many drug release fashion like, controlled, pulsatile, sustain etc. Due to large molecular weight protein, peptide based drug delivery are not the limitation of conventional noninvasive procedure. According to medical practitioner, biocompatibility is a key factor for drug release, which can be achieved by hydrogel. By inspiring the excellent properties of hydrogel and its capability to overcome the challenges in noninvasive delivery, this research has been focus on hydrogel to use it as noninvasive drug dispenser.

References

[1] I. I. Tabata, "The importance of drug delivery systems in tissue engineering," *Pharm Sci Technolo Today*, vol. 3, no. 3, pp. 80–89, 2000.

[2] R. Daneman and A. Prat, "The Blood – Brain Barrier," pp. 1–24, 2018.

[3] R. K. Upadhyay, "Drug delivery systems, CNS protection, and the blood brain barrier," *Biomed Res. Int.*, vol. 2014, pp. 203–223, 2014.

[4] T. Hetal, P. Bindesh, and T. Sneha, "A review on techniques for oral bioavailability enhancement of drugs,"*Inter. J. Pharma. Sc. Rev. Res.*, vol. 4, no. 3, 2010.

[5] L. V. Andel, Z. Zhang, L. Hughes, V. Kansra. M. Sanghvi, M. M. Tibben, A. Gebretensae, J. H. M. Schellens, "Determination of the absolute oral bioavailability of niraparib by simultaneous administration of a 14 C-microtracer and therapeutic dose in cancer patients," *Cancer Chemother. Pharmacol.*, vol. 81, no. 1, pp. 39–46, 2018.

[6] G. Tiwari, R. Tiwari, B. Sriwastawa1, L Bhati, S Pandey, P Pandey, S. K Bannerjee, "Drug delivery systems : An updated review," *Inter. J. of Pharma. Invest.*, vol. 2, no. 1, pp. 2–11, 2016.

[7] A. Z. David Rabago, Andrew Slattengren, "Prolotherapy in Primary Care Practice," *Prim. Care*, vol. 37, no. 1, pp. 65–80, 2010.

[8] D. Yorston, "Anti-VEGF drugs in the prevention of blindness," *J. community eye Heal.*, vol. 27, no. 87, 2014.

[9] P. Susvar, "Intravitreal Injections : Guidelines for Injections in Noninfective Retinal Conditions," *World J. Retin. Vitr.*, vol. 1, no. 1, pp. 33–35, 2011.

[10] M. P. Davis, D. Walsh, S. B. Legrand, and M. Naughton, "Symptom control in cancer patients : the clinical pharmacology and therapeutic role of suppositories and rectal suspensions," *Support Care Cancer*, vol. 10, pp. 117–138, 2002.

[11] W. H. keong Tan, T. Lee, and C. Wang, "Simulation of Intratumoral Release of Etanidazole :," *J. Pharm. Sci.*, vol. 92, no. 4, pp. 773–789, 2003.

[12] T. Morçöl, P. Nagappan, L. Nerenbaum, A. Mitchell, and S. J. D. Bell, "Calcium phosphate-PEG-insulin-casein particles as oral delivery systems for insulin," *Int. J. Pharm.*, vol. 277, pp. 91–97, 2004.

[13] L. Nordquist, N. Roxhed, P. Griss, and G. Stemme, "Novel Microneedle Patches for Active Insulin Delivery are Efficient in Maintaining Glycaemic Control ," *Pharm. Res.*, vol. 24, no. 7, pp. 1381–1388, 2007.

[14] L. P. Aiello, R. L. Averi, P. G. Arrigg, B. A. Keyt, H. D. Jampel, S. T. Shah, H.

Thieme,J. E. Park, H. V. Nyugen, L. M. Aiello, G. L. King, "Vascular Endothelial Growth Factor in ocular fluid of patients with diabetic retinopathy and other retinal disorder," *Newzel. J. Med.*, vol. 331, no. 22, pp. 1480–1487, 1994.

[15] D. M. Dairo and O. E. Osizimete, "Factors affecting vaccine handling and storage practices among immunization service providers in Ibadan , Oyo State , Nigeria .," *African Heal. Sci. Vol*, vol. 16, no. 2, pp. 576–583, 2016.

[16] R. F. Donnelly, T. Raghu Raj Singh, and A. D. Woolfson, "Microneedle-based drug delivery systems: Microfabrication, drug delivery, and safety," *Drug Deliv.*, vol. 17, no. 4, pp. 187–207, 2010.

[17] S. Sangwan, J. M. Agosti, L. A. Bauer, B. A. Otulana, R. J. Morishige, D. C. Cipolla, J. D. Blanchard, and G. C. Smaldone , "Aerosolized Protein Delivery in Asthma ," *J. aerosol Med.*, vol. 14, no. 2, pp. 185–195, 2001.

[18] E. Marttin, N. G. M. Schipper, J. C. Verhoef, and F. W. H. M. Merkus, "Nasal mucociliary clearance as a factor in nasal drug delivery," *Adv. Drug Deliv. Rev.*, vol. 29, pp. 13–38, 1998.

[19] A. Z. Alkilani, M. T. C. Mccrudden, and R. F. Donnelly, "Transdermal Drug Delivery: Innovative Pharmaceutical Developments Based on Disruption of the Barrier Properties of the stratum corneum," *Phama*, vol. 7, pp. 438–470, 2015.

[20] M. N. Pastore, Y. N. Kalia, M. Horstmann, and M. S. Roberts, "Transdermal patches : history , development and pharmacology," *Br. J. Pharmacol.*, vol. 172, no. 9, pp. 2179–2209, 2015.

[21] M. Morishita and N. A. Peppas, "Is the oral route possible for peptide and protein drug delivery ?," *Drug Discov. Today*, vol. 11, no. 19/20, pp. 905–910, 2006.

[22] L. A. Sharpe, A. M. Daily, S. D. Horava, and N. A. Peppas, "Therapeutic applications of hydrogels in oral drug delivery," *Expert Opin Drug Deliv*, vol. 11, no. 6, pp. 901–915, 2014.

[23] S. Sant, S. L. Tao, O. Fisher, Q. Xu, N. A. Peppas, and K. Ali, "Microfabrication Technologies for Oral Drug Delivery," *Adv. Drug Deliv. Rev.*, vol. 64, no. 6, pp. 496–507, 2012.

[24] J. Du, P. Du, and H. D. Smyth, "Hydrogels for controlled pulmonary delivery," *Ther. Deliv*, vol. 4, no. 10, pp. 1293–1305, 2013.

[25] S. Anjali, D. Rameshwar, D. Shivani, and S. Ranjit, "Hydrogels in ophthalmic drug delivery system" *Asian Pacific J. Heal. Sci.*, vol. 5, no. 2, pp. 96–104, 2018.

[26] D. Patel, S. A. Chaudhary, B. Parmar, and N. Bhura, "Transdermal Drug Delivery System : A Review," *Pharma Innov.*, vol. 1, no. 4, pp. 66–75, 2012.

[27] H. Tanwar, "A Review: Physical Penetration Enhancers For Transdermal Drug Delivery Systems," *IOSR J. Pharm. Biol. Sci.*, vol. 11, no. 1, pp. 101–105, 2016.

[28] T. Billiet, M. Vandenhaute, J. Schelfhout, S. Van Vlierberghe, and P. Dubruel, "A review of trends and limitations in hydrogel-rapid prototyping," *Biomaterials*, vol. 33, no. 26, pp. 6020–6041, 2012.

[29] A. S. Hoffman, "Hydrogels for biomedical applications," *Adv. Drug Deliv. Rev.*, vol. 64, pp. 18–23, 2012.

[30] Z. Maolin, L. Jun, Y. Min, and H. Hongfei, "The swelling behavior of radiation prepared semi- interpenetrating polymer networks composed of polyNIPAAm and hydrophilic polymers," *Radiat. Phys. Chem.*, vol. 58, pp. 397–400, 2000.

[31] A. K. Bajpai, S. K. Shukla, S. Bhanu, and S. Kankane, "Responsive polymers in controlled drug delivery," *Prog. Polym. Sci.*, vol. 33, pp. 1088–1118, 2008.

[32] D. J. Overstreet, R. Y. Mclemore, B. D. Doan, A. Farag, and B. L. Vernon, "Temperature-Responsive Graft Copolymer Hydrogels for Controlled Swelling and Drug Delivery," *Soft Mater.*, vol. 11, no. 3, pp. 294–304, 2013.

[33] M. Yang, C. Liu, Z. Li, G. Gao, and F. Liu, "Temperature-Responsive Properties of Poly (acrylic acid- co -acrylamide) Hydrophobic Association Hydrogels with High Mechanical Strength," *Macromolecules*, vol. 43, pp. 10645–10651, 2010.

[34] S. K. De, N. R. Aluru, B. Johnson, W. C. Crone, D. J. Beebe, and J. Moore, "Equilibrium Swelling and Kinetics of pH-Responsive Hydrogels" *J.Micro Electromech. Sys.*,vol. 11, no. 5, pp. 544–555, 2002.

[35] A. G. Mayes, J. Blyth, R. B. Millington, and C. R. Lowe, "Metal Ion-Sensitive Holographic Sensors," *Anal. Chem.*, vol. 74, no. 15, pp. 3649–3657, 2002.

[36] J. H. Holtz and S. A. Asher, "Polymerized colloidal crystal hydrogel films as intelligent chemical sensing materials," *Nature*, vol. 389, pp. 829–833, 1997.

[37] M. Bonini, S. Lenz, R. Giorgi, and P. Baglioni, "Nanomagnetic Sponges for the Cleaning of Works of Art," *Langmuir*, vol. 23, no. 11, pp. 8681–8685, 2007.

[38] N. S. Satarkar, W. Zhang, R. E. Eitel, and J. Z. Hilt, "Magnetic hydrogel nanocomposites as remote controlled microfluidic valves," *Lab Chip*, vol. 9, pp. 1773–1779, 2009.

[39] K. Peng, I. Tomatsu, B. van den Broek, C. Cui, A. V. Korobko, J. van Noort, A. H. Meijer, H. P. Spaink and A.r Kros, "Dextran based photodegradable hydrogels formed via a Michael addition ," *Soft Matter*, vol. 7, pp. 4881–4887, 2011.

[40] Y. Qiu and K. Park, "Environment-sensitive hydrogels for drug delivery," *Adv. Drug Deliv. Rev.*, vol. 64, pp. 49–60, 2012.

[41] A. Mamada, T. Tanaka, D. Kungwatchakun, and M. Irie, "Photoinduced Phase Transition of Gels," *Macromolecules*, vol. 23, pp. 1517–1519, 1990.

[42] K. G. Yager and C. J. Barrett, "Novel photo-switching using azobenzene functional materials," *J. Photochem. Photobiol. A Chem.*, vol. 182, pp. 250–261, 2006.

[43] A. Szilagyi, K. Sumaru, S. Sugiura, T. Takagi, T. Shinbo, M. Zrı́nyi, and T. Kanamori, "Rewritable Microrelief Formation on Photoresponsive Hydrogel Layers," *Chem. Mater.*, vol. 19, no. 11, pp. 2730–2732, 2007.

[44] A. Suzuki and T. Tanaka, "Phase transition in polymer gels induced by visible light," *Nature*, vol. 346, pp. 345–347, 1990.

[45] H. J. Chung and T. G. Park, "Self-assembled and nanostructured hydrogels for drug delivery and tissue engineering," *Nano Today*, vol. 4, no. 5, pp. 429–437, 2009.

[46] W. E. Hennink and C. F. van Nostrum, "Novel crosslinking methods to design hydrogels," *Adv. Drug Deliv. Rev.*, vol. 64, no. SUPPL., pp. 223–236, 2012.

[47] A. D. Baldwin and K. L. Kiick, "Polysaccharide-Modified Synthetic Polymeric Biomaterials," *Biopolymers*, vol. 94, no. 1, pp. 128–140, 2010.

[48] A. J. Sami, M. Khalid, T. Jamil, S. Aftab, S. A. Mangat, A.R. Shakoori, S. Iqbal, "Formulation of novel chitosan guargum based hydrogels for sustained drug release of paracetamol," *Int. J. Biol. Macromol.*, vol. 108, pp. 324–332, 2018.

[49] C. Lin and A. T. Metters, "Hydrogels in controlled release formulations : Network design and mathematical modeling ☆," *Advance*, vol. 58, pp. 1379–1408, 2006.

[50] K. P. R. Chowdhary and Y. S. Rao, "Mucoadhesive Microspheres for Controlled Drug Delivery," *Biol. Pharm. Bull*, vol. 27, no. 11, pp. 1717–1724, 2004.

[51] M. Beck-broichsitter, M. Rieger, R. Reul, T. Gessler, W. Seeger, and T. Schmehl, "Correlation of drug release with pulmonary drug absorption profiles for nebulizable liposomal formulations," *Eur. J. Pharm. Biopharm.*, vol. 84, no. 1, pp. 106–114, 2013.

[52] E. Secret, S. J. Kelly, K. E. Crannell, and J. S. Andrew, "Enzyme-Responsive Hydrogel Microparticles for Pulmonary Drug Delivery," *ACS Appl. Mater. Interfaces*, vol. 6, pp. 10313–10321, 2014.

[53] B. A. Aderibigbe, "In Situ-Based Gels for Nose to Brain Delivery for the Treatment of Neurological Diseases," *Pharmaceutics*, vol. 10, no. 40, pp. 1–17, 2018.

[54] H. Nazar, D. G. Fatouros, S. M. Van Der Merwe, N. Bouropoulos, G. Avgouropoulos, and J. Tsibouklis, "Thermosensitive hydrogels for nasal drug delivery," *Eur. J. Pharm. Biopharm.*, vol. 77, pp. 225–232, 2011.

[55] K. S. Rathore, "in - situ gelling ophthalmic drug delivery system : an overview," *Int.*

J. Pharm. Pharm. Sci., vol. 2, no. 4, pp. 30–34, 2010.

[56] M. Alami-milani, P. Zakeri-milani, H. Valizadeh, R. Salehi, S. Salatin, and A. Naderinia, "Novel Pentablock Copolymers as Thermosensitive Self-Assembling Micelles for Ocular Drug Delivery," *Adv. Pharm. Bull.*, vol. 7, no. 1, pp. 11–20, 2017.

[57] S. Y. Yang, E. D. O'Cearbhaill, G. C. Sisk, K. M. Park, W. K. Cho, M. Villiger, B. E. Bouma, B. Pomahac, and J. M. Karp, "A bio-inspired swellable microneedle adhesive for mechanical interlocking with tissue," *Nat. Commun.*, vol. 4, pp. 2–11, 2013.

Chapter 2

Literature Review

Chapter 1 showed, the hydrogel is advantageous in non-invasive delivery for overcoming the existing challenges. This chapter contains the contribution of hydrogel in non-invasive delivery by different formulations. Drug release efficiency and way of overcoming the challenges of conventional non-invasive delivery are discussed here. The gaps in the existing researches and proposed scope of research are discussed at the end of this chapter.

2.1 Introduction

For executing any therapeutic actions, selection of dose of the drug is important to deliver a specific amount of therapeutic agent at a given time. Wrong dosage of drug consequences perilous effects in infants, old aged and cancer survivors with low immunity. Dosage formulations are another key factor, by which the drugs are being released at targeted sites. The dosage formulations provide some plus points during release like[1]: (i) accurate dose, (ii) protection to the drug gastric acid, degradation e.g. coated tablets, sealed ampoules, capsules, (iii) easy administration of drugs within body tissues, (iv) controlled release mechanism, (v) prolonged and sustained medication as per requirements, (vi) usage of desired vehicle for insoluble drugs. The dosage forms are being decided according to routes of administrations which are already discussed in Chapter 1 for non-invasive delivery like oral, pulmonary, nasal, ocular and dermal routes. Some tentative problems are cannot be ignored in conventional noninvasive medications and those are:

i. Conventional oral formulations are instable in the variation of pH environment and experiences enzymatic degradation in the area of absorption of gastro intestinal (GI) tract makes the drug poor absorption capability into intestinal membrane.
ii. During pulmonary delivery, the inhaled drug particles are struggled with their number, non-uniform sizes, shape and density etc. The struggling points of drug

[1] http://www.srmuniv.ac.in/sites/default/files/downloads/Dosage_forms.pdf

particles affect the drug solubility in mucocilliary body and drug diffusion into epithelial lining for which drug produces lower bioavailability, lack of applied dosage for therapeutic effect as well as toxic effect in mucocilliary body.

iii. The main drawback in intranasal delivery is the nasal mucociliary clearance (NMC) which produces mucus layer which varies patient to patient. Due to NMC drug particles get cleared from the nose before complete absorption through nasal mucosa for which the drug creates lack of dosage and repeated administration with overdose effect.

iv. For ocular drug delivery, the administered eye drop sometimes overflows with blinking of eyes which is a loss of drug and poor bioavailability. For that reason, frequent dosing of drug requires to achieve the therapeutic effect. Dose of ocular gel is uncontrollable by patients, can cause overdosing effect. Due to thicken form of eye gel, drug would not reach in the required site of action.

v. The transdermal patch cannot deliver ionic and large molecule drug due to low membrane permeability. The patch cannot be used for pulsatile and on-demand delivery due to continuous drag transport from patch to skin. Heat is transdermal delivery enhancer by increasing skin and membrane permeability, drug solubility and diffusion rate of drug through microneedle to skin. For this reason it has been suggested that no heating element should be present near of transdermal patch.

The drawbacks of traditional non-invasive delivery, have been influenced the researchers to use hydrogel. The hydrogel has good permeability to handle both low and high molecule drug. The mucoadhesivity of polymer provides gastroretentive drug delivery by retaining the polymer at the released site. The polymer aims to pulsatile, sustain, controlled and on-demand release due to stimuli sensitivity of polymer. This chapter focuses on different dosage formulations of hydrogel and their way of applicability in different noninvasive routes of delivery.

2.2 Different Hydrogels Based Dosage Formulations

Hydrogel has been used in medical application in 1960 by Wichterle in the form of soft contact lens by using hydroxyethyle methacrylate. Since hydrogel have many plus points for overcoming the challenges in drug delivery so this section is giving the idea about different hydrogel based dosage formulations and their working principle. The stimuli responsive drug release process is also described for all dosage formulation.

***In-situ* Gel:** The *in-situ* gelling formulation of polymer is stable in solution form before contact with the body. Under the physiological condition, the solution converts itself into gel. This sol-gel transition depends on the modulation in stimuli like pH, temperature, photo irradiation and the presence of specific ions or molecules. This kind of stimuli triggered gelling technique is widely used in sustained delivery because of some advantages like, simple fabrication, less and easily administrable, making the drug bioavailable, good patient compliance. Some researches stated that *in-situ* gel delivers accurate dose of drug and prolonged the residence time of drug at the site of administration [1]. With all these plus points, *in-situ* gel can be administered into patients and the hydrophobic nature of gel with prolonged residence time impart the increased therapeutic activity [2]. *In-situ* gels can be applied for non-invasive drug administration. The formations of *in-situ* gel (Fig. 2.1) with drug release mechanism by external triggers are discussed below

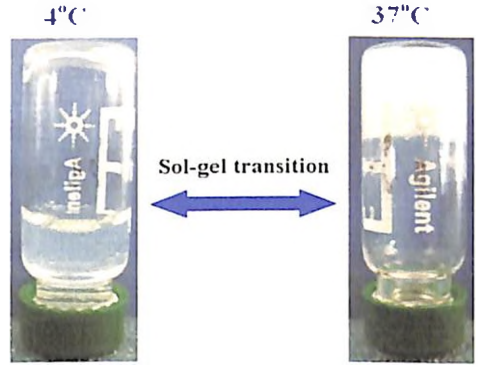

Fig. 2.1: sol-gel transition of PEG based *in-situ* polymer [3]

1 **Gelation Due To Physiological Stimuli:** When the polymer exhibits the physical changes i.e. sol-gel transition by responding to small alterations in their surrounding conditions, they termed as stimuli sensitive, intelligent, smart polymers. These polymers sense and decide the intensity of stimuli as a signal, then transform their chain conformation in response [4].

➢ **Temperature Triggered *in-situ* Gel:** Temperature is such stimulus which is easily controllable and applicable to both *in-vitro* and *in-vivo*. Thermo sensitive polymer has a phase transition temperature called critical solution temperature (CST). When the polymer is stable as gel and converts into solution above CST, this polymer is called positive *in-situ* hydrogel and the CST is termed as upper critical solution temperature (UCST). The vice versa thermo sensitive property makes the polymer to be called

negative *in-situ* hydrogel and the CST is termed as lower critical solution temperature (LCST). The temperature of the solution of the *in-situ* system exists in room temperature (20-25 °C) and gelation occurs in contact with body fluid (35-37 °C). In solution form the polymer chain makes the hydrogen bonds with surrounding solvent and/or drug and during gel formation built hydrogen bonds disrupt and the solvents and/or drug releases [5]. For instance, poloxamers/pluronics, cellulose derivatives [HPMC, ethyl (hydroxy ethyl) cellulose (EHEC), methyl cellulose, xyloglucan, tetronics, etc are the temperature sensitive polymer.

- **pH Triggered *in-situ* Gel:** pH is another physiological stimulus behind the formation of *in-situ* gel. Polymers contain large number of ionisable groups and called as polyelectrolyte. Polymers contain weakly acidic groups (anionic) or basic (cationic) groups which either accept or release protons after exposing to different environmental pHs. The polymer with weakly acidic (anionic) groups exhibits solution form increases as the external pH increases, but polymer contains weakly basic (cationic) groups forms gel with elevated external pH [6]. For example, Polyacrylic acid (Paac) or Carbopol is a pH sensitive polymer which displays a sol-gel phase transition. The -COOH- group in Paac chain accepts protons at low pH and releases in high pH. Therefore, at high pH, the Paac exhibits solution form due to the electrostatic repulsion of the cationic groups, and this mechanism of Carbopol is mostly exploited in ophthalmic delivery [7].

The ophthalmic formulation is stable in solution form at pH 4.4, the formulation exists as a normal solution but gelation occurs at pH 7.4, i.e. the pH of tear fluid. Other pH induced *in-situ* gelling polymers are cellulose acetate phthalate (CAP) latex, polymethacrylic acid (PMMaac), polyethylene glycol (PEG), etc.

2 *In-situ* Gelation by Ion-activated System: Ion sensitive polymers are used for this mechanism where drug loaded polymer solution forms gel in the presence of ions like Na^+, K^+, Ca^{2+} and Mg^{2+}. The anionic polymer solution and/or drug are administered at the targeted site where solution senses the cation strength (monovalent or divalent). The difference in ionic strength between drug loaded polymer solution and surrounding fluid at targeted site creates the osmotic gradient [8]. The aqueous polymer solution forms a clear gel and released the drug in the presence of the mono or divalent cations. This phenomenon is typically found during ocular drug administration. The electrolyte tear

fluid contains different cations like Na^{+}, K^{+}, Ca^{2+} and Mg^{2+} in where installed drug leaded polymer solution formed a layer of gel and released the ophthalmic drug.

3 Photo Polymerization: In this process, the solution of reactive monomer and photoinitiator is installed at targeted site and electromagnetic radiation is applied to form gel. The photopolymerization can be done either by using photoinitiator or by dispersing nanomaterial. Photoinitiator initiates the polymerization after light radiation. Azobisisobutyronitrile (AIBN) is UV light sensitive photoinitiator but this short wave length light has less tissue penetration ability for injectable *in-situ* polymer and moreover it is biologically harmful to use in non-invasive delivery. Camphorquinone in combination with a benzyl alcohol is a visible light sensitizer to initiate cationic photopolymerization [9].

Polymeric Micro/nanoparticle(PNP): In drug delivery system, PNP is termed as revolutionary drug delivery vehicle. Due to biodegradability, biocompatibility, controlled released behavior, design flexibility based on functionalization, and polymer diversity PNP is widely used as drug dispenser [10], [11]. Depending upon the preparation method, PNP offers nanospheres, nanocapsules etc. where drug can be encapsulated, or attached to a nanoparticle matrix (Fig. 2.2). The nanosphere is non-cavity based particle with porous polymer where the drugs are entrapped physically and uniformly inside the pores of the polymer whereas nanocapsules are cavity based systems surrounded by a porous polymer membrane in which the drug is encapsulated into a cavity [12]. Due to some advantageous points, PNP is famous in drug delivery and those are [13]: (i) easy manipulation of particle size and surface characteristics to achieve drug targeting after administration,(ii) control and sustain release capability of the drug at the site of localization, (iii) fast therapeutic efficacy and less side effects, (iv) modulation of particle degradation by the variation of polymer matrix and drugs can interact with the systems without involvement of any chemical reaction. Particle size is a key factor for drug release. Smaller particles have larger surface area and larger particles have lower surface area. The smaller particles (sphere) have relatively smaller pores, mesh size and tortuous path than larger particles (sphere) for which drugs are available at or near the surface of the sphere, leading to fast drug release. Whereas, larger spheres have large pores which allow more drug to be entrapped than smaller spheres but drugs have to move longer tortuous path to come near the surface of the sphere and diffuse out [14].

Fig. 2.2: Polymeric nanoparticle[2]

In case of smaller nanocapsule, drug release is faster due to smaller core and least path transportation from core to outer surface of whereas drug release from larger nanocapsules have bigger core and long transportation path with low diffuse out. Generally, nanoparticles are loaded with drugs during synthesis and the drug delivery happens at the targeted site by below discussed physico-chemical mechanisms.

1 **Swelling of PNP by Hydration**: The drug loaded particle is dispersed in released medium (lets' say pH 7 buffer medium) for drug release. In this case the dry polymer is swelled by hydration by which the encapsulated or entrapped drug can be released through diffusion which called drug dissolution [15]. The release solvent can be used either acidic or neutral or basic.

2 **Enzymatic Reaction:** In the presence of enzyme, the enzyme responsive polymer offers reversible or irreversible changes in chemical structures and/or properties of polymeric materials for the treatment of cancer and diabetes. The on-site enzyme assisted rupture or cleavage of the polymer results the degradation of particle and leads to drug release from the entrapped inner core [16]. Some enzyme-responsive, multilayered nanoparticles allowed the drug delivery by spatial changing in size.

3 **Drug Dissociation from PNP:** In this process the drug loaded swelled nanoparticles are explored for stimuli responsive drug release efficiency using pH, temperature, light etc. The pH sensitive PNP based drug delivery is the most promising and the drug is released in a slightly acidic environment, which occurs in inflammatory tissues and

[2] https://www.precisionnanosystems.com/areas-of-interest/formulations/polymeric-nanoparticles

tumors. The pH sensitive polymers contain acidic or basic groups to accept or donate protons in response to pH of release medium. Swelling of PNP increased as the external in the case of weak acidic groups, but PNP shrink if polymer contains weak basic groups [17]. Thermosensitive PNP contains certain volume phase transition temperature (VPTT). The negative PNP collapsed and release the drug above VPTT whereas positive nanogels behave opposite i.e drug release obtained below VPTT.

Liposome: Polymeric liposomes (PL) are the mimic of vesicle from cell biology. The biological vesicle is liquid encapsulated e spherical structure which presents within or outer the cell, made up of lipid layer. The capability of uptake and release of the content outside and/or inside of the cell by vesicle, has been encouraged to researcher to developed the mimic structure by polymer and/or copolymer with one lipophilic (combine with or dissolve in lipids) component. This artificial vesicle is called liposome which is the bilayers of amphiphilic material in which one or many hydrophilic layers are fit in between hydrophobic lipid (Fig:2.3) (major component of cell membrane). The hydrophilic reservoir of liposome is suitable for hydrophilic drugs and it protects the drug from the acid degradation, acid metabolism by its hydrophobic wall, which is one of the advantages of liposome. Hydrophobic molecules are inserted into the bilayer membrane. Another advantage is that, hydrophobic wall manipulates the diffusion of the drug molecules in and out of the liposome by controlling the permeation of the wall. As a drug delivery system, another plus points are, biocompatibility, capacity for self-assembly, ability and a wide range of physicochemical and biophysical properties that can be modified to control their biological characteristics [18], [19]. The deformable liposomes are known as Transfersomes.

The pH responsive liposomes is employed at different pathological sites to release the drug by sensing the site specific pHs. Some pathological sites have different pH than normal tissues, like tumors are often slightly more acidic than healthy tissue. The pH modulations trigger the liposomal membrane permeability by protonation/deprotonation of functional groups and induce morphological changes in the lipid bilayers[3]. As an example, cholesterol based poly-(acrylic acid) (Chol-Paac), crosslinked with 2,2′-(ethylenedioxy)-bis(ethylamine), created a membrane to promote the leakage of

[3] https://www.ncbi.nlm.nih.gov/pmc/articles/PMC5557698/

encapsulated molecule through an acid triggered conformational collapse upon protonation of the functional groups [20]. Enzyme sensitive liposomes release the molecule by sensing the elevated enzyme expression and initiate the biochemical transformation to activate drug release at specific tumor microenvironments. Enzymatic cleavage on the liposomal membrane produces a gap in the lipid bilayer packing to enhanced diffusion and release.

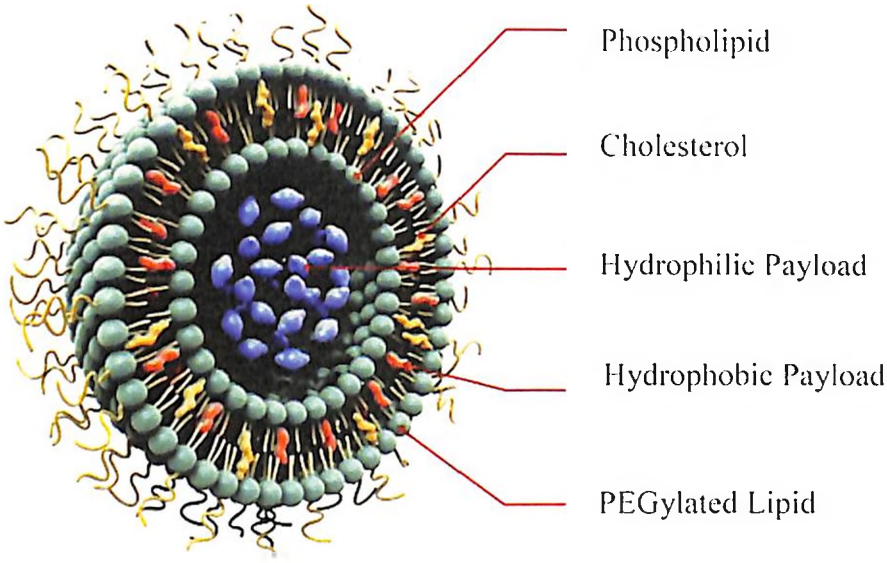

Fig. 2.3: Polymeric liposome[4]

Light is used as an on-demand, physical stimulus to release liposome encapsulated molecules. The main aim is to use the light where activated photons are safe to biological tissue and easy penetrable. The visible to near infrared light range is transmissible deep into biological tissues due to low scattering and small absorption coefficients [21]. Photosensitizer agent is attached with polymer chain and these are hydrophobic for which they are widely used in liposomes. Photosensitizer transfers the photon energy to molecular reactive oxygen species which reacts with the liposomes to induce contents release or photodynamic cancerous tumor therapy [22]. Photo chemical reaction induces the photo cleavage of a reactive amphiphilic polymer molecule in the lipids to trigger release via a localized increase in membrane permeability.

The temperature sensitive liposomes exhibit either LCST or UCST. LCST based liposomes exerts a mechanical stress on the liposomal membrane due to heat elevated contraction for drug release due to membrane immobilization. The UCST based

[4] https://www.precisionnanosystems.com/areas-of-interest/formulations/liposomes

liposomes behave opposite of LCST based liposomes. For example a biocompatible hyperbranched poly(glycidol) (HPG) polymer with temperature-sensitive oligo(ethylene glycol)s (OEGs) based liposome was destabilized under mildly elevated temperature (30–40 °C). Hydrogen bond formation between the polymer carboxyl groups and the phospholipid head groups were also believed to contribute to liposome destabilization [23].

Micelle: Polymeric micelles (PM) are one type of the nanoparticles which has a core-shell structure. Generally, PM formed by self-assembly of copolymers in spherical shape and the size of 10–100 nm [24]. PM is amphiphilic in nature where one part of block copolymers is hydrophobic and other one is hydrophilic. The PM exhibits the sol-micelle and /or micelle-sol forms and the transition depends on applied stimuli as well as the solvent (polar and/or nonpolar). Due to amphiphilic nature PM is suitable to encapsulate both hydrophilic drug as well as hydrophobic drug. PM has some advantages for which it is used in drug delivery and those are [25]: (i) solubilization of amphiphilic drugs and its improved bioavailability, (ii) reduction of toxicity and other adverse effects, (iii) enhanced permeability and favorable biodistribution in drug, (iv) easy penetrations in the interstitial space of small size micelle by enhanced permeability, (v) PM encapsulated drug protects the undesirable side effects on non-targeted organs and tissues.

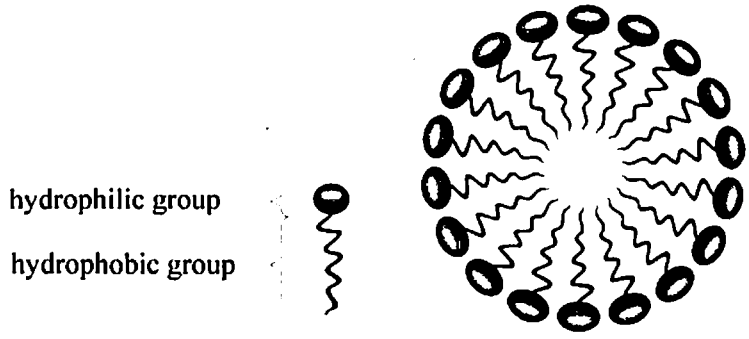

Fig. 2.4: Core-Shell Micelle in nonpolar solvent[5]

According to Kataoka *et al.* [26] in polymeric solution stage the hydrophobic parts of the block copolymers are self assembled and the outer hydrophilic shell stables in hydrated form by creating hydrogen bonds with water and/or hydrophilic drug (Fig. 2.4). The hydrogen bonds breaks and hydrophobic block creates the shell with hydrophilic inner core, leads to drug release.

[5] http://eng.thesaurus.rusnano.com/wiki/article1199

The thermosensitive micelle forming polymer block contains one hydrophilic block and another is thermosensitive block which shows the hydrophobic nature above the temperature of its critical solution temperature (CST). For instances, Poloxamer 407 is a triblock copolymers of poly(ethylene glycol-block-propylene oxide-block-ethylene glycol) (PEG-PPO-PEG) is thermosensitive where PEG is hydrophilic and PPO is hydrophobic. Poloxamer 407 (P407) and hydrophilic carboxymethyl cellulose sodium (CMCs) form micelle structure by self-assembling its hydrophilic core-hydrophobic corona from aqueous state at its CST and beyond that CST gel network forms. The micelle formation temperature was 21 ^{0}C and above this transition temperature micelles were self assembled to form gel matrix with released of drug [27].

In pH sensitive micelle, the ionization of pH sensitive functional group in hydrophobic segment leads the protonation and/or deprotonation to release the drug. Another co-polymer of 1,2-distearoyl-sn-glycero-3-phosphoethanolamine and N-[methoxy(polyethylene glycol)] conjugated poly(β-amino esters) (DSPE-b-PEG-b-PAE-b-PEG-b-DSPE), able to exhibit self-assembled core/shell polymeric micelles in aqueous solution at the change in pH environment [28]. At low pH, the drug release was occurred due to ionization of amine group in PAE segment, leading degradation of the polymeric micelles and resulting in accelerated drug release rate. The micelle to sol transformation is suitable for hydrophilic drug release. The light sensitive degradation of micelle to release the hydrophobic drug was observed by Cao *et al.* [29] hydrophilic chitosan based NIR sensitive amphiphilic micelles containing NIR sensitive 2-nitrobenzyl succinyl ester as the hydrophobic block. The drug was loaded into hydrophobic core of micelle but dissociated under NIR illumination, enabling a controlled fast release of loaded hydrophobic species in the micelles. NIR sensitive dye, cypate accelerated the release of loaded drug.

Nanogel: Nanogels, the drug carrier dosage formulation to deliver at targeted site. When physically or chemically crosslinked, hydrophilic polymeric nanoparticles are offer a colloidal form of hydrogel that called nanogels. According to Garg *et al.* [30] the size of nanoparticles in nanogels are ~100–200 nm. Nano pore sized three dimensional hydrogel with a high water holding capacity and without dissolving into the aqueous medium also called as nanogel. The porous structure of nanogels can encapsulate the micromolecules or macromolecules [31]. Due to some good points, nanogel is called as next generation

of drug delivery and those are: (i) biocompatible and biodegradable nature, (ii) controlled and sustained drug release, (iii) controllable particle size, pore size of gel [32], (iv) easily dispersible in aqueous media [32], (v) easy administrable, (vi) prevention of unexpected drug leakage [33], (vii) encapsulatation of both hydrophilic and hydrophobic drugs. Nanogel contains spherical, core-shell hollow shell, multilayred. Biopolymeric nanogels are prepared from collagen, albumin and fibrin, and polysaccharide polymers such as chitosan, hyaluronic acid (HA), heparin, agarose and alginate. Synthetic nanogels are Poly(lactic acid), poly(lactic)–poly(glycolic) copolymers, poly(e-caprolactone). The optical and TEM image of polymeric nanoparticle reinforced nanostructured nanogel is displaced in Fig. 2.5.The bigger circle in the TEM image is the nanostructured hydrogel and the black dots are the polymeric nanoparticle [34].

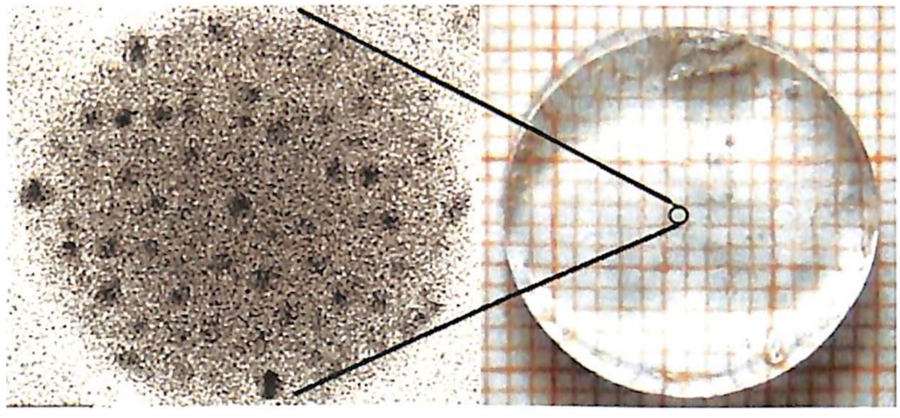

Fig. 2.5: optical and TEM image of polymeric nanoparticle reinforced nanogel [34]

Besed on stimuli sensitivity nanogel can deliver the therapeutic agent which is discussed below:

1 pH Responsive Nanogel: pH sensitive nanogel contains pH sensitive functional groups deionized and/or ionized in the gel network results intermolecular electrostatic force inside the polymer network and drug molecule. This force results the change in osmotic pressure, swelling-deswelling and porosity of the nanogel which triggers the absorption and release of the therapeutic molecules [35].

2 Thermosensitive Nanogel: Thermosensitive nanogels are reactive to a specific volume phase transition temperature (VPTT) for which they display a change in volume according to the temperature. The negative thermosensitive nanogels become hydrated and swelled with loaded drug solution below VPTT and above VPTT they collapsed and release the drug whereas positive thermosensitive nanogels behave opposite to elevated

temperature than VPTT. The Drug release depends on the drug dissolution and built hydrogen bonding between nanogel and drug molecule.

3 Photoisomerized Nanogel: Photoisomerization is a type of photochemical process which leads some conformational changes in the photosensitive functional groups in the nanogel due to light exposure. For instances, photosensitizer isomerizes from a *trans* to *cis* orientation on light irradiation [36]. Photosensitizer loaded nanogel become photo chemically excited and they produce the reactive oxygen which can result in oxidation in the cellular compartment walls that highly influence the release of therapeutic agents.

2.3 Utilization of Dosage Formulations Non-invasively

In this section we have been discussed the drug release efficiency of different hydrogel based formulations in different non-invasive applications. The drug release methods also have been discussed.

Oral Drug Delivery

Like anticancer drug release activities, the large molecule drug such as insulin has limitations on clinically routine administration through injection. Nevertheless, some adverse effect like inflammation, skin allergies etc happened after injection of routine administration. To overcome these drawbacks on insulin administration, the polymeric nanoparticle acts as insulin carrier. A pH-responsive polymeric nanoparticle (NP) based drug carrier was developed by chitosan and poly(γ-glutamic acid) conjugated ethylene glycol tetraacetic acid (γPGA–EGTA) for oral insulin delivery in diabetic rats [37]. γPGA–EGTA was protected the insulin from systemic degradation. Insulin is easily degradable by trypsin, which is advantageous for routine administration to control the blood sugar. Trypsin is a Ca^{2+}-dependent protease present in the small intestine which degrades insulin. The groups on EGTA were deprotonated in intestinal pH (pH 6.4–7.4) and accelerated their association kinetics of Ca^{2+}.

Probiotic lactic acid bacteria is consumed as living microorganism supplements due to have many health benefits [38]. After oral administration, before reaching to small intestine the proliferation of bacteria starts reducing in low pH gastric acid. So it is important to design a protective bacteria carrier to release viable bacteria to small intestine with good therapeutic effect. Mei *et al.* [39] developed low pH protective, pH

sensitive, intestinal targeted drug vehicle. The vehicle was a core shell structured formulation with Ca-alginate/protamine (Ca-AlgP) composite shell with Ca-alginate (Ca-Alg) core. Lactobacillus-casei was the model lactic acid bacterium which was encapsulated with the Ca-alginate (Ca-Alg) core. Ca-AlgP shell offered the protection to the bacteria lactic acid and increased the residence time in the stomach with rapid release of Lactobacillus-casei. In the strong acidic environment of stomach, the diffusion channels in the Ca-Alg networks are obstructed with protamine molecules for which the gastric acid struggled to diffuse inside Ca-AlgP composite shell. But in the neutral small intestine the drug vehicle dissolved rapidly and Lactobacillus-casei was quickly released.

The nanogel is nano structured three dimensional networks and has higher specific surface area than bulk hydrogels. The nanogels are synthesized by emulsion polymerization technique, which contains large amount of organic solvents and surfactants as residue and harmful to drug. To overcome these limitations, the thermoresponsive and pH sensitive hydroxypropyl methylcellulose (HPMC) hybrid nanogels were developed for controlled release of insulin [40]. Insulin was loaded in HPMC hybrid nanogel during synthesis and 21.3% of insulin loading with 95.7% entrapment efficiency found in HPMC hybrid gels. The pH responsive release of insulin was investigated at pH 1.2 and pH 7.4 in incubate shaker at 37 °C and temperature sensitive release was done in incubator at different temperatures of 27 °C, 32 °C, 37 °C and 42 °C at pH 7.4.

For treating various diseases through oral route, microsphere is studied as desirable way to deliver of a wide variety of therapeutics. The absorption of therapeutic particulate system experiences many physiological barriers in the gastrointestinal (GI) tract, such as the intestinal mucus layer [41] which results in low oral absorption efficiencies. The fabrication of microsphere and its deliverance of therapeutic agent in intestine is highly challenging due to some reasons and they are: (i) it is difficult to cost-effectively synthesize the sphere with tailored molar mass and structures [42], (ii) pH-responsive sphere shows delayed and non-sharp profiles to pH fluctuation, for which control of drug release via pH is undesirable. For the management of these issues, a multiple non-covalent interactions-mediated assembly strategy was reported in formation of microparticles with carboxyl bearing compounds (CBCs) as guest molecules and poly(N-isopropylacrylamide) (PNIPaam) served as a host polymer [43]. The encapsulation of

theraputic agent was achieved by self-assembly approach, led to higher drug holding capacity of microspheres as compared to microspheres based on poly(D,L-lactide-coglycolide) (PLGA) and an enteric coating polymer Eudragit S 100 (ES100). Indomethacin (IND), was model drug for gastroretentive drug release. The pH environment for drug release was initially conducted at pH 1.2 and after 2 hrs, the release medium was switched into pH 7.4. Rapid *in-vitro* release occurred at pH 7.4 than pH 1.2, and IND was almost completely released within 24 hrs. At 37 °C PNIPaam chains became more hydrophobic due to dehydration of amide groups so the combined effect of hydrophobic IND and PNIPaam caused negligible IND release in the stomach-relevant acidic solution but at pH 7.4, dissociation of IND was dramatically enhanced its dissolution. The anticancer, hydrophobic drug Paclitaxil (PTX) was also employed for oral delivery and the hydrophobic repulsion between drug and PNIPaam was responsible for drug dissolution. The pH-responsive therapeutic microspheres and their intestinal delivery were examined in mice body of inflammation and tumor.

A phase-transitional shielding layer of poly [(methyl methacrylate)-co-(methyl acrylate)-co-(methacrylic acid)]-poly(D,L-lactide-co-glycolide) (PMMMaac-PLGA), was reported as oral vaccine which protects antigens in the gastro-intestinal tract and achieved targeted vaccination in the large intestine [44]. The pH triggered phase transition and repulsion of the surface negative charge from ionized -COOH in Maac at weak alkaline was the reason behind pH sensitivity of polymeric micelle. Trypsin was employed as the model antigen for oral vaccination against group B Streptococcus (GBS) bacteria. The polymer/antigen nanoparticle was applied as oral vaccine to the large intestine of tilapia.

Large molecule protein and peptide drugs have low oral bioavailability due to their enzymatic degradation in gastrointestinal (GI) tract and low absorption through intestinal membrane [45]. pH sensitive hydrogel is not only efficient for delivery of antitumor drugs but also efficient in oral drug administration where transportation of the drug faces drastic pH alteration occurs through GI tract [46], [47]. A pH responsive poly(methacrylic acid-co-N-vinylpyrrolidone) nanogel was developed by crosslinking with biodegradable oligopeptide [48]. The gel was exhibited pH-responsive oral delivery of siRNA and trypsin. The gel was subsequently exposed to pH 7.4 plus trypsin, after which they displayed a similar loss in turbidity, indicating degradation due to presence of trypsin. The polymer demonstrated successfully pH-dependent loading of the protein

insulin for oral delivery to the small intestine and degradation of drug carrier in small intestine in presence of trypsin.

Camptothecin (CPT) is a powerful anticancer agent but due to its high hydrophobicity it is limited for clinical application. In order to solve these drawbacks, the combination between poly(anhydride) nanoparticles and cyclodextrins was evaluated. CPT-loaded nanoparticles, prepared in the presence of 2-hydroxypropyl-β-cyclodextrin, (HP β-CD-NP) [49]. CPT was not released in gastric pH but in intestinal conditions, about 90% of the drug content was released 18 hrs. In an aqueous environment, the anhydride groups of the nanoparticles are hydrolyzed and create two carboxylic acid residues. When nanoparticles are in an acidic environment, these carboxylic acids cannot be ionized and decreasing the porosity of the nanoparticles but in neutral aqueous medium, nanoparticles would swell due to an ionization of the carboxylic acids residues for which drug dissolution was occurred [50].

The natural polysaccharides are widely applicable biomaterials as drug carriers for nontoxicity, biodegradability, easily availability and economical. Boppana *et al.* [51] developed a pH-responsive polyacrylamide-grafted-TSP (Paam-*g*-TSP) copolymer with sodium alginate (NaAlg) due to its biocompatibility, mucoadhesivity and non-carcinogenicity for *in-vitro* and *in-vivo* gastro-protective delivery of Ketoprofen. The model drug Ketoprofen was loaded into polymer during synthesis of microbeads and *in-vitro* release was performed in dissolution test apparatus in pH 1.2 and pH 7.4 buffer solution at 37 ^{o}C with 100 rpm paddle rotation. The pH controlled drug release upto 12 h. was observed for microbeads containing Paam-*g*-TSP and NaAlg, while 39.9% and 91.1% of Ketoprofen release happened from IPN microbeads of native TSP and NaAlg in pH 1.2 in first 2 hrs. and pH 7.4 in 6 hrs. respectively.

Poly (D,L-lactide-co-glycolide)-poly (ethylene glycol)-poly (D,L-lactide-co-glycolide) triblock copolymers (PLGA-PEG-PLGA) micelle has been developed for anti-cancer drug delivery by oral route [52]. As oral dosage formulation, PLGA-PEG-PLGA micelle was loaded with chemo preventive agent US597. 25.9–28.5% of US597 was loaded into carrier micelle and ~90% of loaded drug was released in sustained manner.

pH-sensitive carrier based on Ca-alginate/protamine microcapsules was developed for drug release in gastrointestinal environments [39], which enhanced the survival of probiotics in the stomach and their release in small intestine. But these microcapsules have the limitation due to complicated process and higher production cost. The making of Ca-alginate/protamine microcapsules as oral formulation is challenging due to the uneven and oversized diameter of probiotic microcapsules, poor sensitivity [53]. To overcome these limitations, a pH-responsive ethylene diaminetetra acetic-calcium-alginate (EDTA-Ca-Alg) hydrogel microsphere to encapsulate L. Rhamnosus ATCC53103 for oral controlled release of probiotics [54]. To investigate the release behaviour of probiotic, the L. Rhamnosus ATCC53103 encapsulated into microsphere was incubated in simulated gastric fluid (SGF) and simulated intestinal fluid (SIF). The encapsulated probiotics were released less than 20% after 2 hrs. in SGF, whereas, 100% release happened from SIF after 4 hrs. It was observed that, the microspheres maintained stable structure in SGF at pH 2.0 and dissolved in SIF at pH 7.4, which confirmed the pH sensitivity of developed EDTA-Ca-Alg microsphere for protection in gastric acid and controlled release in neutral intestinal environment.

Sami *et al.* [55] developed chitosan and guar gum based biopolymer for controlled and sustained release of analgesic Paracetamol. Swelling of polymer was performed in pH 4, 7.4 and 10 and it was seen that the polymer swelling ratio (wt/wt) was decreasing with increasing pH. The biohydrogel was efficient to release drugs at a predetermined rate through the skin. The drug was loaded in the beads during the incubation time of gelation. For releasing, Paracetamol loaded hydrogel was kept in 7.4 buffer solution and also in chicken skin model along with 7.4 buffer solution. In both of the cases the drug loaded gel was kept in mechanical shaker at 200 rpm. The effect of pH for drug release was meaningless as the 25% drug was released only because of mechanical vibration at 160 min.

Pulmonary Drug Delivery

Platinum containing chemotherapeutic agents like Cisplatin, Carboplatin, Paclitaxel, Docetaxel are widely used in case of lungs carcinoma. Another chemotherapeutic agents, doxorubicin shows numerous side-effects including severe cardio-toxicity when it is used in alone or in combination with other drug [56]. Liposome is good for cancer treatment

due to their enhanced permeability. This nanocarrier passes through the long systemic circulation for which hydrophilic polymers, polyethylene glycol (PEG) has to be incorporated but PEG reduced the cell internalization property of liposome which is very important character for accumulation in tumor. To resolve this issue PEG based liposome was modified octa-arginine (R8) which is a cell penetrating peptide and increases the cell internalization [57]. R8-conjugated amphiphilic poly(ethylene glycol)-dioleoyl phosphatidylethanolamine (R8-PEG-DOPE) was encapsulate the doxorubicin.

A porous poly-L-lactide (PLLA) microspheres (PLLA PMs) has been developed as a potential pulmonary drug carrier [58]. Methotrexate (MTX) as a model drug was encapsulated into microspheres during synthesis. *In-vitro cytotoxicity* investigation showed that the microspheres were not toxic and the porous structure showed sustained release profile with 81.6% encapsulated drug. Drug loading behaviors and *in-vitro* inhibitory activity against A549 lung cancer cells were also evaluated. 38.0% of the total drug in the MTX-PLLA PMs was released in 10 hrs. due to the sustained-release effect of the PLLA matrix. No obvious *cytotoxicity* was detected for the PLLA PMs, and the MTX-PLLA PMs.

Hydrogels microparticles are attractive for pulmonary delivery because their size can be easily tuned for delivery into the bronchi and swelling of polymer avoided clearance by alveolar macrophages in lungs. Poly(ethylene glycol) based enzyme responsive hydrogel microparticles were developed for pulmonary drug delivery [59]. During pulmonary disease matrix metalloproteinase (MMP) enzyme is become elevated. That's why the PEG microparticle has been used to release the drug by sensing MMP enzyme. After realize the contact of MMP, the mesh size of polymer was increased and preceded for degradation. Another strategy for lung delivery by avoiding rapid clearance was developed by nano-in-micro hydrogel particle formulation which showed advantages of both nanoparticles and swellable microparticles [60]. A copolymer of polyethylene glycol and phthaloyl chitosan (PEG-g-PHCs) was self-assembled with ciprofloxacin to form drug-loaded nanoparticles. The drug loaded nanoparticle suspension was mixed with sodium alginate solution to form microparticle. The dry hydrogel nano-in-micro hydrogel particles were delivery into rat by intra-tracheal insufflations where microparticle were swelled in lung fluid and released the drug. *In-vivo* pharmacokinetic study showed that approximately 45% drug released at 250 hrs.

In anti-tubercular therapy, sometimes multi drugs are being administered but due to patient noncompliance issue multi drug resistance creates as well as low bioavailability. Mane *et al.* [61] developed pH-responsive nanoparticle using norbornene (NOR) and PEG where NOR was the hydrophobic core. Isoniazid (INZ) and Rifampicin (RIF) were used for dual drug delivery. The drug release was occurred in mild acidic condition where as cancerous cell lines, 4T and A549 were used for their acidic nature. 55% drug released was observed in acidic medium for 24 hrs. According to author the micro/nano particle had potential application in treating both pulmonary TB and lung cancer due to TB.

Carboplatin, a anti-lung cancer drug release was observed from PNIPaam block poly (ε-caprolactone) [62]. LCST of polymer 32 ^{o}C and the micelle was changed its thermosensitive amphiphilicity by appearing as solution below LCST and hydrophobic globule. Carboplatin was slowly released at 37 ^{o}C than 25 ^{o}C due to LCST nature of micelle. The 60% drug release was observed from gel in 20 h. after administration as the polymer solution.

The magnetic polymer particle is used in drug delivery field to enhance the localized and controlled drug delivery, but these are core shelled non-porous structure. Gao *et al.* [63] has developed porous microspheres of poly-caprolactone (PCL) which were loaded with Indomethacin and magnetic nanoparticles (Fe_3O_4 NPs). ~75% to 98% drug was encapsulated into porous microsphere. The external alternating magnetic fields (AMF, 40 kHz) was facilitate the drug release from magneto-responsive microspheres.~35% cumulative release of the drug was observed from microsphere in 16 days. According to author this magnetic field responsive nanoparticles have the potencies for treating lungs carcinoma.

Survivin siRNA is a multifunctional protein which inhibits the spreading of carcinoma. Xu *et al.* [64] prepared a pH-sensitive delivery of Doxorubicin (DOX) and Survivin. Hydrazine bond between (3-maleimidopropionic acid hydrazide, BMPH), polyethylenimine (PEI) and drug was the reason of particle formation. Acid sensitive hydrazine bond between polymer and drug was helped the polymer to be released the drug in acidic medium. 80% cumulative drug released was observed in acidic pH in 72 hrs. which is suitable for a cancerous tumor.

Recurrence of pulmonary infections is caused by cystic fibrosis (CF) disorder, which is the human genetic disorder and this recurrence involve the repeated administration of inhalable antibiotics. Islan *et al.* [65] has developed an inhalable microparticles using sodium alginate. To enhance the porosity and drug loading capability, the microparticles were functionalized with alginate lyase (AL). 67% mucolytic agent, DNase and 40% antibiotic, Levofloxacin (LV) were loaded into microparticles. Microparticles were release the 30–50% DNase for 24 hrs., and LV was released in 3 days.

Amine-modified poloxamines was functionalized with maleimide for controlled antibody delivery to lungs [66]. The polymer stable in solution mode but exhibited an immediate gelation at a temperature above 37 ^{o}C. Model antibody, Bevacizumab was used to evaluate controlled delivery by *in-situ* forming gel. Approximately 87% of the released antibody was intact and displayed functional effect. In the next part, hydrogel stability was analyzed and *cytotoxicity* was assessed. Bevacizumab was selected as intra-vitreal injections of this antibody are currently used to treat neo-vascular age-related macular degeneration and the treatment might benefit from controlled long-term release.

Pulmonary drug and gene delivery is very important for acute lung injury (ALI). Kim *et al.* [67] developed cholesterol-conjugated polyamidoamine (PAM-Chol) micelles as drug dispenser of anti-inflammatory gene and drug into the lungs by inhalation. The PAM-Chol formed self-assembled micelles in an aqueous solution. An anti-inflammatory drug, Resveratrol and Heme oxygenase-1 (pHO-1) gene was loaded into the cores of the PAM-Chol micelles during synthesis process. The powder form of drug loaded micelles was inhaled by ALI animals and the anti inflammation efficiency was recorded by immune histochemical studies.

Nasal Drug Delivery

Peptide and protein drugs are exhibit low bioavailability due to gastro enzymatic degradation and this problem is overcomes by intravenous injection. Another non-invasive route is nasal, is proven as a route for peptide and protein delivery, despite of mucocilliary clearance as challenge for drug delivery. Cheng *et al.* [68] has prepared phenylboronic acid based core-shell nanoparticle for nasal route delivery because phenylboronic acid compounds are capable of covalent interactions with sugars. The ingredients of nanoparticle were poly(3-acrylamidophenylboronic acid) (PAPBA) and

hydroxyl groups of poly (2-lactobionamidoethyl methacrylate) (PLAMA). Insulin was loaded into particle during synthesis and 30% release of the drug was observed.

N-trimethyl chitosan chloride (TMC) is a potential drug carrier network for the intranasal delivery of insulin and by utilizing this property of TMC. Nazar *et al.* [69] prepared *in-situ* thermogel with mucoadhesive property for the transmucosal delivery of insulin via the nasal route. The TMC was blended with glycerophosphate (GP) and poly(ethylene) glycol (PEG) where PEG was thermosensitive polymer and provided the hydrophilic property with hydrogen bonding. The *in-situ* gelling temperature was ~35 °C and 70% insulin was loaded into formulation. GP provided the hydration to the TMC chains at low temperatures and favored hydrophobic interactions at 35 °C, to form of hydrogel network. The rapid sol-gel transition (8 min) started the release of the therapeutic cargo was taking place.45% drug release was observed from hydrogel in 2 hrs. The nasal formulation was administered on diabetic-rat as once-a-day.

In drug delivery field silica nanoparticles are good drug carriers with controlled release pattern because of the versatility and stability of these mesoporous matrices. The pores of these matrices can absorb the drug molecule. The mesoporous nanoparticles are being utilized to overcome the challenges in oral administration of drug for the treatment of rhino sinusitis which is a disease of nasal mucosa. Munoz *et al.* [70] prepared the mesoporous silica nanoparticle using pluronic P123. Corticoid(methyl prednisolone hemi succinate) was encapsulated for slow release. 80-90% drug was released in ~24hrs.

In chapter 1, it was discussed that, due to many difficulties, recent trends have been influenced the researchers to deliver the drug to brain through nasal route. Bhatt *et al.* [71] prepared solid lipid nanoparticles using citric acid, lecithin and poloxamer 188 to investigate the intranasal delivery of Astaxanthin for neurological disorders. Radio labeling studies were evaluated the biodistribution pattern of drug loaded particle after administration and it was found that the particles were uniformly distributed and 96–98% stable even after 48 hrs. of administration with higher concentration of drug. This result confirmed that nasal route is a suitable path for drug delivery to brain. After 48 hrs. of administration 81.40% of drug was released with sustained and controlled pattern.

Asenapine was delivered from lipid nanoparticles for the delivery of drugs in the brain by an intranasal route by Singh *et al.* [72]. Glyceryl monostearate (solid lipid) and oleic acid (liquid lipid) was used for making the nanoemulsion of nanoparticles with different size. 80% drug release was observed in 24 hrs. These findings demonstrate that nanostructured lipid carriers could be a new promising drug delivery system for intranasal delivery of Asenapine in the treatment of schizophrenia.

Chitosan is a unique polysaccharide cum biopolymer for its remarkable usefulness as a vaccine adjuvant to prevent the side effect of hepatitis B virus (HBV) vaccination. Wang *et al.* [73] used chotosan and hepatitis B surface antigen (HBsAg) as a model vaccine for intranasal administration. HBsAg was perfectly encapsulated into chitosan particles and the positive charge on the particle surface provided the strong adhesive effect with prolonged residence time in the nasal cavity. The acidic pH helped the antigen to be escaped. 15% antigen was released in 55 hrs.

Another polymeric nanoemulsion assisted drug delivery system has been investigated for nasal route delivery for delivering the drug to brain by Ahmad *et al.* [74]. The transportation of drug was possible using nanoemulsions (NEs) as model carriers. Nanoemulsion was consisting of polymer particle with different size. Mixture of poloxamer 407 and poloxamer 188 exhibited the sol-gel transition temperature of 30 °C. Chitosan was used as coating on NE to impart meucoadhesivity and extension of drug residence time so that high amount of drug can transport from nasal to brain.

Geniposide is the therapeutic agent for therapy of the neurodegenerative diseases but mucocilliary clearance is the obstacle for nasal route administration. In order to overcome the mucocilliary clearance issue, Wang *et al.* [75], developed a mucoadhesive, thermoreversible *in-situ* nasal gel encapsulated with Geniposide. As thermoreversible and mucoadhesive polymers, the poloxamers (P407, P188) and the hydroxypropyl methylcellulose were used respectively. Borneol was used as a permeation enhancer. Polymer solution was stable in 4 °C and gelation temperature was 29.6-31.3 °C after addition of Benzalkonium Chloride (BC), sodium chloride (NaCl), Borneol and geniposide. The cumulative release of drug from the gel was 95.2% after 6 hrs. after administration the cold polymer solution, it converted into gel just after sensing the nasal

temperature and drug was released as because of the mucoadhesivity of gel was protected from mucocilliary clearance and drug residence time was increased.

Mekawy *et al.* [76], prepared chitosan–ZnO nanocomposite hydrogel to use as insulin Mixtard 30 carrier to decrease the blood glucose concentration by hydrogel based formulation without the injection. Insulin loaded hydrogel nanocomposites were administered into the rat nasal cavity. The hydrogels decreased the blood glucose concentration (50–65% of initial blood glucose concentration) within 4–5.5 h. of administration, with *cytotoxic* effect.

Tazaki *et al.* [77], developed gold nanosphere (AuNPs), gold nanorods (AuNRs) scaffold polyinosinic-polycytidylic acid based adjuvant for the intranasal influenza vaccination. The AuNP–PICs were administrated subcutaneously or intranasally with influenza virus hemagglutinin. The shape- and size-related effects of the AuNPs were found to be dependent on the administration route and antigen dose.

Ocular drug delivery

PVA has wide applications in biomedical applications with the sol–gel transition temperature of PVA is 120 °C [78]. Pure MC showed sol–gel transition at 61.2 °C [79]. When PVA modified with methyl cellulose (MC) and sodium chloride (NaCl) the hydrogel showed lower gelation temperature than the individual gelation temperature or critical solution temperature of MC and PVA. Bain *et al.* [80] prepared the same polymer with said ingredients to see the sustained drug release profile of Ketorolac tromethamine (KT) which is an ophthalmic drug. The gelation temperature of PVA-MC polymer was reduced to 37 °C after addition of a salt. NaCl competed with MC chains for attracting the water molecules, and they attracted more water molecules due to their stronger hydration abilities. As a result, there were more hydrophobic aggregates of MC in a salted MC solution. Thus, upon CST, salted MC solution aggregated enough number of hydrophobic chains to form a gel, so that the sol–gel transition occurred at physiological temperature. ~95% drug was released in 8 hrs.

The rapid secretion and drainage of lachrymal fluid eliminates conventional eye drop rapidly which decreases residence time and low bioavailability of the ophthalmic drug at ocular surface [81]. To avoid these problems frequent administration of drug with

different formulation like viscous solutions, ointments, gels, suspension is required and various ophthalmic vehicles are used but these may cause side effects like blurred vision [82]. Poloxamer is known to exhibit reverse thermal gelation property at body temperature; remaining as solution at low temperature and gelation occurs when temperature increases. The poloxamer gel has mucoadhesive property but modification by carbopol or chitosan, the resulted gel offers suitable gel strength and prevents rapid precorneal elimination by increasing mucoadhesive property which improves the bioavailability [81]. The improved property of poloxamer, Bhowmik *et al.* [83] was inspired to develop xanthan gum (XG) and guar gum (GG) modified poloxamer-407 (PM) with thermosensitive *in-situ* gelling property for the sustained release of an ophthalmic drug. Atropine sulphate eye drop, Topin® was used to release in rabbit's eye. During *in-vitro* testing, the drug released about 53% after 4 hrs. and approximately 88% of the drug released after 8 hrs. of application.

Ophthalmic drugs are available in the form of suspensions, gels, ointments and polymeric inserts. After administration, the formulations show post-administration eye irritation. To compensate the drawbacks, researches have shown that stimuli sensitive *in-situ* sol-gel ophthalmic formulations with methylcellulose (MC). Due to presence of hydroxyl group, MC is water soluble and exhibits thermoreversible sol–gel-sol transition at 61 °C due to hydrogen bonding between hydroxyl groups and water molecules [79]. The mixture of MC and i-carrageenan formed a gel with low phase transition temperature [82]. This gelling technique was inspired Dipankar Chattopadhyay and group [84] to prepare an ophthalmic drug delivery system for release of Pilocarpine hydrochloride with *in-vitro* and *in-vivo* studies. I-carrageenan and potassium chloride reduced gelling temperature from 60 °C to 33.5 °C. So when the drug loaded polymer solution came to tear solution at 37 °C the solution was converted into gel and started release the drug. ~80% cumulative drug release was observed in 8 hrs.

Polymer–surfactant nanoparticles are used in ocular drug delivery as they encapsulate hydrophilic as well as hydrophobic agent to deliver at the specific target location with a steady rate for a prolonged time period. Pokharkar *et al.* [85] has been developed nanoparticulate system, using Aerosol OT (AOT) and gellan gum for ophthalmic delivery of Doxycycline hydrochloride (DXY).The electrolytes of the tear fluid, especially cations were initiate gelation of the polymer when instilled as a liquid solution

on the ocular surface and facilitated the drug release. Drug loaded nanoparticle showed 80% release after 24 h.

An *in-situ* forming ocular gel was developed for the delivery of Norfloxacin, for the treatment of conjunctivitis. Norfloxacin is effective therapeutic agent to treat ocular infections like conjunctivitis and ocular irritation. An *in-situ* ocular gel for Norfloxacin releasing was composed by Carbopol-940 and Hydroxypropylmethyl cellulose (HPMC) [86]. The gelling temperature was 37 °C and below that temperature polymer was in solution form. The loaded drug contents of the formulation was found to range between 98.30- 99.97% whereas 70-90% drug was released in 8 h.

Ocular drug delivery through hydrogel contact lenses is another good option for treating ocular diseases according to patients need. By directly placing on the ocular surface, delivery of drug with right concentration can be feasible. Antimicrobial peptide, Polymyxin B is widely used antibiotic for the treatment of many ocular infections. According to Malakooti *et al.* [87], delivery of Polymyxin B was not been attempted before them. So they prepared a contact lens by 2-hydroxyethyl methacrylate (HEMA) hydrogels. Acrylic acid was functionalized with HPMC to facilitate the higher loading of Polymyxin B. Another antimicrobial peptide Vancomycin was also used for evaluate the sustained release profile. 50-90% drug release was observed in 14 days in NaCl medium because NaCl medium weakened the drug–polymer interactions.

Poly(2-hydroxyethylmethacrylate) (PHEMA) based contact lens was prepared with loading of vitamin E and/or vitamin A [88]. The incorporation of Alexa Fluor 488 dye was made the polymer capable to load hydrophilic drug where as Vitamin A and Emade the polymer to encapsulate lipophilic drug. Timolol and brimonidine were model glaucoma drugs for releasing. Both of the drugs were released 100% in 4 hrs. due to hydrophilic attraction between drug and buffer solution.

An ocular drug, Diclofenac sodium was released from the thermosensitive triblock copolymer of polyethylene glycol and poly carpolactone, PEG–PCL–PEG (PECE) [89]. Polymer exhibited sol-gel phase transition at 35 °C. Drug loaded polymer solution was injected to rabbit eye with 4 °C and the polymer solution formed gel when polymer temperature reached body temperature (37 °C). The sustained release was observed since

7 days with 60–100% of total drug being released from different formulations after administration.

Methoxy poly(ethylene glycol) and hydrophobic poly carpolactone(PCL) was modified with α-cyclodextrin (α-CD) to prepare micellar supramolecular hydrogel through host–guest inclusion, for ocular drug delivery [90]. The aqueous polymer micelle (PEG-PCL) was added into the α-CD aqueous solution and host–guest molecular inclusion was created. The inclusion complex was the resulting effect of the hydrogel based micelle formation. Diclofenac (DIC) was the model drug for releasing. The drug was encapsulated with PEG micelles. After administration of supramolecular hydrogel as ocular gel onto the corneal surface, the micelles with encapsulated drugs was rapidly escape from α-CD modified hydrogel by blinking, providing 100% sustained drug release in 216 h.

Recent years the ophthalmic eye drops are being replaced by hydrogel solution which is liquid before instillation and changes into gel when exposed to body temperature or by changes in pH and ionic configuration. The *in-situ* hydrogels are capable of maintaining the constant drug level in plasma by releasing the drugs in a sustained manner [91]. Conjunctivitis is one of the most common eye infections and without treatment, the infection may worsen to cause corneal ulceration, scarring, and sometimes it leads to blindness. Neomycin is a wide spectrum amino glycoside antibiotic and Betamethasone is a corticosteroid. Combination of these two drugs is used in effective treatment of conjunctivitis. Deepthi *et al.* [92] has developed poloxamer and chitosan containing hydrogel to release Neomycin and Betamethasone for the treatment of conjunctivitis. The polymer was in solution state at 25 °C and converted into gel at 37 °C. 95.46% for neomycin and 94.90% for β-Methasone were released in ~8 hrs.

Drug loaded amphiphilic nanoparticles, composed of poly(ethylene oxide) (PEO) and poly(lactic acid) (PLA) were loaded into the biohydrogel of hyaluronic acid (HA) and methylcellulose (MC) to observe the drug released from stimulus-responsive, *in-situ* forming hydrogel onto the ocular surface [93]. Cannabigerolic acid (CBGA) was the model drug to be released. Sol-gel temperature of polymer was 32 °C at ocular surface. The polymer solution rapidly converted into gel at ocular surface temperature and created a coating. With the gelation of hydrogel lipophilic drug, CBGA loaded

nanoparticle penetrated the cornea. The drug was released by diffusion from amphiphilic nanoparticle.

Transdermal Drug Delivery

Transdermal route is advantageous approach due to its avoidance of gastric degradation and hepatic first-pass metabolism of drug. Maji *et al.* [94], developed chitosan-poly vinyl alcohol (PVA) hydrogel matrix for transdermal drug delivery of Alprozolam for prolong duration of action. Alprazolam, is used to treat anxiety disorders and panic attacks. The drug was dispersed into the polymeric patch. Maximum 93% drug was encapsulated and 54% drug release was released.

Nanoemulsion (NE) enhances drug solubility, and transdermal ability but due to having low viscosity it is constrained in transdermal application. Arora *et al.* [95], developed a nanoemulsion gel using polyacrylic acid (Carbomer 940) to deliver poorly water soluble drug Ketoprofen through transdermal route to overcome the troubles associated with its oral delivery and facilitated drug permeation through the skin without use of skin permeation enhancer. The nanoemulsion was formed the three-dimensional gel network due to noncovalent intermolecular associations such as coulombic, van der waals, and hydrogen bond interaction with drug released phenomena.

Piroxicam is an anti-inflammatory drug, poorly soluble and is associated with undesirable side effects on the stomach and kidneys in addition to gastric mucosal damage. Dhawan *et al.* [96] developed a nanoemulsion system of Piroxicam with better permeation potential through the skin. Carbopol 934 was one of the ingredients for the formation of nanoemulsion into nanoemulgel. The nanoemulsion gel increased the skin permeation during drug delivery.

Liposomes are potential material in drug delivery field. To increase its therapeutic effect Ferreira *et al.* [97] developed deformable liposomes for transdermal delivery of Piroxicam. Deformable liposomes allow the anti-inflammatory drug to penetrate through skin, optimize the side effect of drug. The deformable liposomes are known as Transfersomes. Lipid and β-cyclodextrin were employed to prepare the transfersome. β-cyclodextrin imparted the aqueous solubility due to formation of inclusion complexes with drug in its hydrophobic cavity. 63.27% drug was entrapped in transfersome.

For the treatment of eczema conventional medication is the use of corticosteroids, which has severe side effects such as striae, hypertension and atrophy. Along with alternative therapies like acupuncture, homeopathy, probiotics, massage therapy the conventional functionalized textiles wrap is used for eczema associated bacterial reduction. But these funtionalized textiles are de-moisturized the skin. Wang *et al.* [98] developed a dual functioned hydrogel based transdermal drug delivery system. Thermosensitive Poloxamer 407 (Pluronic F127) was exhibited sol-gel transition at 37 °C. The hydrophilic drug, Cortex moutan (CM) was loaded 50% into polymer solution. Carboxymethyl cellulose sodium provided bioadhesive property as well as hydrophilic nature which impart the moisturization to the skin to keep it wet. This wet-wrap was released 90% drug into skin. To reduce the resistance of drug transport, enhancement of drug permeability a porous channel structure was composed of poloxamer 407 (P407) blended with carboxymethyl cellulose sodium (CMCs) was proposed [27]. The micelle formation temperature was 21 °C and beyond this transition temperature micelles were self assembled to form gel matrix with released of drug by exdiffusion. Gallic acid (GA) loaded hydrogel matrix was penetrated through porcine ear skin and it was observed that, the *in-vitro* cumulative release of drug was ~10% in 50 h. Transdermal studies showed that P407/CMCs had significant increase in drug permeability across the skin.

Cellulose nanofibrils (CNFs) and chitosan are used in controlled release mechanism for their highly hydrophilicity and biocompatibility. Sarkar *et al.* [99], utilized these two materials for the release of Ketorolec Tromethamine (KT) through transdermal route. The researcher prepared a transdermal film with CNF/chitosan matrix. The plan was to release the therapeutic drug with an appropriate rate, balancing the minimum effective dose and toxic threshold dose. 80 % drug was encapsulated into film. *In-vitro* drug release profile was observed in Franz diffusion cell with artificial physiological conditions where 95–98% of the drug was released within 10 h.

Frequent and regular insulin injections and self-monitoring of blood glucose by patients themselves are inconvenient, painful, and prone to local infection and nerve damage. Transdermal delivery offers the painless, efficient, low cost delivery to patients with avoidance of first-pass metabolism and enzymatic degradation of drugs. Zhang *et al.* [100], developed arginine-based poly(ester amide) (Arg-PEA) and polyethylene glycol diacrylamide (PEG-DA) hybrid hydrogel for transdermal drug delivery. 80 % drug

release was observed by *in-vitro* method. The blood glucose level was reduced 80% after 2 h. of administration.

Melanoma is a type of skin cancer originated in the bottom layer of the epidermis due to high metastasis of melanin forming cell and include conventional chemotherapy and radiotherapy. Although transdermal administration is the either way to treat melanoma with maximum therapeutic efficacy but some challenges including tumor microenvironment, and cellular barriers obstruct the efficiency of transdermal drug delivery. Jiang *et al.* [101], proposed a paintable oligopeptide hydrogel based transdermal delivery system to deliver Paclitaxel (PTX)-encapsulated cell-penetrating-peptide (CPP)-modified transfersomes (PTX-CTs) melanoma treatment. The PTX-CTs-embedded hydrogel (PTX-CTs/Gel) patch was placed on the outer surface of skin above the melanoma tumor. The CPP enhanced the skin permeability and tumor stoma to facilitate PTX-CT penetration. The cell viability was decreased with the increasing concentration of released PTX. The size of the tumor in melanoma rat body was decreased due to released PTX.

Eudragit S 100 (ES100) a pH-responsive polymer, has the dissolution threshold at pH 7. This polymer is insoluble in acidic medium but soluble at pH 7.4. This pH dependent dissolution behavior makes the polymer to act as a drug delivery vehicle. According to Qindeel *et al.* [102] pH sensitive polymer especially ES100 has not been explored for transdermal delivery. So they exploited the pH sensitive release of Piroxicam through transdermal route. The pH difference at the skin surface and blood circulation was been explored. ES100 based pH sensitive nanoparticles was prepared with incorporation of poly vinylalcohol (PVA). ~88% drug was encapsulated into nanoparticle and 65% of drug was released within 8 h.

Non-invasive Alternative of Invasive

Poly(N-isopropylacrylamide) (PNIPaam) is a thermosensitive polymer with a lower critical solution temperature (LCST) of ~32 °C and also exhibit UCST [103] when dimethylsulfoxide (DMSO)/water mixtures are reacts with PNIPaam. PNIPaam was crosslinked with PEG diacrylate (PEG-DA) due to the thermo-responsive and sustained release characteristics of the co-polymer [104]. The polymer solution was injected into the vitreous chamber of rat's eyes and retinal function including retinal thickness, intra

ocular pressure (IOP) was being monitored. The changes observed in retinal parameters, such as diameter, thickness and IOP, did not persist after 2 weeks post-injection. These changes were likely due to an acute inflammatory response after hydrogel injection, as no indications of a chronic response were observed.

Polymeric nanoparticles are good drug carriers, whose physicochemical properties can be tuned with varying molar mass or chemical properties [105]. But nanoparticles are struggles with the unexpected burst release of loaded drugs in physiological conditions as well as the stability of nanoparticles in blood is critical for efficient tumor-targeted delivery [106]. These problems reduce the drug accumulation in cancerous cell and toxicated the healthy cells. To resolve these issues, Yoon *et al.* [107] developed UV crosslinked hyaluronic acid based nanoparticles (c-HANPs) with improved structure stability for *in-vivo* tumor targeted drug delivery. Paclitaxel (PTX), a hydrophobic model drug was employed for evaluating the *in-vitro* stability and release behaviour from particle. 80% drug was released and release pattern was linear. No burst release was observed. The application of combination of two anti cancer drugs for cancer treatment became interesting and both Doxorubicin and Paclitaxel are using for breast cancer treatment [108]. The polymer nanoparticles assembled from amphiphilic block copolymers became a potent carrier as drug delivery system for cancer chemotherapy due to their nanosized and ability to solubilise water insoluble drugs [109]. However, combined anticancer drug therapy increased toxic effect. To overcome these drawbacks, a pH sensitive poly(caprolactone)-heparine bio-conjugates were developed for sustain release of binary anti-cancer drugs [110]. The Paclitaxel and Doxorubicin were used as model binary drugs, where paclitaxel is lipophilic and neutral in nature and Doxorubicin is hydrophilic and positively charged in nature. The paclitaxel was loaded into synthesized bio-conjugate finally freeze drying was applied, whereas, Doxorubicin was loaded into the negative shell through the electrostatic interaction in aqueous solution. The release of Paclitaxel and Doxorubicin were done in citrate buffer of pH 5.0 and phosphate buffer of pH 7.4 at 37 ^{o}C. The Doxorubicin showed the pH dependent release than Paclitaxel. The poly(caprolactone)-heparine bio-conjugates released about 24% and 45% doxorubicin at pH 7.4 and pH 5.0 in 15 h. respectively, whereas, about 25% of paclitaxel was released in 50 hrs. from both pH 5.0 and pH 7.4. The developed

poly(caprolactone)-heparine bio-conjugates have the potential application for sustain release of binary anti-cancer drugs.

Tissue and organ adhesions are abnormal and unexpected problems after surgery, infection and other harmful events. So, prevention of adhesions has been made at post-surgical but these are proven as temporary. Polyethylene glycol (PEG), and methyl cellulose (MC) have been tested in animals as an anti-adhesive material. Thermosensitive methyl cellulose (MC)-based injectable hydrogels for post-operation anti-adhesion were prepared by integrating polyethylene glycol (PEG), carboxymethyl cellulose (CMC) and chitosan sulfate (CS-SO3) [111]. The gelation temperature of polymer solution was body temperature i.e. 37 °C. The polymer solution was injected to damaged rat caecum surface for 14 days. On 15th day the post injection anti-adhesion between organs was noted and no adhesion between tissues and organs was observed. The efficacy of the MC-based injectable hydrogels was successfully used as barriers for reducing postsurgical adhesions.

In the case of sol-gel transition of hydrogel, due to the direct solubility of drug became toxic leading to skin irritation and damage of healthy tissues. To solve these problems, a dual-reverse thermosensitive nanomicelle (DRTN) system was developed. The DRTN system was drug loaded, solid-lipid based thermosensitive nanoparticle of poloxomer. [112]. The SLNs and poloxamer gels prevented toxication of drug. At 25 °C, SLNs were solid form and transform into liquid at body temperature (34.7 °C).

Poloxamer 407 (P407) is technically known as pluronic, commonly used polymer to form thermosensitive gel for prolonged drug delivery due to its suitable reverse thermo sensitive property. P407 is a triblock copolymers from the family of poly(ethylene glycol-block-propylene oxide- block -ethylene glycol) (PEG-PPO-PEG). This polymer is useful in controlled delivery as its molecular weight effects on macromolecular therapeutic agent during release, but research showed that effect of molecular weight on release of intramuscular injection was missing. To improve that limitation the conventional Poloxamer 407 was modified with another grade of Poloxamer 188 [113]. As the polymer was injectable so sol-gel transition of polymer was observed and solution temperature was kept at 4 °C where as gelation temperature was 37 °C. Drug release was

observed by *in-vivo* and *in-vitro*, both methods. The rat was utilized as targeted place for drug release and the drug was released 100% from the in situ formed gel in 12 h.

Alginate is an anionic polysaccharide composed of two saccharides: epimeric β-d-mannuronate (M) and α-l-guluronate (G). Alginate based hydrogels offer high water absorption, elasticity, ability to maintain a physiologically moist microenvironment in the wound bed [114]. However, GG block modified alginates can incorporate more ionic interactions between chains and usually form a gel. The alginate and cyclodextrin conjugate with mild mechanical compression is known to be perfect material for drug delivery because of the host–guest inclusion ability of CD moieties for accommodating drug molecules and stimuli responsive nature of alginate like pH [115]. Chiang *et al.* [116], developed a photoresponsive β- CD-grafted alginate (β-CD-g-Alg)-co-azobenzene modified poly(ethylene glycol) (Az-PEG). Moreover, UV light irradiation induced the polymer chain *trans*-to-*cis* isomerization due to presence of azobenzene and switched back to the initial *trans* state under visible light. This photosensitive behavior enabled dissociation of the inclusion complex and gel degradation initiated release the drug. Due to ionic nature of alginate incident light with higher power and mild acidic environment are capable of accelerating the photo-triggered release, thus allowing the potential applications toward acute wound healing.

Chronic wound healing is a challenging task because of humidity and lack of angiogenic conditions are two important factors to interrupt the healing process [121]. Zeng *et al.* [117] was encouraged to develop a wound healing system using bioglass (BG) and agarose–alginate (AA) to improve the negative reason behind not healing the wound. Bioglass (BG) is a silicate-based inorganic material, which binds to soft tissues and promotes angiogenesis condition *in-vitro* and *in-vivo*. Alginate is also a wound dressing material, and a thermosensitive component, by combined with agarose. The BG/AA copolymer was appeared as solution at 50 ^{o}C and was injected into rabbits. The polymer solution formed into gel within 60s, at 37 ^{o}C by forming hydrogen bond between the hydroxyl group of agarose and alginate by releasing calcium ions (Ca^{2+}) from bioglass.

Keloid is dermal disease, which arises after an abnormal wound healing process. The treatment of keloid is challenging and need of frequent steroids injection. A thermosensitive hydroxybutyl chitosan (HBC) hydrogel as a cell delivery matrix was

developed [118]. Hydroxybutyl chitosan (HBC) was synthesized connecting hydroxybutyl groups to the hydroxyl and amino groups of chitosan, to possess reversible temperature responsive properties with maintaining the biocompatibility of chitosan. The polymer was appeared as solution at 4 °C where as gelation temperature of the HBC hydrogel was 25.7 °C, and at 37 °C polymer was appeared as complete gel form by hydrogen bond formation-destruction with surrounding solvent and drugs were released. The HBC hydrogel showed sustained drug release capacity (5-FU, 89.3%; DEXSP, 95.6%) for duo drug delivery.

Wang *et al.* [119], developed a chitosan modified PNIPaam for thermo responsive and photo responsive drug delivery application. The polymer was injectable and biodegradable due to presence of chitosan. Thermo responsivity was confirmed as PNIPaam itself is thermosensitive polymer. Photo thermal carbon solution was loaded into hydrogel for developing photo sensitive polymer. The polymer swelled at 26.5 °C and shrank at 45 °C also the transmittance was observed below LCST (32 °C) and gelation formed above that temperature. Doxorubicin was used as model drug to release by near infrared (NIR) irradiation. Maximum 62% drug was released from polymer in 67 h. after applying temperature and 80% drug release was observed after NIR irradiation. The polymer patch was adhered on the skin patch and conducted all experiments.

Luan *et al.* [120] developed a pH sensitive nano micelles of Konjacglucomannan (KGM) based amphiphilic polymers for cancer therapy. The presence of Schiff's base into KGM based amphiphilic polymer attributed for the pH sensitivity in nature. Curcumin was used as reference drug for *in-vitro* release behaviour. The water soluble KGM is advantageous to use in targeted drug delivery applications due to its low cost, good biocompatibility and biodegradability over limitations of several other natural polysaccharides. The release of Curcumin from loaded KGM based amphiphilic micelles was performed at two different pH values of 5.0 and 7.4 at 37 °C for 48 hrs. The rate of drug release was faster in pH 5.0 than pH 7.4 in first 24 h. Subsequently, 83.9% drug release was found at pH 5.0 after 48 h., while only 55.9% release happened at pH 7.4 after same time duration. The pH 5.0 medium stimulate the breakage of internal linkages between primary amine of octylamine and aldehyde group of KGM based amphiphilic

micelles, which results the faster rate of drug release with higher percentage of drug release in pH 5.0 than pH 7.4.

The increasing number of post joint surgical infections between intercellular mucosal films due to the microbial infection. To limit this problem a system with antimicrobial activity as well as antibiotic release property for prolonged time can be a good pathway. That's why a thermoresponsive, biodegradable, polymeric antibiotic delivery system was synthesized by hydroxypropyl methacrylamide monolactate (HPMAm-lac)/PEG copolymers hyaluronic acid (HA) [121], for the avoidance of implant-associated infections. An antibiotic Daptomycin was encapsulated in hydrogel network. The polymer exhibited sol (4 °C)-gel (37 °C) and this thermosensitive gelation helped the polymer to release the drug. 60% drug release was observed in 250 h. The thermo sensitive hydrogels were successfully demonstrated the antibiotic release.

Although, conventional colon specific drug delivery has been an invasive techniques but employment of hydrogel make possible the treatment of the colon disease through noninvasive approach. Sagar Pal and his group developed polyacrylamide grafted guar gum (GG-g-Paam) as matrix for the release of 5-amino salicylic acid to treat ulcerative colitis [122]. Drug was encapsulated by compression method of the mixture of drug and crushed polymer. *In-vitro* pH responsive release of drug loaded pellet was studied by USP dissolution method in pH 2, 7.2 and 10. 35-55% drug release was observed in pH 2 and 7.2 but 55-75 % drug was released in pH 10 after 10 h. Shahid *et al.* [123] used the same polymeric materials to release triamcinolone in colonic system (pH 7.2) and in gastro-enteric system (pH 1.2). Encapsulation of drug with polymer was followed the same process i.e compression method. 100 % drug was released in colonic system for 12 h. whereas 90% drug release was observed in gastric system in 7 h. Gowrav *et al.* [124], prepared pH-sensitive pellets of Polyacrylamide-grafted-guar gum (GG-g-Paam) to colon specific release of an anti-diabetic drug, glimepiride. Drug was encapsulated during preparation of pellet. 95.91% drug entrapment efficiency was observed and dry pellet was placed in pH 1.2 buffer first and then pH 7.2 solution to observe pH responsive drug release. Almost 95% drug was released by in-vitro method. The pellets of MCC and GG-g-Paam were suitable for pH sensitive colonic delivery of glimepiride. When pH sensitive drug dissolution has been captured the researchers' attention, Sagar Pal and his group [125] demonstrated glycogen (Gly), N-isopropylacrylamide

(PNIPaam) and ethylene glycol dimethacrylate (EGDMA) based crosslinked hydrogel (Gly/PNIPaam) for controlled release of colon targeted drugs. The temperature sensitive sol-gel transition was observed in 32 °C due to lower critical solution temperature (LCST) of PNIPaam. To load the drug (5-ASA and ornidazole) into polymer matrix the environmental conditions were kept at pH 9 and 25 °C. The dried hydrogel and drug mixed in buffer solution and centrifuged at 8000 rpm to precipitate the drug loaded hydrogel. The drugs were release in a controlled way (~53% ornidazole and ~73% 5-ASA were released after 24 h). The pH sensitive drug dissolution (cumulative release) was also performed at pH 1.2/7.4 where 5-ASA was released 70% and ornidazole was released 45%. The crosslinked hydrogel (Gly/PNIPaam) had been promising carrier for the controlled release of colonic drugs.

Table 2.1: Summarization of reported works on hydrogel based dosage formulation for noninvasive delivery

Route	Material	Stimuli	Drug used	Dosage formulation	Loading efficiency	Release efficiency	Ref. #	Remarks
Oral	Chitosan, poly(γ-glutamic acid),	pH	Insuline	Nanoparticle	77.40%	Not available	[37]	---
Oral	Ca-alginate, protamine	pH	Lactobacillus-casei becteria	Core-shell bead		100% release rate in pH 7 (approx)	[39]	---
Oral	HPMC	Thermo and pH	Insuline	Nanogel	21.30%	32% at 32 °C 48% at 37 °C 49% at pH 7.4 8% at pH 1.2	[40]	---
Oral	PNIPaam, PLGA	pH	Indomethacin Pactlitaxil	Microsphere	84%	90% approx at pH 7.4	[43]	---
Oral	PMMMAA-PLGA	pH	Trypsin	Nanoshell		0.7 μgm/mL approx	[44]	---
Oral	Methacrylic acid, N-vinylpyrrolidone	pH	siRNA and Trypsin	Nanogel	0.4 mg siRNA per mg nanogel in 4μM siRNA concentrate solution	---	[48]	---
Oral	2-hydroxypropyl-β-cyclodextrin, Poly(anhydride)	pH	Camptothecin	Nanoparticle	50μ gm/mg nanoparticle	90% at intestinal condition (pH 7.4)	[49]	---
Oral	Tamarind seed polysaccharide, Paam, NaAlg	pH	Ketoprofen	microbeads	20% (w/w)	39.9 % at pH 1.2, 91.1 % at pH 7.4	[51]	---
Oral	PLGA,PEG	pH	US597	Micelle	25.9-28.5%	90% approx	[52]	---
Oral	Ca-alg, EDTA	pH	L. Rhamnosus ATCC53103	Microsphere	---	20% in pH 2 100% in pH 7.4 (approx)	[54]	---
Oral	Chitosan, Gaur gum	pH	Paracetamol	Circular disc		0.25% at pH 7.4	[55]	---
Pulmonary	PEG, DOPE, Octa-arginine(R8)	Not Available	Doxorubicine (DOX)	Liposome	100μg/ml	---	[57]	Cancer cell viability was decreased with enhanced cancer cell penetration capability of R8-modified PLD

Route	Material	Stimuli	Drug used	Dosage formulation	Loading efficiency	Release efficiency	Ref. #	Remarks
Pulmonary	PLLA	Not Available	Methotrexate (MTX)	Microsphere	81.6%	38%	[58]	Drug loaded microsphere was immersed in buffer solution bath (37 °C and 60 rpm).
Pulmonary	PEG	Enzyme	---	Microparticle	---	---	[59]	MMP was used as model enzyme to observe the enzymatic degradation of microparticle in lung cancer therapy
Pulmonary	PEG-g-PHCs	---	Ciprofloxacine	Nanoparticles (NP)	30% w/w	45% approx in-vitro and 80% *in-vivo*	[60]	Drug loaded NP powder was immersed in pH7.4 buffer medium to evaluate the drug dissolution and release
Pulmonary	NOR, PEG	pH	Isoniazid, Rifampicin	Micro-/Nanoparticle	2.7×10^{-3} mol% in 1mg polymer	55% approx	[61]	---
Pulmonary	PNIPaam,poly(ε-caprolactone)	Temperature	Carboplatine	Micelle	---	60% approx	[62]	*In-vivo* biodistribution of drug was evaluated by micelle where 2.5-3.4 µg/mg of carboplatin was biodistributed
Pulmonary	PCL with Fe_3O_4 NPs	Magnetic field	Indomethacine	Fe_3O_4 NPs reinforced Microsphere	75%-98%	30%	[63]	---
Pulmonary	BMPH, PEI	pH	Doxorubicine(DOX),	Nanoparticle	30 mg DOX	80% in acidic medium	[64]	---
Pulmonary	Na-algenate, Algenate lyase	---	DNase, Levofloxacine	Nanoparticle	67% DNase 40% levofloxacine	30-50%	[65]	Loaded dry microparticles were incubated in 1.0 ml of physiological solution (pH = 7.0) at 37°C for 72 h. The drug was

Route	Material	Stimuli	Drug used	Dosage formulation	Loading efficiency	Release efficiency	Ref. #	Remarks
								released due to swelling of the microparticles by dissolution of drug
Pulmonary	Poloxamines, Maleimide	Temperature	Bevacizumab	*In-situ* gel	6.25 mg mL^{-1}	87%	[66]	---
Pulmonary	PAM-Chol	---	Resveratrol, Heme oxygenase-i	Micelles	46.45%	---	[67]	The drug loaded dry micelle powder was injected through intratracheal injection and the inflammatory action of drug loaded micelle was evaluated by animal lung injury model
Nasal	PAPBA, PLAMA	---	Insuline	Nanoparticle (NP)	31.4% to 57.9%	30%	[68]	The drug was released from the drug loaded nanoparticle by diffusion and swelling of NP
Nasal	N-trimethyle chitosan chloride (TMC) blended with GP and PEG	Temperature	Insuline	*In-situ* gel	70%	45%	[69]	---
Nasal	Pluronic P123, MSN	pH	Corticoid (methylpredniso lone hemisuccinate)	Meshoporous nanoparticle	40 wt%	80-90%	[70]	---
Nasal	Poloxamer 188, lecithin, citric acid	---	Astaxanthin	Solid lipid nanoparticle	77.42%	81.40%	[71]	The drug was released from the drug loaded nanoparticle by diffusion and swelling of NP

Route	Material	Stimuli	Drug used	Dosage formulation	Loading efficiency	Release efficiency	Ref. #	Remarks
Nasal	Glyceryl monostearate, Oleic acid	---	Asenapine	Lipid nanoparticle	83.50%	80%	[72]	The drug was released from the drug loaded nanoparticle by diffusion and swelling of NP
Nasal	Chitosan	pH	HBsAg	Particle	2 µg HBsAg	15% in acidic medium	[73]	---
Nasa	Poloxamer 407, Poloxamer 188, Chitosan	Temperature	DiR and coumarin-6 (C6)	Nanoemulsion	---	---	[74]	nose-to-brain transportation of nanoparticles was tracked by fluorescent bioimaging strategies. Confocal microscopy confirmed translocation of NEs
Nasal delivery	Poloxamer 407, Poloxamer 188, Hydroxypropyl methylcellulose	Temperature	Geniposide	In- situ	20 µL	95.2%	[75]	---
Nasal delivery	Chitosan-ZnO nanocomposite	pH	Insuline	Nanocompo-site film	8 mg mL^{-1}	50-65% reduction of blood glucose concentration diabetic rat	[76]	---
Nasal delivery	Gold nanosphere, nanorod scaffold polyionosinic-polycytidylic acid	---	---	---	---	---	[77]	The AuNPs based polymeric material was used as an adjuvant to boost the immune response. Conjugation with gold nanorods increased adjuvanticity of polymer than conjugated with spherical nanoparticle
Occular	PVA, MC	Temperature	ketorolac tromethamine (KT)	Sol-gel	0.5 wt%	95%	[80]	---

Route	Material	Stimuli	Drug used	Dosage formulation	Loading efficiency	Release efficiency	Ref. #	Remarks
Ocular	Xanthan gum (XG), guar gum (GG) and poloxamer-407	Temperature	Atropine sulphate eye drop (Topin®)	Sol-gel	1%	53% -88%	[83]	---
Ocular	Methyl cellulose and i-carrageenan	Temperature	Pilocarpine hydrochloride	Sol-gel	2%	~80%	[84]	---
Ocular	Gellangum	Ion stimuli	Doxycycline hydrochloride	Sol-nanoparticle	45–80%	80%	[85]	---
Ocular	Carbopol-940, HPMC	Temperature	Norfloxacine	Sol-gel	98.30-99.97%	70-90%	[86]	---
Ocular	HEMA, Acrylic acid	Ion sensitive	Polymyxin-B, Vancomycin	Contact lens	2 mL Polymyxin-B, 2 mL of vancomycin	50-90%	[87]	---
Ocular	Poly-HEMA	---	Timolol,Brimonidine	Contact lens	19.1%, and 18.7% respectively	100%	[88]	Drug loaded contact lens was immersed in buffer solvent for drug release by diffusion
Ocular	triblock copolymer, PEG–PCL–PEG (PECE)	Thermo	diclofenac sodium	Sol-gel	0.1% (w/v)	60–100%	[89]	---
Ocular	PEG, PCL, α-CD	Temperature	Diclofenac	Micelle, sol-gel	0.1(w/v)%	100%	[90]	---
Ocular	Poloxamer, chitosan	Temperature	Neomycin, Betamethasone	Sol-gel	91–95% for betamethasone and 90–98% for neomycin	95.46% for neomycin; 94.90% for betamethasone	[92]	---
Ocular	PEO, PLA, HA, MC	Temperature	Cannabigerolic acid	Sol-nanopartticle	231 µg/mL	200 µg/mL	[93]	---
Transdermal	Chitosan, PVA	---	Alprazolam	Patch	93%	54%	[94]	The *in vitro* skin permeation property was used for release
Transdermal	Poly acrylic acid (Carbomer-940)	---	Kotoprofen	Nano emulsion	97.96% to 100.05%.	1.6mg/cm^2 drug was permeated	[95]	The *in vitro* skin permeation property was used for release

Route	Material	Stimuli	Drug used	Dosage formulation	Loading efficiency	Release efficiency	Ref. #	Remarks
Transdermal	Carbopol-934	---	Piroxicam	Nano emulsion	96.9-99.6%	0.8-1 mg/cm^2 drug was permeated	[96]	The *in vitro* skin permeation property was used for release
Transdermal	β-CD	---	Piroxicam	Transfersome	63.27%	8 mg/cm2 drug was permeated	[97]	The permeation of the deformable liposomes incorporating Piroxicam was performed on the pig skin
Transdermal	Poloxomer 407	Thermo	Cortex moutan	Sol-gel	50%	90%	[98]	---
Transdermal	Poloxomer 407, CMC	Thermo	Gallic acid(GA)	Micelle	15% (w/w)	10% approx	[27]	---
Transdermal	Cellulose nanofibrilis, Chitosan	---	Ketorolec tromethamine	Transdermal film	80%	95-98%	[99]	Drug loaded film was kept in Franz diffusion cell with dialysis bag and the drug release was observed by diffusion process
Transdermal	Arg-PEA, PEG-DA	---	Insulin	Transdermal film	5 mg/mL	80%	[100]	Drug loaded film was kept in Franz diffusion cell with dialysis bag and the drug release was observed by diffusion process
Transdermal	PTX-CTs	---	Paclitaxel	Transfersome	99%	30%	101	The cancer cell viability and volume reduction by drug loaded transfersome was observed
Transdermal	PVA,ES-100	pH	Piroxicam	Nanoparticle	88%	65%	[102]	---
Alternative rout of Invasive	PNIPaam,PEG-DA	Temperature	---	Injectable sol-gel	---	---	[104]	The purpose of this research was to investigate the effect of hydrogel injection on

Route	Material	Stimuli	Drug used	Dosage formulation	Loading efficiency	Release efficiency	Ref. #	Remarks
								retinal function
Alternative rout of Invasive	c-HANPs	UV light	Paclitaxel	Nanoparticle	$2.2x10^{5}$ mg	80%	[107]	---
Alternative rout of Invasive	Poly(caprolactone)-heparine	pH	Paclitaxel (PTX), Doxorubicin (DOX)	Nanoparticle	10 mg PTX 10 mL aqueous solution (1 mg/mL) DOX	24% doxorubicin in pH 7.4 & 45% in pH 5 25% PTX in both pH 5 and 7.4	[110]	---
Alternative rout of Invasive	PEG, CMC, Chitosan sulphate	temperature	NIL	Sol-gel	Anti-adhesion properties investigated	Anti-adhesion properties investigated	[111]	---
Alternative rout of Invasive	Poloxamer	Temperature	Flurbiprofen	Sol-micelle	Flurbiprofen (100 g) was added into 150 g of a lipid	~80%	[112]	---
Alternative rout of Invasive	Poloxamer-407,Poloxamer-188	Temperature	5-40KDa PEG	Sol-gel	0.5ml	100%	[113]	---
Alternative rout of Invasive	β-CD grafted algenate, Azo-benzene modified PEG	pH, UV light	Red-colored Rhodamine B (RhB)	Trans-to-sis isomerization	10^{-2}M,0.5mL	100%	[116]	Degradation of formulation enhanced the
Alternative rout of Invasive	Bio-glass, Agarose, Algenate	Temperature	---	Sol-gel	---	---	[117]	bioglass (BG) and agarose–alginate (AA) have been used for wound healing system.
Alternative rout of Invasive	HBC	Temperature	5-Fluorouracil, DEXSP	Sol-gel	---	---	[118]	This material has been used as cell delivery matrices.
Alternative rout of Invasive	Chitosan, PNIPaam, photo thermal carbon solution	pH, Temperature , photo	Doxorubicin	Sol-gel	0.5 mg/mL	62% release by temperature, 80% release by NIR irradiation	[119]	---
Alternative	Konjacglucomannan	pH	Curcumin	Nano micelle	34.5%	83.9% at pH5,		---

Route	Material	Stimuli	Drug used	Dosage formulation	Loading efficiency	Release efficiency	Ref. #	Remarks
rout of Invasive						55.9% at pH7.4	[120]	
Alternative rout of Invasive	HPMAm-lac,PEG	Thermo	Daptomycin	Sol-gel	28 mg/mL	60%	[121]	---
Alternative rout of Invasive	Polyacrylamide grafted guar gum	pH	5-amino salicylic acid	tablet	20.8	35-55% in pH2 and pH7.2 55-75% in pH10.	[122]	---
Alternative rout of Invasive	Polyacrylamide grafted guar gum	pH	Triamcinolone	tablet	---	100% in pH7.2 90% in pH1.2	[123]	---
Alternative rout of Invasive	Polyacrylamide grafted guar gum	pH	Glimepiride	tablet	95.91%	95%	[124]	---
Alternative rout of Invasive	EGDMA based Gly/PNIPaam	pH, Temperature	5-ASA, Ornidazole	Sol-gel	~96–97%	53% release for Ornidazole 73% for 5-ASA	[125]	---

2.4 Gaps in Existing Research

From previous reviewed section, it is found that the biopolymer has a vital role as carrier in drug delivery applications. Drug delivery has been executed in different routes by polymeric formulations. The transdermal drug delivery is occurred by temperature and light triggering of polymer where as the oral delivery was realized by pH stimuli. But in these two delivery methods, the current research pointed out some gaps which are summarizes below:

1. Grafting of natural saccharide to synthetic polymer is an important step to modify the synthetic gel for improving its solvent encapsulation ability and biocompatibility. 100% grafting efficiency is expectable for synthesizing a good biopolymer whereas some researchers offered <100% grafting efficiency. For instances, Agüeros *et al.* [50] reported 91.3 ± 3.1% grafting efficiency, Sen *et al.* [122] reported the grafting efficiency 23%-58%, Shahid *et al.* [123] observed 22% to 55% grafting efficiency, Gowrav *et al.* [124] showed the grafting efficiency from 60.1%-84.3%. Zeng *et al.* [128] synthesized the microsphere with 20% grafting efficiency. The lower grafting efficiency signifies the possibilities to presence of synthetic monomers in the gel network. Therefore preparation of biopolymer with 100% grafting efficiency is needed to improve the solvent encapsulation capability and biocompatibility.

2. Polymerization with nontoxic solvents, develops a biocompatible polymer as drug delivery vehicle without toxication of drugs. Whereas most of the researchers used emulsion polymerization in drug delivery [37], [39], [48], [74], [85], [90], [95]-[97], [101], [102], [127], which occurs in presence of organic solvent like dichloromethane, chloroform and stabilizer. Organic solvents and stabilizer are toxic which are difficult to remove from synthesized polymer and make the polymer impure [129]. Stabilizer may react with encapsulated drug and makes the drug toxic [130]. Particle aggregation creates difficult physical handling in liquid and dry form [131]. So there is needed to replace the emulsion polymerization by thermally assisted bulk polymerization with aqueous or nontoxic chemicals to prepare polymeric drug vehicle.

3. Oral administered drugs could be instable in the variation of pH environment due to chemical reaction with gastric and intestinal acid as well as chemical cleavage in its structure. This reason creates low bioavailability of drug. To protect the drug from acid metabolism, the hydrogel as carrier material need to stable in gastrointestinal acid to prevent the acid degradation, burst release of drug from gel network and poor bioavailability which have not investigated in reported research [37], [39], [48], [49], [51], [52], [55] [126], [132]-[134]. Therefore, the acid stability investigation of the carrier polymer is an important to make the delivered drug more bioavailable in the targeted zone, which is one of investigating point in current research.

4. Antibiotics like Ciprofloxacin, Norfloxacin, Levofloxacin etc. have their thermal stability upto 30 °C. For that reason antibiotics are limited to be released by the reported thermosensitive hydrogels drug carrier [3], [62], [66], [74], [75], [80], [83], [86], [90], [92], [98], [104], [112], [121]. Because, the reported gels were deswelled above their phase transition temperature (say LCST) at 37 °C to release the drugs. Therefore to prevent the thermal degradation of antibiotics, replacement of the LCST based hydrogel by UCST based polymer which will deswell at below 30 °C for studying the antibiotics release profile is another aim of current research.

5. The drug encapsulation and release by stimuli activated hydrogels need to be done with controlled dose and on-demand basis which makes the delivery vehicle good patient compliance. But in reported pH and thermosensitive hydrogel [58], [60], [65], [67], [68], [71], [72], [88], [99]-[101], drug was encapsulated within the polymer during synthesis. The synthesized dry polymer released the drug in different temperature zone and/or pH zone by drug dissolution process. Therefore, on-demand encapsulation-release with controlled dose was limited. So it is need to utilize the stimuli responsivity of hydrogel, which could be able to intake and release the drugs based on the applied external stimulus and/or stimuli on-demand basis. This could overcome the encapsulation limitation of the drug into polymer network.

6. The reported hydrogel based transdermal patch [94], [99], [100] offered continuous drag transport from patch to skin even without applied stimuli. Continuous and uncontrollable drug release creates overdosing effect or some skin rash, which is

needed for further research to overcome. Therefore, present research is aimed to develop a stimuli responsive drug delivery vehicle which can offer a pulsatile volumetric expansion-contraction to encapsulate-release the drug.

7. The reported photoresponsive polymers involved stimulation of photosensitive chromophores by ultraviolet (UV) light [107], [116]. The chromophore salts are carcinogenic and UV is not safe for mammalian tissue, which may cause damage to biological samples and limit the biomedical applications. According to the discussions in previous reviewed section the visible light triggered drug delivery has not been investigated, which is the aim in current research.

8. In reported literatures [49], [50], [58], [63], [85], [90], [122]-[124], [126] mechanical shaker was used along with the external stimuli like temperature, pH and light for *in-vitro* drug delivery. Therefore it is debatable whether the drug was released by stimuli or mechanical vibration. Due to presence of mechanical vibrator, the whole system becamos bulky. So, the biopolymeric drug delivery vehicle excluding any role of external mechanical shaker will make the system simpler and more effective on stimuli. Hence, the development of stimuli responsive biopolymer and its investigational responses over the applied different external stimuli i.e pH, temperature, light are also an interesting aim in current research to eliminate the shaker functionality.

The above limitations on the existing researches on hydrogel based noninvasive drug delivery systems motivated us to develop such multi stimuli bio-material to overcome the challenges in reported formulations, transdermal as well as oral route administrations

2.5 Scope of Research

On the deliberate and extensive literature review, the stimuli responsive polymer has a wide spread application in biomedical application, especially in the field of drug delivery activities. Different external stimuli were reported for different drug release applications. Due to existence of some limitations on different biocompatible polymers, this thesis work is aimed for designing a natural biocompatible smart polymer for sensing, transducing and actuation for drug delivery purposes. Efficacy of designed biopolymer on different stimuli like medium pH, environmental temperature and visible light also aimed for investigation. Considering state of art after comprehensive literature review,

this research work briefly describe the scope of investigations on the following aspect of the issues for challenging in noninvasive drug delivery applications.

1 The gap in existence research, the limitation on grafting efficiency for gel synthesis can be overcome by using temperature assisted bulk polymerization, which can improve the yield of synthesized gel.

2 To avoid the polymer toxication by emulsion method this research is proposed the free radical bulk polymerization in aqueous medium. Further extensive purification by refluxing method can be implemented to remove the impurities like un-reacted monomers, cross linkers etc.

3 The acid degradation of oral administered drugs can be overcome by using a polymeric carrier. The carrier material should have acid stability so that it can protect the encapsulated drug from its degradation at the targeted location. The pH stability issue of drug carrying material can be evaluated by acid hydrolysis. This could fulfill the issues of oral administration.

4 Development of the low thermal volume phase transition based positive gel can overcome the issue of antibiotic release at the temperature above their thermal stability zone. By utilizing the positive nature to temperature the drug can be release by lowering the temperature.

5 To overcome the probability of solvent/drug toxication during synthesis and uncontrollable loading dose titration, this research work is aimed to develop a biocompatible hygrogel, which can entrap the solvent/drug in terms of its volume alteration by external stimuli like temperature, visible light.

6 This work is proposed to use the stimuli sensitive material as drug dispenser for transdermal delivery to control the drug release in pulsatile mode by applying and/ or off the stimuli on-demand. The elevated temperature will be supportive to control the dose of loaded drug. This could overcome the challenges of the transdermal delivery.

7 To avoid the use of usage of chromophores and UV light, this research work is proposed to develop the visible light sensitive polymer which is safe for mammalian tissue. In order to avoid the chromophore salt, gold nanoparticle reinforced (AuNP) polymer nanocomposite development is proposed.

8 This work is aimed to demonstrate the efficacy of the responsiveness of applied external stimuli for drug release to avoid the usage of mechanical apparatus. The

deswelling properties of synthesized gel with the applied stimuli are intended to demonstrate the release of drug to avoid any mechanical assistance. Another approach can be applied to avoid the mechanical shaker and that is the simultaneous application of pH and temperature on the polymer during drug release.

The existing research confirmed the bioactivity of the released drug by performing *in-vivo* testing on animals, while the current research confirmed the noninvasive bioactivity of release drug by performing in-vitro testing on bacteria and mouse breast cancer cell.

2.6 Methodology

A broad literature review was presented, on synthetic and semi-synthetic and/or biopolymer for invasive drug delivery applications. The reported researches exhibited some drawbacks which motivated us to prepare the scope of work. In the view of executing the objectives of work we have planned the pathway which is shown in below flow chart in crisp.

Material Selection:

Material selection and infrastructure development is the foremost and important step prior to start the thesis work. We will develop positive stimuli responsive hydrogels for drug delivery application. This thesis will be aimed for investigate the drug release efficacy through UCST and non UCST based positive hydrogel with low working temperature zone (10 °C to 40 °C). The nanoparticle (NP) reinforced positive nanocomposite will be prepared to make the photosensitive gel, The application of the polymer as non-invasive drug delivery will be confirmed by using ciprofloxacin and insulin as model drug. The detail on material selection and infrastructure development are described in Chapter 3.

Protocol Definition and Gel Synthesis:

In step 2, a proper gel synthesis protocol is designed, followed by the selection of the required base material. The free radical reaction mechanism is proposed for synthesis. The gel synthesis process will be carried out by means of defined synthesis protocol. The graft and interpenetrating networked polymer will be synthesized by following pre-

determined unit composition, decided in synthesis protocol. The detailing of synthesis protocol is described in Chapter 4.

Morphological Characterization and Analysis for Gel Formation:

The different characterizations will be done on both graft and interpenetrating networked polymer sample to understand the proper fabrication of synthesized gels. The data from characterization tools will be analyzed to investigate the correctness of synthesized gels according to our requirement. The chemical reaction synthesis process/activity may be modifying till getting the suitable gels, which will be confirmed by characterization tools. The detailing of characterization analysis is described in Chapter 4.

Functional Characterization of Polymer to Optimize User Condition:

After completion of characterization process on synthesized gels, the investigation of different responsive properties with different stimuli of synthesized gels will commence. To execute the analysis of responsivity, the experimentation on the equilibrium swelling (ES) studies and reversible shape/mass effect of gel on different external stimuli like variation of medium pH, environmental temperature, dual (combination of pH and temperature) and visible light will be performed. The experimental data is analysed to evaluate the efficiency of synthesized gels under different stimuli conditions for both activities (A) and (B). The variation pH of medium is selected as pH 4, pH 7 and pH 9.2. The experimental working temperature range kept at 10 °C to 40 °C as environmental temperature stimuli. The effects of different physical parameters of gel are also analyzed on the basis of experimental data. The detail of experimental activities and analysis are described in Chapter 5.

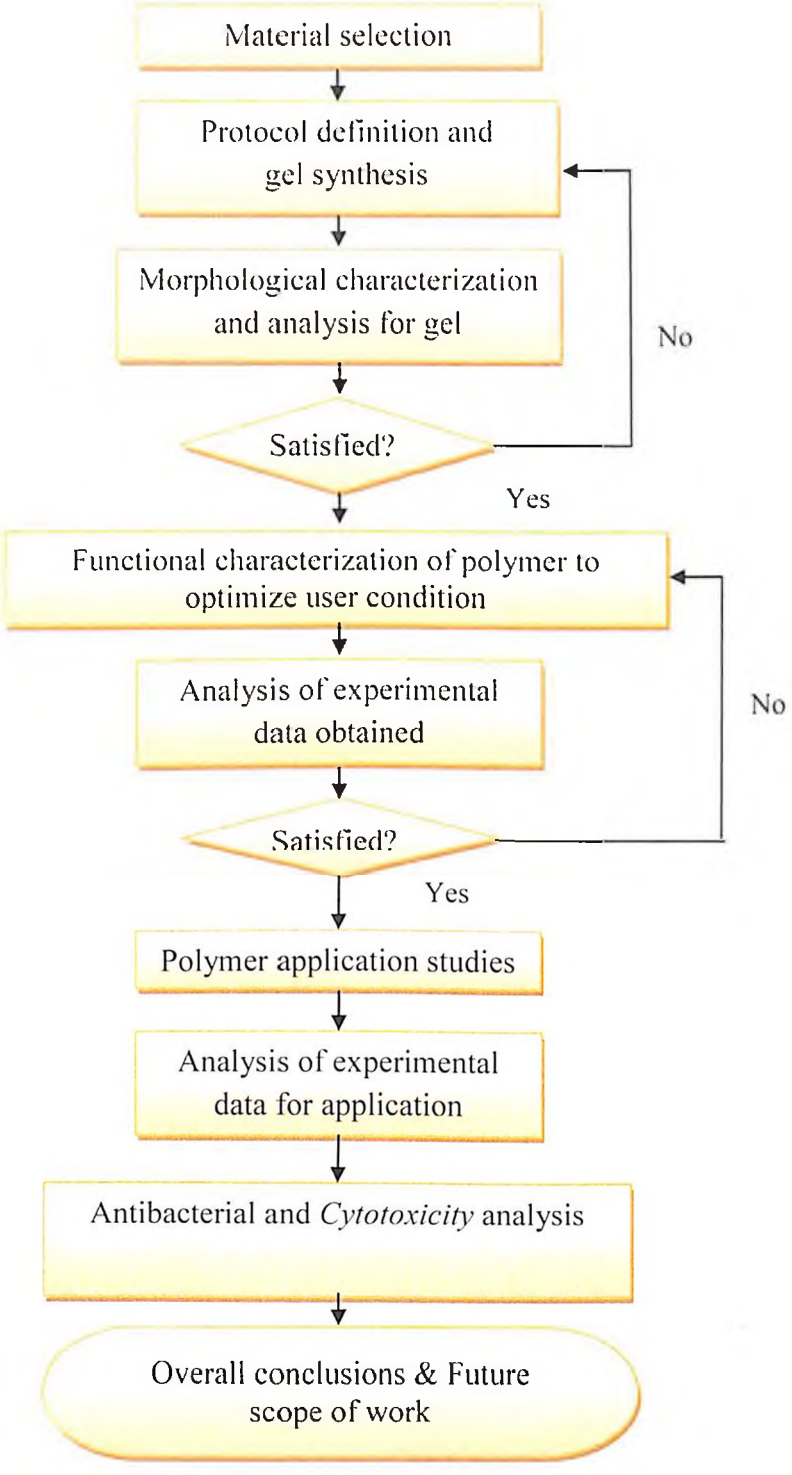

Scheme 1: Flow chart of thesis methodology

Polymer Application Studies:

The drug entrapment and release commotion were performed on graft and the best responsive double crosslinked gel samples under reverse pulsatile temperature stimuli phenomenon. The drug release activities under three specific stimuli cases: Case I- temperature assisted loading and releasing, Case II- temperature assisted loading and pH assisted releasing and Case III- visible light assisted loading and releasing. The loading and releasing kinetics were also investigated. The efficacy of the synthesized gel was also correlated with the possibility applicability on controlled and sustained drug delivery activities. The effects of different physical parameters of gel are also analyzed on the basis of experimental data. The detail of drug delivery efficacies are described in Chapter 6.

Antibacterial and *Cytotoxicity* Analysis:

The anti-bacterial and *cytotoxicity* testing are performed to check the bio-compatibility of the gel. The anti-bacterial studies are performed on both gram +ve and gram –ve bacteria. The cell viability experimentation will be carried out on 4T1 mouse breast cancer cell to demonstrate the *cytotoxicity* activities to confirm the biocompatibility of the gel. The detail procedure and analysis are described in Chapter 7.

Over all Conclusions and Future Scope of Work

Finally, the overall conclusions and the future scope of the work are discussed in Chapter 7.

References

[1] N. A. A. Khatera, O. A. Soliman, and E. A. Mohamed, '*In-Situ* Gelling Ophthalmic Formulations for Sustained Release and Enhanced Ocular Delivery of Fluconazole', *IOSR J. Pharm. Biol. Sci.*, vol. 11, no. 2, pp. 43–51, 2016.

[2] D. Mohanty, V. Bakshi, N. Simharaju, M. A. Haque, and C. K. Sahoo, 'A Review on in situ Gel: A Novel Drug Delivery System', *Int. J. Pharm. Rev. Res.*, vol. 50, no. 1, pp. 175–181, 2018.

[3] Z. Luo, L. Jin, L. Xu, Z. L. Zhang, J. Yu, S. Shi, X. Li, H. Chen 'Thermosensitive PEG – PCL – PEG (PECE) hydrogel as an in situ gelling system for ocular drug delivery of diclofenac sodium', *Drug Deliv.*, vol. 23, no. 1, pp. 63–68, 2016.

[4] A. Kant, S. Reddy, .M.M Shankraiah, J. . Venkatesh, and C. Nagesh, 'In Situ Gelling System - An Overview', *Pharmacologyonline*, vol. 2, pp. 28–44, 2011.

[5] T. R. Hoare and D. S. Kohane, 'Hydrogels in drug delivery: Progress and challenges', *Polymer (Guildf).*, vol. 49, no. 8, pp. 1993–2007, 2008.

[6] Y. Qiu and K. Park, 'Environment-sensitive hydrogels for drug delivery', *Adv. Drug Deliv. Rev.*, vol. 64, pp. 49–60, 2012.

[7] H. Almeida, M. H. Amaral, P. Loba, and M. S. Lobo, 'In situ gelling systems : a strategy to improve the bioavailability of ophthalmic pharmaceutical formulations', *Drug Discov. Today*, vol. 19, no. 4, pp. 400–412, 2014.

[8] S. R. Devasani, A. Dev, S. Rathod, and G. Deshmukh, 'An overview of in situ gelling systems', *Pharm. Biol. Eval.*, vol. 3, no. 1, pp. 60–69, 2016.

[9] J. V Crivello, 'A New Visible Light Sensitive Photoinitiator System for the Cationic Polymerization of Epoxides', *J. Polym. Sci. Part A Polym. Chem.*, vol. 47, no. November 2008, pp. 866–875, 2009.

[10] V. Delplace, P. Couvreur, and J. Nicolas, 'Polymer Chemistry Recent trends in the design of anticancer polymer prodrug nanocarriers', *Polym. Chem.*, vol. 5, pp. 1529–1544, 2014.

[11] J. K. Twibanire and T. B. Grindley, 'Polyester Dendrimers: Smart Carriers for Drug Delivery', *Polymers (Basel).*, vol. 6, no. 1, pp. 179–213, 2014.

[12] K. S. Soppimath, T. M. Aminabhavi, A. R. Kulkarni, and W. E. Rudzinski, 'Biodegradable polymeric nanoparticles as drug delivery devices', *J. Control. Release*, vol. 70, pp. 1–20, 2001.

[13] V. J. Mohanraj and Y. Chen, 'Nanoparticles – A Review', *Trop. J. Pharm. Researc*, vol. 5, no. 1, pp. 561–573, 2006.

[14] H. M. Redhead, S. S. Davis, and L. Illum, 'Drug delivery in poly (lactide-co-

glycolide) nanoparticles surface modified with poloxamer 407 and poloxamine 908 : in vitro characterisation and *in-vivo* evaluation', *J. Control. Release*, vol. 70, pp. 353–363, 2001.

[15] D. Heng, D. J. Cutler, H. Chan, J. Yun, and J. A. Raper, 'What is a Suitable Dissolution Method for Drug Nanoparticles ?', *Pharm. Res.*, vol. 25, no. 7, pp. 1696–1701, 2008.

[16] Q. Hu, P. S. Katti, Z. Gu, C. Hill, and C. Hill, 'Enzyme-Responsive Nanomaterials for Controlled Drug Delivery', *Nanoscale*, vol. 6, no. 21, pp. 12273–12286, 2015.

[17] A. Lavasanifar, J. Samuel, and G. S. Kwon, 'Poly (ethylene oxide) - block -poly (L -amino acid) micelles for drug delivery', *Adv. Drug Deliv. Rev.*, vol. 54, pp. 169–190, 2002.

[18] D. D. T. Vol and N. June, 'Targeted drug delivery systems for the intracellular delivery of macromolecular drugs', *Drug Discov. Today*, vol. 8, no. 11, pp. 2699–2700, 2003.

[19] S. Hua and S. Y. Wu, 'The use of lipid-based nanocarriers for targeted pain therapies', *Front. Pharmacol.*, vol. 4, no. November, pp. 1–7, 2013.

[20] S. Lee, O. Lee, T. V. O. Halloran, G. C. Schatz, S. T. Nguyen, and L. E. E. E. T. Al, 'Triggered Release of Pharmacophores Caged Nanobin Enhances Pro-apoptotic Activity : A Combined Experimental and Theoretical Study', *ACS Nano*, vol. 5, no. 5, pp. 3961–3969, 2011.

[21] D. S. Conceição, D. P. Ferreira, and L. F. Vieiraão, 'Photochemistry and Cytotoxicity Evaluation of Heptamethinecyanine Near Infrared (NIR) Dyes', *Int. J. Mol. Sci.*, vol. 14, no. 9, pp. 18557–18571, 2013.

[22] A. Yavlovich, B. Smith, K. Gupta, R. Blumenthal, and A. Puri, 'Light-sensitive Lipid-based Nanoparticles for Drug Delivery: Design Principles and Future Considerations for Biological Applications', *Mol. Membr. Biol.*, vol. 27, no. 7, pp. 364–381, 2011.

[23] K. Kono, T. Kaiden, E. Yuba, Y. Sakanishi, and A. Harada, 'Synthesis of oligo (ethylene glycol) -modified hyperbranched poly (glycidol) s for dual sensitization of liposomes to pH and temperature', *J. Taiwan Inst. Chem. Eng.*, vol. 45, no. 6, pp. 3054–3061, 2014.

[24] H. Cabral, Y. Matsumoto, K. Mizuno, Q. Chen, M. Murakami, M. Kimura, Y. Terada, M. R. Kano, K. Miyazono, M. Uesaka, N. Nishiyama, K. Kataoka 'Accumulation of sub-100 nm polymeric micelles in poorly permeable tumours depends on size', *Nat. Nanotechnol.*, vol. 6, no. 12, pp. 815–823, 2011.

[25] S. Rana, J. Bhattacharjee, K. C. Barick, G. Verma, P. A. Hassan, and J. V Yakhmi, *Chapter 7 - Interfacial engineering of nanoparticles for cancer*

therapeutics. Elsevier Inc., 2017.

[26] K. Kataoka, A. Harada, and Y. Nagasaki, 'Block copolymer micelles for drug delivery : design , characterization and biological significance', *Adv. Drug Deliv. Rev.*, vol. 47, pp. 113–131, 2001.

[27] W. Wang, P. C. L. Hui, E. Wat, F. S. F. Ng, C-W Kan, C. B. S. Lau, P-C Leung, 'Enhanced Transdermal Permeability via Constructing the Porous Structure of Poloxamer-Based Hydrogel', *Polymers (Basel).*, vol. 8, no. 406, pp. 1–16, 2016.

[28] X. X. Zhou, L. Jin, R. Q. Qi, and T. Ma, 'pH-responsive polymeric micelles self-assembled from amphiphilic copolymer modified with lipid used as doxorubicin delivery carriers', *R. Soc. Open Sci.*, vol. 5, no. 3, pp. 1–13, 2018.

[29] J. Cao, S. Huang, Y. Chen, S. Li, X. Li, D. Deng, Z. Qian, L. Tang, Y. Gu 'Near-infrared light-triggered micelles for fast controlled drug release in deep tissue', *Biomaterials*, vol. 34, no. 26, pp. 6272–6283, 2013.

[30] T. Garg, O. Singh, S. Arora, and R. S. R. Murthy, 'Scaffold : A Novel Carrier for Cell and Drug Delivery Scaffold : A Novel Carrier for Cell and Drug Delivery', *Crit. Rev. Ther. Drug Carr. Syst.*, vol. 29, no. 1, pp. 1–63, 2012.

[31] H. Lee, H. Mok, S. Lee, Y. Oh, and T. G. Park, 'Target-specific intracellular delivery of siRNA using degradable hyaluronic acid nanogels', *J. Control. Release 119*, vol. 119, no. 2, pp. 245–252, 2007.

[32] S. Sawada, Y. Sasaki, Y. Nomura, and K. Akiyoshi, 'Cyclodextrin-responsive artificial chaperone peroxidase nanogel as an for horseradish', *Colloid Polym. Sci.*, vol. 289, no. 5–6, pp. 685–691, 2011.

[33] L. G. Guerrero-Ramírеza, S. M. Nu˜no-Donlucas, L. C. Cesteros, and I. Katime, 'Smart copolymeric nanohydrogels : Synthesis , characterization and properties', *Mater. Chem. Phys.*, vol. 112, pp. 1088–1092, 2008.

[34] L. Xia, R. Xie, X. Ju, W. Wang, Q. Chen, and L. Chu, 'Nano-structured smart hydrogels with rapid response and high elasticity', *Nat. Commun.*, vol. 4, pp. 1–11, 2013.

[35] J. P. K. Tan, M. B. H. Tan, and M. K. C. Tam, 'Application of nanogel systems in the administration of local anesthetics', *Local Reg. Anesth.*, vol. 3, pp. 93–100, 2010.

[36] A. A. Nadezda Fomina, Jagadis Sankaranarayanan, 'Photochemical mechanisms of light-triggered release from nanocarriers', *Adv Drug Deliv Rev*, vol. 64, no. 11, pp. 1005–1020, 2012.

[37] E. Chuang, K-J Lin, F-Y Su, F-L. Mi, B. Maiti, C-T. Chen, S-P. Wey, T-C. Yen, J-H. Juang, H-W. Sung 'Noninvasive imaging oral absorption of insulin delivered by nanoparticles and its stimulated glucose utilization in controlling postprandial

hyperglycemia during OGTT in diabetic rats', *J. Control. Release*, vol. 172, no. 2, pp. 513–522, 2013.

[38] R. Fuller, 'Probiotics in man and animals', *J. Appl. Bacteriol.*, vol. 66, pp. 365–378, 1989.

[39] L. Mei, F. He, R-Q. Zhou, C-D. Wu, R. Liang, R. Xie, X-J. Ju, W. Wang, L.-Y. Chu, 'Novel Intestinal-Targeted Ca-Alginate-Based Carrier for pH- Responsive Protection and Release of Lactic Acid Bacteria', *ACS Appl. Mater. Interfaces*, vol. 6, pp. 5962–5970, 2014.

[40] D. Zhao, X. Shi, T. Liu, X. Lu, G. Qiu, and K. J. Shea, 'Synthesis of surfactant-free hydroxypropyl methylcellulose nanogels for controlled release of insulin &', *Carbohydr. Polym.*, vol. 151, pp. 1006–1011, 2016.

[41] D. A. Norris, N. Puri, and P. J. Sinko, 'The effect of physical barriers and properties on the oral absorption of particulates', *Adv. Drug Deliv. Rev.*, vol. 34, pp. 135–154, 1998.

[42] V. J, 'Cancer Nanomedicine', *Nano*, vol. 6, no. 9, pp. 2166–2171, 2008.

[43] X. Zhou, Yang Zhao,†,§ Siyu Chen,† Songling Han,† Xiaoqiu Xu,† Jiawei Guo,† Mengyu Liu,† Ling Che,‖ Xiaohui Li,*,‡ and Jianxiang Zhang, 'Self-Assembly of pH-Responsive Microspheres for Intestinal Delivery of Diverse Lipophilic Therapeutics', vol. 17, pp. 2540–2545, 2016.

[44] L. Zhan, Z. Zeng, C. Hu, S. L. Bellis, W. Yang, Y. Su, X. Zhang, Y. Wu 'Controlled and targeted release of antigens by intelligent shell for improving applicability of oral vaccines', *Biomaterials*, vol. 77, pp. 307–319, 2016.

[45] J. H. Hamman, G. M. Enslin, and A. F. Kotzé, 'Oral Delivery of Peptide Drugs', *BioDrugs*, vol. 19, no. 3, pp. 165–177, 2005.

[46] E. S. Lee, K. Na, and Y. H. Bae, 'Polymeric micelle for tumor pH and folate-mediated targeting', *J. Control. Release*, vol. 91, no. 1–2, pp. 103–113, 2003.

[47] P. N. A. Koetting M C, 'pH responsive and Enzymetically responsive', vol. 91, no. 2, pp. 165–171, 2015.

[48] J. M. Knipe, L. E. Strong, and N. A. Peppas, 'Enzyme- and pH-Responsive Microencapsulated Nanogels for Oral Delivery of siRNA to Induce TNF - α Knockdown in the Intestine', 2016.

[49] J. Huarte, S. Espuelas, Y. Lai, B. He, J. Tang, and J. M. Irache, 'Oral delivery of camptothecin using cyclodextrin / poly (anhydride) nanoparticles', *Int. J. Pharm.*, vol. 506, pp. 116–128, 2016.

[50] M. Agüeros, L. Ruiz-Gatóna, C. Vauthier b, K. Bouchemal b, S. Espuelas a, G. Ponchel b, J.M. Irache 'Combined hydroxypropyl- β -cyclodextrin and poly (anhydride) nanoparticles improve the oral permeability of paclitaxel', *Eur. J.*

Pharm. Sci., vol. 38, pp. 405–413, 2009.

[51] R. Boppana, R. V Kulkarni, G. K. Mohan, S. Mutalik, and T. M. Aminabhavi, 'RSC Advances *In- vitro* and *in- vivo* assessment of novel pH- sensitive interpenetrating polymer networks of a graft copolymer for gastro-protective delivery of', *RSC Adv.*, vol. 6, pp. 64344–64356, 2016.

[52] X. Chen, J. Chen, B Li, X. Y, R. Zeng, Y. Liu, T. Li, R. J.Y. Ho, J. Shao, 'PLGA-PEG-PLGA triblock copolymeric micelles as oral drug delivery system : In vitro drug release and *in- vivo* pharmacokinetics assessment', *J. Colloid Interface Sci.*, vol. 490, pp. 542–552, 2017.

[53] A. De Prisco and G. Mauriello, 'Probiotication of foods: A focus on microencapsulation tool', *Trends Food Sci. Technol.*, vol. 48, pp. 27–39, 2016.

[54] H. Zheng, M. Gao, Y. Ren, R. Lou, H. Xie, W. Yu, X. Liu, X. Ma, 'An improved pH-responsive carrier based on EDTA-Ca-alginate for oral delivery of Lactobacillus rhamnosus ATCC 53103', *Carbohydr. Polym.*, vol. 155, pp. 329–335, 2017.

[55] A. J. Sami, M. Khalid, T. Jamil, S. Aftab, S. A. Mangat, A.R. Shakoori, S. Iqbal, 'Formulation of novel chitosan guargum based hydrogels for sustained drug release of paracetamol', *Int. J. Biol. Macromol.*, vol. 108, pp. 324–332, 2018.

[56] Y. Octavia, C. G. Tocchetti, K. L. Gabrielson, S. Janssens, H. J. Crijns, and A. L. Moens, 'Doxorubicin-induced cardiomyopathy: From molecular mechanisms to therapeutic strategies', *J. Mol. Cell. Cardiol.*, vol. 52, no. 6, pp. 1213–1225, 2012.

[57] S. Biswas, F. Deshpande, Pranali P. Perche, N. S. Dodwadkar, and V. P. Sane, Shailendra D. Torchilin, 'Octa-Arginine-Modified Pegylated Liposomal Doxorubicin: An Effective Treatment Strategy for Non-Small Cell Lung Cancer', *Cancer Lett.*, vol. 335, no. 1, pp. 191–200, 2013.

[58] A. Chen, C. Zhao, S. Wang, Y. Liu, and D. Lin, 'Generation of porous poly-L-lactide microspheres by emulsion-combined precipitation with a compressed CO2 antisolvent process', *J. Mater. Chem. B*, vol. 1, pp. 2967–2975, 2013.

[59] E. Secret, S. J. Kelly, K. E. Crannell, and J. S. Andrew, 'Enzyme-Responsive Hydrogel Microparticles for Pulmonary Drug Delivery', *ACS Appl. Mater. Interfaces*, vol. 6, pp. 10313–10321, 2014.

[60] J. Du, I. M. El-sherbiny, and H. D. Smyth, 'Swellable Ciprofloxacin-Loaded Nano-in-Micro Hydrogel Particles for Local Lung Drug Delivery', *AAPS PharmSciTech*, vol. 15, no. 6, pp. 1535–1544, 2014.

[61] S. R. Mane, K. Chatterjee, H. Dinda, J. Das Sarma, and R. Shunmugam, 'Stimuli responsive nanocarrier for an effective delivery of multi-frontline tuberculosis drugs', *Polym. Chem.*, vol. 5, no. 12, pp. 2725–2735, 2014.

[62] R. S. Lee, C. H. Lin, I. A. Aljuffali, K. Y. Hu, and J. Y. Fang, 'Passive targeting of thermosensitive diblock copolymer micelles to the lungs: Synthesis and characterization of poly(N-isopropylacrylamide)-block-poly(ε-caprolactone)', *J. Nanobiotechnology*, vol. 13, no. 1, pp. 1–12, 2015.

[63] Y. Gao, M. Chang, Z. Ahmad, and J. Li, 'Magnetic-responsive microparticles with customized porosity for drug delivery', *RSC Adv.*, vol. 6, no. 9, pp. 88157–88167, 2016.

[64] C. Xu, H. Tian, P. Wang, Y. Wang, and X. Chen, 'The suppression of metastatic lung cancer by pulmonary administration of polymer nanoparticles for co-delivery of doxorubicin and Survivin siRNA', *Biomater. Sci.*, vol. 4, no. 11, pp. 1646–1654, 2016.

[65] G. A. Islan, M. E. Ruiz, J. F. Morales, M. L. Sbaraglini, A. V. Enrique, G. Burton, A. Talevi, L. E. Bruno-Blanchc, G. R. Castro 'Hybrid inhalable microparticles for dual controlled release of levofloxacin and DNase: physicochemical characterization and *in- vivo* targeted delivery to the lungs', *J. Mater. Chamistry B*, vol. 5, pp. 3132–3144, 2017.

[66] M. Gregoritza, V. Messmann, K. Abstiens, F. P. Brandl, and A. M. Goepferich, 'Controlled Antibody Release from Degradable Thermoresponsive Hydrogels Cross-Linked by Diels – Alder Chemistry', *Biomacromolecules*, vol. 18, pp. 2410–2418, 2017.

[67] G. Kim, C. Piao, J. Oh, and M. Lee, 'Self-assembled polymeric micelles for combined delivery of anti-inflammatory gene and drug to the lungs by inhalation', *Nanoscale*, vol. 10, no. 4, pp. 8503–8514, 2018.

[68] C. Cheng, X. Zhang, J. Xiang, Y. Wang, C. Zheng, Z. Lu and C. Li, 'Development of novel self-assembled poly(3-acrylamidophenylboronic acid)/ poly(2-lactobionamidoethyl methacrylate) hybrid nanoparticles for improving nasal adsorption of insulin', *Soft Matter*, vol. 8, no. 3, pp. 765–773, 2012.

[69] H. Nazar, P. Caliceti, B. Carpenter, A. I. El-Mallah, D. G. Fatouros, M. Roldo, S. M. van der Merwea and J. Tsibouklisa 'A once-a-day dosage form for the delivery of insulin through the nasal route: in vitro assessment and *in- vivo* evaluation', *Biomater. Sci.*, vol. 1, no. 3, pp. 306–314, 2013.

[70] R. A. Garc´ıa-Mu˜noz, V. Morales, M. Linares, P. E. Gonz´alez, R. Sanz, and D. P. Serrano, 'Influence of the structural and textural properties of ordered mesoporous materials and hierarchical zeolitic supports on the controlled release of methylprednisolone hemisuccinate', *J. Mater. Chamistry B*, vol. 2, no. 43, pp. 7996–8004, 2014.

[71] P. C. Bhatt, P. Srivastava, P. Pandey, W. Khan, and B. P. Panda, 'Nose to brain delivery of astaxanthin-loaded solid lipid nanoparticles: fabrication, radio labeling, optimization and biological studies', *RSC Adv.*, vol. 6, no. 12, pp.

10001–10010, 2016.

[72] S. K. Singh, P. Dadhania, P. R. Vuddanda, A. Jain, S. Velaga, and S. Singh, 'Intranasal delivery of asenapine loaded nanostructured lipid carriers: formulation, characterization, pharmacokinetic and behavioural assessment', *RSC Adv.*, vol. 6, no. 3, pp. 2032–2045, 2016.

[73] Z. Wang, P. Shan, S. Z. Li, Y. Zhou, X. Deng, J. L. Li, Y. Zhang, J. S. Gao, J. Xu, 'The mechanism of action of acid-soluble chitosan as an adjuvant in the formulation of nasally administered vaccine against HBV', *RSC Adv.*, vol. 6, no. 99, pp. 96785–96797, 2016.

[74] E. Ahmad, Y. Feng, J. Qi, W. Fan, Y. Ma, and H. He, 'Evidence of nose-to-brain delivery of nanoemulsions : cargoes but not vehicles', *Nanoscale*, vol. 9, no. 3, pp. 1174–1183, 2017.

[75] Y. Wang, S. Jiang, H. Wang, and H. Bie, 'A mucoadhesive , thermoreversible in situ nasal gel of geniposide for neurodegenerative diseases', *PLoS One*, vol. 12, no. 12, pp. 1–17, 2017.

[76] R. E. El-mekawy and R. S. Jassas, 'Recent trends in smart and flexible three-dimensional cross-linked polymers: synthesis of chitosan–ZnO nanocomposite hydrogels for insulin drug delivery', *MedChemComm Res. Artic. View*, vol. 8, no. 5, pp. 897–906, 2017.

[77] T. Tazaki, K. Tabata, A. Ainai, Y. Ohara, and S. Kobayashi, 'Shape-dependent adjuvanticity of nanoparticle- conjugated RNA adjuvants for intranasal inactivated influenza vaccines', *RSC Adv.*, vol. 8, no. 30, pp. 16527–16536, 2018.

[78] M. Bercea, L. E. Nita, S. Morariu, and A. Chiriac, '*In-situ* gelling system based on pluronic f127 and poly (vinyl alcohol) for smart biomaterials', *Rev. Roum. Chim.*, vol. 60, no. 7–8, pp. 787–795, 2015.

[79] Y. Edelby, S. Balaghi, and B. Senge, 'Flow and sol-gel behavior of two types of methylcellulose at various concentrations Flow and Sol-Gel Behavior of Two Types of Methylcellulose at Various Concentrations', *AIP Conf. Proc.*, vol. 1593, pp. 750–754, 2014.

[80] M. K. Bain, B. Bhowmick, D.Maity, D. Mondal, Md. M. R. Mollick, B. K. Paul, M. Bhowmik, D. Rana, D. Chattopadhyay 'Effect of PVA on the gel temperature of MC and release kinetics of KT from MC based ophthalmic formulations', *Int. J. Biol. Macromol.*, vol. 50, no. 3, pp. 565–572, 2012.

[81] H. Qi, W. Chen, C. Huang, L. Li, C. Chen, W. Li, C. Wu., 'Development of a poloxamer analogs / carbopol-based in situ gelling and mucoadhesive ophthalmic delivery system for puerarin', *Int. J. Pharm.*, vol. 337, pp. 178–187, 2007.

[82] M. Bhowmik, S. Das, D. Chattopadhyay, and L. K. Ghosh, 'Study of Thermo-Sensitive In-Situ Gels for Ocular Delivery', *Sci. Pharmaceitica*, vol. 79, pp. 351–

358, 2011.

[83] B. Bhowmick, G. Sarkar, D. Rana, I. Roy, N. R. Saha, S. Ghosh, M. Bhowmik, D. Chattopadhyay, 'Effect of xanthan gum and guar gum on in situ gelling ophthalmic drug delivery system based on poloxamer-407', *Int. J. Biol. Macromol.*, vol. 62, pp. 117–123, 2013.

[84] B. Bhowmick, G. Sarkar, D. Rana, I. Roy, N. R. Saha, S. Ghosh, M. Bhowmik, D. Chattopadhyay, 'Effect of carrageenan and potassium chloride on an in situ gelling ophthalmic drug delivery system based on methylcellulose', *RSC Adv.*, vol. 5, pp. 60386–60391, 2015.

[85] V. Pokharkar, V. Patil, and L. Mandpe, 'Engineering of polymer – surfactant nanoparticles of doxycycline hydrochloride for ocular drug delivery Engineering of polymer – surfactant nanoparticles of doxycycline hydrochloride for ocular drug delivery', *Drug Deliv.*, vol. 22, no. 4, pp. 955–968, 2015.

[86] S. Patil, A. Kadam, S. Bandgar, and S. Patil, 'Formulation and evaluation of an in situ gel for ocular drug delivery of anticonjunctival drug', *Cellul. Chem. Technol.*, vol. 49, no. 1, pp. 35–40, 2015.

[87] N. Malakooti, C. Alexander, and C. Alvarez-lorenzo, 'Imprinted Contact Lenses for Sustained Release of Polymyxin B and Related Antimicrobial Peptides', *J. Pharm. Sci.*, vol. 104, no. 10, pp. 3386–3394, 2015.

[88] D. Lee, S. Cho, H. S. Park, and I. Kwon, 'Ocular Drug Delivery through pHEMA-Hydrogel Contact Lenses Co-Loaded with Lipophilic Vitamins', *Nat. Publ. Gr.*, vol. 6, no. July, pp. 1–8, 2016.

[89] Z. Luo, L. Jin, L. Xu, Z. L. Zhang, J. Yu, S. Shi, X. Li, H. Chen., 'Thermosensitive PEG-PCL-PEG (PECE) hydrogel as an in situ gelling system for ocular drug delivery of diclofenac sodium', *Drug Deliv.*, vol. 23, no. 1, pp. 63–68, 2016.

[90] Z. Zhang, Z. He, R. Liang, Y. Ma, W. Huang, R. Jiang, S. Shi, H. Chen, X. Li 'Fabrication of a Micellar Supramolecular Hydrogel for Ocular Drug Delivery', *Biomacromolecules*, vol. 17, pp. 798–807, 2016.

[91] J. C. Keister, E. R. Cooper, P. J. Missel, J. C. Lang, and D. F. Hager, 'Limits on Optimizing Ocular Drug Delivery', *Am. Pharm. Assoc.*, vol. 80, no. 1, pp. 1989–1992, 1991.

[92] S. Deepthi and J. Jose, 'Novel hydrogel-based ocular drug delivery system for the treatment of conjunctivitis', *Int. Opthalmology*, pp. 1–12, 2018.

[93] M. Kabiri, S. H. Kamal, S. V. Pawar, P. R. Roy, M. Derakhshandeh, U. Kumar, S. G. Hatzikiriakos, S. Hossain, V. G. Yadav, 'A stimulus-responsive, in situ-forming, nanoparticle-laden hydrogel for ocular drug delivery', *Drug Delivbery Transl. Res.*, vol. 8, pp. 484–495, 2018.

[94] P. Maji, A. Gandhi, S. Jana, and N. Maji, 'Preparation and Characterization of Maleic Anhydride Cross-Linked Chitosan-Polyvinyl Alcohol Hydrogel Matrix Transdermal Patch', *J. PharmaSciTech*, vol. 2, no. 2, pp. 62–67, 2013.

[95] R. Arora, G. Aggarwal, S. L. Harikumar, and K. Kaur, 'Nanoemulsion Based Hydrogel for Enhanced Transdermal Delivery of Ketoprofen', *Adv. Pharm.*, vol. 2014, pp. 1–12, 2014.

[96] B. Dhawan, G. Aggarwal, and S. L. Harikumar, 'Enhanced transdermal permeability of piroxicam through novel nanoemulgel formulation', *Int. J. Pharm. Investig.*, vol. 4, no. 2, pp. 65–76, 2014.

[97] H. Ferreira, A. Ribeiro, and R. Silva, 'Deformable Liposomes for the Transdermal Delivery of Piroxicam', *J. Pharm. Drug Deliv. Res.*, vol. 4, no. 4, pp. 1–6, 2015.

[98] W. Wang, E. Wat, P. C. L. Hui, B. Chan, F. S. F. Ng, C. W. Kan, X. Wang, H. Hu, E. C.W.Wong, C. B. S. Lau, P. C. Leung, 'Dual-functional transdermal drug delivery system with controllable drug loading based on thermosensitive poloxamer hydrogel for atopic dermatitis treatment', *Sci. Rep.*, vol. 6, pp. 1–10, 2016.

[99] G. Sarkar, J. T. Orasugh, N. R. Saha, I. Roy, A. Bhattacharyya, A. K. Chattopadhyay, D. Ranad, D. Chattopadhyay 'Cellulose nanofibrils/chitosan based transdermal drug delivery vehicle for controlled release of ketorolac tromethamine Gunjan', *New J. Chem.*, vol. 41, no. 24, pp. 15312–15319, 2017.

[100] Z. Gu and J. Wu, 'Poly(ester amide)-based hybrid hydrogels for efficient transdermal insulin delivery', *J. Mater. Chamistry B*, vol. 6, no. 42, pp. 6723–6730, 2018.

[101] T. Jiang, T. Wang, T. Li, S. Shen, B. He, and R. Mo, 'Cite This: ACS Nano 2018, 12, 9693−9701 www.acsnano.org Enhanced Transdermal Drug Delivery by Transfersome-Embedded Oligopeptide Hydrogel for Topical Chemotherapy of Melanoma', *ACS Nano*, vol. 12, no. 10, pp. 9693–9701, 2018.

[102] Q. Maimoona, A. Naveed, S. Fakhara, K. Samiullah, and R. Asim, 'Development of Novel pH-sensitive Nanoparticles Loaded Hydrogel for Transdermal Drug Delivery', *Drug Dev. Ind. Pharm.*, vol. 45, no. 4, pp. 1–15, 2019.

[103] H. Yamauchi and Y. Maeda, 'LCST and UCST behavior of poly(N-isopropylacrylamide) in DMSO/water mixed solvents studied by IR and micro-raman spectroscopy', *J. Phys. Chem. B*, vol. 111, no. 45, pp. 12964–12968, 2007.

[104] S. B. Turturro, M. J. Guthrie, A. A. Appel, P. W. Drapala, E. M. Brey, V. H. Pérez-Luna, W. F. Mieler, J. J. Kang-Mieler, 'The effects of cross-linked thermo-responsive PNIPAAm-based hydrogel injection on retinal function', *Biomaterials*, vol. 32, no. 14, pp. 3620–3626, 2011.

[105] T. Lammers, F. Kiessling, W. E. Hennink, and G. Storm, 'Nanotheranostics and

Image-Guided Drug Delivery: Current Concepts and Future Directions', *Mol. Pharm.*, vol. 7, no. 6, pp. 1899–1912, 2010.

[106] S. J. Lee, , H. Koo, H. Jeong, M. S. Huh, Y. Choi, S. Y. Jeong, Y. Byun, K. Choi, K. Kim, I. C. Kwon 'Comparative study of photosensitizer loaded and conjugated glycol chitosan nanoparticles for cancer therapy', *J. Control. Release*, vol. 152, no. 1, pp. 21–29, 2011.

[107] H. Y. Yoon, H. Koo, K. Y. Choi, I. C. Kwon, K. Choi, J. H. Park, K. Kim, 'Photo-crosslinked hyaluronic acid nanoparticles with improved stability for *in-vivo* tumor-targeted drug delivery', *Biomaterials*, vol. 34, pp. 5273–5280, 2013.

[108] M. C. Cochran, J. Eisenbrey, R. O. Ouma, M. Soulen, and M. A. Wheatley, 'Doxorubicin and paclitaxel loaded microbubbles for ultrasound triggered drug delivery', *Int. J. Pharm.*, vol. 414, pp. 161–170, 2011.

[109] E. Ruoslahti, S. N. Bhatia, and M. J. Sailor, 'Targeting of drugs and nanoparticles to tumors', *J. Cell Biol.*, vol. 188, no. 6, pp. 759–768, 2010.

[110] L. Ye, Z. Gao, Y. Zhou, X. Yin, X. Zhang, A. Zhang, Z. Feng., 'A pH-sensitive binary drug delivery system based on poly (caprolactone)– heparin conjugates', *Soc. biometerials*, vol. 102A, no. 3, pp. 880–889, 2013.

[111] Y. Zhang, C. Gao, X. Li, C. Xu, Y. Zhang, Z. Sun,Y. Liu, J. Gao, 'Thermosensitive methyl cellulose-based injectable hydrogels for post-operation anti-adhesion', *Carbohydr. Polym.*, vol. 101, pp. 171–178, 2014.

[112] F. Din, R. Rashid, O. Mustapha, D. W. Kim, J. H. Park, S. K. Ku, Y. K. Oh, J. O. Kim, Y. S. Youn, C. S. Yong, H. G. Choi, 'Development of a novel solid lipid nanoparticles loaded dual-reverse thermosensitive nanomicelle release and reduced toxicity', *RSC Adv.*, vol. 5, pp. 43687–43694, 2015.

[113] K. Zhang, X. Shi, X. Lin, C. Yao, L. Shen, and Y. Feng, 'Poloxamer-based in situ hydrogels for controlled delivery of hydrophilic macromolecules after intramuscular injection in rats', *Drug Deliv.*, vol. 22, no. 3, pp. 375–382, 2015.

[114] J. Sun and H. Tan, 'Alginate-Based Biomaterials for Regenerative Medicine Applications', *Materials (Basel).*, vol. 6, pp. 1285–1309, 2013.

[115] H. Izawa, K. Kawakami, M. Sumita, Y. Tateyama, J. P. Hill, and K. Ariga, 'b-Cyclodextrin-crosslinked alginate gel for patient-controlled drug delivery systems: regulation of host–guest interactions with mechanical stimuli† Hironori', *J. Mater. Chem. B*, vol. 1, pp. 2155–2161, 2013.

[116] C. Chiang and C. Chu, 'Synthesis of photoresponsive hybrid alginate hydrogel with photo-controlled release behavior', vol. 119, pp. 18–25, 2015.

[117] Q. Zeng, Y. Han, H. Li, and J. Chang, 'Design of a thermosensitive bioglass/agarose–alginate composite hydrogel for chronic wound', *J. Mater.*

Chem. B, vol. 3, pp. 8856–8864, 2015.

[118] Z. Bao, C. Jiang, Z. Wang, Q. Ji, G. Sun, S. Bi,Y. Liu, X. Chen, 'The influence of solvent formulations on thermosensitive hydroxybutyl chitosan hydrogel as a potential delivery matrix for cell therapy', *Carbohydr. Polym.*, vol. 170, pp. 80–88, 2017.

[119] L. Wang, B. Li, F. Xu, Z. Xu, D. Wei, Y. Feng, Y. Wang, D. Jia, Y. Zhou, 'UV-crosslinkable and thermo-responsive chitosan hybrid hydrogel for NIR-triggered localized on-demand drug delivery', *Carbohydr. Polym.*, vol. 174, pp. 904–914, 2017.

[120] J. Luan, K. Wu, C. Li, J. Liu, X. Ni, M. Xiao, Y. Xu, Y. Kuang, F. Jiang, 'pH-Sensitive drug delivery system based on hydrophobic modified konjac glucomannan', *Carbohydr. Polym.*, vol. 171, pp. 9–17, 2017.

[121] C. Casadidio, M. Eugenia, A. Trampuz, M. Di, R. Censi, and P. Di, 'Daptomycin-loaded biodegradable thermosensitive hydrogels enhance drug stability and foster bactericidal activity against Staphylococcus aureus', *Eur. J. Pharm. Biopharm.*, vol. 130, pp. 260–271, 2018.

[122] G. Sen, S. Mishra, U. Jha, and S. Pal, 'Microwave initiated synthesis of polyacrylamide grafted guar gum (GG-g-PAM)— Characterizations and application as matrix for controlled release of 5-amino salicylic acid', *Int. J. Biol. Macromol.*, vol. 47, no. 2, pp. 164–170, 2010.

[123] M. Shahid, S. A. Bukhari, Y. Gul, H. Munir, F. Anjum, M. Zuber, T. Jamil, K. M.Zia 'Graft polymerization of guar gum with acryl amide irradiated by microwaves for colonic drug delivery', *Int. J. Biol. Macromol.*, vol. 62, pp. 172–179, 2013.

[124] M. P. Gowrav, U. Hani, H. G. Shivakumar, R. A. M. Osmani, and A. Srivastava, 'Polyacrylamide grafted guar gum based glimepiride loaded pH sensitive pellets for colon specific drug delivery: Fabrication and characterization', *RSC Adv.*, vol. 5, no. 97, pp. 80005–80013, 2015.

[125] P. Patra, A. P. Rameshbabu, D. Das, S. Dhara, A. B. Panda, and S. Pal, 'Stimuli-responsive, biocompatible hydrogel derived from glycogen and poly(: N - isopropylacrylamide) for colon targeted delivery of ornidazole and 5-amino salicylic acid', *Polym. Chem.*, vol. 7, no. 34, pp. 5426–5435, 2016.

[126] D. Zhao, X. Shi, T. Liu, X. Lu, G. Qiu, and K. J. Shea, 'Synthesis of surfactant-free hydroxypropyl methylcellulose nanogels for controlled release of insulin, *Carbohydr. Polym.*, vol. 151, pp. 1006–1011, 2016.

[127] W. Y. Wang, P. C. L. Hui, E. Wat, F. S. F. Ng, C-W Kan, C. B. S. Lau, and P.-C. Leu 'Enhanced transdermal permeability via constructing the porous structure of poloxamer-based hydrogel', *Polymers (Basel).*, vol. 8, no. 11, 2016.

[128] J. Zeng, H. Huang, S. Liu, H. Xu, J. Huang, and J. Yu, 'Hollow nanosphere fabricated from beta-cyclodextrin-grafted alpha, beta-poly(aspartic acid) as the carrier of camptothecin', *Colloids Surfaces B Biointerfaces*, vol. 105, pp. 120–127, 2013.

[129] P. Ahlin Grabnar and J. Kristl, 'The manufacturing techniques of drug-loaded polymeric nanoparticles from preformed polymers', *J. Microencapsul.*, vol. 28, no. 4, pp. 323–335, 2011.

[130] J. M. Irache, L. Bergougnoux, I. Ezpeleta, J. Gueguen, and A. M. Orecchioni, 'Optimization and in vitro stability of legumin nanoparticles obtained by a coacervation method', *Int. J. Pharm.*, vol. 126, no. 1–2, pp. 103–109, 1995.

[131] N. Jawahar and M. Sn, 'Polymeric nanoparticles for drug delivery and targeting : A comprehensive review', *Int. J. Heal. Allied Sci.*, vol. 1, no. 4, pp. 217–223, 2012.

[132] X. Zhou, Y. Zhao, S. Chen, S. Han, X. Xu, J. Guo, M. Liu, L. Che, X. Li, J. Zhang, 'Self-assembly of pH-responsive microspheres for intestinal delivery of diverse lipophilic therapeutics', *Biomacromolecules*, vol. 17, no. 8, pp. 2540–2554, 2016.

[133] L. Zhang, Z. Zeng, C. Hu, S. L. Bellis,W. Yang, Y. Su, X. Zhang, Y. W, 'Controlled and targeted release of antigens by intelligent shell for improving applicability of oral vaccines', *Biomaterials*, vol. 77, pp. 307–319, 2016.

[134] H. Zheng, M. Gao, Y. Ren, R. Lou, H. Xie, W. Yu, X. Liu, X. Ma., 'An improved pH-responsive carrier based on EDTA-Ca-alginate for oral delivery of Lactobacillus rhamnosus ATCC 53103', vol. 155, pp. 329–335, 2017.

Chapter 3

Material Selection

This chapter contains the selection of raw materials for hydrogels synthesis. For fulfillment of material selection criterion based on our aim (as described in Section 2.4 and 2.5), the responsiveness and type of polymer towards applied external stimuli with justification is discussed here. Selection of polymerization assisted materials is also conferred in this chapter.

3.1 Introduction

In Chapter 2, it has been discussed that this research is aimed to overcome the gaps in existing researches, by a non-invasive drug delivery system with stimuli triggered biopolymer based drug dispenser. This research work developed such biomaterial, in which the stimuli sensitive synthetic material was modified with natural saccharide. The aim of resulting biomaterial was to load the solvent and/or therapeutic with increasing intensity of applied stimuli and to release the loaded solvent and/or therapeutic agent by lowering the intensity of stimuli. This kind of polymer termed as positive hydrogel. The positive stimuli triggering help to control the loading-releasing dose of the therapeutic cargo, which makes the material patient compatible and patient, will be able to load and release the drug according to on-demand basis with prescribed dose. For drug delivery, a biopolymer should be biocompatible, chemically stable and highly porous. This chapter is selecting the raw materials based on our demands.

3.2 Selection of Material

The proposed positive hydrogel have been divided into two categories and they are Upper Volume Phase Transition Temperature (UVPTT) based hydrogel and Non-Upper Volume Phase Transition Temperature (Non-UVPTT) based hydrogel. pH, temperature and light were used as external stimuli because, pH is assumed as physiological stimuli and moreover temperature and light are such kind of stimuli which don't affect the self pH of therapeutic cargo. The acidic (pH 4), neutral (pH 7) and basic (pH 9.2) buffer mediums were used as pH stimuli. The experimental temperature was ranged from 10 °C

to 40 °C. The way of choosing materials as ingredients of the hydrogel is described in the subsequent sections. The selection of raw material is the prime step prior to synthesis of polymer. This research is aimed to develop positive stimuli responsive hydrogels to investigate the drug release efficacy through UVPTT and non-UVPTT based positive hydrogel with low working temperature zone (10 °C to 40 °C).

3.2.1 Upper Volume Phase Transition Temperature(UVPTT) based Hydrogel

UVPTT hydrogel offers a volume phase transition temperature (VPTT) at 32 °C-37 °C for which the polymer exhibits swelling-deswelling transition. Above the VPTT, polymer swells and below VPTT, polymer deswells. Co-polymer of acrylamide and acrylic acid (Paam-*co*-Paac) is well known UVPTT based polymer which forms intermolecular complexes via hydrogen bonding at temperatures lower than the VPTT with deswelling state, whereas hydrogen bond dissociates at temperatures higher than the VPTT with swelling state. Paam-*co*-Paac is superabsorbent hydrogels [1] with fast swelling-deswelling as well as pH and temperature sensitive. Zhou *et al.* [2] has reported the pH sensitive Paam-*co*-Paac where the drug loaded dry gel was placed in different pH solvent and drug release was increased in higher pH than lower one because of more swelling in higher pH. When the drug loaded dry hydrogel was immersed in pH solvents due to more swelling in elevated pH, more quantity of drug was diffused out or drug dissolution was more than low pH. This work motivated us to use Paam-*co*-Paac for stimuli responsive positive release of drug i.e swelling in high pH and or temperature and releasing at low pH and or temperature. Shirakura *et al.* [3] and Alvarado *et al.* [4] prepared Paam-*co*-Paac nanoparticle with 37 °C UVPTT for releasing of chemotherapeutic agent. The polymer nanoparticle swelled at high pH and temperature but shrank at low pH and temperature. These examples motivated us to utilize the positive stimuli responsive property of Paam-*co*-Paac at saccharide backbone. Therefore to develop a UVPTT based biohydrogel, the selection of saccharide was executed.

In literature review chapter, it was observed that, the polysaccharides are provided many plus points to modified semi-synthetic and or biopolymer but individually they exhibit some limitations, which hampers the drug release efficiency. For instances: (i) chitosan is mostly used polysaccharide in drug delivery field, for its non-toxic, biocompatible, biodegradable nature, mucoadhesive and permeation enhancing properties. But it suffers from limited solubility at physiological pH and causes first pass metabolism of drugs in

intestinal and gastric fluids in the presence of proteolytic enzymes [5]. (ii) Sodium alginate (NaAl) is a hydrophilic, nontoxic in nature, orally administrable and also acts as protective layer on upper gastrointestinal mucous membrane but the derivative of alginate gel with chitosan, erodes slowly in pH 6.8 which leads to suppress the drug release rate [6]. Porous structure of alginate gel exhibits fast release pattern of incorporated drugs which is not suitable for sustained drug release. Also NaAl has very low encapsulation capability of the drug with low molar weight [7]. (iii) Carrageenan gum is not suitable for sufficient sustained release due to rigid structure and limited exdiffusion [8]. (iv) The increasing amount of gum acacia diminishes the rate of drug release [9] from the pellet. Due to these limitations of macromolecular polysachharide, the cyclodextrin (CD) is another macromolecular complexation [10] has been explored became the matter of interest. CDs are cone shaped cyclic oligosaccharides of glucopyranose, with hydrophobic central cavity and hydrophilic outer surface [11], [12], produced by enzymatic degradation of starch. Due to the molecular structure and shape (Fig. 3.1), CD acts as molecular host chest by entrapping hydrophobic guest molecules in their internal cavity. The parent CDs consist of 6, 7 or 8 glucopyranose units and are referred to as alpha, beta and gamma CD, respectively [13], [14]. The cone shaped 3D CD molecule has two opening faces called primary and secondary face (Fig. 3.2). The hydroxyl groups are attached at the C_2 and C_3 positions of the glucopyranose unit at wide secondary opening called secondary hydroxyl group where as the narrow primary narrow face consists of hydroxyl groups at C_6 positions of the glucopyranose unit called primary hydroxyl groups. In drug delivery field, CDs have some advantages like: (i) The poorly soluble or completely hydrophobic drugs become aqueous soluble by forming inclusion complexes between their functional groups with interior cavity of the CD, while the hydrophilic hydroxyl groups exposed to the environment. In addition, by improving solubility of drug, inclusion complexes prevent the crystallization of individual drug molecules so that they can no longer self-assemble [12], [15]. (ii) The poorly soluble drug offers poor bioavailability. When drug is complexed with CD, dissolution rate and absorption by physiological tissue are enhanced [14], [16]. (iii) By improving solubility, bioavailablity of hydrophobic drug, CD inclusion complex improves the chemical, physical and thermal stability of drugs.

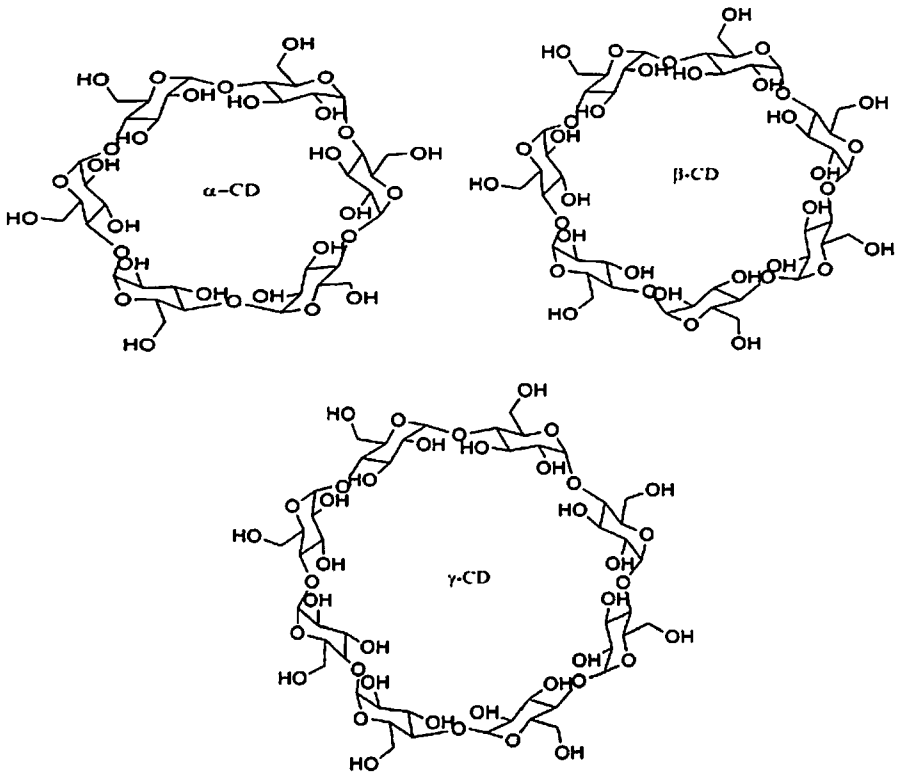

Fig. 3.1: Structure of Cyclodextrin

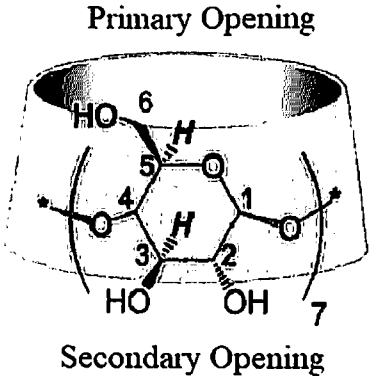

Fig. 3.2: Primary and secondary opening of β-Cyclodextrin[1]

When a guest molecule is entrapped within the CD cavity, it is difficult for the reactants like oxygen, water, radiation or heat, chemical reactions etc. to diffuse into the cavity and react with the protected guest [15], [17]. (iv) The CD complex reduces the local concentration of free drug. The free drug can irritates the stomach, skin or eye which are possible to resolve by CD complex. As the complex gradually dissociates and the free drug is slowly released, it gets absorbed into the body with reduced concentration of local free drug [16], [18].

[1] https://www.beilstein-journals.org/bjoc/articles/13/157

Among all three cyclodextrins, β-CD is widely used in pharmaceutical field. β-CD consists of seven glucopyranose units and is partially water soluble due to intermolecular hydrogen bonding. Derivatives of β-CD or the certain ratio of water and organic solvent break this hydrogen bond and become water soluble [17], [18]. Hydrophilic outer surface of β-CD helps to enter the hydrophilic molecules into β-CD modified macromolecules which termed as exclusion complexes (Fig. 3.3(a)), whereas a lipophilic central cavity increases solubility of the incorporated drug, enhanced permeation for macromolecular drugs [19] and inhibition of certain protease activities [20] by accommodate the hydrophilic and lipophilic drugs into its cavity, called inclusion complexes (Fig. 3.3(b)). Although β-CD has limited aqueous solubility but this was overcome by preparing the derivative of β-CD such as hydroxypropyl (HP)-β-CD [21], methyl (M)-β-CD [22] and sulfobutyl ether (SBE) β-CD [23] and these substituent have been commercially used as pharmaceutical participants. When the solubility issue has been resolved, β-CD exhibits some benefits in pharmaceutical field and those are (i) The natural α- and β-CD cannot be hydrolyzed by human saliva and pancreatic amylases [24]. (ii) The molecular weight of β-CD is higher than α-CD and the cavity size of β-CD is more suitable than other CDs to encapsulate a wide range of molecules [25], [26]. (iii)Although the molar mass of β-CD is less than γ-CD but the derivatives of β-CD offers higher molecular weight than γ-CD (molecular weight (MW) over 2000 Daltons). (iv) β-CD is less irritating than α-CD after intramuscular injection [27]. Orally administrated beta CD and/or its complexes are absorbed in very small amount by the upper gastrointestinal wall which is an expected property of any drug loaded macromolecular carrier[2]. β-CD encapsulates the water insoluble ocular drug such as Nepafenac by creating molecular inclusion complex with drug for non invasive ocular delivery and makes the drug soluble in water based ocular drop[3]. The β-CD based nanoparticle, liposome, microsphere create the inclusion and/ or exclusion complex with polar and non polar drug both for nasal and pulmonary drug delivery [28]. So the non-invasive drug delivery application capability of β-CD and the pH and thermosensitivity properties of Paam-*co*-Paac, have been motivated us to use β-CD as backbone of Paam-*co*-Paac to develop UVPTT based positive thermosensitive hydrogel.

[2] http://shodhganga.inflibnet.ac.in/bitstream/10603/219226/10/10%20chapter%201%20(parti&ii).pdf
[3] https://etd.auburn.edu/bitstream/handle/10415/6352/HRS_Dissertation%20OG.pdf?sequence=2&isAllowed=y

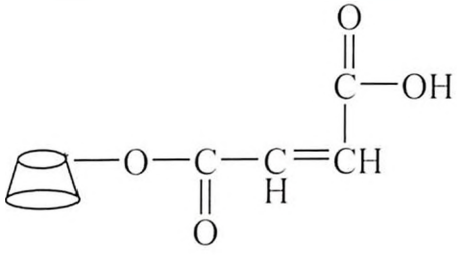

Fig. 3.2(a): Molecular exclusion of β-CD with Maleic Anhydride

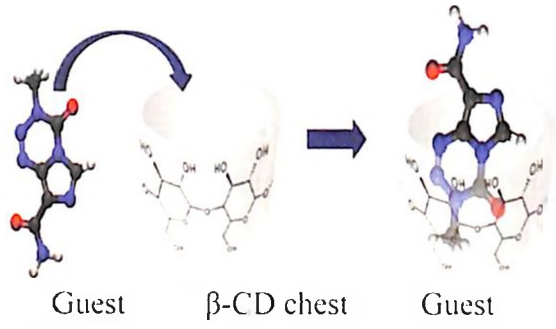

Fig. 3.2(b): Molecular inclusion of β-CD[4]

3.2.2 Non-Upper Volume Phase Transition Temperature (Non-UVPTT) based Hydrogel

Non-UVPTT hydrogel also exhibits volume transition temperature but does not fall on working temperature of polymer (say: from 10 °C to 40 °C) which the polymer offers swelling-deswelling transition. If the UVPTT is higher than working temperature of polymer, then during heating the polymer from 10 °C to 40 °C or vice versa, there will not be any physicochemical change but morphological parameters of polymer network like: mesh size, tortuosity, porosity will respond to external stimuli and help the polymer to swell-deswell. As synthetic polymer, Paac and Paam were already been selected and both are pH sensitive but sole polyacrylic acid is not thermosensitive. Guar gum modified polyacrylamide was developed for prolonged colonic drug delivery application [29]-[32]. The drug released was observed at different pH mediums. The temperature sensitive swelling of synthetic Paam was observed by Boyde *et al.* [33] for electrophoresis apparatus in chromatography. This only evidence motivated us to use Paam as one of the ingredients for Non-UVPTT hydrogel.

Here, the current research is aimed to design the positive thermosensitive Non-UVPTT based hydrogel and for that we have chosen a polysaccharide based natural hydrogel. In the class of plant polysaccharide, the galactomannan e.g guar gum (composed of galactose and mannose) is extensively employed for pharmaceutical applications, which is extracted from seed coating or endosperm of leguminous plants.

Galactomannan consists of α (1, 4)-linked β- D-mannopyranose backbone with branch points from their 6- positions (Fig. 3.3). Guar gum (GG) is well-accepted

[4] http://www.scielo.br/scielo.php?script=sci_arttext&pid=S1984-82502018000200606

galactomannan, have an efficacy of the therapy in the field of drug delivery. It hydrates rapidly in water, which gives highly viscous pseudoplastic solutions of low-shear viscosity [34]. The viscosity of GG solution decreases when heated for longer periods of time.

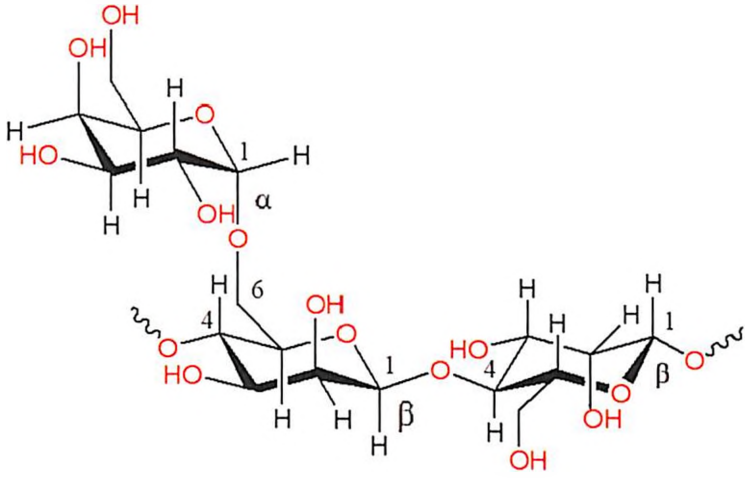

Fig. 3.3: Structure of guar gum (GG)

Guar gum is high molecular weight polysaccharide than all the other galactomannan. It has highest degree of galactose side chain than other galactomannan polysaccharides which acts as a hydrophilic backbone during grafting with the synthetic stimuli sensitive polymer like, poly(n-isopropylacrylamide) (PNIPaam) [35], [36], poly(ethylene glycol)(PEG) [37], polyacrylic acid (Paac) [38]. Research has shown that synthetic polymers convert into nontoxic, drug-compatible after blended with galactomannan polysaccharide. The mass ratio of polymer/polysaccharide significantly impacts the physicochemical properties of the resulting networks, for example, swelling-deswelling, drug loading-releasing, and thermal responsiveness. Guar gum based polymers are noninvasive in nature. The swelling-deswelling of the guar gum based polymer, which helps in drug loading-releasing, depends upon external temperature stimuli. So guar gum was the polysaccharide to modify the synthetic gel.

3.2.3 Polymerization Assisted Material

Crosslinker: To synthesis the polymer, the selection of crosslinking agent is an important and and challenging task. Crosslinking agent forms the covalent bond between molecular chains. The target of covalent crosslinking of polymer is to enhance the properties like glass transition temperature, melting point, crystalline temperature, etc. Crosslinking agent is used in the synthesis of stimuli-responsive hydrogels from

polymermolecules containing polar or nonpolar groups. Water soluble hydrogel becomes insoluble by variation of concentration of crosslinking agent or by a second reaction following that of polymerization of the starting monomers.

There are classes of crosslinker available according to the type of functional groups presence in monomer. For instance, derivatives of ethylene glycol di(meth)acrylateis used to crosslinked acrylate, methaacrylate, methylacrylate [39]-[41]. Like that, as Paam is the raw material for both UVPTT and non-UVPTT based polymers so, methylene bis acrylamide was used as crosslinker. Glutaraldehyde is another crosslinker which is generally used in chemical sterilization [42], biomedical and pharmaceutical sciences [43]. Due to sterilizing effect, gluteraldehyde is used to crosslink the polysaccharide and protect the natural polymer from affected by microorganisms. For this reason we are going to use glutaraldehyde for guar gum crosslinking.

Initiator: As we are planning to conduct a thermal free radical analysis, so free radical initiator must be used to initiate the polymerization. Sodium bisulfites (SBS), ammonium persulfate (APS), potassium persulfate (KPS), ammonium cerium (IV) sulphate (ACS) are the examples of radical initiator. A thermal free radical initiator is stable at room temperature for which it cannot be decomposed to create the free radicals for initiating the reaction but decomposes rapidly at the polymer processing temperature or high temperature.

3.2.4 Hydrogel Nanocomposite

The pH and temperature sensitive polymer can easily tune its spatial alteration by means of drug delivery as non-invasive application. The noninvasive stimuli sensitive polymer can senses the physiological parameter of biological body and releases the therapeutic agents by means of their spatial alterations. The polymeric drug delivery vehicles are available in non-invasive drug delivery through different forms like sol-gel [44], [45], particle [46], [47], microsphere [48], micelle [49], [50]. Sometimes this kind of formulated drug delivery system creates unexpected release of drug which termed as "drug leakage". The leakage of drug can be occurred at healthy cells which can creates the side effects and offer less bioavailability to targeted area. When the drug delivery is depends upon the biological parameters of targeted point, the rate of drug release can be affected by physiological barrier of patient's body which can be varied from patients to

patients. In front of these significant limitations of stimuli triggered polymer, light is another external stimulus with some benefits. Intensity of light, incident time,can be easily controlled and regulated by external apparatuses, by offering the dynamic spatial alterations of polymeric drug carrier [51], [52]. The presence of photosensitive moieties inside the polymer network, induce the photochemical or photoisomerization, photo-thermal or photomechanical actions of polymer.

As discussed in review chapter, it was discovered that, many researchers have been used chromophore salt for making the polymer photo sensitive. For example: Chiang *et al.* [53] developed a photoresponsive β-CD and alginate modified PEG, incorporated with azobenzene. UV light irradiation was induced the polymer chain trans-to-cis isomerization due to presence of azobenzene and switched back to the initial trans- state without UV light. This photoisomerization enabled gel degradation and initiated release the drug for wound healing. Wang *et al.* [54] designed UV light responsive polymer by metha-acrylic acid based hydrophobic spiropyrane (SPMA) and hydrophilic hydroxyethyl methylacrylate (HEMA). The polymer converted to the gel by visible light irradiation and loaded the drug (pyrene), but disassembled into micelle on UV irradiation; the loaded drug was released. The photoreceptor in lyposomes sense the irradiated light energy and breaks covalent bonds by a photochemical reaction by which lipid's hydrophilic/hydrophobic alteration triggers the release of drugs. The UV light-responsive micelles were also used for the triggered release of Rifampicin and Paclitaxel due to presence of coumarin.

The photosensitive chromophores are sensitive to ultraviolet light (250–380 nm) but UV radiation has a relatively high energy (6 eV) [55] which is harmful to mammalian tissue and obstruct the biological applications of photo-responsive polymers containing chromophor salt. Hence, development of polymer containing photochromic moieties with a low energy excitation wavelength, such as visible light (400–700 nm, <6 eV) and or near infrared light (800–2,500 nm) is obvious necessary. Although, in previous, the researchers were focused to design such kind of photochemical moieties which can be triggered by visible as well as NIR light [56], [57] in drug delivery vehicle which has deep tissue penetration than UV light. For instance, polymeric micelles of hydrophilic PEO block and hydrophobic PGA block, linking with coumarin exhibited NIR absorption to form the micelle with hydrophobic corona for drug release. Upon removal

of light irradiation converted the PGA block back to being hydrophilic, thereby destabilizing the hydrophilic/hydrophobic balance [58]. However, the photochemically triggered polymer suffers from some challenges. Photochemical triggering usually creates an irreversible change drug vehicle, which makes these systems 'one time use' [59], which require multiple administrations of the drug carrier, and for those that have demonstrated pulsatile release, they fail to produce uniform release profiles from each light exposure [60]. Some degradable chromophore or photoreceptor salt, including nitrobenzene, are considered toxic which also toxicated the carrier and the drug [61], [62].

Photothermally triggered polymeric drug delivery vehicle is the combination of such material which generates heat upon photoexcitation and thermally sensitive components which absorb the produced heat and stimulates the drug loading or release. Conventionally chromophore converts photo energy into heat energy; and the hydrogel with thermo sensitive moiety rapidly responds on change of temperature in some manner, and leads to drug release. But to avoid negative points of chromophores, nanomaterials are being the matter of interest. Inorganic nanoparticles offer the broad light spectrum (from UV to NIR) sensitivity according their material and they are silver nanoparticle, gold nanoparticles, gold nanorod, silica nanoparticles and Fe_3O_4 nanoparticles etc. These nanomaterials reinforced polymer have shown their interest and efficiency in drug delivery due to their excellent unique biocompatibility and chemical stability. Among all nanomaterials, gold nanoparticles are popular due to inert and nontoxic nature [63]. Depending upon their size and shape, they have tunable optical and photothermal, as well as they offered broad absorbance from UV to NIR region of the photo spectrum [64]. Using gold nanomaterial, most of the researchers have been use Pnipaam and its copolymer for triggered drug-delivery systems. As example a selected mixture of PNIPaam and acrylic acid (Aac) in the presence of the silica core gold nanoshell core showed near-infrared wavelengths (800–1200 nm) absorbance as photothermally responsive drug-delivery vehicles [65]. The polymer was collapsed by exposure of light via excitation of the strong plasmon resonance of the gold shell/silica core and releases the drug.

This chapter is focused on to prepare visible light sensitive gold nanoparticle reinforced hydrogel nanocomposite. The reinforcement of AuNP was performed in both hydrogels i.e. UVPTT based β-CD modified positive hydrogel and Non-UVPTT based guar gum

modified positive hydrogel. Ciprofloxacin was used as model drug for photomechanical activity.

3.3 Detailing of Materials

The Table 3.1 shows the complete list of materials, which have been used for synthesis of UVPTT based, Non-UVPTT based and nanocomposite positive hydrogels.

Table 3.1: List of materials

Name of the chemicals used	Description
Acrylic acid (Aac)	Anhydrous, assay 99%, Sigma Aldrich
Acrylamide (Aam)	Puriss: ≥ 98.0%, Sigma Aldrich
Ammonium cerium(IV) sulphate dehydrate GR	GR grade, Merck Specialities Private Limited
Ammonium Persulfate (APS)	Reagent grade, 98%, Sigma Aldrich
Acetone	HPLC grade, MolyChem
β-cyclodextrin(β-CD)	≥ 97.0%, Sigma Aldrich
Chloroform	Merck
Guar gum	Moly Chem
Glutaraldehyde	25% aq. Soln., Alfa Aesar
Maleic Anhydride (MAH)	Puriss: ≥ 99.0% (NT), Sigma Aldrich
N-Cetyl-N,N,N-Trimethyl ammonium bromide	Central Drug House Pvt. Ltd.
N, N'-Methylenebis(acrylamide)(MBA)	Assey: 99%, Sigma Aldrich
N,N-Dimethylformamide (DMF)	RANKEM
Sodium Bisulfite (SBS)	ACS reagent, Sigma Aldrich
Sodium borohydride	Merck Life science Private Limited
Hydrogen tetrachloroaurate (III) trihydrate	ACS 99.99% (metal basis), Au 49.0%, Alfa Easer

3.4 Conclusion

From the discussions, the two types of the positive hydrogels are selected to be synthesized to fulfil the objective of this thesis. The Paam-*co*-Paac will be modified with β-cyclodextrin saccharide to form positive upper volume phase transition temperature (UVPTT) based hydrogel and Paam will be modified with guar gum to prepare the non-upper volume phase transition temperature (non-UVPTT) based positive hydrogel. The glutaraldehyde will also be used as another crosslinker to understand the cross linking

effect on guar gum based non-UVPTT positive hydrogel. Furthermore, the AuNP will be reinforced into both prepared positive hydrogel network to make it visible light responsive in nature.

References

[1] R. A. Gemeinhart, J. Chen, and K. Park, "pH-sensitivity of fast responsive superporous hydrogels," *J. Biomat. Sc. Polym. Ed.* ol 11, no 12, pp. 1371–1380, 2012.

[2] X. Zhou L. Weng, Q. Chen, J. Zhang, D. Shen, Z. Li, M. Shao and J. Xu ., "Investigation of pH sensitivity of poly(acrylic acid-co-acrylamide) hydrogel," *Polym. Int.*, vol. 52, no. 7, pp. 1153–1157, 2003.

[3] T. Shirakura, T. J. Kelson, A. Ray, A. E. Malyarenko, and R. Kopelman, "Hydrogel Nanoparticles with Thermally Controlled Drug Release," *ACS Macro Lett.*, vol. 3, no. 7, pp. 602–606, 2014.

[4] A. G. Alvarado, J. Cortés, L. A. Pérez-Carrillo, M. Rabelero, J. Arellano, J. Carlos S.-Díaz, J. E. Puig & M. Arellano, "Temperature and pH-Responsive Polyacrylamide/Poly(Acrylic Acid) Interpenetrating Polymer Network Nanoparticles," *J. Macromol. Sci. Part B Phys.*, vol. 55, no. 11, pp. 1086–1098, 2016.

[5] S. Chopra, S. Mahdi, J. Kaur, Z. Iqbal, S. Talegaonkar, and F. J. Ahmad, "Advances and potential applications of chitosan derivatives as mucoadhesive biomaterials in modern drug delivery," *J. Pharm. Pharmacol.*, vol. 58, no. 8, pp. 1021–1032, 2006.

[6] Y. Murata, T. Maeda, E. Miyamoto, and S. Kawashima, "Preparation of chitosan-reinforced alginate gel beads - effects of chitosan on gel matrix erosion," *Int. J. Pharm.*, vol. 96, no. 1–3, pp. 139–145, 1993.

[7] G. P fister, M. Bahadir, and F. Korte, "Release Characteristics of Herbicides from Ca Alginate Gel Formulation", J. Cont. Rel", vol. 3, no-1,pp. 229–233, 1986.

[8] J. S.Areevath, D. L. Munday, P.J. Cox, K. A. Khan, "Release characteristics of diclofenac sodium from encapsulated natural gum mini-matrix formulations," *Int. J. Pharm.*, vol. 139, no. 1–2, pp. 53–62, 1996.

[9] V. Batra, A. Bhowmick, B. K. Behera, and A. R. Ray, "Sustained release of ferrous sulfate from polymer-coated gum arabica pellets," *J. Pharm. Sci.*, vol. 83, no. 5, pp. 632–635, 1994.

[10] J. Breitenbach, "Melt extrusion: from process to drug delivery technology," *Eur. J. Pharm. Biopharm.*, vol. 54, pp. 107–117, 2002.

[11] F. Ahsan, J. J. Arnold, E. Meezan, and D. J. Pillion, "Mutual inhibition of the insulin absorption-enhancing properties of dodecylmaltoside and dimethyl-β-cyclodextrin following nasal administration," *Pharm. Res.*, vol. 18, no. 5, pp. 608–614, 2001.

[12] H. A. Archontaki and M. V Vertzoni, "Study on the inclusion complexes of bromazepam with b-," *J. Pharm. Biomed. Anal.*, vol. 28, pp. 761–769, 2002.

[13] A. Vyas, S. Saraf, and S. Saraf, "Cyclodextrin based novel drug delivery systems," *J.*

Incl. Phenom. Macrocycl. Chem., vol. 62, no. 1–2, pp. 23–42, 2008.

[14] H. Arima, K. Yunomae, K. Miyake, T. Irie, F. Hirayama, and K. Uekama, "Comparative studies of the enhancing effects of cyclodextrins on the solubility and oral bioavailability of tacrolimus in rats," *J. Pharm. Sci.*, vol. 90, no. 6, pp. 690–701, 2001.

[15] H. Arima, T. Miyaji, T. Irie, F. Hirayama, and K. Uekama, "Enhancing effect of hydroxypropyl-β-cyclodextrin on cutaneous penetration and activation of ethyl 4-biphenylyl acetate in hairless mouse skin," *Eur. J. Pharm. Sci.*, vol. 6, no. 1, pp. 53–59, 1998.

[16] G. Tiwari, R. Tiwari, and A. Rai, "Cyclodextrins in delivery systems: Applications," *J. Pharm. Bioallied Sci.*, vol. 2, no. 2, p. 72, 2010.

[17] S. Ho, Y. Y. Thoo, D. J. Young, and L. F. Siow, "Cyclodextrin encapsulated catechin: Effect of pH, relative humidity and various food models on antioxidant stability," *LWT - Food Sci. Technol.*, vol. 85, pp. 232–239, 2017.

[18] A. K. Chatjigakis, C. Donzé, A. W. Coleman, and P. Cardot, "Solubility Behavior of β-Cyclodextrin in Water/Cosolvent Mixtures," *Anal. Chem.*, vol. 64, no. 14, pp. 1632–1634, 1992.

[19] Y. Yang, J. Gao, X. Ma, and G. Huang, "Inclusion complex of tamibarotene with hydroxypropyl-β-cyclodextrin: Preparation, characterization, in-vitro and in-vivo evaluation," *Asian J. Pharm. Sci.*, vol. 12, no. 2, pp. 187–192, 2017.

[20] X. Hou, W. Zhang, M. He, Y. Lu, K. Lou, and F. Gao, "Preparation and characterization of β-cyclodextrin grafted N-maleoyl chitosan nanoparticles for drug delivery," *Asian J. Pharm. Sci.*, vol. 12, no. 6, pp. 558–568, 2017.

[21] M. Hiral, D. Akhilesh, P. Prabhakara, and J. V Kamath, "Enhancement of solubility by complexation with cyclodextrin and nanocrystallisation," *Int. Res. J. Pharm.*, vol. 3, no. 5, pp. 100–105, 2012.

[22] P. Saokham, C. Muankaew, P. Jansook, and T. Loftsson, "Solubility of cyclodextrins and drug/cyclodextrin complexes," *Molecules*, vol. 23, no. 5, pp. 1–15, 2018.

[23] D. R. Luke, K. Tomaszewski, B. Damle, H. T. Schlamm "Review of the Basic and Clinical Pharmacology of Sulfobutylether-b-Cyclodextrin," *J. Pharm. Sci.*, vol. 99, no. 8, pp. 340–347, 2010.

[24] M. M. and T. L. A. Magnúsdóttir, "Cyclodextrins," vol. 44, no. c, pp. 213–218, 2002.

[25] J. Szejtli, "Introduction and General Overview of Cyclodextrin Chemistry," *Chem. Rev.*, vol. 98, no. 5, pp. 1743–1754, 1998.

[26] F. B. De Sousa, A. C. Lima, A. M. L. Denadai, C. P. A. Anconi, W. B. De Almeida, W. T. G. Novato, H. F. Dos Santos, C. L. Drum, R. Langer and R. D. Sinisterra, "Superstructure based on β-CD self-assembly induced by a small guest molecule," *Phys. Chem. Chem. Phys.*, vol. 14, no. 6, pp. 1934–1944, 2012.

[27] E. M. M. Del Valle, "Cyclodextrins and their uses: A review," *Process Biochem.*, vol. 39, no. 9, pp. 1033–1046, 2004.

[28] C. Muankaew and T. Loftsson, "MiniReview Cyclodextrin-Based Formulations : A Non-Invasive Platform for Targeted Drug Delivery," *basic Clin. Pharmacol. Toxic.*, vol. 122, pp. 46–55, 2018.

[29] M. Shahid, S. A. Bukhari, Y. Gul, H. Munir, F. Anjum, M. Zuber, T. Jamil, "International Journal of Biological Macromolecules Graft polymerization of guar gum with acryl amide irradiated by microwaves for colonic drug delivery," *Int. J. Biol. Macromol.*, vol. 62, pp. 172–179, 2013.

[30] K. S. Soppirnath and T. M. Aminabhavi, "Water transport and drug release study from cross-linked polyacrylamide grafted guar gum hydrogel microspheres for the controlled release application q," vol. 53, pp. 87–98, 2002.

[31] M. P. Gowrav, U. Hani, H. G. Shivakumar, and R. A. M. Osmani, "loaded pH sensitive pellets for colon speci fi c drug delivery : fabrication and characterization," pp. 80005–80013, 2015.

[32] P. B. Kajjari, L. S. Manjeshwar, and T. M. Aminabhavi, "Novel interpenetrating polymer network hydrogel microspheres of chitosan and poly(acrylamide)- grafted - guar gum for controlled release of ciprofloxacin," *Ind. Eng. Chem. Res.*, vol. 50, no. 23, pp. 13280–13287, 2011.

[33] T. R. C. Boyde, "Swelling and contraction of polyacrylamide gel slabs in aqueous solutions," *J. Chromatogr. A*, vol. 124, no. 2, pp. 219–230, 1976.

[34] T. Hongbo, L. Yanping, S. Min, and W. Xiguang, "Preparation and property of crosslinking guar gum," *Polym. J.*, vol. 44, no. 3, pp. 211–216, 2012.

[35] Y. Lang, T. Jiang, S. Li, and L. Zheng, "Study on Physicochemical Properties of Thermosensitive Hydrogels Constructed Using Graft-Copolymers of Poly (N - isopropylacrylamide) and Guar Gum," 2008.

[36] Y. Y. Lang, S. M. Li, W. S. Pan, and L. Y. Zheng, "Thermo- and pH-sensitive drug delivery from hydrogels constructed using block copolymers of poly(N-isopropylacrylamide) and Guar gum," *J. Drug Deliv. Sci. Technol.*, vol. 16, no. 1, pp. 65–69, 2006.

[37] M. Tizzotti, M.P. Labeau, T. Hamade, E. Drockenmullar, A. Charlot, "Synthesis of

Thermosensitive Guar-Based Hydrogels with Tunable Physico-Chemical Properties by Click Chemistry," *J. Polym. Sci. Part A Polym. Chem.*, vol. 48, pp. 13–14, 2010.

[38] S. B. Shruthi, C. Bhat, S. P. Bhaskar, G. Preethi, and R. R. N. Sailaja, "Microwave Assisted Synthesis of Guar Gum Grafted Acrylic Acid/Nanoclay Superabsorbent Composites and Its Use in Crystal Violet Dye Absorption," *Green Sustain. Chem.*, vol. 06, no. 01, pp. 11–25, 2016.

[39] L. Gang, W. Ting, H. Maofang, G. Tianming, and F. Xin, "Effect of ethyleneglycol dimethacrylate crosslinker on the performance of core-double shell structure poly(vinyl acetate-butyl acrylate) emulsion," *J. Appl. Polym. Sci.*, vol. 132, no. 17, pp. 1–11, 2015.

[40] H. J. Naghash, A. R. Massah, R. J. Kalbasi, "Crosslinked Methyl Methacrylate/Ethylene Glycol Dimethacrylate Polymer Compounds with a Macroazoinitiator," *J. Appl. Polym. Sci.*, vol. 116, pp. 382–393, 2010.

[41] B. C. F. Wong, A. Ahmad, S. A. Hanifah, and N. H. Hassan, "Effects of ethylene glycol dimethacrylate as cross-linker in ionic liquid gel polymer electrolyte based on poly(glycidyl methacrylate)," *Int. J. Polym. Anal. Charact.*, vol. 21, no. 2, pp. 95–103, 2016.

[42] S. P. Gorman, E.M. Scott, "Antimicrobial activity, uses and mechanism od action of glutaraldehyde," *J. Appl. Bacteriol.*, vol. 48, pp. 161–190, 1980.

[43] M. E. Nimni, D. Cheung, B. Strates, M. Kodama, and K. Sheikh, "Chemically modified collagen: A natural biomaterial for tissue replacement," *J. Biomed. Mater. Res.*, vol. 21, no. 6, pp. 741–771, 1987.

[44] E. Khodaverdi, F. Kheirandish, F. S. Mirzazadeh Tekie, B. Z. Khashyarmanesh, F. Hadizadeh, and H. Moallemzadeh Haghighi, "Preparation of a Sustained Release Drug Delivery System for Dexamethasone by a Thermosensitive, In Situ Forming Hydrogel for Use in Differentiation of Dental Pulp," *ISRN Pharm.*, vol. 2013, pp. 1–6, 2013.

[45] P. Ni, Q. X. Ding, M. Fan, J. F. Liao, Z. Y. Qian, J. C. Luo, X. Q. Li, F. Luo, Z. M. Yang, Y. Q. Wei., "Injectable thermosensitive PEG-PCL-PEG hydrogel/acellular bone matrix composite for bone regeneration in cranial defects.," *Biomater.*, vol. 35, pp. 1–13, 2013.

[46] M. Kamimura, T. Furukawa, S. I. Akiyama, and Y. Nagasaki, "Enhanced intracellular drug delivery of pH-sensitive doxorubicin/ poly(ethylene glycol)-block-poly(4-vinylbenzylphosphonate) nanoparticles in multi-drug resistant human epidermoid KB carcinoma cells," *Biomater. Sci.*, vol. 1, no. 4, pp. 361–367, 2013.

[47] Z. Q. Cao and G. J. Wang, "Multi-Stimuli-Responsive Polymer Materials: Particles,

Films, and Bulk Gels," *Chem. Rec.*, pp. 1398–1435, 2016.

[48] X. Zhou, Y. Zhao, S. Chen, S. Han, X. Xu, J. Guo, M. Liu, L. Che, X. Li and J. Zhang., "Self-assembly of pH-responsive microspheres for intestinal delivery of diverse lipophilic therapeutics," *Biomacromol*, vol. 17, no. 8, pp. 2540–2554, 2016.

[49] M. Nakayama, T. Okano, T. Miyazaki, F. Kohori, K. Sakai, and M. Yokoyama, "Molecular design of biodegradable polymeric micelles for temperature-responsive drug release," *J. Control. Release*, vol. 115, no. 1, pp. 46–56, 2006.

[50] Y. Sun , Y. Li, H. Huang, Y. Wang, Z. Sa, J. Wang & X. Chen., "pH-Sensitive Poly(itaconic acid)-poly(ethylene glycol)-poly(L-histidine) Micelles for Drug Delivery," *J. Macromol. Sci. Part A Pure Appl. Chem.*, vol. 52, no. 11, pp. 925–933, 2015.

[51] J. F. Gohy and Y. Zhao, "Photo-responsive block copolymer micelles: Design and behavior," *Chem. Soc. Rev.*, vol. 42, no. 17, pp. 7117–7129, 2013.

[52] N. Fomina, J. Sankaranarayanan, "Photochemical mechanisms of light-triggered release from nanocarriers," *Adv Drug Deliv Rev*, vol. 64, no. 11, pp. 1005–1020, 2012.

[53] C. Y. Chiang and C. C. Chu, "Synthesis of photoresponsive hybrid alginate hydrogel with photo-controlled release behavior," *Carbohydr. Polym.*, vol. 119, pp. 18–25, 2015.

[54] B. Wang, K. Chen, R. Yang, F. Yang, and J. Liu, "Stimulus-responsive polymeric micelles for the light-triggered release of drugs," *Carbohydr. Polym.*, vol. 103, no. 1, pp. 510–519, 2014.

[55] M. Korbelik, "PDT-Associated Host Response and its Role in the Therapy Outcome," *Laser Surg. Med.*, vol. 38, pp. 500–508, 2006.

[56] G. S. Kumar and D. C. Neckers, "Photochemistry of Azobenzene-Containing Polymers," *Chem. Rev.*, vol. 89, no. 8, pp. 1915–1925, 1989.

[57] M. Dong, A. Babalhavaeji, S. Samanta, A. A. Beharry, and G. A. Woolley, "Red-Shifting Azobenzene Photoswitches for in Vivo Use," *Acc. Chem. Res.*, vol. 48, no. 10, pp. 2662–2670, 2015.

[58] S. Kumar, J. F. Allard, D. Morris, Y. L. Dory, M. Lepage, and Y. Zhao, "Near-infrared light sensitive polypeptide block copolymer micelles for drug delivery," *J. Mater. Chem.*, vol. 22, no. 15, pp. 7252–7257, 2012.

[59] M. Eeman, "From biological membranes to biomimetic model membranes," *Biotechnol. Agron. Soc. Env.*, vol. 14, no. 4, pp. 719–736, 2010.

[60] A. Y. Rwei, J.-J. Lee, C. Zhan, Q. Liu, M. T. Ok, S. A. Shankarappa, R. Langer, and D. S. Kohane, "Repeatable and adjustable on-demand sciatic nerve block with phototriggerable liposomes," *Proc. Natl. Acad. Sci.*, vol. 112, no. 51, p. 201518791, 2015.

[61] C. A.Lorenzo, L. Bromberg, and A. Concheiro, "Light-sensitive intelligent drug delivery systems," *Photochem. Photobiol.*, vol. 85, no. 4, pp. 848–860, 2009.

[62] J. M. Joseph, H. Destaillats, H. M. Hung, and M. R. Hoffmann, "The Sonochemical Degradation of Azobenzene and Related Azo Dyes: Rate Enhancements via Fenton's Reactions," *J. Phys. Chem. A*, vol. 104, no. 2, pp. 301–307, 2000.

[63] A. M. Alkilany and C. J. Murphy, "Toxicity and cellular uptake of gold nanoparticles: What we have learned so far?," *J. Nanoparticle Res.*, vol. 12, no. 7, pp. 2313–2333, 2010.

[64] S. Link and M. A. El-sayed, "Shape and size dependence of radiative, non-radiative and photothermal properties of gold nanocrystals," *Int. Rev. Phys. Chem.*, vol. 19, no. 3, pp. 409–453, 2000.

[65] J. Kim and T. R. Lee, "Thermo-Responsive Hydrogel-Coated Gold Nanoshells for In Vivo Drug Delivery," *J. Biomed. & Pharma. Eng.* vol. 1, pp. 29–35, 2008.

Chapter 4

Gel Synthesis and Morphological Characterization

In Chapter 3, the selection of monomers, crosslinkers and initiators have been discussed. This chapter deals with the synthesis of both the UVPTT and non-UVPTT based positive hydrogels. Next to the gel synthesis, prepared gels were characterized to verify the proper making of grafts as well as IPN gels.

4.1 Introduction

Polymers are made of monomers, which are covalently assembled with one another by different mechanisms to form macromolecules of several thousand monomer units. The polymerization techniques are: (i) Microwave (MW) assisted polymerization, (ii) Oil-water emulsion process, (iii) free radical bulk polymerization. In MW assisted polymerization, microwave irradiation is a common heat source. The advantages of this technology include highly accelerated rate of the reaction, shorter reaction time and reduction of side reactions compared with syntheses performed under conventional heating [1]. Whereas, in conventional heating, synthesis usually needs longer heating time, large apparatus setup etc. MW assisted organic synthesis has been introduced in the year of 80's but since the beginning MW assisted reaction has been experienced some drawbacks and they are: (i) initially MW assisted synthesis was carried out in open vessel for which the reaction solvent with lower boiling point was limit the reaction and that is why the reaction was only limited to high boiling point solvent[1]. (ii) Inflammability of organic solvent due to high temperature creation is another obstacle for employment of organic solvent in MW chamber. (iii) Closed vessel MW reactor sometimes creates over heating of reaction mixture which disturbs the reaction temperature. (iv) Microwave reactors are expensive and produced overheating. (v) Metals are reflective to microwaves. Due to this, metal particles or metals have to be avoided inside the microwave oven because there is always a possibility of an electric spark in the oven[2].

[1]https://wiki.anton-paar.com/en/microwave-assisted-synthesis/
[2]http://shodhganga.inflibnet.ac.in/bitstream/10603/79450/5/05_chapter%201.pdf

Emulsion polymerization is a type of polymerization where oil-in-water or water-in-oil emulsion method uses. The main ingredients of emulsion polymerization are organic solvents and/or oil, monomers, stabilizer, surfactant. In the case of emulsion polymerization, droplets of monomer (oil phase) are emulsified (with surfactants) in a continuous phase of water. Water-soluble polymers are used as emulsifiers in the water-in-oil method. The emulsion polymerization are widely used method for synthesizing polymeric micelles, particles, lyposomes etc. because of (i) rapid polymerisation of polymer with low polydispersity, (ii) low viscosity of polymer emulsion, (iii) synthesized form of polymer can be easily removed from reactor due to low viscosity, (iv) reaction temperature can be controlled and overheating is avoided due to water as heat sink. When these plus points motivate the researchers to use emulsion polymerization, the unexpected drawbacks cannot be ignored and those are (i) Surfactants and other polymerization adjuvant remain in the polymer or are difficult to remove[3], (ii) polymer can easily be contaminated by the trace of emulsifier, (iii) due to present of oil, drying of synthesized product is an energy-intensive process, (iv) the polymer with lower glass transition temperature than polymerization temperature, are difficult to be employed due to aggregation of particulate polymer[4], (v) Stabilizer may react with encapsulated cargo and makes them toxic [2], (vi) particle aggregation creates difficult physical handling in liquid and dry form [3]

When the drawbacks of microwave assisted and emulsion polymerization obstruct the researchers to use these methods, bulk polymerization motivates the researchers due to production of relatively pure product with minimum contamination. In bulk polymerization shape of polymer not limited like emulsion polymerization. It is before mentioned that emulsion polymerization is famous for the formation of micelles, particles, lyposomes. Non-spherical structure like slab, cube, cylinder, disc etc. can be achieved by MW assisted and bulk polymerization. As limitations of MW assisted polymerization are not reported for bulk polymerization method, so in this research polymer has been synthesized by bulk polymerization method which is discuss in the next section.

[3] https://www.coursehero.com/file/p54e2mi/Disadvantages-of-emulsion-polymerization-include-Surfactants-and-other/
[4] https://web.stanford.edu/class/cheme160/lectures/lecture13.pdf

4.2 Bulk Polymerization Synthesis Process

In bulk polymerization, the reaction mixture consists of monomers, initiator according to type of polymerization like free-radical or ionic (cationic and/ or anionic) or catalytic (Fig 4.1). Crosslinker is another ingredient of bulk polymerization. The bulk polymerization used to make the macromolecular long chain from small monomer molecules with C=C bond, like vinyl monomers (styrene, methyl methaacrylate, vinyl acetate, ethylene, acrylamide etc.). The reaction is initiated by heating or exposing to radiation. This polymerization offers many plus points over other polymerization process and they are: (i) the reactor is simple and yield of gel can be adjusted by the size of reactor, (ii) molecular weight of polymer can be easily tuned by changing the molar concentration of monomers[5].

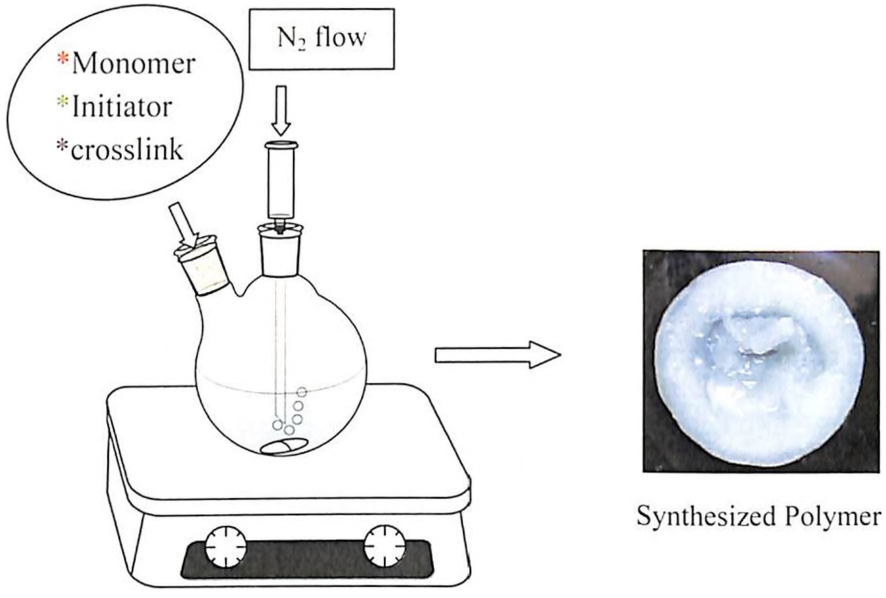

Fig 4.1: Schematics of bulk polymerization setup

(iii) reaction time can be easily adjusted by initiator with varying molar concentration, (iv) reaction temperature is easily controllable. Although conventional bulk polymerization was conducted without solvent, but this polymerization process is often exothermic and can't dissipate the heat after gelling due to increment of viscosity[6] but in recent years solvents are being used for polymerization as thermal insulator. Another major drawback of bulk polymerization is the removal of remained traces of monomers and other reagents from highly viscous gel. The unreacted monomers are often toxic and could leach out from

[5] http://polymerdatabase.com/polymer%20chemistry/Bulk%20Polymerization.html
[6] https://www.list.ch/processes/bulk-polymerization/

the hydrogels continuously, but these can be overcome by extraction using water and volatile solvent like ethanol, acetone, methanol etc. [4]. Without extraction, the purification can be achieved by post-polymerization curing (e.g. by thermal treatment or irradiation of the resulting products) [5], [6]. Selection of nontoxic monomers is another way to get prepared nontoxic polymer. Modification of synthetic polymer with natural polysaccharide and oligosaccharide is the recent years trend to prepare nontoxic gel [7], [8].

In bulk polymerization, free radical reaction mechanism is mostly used technique than ionic method. Some advantages of radical polymerizations than other techniques are the relative insensitivity to impurities, the moderate reaction temperatures [9]. Free radical polymerization (FRP) is a chain growth polymerization, where polymer chain is made by successive addition of the monomer units by breaking of a double bond of the monomer unit, adding them to form a long chain [10]. Free radical polymerization does not require stringent process conditions and can be used for the copolymerization of a wide range of vinyl monomers [11]. The chain growth reactions, free radical polymerizations proceed via three distinct processes:

Initiation: In this first step, a reactive site is created from which the generation of polymer chain starts. Radical initiation is suitable on the carbon–carbon double bond of vinyl monomers and the carbon–oxygen double bond in aldehydes or ketones[7]. Initiation process is being executed in two steps. In first step, radical molecules are created from initiator by temperature or light or metal ions or electromagnetic radiations. The initiating molecules fall apart and when they split, the pair of electrons in the bond is broken and separate. The unpaired electrons are called free radicals and the breaking of bonds is called dissociation of monomer. In second step, the radicals are attached to monomers unit and create the radical site at the monomer chain. This process is called association.

$$I \longrightarrow R^{*} \quad \text{Dissociation}$$

$$R^{*} + M \longrightarrow M^{*} \quad \text{Association}$$

Step 1: initiation process of FRP

The initiation step 1 is presented above where I means initiator, R* means free radical and M* means radical site at monomer.

[7] http://www.carborad.com/Volume%20II/Chapter%2010/Aldehydes%20and%20Ketones.pdf

Propagation: Once the free radical of initiator creates the radical site at monomers chain, it means polymerization is initiated and the reactive monomer molecules added one by one to the active chain end which called propagation step. The reactive site regenerated after each addition of monomer. The propagation step (Step 2) would continue until all monomers are utilized.

$$M^* + M \longrightarrow M_1^*$$
$$M_1^* + M \longrightarrow M_2^*$$
$$M_2^* + M \longrightarrow M_3^*$$
$$\vdots$$
$$M_n^* + M \longrightarrow M_{n+1}^*$$

Step2: Propagation process of FRP

Termination: Chain termination occurs when two free radical species react with each other to form a stable, non-radical adducts. The pairs of radicals also have a tendency to react with each other and thus eradication of active sites leads to "terminated," or inert, macromolecules. This process is called combination or coupling.

$$M_{n+1}^* + M_{m+1}^* \longrightarrow P_{(n+1)+(m+1)}$$

Step3: Termination process of FRP

The process of synthesis protocol for producing both UVPTT based β-cyclodextrin modified and non-UVPTT based guar gum modified positive hydrogels is defined in the next sections as a foremost key step. The above discussed reaction mechanism is followed during the synthesis.

4.2.1 Synthesis Protocol for UVPTT based β-CD Modified Positive Hydrogel

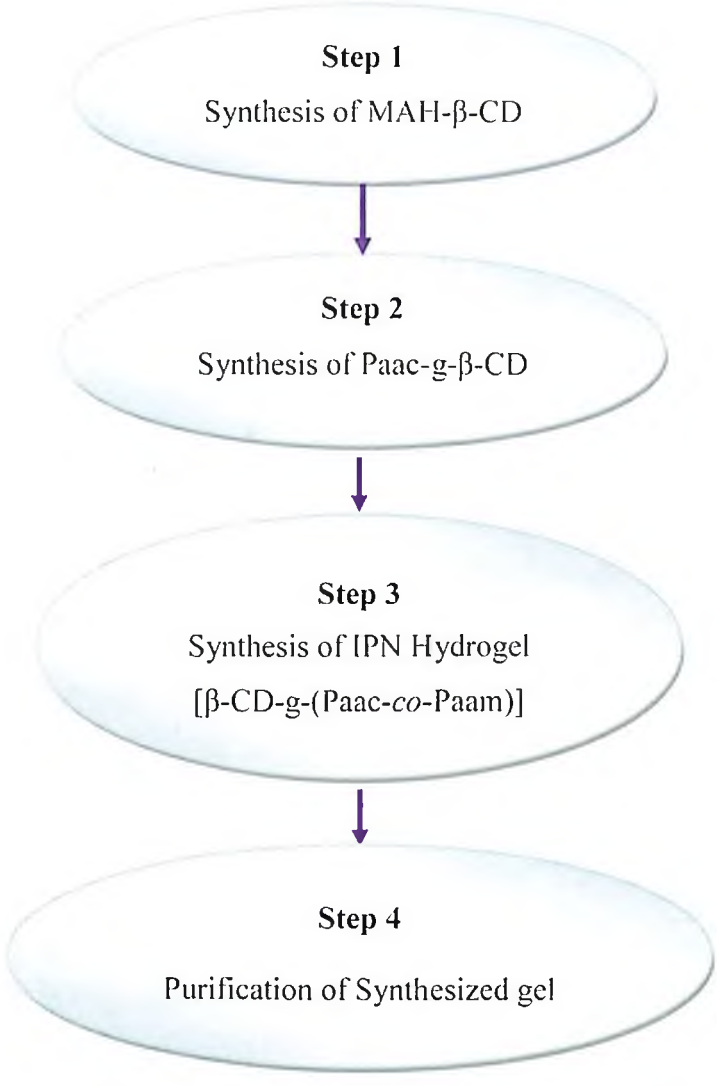

Fig. 4.2: Schematic of Synthesis protocol of β-CD modified hybrid UVPTT hydrogel

The β-cyclodextrin (β-CD) modified hybrid UVPTT hydrogel was synthesized by following process flow shown in the schematic (Fig. 4.2). The synthesis protocol involves four process steps: in 1st step, the synthesis of β-CD based reactive monomer (MAH- β-CD) will be performed; in 2nd step, the poly(acrylic acid)-graft-β-cyclodextrin (Paac–g–β–CD) will be synthesized, in 3rd step, the IPN hydrogel β-CD-g-(Paac-co-Paam) will be synthesized and the 4th and last step involved the purification of the synthesized gel. Therefore in short, the poly(acrylic acid) grafted β-CD (Paac-g-β-CD) was made, followed by Paam was introduced to Paac-g-β-CD graft gel to produce interpenetrating gel network (IPN) of UVPTT based β-CD modified positive hydrogel. The purification is most vital step to get the purest form of synthesized gel.

The detail process of synthesis to form β-CD modified hybrid UVPTT hydrogel is described in below section.

4.2.2 Synthesis Protocol for Non-UVPTT Based Guar Gum Modified Positive Hydrogel

Based on the selection of guar gum as base material as discussed in Chapter 3, a non-UVPTT based positive hydrogel was developed by synthesizing both graft gel sample and the double cross linked gel samples. The perform the synthesis activities, the guar gum based graft and double cross linked gels were synthesized by free radical reaction mechanism. The overall synthesis protocol is defined as given in Fig. 4.3. In Step I, the guar grafted polyacrylamide (GG-g-Paam) was synthesized (detail synthesis process is discussed in Section 4.3.2.1). The efficiency of grafting was scrutinized by using ammonium cerium sulphate (ACS) and APS as initiator during gel synthesis. The synthesis of GG-g-Paam is sub-divided into two cases; Case I – reaction synthesis was performed by using APS as initiator and Case II – the ACS was used as initiator to perform the chemical gel synthesis. Both APS and ACS were used as initiator during graft polymerization to investigate the grafting efficiency and the quality of the graft gel. The detail discussion on usefulness of APS and ACS are discussed in Section 4.3.2.1. In Step II, the synthesized graft gel was further crosslinked by glutaraldehyde (GA) and the gel purification process was performed as final in Step III. Therefore, in brief, the non-UVPTT based guar gum modified positive hydrogel was prepared by grafting of guar gum with Paam (GG-g-Paam) (Step I) and thereafter, in Step II, the glutaraldehyde was introduced into graft gel GG-g-Paam network to make it double cross linked interpenetrating hydrogel (DC-GG-Paam$_{GAi}$) network.The molar concentration of GA was varied to understand the double crosslinking effect on external stimuli responsiveness.

The above UVPTT and non-UVPTT polymers are not photo responsive as the polymers are not contain any photosensitizer. So to actuate the polymers by light irradiation next section is describe the method of gold nanoparticle reinforcement inside polymer network. Gold is biocompatible is gold nanoparticle is visible light sensitive and compatible to mammalian tissue.

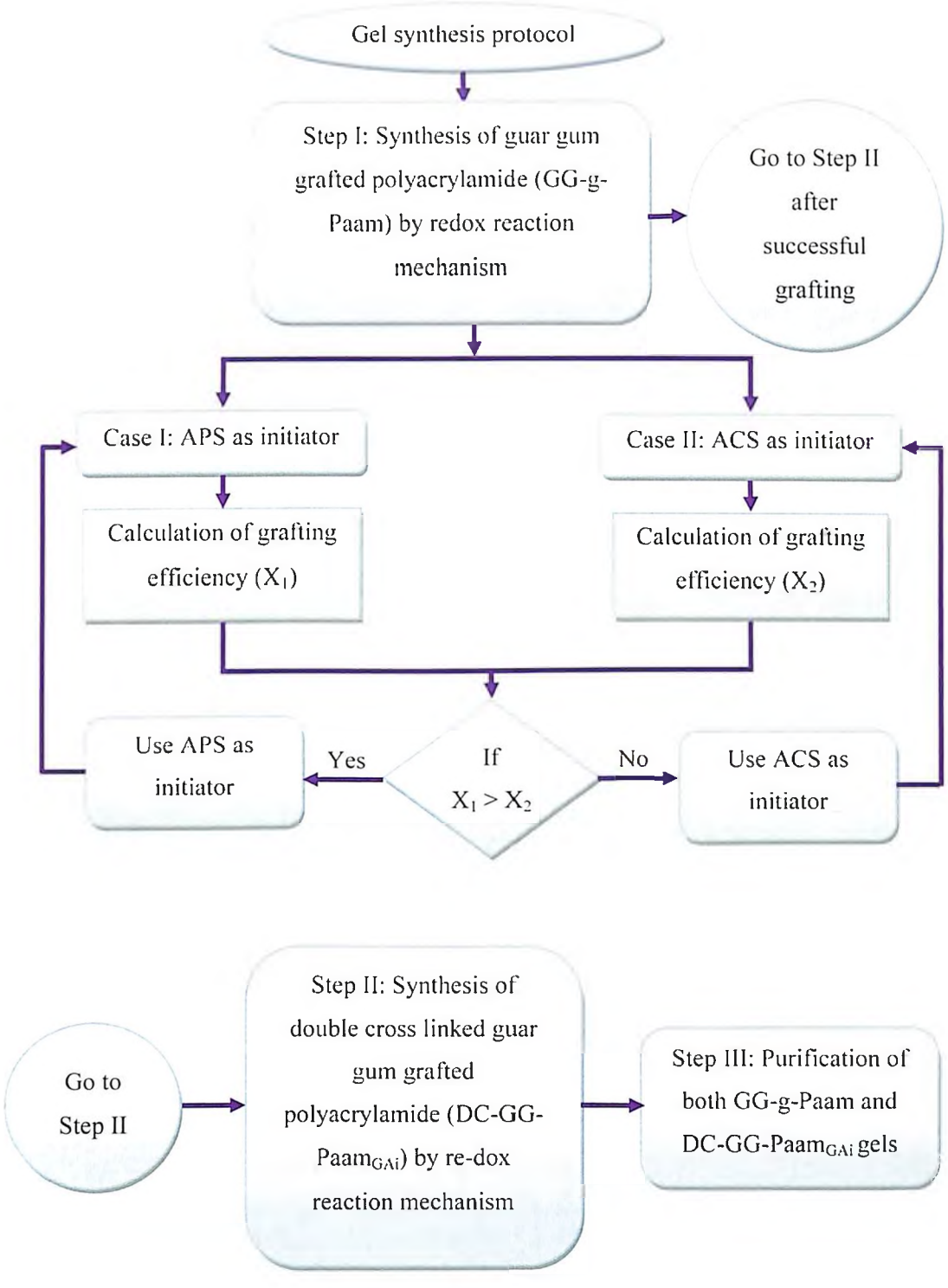

Fig. 4.3: Schematic for non-UVPTT gel synthesis protocol

4.2.3 Synthesis Protocol for Hydrogel Nanocomposite

The synthesized positive hydrogels are prepared as hydrogel nanocomposite by reinforcement of gold nanoparticle (AuNP) into the polymer network. The AuNP reinforcement was executed in two different approaches – Case I: Dip method and Case II: *In-situ* synthesis method. Both dip method and the *In-situ* method are schematically shown in Fig. 4.4 and Fig.4.5 respectively.

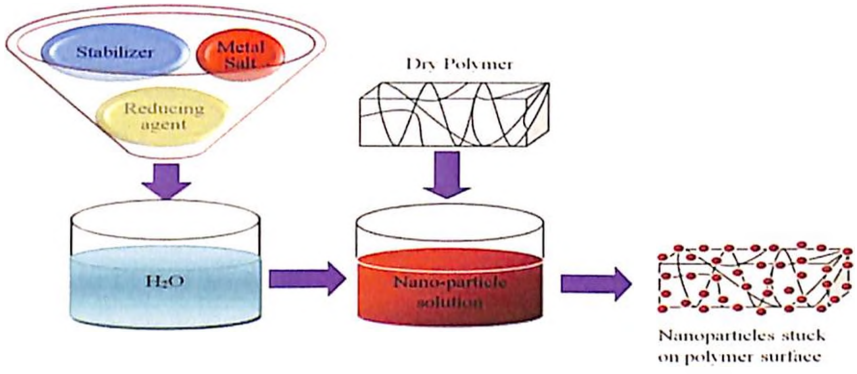

Fig. 4.4: Schematics of AuNP reinforcement into polymer by Dip method

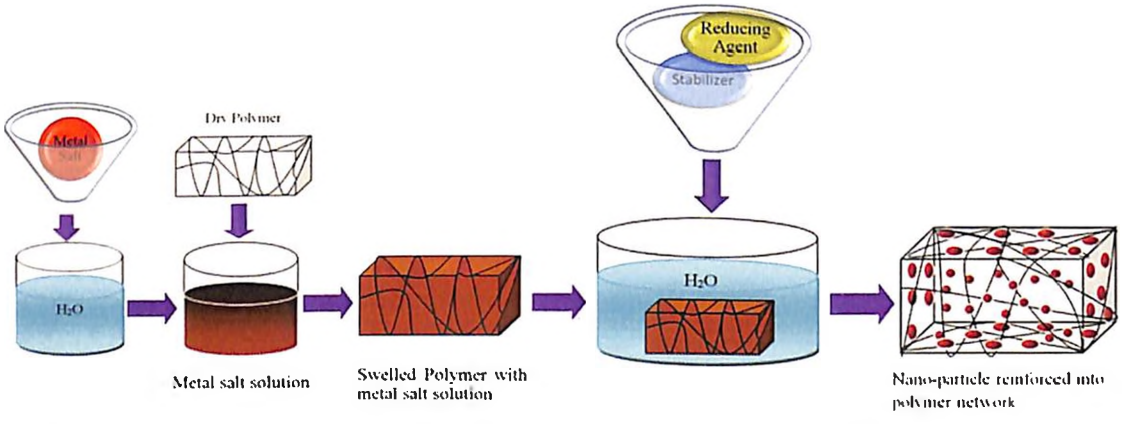

Fig. 4.5: Schematics of AuNP reinforcement into polymer by *in-situ* synthesis method

In the 1st approach, Case I (Fig. 4.4), the predefined fixed dimensional synthesized dry IPN gel was immerged into the solution of mono-dispersed AuNP solution, stabilizer and reducing agent until the dry gel sample reached its equilibrium swelled state, whereas, in *in-situ* method (Fig. 4.5), nanoparticles were synthesized inside the polymer network. The dry polymer samples were immersed into differently concentrated Au(III) solution until its maximum and constant swelling. After that the swelled polymers with incorporated metal ion were shifted into fresh DI water. Finally the reinforced Au^{3+} ions were reduced and formed Au (0) by diffusing in 1 ml of 10^{-1}

mol.lt^{-1} $NaBH_4$ from 1.0 mol.lt^{-1} concentrated 10 ml stock solution of $NaBH_4$ solution as reducing agent.

4.3 Polymer Synthesis

The synthesis of both UVPTT and non-UVPTT gels were done by following the defined protocol in the last section.

4.3.1 Synthesis of UVPTT based β-Cyclodextrin Modified Positive Hydrogel

The UVPTT based β-CD modified positive hydrogel synthesis process steps are briefly described as below.

Preparation of Reactive Monomer (MAH-β-CD)

In order to graft the Paac with β–CD, a reactive monomer of β–CD was synthesized which can be copolymerized and cross-linked with Paac component, a modified β-CD carrying five vinyl carboxylic acid groups was designed and synthesized. Specifically, 5.68 gm of β–CD (0.005 mol) was dissolved in 100 ml DMF, and 4.90 gm (0.05 mol) of Maleic Anhydride (MAH) was added afterwards. The mixture solution was heated at 80°C for 10 hrs under the vigorously stirring. After the reaction was completed, the mixture was allowed to cooling to room temperature and then, 150 ml of trichloromethane was added. A white precipitate obtained was filtrated, and washed using acetone; finally, dried in a vacuum oven at room temperature for 24 hrs. Fig. 4.6 depicts the reaction schematic for the synthesis of reactive monomer MAH-β-CD.

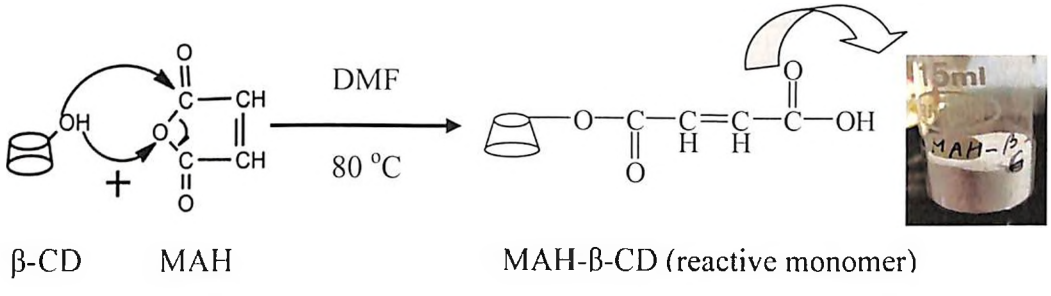

β-CD MAH MAH-β-CD (reactive monomer)

Fig. 4.6: Reaction schematic for the synthesis of reactive monomer MAH-β-CD

Preparation of Poly(acrylic acid)-graft-β-Cyclodextrin (Paac-g-β-CD)

A reactive monomer, MAH–β–CD and Aac in an aqueous solution were reacted at 20 °C with an APS–SBS redox system as the initiator for 12 hrs. Thereafter, 1 mol of MAH–β-CD and Aac (9 mol) was dissolved in 18 ml of distilled water. The 0.08 gm of SBS (0.768 mol) solution in 1 ml DI water and 0.32 gm APS (1.4 mmol) solution in 1 ml DI water were added. The reaction was conducted in nitrogen environment to eliminate oxygen. After the reaction was completed, synthesized product was immersed in distilled water at room temperature and kept there until its volume did not change anymore; it was dialyzed with DI water for 72 hrs. to eliminate residual chemicals and then dried to a constant weight at 40 °C. Fig. 4.7 depicts the reaction schematic for the synthesis of poly(acrylic acid)-graft-β-Cyclodextrin (Paac-g-β-CD). The 101.59±8.46% (n=10) of grafting efficiency was found.

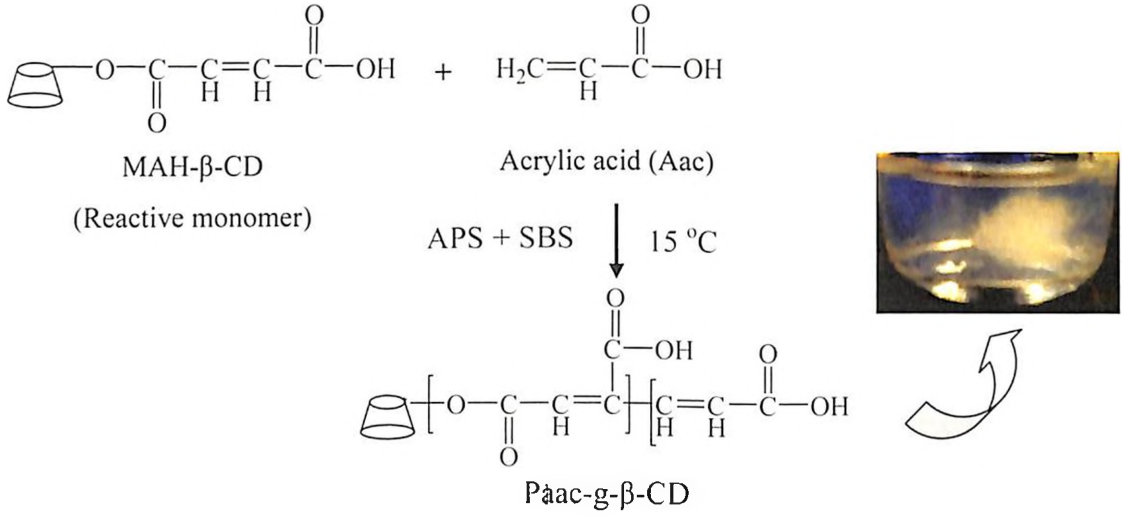

Fig. 4.7: Reaction schematic for the synthesis of Paac-g-β-CD

Preparation of the IPN Hydrogel β-CD-g-(Paac-co-Paam)

The IPN hydrogel was finished by a method of sequential IPN synthesis, in which the IPN hydrogel with β-CD-g-Paac and Paam were synthesized as the initial matrix and the secondary gel, respectively. Paac-g-β-CD was immersed in water at 50 °C until the polymer was completely swollen. Then, 9.85 mmol of the monomer Aam per gm of graft polymer, containing the initiator (APS; 0.3 wt % of the total monomer), was added at room temperature in a nitrogen environment. After the monomer Aam was subsequently polymerized within the initial Paac-g-β CD matrix at 60 °C for 24 hrs., the IPN hydrogel that was obtained was immersed in deionized water at room temperature for 96 hrs., and the water was changed every several hours. Finally, the IPN hydrogel was dried to a

constant weight in vacuum oven at 40 °C. Fig. 4.8(a)-(b) depicts the reaction schematic for the synthesis of IPN hydrogel β-CD-g-(Paac-*co*-Paam). The thermal initiated free radical redox reaction was performed for the synthesis of β-CD-g-(Paac-*co*-Paam). In thermal decomposition of initiator (APS), per sulfate ions ($S_2O_8^{2-}$) ripped into sulphate free radicals (SO_4^{-}). The sulphate free radicals created the radical site at acrylamide and β-CD-g-Paac by breaking the pi bond (π) into sigma bond (σ) of Aac and Aam to initiate the reaction. Chain propagation started when initiated Aam monomers attached with β-CD-g-Paac at its radical site until there were no more radical Aam left. When no more radical sites are present in the reaction and chain length augmentation, is called termination. For preparation of natural polymers, grafting between natural gum and synthetic monomer is most important step.

Thermal Decomposition of APS

$$(NH_4)_2S_2O_8 \xrightarrow{60^oC} (S_2O_8)^{2-} \xrightarrow{-e^-} 2\,SO_4^{-*}\,(R^*)$$

Initiation Process

$$H_2C{=}CHX \xrightarrow{R^*} H_2C{-}CHX^*\ \text{(Radical monomer)}$$

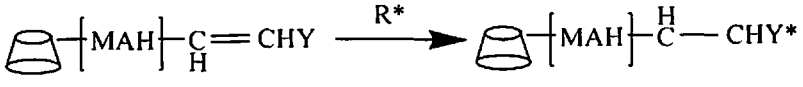

Propagation Process

X is $HC(=O)-NH_2$ Y is $HC(=O)-OH$

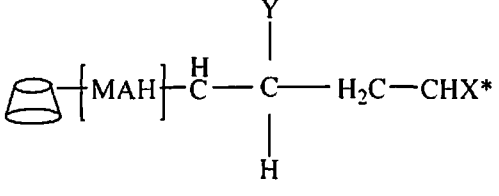

Termination Process

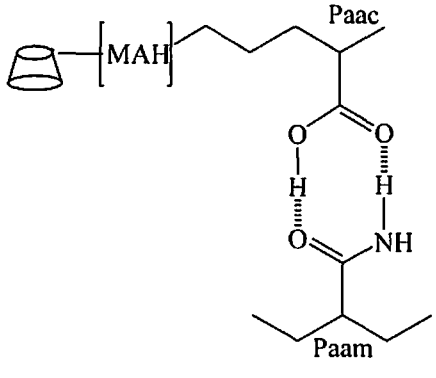

Fig. 4.8 (a): Copolymerization method between β-CD-g-Paac and Paam

Polymer Purification

Purification of synthesized monomer is as important however is difficult because of DMF which is difficult to remove from any reacted product. After drying the powder, the monomer was again stirred at 45 °C in trichloromethane for 24 hrs. to extract the DMF residues in the monomer if any. Final purification was performed by evaporating the acetone at its boiling points by using rotaevaporator.

Graft gel was temperature sensitive and it was degraded above 40 °C for which it was washed in ice cold DI water. The copolymer was immersed in DI water at 20 °C for 96 hrs. Water was keep changing every day. Then samples were taken out from hot water, cut into pieces and dried. Washed samples were dried at 40 °C up to constant weight. The final purified prepared samples were shaped in the dimension of 5mm (L) x 5mm (W) x 0.25 mm (H) for all experimental purposes.

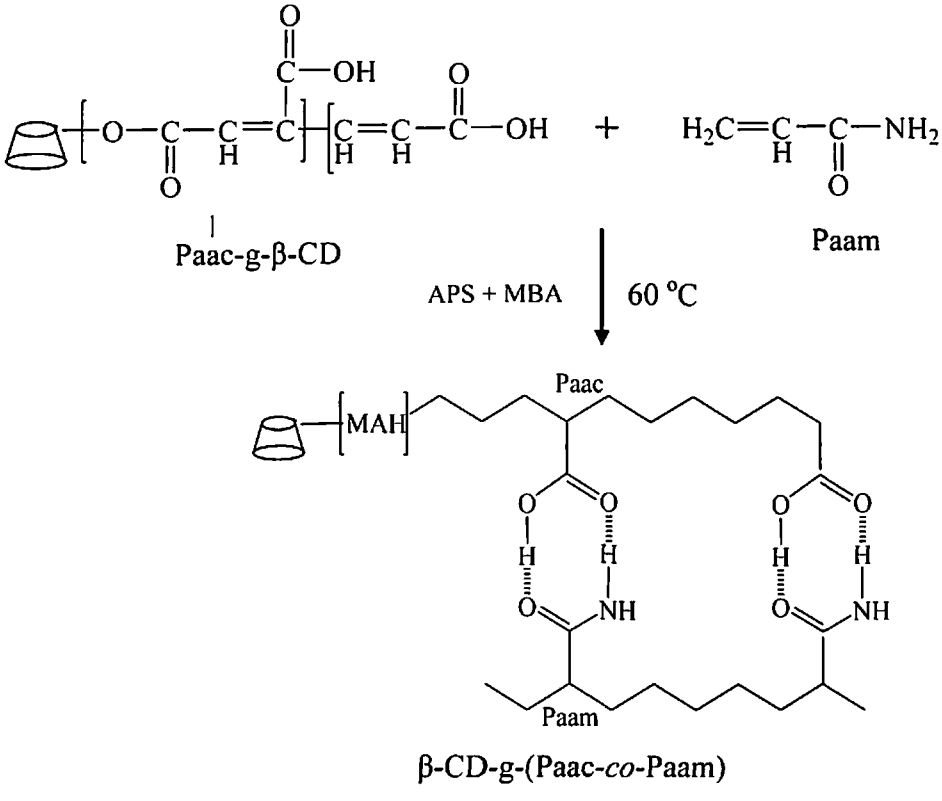

Fig. 4.8(b): Reaction schematic for the synthesis of β-CD-g-(Paac-*co*-Paam)

4.3.2 Synthesis of Non-UVPTT based Guar Gum Modified Positive Hydrogel

This section is aimed to describe the synthesis process of non-UVPTT based hydrogels.

4.3.2.1 Preparation of Guar Gum Grafted Polyarylamide (GG-g-Paam) Gel

0.995 mmol guar gum was dissolved in 50 ml DI water and stirred upto 24 hrs. to form a uniform solution. After 24 hrs., 56 mmol of acrylamide solution with 10 ml of DI water was added with guar gum solution. To that solution 1.04 mmol MBA with 10 ml DI water was added followed by the addition of 0.701 mmol APS in 10 ml DI water and was added into the reactor to initiate the grafting reaction. The reaction was carried out in the nitrogen environment at 60°C. The reaction time was varied from 30 min to 180 min in the step of 30 min to determine the higher percentage of grafting and entanglement between monomers by keeping the amount of monomer, crosslinkers and initiator constant. The formulation of polymer was termed as Time Gel 1 (TG 1) to Time Gel 6 (TG 6) by the variation of reaction time from 30 min to 180 min. Five trials were performed for the synthesis of each TG. The percentage of grafting efficiency was determined by Eq (1). The optimized reaction time was decided from grafting percentage.

$$\%\text{Grafting efficiency} = \left(\frac{\text{Mass of TG}}{\text{Mass of Aam} + \text{Mass of CG}} \right) \times 100 \qquad (4.1)$$

where, TG denotes Time Gel. The compositions of all time gels are detailed in Table 4.1.

Table 4.1. Composition of all TGs

Formulation code	GG (mmol)	Aam (mmol)	MBA (mmol)	APS (mmol)	Reaction time (min)
TG1	0.995	56.0	1.04	0.701	30
TG2	0.995	56.0	1.04	0.701	60
TG3	0.995	56.0	1.04	0.701	90
TG4	0.995	56.0	1.04	0.701	120
TG5	0.995	56.0	1.04	0.701	150
TG6	0.995	56.0	1.04	0.701	180

The thermal initiated free radical redox reaction was performed for the synthesis of GG-g-Paam. Thermal associated free radical created on guar gum backbone thus synthesis was based on free radical mechanism. For preparation of natural polymers, grafting between natural gum and synthetic monomer is most important step. Chain initiation process involved thermal decomposition of initiator (APS) as well as thermal initiation of monomers, acrylamide and guar gum. After thermal decomposition of APS,

persulfate ions ($S_2O_8^{2-}$) ripped into sulphate free radicals (SO_4^{-}). During thermal initiation of acrylamide, the pi bond (π) of vinyl group in monomer was converted into sigma bond (σ) and thus the monomer been initiated [12]. The sulphate free radical extracted the hydrogen from –OH groups of 1–6,α–D-galactose linkage of GG as that –OH group is highly polar other than other connected –OH bond and thus thermal initiation of guar gum was started. Chain propagation starts when two initiated monomers attached together at their radical site until there were no more vinyl monomers left or until termination or chain length augmentation occurred. Fig.4.9 shows the grafting mechanism. Atmospheric oxygen is a dramatic inhibitor of polymerization. Hence, nitrogen (N_2) gas was purged throughout the reaction process. The polyacrylamide long chains for entangled between the GG chains are linked by MBA units.

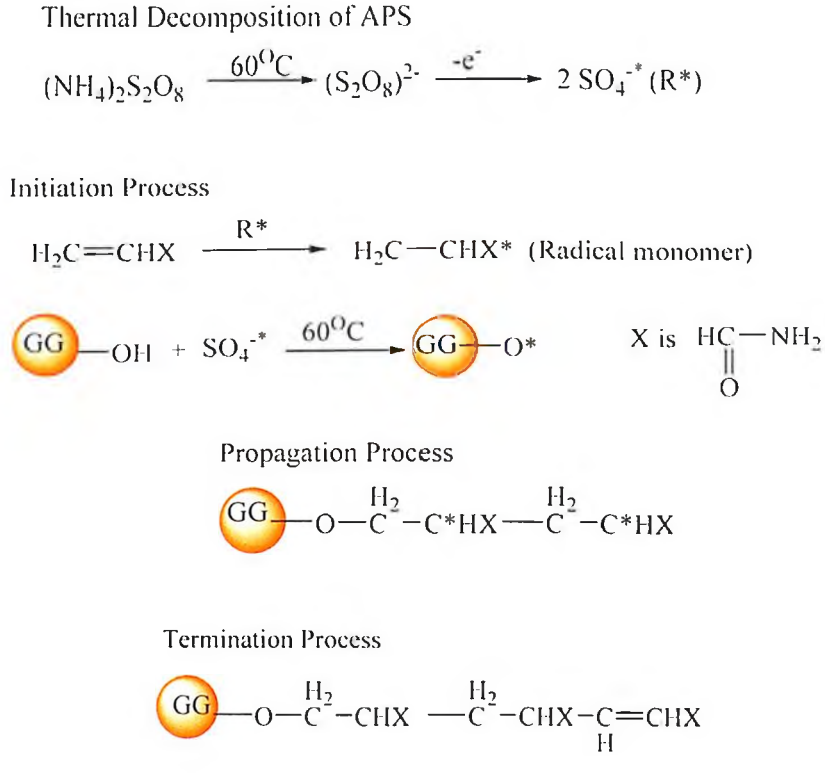

Fig. 4.9: Grafting method between GG and Paam

This gel possessed appreciable hydrophilic character due to the presence of primary and secondary amide of long MBA crosslinked Paam chains and the hydroxyl group of guar gum. The Fig. 4.10 depicts the structure of synthesized graft polymer (GG-*g*-Paam), which was expected to be formed using MBA as solo crosslinking agent. The percentage of grafting efficiency of acrylamide on guar gum backbone has been investigated by

varying time of thermal exposure from 30 min to 180 min during synthesis, keeping other polymerization parameter constant as mentioned in Table 4.2. The Table 4.2 shows the percentage of grafting efficiency for each TGs corresponding to their stipulated reaction time duration.

Table 4.2: Percentage of Grafting efficiency for all TGs.

Sample Code	Grafting efficiency (%)					Avg. Grafting efficiency (%)
	Trial 1	Trail 2	Trail 3	Trial 4	Trial 5	
TG 1	87.92	88.13	87.50	85.35	89.79	87.74 ± 1.59*
TG 2	92.29	93.10	91.69	91.92	95.08	92.82 ± 1.38*
TG 3	99.38	100.85	100.21	100.00	98.33	99.75 ± 0.95*
TG 4	102.71	104.42	106.71	103.33	102.29	103.89 ± 1.77*
TG 5	106.67	108.81	107.65	105.31	108.96	107.48 ± 1.53*
TG 6	100.63	102.13	104.27	104.42	100.38	102.36 ± 1.93*

* SD (n=5) of average percentage of grafting efficiency

The grafting efficiency was increased as reaction time increased, and the maximum (107.48±1.53)% of grafting efficiency was obtained for TG5 when reaction time was 150 min. The increment of grafting efficiency (Fig. 4.11) might be due to increasing additions of vinyl monomer molecules to the growing grafted chains. But on further increasing time period (for 180 min) grafting efficiency was decreased. This behaviour can be explained that, all the active sites have been exhausted after 150 min and beyond this time period can damage the backbone of polysaccharide and also may promote more acrylamide homo polymerization rather than grafted copolymer [13].

Therefore, the optimum reaction time duration of 150 minutes is considered for all synthesis runs to get maximum percentage of grafting efficiency and thus proper grafted gel GG-g-Paam.

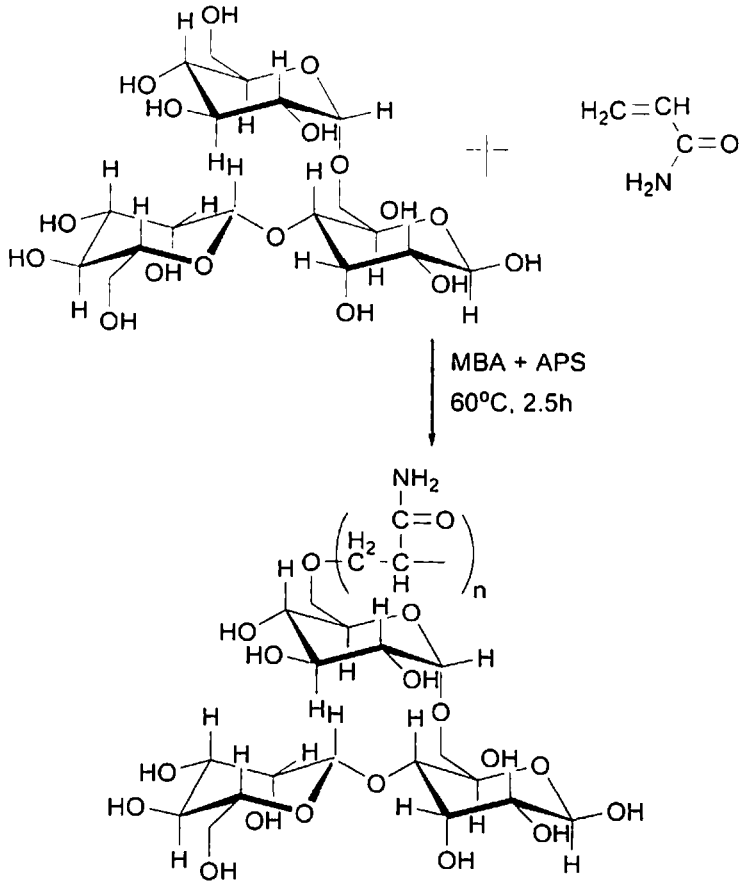

Fig. 4.10: Structure of synthesized graft polymer (GG-*g*-Paam)

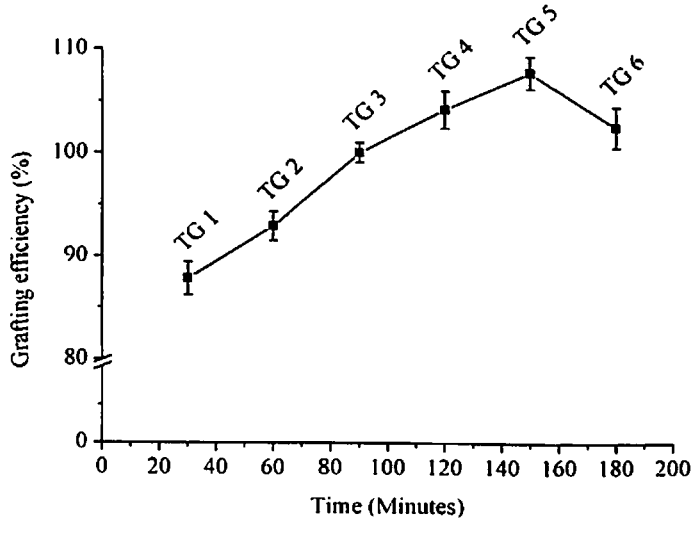

Fig. 4.11: Percentage of grafting efficiency of TGs

The ACS was also used as initiator in place of APS keeping all other synthesis parameters fixed with reaction time duration of 150 minutes. After completing the reaction till 150 minutes, no gel was formed, but the precipitation was observed at the bottom of the beaker (Fig. 4.12(a)). Afterwards, the reaction time was increased to 300

minutes keeping other parameter unaltered and the gel was visible to be formed (Fig. 4.12(b)).

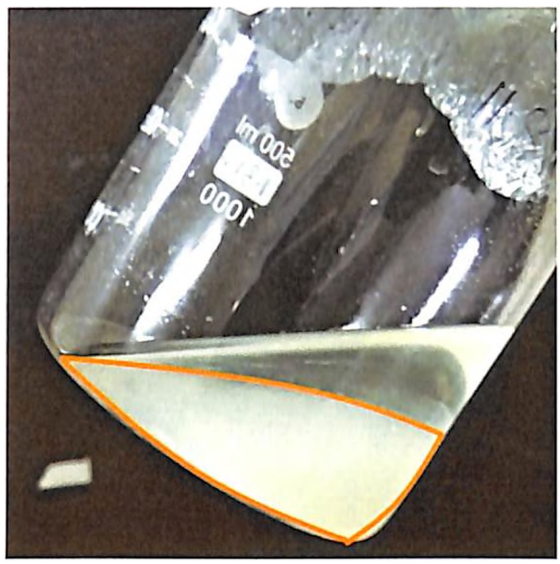

Fig. 4.12(a): Precipitation during synthesis with ACS with 150 minutes

The percentage of grafting was calculated by Eq. (4.1) and was improved upto (76.25±1.83)% than reported work [14]. Therefore, the APS was used as an alternate redox initiator in place of ACS to synthesis of all formulated gels.

Fig. 4.12(b): Gel formation with ACS with 300 minutes

4.3.2.2 Preparation of Double Cross Linked Guar Gum Grafted Polyacrylamide ($DC\text{-}GG\text{-}Paam_{GAi}$) gel

The 0.995 mmol guar gum was dissolved in 50 ml DI water and stirred for 24 hrs, followed by solution of 56 mmol of acrylamide with 10 ml DI water was added. Thereafter, mixture of 1.04 mmol MBA and 10 ml DI water was

added. The molar concentration of GA ("i") was varied from 0.80 mmol to 6.59 mmol and those were dissolved in 10 ml DI water. Each of differently concentrated GA solutions was mixed separately in separate set of experiments, to the guar and acrylamide solution containing previously mentioned same weight of APS solution was added into the reactor to initiate the grafting reaction. Dry nitrogen was bubbled through the mixture and the reactor kept sealed firmly until the complete polymerization for the optimized time period of 150 minutes. With optimized reaction time (150 min), the formulation codes of synthesized polymers with concentrations of GA variation are named as DC-GG-Paam$_{GA0.80}$, DC-GG-Paam$_{GA1.60}$, DC-GG-Paam$_{GA2.20}$, DC-GG-Paam$_{GA4.39}$ and DC-GG-Paam$_{GA6.59}$. The reproducibility of the above mentioned synthesized polymers was confirmed by the repeatable replication of polymerization. The compositions of all differently formulated polymers are given in Table 4.3.

Table 4.3. Compositions of differently formulated polymer samples

Formulation code	GG (mmol)	AAm (mmol)	MBA (mmol)	APS (mmol)	GA (mmol)	Reaction time (min)
GG-g-Paam	0.995	56.0	1.04	0.701	-	150
DC-GG-Paam$_{GA0.80}$	0.995	56.0	1.04	0.701	0.80	150
DC-GG-Paam$_{GA1.60}$	0.995	56.0	1.04	0.701	1.60	150
DC-GG-Paam$_{GA2.20}$	0.995	56.0	1.04	0.701	2.20	150
DC-GG-Paam$_{GA4.39}$	0.995	56.0	1.04	0.701	4.39	150
DC-GG-Paam$_{GA6.59}$	0.995	56.0	1.04	0.701	6.59	150

When GA was used along with MBA, an interpenetrating network (IPN) was formed, in which the GG units of different chains are linked by GA and the acrylamide units by MBA. The double cross linked IPN was expected to show more rigidity when compared to the graft system as the chains is held more tightly. The hydrophobic nature of IPN gel may get enhanced due to the involvement of free –OH groups in cross linking reaction with GA and that represented in Fig. 4.13. The structure of synthesized double cross linked (DC-GG-Paam$_{GAi}$) polymer is shown in Fig. 4.14.

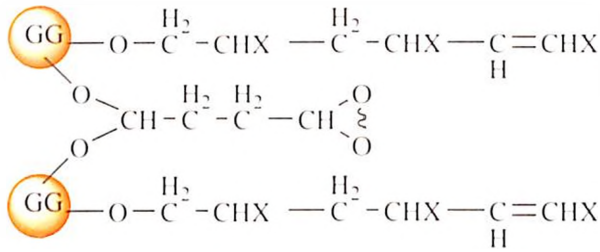

Fig. 4.13: IPN formation by cross linking with GG and GA

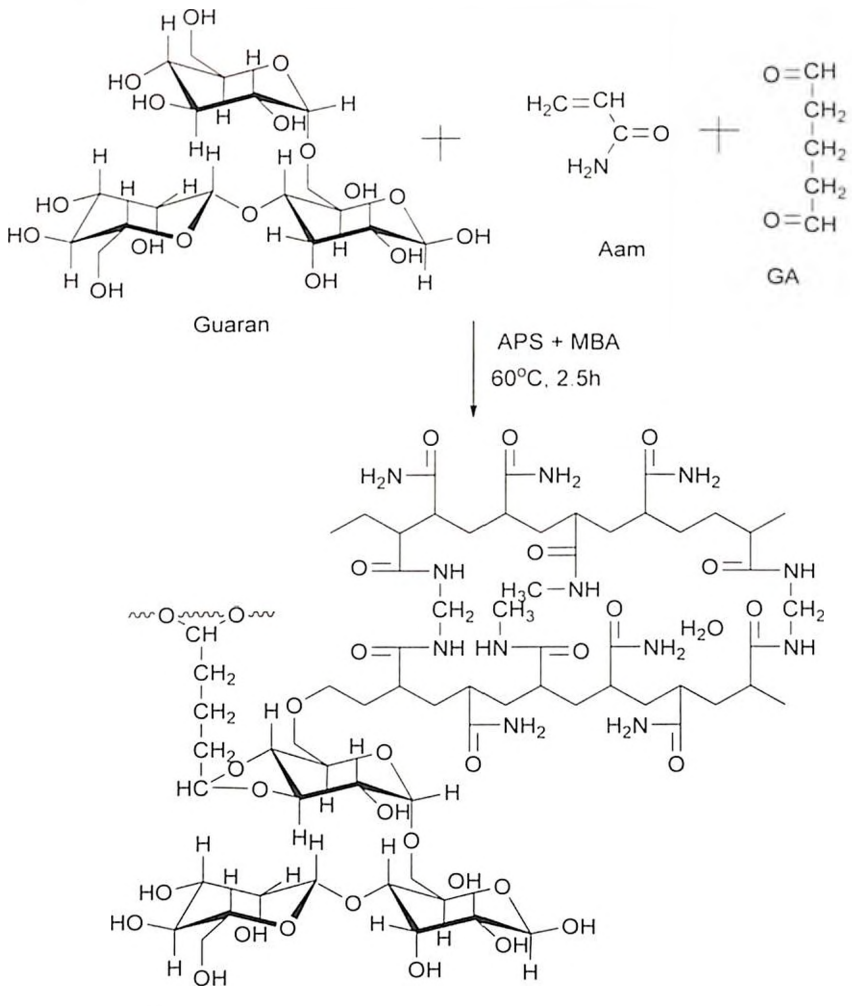

Fig. 4.14: Structure of synthesized double crosslinked (DC-GG-Paam$_{GAi}$) polymer

Polymer Purification

The gel purification process step is the most vital to remove the unreacted residues from polymer network and it was performed for both grafting and double crosslinking polymerization method. To remove the residues, the dried samples were further washed through soxhlet extractor with boiling water and ethanol at 170 °C successively. Washed samples were dried at 40 °C up to constant weight.

The final purified prepared samples were shaped in the dimension of 5mm (L) x 5mm (W) x 1mm (H) for all experimental purposes.

4.3.3 Preparation of Hydrogel Nanocomposite

AuNP reinforcement was executed in two methods: Dip method and *In-Situ* synthesis method. In Dip method, at first the 10 ml mono-dispersed AuNP solution was prepared by taking different concentration of Au(III) solution from the stock solution of $HAuCl_4$, $3H_2O$ salt. After that, 2 ml of 10^{-1} mol.ltr^{-1} CTAB solution from $5x10^{-1}$ mol.ltr^{-1} concentrated 10 ml stock solution was to each concentrated Au(III) solution as surfactant and stabilizer. Finally the Au^{3+} ions were reduced and formed Au(0) by adding 1 ml of 10^{-1} mol.ltr^{-1} $NaBH_4$ from 1 mol.ltr^{-1} concentrated 10 ml stock solution of $NaBH_4$ solution as reducing agent. After that the dry polymer with the dimension of 5mm (L) x 5mm (W) x 1mm (H) was dipped into differently concentrated AuNP solution until the weight of polymer was saturated. The reinforcement of AuNP into polymer matrix was checked by colour changing of polymer and UV-Vis spectrometer, whereas in *in-situ* method, nanoparticles were synthesized inside the polymer network. The dry polymer samples were immersed into differently concentrated Au(III) solution until its maximum and constant swelling. After that the swelled polymers with incorporated metal ion were shifted into fresh DI water. Finally the reinforced Au^{3+} ions were reduced and formed Au(0) by diffusing in 1 ml of 10^{-1} mol.ltr^{-1} $NaBH_4$ from 1 mol.ltr^{-1} concentrated 10 ml stock solution of $NaBH_4$ solution as reducing agent. In *in-situ* synthesis method, CTAB stabilizer was not added as guar gum inside the gel network acted as stabilizer and surfactant [12]. The reinforcement of AuNP into polymer matrix was checked by colour changing of polymer and UV-Vis spectrometer. In both methods just after adding reducing agent to stabilized Au(III), The yellow colour of Au(III) solution was converted to wine reddish colour. The concentrations of Au(III) solution for both methods were 1×10^{-3} mol.ltr^{-1}, $1x10^{-4}$ mol.ltr^{-1}, 3×10^{-4} mol.ltr^{-1} and 5×10^{-4} mol.ltr^{-1} to optimize the best AuNP reinforced polymer in terms of photomechanical response of polymer. Fig. 4.15(a) and Fig. 4.15(b) represent the visual appearance of mono-dispersed AuNP solution and AuNP reinforced polymer composite respectively. For preparing AuNPs, the reduction of Au^{+} or Au^{3+} salts have been accomplished in water, at room temperature, with strong

reducing agent (sodium borohydride) to "seed" particles. In dip method, CTAB was used as surfactants which acted as capping agents, bonded themselves with nanoparticles and caged them. It prevented the interaction of nanoparticles with one another (Fig 4.15(c)).

Fig. 4.15(a): Monodispersed solution of AuNP

Fig. 4.15(b): AuNP reinforced polymer composite

Nanoparticles agglomerate and lose their size and shape. But during *in-situ* method, no surfactant was used to stabilize the AuNP due to presence of guar gum as it was stabilized the nanoparticle to be agglomerated. We demonstrate that when guar gum and/or β-CD were added to gold salt solution and sodium borohydride were used together, a brown coloured colloid results from small spherical particles (Fig 4.15(d)). Before the addition of the reducing agent, the gold was in the Au^{+3} form. When the reducing agent was added, gold atoms were formed in the solution, and their concentration increased rapidly until the solution exceeded saturation. Particles then formed in a process called nucleation. The remaining dissolved gold atoms bind to the nucleation sites and growth occurred to form Au(0). Growth is defined as a process in which additional material deposits on this particle causing it to increase in size. The concentration of gold salt was selected as $1x10^{-3}$ $mol.ltr^{-1}$ and its multiplications but it was observed that the metal salt precipitated into polymer network (Fig 4.15(e)) which didn't reduced by $NaBH_4$ but when the concentration of gold salt solution was used $1x10^{-4}$ $mol.ltr^{-1}$ the gold ion was uniformly distributed into polymer network (Fig 4.15(f)). The same phenomenon was observed when the concentration of gold salt solution was used 8×10^{-4} $mol.ltr^{-1}$ and that is why the maximum concentration was kept 5×10^{-4} $mol.ltr^{-1}$.

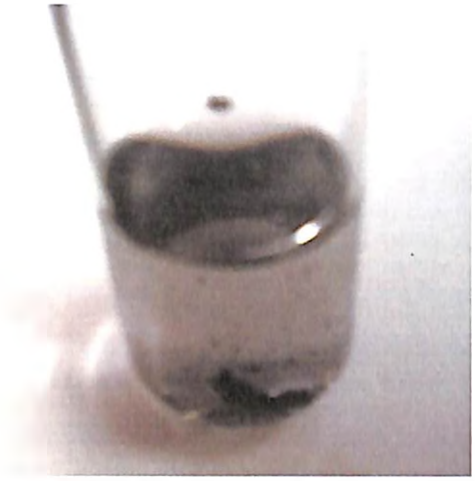

Fig. 4.15(c): Agglomerated nanoparticle without CTAB

Fig. 4.15(d): Monodispersed AuNP solution using guar gum and/or β-CD as stabilizer

Fig. 4.15(e): Precipitation of gold salt in polymer network

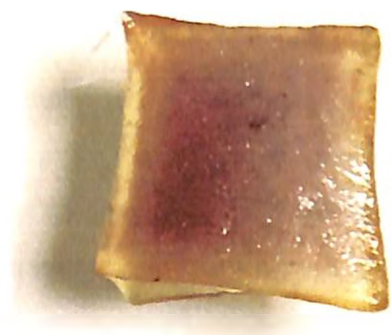

Fig. 4.15(f): Monodispersed AuNP solution using guar gum and/or β CD as stabilizer

4.4 Formulation Codes of Synthesized Gels

The synthesized gels can be coded depending on the synthesis process and variation of cross linker used. The Table 4.4 depicts the brief of formulation code of the gels.

Table. 4.4: Gel formulation code

Formulation code	Description
β-CD modified UVPTT based gels	
β-CD-g-(Paac-*co*-Paam)	IPN hydrogel
β-CD-g-(Paac-*co*-Paam)-1	β-CD modified IPN composite containing 1×10^{-4} mol.l^{-1} Au^{3+} concentration
β-CD-g-(Paac-*co*-Paam)-3	β-CD modified IPN composite containing 3×10^{-4} mol.l^{-1} Au^{3+} concentration
Guar gum modified non-UVPTT based gels	
GG-g-Paam	Guar gum modified graft gel
DC-GG-Paam$_{GA0.80}$	Guar gum modified double cross linked gel with 0.80 mmol GA

Formulation code	Description
DC-GG-Paam$_{GA1.60}$	Guar gum modified double cross linked gel with 1.60 mmol GA
DC-GG-Paam$_{GA2.20}$	Guar gum modified double cross linked gel with 2.20 mmol GA
DC-GG-Paam$_{GA4.39}$	Guar gum modified double cross linked gel with 4.39 mmol GA
DC-GG-Paam$_{GA6.59}$	Guar gum modified double cross linked gel with 6.59 mmol GA
DC-GG-Paam$_{GA4.39}$-1	Guar gum modified composite containing 1×10^{-4} mol.l^{-1} Au^{3+} concentration
DC-GG-Paam$_{GA4.39}$-3	Guar gum modified composite containing 3×10^{-4} mol.l^{-1} Au^{3+} concentration
DC-GG-Paam$_{GA4.39}$-5	Guar gum modified composite containing 5×10^{-4} mol.l^{-1} Au^{3+} concentration

4.5 Morphological Characterization

This section is intended to analyze the synthesized gels through different characterization tools. The Attenuated Total Reflectance (ATR), thermogram (DSC and TGA), Nuclear Magnetic Resonance (NMR) Spectroscopy and Environmental Scanning Electron Microscopy (ESEM) were analyzed for both β-CD modified UVPTT based gels and guar gum modified non-UVPTT gels. The ATR and NMR were performed to understand the forming of graft gels perfectly. The thermal stability was analyzed via thermogram. The pores (size) were examined through ESEM on equilibrium swelled (ES) samples. Lastly, the reinforced AuNP particle size and the density (depending on the variation of Au^{3+} concentration during synthesis) into the composite gels were investigated by Transmission Electron Microscopy (TEM).

4.5A β-Cyclodextrin Modified UVPTT Based Hydrogel

The morphological analysis of β-CD modified UVPTT IPN gel is described in below subsequent subsections.

4.5.1A Attenuated Total Reflectance (ATR)

The ATR was performed to verify the formation of β-CD-g-(Paac-*co*-Paam). The ATR spectra of Paam, β–CD and the synthesized final IPN gel are given in Fig. 4.16(a)-(b). In case of the Paam the absorption band at 3332.99 cm^{-1} (A) and 3201.83 cm^{-1} (B) are due to the asymmetric and symmetric stretching vibration bands of N–H of NH_2 group respectively [15]. The CH_2 stretching vibration band found at 2931.80 cm^{-1} (C) [16].

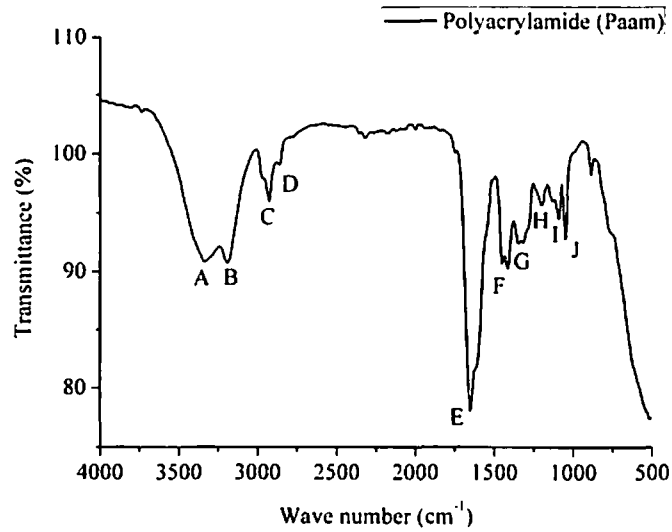

Fig. 4.16(a): ATR spectra of Polyacrylamide (Paam)

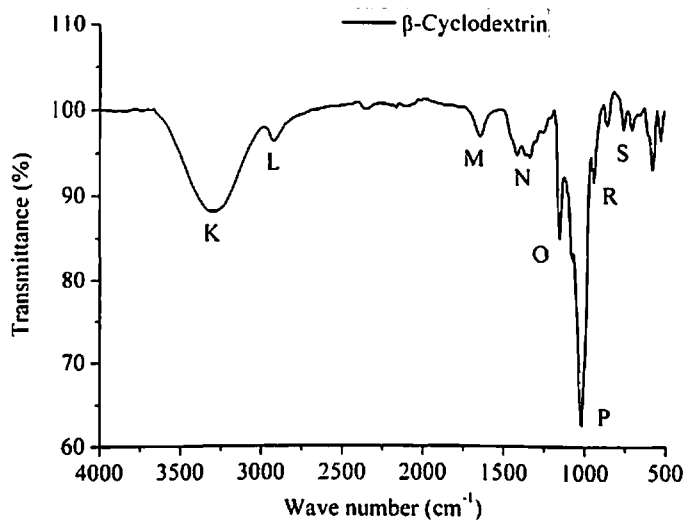

Fig. 4.16(b): ATR spectra of β-Cyclodextrin (β-CD)

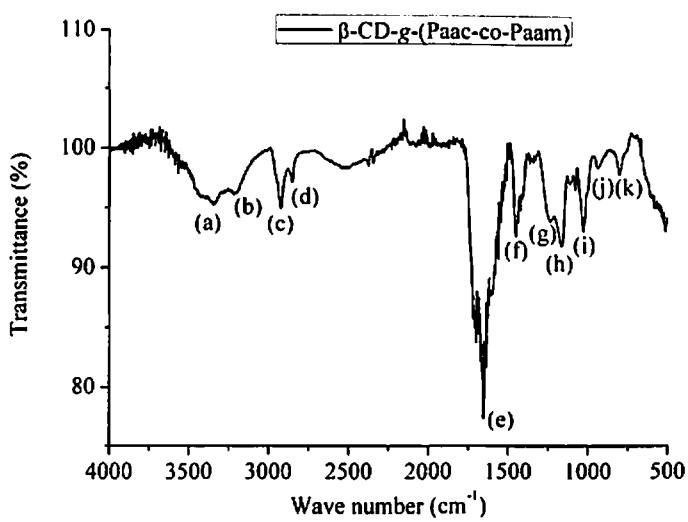

Fig. 4.16(c): ATR spectra of β-CD-g-(Paac-*co*-Paam) IPN

Two other bands around 1651.07 cm^{-1} (E) and 1419.60 cm^{-1} (F) are due to C=O stretching [17] and C–N stretching respectively [18]. In case of β-cyclodextrin (β–CD), the peaks at 3317.56 cm^{-1} (K) and 2924.09 cm^{-1} (L) are demonstrated the characteristics stretching vibration of C–OH and asymmetric vibration of $-CH_2$ [19]. The C–O–C and C–O vibrations are occurred at absorption band at 1026.13 cm^{-1} (P) and 1145.57 cm^{-1} (O) respectively [20]. For IPN gel, β-CD-g-(Paac-*co*-Paam) (Fig. 4.16(c)), band around 2924.09 cm^{-1} (c) indicates the presence of $-CH_2$ stretching vibration band of Paam [16], the absorption peak at 1155.36 cm^{-1} (h) and 1028.06 cm^{-1} (i) confirmed the presence of stretching vibration of C–O and C–O–C of β–CD [21]. The occurrence of new absorption peak at 1654.92 cm^{-1} (e) depicts the presence of stretching vibration of C=O of Paac [21], which proves the formation of interpenetrating gel network of β-CD-g-(Paac-*co*-Paam).

4.5.2A NMR-Spectroscopy

The solid state ^{13}C NMR was performed for β-CD modified UVPTT based IPN gel, (Fig.4.17).41.892 ppm and 101.540 ppm are attributed the CH_2 group and CH group from both polyacrylic acid and polyacrylamide respectively [22]. 60.035 to 103.436 ppm is a traced of β-CD [23]. The signals at 259.633 ppm and 179.988 ppm are attributed for COOH from Paac network and $-CONH_2$ group of C's from polyacrylamide network [24], which are the evidence of copolymerization of Paac and Paam. So it was seen that β-CD and Paac-co-Paam both were traced in the NMR spectra of IPN gel which confirmed the formation of β-CD-g-(Paac-*co*-Paam).

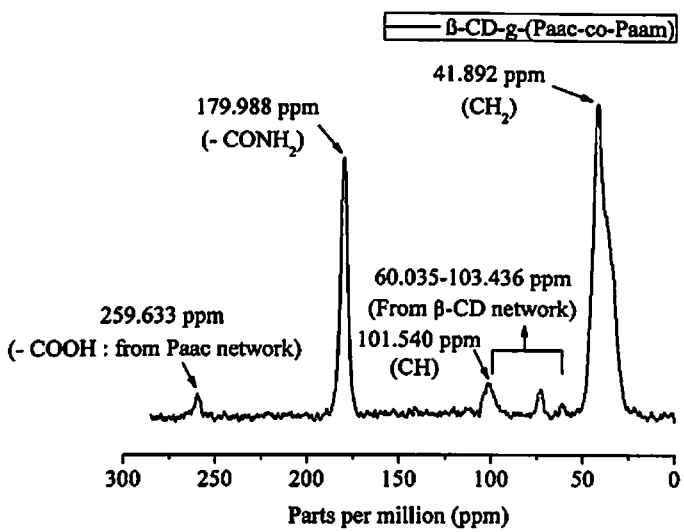

Fig. 4.17: Solid state ^{13}C NMR spectra for β-CD-g-(Paac-*co*-Paam) IPN

4.5.3A DSC Thermogram

The DSC analysis was performed to understand the thermal behaviour of the synthesized IPN hydrogel from 10 to 150 °C. The results are shown in Fig. 4.17. The DSC thermogram indicates two sharp endothermic peaks at 35.01 °C and 125.88 °C. These are attributed for phase transition [25] and glass transformation temperature [26]. A great volume phase transition occurred during swelling experiment due to the synthesized IPN exhibited a phase transition temperature at 35.01°C.

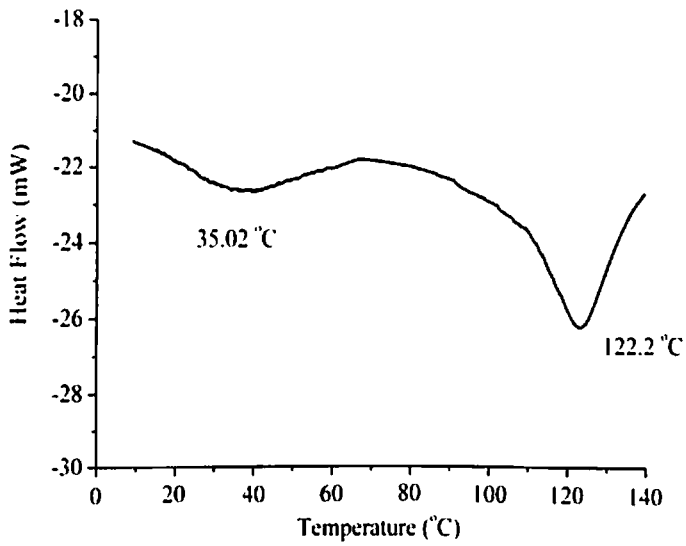

Fig. 4.18: DSC thermogram of β-CD-g-(Paac-*co*-Paam) IPN

4.5.4A Environmental SEM Analysis (ESEM)

ESEM images (Fig.4.19) was taken on all β-CD-g-(Paac-*co*-Paam) IPN to investigate the pores inside the equilibrium swelled (equilibrium swelling phenomenon is briefly described in Section 5.3 in Chapter 5) polymers. Polymer samples were prepared with the dimension of 10 mm x 10 mm x 1mm with a perfectly flat surface and were allowed to equilibrium swell in neutral buffer solution. After that samples were taken out from liquids and surface adhered liquids were blotted out.

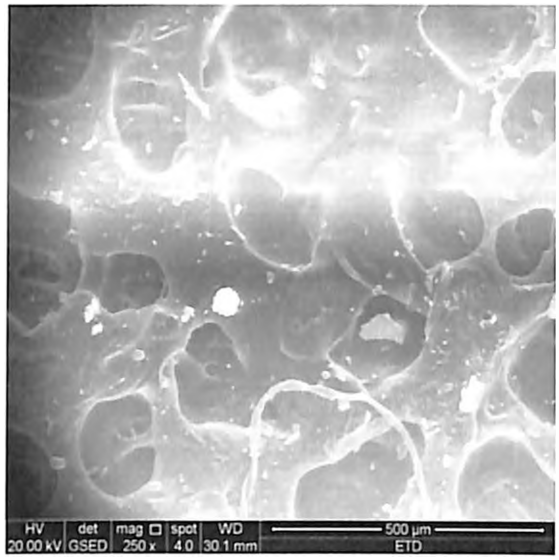

Fig. 4.19: ESEM of β-CD-g-(Paac-*co*-Paam) IPN

4.5B Guar Gum Modified Non-UVPTT Based Hydrogel

The morphological analysis of guar gum modified graft and double cross linked gels are briefly described in the below subsections.

4.5.1B Attenuated Total Reflectance (ATR)

ATR was performed to verify the grafting mechanism for acrylamide as a monomer in Fig. 4.20(a). In the case of acrylamide (Aam) monomer, the absorption band at 3352.28 cm^{-1} (A) and 3167.11 cm^{-1} (B) are due to the asymmetric and symmetric stretching vibration bands of N–H of the NH_2 groups [27]. A band at 2978.09 cm^{-1} (C) indicates the CH_2 stretching vibration [28]. The C–H stretching vibration has occurred at absorption band at 2808.35 cm^{-1} (D) [29]. Two other bands around 1658.78 cm^{-1} (E) and 1600.91 cm^{-1} (F) are due to C=O stretching [18] and N–H bending [30] respectively. The band at 1419.60 cm^{-1} (G) indicates for the C–N stretching vibrations [18]. In-plane NH_2 bending scissoring vibration and out-of-plane NH_2 wagging vibration found at absorption bands at 1346.31 cm^{-1} (H) and 1276.87 cm^{-1} (I) respectively [31]. CH_2 bending scissoring vibration happened at the absorption band of 1130.28 cm^{-1} (J) and CH_2 wagging are visible at 972.12 cm^{-1} (K) and 833.24 cm^{-1} (L) [28]. For crude guar gum (Fig. 4.20(b)), a peak at 3329.13 cm^{-1} (M) attributed to O–H stretching vibration [32] which shows the presence of a large number of hydroxyl molecule in guar backbone while the peak at 2881.65 cm^{-1} (N) corresponds to C–H stretching vibrations of the CH_2 group [13]. Additional information from the characteristic absorption bands of GG appears at 1411.89 cm^{-1}

(O) is representing the C-H bending [33]. Similarly, absorbance band at 1010.69 cm^{-1} (P) is due to O–H bending vibrations [33]. On grafting of Paam with crude GG (Fig. 4.20(c)), GG-g-Paam an additional peak observed at 3186.40 cm^{-1} (Q) (O–H stretching vibration) near to the O–H symmetric stretching band of 3329.13 cm^{-1}, which are correlated with the earlier reported work [34] and indicates that, the grafting of Paam with guar gum forming GG-g-Paam.

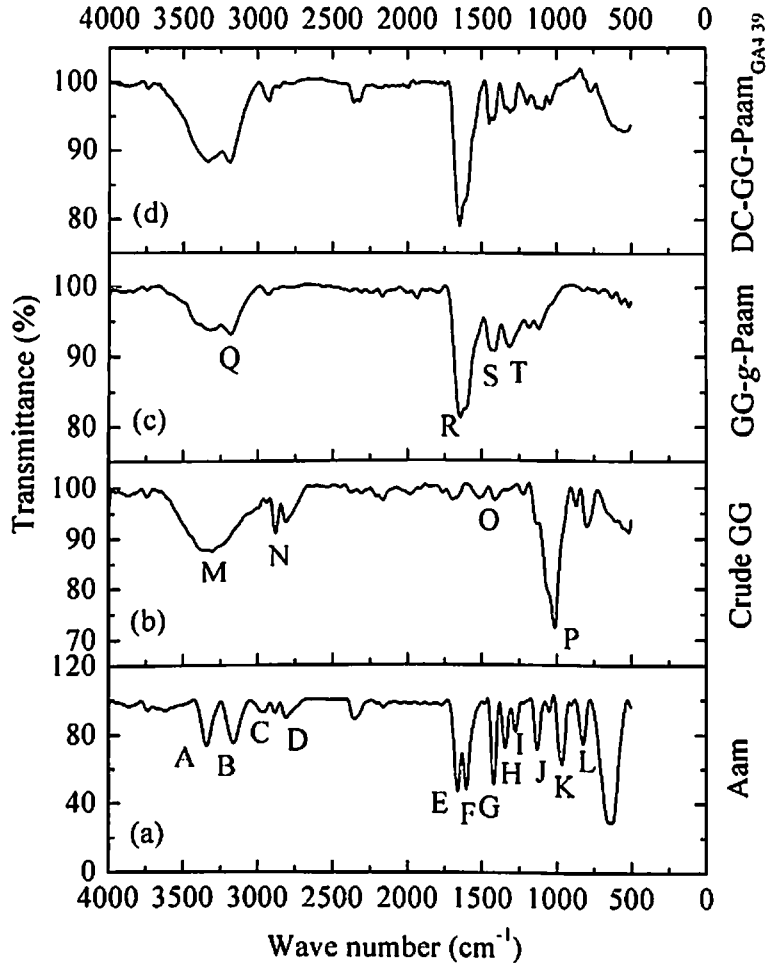

Fig. 4.20: ATR spectra of (a) acrylamide (Aam), (b) crude guar gum, (c) graft polymer (GG-g-Paam) and (d) double crosslinked polymer (DC-GG-Paam$_{GA4.39}$)

Moreover, the appearance of another band at 1643.35cm^{-1} (R) corresponds to C=O stretching vibration from Paam network [34], confirms the forming of GG-g-Paam by means of grafting of Paam with crude guar gum. A new peak 1431.18 cm^{-1} (S) depicts the dominating of Paam containing C–N stretching vibrations [35] over crude GG containing C–H bending, indicates the forming of GG-g-Paam by the grafting of Paam with crude GG. The occurrence of a new absorption band ranging 1114.86-1311.59 cm^{-1} (T) (due to the presence of ether linkage formed by –OH group of guar

gum and acrylamide [34] proves the grafting of Paam with crude guar gum. The occurrence of a new absorption band at 1311.59cm^{-1} (T) (due to In-plane NH_2 bending vibration from Paam network) [36] proves the grafting of Paam with crude guar gum. Thus, the existence of these bands in case of grafted guar gum compared to that of pure guar gum confirms the successful grafting of Paam chains on the backbone of GG. For DC-G-Paam$_{GA4.39}$ (Fig. 4.20(d)), the increases of peak intensities at 2924.09 cm^{-1} and 3356.14-3178.69 cm^{-1} are related to the C–H stretching vibration of the alkyl chain and aldehyde, which indicates GA introduced into gel network to perform successful double cross linking polymerization [37].

4.5.2B NMR-Spectroscopy

The solid state ^{13}C NMR was performed for crude guar gum (Fig. 4.21(a)), polyacrylamide (Paam) (Fig. 4.21(b)), guar gum grafted polyacrylamide (GG-*g*-Paam) (Fig. 4.21(c)) and 4.39 mmol GA containing double cross linked polymer (DC-GG-Paam$_{GA4.39}$) (Fig. 4.21(d)). In Fig. 4.21(c), the signals at 41.976 ppm and 179.986 ppm are attributed for CH_2 and $-CONH_2$ group of C's in guar gum grafted polyacrylamide (GG-*g*-Paam) network [36], which are not visible in crude guar gum spectrum (Fig. 4.21(a)) but detectable in polyacrylamide spectrum (Fig. 4.21(b)). Additionally, the signals at 70.945 ppm to 100.692 ppm are noticeable in Fig. 4.21(c) for different Cs of galactose and mannose from crude guar gum, however, the signal for C_6 of galactose and mannose at around 62.827 ppm vanishes from graft network in Fig. 4.21(c) [38].

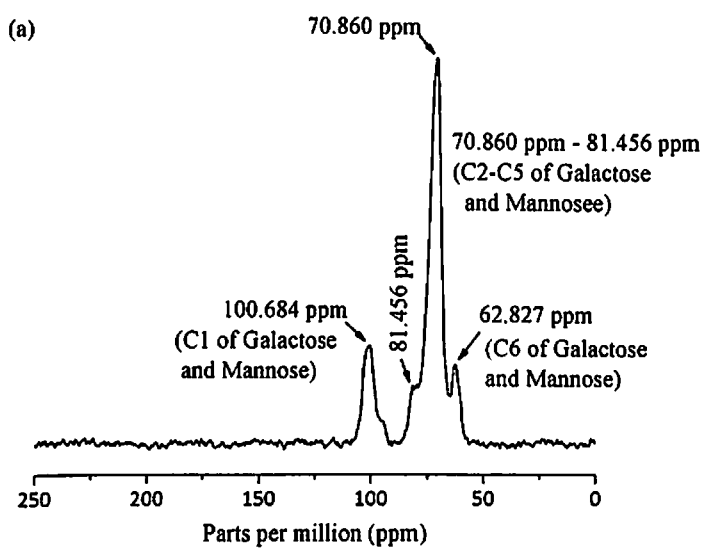

Fig. 4.21(a): Solid state ^{13}C NMR spectra for crude guar gum

Therefore, from Fig. 4.21(a)-(c), it is confirmed that, the polyacrylamide has been grafted perfectly in the backbone of crude guar gum network. Furthermore, an extra signal at 100.000 ppm found in double cross linked gel (DC-GG-Paam$_{(GA4.39)}$) network due to further cross linking of guar gum grafted polyacrylamide gel (GG-g-Paam) with glutaraldehyde to get DC-GG-Paam$_{(GA4.39}$ and hence the 2nd stage cross link happened between GG-g-Paam and DC-GG-Paam$_{(GA4.39}$.

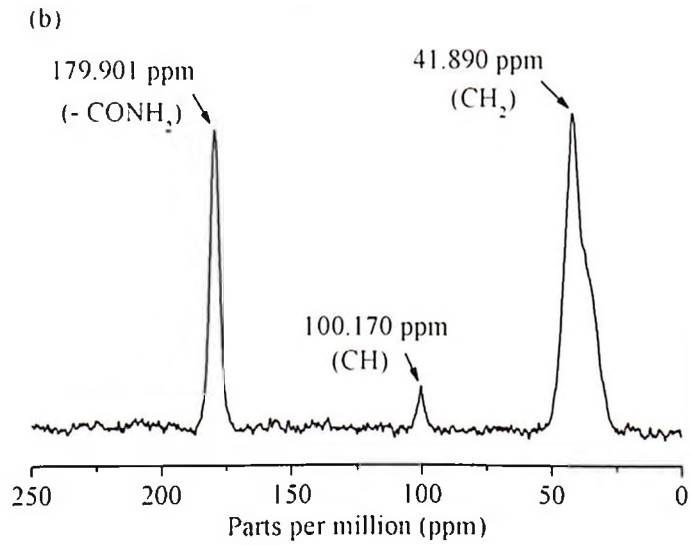

Fig. 4.21(b): Solid state ^{13}C NMR spectra for polyacrylamide (Paam)

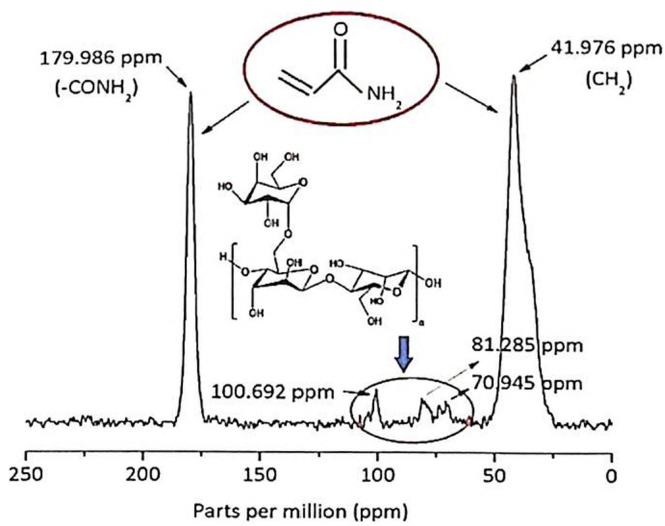

Fig. 4.21(c): Solid state ^{13}C NMR spectra for GG-g-Paam

To confirm grafting of Paam onto guar gum network, ^{1}H NMR was performed (Fig. 4.21(e)). The protons of GG network were found in the resonance range of 3.454 ppm to 5.179 ppm [39]. The hydrogen from amide group of polyacrylamide is visible at 6.067 ppm [40]. The –CH and CH_2 groups from Paam attributed at

2.079 ppm and 1.497 ppm respectively [41]. Thus successful grafting of polyacrylamide into guar gum backbone confirmed.

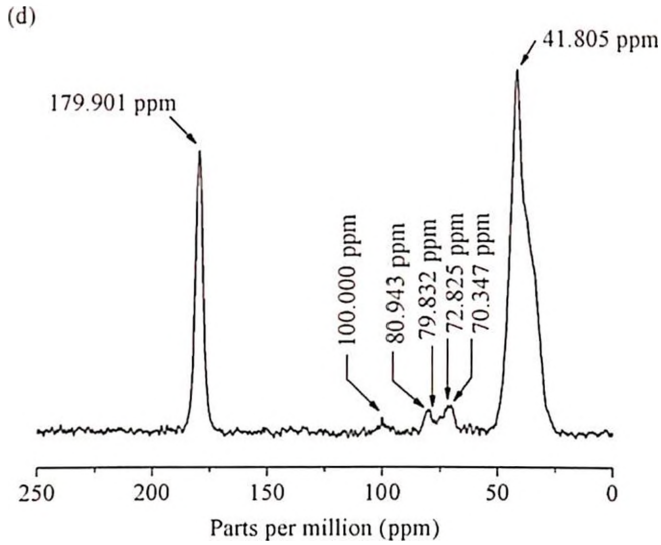

Fig. 4.21(d): Solid state ^{13}C NMR spectra for DC-GG-Paam$_{GA4.39}$

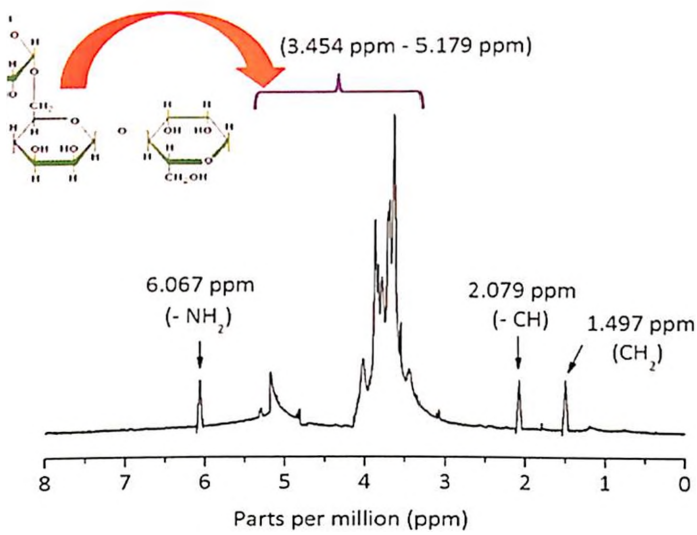

Fig. 4.21(e): ^{1}H NMR spectra for GG-g-Paam

4.5.3B. Thermal Study: DSC and TGA Analysis

The Thermal behavior of crude guar gum (GG), Acrylamide (Aam), guar gum grafted polyacrylamide (GG-g-Paam) and GA containing double crosslinked grafted polymer (DC-GG-Paam$_{GA4.39}$) were investigated through DSC (Fig. 4.22(a)-(d)) and TGA (Fig. 4.23(a)-(d)) analysis. The DSC thermogram of crude GG (Fig. 4.22(a)) indicates two endotherms at 87.78 ^{o}C and 242.59 ^{o}C and one exotherm at 309.34 ^{o}C. The first endotherm due to glass transition temperature (T_{gGG}), whereas, other two indicate

crystalline temperature $(T_{C_{GG}})$ and melting temperature $(T_{m_{GG}})$ respectively [42]. The monomer, Acrylamide (Fig. 4.22(b)) presents three events of thermal degradation. First one, a sharp endothermic peak occurs at 89.76 °C due to the glass transition temperature of acrylamide $(T_{g_{Aam}})$ for relaxation process due to the micro Brownian motion of the main chain backbone of acrylamide and then an exothermic event is observed at 148.76 °C related to the release of energy caused by mass loss where as the third event occurs at 240.09 °C in endothermic nature, is attributed to the melting temperature $(T_{m_{Aam}})$ [39].

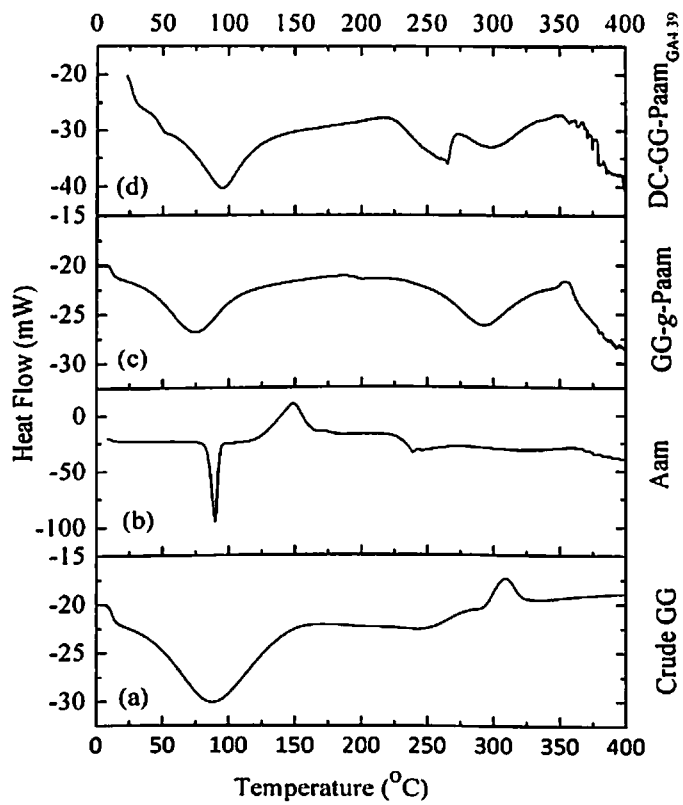

Fig. 4.22: DSC Thermogram of (a) Crude guar gum (GG), (b) Acrylamide (Aam), (c) Graft polymer (GG-*g*-Paam) and (d) Double crosslinked polymer (DC-GG-Paam$_{GA4.39}$)

Whereas, guar gum grafted polyacrylamide (GG-g-Paam) (Fig. 4.22(c)) exhibits two endothermic transitions at 74.81 °C and 293.16 °C, which are attributed to glass transition temperature $(T_{g_{GG-g-Paam}})$ and crystalline temperature $(T_{c\,GG-g-Paam})$ respectively more over lastly, an exothermic event occurred at 354.41 °C due to melting temperature $(T_{m\,GG-g-Paam})$ [43]. The higher values of crystalline temperature and melting temperature of GG-g-Paam than crude guar gum reflect the grafting interaction between carbonyl group of polyacrylamide and hydroxyl group of guar gum.

The DSC thermogram of doubly crosslinked DC-GG-Paam$_{GA4.39}$ (Fig. 4.22(d)) exhibits three endothermic transitions at 96.34 °C, 264.93 °C, and 298.64 °C. The first and third transitions are due to glass transition temperature ($T_{g_{DC-GG-PaamGA4.39}}$) and crystalline temperature ($T_{C_{DC-GG-PaamGA4.39}}$) respectively, whereas, the 2nd transition at 264.93°C may be due to cross-link effect of GA with GG-g-Paam. An exothermic event occurred at around 353.91 °C, which is attributed to melting temperature ($T_{m\ DC-GG-PaamGA4.39}$).

The higher values of glass transition temperature, crystalline temperature and melting temperature of DC-GG-Paam$_{GA4.39}$ than GG-g-Paam, signifies DC-GG-Paam$_{GA4.39}$ is much more thermally stable than graft copolymer due to double crosslinked polymerization.

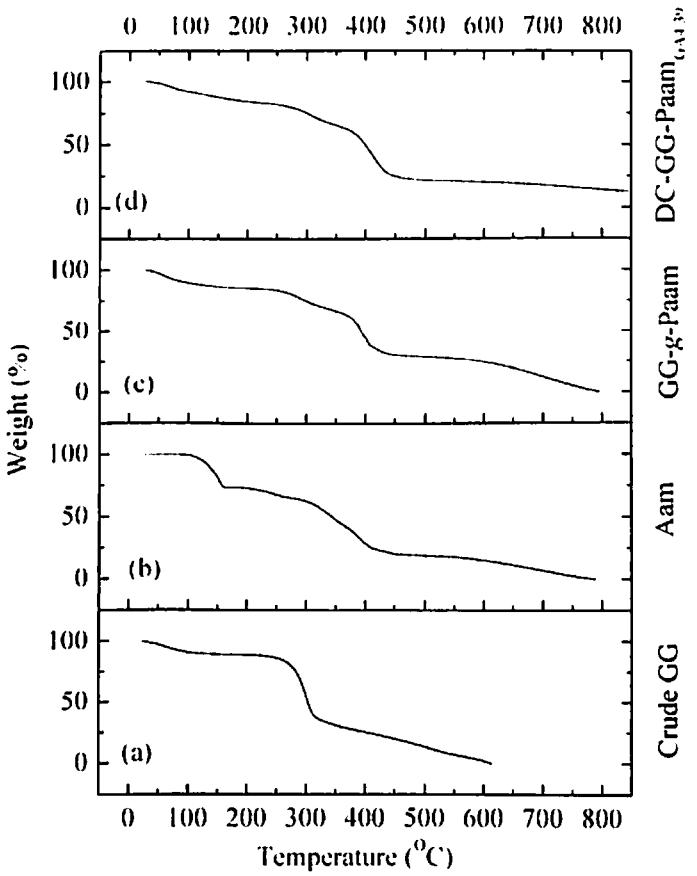

Fig. 4.23: TGA of (a) Crude guar gum (GG), (b) Acrylamide(Aam), (c) Graft polymer (GG-*g*-Paam) and (d) GA containing double crooslinked polymer (DC-GG-Paam$_{GA4.39}$)

In contrast to TGA, Fig. 4.23(d), DC-GG-Paam$_{GA4.39}$ degrades 87% of its weight at 824.65 °C. Whereas up to 99.5% weight loss happened for both crude guar gum and GG-g-Paam at 609.5 °C and 787.5 °C [13] respectively, which confirmed GA containing double cross-linked grafted polymer (DC-GG-Paam$_{GA4.39}$) is much more thermally stable than crude guar gum and acrylamide grafted copolymer (GG-g-Paam).

4.5.3B Environmental SEM Analysis (ESEM)

ESEM images (Fig.4.24(a)-(f)) were taken on all formulated guar gum modified gels to investigate the spatial changes of pores inside the equilibrium swelled (equilibrium swelling phenomenon is briefly described in Section 5.3 in Chapter 5) polymers. Polymer samples were prepared with the dimension of 10mm x 10mm x 5mm with a perfectly flat surface and were allowed to equilibrium swell in neutral buffer solution. After that samples were taken out from liquids and surface adhered liquids were blotted out.

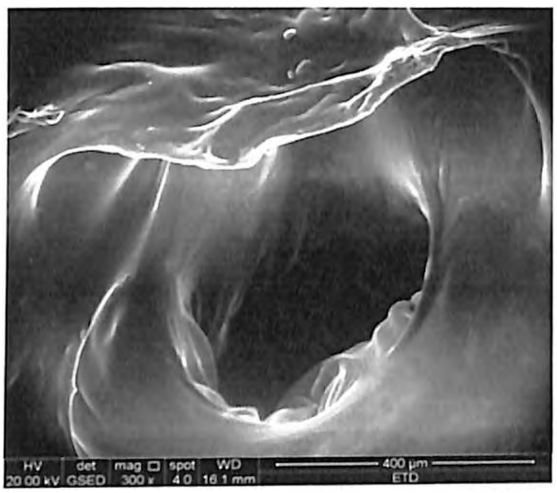

Fig. 4.24(a): ESEM image of GG-g-Paam

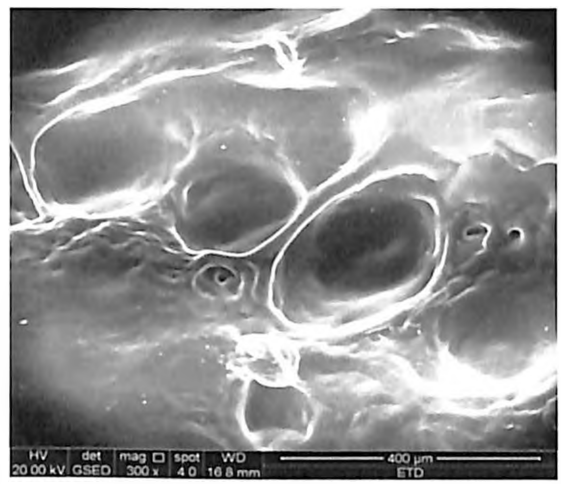

Fig. 4.24(b): ESEM image of DC-GG-Paam$_{GA0.80}$

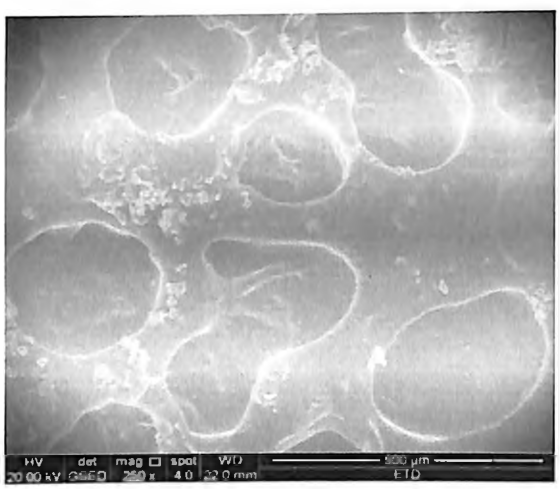

Fig. 4.24(c): ESEM image of DC-GG-Paam$_{GA1.60}$

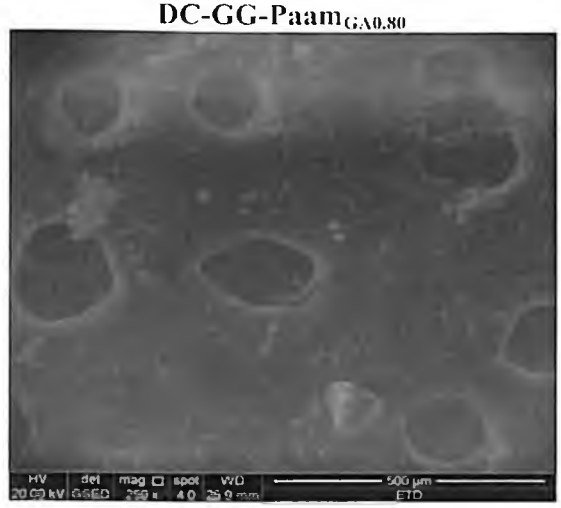

Fig. 4.24(d): ESEM image of DC-GG-Paam$_{GA2.20}$

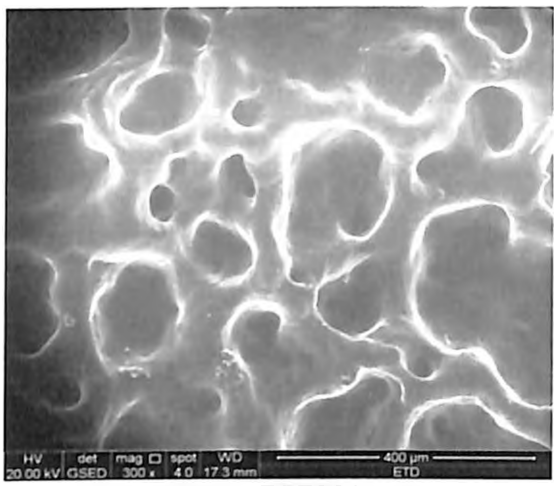

Fig. 4.24(e): ESEM image of DC-GG-Paam$_{GA4.39}$

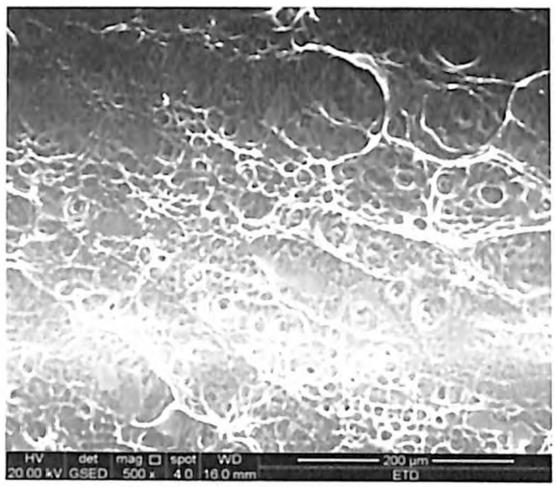

Fig. 4.24(f): ESEM image of DC-GG-Paam$_{GA6.59}$

The largest pore size found in graft gel and the pore sizes were reduced with intensifying the GA concentration into the synthesized gels.

4.6 Morphological Characterization of Gel Nanocomposites

The Transmission Electron Microscopy (TEM) and UV-vis Spectroscopy were performed for both UVPTT and non-UVPTT based composites. The Fig. 4.25(a)-(b) depicts the TEM micrograph of β-CD-g-(Paac-*co*-Paam)-1 and β-CD-g-(Paac-*co*-Paam)-3 UVPTT based composites. TEM was performed in FEI Technai G2 with 200KeV having LaB_6 filament. The ultrathin carbon coated 300-mesh Cu grids (Ted Pella. Inc, USA) were subjected to glow discharge treatment at atmospheric conditions. The Fig.4.26(a)-(c) depicts the TEM micrograph of DC-GG-Paam$_{GA4.39}$-1, DC-GG-Paam$_{GA4.39}$-3 and DC-GG-Paam$_{GA4.39}$-5 non-UVPTT based composites. From TEM images for all composites and it was found that the size of the particle was below 20nm. The structure of particle was spherical but the distribution of nanoparticles was non-uniform and that because of non-uniform pore sizes which allowed the gold salt solution. As the molar concentration of gold salt was increased, the concentration of AuNP was also increased. The particle size distribution was analyzed by Malvern Zeta Sizer 6.1 and it was found that the diameter of AuNP was in the range of 2-10 nm Fig. 4.26(d). Fig. 4.26(e)-(f) depicts the UV-vis spectra for both UVPTT and non-UVPTT composites. For both of the polymer it was seen that, the UV-vis absorbance is increased with the elevating concentration of AuNP. The Photo absorbance of both polymer was within 500nm to 550nm. For this reason the photo mechanical action of polymers was observed vu using 530nm visible laser source.

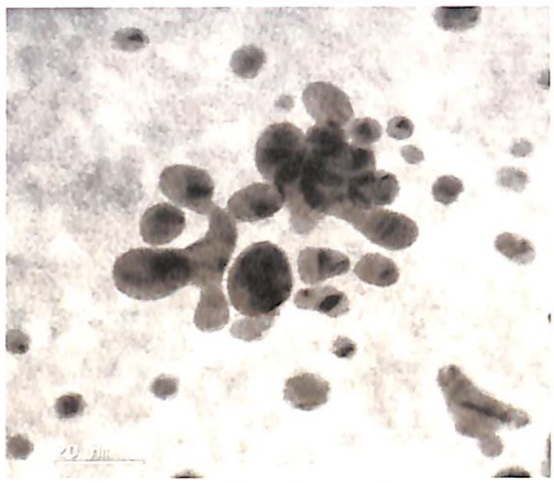

Fig. 4.25(a): TEM of β-CD-g-(Paac-*co*-Paam)-1 composite

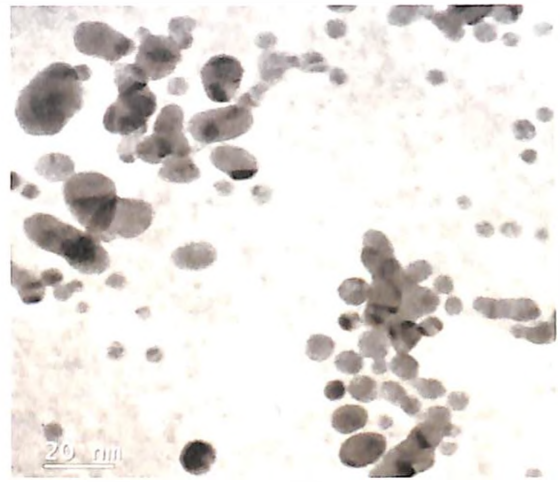

Fig. 4.25(b): TEM of β-CD-g-(Paac-*co*-Paam)-3 composite

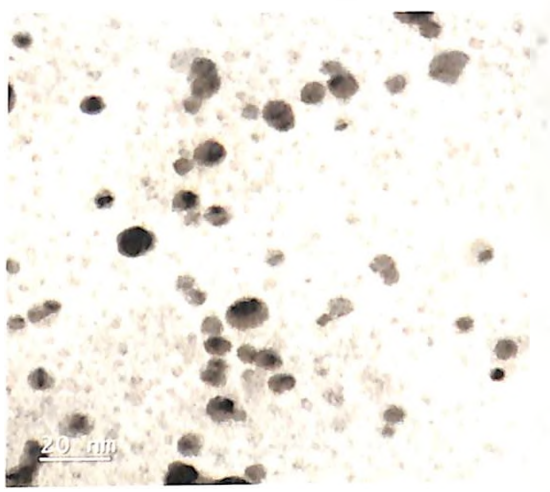

Fig. 4.26(a): TEM of DC-GG-Paam$_{GA4.39}$-1 composite

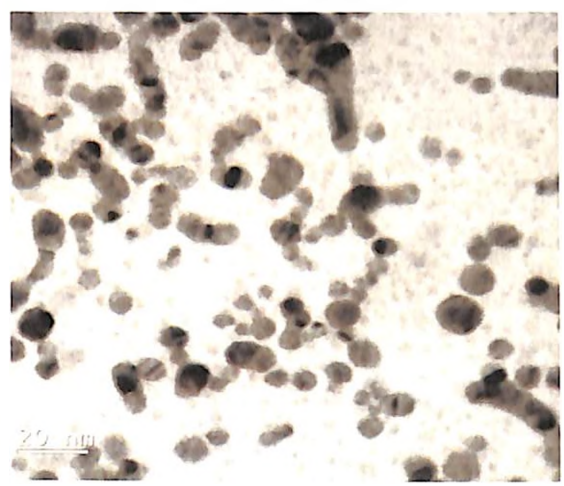

Fig. 4.26(b): TEM of DC-GG-Paam$_{GA4.39}$-3 composite

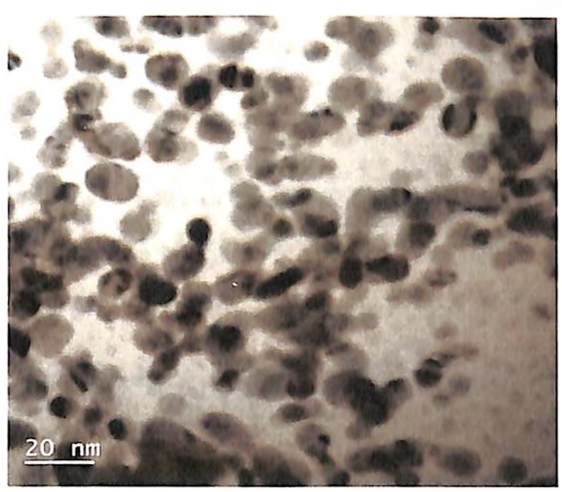

Fig. 4.26(c): TEM of DC-GG-Paam$_{GA4.39}$-5 composite

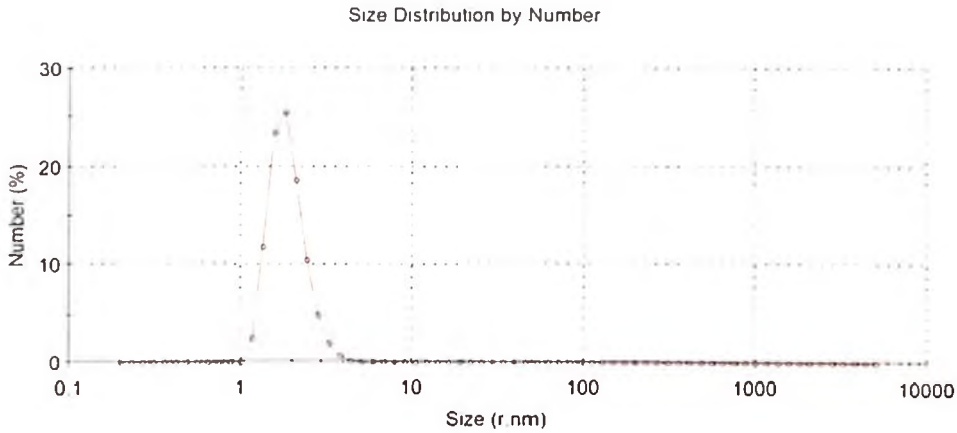

Fig. 4.26(d):AuNP size distribution of polymer composites

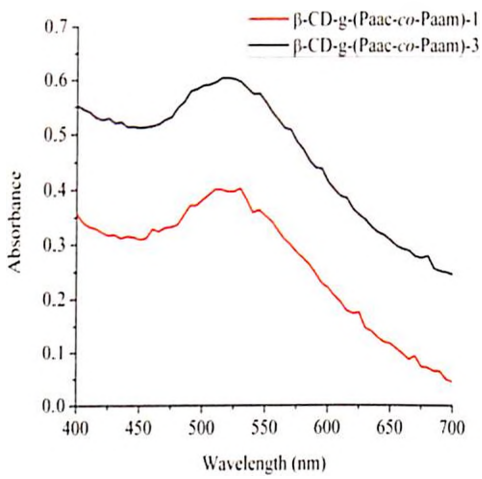

Fig. 4.26(e): UV-vis Spectra of β-CD-g-(Paac-*co*-Paam) composites

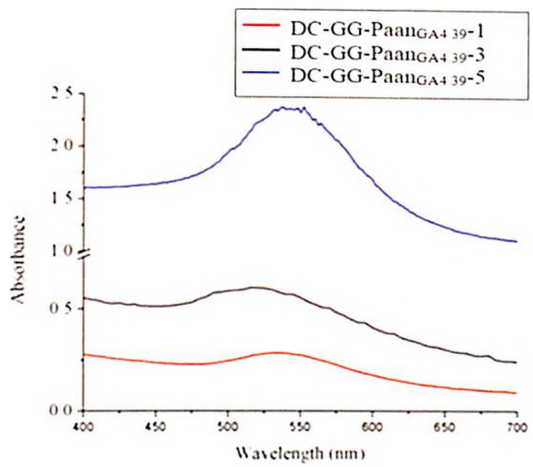

Fig. 4.26(f): UV-vis Spectra of DC-GG-Paam$_{GA4.39}$ composites

4.7 Stability in Acidic Medium

The UVPTT and non-UVPTT samples were equilibrium swelled in 1mM HCl solution at room temperature and washed properly in ethanol. Finally the prepared sample dried for ATR characterization. For β-CD modified IPN gel (Fig. 4.27), the absorption bands at 3336.28 cm^{-1} (a') and 3202.62 cm^{-1}(b') are due to the asymmetric and symmetric stretching vibration bands of N–H of NH_2 group respectively. The $-CH_2$ stretching vibration band found at 2925.29 cm^{-1} (c'). Two other bands around 1654.92 cm^{-1} (e') isobtained due to C=O stretching. The absorption peak at 1155.36 cm^{-1} (h') and 1027.27 cm^{-1} (i') confirmed the presence of stretching vibration of C–O and C–O–C. The ATR spectra of acid hydrolysed β-CD modified IPN (β-CD-g-(Paac-*co*-Paam)) shows the identical as without hydrolysedgel (Fig. 4.16(b)), this confirm that there is no

chemical changes in gel network on acid hydrolysis. Thus, the β-CD-g-(Paac-*co*-Paam) sample is stable in acidic medium. Similarly, the ATR sprectra for acid hydrolyzed guar gum modified non-UVPT based graft gel (GG-g-Paam) and the double cross linked (DC-GG-Paam$_{(GA4.39)}$) (Fig 4.28) gels made available all the functional absorption bands at identical wavenumbers as described in Fig. 4.20(c)-(d). Therefore, both graft and double cross linked guar gum modified non-UVPTT gels have the stability in acidic environment also.

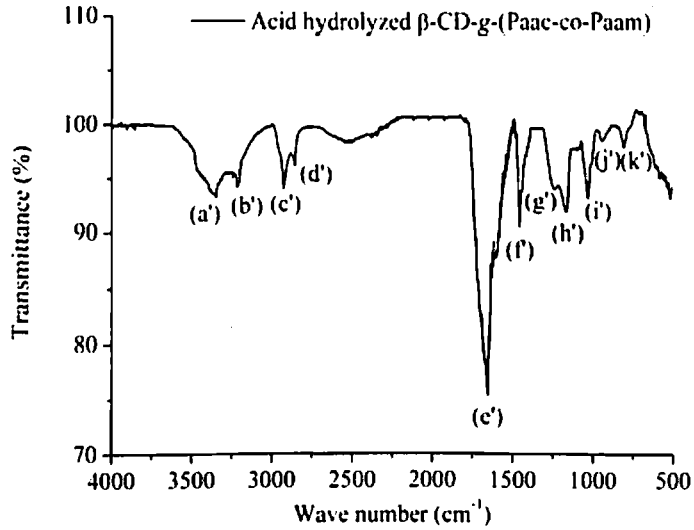

Fig. 4.27: ATR spectra of IPN β-CD-g-(Paac-*co*-Paam)

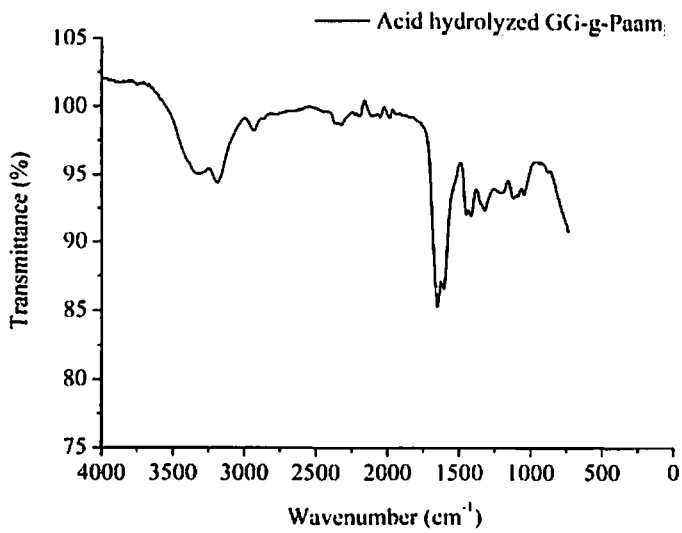

Fig. 4.28(a): ATR Spectra of acid hydrolyzed GG-g-Paam

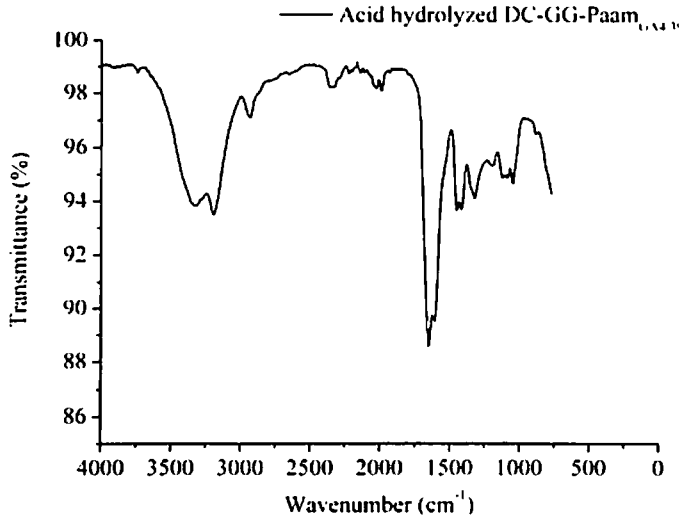

Fig. 4.28(b): ATR Spectra of acid hydrolyzed DC-GG-Paam$_{GA4.39}$

4.8 Conclusions

This chapter described the synthesis process and mechanism for both UVPTT based β-cyclodextrin modified positive hydrogel and the non-UVPTT based guar gum based positive hydrogel. Grafting of natural saccharide to synthetic polymer is a foremost step to modify the synthetic gel. Some researchers offered less than 100% grafting efficiency. For instances, Sen *et al.* [13] reported the grafting efficiency 23%-58%, Gowrav *et al.* [34] showed the grafting efficiency from 60.1%-84.3%, Agüeros *et al.* [44] reported 91.3±3.1% grafting efficiency, Zeng *et al.* [45] synthesized the microsphere with 20% grafting efficiency, Shahid *et al.* [46] observed 22% to 55% grafting efficiency. The current research improved the grafting efficiency upto 101.59±8.46% and 107.48±1.53% for UVPTT and non-UVPTT based graft gels respectively, in contrast with the aforementioned researches. Higher grafting efficiency eliminated the possibilities to presence of synthetic monomers in the gel network. Further, the APS and ACS initiators were used during grafting of non-UVPTT based graft gel to examine the higher grafting efficiency. The grafting efficiency of 76.25±1.83% observed in case of ACS initiator (with a reaction time duration of 300minutes) than reported grafting efficiency 65.34% [14].

The morphological characterization was performed after synthesizing both the UVPTT based and non-UVPTT positive hydrogels. The DSC thermogram for UVPTT based β-CD modified IPN gel showed phase transition temperature and glass transition temperature at 35.02 °C and 125.88 °C respectively.

In case of non-UVPTT based guar gum modified gels are more thermally stable with containing of the higher percentage GA concentration and the minimum glass transition temperature of 74.81 °C was found for guar gum based graft gel, whereas, 96.34°C glass transition temperature was observed for DC-GG-Paam$_{GA4.39}$ gel.

The ATR and solid state ^{13}C NMR confirmed the grafting and cross linking performance for both the synthesized positive hydrogels. The polymer–AuNp composite with variable concentration of gold for both UVPTT based and non-UVPTT positive hydrogels was also successfully prepared which was confirmed by TEM analysis. The next chapter will be focused on the experimental activities under different conditions.

References

[1] S. Sinnwell and H. Ritter, 'Recent Advances in Microwave-Assisted Polymer Synthesis', *Aust. J. Chem.*, vol. 60, no. January, pp. 729–743, 2007.

[2] J. M. Irache, L. Bergougnoux, I. Ezpeleta, J. Gueguen, and A. M. Orecchioni, 'Optimization and in vitro stability of legumin nanoparticles obtained by a coacervation method', *Int. J. Pharm.*, vol. 126, no. 1–2, pp. 103–109, 1995.

[3] N. Jawahar and M. Sn, 'Polymeric nanoparticles for drug delivery and targeting : A comprehensive review', *Int. J. Heal. Allied Sci.*, vol. 1, no. 4, pp. 217–223, 2012.

[4] A. M. Mathur, S. K. Moorjani, and A. B. Scranton, 'Methods for Synthesis of Hydrogel Networks : A Review', *J. Macromol. Sci. Part C*, vol. 36, no. 2, pp. 405–430, 1996.

[5] K. R. Park and Y. C. Nho, 'Synthesis of PVA / PVP hydrogels having two-layer by radiation and their physical properties', *Radiat. Phys. Chem.*, vol. 67, pp. 361–365, 2003.

[6] J. M. Rosiak, I. P. Ulanski, L. A. Pajewski, F. Yoshi, and K. Makuuchi, 'Radiation formation of hydrogels for biomedical purposes. Some remarks and comments', *Radiat. Phys. Chem.*, vol. 46, no. 2, pp. 161–168, 1995.

[7] P. A. G. Soares, A. I. Bourbon, A. A. Vicente, C. A. S. Andrade, W. B. Jr., M. T.S. Correia, A. P. Jr., M. G. Carneiro-da-Cunha 'Development and characterization of hydrogels based on natural polysaccharides : Policaju and chitosan', *Mater. Sci. Eng. C*, vol. 42, pp. 219–226, 2014.

[8] M. K Younis., A. Z Tareq, 'Optimization Of Swelling , Drug Loading And Release From Natural Polymer Hydrogels', *IOP Conf. Ser. Mater. Sci. Eng.*, vol. 454, no. 012017, pp. 1–15, 2018.

[9] V. Mishra and R. Kumar, 'Living radical polymerization: A review', *J. Sci. Res.*, vol. 56, pp. 141–176, 2012.

[10] G. Moad, J. Chiefari, R. T.A. Mayadunne, C. L. Moad, A. Postma, E. Rizzardo, S. H. Thang 'Initiating free radical polymerization', *Macromol. Symp.*, vol. 182, pp. 65–80, 2002.

[11] K. Matyjaszewski and J. Spanswick, 'Controlled / living radical polymerization', *Mater. Today*, vol. 8, no. 3, pp. 26–33, 2005.

[12] K. E. Lee, T. L. Goh, and N. Simon, 'Response surface modeling of polyacrylamide redox polymerization', *Int. J. ChemTech Res.*, vol. 7, no. 6, pp. 2697–2710, 2015.

[13] G. Sen, S. Mishra, U. Jha, and S. Pal, 'Microwave initiated synthesis of polyacrylamide grafted guar gum (GG-g-PAM)— Characterizations and application as matrix for controlled release of 5-amino salicylic acid', *Int. J. Biol. Macromol.*, vol. 47, no. 2, pp. 164–170, 2010.

[14] P. Chowdhury, S. Samui, T. Kundu, and M. M. Nandi, 'Graft polymerization of methyl methacrylate onto guar gum with ceric ammonium sulfate/dextrose redox pair', *J. Appl. Polym. Sci.*, vol. 82, pp. 3520–3525, 2001.

[15] M. A. Moharram, S. M. Rabie, and H. M. El-Gendy, 'Infrared spectra of γ-irradiated poly(acrylic acid)-polyacrylamide complex', *J. Appl. Polym. Sci.*, vol. 85, no. 8, pp. 1619–1623, 2002.

[16] S. A. Asgharzadehahmadi, I. I. Muhamad, N. Khairuddin, D. N. A. Zaidel, and E. Supriyanto, 'Synthesis and Characterization of Polyacrylamide Based Hydrogel Containing Magnesium Oxide Nanoparticles for Antibacterial Applications', *Int. J. Biol. Biomed. Eng.*, vol. 7, no. 3, pp. 108–113, 2013.

[17] S. Nesrinne and A. Djamel, 'Synthesis , characterization and rheological behavior of pH sensitive poly (acrylamide-co-acrylic acid) hydrogels', *Arab. J. Chem.*, vol. 10, no. 7, pp. 539–547, 2017.

[18] A. S. G. Magalhães, M. P. A. Neto, M. N. Bezerra, N. M. P. S. Ricardo, and J. P. A. Feitosa, 'Application of ftir in the determination of acrylate content in poly(sodium acrylate-CO-acrylamide) superabsorbent hydrogels', *Quim. Nova*, vol. 35, no. 7, pp. 1464–1467, 2012.

[19] S. Selvam, B. Balamuralitharan, S. N. Karthick, A. Dennyson Savariraj, K. V. Hemalatha, S. K. Kima and H. J. Kim 'Novel high-temperature supercapacitor combined dye sensitized solar cell from a sulfated β-cyclodextrin/PVP/$MnCO_3$ composite', *J. Mater. Chem. A*, vol. 3, no. 19, pp. 10225–10232, 2015.

[20] M. B. Povea, W. A. Monal, J. V. Cauich-Rodríguez, A. M. Pat, N. B. Rivero, and C. P. Covas, 'Interpenetrated Chitosan-Poly(Acrylic Acid-Co-Acrylamide) Hydrogels. Synthesis, Characterization and Sustained Protein Release Studies', *Mater. Sci. Appl.*, vol. 02, no. 06, pp. 509–520, 2011.

[21] H. Rachmawati, C. A. Edityaningrum, and R. Mauludin, 'Molecular inclusion complex of curcumin-β-cyclodextrin nanoparticle to enhance Curcumin skin permeability from hydrophilic matrix gel', *AAPS PharmSciTech*, vol. 14, no. 4, pp. 1303–1312, 2013.

[22] S. Maeda, Y. Fujiwara, C. Sasaki, and K. K. Kunimoto, 'Structural analysis of microbial poly(ε-L-lysine)/poly(acrylic acid) complex by FT-IR, DSC, and solid-state 13C and 15N NMR', *Polym. J.*, vol. 44, no. 2, pp. 200–203, 2012.

[23] T. Endo, H. Nagase, H. Ueda, S. Kpbayashi, and T. Nagai, 'Isolation, Purification and Characterization of Cyclomaltodecaose, Cyclomaltoundecaose, Cyclomaltotridecaose', *Chem. Pharm. Bull.*, vol. 45, no. 3, pp. 532–536, 1997.

[24] S. Kaity, J. Isaac, P. M. Kumar, A. Bose, T. W. Wong, and A. Ghosh, 'Microwave assisted synthesis of acrylamide grafted locust bean gum and its application in drug delivery', *Carbohydr. Polym.*, vol. 98, no. 1, pp. 1083–1094, 2013.

[25] H. Dai, Q. Chen, H. Qin, Y. Guan, D. Shen, Y. Hua, Y. Tang, J. Xu 'A temperature-responsive copolymer hydrogel in controlled drug delivery', *Macromolecules*, vol. 39, no. 19, pp. 6584–6589, 2006.

[26] Y. Xu, O. Ghag, M. Reimann, P. Sitterle, P. Chatterjee, E. Nofen, H. Yu, H. Jiang , L. L. Dai 'Development of visible-light responsive and mechanically enhanced "smart" UCST interpenetrating network hydrogels', *Soft Matter*, vol. 14, no. 1, pp. 151–160, 2018.

[27] G. Craciun, D. Ighigeanu, E. Manaila, and M. D. Stelescu, 'Synthesis and characterization of Poly(Acrylamide-Co-Acrylic Acid) flocculant obtained by electron beam irradiation', *Mater. Res.*, vol. 18, no. 5, pp. 984–993, 2015.

[28] R. Murugan, S. Mohan, and A. Bigotto, 'FTIR and Polarised Raman Spectra of Acrylamide and Polyacrylamide', *J. Korean Phys. Soc.*, vol. 32, no. 4, pp. 505–512, 1998.

[29] J. Šebek, R. Knaanie, B. Albee, E. O. Potma, and R. B. Gerber, 'Spectroscopy of the C-H stretching vibrational band in selected organic molecules', *J. Phys. Chem. A*, vol. 117, no. 32, pp. 7442–7452, 2013.

[30] D. Mishra, M. Nagpal, and S. Singh, 'Superporous hybrid hydrogels based on polyacrylamide and chitosan: Characterization and in vitro drug release', *Int. J. Pharm. Investig.*, vol. 3, no. 2, p. 88, 2013.

[31] M. E. Mohamed and A. M. A. Mohammed, 'Experimental and Computational Vibration Study of Amino Acids', *Int. Lett. Chem. Phys. Astron. ISSN*, vol. 10, no. 1, pp. 1–17, 2013.

[32] X. Wan, Y. Li, X. Wang, S. Chen, and X. Gu, 'Synthesis of cationic guar gum-graft-polyacrylamide at low temperature and its flocculating properties', *Eur. Polym. J.*, vol. 43, no. 8, pp. 3655–3661, 2007.

[33] S. S. Prasad, K. M. Rao, P. R. S. Reddy, N. S. Reddy, K. S. V. K. Rao, and M. C. S. Subha, 'Synthesis and Characterisation of Guar Gum-g-Poly (Acrylamidoglycolic acid) by Redox Initiator', *Indian J. Adv. Chem. Sci.*, vol. 1, pp. 28–32, 2012.

[34] M. P. Gowrav, U. Hani, H. G. Shivakumar, R. A. M. Osmani, and A. Srivastava,

'Polyacrylamide grafted guar gum based glimepiride loaded pH sensitive pellets for colon specific drug delivery: Fabrication and characterization', *RSC Adv.*, vol. 5, no. 97, pp. 80005–80013, 2015.

[35] P. B. Kajjari, L. S. Manjeshwar, and T. M. Aminabhavi, 'Novel interpenetrating polymer network hydrogel microspheres of chitosan and poly(acrylamide)- grafted - guar gum for controlled release of ciprofloxacin', *Ind. Eng. Chem. Res.*, vol. 50, no. 23, pp. 13280–13287, 2011.

[36] K. Dutta, B. Das, D. Mondal, A. Adhikari, and D. Rana, 'An ex situ approach to fabricating nanosilica reinforced polyacrylamide grafted guar gum nanocomposites as an efficient biomaterial for transdermal drug delivery application', *New J. Chem.*, vol. 41, pp. 9461–9471, 2017.

[37] Y. Pan, C. Peng, W. Wang, K. Shi, Z. Liu, and X. Ji, 'Preparation and absorption behavior to organic pollutants of macroporous hydrophobic polyvinyl alcohol-formaldehyde sponges', *RSC Adv.*, vol. 4, no. 67, pp. 35620–35628, 2014.

[38] C. K. S. V Poorna, A. Singh, A. Rathore, and A. Kumar, 'Novel cross linked guar gum-g-poly(acrylate) porous superabsorbent hydrogels: characterization and swelling behaviour in different environments', *Carbohydr. Polym.*, 2016.

[39] J. Gao and B. P. Grady, 'Reaction Kinetics and Subsequent Rheology of Carboxymethyl Guar Gum Produced from Guar Splits', *Ind. Eng. Chem. Res.*, vol. 57, no. 22, pp. 7345–7354, 2018.

[40] A. H. Liu, S. Z. Mao, M.L. Liu, Y. X. Zhang, F. P. Wu, M. Z. Li, E. J. Wang, G. Z. Cheng, Y. R. Du '^{1}H NMR study on microstructure of a novel acrylamide/methacrylic acid template copolymer in aqueous solution', *Colloid Polym. Sci.*, vol. 285, no. 4, pp. 381–388, 2007.

[41] A. M. Al-Sabagh, N. G. Kandile, R. A. El-Ghazawy, M. R. Noor El-Din, and E. A. El-sharaky, 'Synthesis and characterization of high molecular weight hydrophobically modified polyacrylamide nanolatexes using novel nonionic polymerizable surfactants', *Egypt. J. Pet.*, vol. 22, no. 4, pp. 531–538, 2013.

[42] A. Kumar, A. De, and S. Mozumdar, 'Synthesis of acrylate guar-gum for delivery of bio-active molecules Synthesis of acrylate guar-gum for delivery of bio-active molecules', no. March, 2016.

[43] D. Mudgil, S. Barak, and B. S. Khatkar, 'X-ray diffraction, IR spectroscopy and thermal characterization of partially hydrolyzed guar gum', *Int. J. Biol. Macromol.*, vol. 50, no. 4, pp. 1035–1039, 2012.

[44] M. Agüeros, L. Ruiz-Gatóna, C. Vauthier, K. Bouchemal, S. Espuelas, G. Ponchel, J.M. Irache 'Combined hydroxypropyl- β -cyclodextrin and poly (anhydride)

nanoparticles improve the oral permeability of paclitaxel', *Eur. J. Pharm. Sci.*, vol. 38, pp. 405–413, 2009.

[45] J. Zeng, H. Huang, S. Liu, H. Xu, J. Huang, and J. Yu, 'Hollow nanosphere fabricated from beta-cyclodextrin-grafted alpha, beta-poly(aspartic acid) as the carrier of camptothecin', *Colloids Surfaces B Biointerfaces*, vol. 105, pp. 120–127, 2013.

[46] M. Shahid, S. A. Bukhari, Y. Gul, H. Munir, F. Anjum, M. Zuber, T. Jamil, K. M.Zia 'Graft polymerization of guar gum with acryl amide irradiated by microwaves for colonic drug delivery', *Int. J. Biol. Macromol.*, vol. 62, pp. 172–179, 2013.

Chapter 5

Functional Characterization of Polymer

Chapter 4 dealt with the preparation of the gel by morphological characterization. The functional characterization i.e. the stimuli triggered functionality of synthesized polymer will be discussed in this chapter. The reason behind the stimuli sensitivity, swelling and/or deswelling kinetics are discussed in detailed for UVPTT, non-UVPTT and polymer nanocomposites.

5.1 Introduction

Functional characterization is to observe the functionality of polymer, response to applied stimuli in terms of their reversible volume alterations. The synthetic Poly(Aac-*co*-Aam) is the UVPTT polymer but after modification with β-CD the same thermosensitive nature was reflected or not that has been evaluated in this chapter as well as pH sensitivity of β-CD modified Poly(Aac-*co*-Aam) has been investigated. In Chapter 2, it was discussed that the reported guar gum grafted polyacrylamides have been functionally characterized in different pH by means of their equilibrium swelling with release of encapsulated solute by dissolution method. Chapter 3 gave information about temperature dependent irreversible swelling of synthetic Paam for gel chromatography application. These examples motivated us to investigate the reversible volume expansion nature of guar modified Paam by applying temperature and pH. If we rewind the reported work on dual stimuli responsive polymer, it was observed that, the researchers have been applied the stimuli separately i.e the dual stimuli responsivity of polymer was studied by applying solo stimuli at a time. For instances, Zhau *et al.* [1] developed hydroxypropyl methylcellulose (HPMC) hybrid nanogel for insulin release. The pH and temperature were assisted for drug release separately and both solo stimuli triggered released were performed in incubator shaker. The pH and temperature were applied separately at a time on dual-responsive copolymer of poly(N-(2-hydroxypropyl) methacrylamide dilactate)-co-(N-(2-hydroxypropyl)methacrylamide-*co*-histidine) and PEG [2] which was applied invasively in cancerous mouse model to release Paclitaxel and Imidazol. Hong *et al.* [3] illustrated dual responsivity of poly(L-histidine)(PHis) with

poly(ethylene glycol) (PEG) and poly(D,L-lactide-*co*-glycolide) (PLGA) micelle. When temperature responsivity was being observed, pH was kept constant and vice versa to release Doxorubicin. A temperature and pH dual responsive PNIPaam and Acrylic acid (Aac) copolymer and Silica nanoparticle based PNIPaam/Aac @SiO_2 particles were fabricated for efficient cancer treatment [4]. Wang *et al.* [5] developed an injectable and biodegradable chitosan modified poly(n-isopropylacrylamide) for thermoresponsive and photo responsive drug delivery application. Due to presence of PNIPaam, the hydrogel deswelled with the elevated intensity of applied stimuli like temperature and light. Photo thermal carbon solution was loaded into hydrogel to introduce NIR photo sensitivity. The stimuli triggered shrinking and drug release method helped the polymer to act as transdermal film. The above reported researches offered the negative natures towards applied stimuli i.e. the encapsulated cargo was released at elevated stimuli intensity. Because of PNIPaam, PEG the particle diameter shrank at the temperature, above the volume transition temperature as well as light but in pH medium the samples were working in opposite manner. Whereas this research aimed to explore the positive sensitivity of both UVPTT and non- UVPTT towards applied stimuli like temperature, pH and light. In order to avoid mechanical shaker in dual responsive polymer, we have applied pH and temperature simultaneously. The visible light sensitivity of gold nanoparticle reinforced polymer nanocomposite has been investigated with positive photothermal property which is different from reported negative photothermal hydrogel [5].

5.2 Experimental Procedure: Effects of Stimuli on Equilibrium Swelling (ES) Studies

The investigation of equilibrium swelling properties of a hydrogel is the key step to understand the swelling behaviour under applied stimuli. The equilibrium swelling (ES) of the positive stimuli responsive gel indicates the state at which it reaches at maximum stable weight by uptaking the solvent. This section is aimed to analyse the effect of external stimuli on ES gels. The ES experimentations were done by employing three types of external stimuli; such as pH, temperature and visible light laser (532 nm, 500 mW) irradiation. The effects of these stimuli on ES are discussed in next successive sections. Before start the ES experiment, the dimension and weight of dry polymer was maintained as mentioned in Table 5.1.

Table 5.1: Dry/Initial Sample parameters

Sample Code	Sample dimension, L × W × H (in mm)	Avg. weight of the dry gel, W_{dry} (in gm)*
PART I (UVPTT based)		
β-CD-g-(Paac-*co*-Paam)	5 × 5 × 0.25, ± 0.001	0.021 ± 0.001
β-CD-g-(Paac-*co*-Paam)-1	5 × 5 × 0.25, ± 0.001	0.041 ± 0.001
β-CD-g-(Paac-*co*-Paam)-3	5 × 5 × 0.25, ± 0.001	0.045 ± 0.001
PART II (non-UVPTT based)		
GG-g-Paam	5 × 5 × 1, ± 0.01	0.084 ± 0.003
DC-GG-Paam$_{GA0.80}$	5 × 5 × 1, ± 0.01	0.082 ± 0.003
DC-GG-Paam$_{GA1.60}$	5 × 5 × 1, ± 0.01	0.0826 ± 0.003
DC-GG-Paam$_{GA2.20}$	5 × 5 × 1, ± 0.01	0.0831 ± 0.003
DC-GG-Paam$_{GA4.39}$	5 × 5 × 1, ± 0.01	0.0837 ± 0.002
DC-GG-Paam$_{GA6.59}$	5 × 5 × 1, ± 0.01	0.0843 ± 0.003
DC-GG-Paam$_{GA4.39}$-1	5 × 5 × 1, ± 0.01	0.088 ± 0.002
DC-GG-Paam$_{GA4.39}$-3	5 × 5 × 1, ± 0.01	0.094 ± 0.001
DC-GG-Paam$_{GA4.39}$-5	5 × 5 × 1, ± 0.01	0.097 ± 0.001

*SD (n=5)

5.2.1 Effect of Medium pH on ES

The three types of pH mediums; such as acidic (pH 4 buffer solution), neutral (pH 7 buffer solution) and alkaline (pH 9.2 buffer solution) were used for ES experimentations. The pH assisted ES experimentation was performed as shown in Fig. 5.1. The dry samples were immersed into three buffer solutions separately at room temperature 25 °C until the sample reached at constant weight. The sample weight was taken at every hour by using an electronic weighing balance (Shimadzu Corporation, Japan, Model AUX220) with the accuracy of 0.001 gm. The samples with maximum swelled state, were taken out from the medium, excess surface adhered liquid was blotted out. The volume of the ES sample was measured. The percentages of equilibrium swelling in terms of weight as well as volume were calculated by Eq. (5.1) and (5.2) respectively.

$$\% W_{es\,(i)} = \frac{W_{swell\,(i)} - W_{dry}}{W_{dry}} \times 100\,\% \tag{5.1}$$

$$\% V_{es\,(i)} = \frac{V_{swell\,(i)} - V_{dry}}{V_{dry}} \times 100\,\% \tag{5.2}$$

Where, $W_{swell\,(i)}$ and W_{dry} are the weights of the swelled and dry polymer sample respectively and are expressed in gm. "i" indicates the applied stimuli i.e pH 4/pH 7/pH

9.2. Similarly, $V_{swell\ (i)}$ and V_{dry} are the volumes of the swelled and dry polymer sample respectively and are expressed in cubic centimetre (cc). The equilibrium swelling time, (t_{es}) i.e. the time taken to reach the sample in equilibrium swelling (ES) state was also recorded for each performed experiment. The density of the dry gel (ρ_{dry}) and the equilibrium swelled polymer sample ($\rho_{es\ (i)}$) were calculated by the Eq. (5.3) and (5.4) with the help of experimental measured values of W_{dry}, V_{dry}, $W_{es\ (i)}$ and $V_{es\ (i)}$ respectively.

$$\rho_{dry} = \frac{W_{dry}}{V_{dry}} \tag{5.3}$$

$$\rho_{es\ (i)} = \frac{W_{es\ (i)}}{V_{es\ (i)}} \tag{5.4}$$

The ρ_{dry} and $\rho_{es\ (i)}$ both are expressed in $gm.cc^{-1}$.

5.2.2 Effect of Medium Temperature on ES

The temperature assisted ES experimentation was performed at different temperatures such as 10 °C and 40 °C in neutral buffer solution. The Fig. 5.1 shows the schematic of the temperature based ES experiment. The dry samples were immersed into neutral buffer medium and allowed to reach at ES state with temperature stimuli of 10 °C and 40 °C respectively. The weight of the sample was taken at every hour. The equilibrium swelled polymers were taken out from the medium, excess surface adhered liquid was blotted out. The percentages of equilibrium swelling in terms of weight as well as volume were calculated by Eq. (5.1) and (5.2) respectively. Where, "i" considered as the applied stimuli e.g. 10 °C/40 °C. The equilibrium swelling time, (t_{es}) was also recorded for each experiment. Similarly, the densities of dry gel samples and the equilibrium swelled polymer samples were calculated by the Eq. (5.3) and Eq. (5.4) respectively, where "i" considered as the applied stimuli e.g. 10 °C/40 °C. Both the densities are expressed in $gm.cc^{-1}$.

5.2.3 Effect of Visible Light on ES

The continuous visible light laser with 532 nm, 500 mW was used for ES experimentation. The polymer-AuNP nanocomposites were employed for this photo sensitive ES studies. The positive photosensitivity of both UVPTT and non-UVPTT hydrogels were directed for equilibrium swelling under laser irradiation duration. The neutral buffer medium was used as solvent medium. As discussed in Section 5.2.1 and 5.2.2, after the sample reached at ES state, the samples were taken out from the medium

by removing excess surface adhered liquid. The percentages of equilibrium swelling in terms of weight as well as volume were calculated by Eq. (5.1) and (5.2) respectively. Where, "i" considered as the applied laser irradiation on different AuNP concentrated composites. The equilibrium swelling time, (t_{es}) was also recorded for each experiment. Similarly, the densities of dry gel samples and the equilibrium swelled polymer samples were calculated by the Eq. (5.3) and Eq. (5.4) respectively and are expressed in gm.cc^{-1}. The Fig. 5.1 shows the schematic of the stimuli based ES experiment.

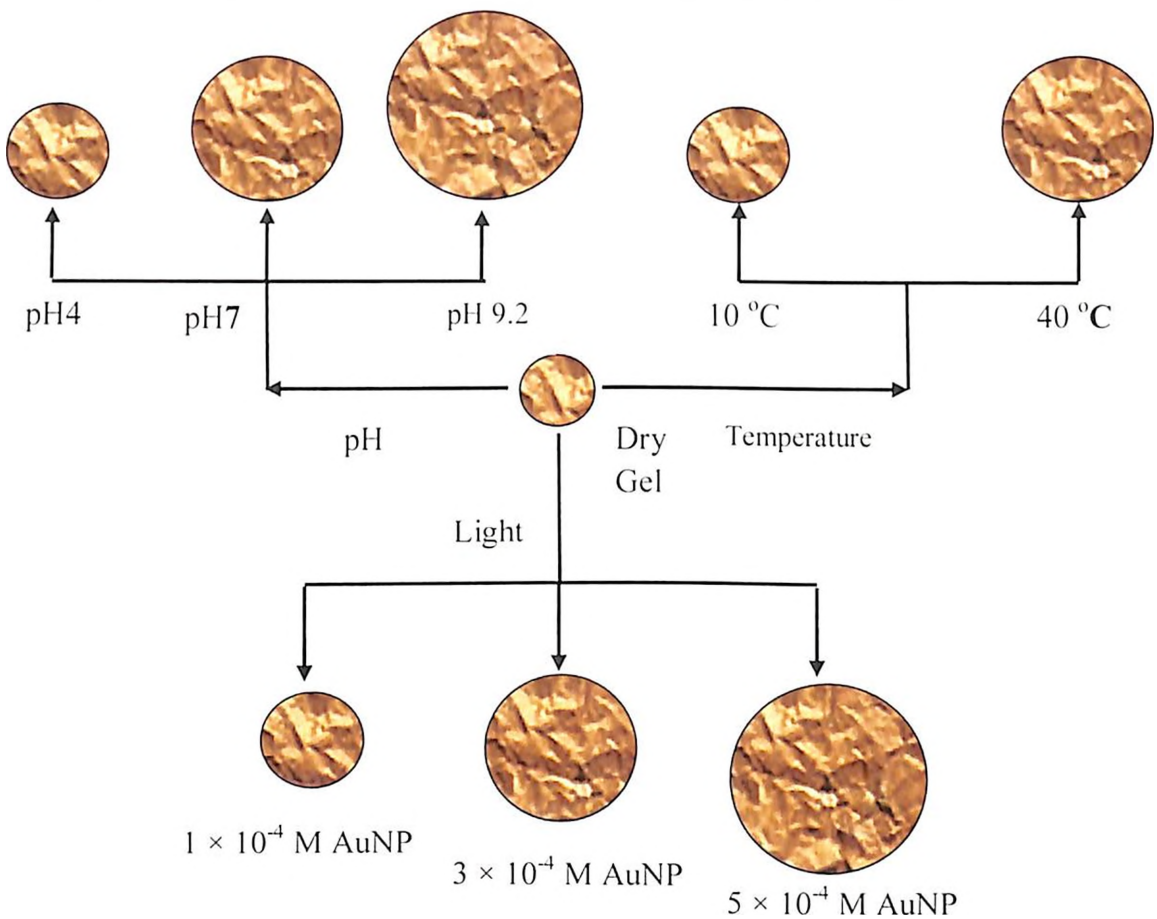

Fig. 5.1: Schematic illustration of stimuli triggered ES phenomenon

5.3 Results and Discussions: Effects of Stimuli on Equilibrium Swelling (ES) Studies

As described in last Section 5.2, the ES experimentations were carried out for both β-CD modified UVPTT gel and guar gum modified non-UVPTT gels to standout the ES effect on all applied external stimuli. We divided into two parts to discuss the results for two types of gels; Part A for β-CD modified UVPTT and Part B is for guar gum modified non-UVPTT polymers. The subsequent subsections are

analyzed the ES response of all the above formulated gels on different applied stimuli.

PART A β-CD Modified UVPTT Based Hydrogel

This section is objected for exploring the ES phenomenon of β-CD modified gel on the applied external stimuli.

5.3.1A Effect of Medium pH on ES

The ES response of UVPTT based β-CD-g-(Paac-*co*-Paam) IPN was carried out in acidic, neutral and alkaline mediums as described in Section 5.2.1. The (wt/wt) and (v/v) percentages of ES gels were calculated by Eq. (5.1) and Eq. (5.2) respectively. The IPN gel reached its ES state in 7 h for all pHs. The dynamic swelling response of the gel in different mediums stimuli are shown in Fig. 5.2. The (wt/wt) percentage of equilibrium swelling was increased with the swelling medium varied from acidic to alkaline in nature. The gel performed 594.77±36.27%, 718.77±41.36% and 750.43±39.87% of ES in acidic, neutral and alkaline buffer mediums respectively.

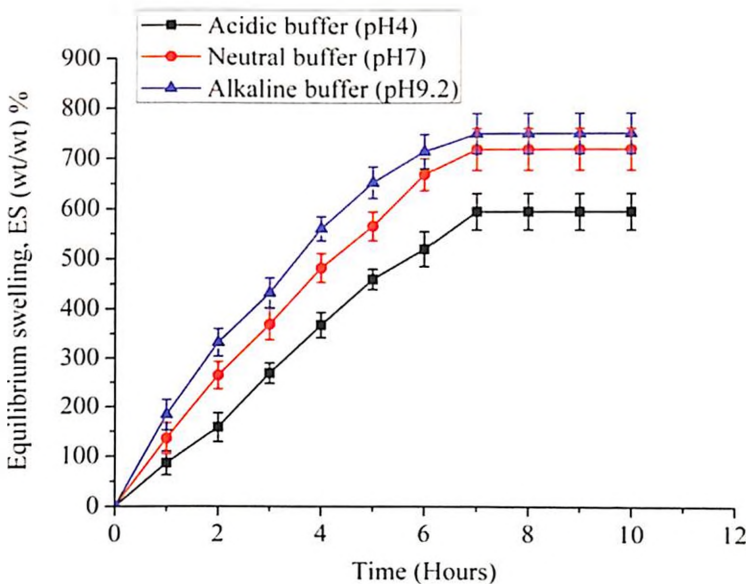

Fig. 5.2: Equilibrium swelling, ES (wt/wt) % in different medium stimuli

The elevating percentage of volumetric ES was observed with the change of medium from acidic (722.03±34.92%) to alkaline (2496.32±86.05%) (Fig. 5.3). The density of the equilibrium swelled sample (ρ_{es}) decreased with the increase of volumetric equilibrium swelling capability with the pH of the medium stimuli.

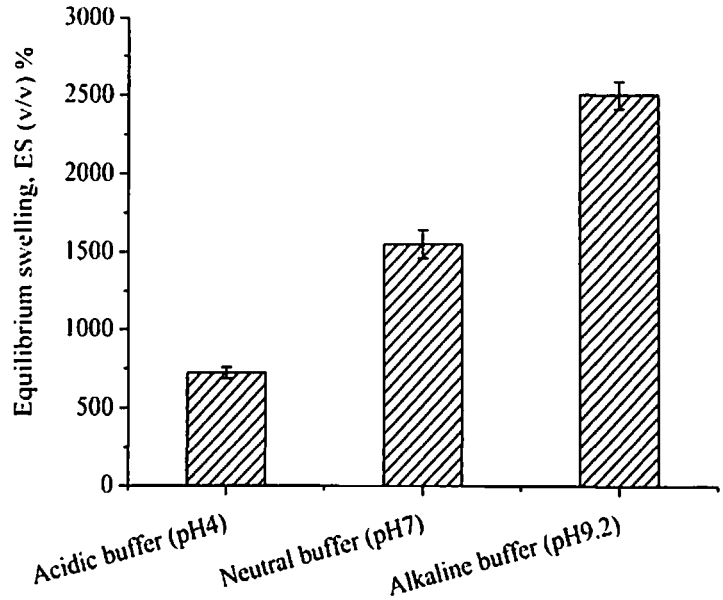

Fig. 5.3: Volumetric equilibrium swelling, ES (v/v)% in different pH stimuli

5.3.2A Effect of Medium Temperature on ES

The 10 °C and 40 °C were applied as temperature stimuli to investigate the thermal ES response of UVPTT IPN in neutral solvent as described in Section 5.2.2. The (wt/wt) and (v/v) percentages of ES gel were calculated by Eq. (5.1) and Eq. (5.2) respectively. The IPN gel reached its ES state in 7 h in both temperature stimuli. The dynamic swelling response of the gel in different temperature stimuli are shown in Fig. 5.4.

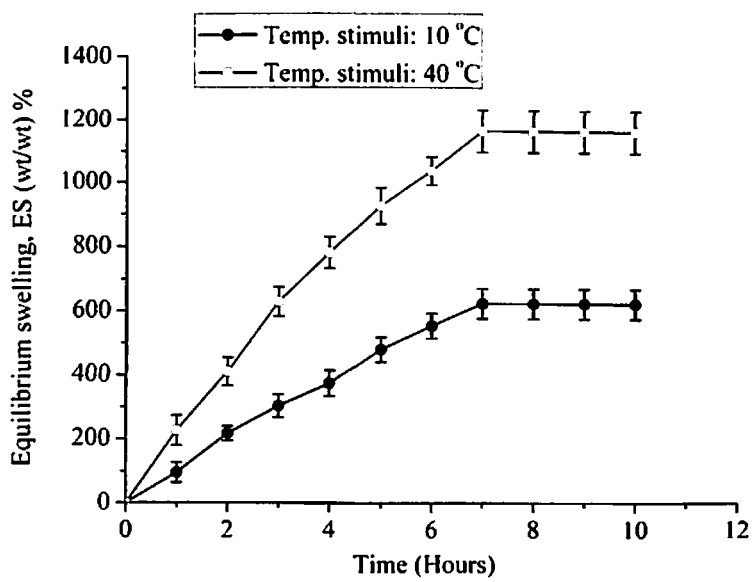

Fig. 5.4: Equilibrium swelling, ES (wt/wt)% at temperature stimuli

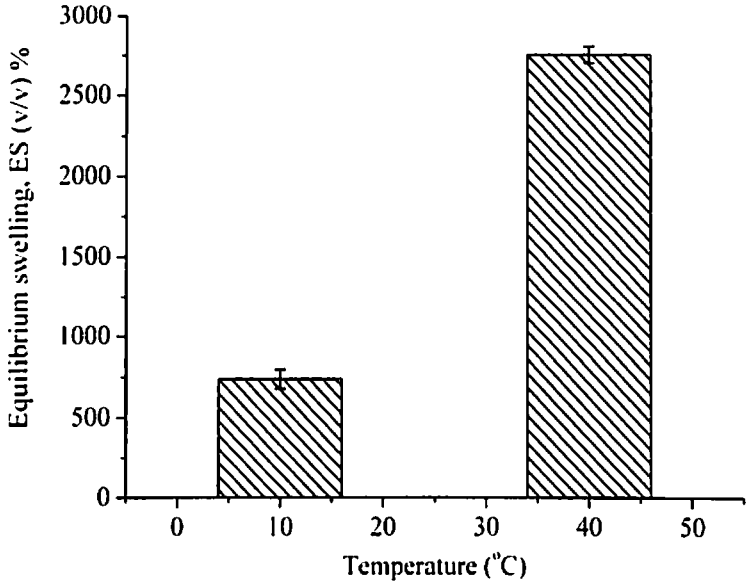

Fig. 5.5: Volumetric equilibrium swelling, ES (v/v)% at different temperature

The (wt/wt) percentage of equilibrium swelling was enhanced at higher temperature (40 °C) than low temperature (10 °C). The gel performed 626.88±46.67% and 1167.16±66.69% of ES in (wt/wt) at 10 °C and 40 °C respectively. The percentage of volume change was higher at 40 °C (2751.60±52.32%) than 10 °C (737.81±58.45%) (Fig. 5.5). The density of the equilibrium swelled sample (ρ_{es}) lowered at higher external temperature (40 °C) than at lower temperature (10 °C).

5.3.3A Effect of Visible Light on ES

The visible light assisted ES studies were performed on both AuNP composite IPNs (β-CD-g-(Paac-*co*-Paam)-1 and β-CD-g-(Paac-*co*-Paam)-3). The experiments were performed as described in Section 5.2.3. The percentages of ES in terms of weight and volume were calculated by Eq. (5.1) and (5.2) respectively. The Fig. 5.6 depicts the dynamic equilibrium swelling profile under the irradiation of the laser source. Fig. 5.7 represents that the higher concentrated AuNP composite IPN (β-CD-g-(Paac-*co*-Paam)-3) gives higher percentage of volumetric equilibrium swelling of 3365.60±16.63% than lower AuNP concentrated β-CD-g-(Paac-*co*-Paam)-1 (1832.86±22.28%). This shows the higher capacity to intake the solvent during swelling. This is happened due to generating more localize heat inside the gel network during laser irradiation by the NPs. Thus larger volumetric expansion occurred in β-CD-g-(Paac-*co*-Paam)-3 than β-CD-g-(Paac-*co*-Paam)-1 (Fig. 5.7).

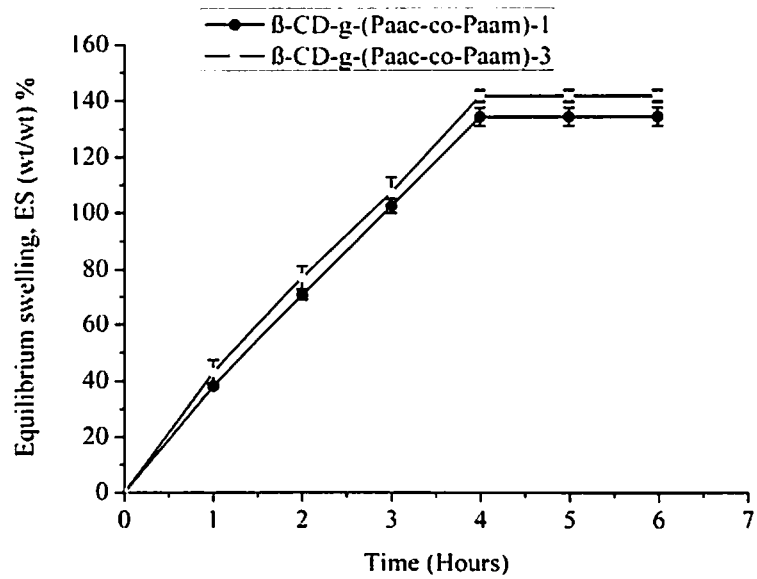

Fig. 5.6: Equilibrium swelling, ES (wt/wt)% at visible light stimuli

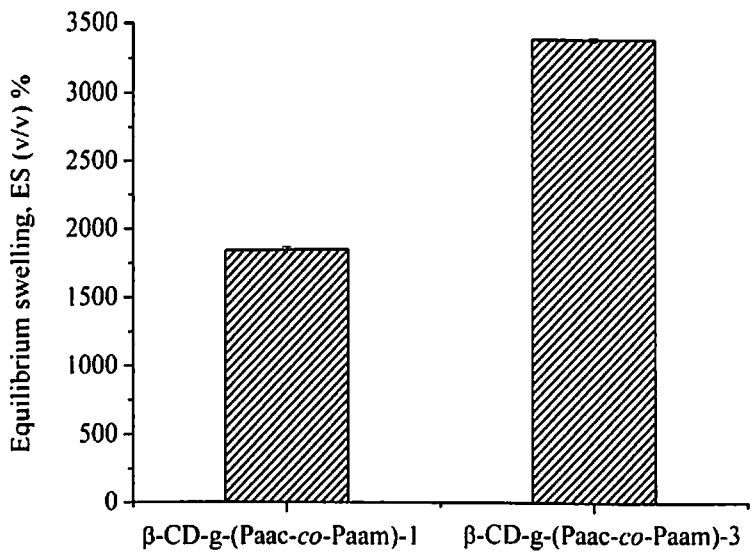

Fig. 5.7: Equilibrium swelling, ES (v/v)% at visible light stimuli

Further, the lower ES time (t_{es}) of 4 hours was observed to reach the IPN composites to ES state by the visible light stimuli phenomenon than other two external stimuli (pH and the temperature) assisted ES activities.

PART B Guar Gum Modified Non-UVPTT Based Hydrogel

This section is aimed to investigate the ES phenomenon of guar gum modified gels on the applied external stimuli.

5.3.1B Effect of Medium pH on ES

The ES response of non-UVPTT based guar gum modified GG-g-Paam and DC-GG-Paam$_{GA\ (i)}$ IPN was carried out in acidic, neutral and alkaline mediums as described in Section 5.2.1. The (wt/wt) and (v/v) percentages of ES were calculated by Eq. (5.1) and Eq. (5.2) respectively. The ES profile for each gels under applied pH stimuli are shown in Fig. 5.8(a)-(c) respectively.

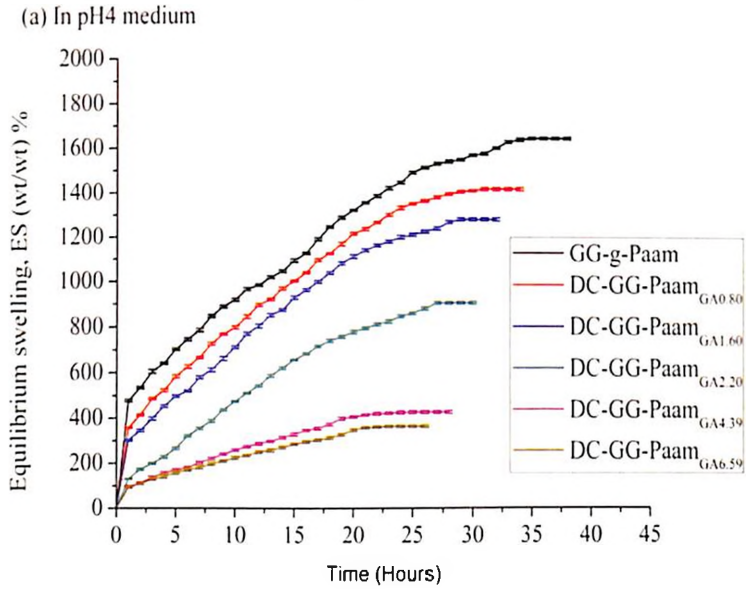

Fig. 5.8(a): Equilibrium swelling, ES (wt/wt)% in pH 4 buffer medium

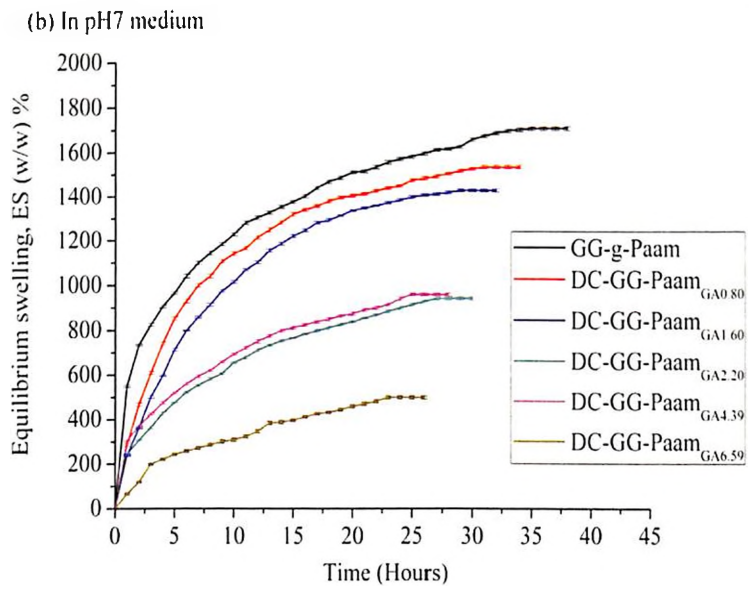

Fig. 5.8(b): Equilibrium swelling, ES (wt/wt)% in pH 7 buffer medium

The gels reached its ES state at different time span. From, Fig. 5.8(a)-(c), irrespective of the medium stimuli, the maximum equilibrium swelling time, t_{es} found for graft sample,

whereas, the t_{es} decreased with the gels containing higher concentration of GA, i.e. DC-GG-Paam$_{GA6.59}$ reached to its ES state in lowest time duration.

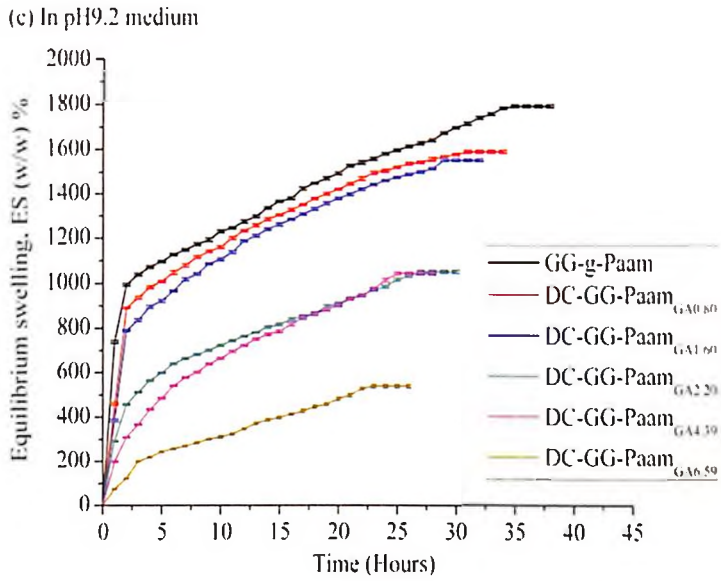

Fig. 5.8(c): Equilibrium swelling, ES (wt/wt) % in pH 9.2 buffer medium

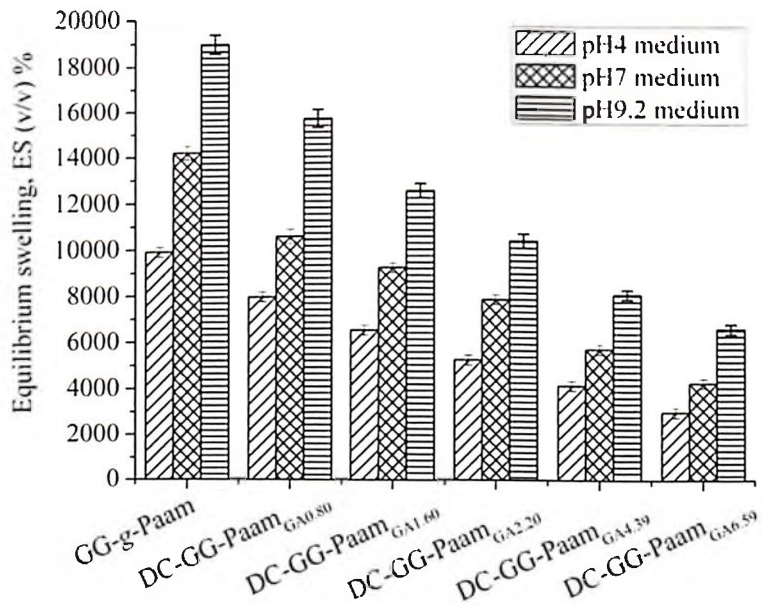

Fig. 5.9: Volumetric equilibrium swelling, ES % in pH 4, pH 7 and pH 9.2 medium

Further, the graft gel performed highest swelling capability among other guar gum modified gels in all medium stimuli, and the (wt/wt)% of ES reduced with the increase of GA concentration inside the double cross linked samples. Subsequently, the volumetric percentage of equilibrium swelling diminishes with the increase of GA concentration present in the gel network (Fig. 5.9) in all medium stimuli.

Furthermore, all the formulated gel samples endow with higher volumetric expansion in terms of percentage of equilibrium swelling in alkaline buffer medium, and decreased

with the pH of the medium. It signifies that, the gel network is capable to up take more solvent/solute of in alkaline medium than acidic one.

5.3.2B Effect of Medium Temperature on ES

The ES response of non-UVPTT based graft and other double cross-linked gels was carried out in neutral buffer medium at 10 °C and 40 °C separately and the experimentation process was followed as described in Section 5.2.2. The (wt/wt)% and (v/v)% of equilibrium swelled gel were calculated by Eq. (5.1) and Eq. (5.2) respectively. The temperature stimulated dynamic swelling response for each formulated ES gels are shown in Fig. 5.10(a)-(b) respectively.

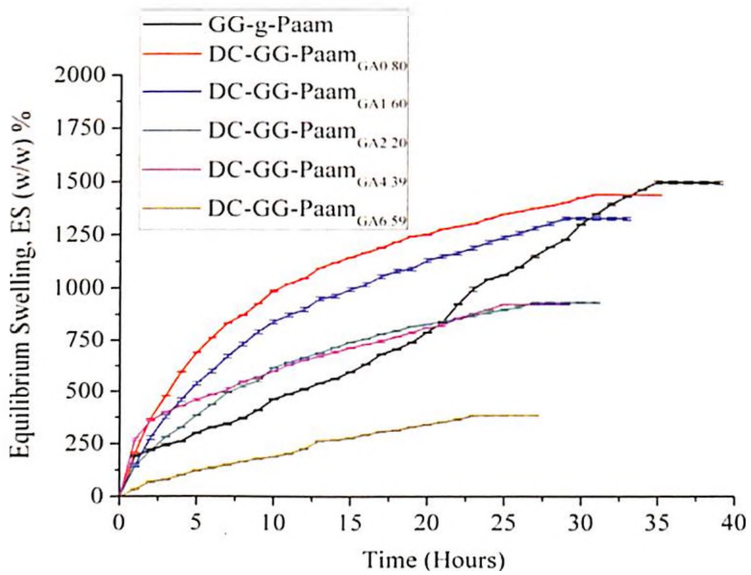

Fig. 5.10(a): Equilibrium swelling (wt/wt)% at 10 °C

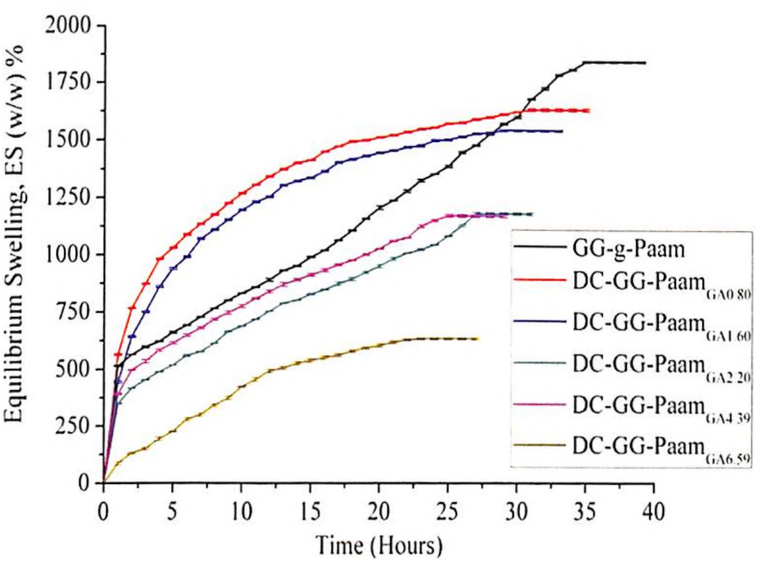

Fig. 5.10(b): Equilibrium swelling (wt/wt)% at 40 °C

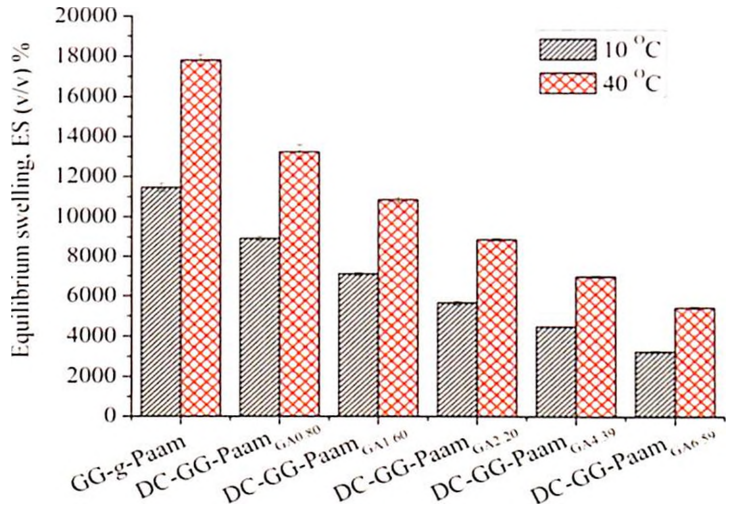

Fig. 5.11: Equilibrium swelling, ES (v/v)% at 10 °C and 40 °C

The graft gel (GG-g-Paam) performed higher (wt/wt) percentage of equilibrium swelling of (1498.33±7.48)% and (1845.71±2.88)% in 10 °C and 40 °C temperatures respectively. The highest t_{es} observed for graft gel and is decreasing with the increasing of GA concentration present in gel network. Same phenomenon was observed in the percentage of volumetric change of equilibrium swelled gels (Fig. 5.11). Therefore, the temperature stimulated equilibrium swelling experiment shows, the higher environmental temperature (40 °C) gives the higher (wt/wt)% and (v/v)% of equilibrium swelling for all formulated gel samples than lower one (10 °C).

5.3.3B Effect of Visible Light on ES

The visible light assisted ES studies were performed on all three non-UVPTT based AuNP composite gels (DC-GG-Paam$_{GA4.39}$-1, DC-GG-Paam$_{GA4.39}$-3 and DC-GG-Paam$_{GA4.39}$-5) as described in Section 5.2.3. The Fig. 5.12 depicts the dynamic equilibrium swelling profile under the irradiation of the laser. The percentage of volumetric change of the ES gel is shown in Fig. 5.13. The higher concentrated AuNP composite gel (DC-GG-Paam$_{GA4.39}$-5) gives higher percentage of equilibrium swelling than lower AuNP concentrated DC-GG-Paam$_{GA4.39}$-1. This shows the higher capacity to intake the solvent during swelling. This is happened due to generating more localize heat inside the gel network during laser irradiation by the NPs.

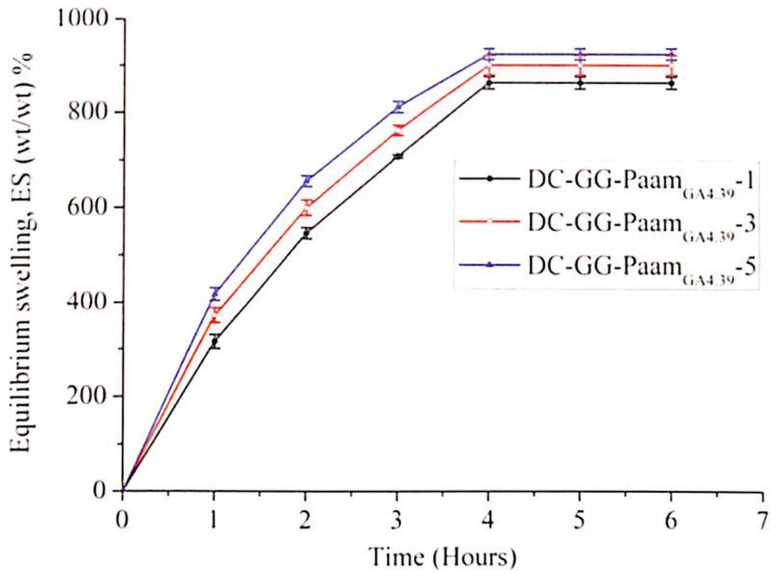

Fig. 5.12: Equilibrium swelling (wt/wt)% under visible light exposure

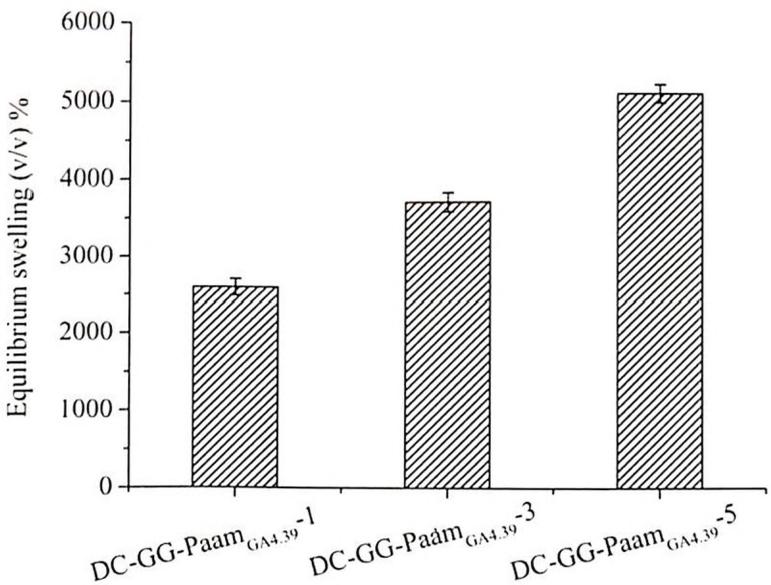

Fig. 5.13: Equilibrium swelling (v/v)% under visible light exposure

5.4 Theoretical Aspect: Equilibrium Swelling Kinetics

After observing the stimuli triggered equilibrium swelling performance of gels, this section is aimed to understand the theoretical background behind the swelling kinetics during ES phenomenon and the stimuli effect on gel network.

To understand the stimuli triggered gel swelling kinetics, the computation of swelling rate constant is the key step to understand. During swelling phenomenon, the polymer can obey either 1st order or 2nd order non-liner kinetics. The swelling rate constants, $k_{1\,(j)}$ and $k_{2\,(j)}$ were measured from experimental equilibrium

swelling data by using well established 1st order[6] and 2nd order [7] nonlinear kinetics Eq. (5.5) and Eq. (6) respectively.

$$S_{t\,(j)} = S_{es\,(j)}\left(1 - e^{-k_{1\,(j)}\cdot t}\right) \tag{5.5.}$$

$$\frac{t}{W_{t\,(j)}} = \frac{1}{k_{2\,(j)}\cdot W_{es\,(j)}^2} + \frac{t}{W_{es\,(j)}} \tag{5.6}$$

Where, $S_{t\,(j)}$ and $S_{es\,(j)}$ represent the solvent uptake at time t and at equilibrium swelled condition at equilibrium swelling time (t_{es}) respectively. The suffix "j" indicates the applied pH/ environmental temperature/visible light stimuli.

Where, $W_{t\,(j)}$ and $W_{t-1\,(j)}$ are the weight of the sample at time t = t and t = (t – 1) during swelling. The $W_{es\,(j)}$ denotes the sample weight at equilibrium swelling time (t_{es}). The $k_{1\,(j)}$ and $k_{2\,(j)}$ are the rate constants in 1st order kinetics and rate constant at 2nd order kinetics respectively for both stimuli conditions.

The nonlinear curve fit named BoxLucas1 technique was used through Origin 8 to calculate 1st order rate constant, $k_{1\,(j)}$. Whereas, to measured the 2nd order rate constant, $k_{2\,(j)}$, the LineMod polynomial nonlinear curve fit technique was applied by simplifying the Eq. (5.6) to Eq. (5.7).

$$y = A\,(t - B) \tag{5.7}$$

Where, A and B are constants getting from curve fitted data and are expressed as $A = \frac{1}{S_{es\,(j)}}$ and $B = A.k_{2\,(j)}^{-1}$ and $y = \frac{t}{S_{t\,(j)}}$.

To understand the suitability of the followed swelling kinetics between 1st order and 2nd order, the obtained Adj. r^2 values (from the fitted data) were analyzed.

5.5 Experimental Aspect: Equilibrium Swelling Kinetics

The 1st order ($k_{1\,(j)}$) and 2nd order ($k_{2\,(j)}$) swelling rate constants are measured from experimental equilibrium swelling data by using Eq. (5.5) and Eq. (5.6) respectively. The rate constants $k_{1\,(j)}$, $k_{2\,(j)}$ and obtained Adj.r^2 value from the fitted curve are given in Table 5.2(A)-Table 5.4(A) and Table 5.2(B)-Table 5.4(B) for UVPTT and non-UVPTT based polymer respectively for medium, temperature and visible light stimulated ES respectively.

Table 5.2A: Swelling rate constant for 1st order and 2nd order kinetics at Equilibrium Swelled (ES) state under applied buffer stimuli for UVPTT based polymer

Sample Code	1st Order Rate constant, k_1* (hr^{-1})	Adj.r^2 value	2nd Order Rate constant, k_2* (hr^{-1})	Adj.r^2 value
ES Condition: pH 4 medium and room temperature (25 °C)				
β-CD-g-(Paac-*co*-Paam)	0.022 ± 0.019	0.996	0.0002	0.680
ES Condition: pH 7 medium and room temperature (25 °C)				
β-CD-g-(Paac-*co*-Paam)	0.102 ± 0.010	0.998	0.209	0.778
ES Condition: pH 9.2 medium and room temperature (25 °C)				
β-CD-g-(Paac-*co*-Paam)	0.194 ± 0.016	0.998	0.211	0.860

Table 5.3A: Swelling rate constant for 1st order and 2nd order kinetics at Equilibrium Swelled (ES) state under applied temperature for UVPTT based polymer

Sample Code	1st Order Rate constant, k_1* (hr^{-1})	Adj. r^2 value	2nd Order Rate constant, k_2* (hr^{-1})	Adj. r^2 value
ES Condition: Temperature (10 °C) in neutral medium .				
β-CD-g-(Paac-*co*-Paam)	0.058 ± 0.013	0.998	0.184	0.752
ES Condition: Temperature (40 °C) in neutral medium				
β-CD-g-(Paac-*co*-Paam)	0.115 ± 0.009	0.999	0.325	0.758

Table 5.4A: Swelling rate constant for 1st order and 2nd order kinetics at Equilibrium Swelled (ES) state under applied visible light (laser irradiation) stimuli for UVPTT based polymer

Sample Code	1st Order Rate constant, k_1* (hr^{-1})	Adj. r^2 value	2nd Order Rate constant, k_2* (hr^{-1})	Adj. r^2 value
β-CD-g-(Paac-*co*-Paam)-1	0.066 ± 0.014	0.999	0.098	0.931
β-CD-g-(Paac-*co*-Paam)-3	0.102 ± 0.030	0.998	0.111	0.932

The Tables 5.2(A,B) depict all the Adj. r^2 values from 1st order kinetics are higher than that of 2nd order for all applied stimuli, therefore, all the formulated gels are followed 1st order swelling kinetics more accurately than 2nd order kinetics. Furthermore, the rate constant of 1st order kinetics (k_1) are increased with the increase of stimuli intensities for all gels, such that, for a particular gel, the highest k_1 obtained for alkaline based ES phenomenon, whereas, lowest rate observed in case of acidic medium. Thus, the higher percentage of ES i.e. the higher solvent uptake capability (in terms of volumetric swelling) found in alkaline medium than acidic (see Fig. 5.3 and Fig. 5.9). Similar

phenomenon were observed for temperature based ES (Table 5.3(A,B)), i.e., for a particular gel, the highest k_1 at 40 °C, whereas, ES at 10 °C provided lowest rate. Thus, the gels are capable to uptake the higher rate of solvent at 40 °C during ES that 10 °C (Fig. 5.5 and Fig. 5.11).

Table 5.2B: Swelling rate constant for 1st order and 2nd order kinetics at Equilibrium Swelled (ES) state under applied medium buffer stimuli for non-UVPTT based polymer

Sample Code	1st Order Rate constant, k_1* (hr^{-1})	Adj. r^2 value	2nd Order Rate constant, k_2* (hr^{-1})	Adj. r^2 value
ES Condition: pH 4 medium and room temperature (25 °C)				
GG-g-Paam	0.093 ± 0.011	0.990	0.089 ± 0.002	0.892
DC-GG-Paam$_{GA0.80}$	0.083 ± 0.009	0.949	0.074 ± 0.010	0.901
DC-GG-Paam$_{GA1.60}$	0.072 ± 0.009	0.959	0.066 ± 0.011	0.921
DC-GG-Paam$_{GA2.20}$	0.041 ± 0.004	0.991	0.039 ± 0.005	0.931
DC-GG-Paam$_{GA4.39}$	0.073 ± 0.012	0.960	0.069 ± 0.013	0.910
DC-GG-Paam$_{GA6.59}$	0.091 ± 0.014	0.947	0.081 ± 0.022	0.897
ES Condition: pH 7 medium and room temperature (25 °C)				
GG-g-Paam	0.176 ± 0.013	0.927	0.136 ± 0.010	0.833
DC-GG-Paam$_{GA0.80}$	0.154 ± 0.005	0.990	0.141± 0.015	0.923
DC-GG-Paam$_{GA1.60}$	0.127 ± 0.003	0.997	0.111 ± 0.013	0.921
DC-GG-Paam$_{GA2.20}$	0.137 ± 0.009	0.969	0.128 ± 0.004	0.902
DC-GG-Paam$_{GA4.39}$	0.166 ± 0.014	0.948	0.154 ± 0.012	0.899
DC-GG-Paam$_{GA6.59}$	0.109 ± 0.010	0.971	0.095 ± 0.002	0.921
ES Condition: pH 9.2 medium and room temperature (25 °C)				
GG-g-Paam	0.229 ± 0.029	0.967	0.207 ± 0.013	0.927
DC-GG-Paam$_{GA0.80}$	0.223 ± 0.022	0.972	0.211 ± 0.020	0.927
DC-GG-Paam$_{GA1.60}$	0.194 ± 0.018	0.902	0.173 ± 0.013	0.871
DC-GG-Paam$_{GA2.20}$	0.184 ± 0.017	0.906	0.168 ± 0.004	0.881
DC-GG-Paam$_{GA4.39}$	0.194 ± 0.008	0.970	0.104 ± 0.010	0.912
DC-GG-Paam$_{GA6.59}$	0.130 ± 0.009	0.965	0.074 ± 0.011	0.915

Table 5.3B: Swelling rate constant for 1st order and 2nd order kinetics at Equilibrium Swelled (ES) conditions under external temperature stimuli for non-UVPTT based polymer

Sample Code	1st Order Rate constant, k_1* (hr^{-1})	Adj. r^2 value	2nd Order Rate constant, k_2* (hr^{-1})	Adj. r^2 value
ES Condition: Temperature 10 °C, neutral buffer as medium				
GG-g-Paam	0.049 ± 0.008	0.908	0.052 ± 0.021	0.839
DC-GG-$Paam_{GA0.80}$	0.064 ± 0.002	0.991	0.073 ± 0.011	0.876
DC-GG-$Paam_{GA1.60}$	0.094 ± 0.003	0.994	0.072 ± 0.027	0.949
DC-GG-$Paam_{GA2.20}$	0.101 ± 0.003	0.995	0.119 ± 0.043	0.899
DC-GG-$Paam_{GA4.39}$	0.126 ± 0.014	0.930	0.206 ± 0.061	0.941
DC-GG-$Paam_{GA6.59}$	0.133 ± 0.020	0.943	0.233 ± 0.041	0.901
ES Condition: Temperature 40 °C, neutral buffer as medium				
GG-g-Paam	0.053 ± 0.008	0.892	0.072 ± 0.027	0.810
DC-GG-$Paam_{GA0.80}$	0.081 ± 0.011	0.971	0.093 ± 0.017	0.887
DC-GG-$Paam_{GA1.60}$	0.194 ± 0.011	0.965	0.192 ± 0.035	0.891
DC-GG-$Paam_{GA2.20}$	0.110 ± 0.014	0.948	0.141 ± 0.043	0.926
DC-GG-$Paam_{GA4.39}$	0.146 ± 0.016	0.941	0.181 ± 0.048	0.913
DC-GG-$Paam_{GA6.59}$	0.135 ± 0.011	0.955	0.142 ± 0.023	0.913

Table 5.4B: Swelling rate constant for 1st order and 2nd order kinetics at Equilibrium Swelled (ES) state under applied visible light (laser irradiation) stimuli for non-UVPTT based polymer

Sample Code	1st Order Rate constant, k_1* (hr^{-1})	Adj. r^2 value	2nd Order Rate constant, k_2* (hr^{-1})	Adj. r^2 value
DC-GG-$Paam_{GA4.39}$-1	0.405 ± 0.137	0.967	0.918	0.822
DC-GG-$Paam_{GA4.39}$-3	0.496 ± 0.143	0.969	1.004	0.866
DC-GG-$Paam_{GA4.39}$-5	0.590 ± 0.145	0.972	1.054	0.899

For visible light stimuli, Table 5.4(A,B), the 1st order kinetics was followed in both UVPTT and non-UVPTT composites. Further, the k_1 was higher in higher AuNP concentrated composites, due to the higher ability to solvent intake via swelling (Fig. 5.7 and Fig. 5.13).

In conclusion, from Table 5.2(A,B), Table 5.3(A,B) and Table 5.4(A,B), the increased 1st order rate constant, $k_{1\,(j)}$ is observed with the increase of stimuli intensities for all

applied stimuli, which facilitated the solvent diffusion process inside polymer network during swelling. Therefore, the gel network parameters are also contributed key role to make the diffusion activities inside the gel, and thus the gel absorbed the solvent from the surroundings.

5.6 Theoretical View: Role of Gel Network and Diffusion on Equilibrium Swelling

To understand the solvent diffusional effect inside the swelled gel, the Fick's 2nd law of diffusion was used. The diffusion rate constant (k_D) of solution was calculated from experimental swelling data by using well defined Eq. (5.8) [8].

$$\frac{W_t}{W_{es}} = k_D \cdot t^n \qquad (5.8)$$

Where, W_t and W_{es} are the weight of the polymer at a time "t" and weight of the polymer at equilibrium swelled time (t_{es}) respectively. "n"denotes the type of diffusion occurred inside the polymer gel network. The other important parameter called, diffusion co-efficient, D_S ($cm^2.hr^{-1}$) of the solvent into polymer gel, indicative of the diffusion mobility was measured by Eq. (5.9) [9].

$$D_S = \frac{k_D h^2}{\Pi^2} \qquad (5.9)$$

where, h represents the thickness of swelled polymer. Π is the constant and taken as 3.14159.

The front velocity of solvent during solvent interaction into polymer network, u ($cm.hr^{-1}$) was calculated using the Eq. (5.10) [10].

$$u = \left(\frac{dv}{dt}\right)\frac{1}{2A} \qquad (5.10)$$

where, dv/dt is the change in volume of per unit time and A represents the surface area of swelled polymer sample and A is multiplied by 2, considering the opposite bi-directional solvent penetration at both side of rectangular sample.

For realization of diffusion phenomenon inside the gel, the swelling behavior of the gel samples was analyzed by Flory-Huggins approach by using experimental swelling studies. The foremost parameter called Florry-Huggin's polymer-solvent interaction parameter, χ is a key parameter to analyze the polymer network, which quantifies the interaction between solvent and polymer network. The χ can be measured according to Xue *et al.* [11], by Eq. (5.11).

$$\chi = \frac{1}{2} + \frac{\phi}{3} \tag{5.11}$$

where, ϕ is the volume fraction of swelled polymer. The polymer volume fraction defined as the fractional ratio of the volume of the polymer to the sum of the volume of polymer and the volume of the solvent used and it is expressed by Eq. (5.12). It can be written as Eq. (5.13).

$$\phi = \frac{V_P}{V_P + V_W} \tag{5.12}$$

$$\phi = \left(1 + \frac{\rho_{P_{dry}}}{\rho_W} \times q_W\right)^{-1} \tag{5.13}$$

where, $\rho_{P_{dry}}$ (expressed in $gm.cc^{-1}$) is the density of dry gel and ρ_W is the density (expressed in $gm.cc^{-1}$) of solvent (water). The density of dry polymer was determined from the direct mass and dimensional measurements by dividing weight of dry hydrogel with the volume of the dry hydrogel. The values of ρ_W with respect to the different experimental temperatures are considered as listed in below Table 5.5.

Table 5.5: Density of water at different temperatures

Experimental temperature (°C)	Value of density of water, ρ_W ($gm.cc^{-1}$)
10	999.7000×10^{-3}
25	997.0470×10^{-3}
40	992.2152×10^{-3}

The q_W is the amount of solvent (in gm) required for per gm of dry sample to reach the required swelled state and it was calculated by Eq. (5.14).

$$q_W = \frac{W_{SP} - W_{dry}}{W_{dry}} \tag{5.14}$$

W_{SP} is the weight of the swelled gel and expressed in gm. The other parameter called the molecular weight of the polymer chain between cross-linking points, M_C (expressed in ($gm.mol^{-1}$) was calculated by using well established Flory and Rehner theory [12][13] from Eq. (5.15).

$$M_C = -V_1 \times \rho_P \times \frac{\phi^{1/3} - \frac{\phi}{2}}{\ln(1-\phi) + \phi + \chi\phi^2} \tag{5.15}$$

V_1 is the molar volume of the solvent, which is defined volume occupied by the one mole of the solvent molecule at a given temperature and pressure. It was calculated by Eq. (5.16).

$$V_1 = \frac{M_W}{\rho_W} \tag{5.16}$$

where, M_W is the molecular weight (18.01528 gm.mol^{-1}) of the solvent.

The other important gel network parameters closely related to the degree of swelling is cross-link density (CLD), ρ_C (mol.m^{-3}) and was calculated by Eq. (5.17) [14].

$$\rho_C = \frac{\rho_P}{M_C} \tag{5.17}$$

Another parameter called mesh size, ζ (Å) defines the average distance between consecutive cross-links and indicates the maximum size of solutes can pass through the polymer network, was calculated according to Canal *et al.* [15] by Eq. (5.18).

$$\zeta = \phi^{-1/3} l \left[\frac{2 C_n M_C}{M_n}\right]^{1/2} \tag{5.18}$$

where, l is the C-C bond length, considered as 1.54 Å. C_n is the Flory characteristic ratio of polyacrylamide, considered as 8.8 [16] and M_n is the average molecular weight of the repeating units into gel and was calculated by Eq. (5.19A) and (5.19B) for UVPTT and non-UVPTT based gels respectively.

For UVPTT gel,

$$M_n = \frac{M_{\beta-CD} n_{\beta-CD} + M_{Paam} n_{Paam} + M_{Paac} n_{Paac} + M_{MBA} n_{MBA}}{n_{\beta-CD} + n_{Paam} + n_{MBA} + n_{Paac}} \tag{5.19A}$$

$M_{\beta-CD}$, M_{Paam}, M_{MBA} and M_{Paac} are the molecular weight of guar gum, Paam, MBA and Paac respectively. $n_{\beta-CD}$, n_{Paam}, n_{MBA} and n_{Paac} are the number of mole used during synthesis for β – CD, Paam, MBA and Paac respectively.

For non-UVPTT gel,

$$M_n = \frac{M_{Guar\,gum} n_{Guar\,gum} + M_{Paam} n_{Paam} + M_{MBA} n_{MBA} + M_{GA} n_{GA}}{n_{Guar\,gum} + n_{Paam} + n_{MBA} + n_{GA}} \tag{5.19B}$$

$M_{Guar\,gum}$, M_{Paam}, M_{MBA} and M_{GA} are the molecular weight of guar gum, Paam, MBA and GA respectively. $n_{Guar\,gum}$, n_{Paam}, n_{MBA} and n_{GA} are the number of mole used during synthesis for guar gum, Paam, MBA and GA respectively.

During solvent-polymer interaction, the solvent intake by the gel network is dependent on the porosity (P) of the polymer network and the tortuosity (τ). The porosity is the fraction of a elementary volume available for the solvent into the polymer network,

whereas, tortuosity is defined as the ratio of the actual distance travelled by the solvent molecule per unit length of the medium. The porosity, P and the tortuosity, τ were assessed by Eq. (5.20) and Eq. (5.21) [17] respectively.

$$P = \frac{W_{es} - W_{dry}}{\rho_W V_{es}} \tag{5.20}$$

$$\tau^2 = 1 + \ln\left(\frac{1}{P^2}\right) \tag{5.21}$$

For the synthesized stimuli responsive hydrogels, the gels were swelled with the stimuli intensities (discussed in Section 5.3) and it depends on the polymer chain elasticity or degree of elongation and polymer-solvent affinity. The low chain elongation leads to low tendency of swelling. Thus, the swelling ability is the combinational effect of the polymer-solvent mixing and the chain elasticity. Hence, there are two opposite types of energies produced inside the polymer network; one is the mixing energy due to polymer-solvent interaction and the elastic energy produced from the chain elasticity. The mixing energy helps the polymer network to intake the solvent and the elastic energy opposes the chain from stretching, tends to limit the swelling. The mixing free energy (ΔG_{mix}) and the elastic free energy (ΔG_{el}) can be evaluated from Florry-Huggin's theory [18], using Eq. (5.22) Eq. (5.23) respectively.

$$\Delta G_{mix} = R\,T\,[\ln(1 - \phi) + \phi + \chi\,\phi^2] \tag{5.22}$$

$$\Delta G_{el} = \phi^{1/3}\,\frac{V_1\,\rho_{SP}\,R\,T}{M_C} \tag{5.23}$$

Where, R is Universal gas constant and is considered as 8.314 $J.mol^{-1}.K^{-1}$ and T is the working temperature in Kelvin. The ΔG_{mix} and ΔG_{el} are expressed in $J.mol^{-1}$.

For equilibrium swelled gels, the mixing free energy is equals to zero[18] having maximum elastic free energy. Thus, considering $\Delta G_{mix} = 0$ and by expanding the natural logarithmic term upto 2nd order in Eq. (5.22), the polymer-solvent interaction parameter (χ) shows the value of 0.5. With the combination of mixing free energy and elastic free energy, the total free energy (ΔG_{Total}) can be expressed as Eq. (5.24).

$$\Delta G_{Total} = R\,T\,[\ln(1 - \phi) + \phi + \chi\,\phi^2] + \phi^{1/3}\,\frac{V_1\,\rho_{SP}\,R\,T}{M_C} \tag{5.24}$$

In the context of the statistical thermodynamic approach, the mixing Gibb's free energy (ΔG_{mix}) can be expressed as Eq. (5.25).

$$\Delta G_{mix} = \Delta H_{mix} - T\Delta S_{mix} \tag{5.25}$$

where, ΔH_{mix} and ΔS_{mix} are the enthalpy heat energy and the energy for entropy of the mixing of solvent developed into the gel network respectively.

According to lattice theory of Flory and Rehner [12], the heat energy of mixing ΔH_{mix} and ΔS_{mix} can estimated from the Eq. (5.26) and Eq. (5.27) respectively.

$$\Delta H_{mix} = K_B T \chi n_s \phi \tag{5.26}$$

$$\Delta S_{mix} = - K_B n_s \ln(1 - \phi) \tag{5.27}$$

Where, K_B is the Boltzman constant (1.3806×10^{-32} $J.K^{-1}$) and n_s is the mole number of the solvent into the swelled gel and can be calculated by Eq. (5.28).

$$n_s = \frac{W_{SP} - W_{dry}}{M_W} \tag{5.28}$$

The swelling or deswelling of gel occurs by stretching or entanglement of the network chains. Hence, the lesser entropy welcomes the retractive force to return the swelled gel network to its original un-stretched state. Commonly, the crosslinked points obstruct the gel network to be elongated. The increasing crosslinked points in the gel network leads to lesser elongation with higher configurational probability (high entropy) than the network with lesser crosslinked points. Hence the chain configurational entropy $\left(\Delta S_{mix\,Chain\,config}\right)$ plays a vital role on the entropy of mixing of solvent and polymer. This can be measured from the experimental data by using Eq. (5.29) [19].

$$\Delta S_{mix\,Chain\,config} = -R\left[\ln(1 - \phi) + \phi + \phi^{1/3} \frac{V_1 \rho_{SP}}{M_C}\right] \tag{5.29}$$

For a Gaussian chain statistics for polymer network, the osmotic pressure plays a role on the chain network during swelling and deswelling under stimuli and the equivalent osmotic pressure, Π_{eq} is given by Eq. (5.30).

$$\Pi_{eq} = \Pi_{mix} + \Pi_{el} \tag{5.30}$$

Where, Π_{mix} and Π_{el} are the osmotic pressure due to oppose the mixing of polymer-solvent and the elastic response of the polymer network chain due to cross-linking which opposes to the chain expansion respectively. Furthermore, according to Orwoll *et al.* [20], the equivalent osmotic pressure, Π_{eq} with respect to the chemical potential can be expressed as Eq. (5.31).

$$\mu_1 - \mu_1^0 = - \Pi_{eq} V_1 \tag{5.31}$$

where, μ_1 and μ_1^0 are the chemical potentials of the solution during the polymer-solvent interaction and the chemical potential of the pure solvent respectively.

Considering the mixing and the elastic gel behaviour, the relation between the total chemical potential and the chemical potential contributions during solvent interaction into the polymer chain network can be expressed as the well-established Eq. (5.32) [19].

$$\mu_1 - \mu_1^0 = (\Delta\mu_1)_{mix} + (\Delta\mu_1)_{el} \tag{5.32}$$

where, the mixing contribution to the chemical potential energy, $(\Delta\mu_1)_{mix}$ and the chain elasticity contributed chemical potential, $(\Delta\mu_1)_{el}$ for the cross-linked polymeric system are and expressed as Eq. (5.33) and Eq. (5.34) respectively.

$$(\Delta\mu_1)_{mix} = RT\left[\ln(1-\phi) + \phi + \chi\phi^2\right] \tag{5.33}$$

$$(\Delta\mu_1)_{el} = RT\left(\frac{V_1}{\upsilon_{SP} M_C}\right)\left(1 - \frac{2M_C}{M_n}\right)\left(\phi^{1/3} - \frac{\phi}{2}\right) \tag{5.34}$$

where, υ_{SP} represents the specific volume of the swelled gel sample and is calculated from the experimental data by using Eq. (5.35).

$$\upsilon_{SP} = \frac{1}{\rho_{SP}} \tag{5.35}$$

where, ρ_{SP} denotes the density of the swelled sample and is expressed in gm.cc^{-1}. Hence, the equivalent osmotic pressure, Π_{eq} can be determined by substituting the Eqs. (5.32), (5.33) and (5.34) into Eq. (5.31) and can be expressed as Eq. (5.36).

$$\Pi_{eq} = -\frac{RT}{V_1}\left\{\ln(1-\phi) + \phi + \chi\phi^2\right\} - RT\left\{\left(\frac{\rho_{SP}}{M_C}\right)\left(1 - \frac{2M_C}{M_n}\right)\left(\phi^{1/3} - \frac{\phi}{2}\right)\right\} \tag{5.36}$$

The next Section will be focused on the effect of stimuli on gel network during equilibrium swelling.

5.7 Experimental Analysis: Role of Gel Network on Equilibrium Swelling Stimuli

The previous section highlighted on the different network parameters and developed energy associated with gel swelling. This section is now aimed to understand the effect of pH, temperature and visible light laser stimuli on polymer network chain behind the occurrence of polymer swelling.

PART A UVPTT Based Hydrogel

This section is confined to the role of gel network parameters on stimuli applied equilibrium swelled β-CD modified UVPTT gel. All the network parameters are

measured from the experimental equilibrium swelling data by using corresponding equations as described in Section 5.5.

5.7.1A Effect on Medium pH and Temperature Stimuli

The equilibrium swelling under different stimuli, are discussed in previous section (Section 5.3). Based on obtained data from experimental ES studies, the role polymer network parameters behind the swelling, are investigated in this section. In Fig. 5.14, the polymer volume fraction, ϕ varied with environmental condition during equilibrium swelling phenomenon. The volume fraction is decreased at higher environmental temperature (40 °C) and the medium changes from acidic to basic which satisfy the Eq. (5.12). On the other hand, the molecular weight between two cross links (M_C) varies linearly with increase of temperature and the pH of medium (Fig. 5.15) due to the addition of molar volume of solvent to polymer segments between crosslink points with increasing stimuli intensities.

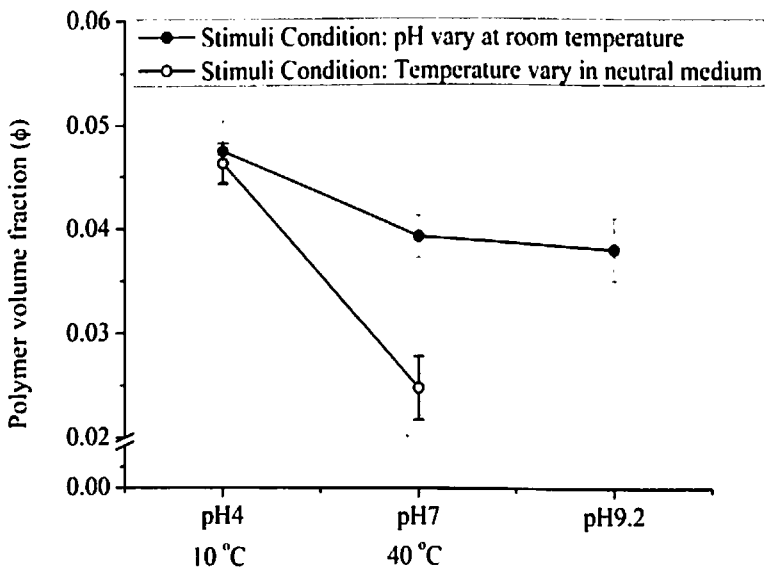

Fig. 5.14: Dependencies of polymer volume fraction, ϕ during ES

From Fig. 5.16, the cross link density is lowered with the increment of external stimuli temperature and the medium changing from acidic to basic, which favoured the dependencies of M_C with the swelling behaviour with the applied external stimuli temperature and pH. Furthermore, the increase of mesh size with increment of temperature and acidic to basic medium (Fig. 5.17) depicts the higher tendency to hold larger amount of solvent.

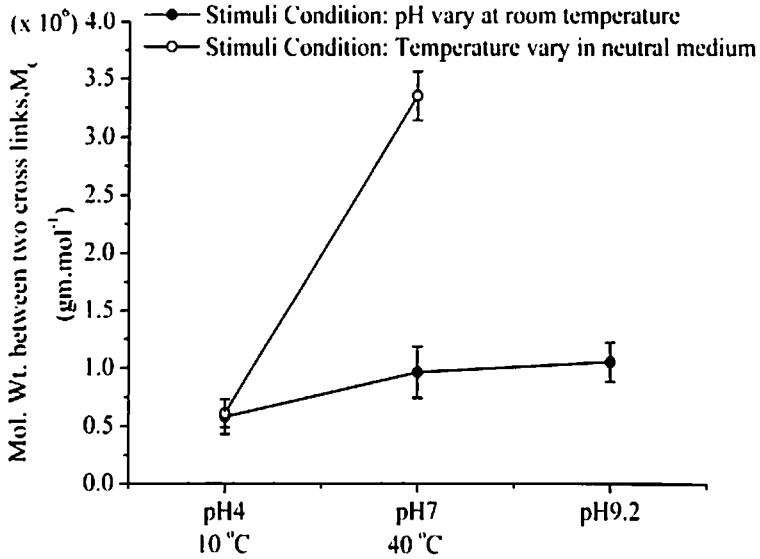

Fig. 5.15: Dependencies of molecular weight between two cross links, M_C during ES

Moreover, the porosity of the gel network has the inverse relationship with both the increment of external stimuli temperature and the alkalinity of the medium (Fig. 5.18). Consequently, the tortuosity increases with the increase of temperature the pH of the medium (Fig. 5.19). In contrast to the free energy effect on gel network during ES phenomenon, the enthalpy was increased with the changing the medium from acidic to basic as well as temperature increases from 10 °C to 40 °C (Fig. 5.20 and Fig. 5.21) and supported by the work done in terms of the volume expansion of the gel.

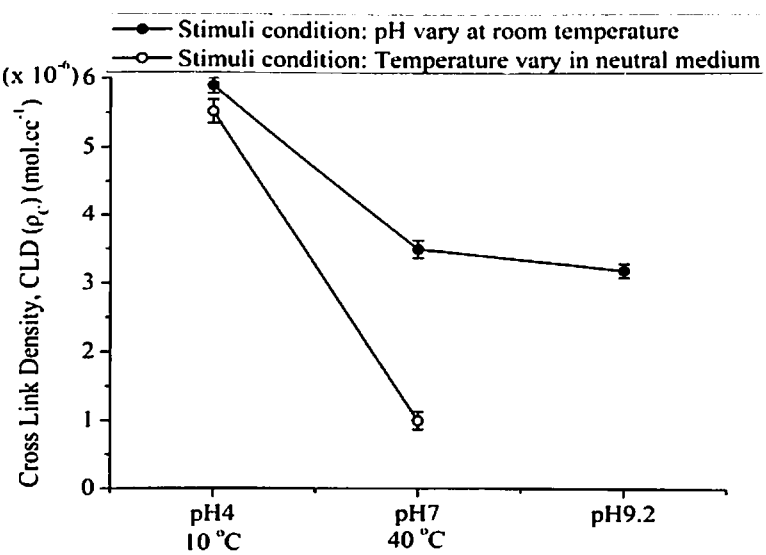

Fig. 5.16: Dependencies of Cross link density, CLD (ρ_C) during ES

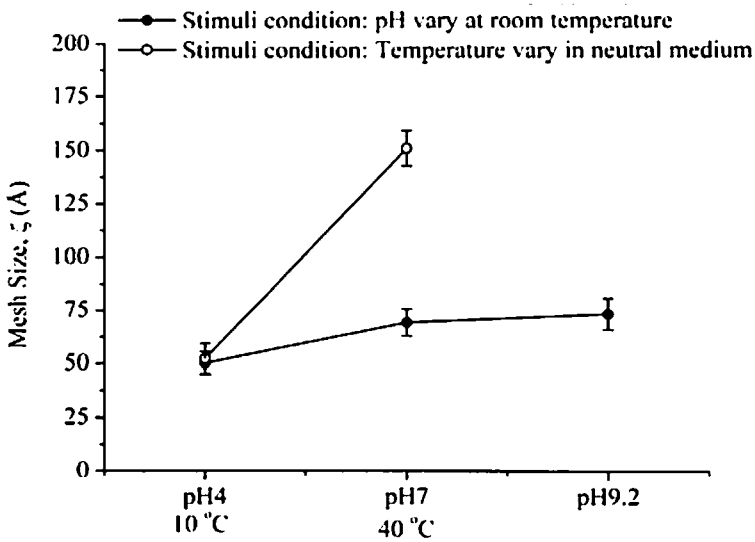

Fig. 5.17: Dependencies of Mesh size, (ζ) during ES

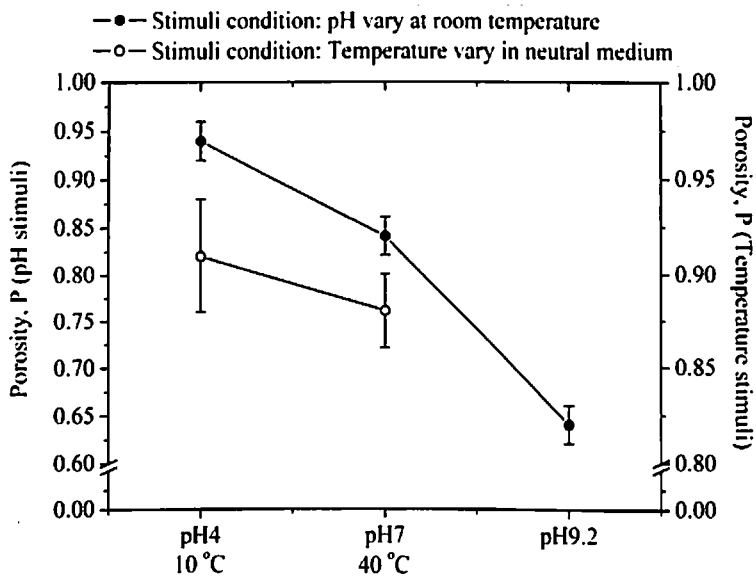

Fig. 5.18: Dependencies of Porosity during ES

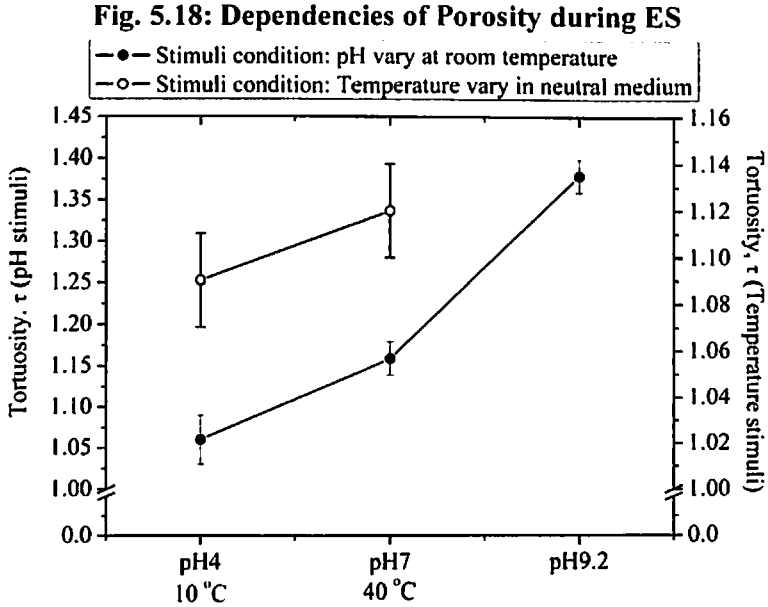

Fig. 5.19: Dependencies of Tortuosity during ES

Hence, the network chain got more stretched and thus enlarged the mesh size as well to hold more solvent/solute molecule with increasing intensity of stimuli. The polymer chains connecting with the cross link points are elongated due to the volume expansion during swelling, thus the chain configurational entropy $\left(\Delta S_{mix\,Chain\,config}\right)$ is reduced with the stimuli intensities (Fig. 5.22) due to the available less probability of configuration in the gel lattice. The lesser chain configurational entropy indicates the lesser disarrangement of the polymer chains at the expanded state of the gel. To oppose this configurational chain entropy, the entropy of mixing of solvent is increased (Fig. 5.20 and 5.21), which favoured the gel to swell upon the higher alkaline medium and higher temperature stimuli.

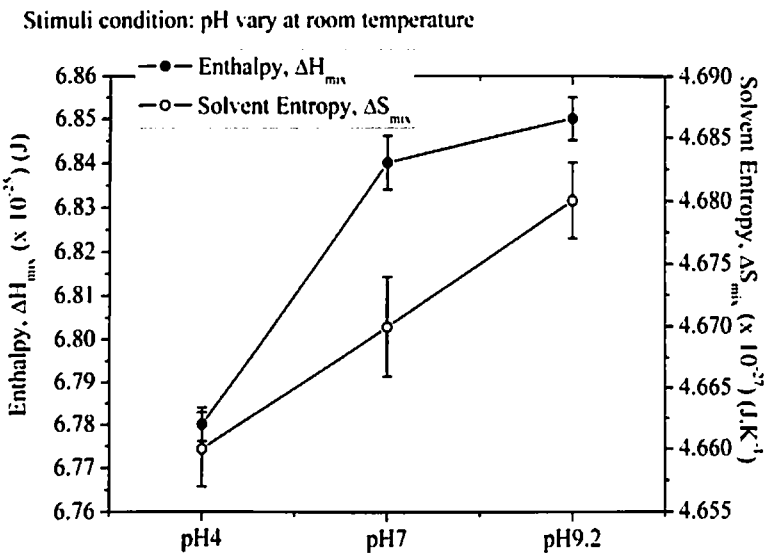

Fig. 5.20: Dependencies of enthalpy and entropy on pH during ES with pH stimuli

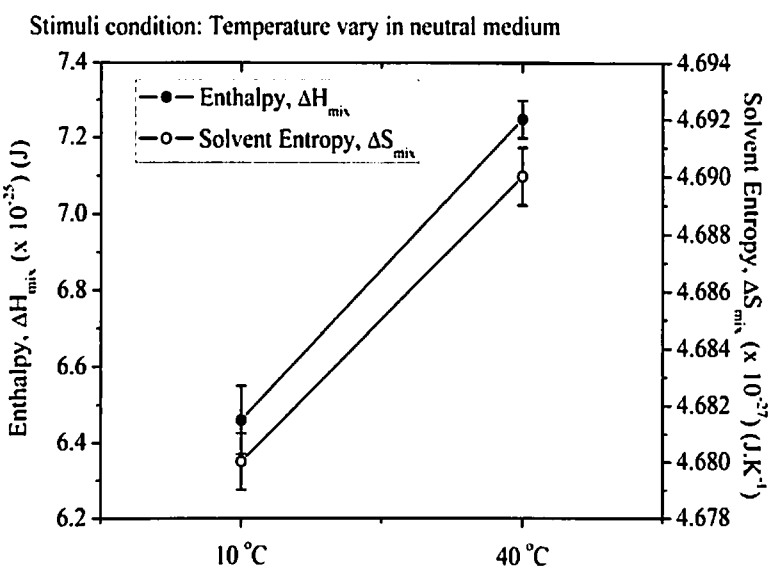

Fig. 5.21: Dependencies of enthalpy and entropy during temperature assisted ES

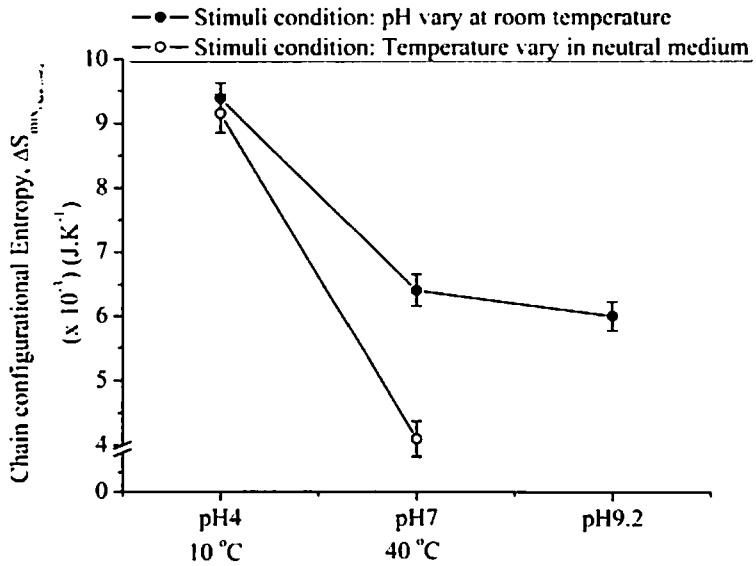

Fig. 5.22: Dependencies of Chain configurational entropy energy $\left(\Delta S_{mix\ Chain\ config}\right)$ on pH and temperature stimulated ES

Thus the enthalpy driven swelling happened into the synthesized UVPTT based IPN network.

5.7.2A Effect of Laser Irradiated Light Stimuli

In case of visible light irradiated ES phenomenon, the polymer volume fraction, ϕ (Table 5.6) decreased for higher AuNP concentrated IPN composite (β-CD-g-(Paac-*co*-Paam)-3) than another lower AuNP concentrated IPN gel composite (β-CD-g-(Paac-*co*-Paam)-1) with identical laser source. As higher concentration of AuNPs are reinforced into β-CD-g-(Paac-*co*-Paam)-3 composite, thus more localized heat is developed inside the β-CD-g-(Paac-*co*-Paam)-3 composite. On the other hand, the molecular weight between two cross links (M_C) (Table 5.6) varies linearly with increase of higher concentration of AuNP containing composite IPN. This helps to hold more solvent inside the gel network and thus higher volumetric expansion (swelling) was observed in β-CD-g-(Paac-*co*-Paam)-3 composite gel than β-CD-g-(Paac-*co*-Paam)-1 (see Fig. 5.7).

Further, the cross link density is lowered with the higher concentration of AuNP containing IPN composite gel (β-CD-g-(Paac-*co*-Paam)-3), which favoured the dependencies of M_C with the swelling behaviour with the applied external stimuli. Furthermore, the increase of mesh size in β-CD-g-(Paac-*co*-Paam)-3 composite depicts the higher tendency to hold larger amount of solvent, which is linearly correlate with M_C.

Table. 5.6.: Measure network parameter of β-CD-g-(Paac-*co*-Paam) composites during light assisted ES

Network parameters	Composite IPN gel	
	β-CD-g-(Paac-*co*-Paam)-1	β-CD-g-(Paac-*co*-Paam)-3
Polymer volume fraction, ϕ	0.1018	0.0887
Molecular weight between two cross links (M_c) ($gm.mol^{-1}$)	1.30×10^5	2.09×10^5
Cross link density, CLD (ρ_c) ($mol.cc^{-3}$)	50.63×10^{-6}	34.38×10^{-6}
Mesh size, ζ (Å)	18.48	24.59
Porosity, P	0.46	0.30
Tortuosity, τ	1.60	1.85

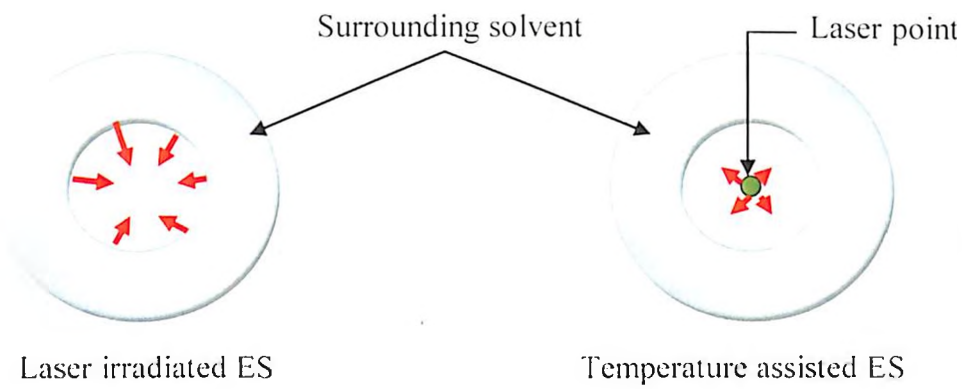

Fig. 5.23: Schematic of temperature and light assisted ES phenomenon

Moreover, the porosity of the composite gel network has the inverse relationship with the increment of localized heat produced in β-CD-g-(Paac-*co*-Paam)-3 composite gels by laser irradiation and consequent the increased tortuosity. This is because of, the inward heat flow (Fig. 5.23, red arrow, outer surface of the gel to centre of the gel) was happened during temperature assisted ES, whereas, the outward heat flow (red arrow, from the localized heat producing zone to surrounding area of the composite) was performed during laser irradiated ES phenomenon.

PART B Non-UVPTT Based Hydrogel

This section is confined to the role of gel network parameters on equilibrium swelled guar gum modified non-UVPTT based gels due to the applied stimuli. All the network parameters are measured from the experimental equilibrium swelling data by using corresponding equations as described in Section 5.5.

5.7.1B Effect on Medium pH Stimuli

In the last section, the volumetric expansion was analyzed on equilibrium swelled gel sample (non-UVPTT based polymers) under different medium stimuli, ranging from acidic to alkaline medium. The maximum solvent intake capability was found in graft gel (GG-g-Paam) than other double cross linked gels in all pH. All the gels have highest swelling ability in alkaline medium i.e pH 9.2 buffer medium than acidic medium. The volumetric expansion of all the gel samples due to the medium stimuli entails the transport of solvent molecule through gel due to random molecular motion of individual molecules through a driving force which involves different phenomenon inside the gel network like sorption, diffusion of solvent molecule. The different network parameters play significant role in spatial alteration with the variation of medium. To analyze the equilibrium swelling performance of all the formulated gels in all medium stimuli, the cross link density (CLD) was measured from the equilibrium swelling experimental data by using Eq. (5.17). Fig. 5.24(a)-(c) indicate that, the CLD is directly related to the presence of GA in the formulated gel samples, whereas the equilibrium volumetric swelling reduces with the increase of concentration of GA into the gel network.

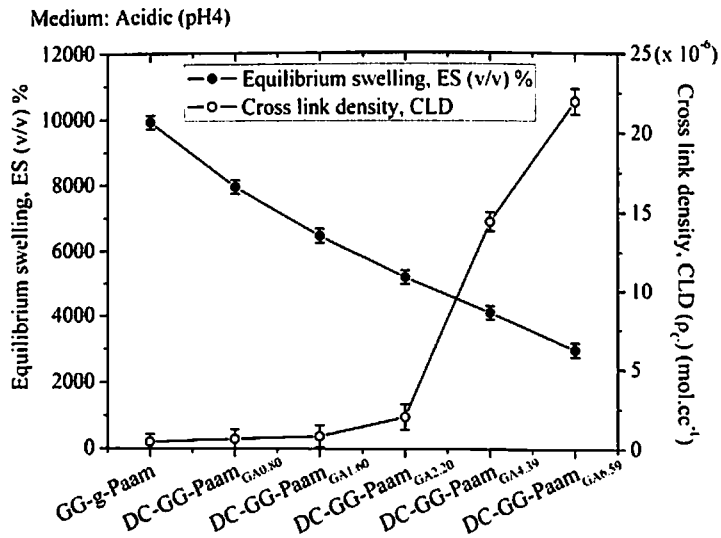

Fig. 5.24(a): Dependencies of ES % and Cross link density on non-UVPTT network in acidic buffer (pH 4) stimuli

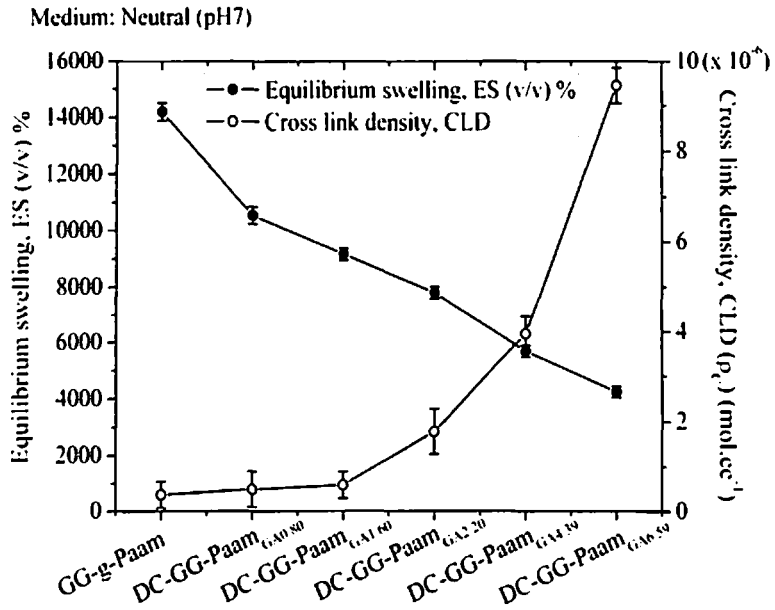

Fig. 5.24(b): Dependencies of ES % and Cross link density on non-UVPTT network in neutral buffer (pH 7) stimuli

The increased CLD means, mole numbers of efficient cross links per unit volume increased for which there is reduction of molar mass between cross link (M_C) from graft sample to highest GA containing gel (DC-GG-Paam$_{GA6.59}$). The M_C was calculated by using Eq. (5.15) and the dependencies of M_C showed in Fig. 5.25(a)-(c). Further, the M_C showed the linear relationship with the medium intensity i.e acidic buffer to alkaline buffer and CLD varied inversely proportional to the medium stimuli for all samples.

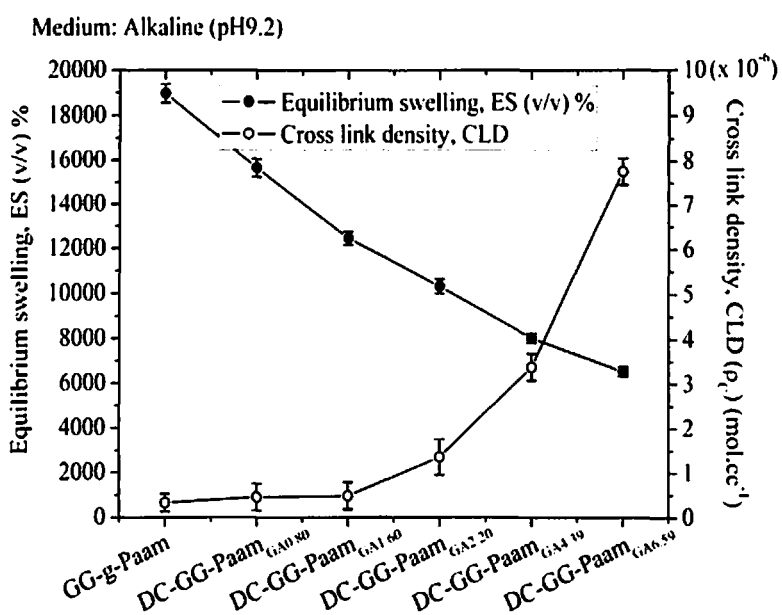

Fig. 5.24(c): Dependencies of ES % and Cross link density on non-UVPTT network in alkaline (pH 9.2) buffer stimuli

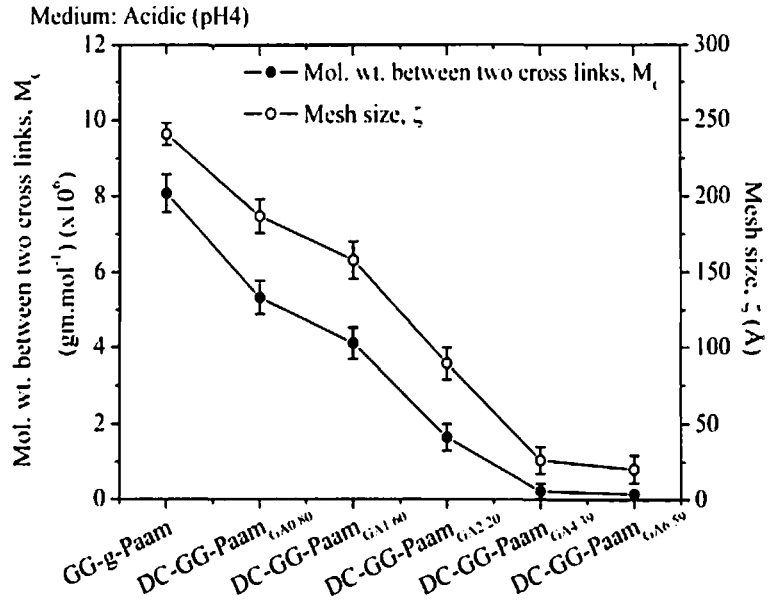

Fig. 5.25(a): Effect of mol. wt. between two cross links (M_C) and mesh size (ζ) on non-UVPTT network in acidic buffer

In addition, the other important parameter called mesh size (ζ) is directly correlated with M_C shrinks with increase of CLD and linearly varied with enhancing the medium alkalinity from acidic for all formulated gels. The mesh size was calculated from ES experimental data using Eq. (5.18). During the ES, the polymer volume fraction (ϕ) is reduced with the changing of medium from acidic to alkaline (Fig. 5.26) as ϕ is reliant on the normalized density of dry gels (normalized by the solvent density) and the amount of water solvent (q_w) required for per gm of dry sample to reach ES state.

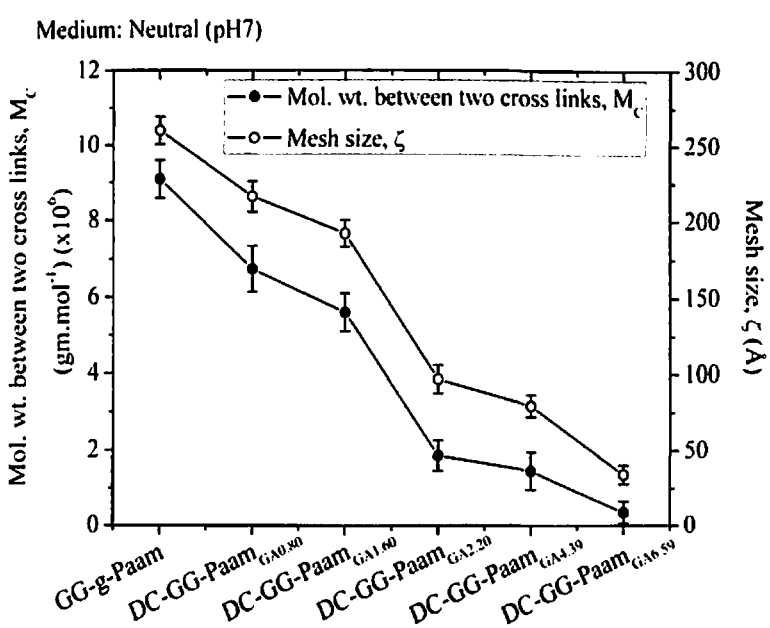

Fig. 5.25(b): Effect of mol. wt. between two cross links (M_C) and mesh size (ζ) on non-UVPTT network in neutral buffer (pH 7)

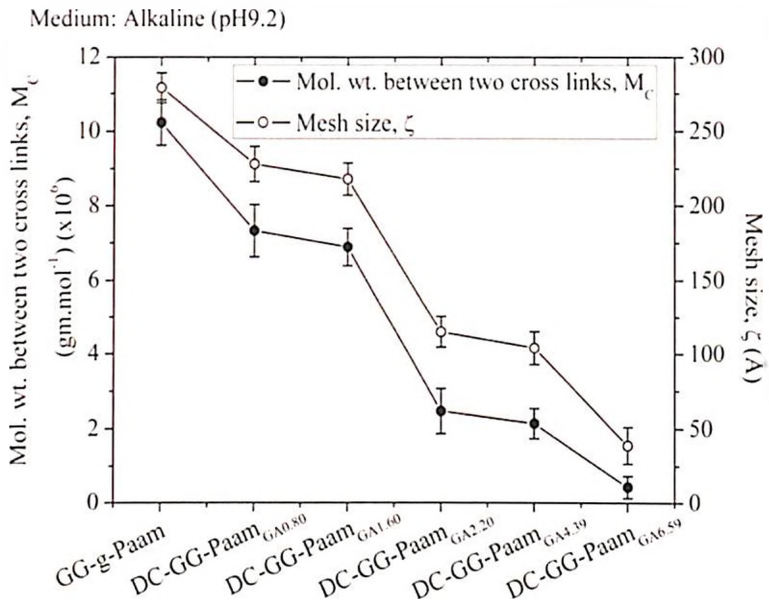

Fig. 5.25(c): Effect of mol. wt. between two cross links (M_C) and mesh size (ζ) on non-UVPTT network in alkaline buffer (pH 9.2)

The polymer volume fraction is increased with the increasing GA quantity into the gel in all medium stimuli. The ϕ was estimated by using Eq. (5.13). Furthermore, the highest porosity (Fig. 5.27) and lowest tortuosity (Fig. 5.28) were found in the double cross linked gel sample with 5.69 mmol GA concentration (DC-GG-$_{PaamGA5.69}$) in all medium stimuli, whereas, vise versa effect observed in case of graft gel. Porosity is reduces with the increasing the basic nature of the medium, whereas higher tortuous path developed in alkaline medium.

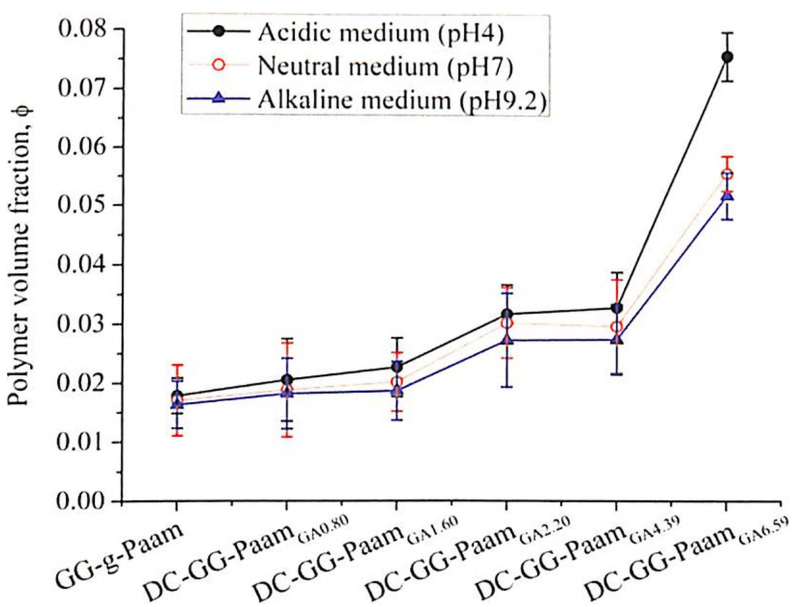

Fig. 5.26: Dependencies of polymer volume fraction (ϕ) in different stimuli medium

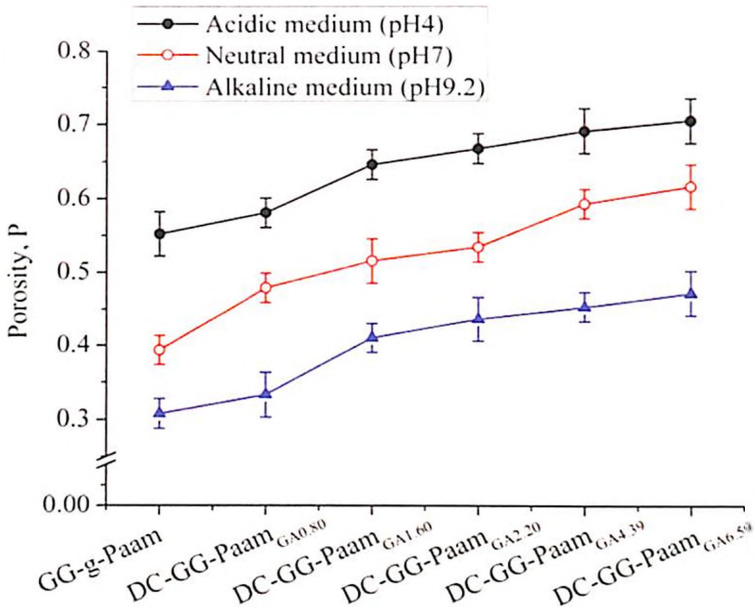

Fig. 5.27: Stimuli effect on porosity in all gels

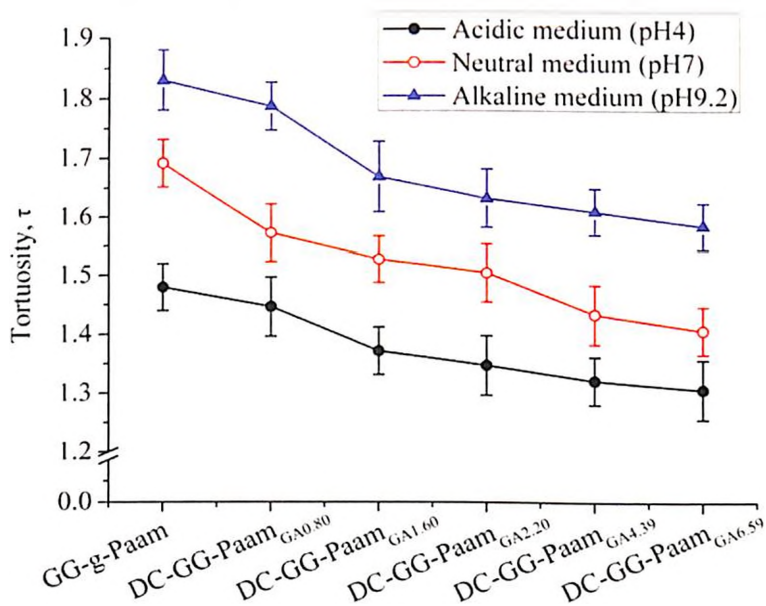

Fig. 5.28: Stimuli effect on tortuosity for all samples

The higher tortuous path helped to enter more solvent molecule into the gel network and thus highest volumetric swelling was observed in alkaline medium stimuli. The porosity and tortuosity were calculated by Eq. (5.20) and Eq. (5.21) respectively.

5.7.2B Effect of Medium Temperature Stimuli

The thermal volumetric expansion of the guar gum modified graft and the other double cross linked gel samples involves the transport of solvent molecule through gel sample due to random molecular motion of individual molecules which facilitates different phenomenon inside the gel network like sorption, diffusion of solvent molecule. The

different network parameters play significant role in spatial alteration with temperature variation. In last section, the highest ES (v/v) % observed in graft gel for both the temperatures, whereas, the ES (v/v)% decreased with the increasing the GA into other double cross linked gel samples. To analyze the equilibrium swelling performance of all the formulated gels in both environmental temperatures, the cross link density (CLD) was measured from the equilibrium swelling experimental data by using Eq. (5.17). Fig. 5.29 (a)-(b) indicate that, the CLD is directly related to the presence of GA in the formulated gel samples for both environmental ES temperature conditions, whereas ES (v/v)% has inverse relationship with the GA concentration containing into the gel network.

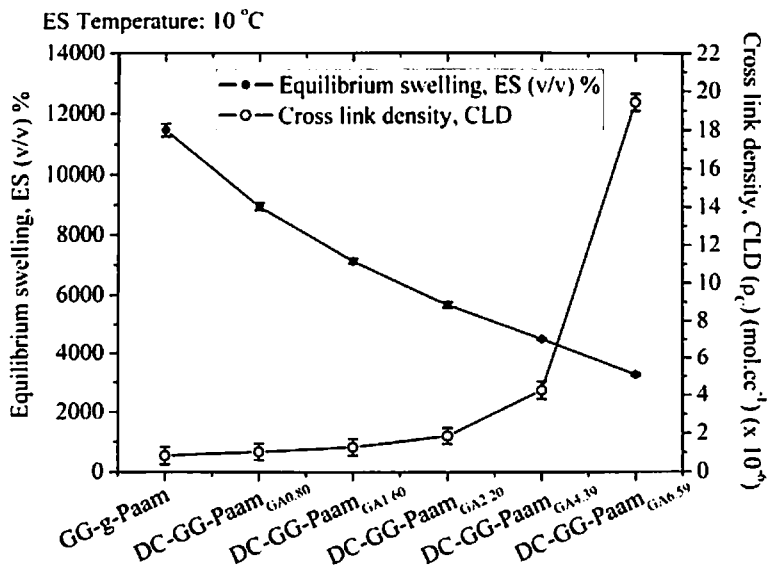

Fig. 5.29(a): Dependencies of ES (v/v)% and CLD on GA into gel network at 10 °C

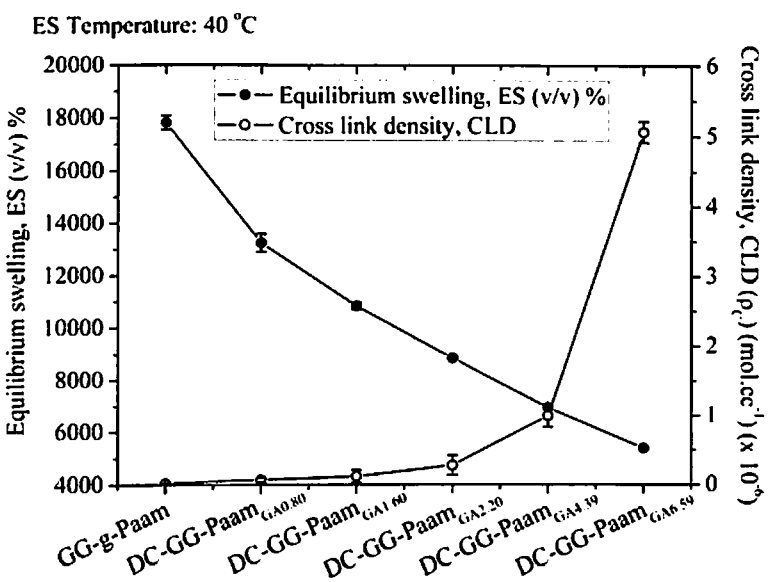

Fig. 5.29(b): Dependencies of ES (v/v)% and CLD on GA into gel network at 40 °C

The graft gel (containing zero concentration of GA) provides highest percentage of volumetric expansion with lowest CLD and for highest quantity of GA containing double cross linked gel sample DC-GG-Paam$_{GA6.59}$ performed lowest percentage of volumetric expansion with highest CLD for both the experimental ES temperature. The increased CLD means, mole numbers of efficient cross links per unit volume increased for which there is reduction of molar mass between cross link (M_C) from graft sample to highest GA containing gel (DC-GG-Paam$_{GA6.59}$). The M_C was calculated by using Eq. (5.15) and the dependencies of M_C showed in Fig. 5.30(a)-(b). Further, the M_C showed the linear relationship with the ES temperature and CLD varied inversely proportional to the experimental ES temperature for all formulated gel samples.

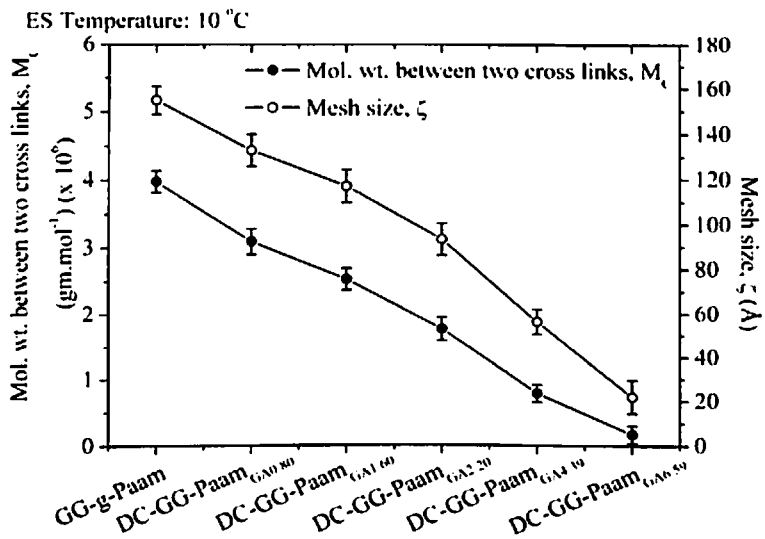

Fig. 5.30(a): Dependencies of molecular weight between two cross links, M_C and Mesh size, ζ on GA into gel network at 10 °C

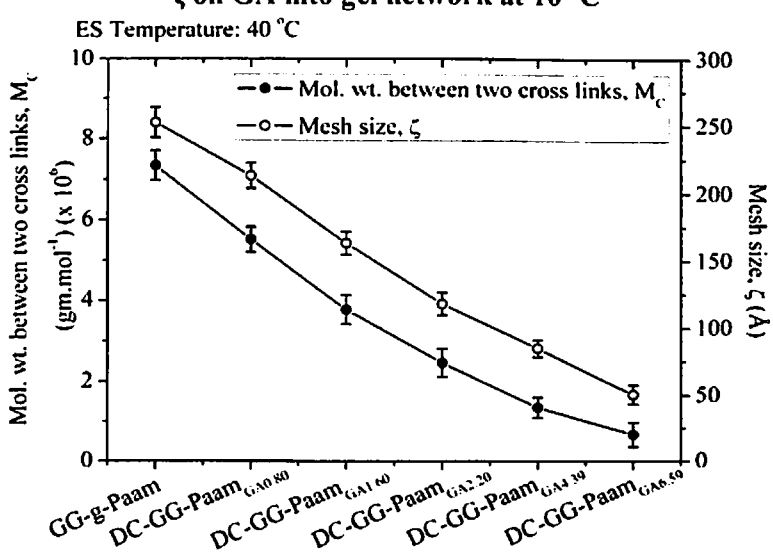

Fig. 5.30(b): Dependencies of molecular weight between two cross links, M_C and Mesh size, ζ on GA into gel network at 40 °C

In addition, the other important parameter called mesh size (ζ) is directly proportional with M_C, and inversely proportional with degree of crosslinking (CLD) with temperature enhance for all formulated gels. The mesh size was calculated from ES experimental data using Eq. (5.18). During the swelling phenomenon in ES, the polymer volume fraction (ϕ) inversely varied with the external temperature (Fig. 5.31) as ϕ is reliant on the normalized density of dry gels (normalized by the solvent density) and the amount of water solvent (q_W) required for per gm of dry sample to reach ES state.

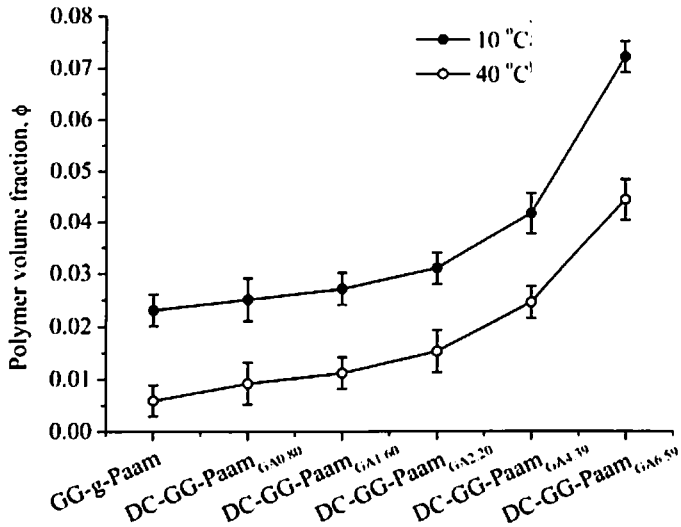

Fig. 5.31: Dependencies of Polymer volume fraction, ϕ on GA into gel network at 10° C and 40° C

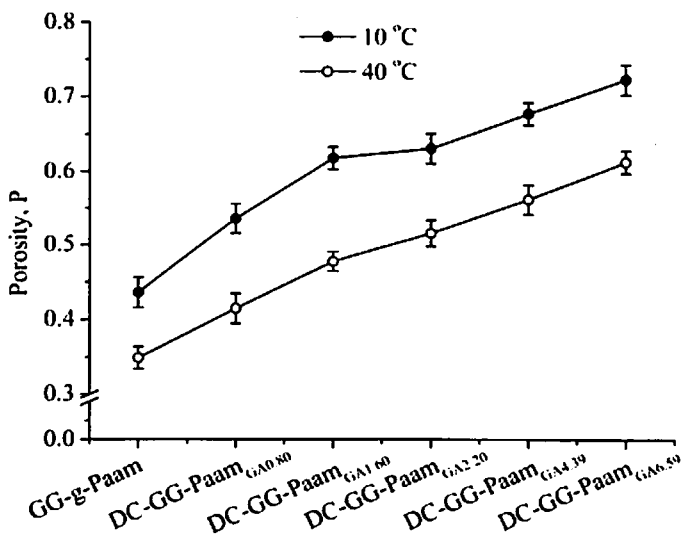

Fig. 5.32: Dependencies of Porosity, P on GA into gel network at 10 °C and 40 °C

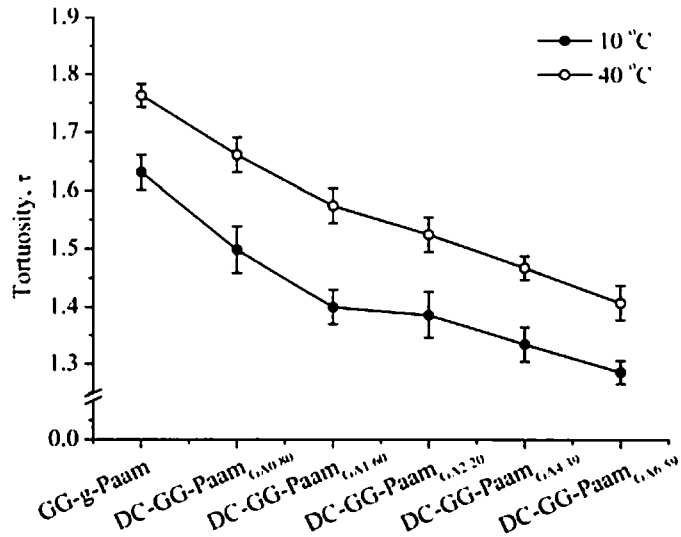

Fig. 5.33: Dependencies of Tortuosity, τ on GA into gel network at 10 °C and 40 °C

Furthermore, the highest porosity (Fig. 5.32) and lowest tortuosity (Fig. 5.33) found in the double cross linked gel sample with 5.69 mmol GA concentration (DC-GG-$_{PaamGA5.69}$) for both ES temperatures, whereas, vise versa effect observed in case of graft gel. Porosity is inversely proportional with the increase of experimental ES temperature and tortuosity is directly proportional with the increase of experimental ES temperature. The tortuosity is the ability of the gel network to create the opening pathway for solvent molecule to enter inside the gel network during swelling.

5.7.3B Effect of Visible Light Stimuli

In case of laser irradiated visible light stimuli ES phenomenon, the polymer volume fraction, ϕ (Table 5.7) decreased for higher AuNP concentrated non-UVPTT composite (DC-GG-Paam$_{GA4.39}$-5) than other two lower AuNP concentrated composites (DC-GG-Paam$_{GA4.39}$-1 and DC-GG-Paam$_{GA4.39}$-3) with identical laser source. As higher concentrations of AuNPs were reinforced into DC-GG-Paam$_{GA4.39}$-5 composite, thus more localized heat is developed inside the DC-GG-Paam$_{GA4.39}$-5 composite. On the other hand, the molecular weight between two cross links (M_C) (Table 5.7) varies linearly with increase of higher concentration of AuNP containing composites. This helps to hold more solvent inside the gel network and thus higher volumetric expansion (swelling) was observed in DC-GG-Paam$_{GA4.39}$-5 composite gel than DC-GG-Paam$_{GA4.39}$-1 and DC-GG-Paam$_{GA4.39}$-3 (see Fig. 5.13).

Table 5.7: Measure network parameter of non-UVPTT based composites during laser irradiated ES

Network parameters	Non-UVPTT based Composite gel		
	DC-GG-Paam$_{GA4.39}$-1	DC-GG-Paam$_{GA4.39}$-3	DC-GG-Paam$_{GA4.39}$-5
ϕ	0.0318	0.0287	0.0272
(M_C) (gm.mol^{-1})	1.74×10^6	2.46×10^6	2.93×10^6
CLD (ρ_c) (mol.cc^{-3})	2.02×10^{-6}	1.53×10^{-6}	1.33×10^{-6}
Mesh size, ζ (Å)	0.92×10^2	1.13×10^2	1.25×10^2
Porosity, P	0.29	0.23	0.18
Tortuosity, τ	1.86	1.99	2.12

Furthermore, the increase of mesh size in DC-GG-Paam$_{GA4.39}$-5 than other two composites depicts the higher tendency to hold larger amount of solvent, which is linearly correlate with M_C. Moreover, the porosity of the composite gel network has the inverse relationship with the increment of localized heat produced in DC-GG-Paam$_{GA4.39}$-5 composite, due to presence of higher AuNP concentration inside the gel. Consequently, the tortuosity increased. Thus the more solvent entered in the network of DC-GG-Paam$_{GA4.39}$-5 than other two composites.

5.7.4 The Laser Assisted Heating Method of AuNP-Polymer Composite

When electromagnetic wave is passing through AuNp, the electric field of incident light polarizes the free electrons (conduction band electrons) on the surface of the metal nanoparticle. According to Link *et al.* [21] the produced in-phase oscillation creates with respect to the much heavier ionic core of a spherical nanoparticle. This electron oscillation around the particle surface causes a charge separation with respect to the ionic lattice of gold, forming a dipole oscillation along the direction of the electric field of the light (Fig. 5.34) [22]. The maximum amplitude of the oscillation at certain frequency is called Surface Plasmon Resonance (SPR). The SPR induced a strong absorption of the incident light which can be measured using a UV–Vis absorption spectrometer. The SPR band is strong for noble metal like Au, Ag etc. The surface enhanced photo illumination generates heat from AuNP. The

SP-mediated heating also induced the scattering of free electrons which involved in the plasma oscillations on gold phonons [23] and this scattering transfers the heat of the NP to the surrounding medium via nonradiative process. The NPs were physically attached with polymer chain, where the chain of both UVPTT and non-UVPTT polymer have shown the temperature sensitivity. The transferred heat increased the local temperature of polymer network was increased. The increased temperature of polymer network helped them to be elongated for which tortuous path of the polymers was widened which increased the diffusion capability of polymer and allowed to swell by light irradiation. The heat generation was increasing with elevated concentration of Au^{3+} as increasing gold ions meant to have increasing number of particle. More number of particles means more free elections, caused more oscillation after light irradiation, which increased the energy difference and heat conversion. Once the laser was in off state, the oscillations of free electrons on the AuNP surface and heat generation were stopped.

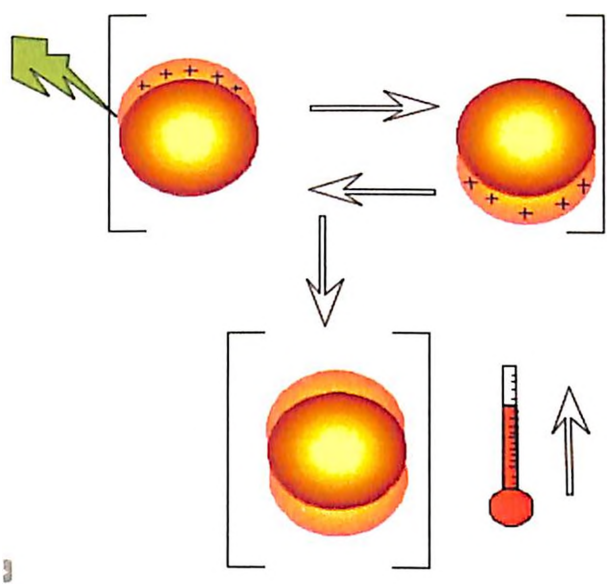

Fig. 5.34: Schematic illustrations of laser assisted nanoparticle heating

5.8 Experimental Analysis: Role of Diffusion on Equilibrium Swelling Stimuli

To Evaluate the Diffusion rate constants (k_D), the experimental data were used. Over the last few decades, there are many mathematical models have been reported for the study of adsorption isotherms at solid-liquid interfaces, such as

solute complexation model [24], metastable-equilibrium adsorption (MEA) theory [25], particle interaction model [26], flocculation model [27], power function (Freundlich-like) model [28], four components adsorption model [29], surface component activity (SCA) model [30]. Apart from these models, the Langmuir and Freundlich isotherm models are also widely used. According to Pan and Liss *et al.* [25], the adsorption equilibrium constant under constant temperature, pressure and medium composition is independent of both adsorbate and adsorbent concentrations in Freundlich model. In case of our experimental analysis described in previous sections, it was observed that, the heterogonous solvent-polymer surface and the exponential distribution of solvent inside polymer network i.e. solvent/solute adsorbs continuously and independently at a constant rate (k_1) during diffusion were occurred. Therefore, Freundlich model was used to evaluate adsorption equilibrium constant i.e. diffusion rate constant (k_D) through Origin Pro 8. The generated corresponding "n" values are also noted to justify the type of diffusion happened inside the gel network. The Eq. (5.8) was used to fit the curve through Classical Freundlich Model. The diffusivity, D_s and the front velocity, u of the solvent were computed by using Eq. (5.9) and Eq. (5.10) respectively. All the evaluated values of k_D, n, $D_s$and u for both UVPTT and non-UVPTT based experimented gels are given in Table 5.8(a)-(c), for medium stimuli (acidic, neutral and alkaline), external temperature (10 °C and 40 °C) and laser irradiated visible light stimuli respectively. For medium assisted ES phenomenon (Table 5.8(a)), the diffusion rate constant is enhanced for all gels in acidic to alkaline medium, which signify the pH of the solvent medium has an effect on gel to diffuse-in the solvent into the gel network. Further, the diffusivity (diffusion co-efficient) also elevated at alkaline medium than acidic for UVPTT and non-UVPTT gels. Thus higher percentage of equilibrium swelling found in alkaline medium, having pH 9.2 in both UVPTT and non-UVPTT based all gels. The diffusional front velocity, u of the solvent is increased in higher alkaline medium, due to larger tortuous path availability during ES in pH 9.2 buffer medium than other acidic and neutral buffer stimuli. As a result, advances the diffusion rate constant, k_D as well. Therefore, the solvent/solute penetrates more into gel samples through wider tortuous path and is getting more swelled at higher medium pH stimuli than lower pH.

For temperature stimulated ES phenomenon (Table 5.8(b)), the diffusion rate constant is enhanced for all gels under higher intensity of temperature stimuli i.e. at 40 °C than 10 °C, which indicate the temperature has an effect on gel to diffuse-in the solvent into the gel network. Further, the diffusivity (diffusion co-efficient) also elevated at higher temperature than lower one for all samples. Thus higher percentage of equilibrium swelling found at higher temperature in both UVPTT and non-UVPTT based all gels.

The diffusional front velocity, u of the solvent is increased with enhancement of temperature, because of the tortuosity increases with increase of temperature (Fig.5.33) in ES phenomenon, as a result, advances the diffusion rate constant, k_D as well.

In case of laser irradiated visible light stimulated ES phenomenon (Fig. 5.8(c)), both UVPTT and non-UVPTT based AuNP composite gels have higher diffusion rate constants in higher concentrated AuNP present in the composite gel. Further, the diffusion co-efficient, and front velocity are also directly related to the NP concentration present inside the gel. The composites containing higher AuNPs developed more localized heat during laser irradiation, thus more solvent penetrate into the composite network through available wider tortuous path. Therefore, the absorption of solvent/solute into the polymer network during swelling is performed by diffusion activities.

Table 5.8(a): Measured values of Diffusion rate constant with Adj.R-square, diffusion co-efficient, diffusion exponent, front velocity and type of diffusion at environmental medium stimuli ES phenomenon

Sample code	Diffusion rate constant, k_D (hr^{-1})	Adj. R-Square	Diffusion exponent, n	Diffusion co-efficient, D_S ($cm^2.hr^{-1}$)	Front velocity, u ($cm.hr^{-1}$)	Diffusion/solvent transport type
Medium stimuli: Acidic (pH 4) buffer						
B-CD-g-(Paac-co-Paam)	0.241±0.011	0.994	0.73±0.03	2.44×10^{-4}	6.27×10^{-3}	Anomalous
Non-UVPTT based gel						
GG-g-Paam	0.235±0.011	0.973	0.41±0.02	2.11×10^{-2}	9.20×10^{-3}	Pseudo-Fickian
DC-GG-$Paam_{GA0.80}$	0.216±0.008	0.985	0.46±0.01	1.07×10^{-2}	11.19×10^{-3}	Pseudo-Fickian
DC-GG-$Paam_{GA1.60}$	0.195±0.009	0.982	0.50±0.02	0.82×10^{-2}	9.34×10^{-3}	Fickian diffusion
DC-GG-$Paam_{GA2.20}$	0.146±0.007	0.988	0.60±0.02	0.67×10^{-2}	9.09×10^{-3}	Anomalous
DC-GG-$Paam_{GA4.39}$	0.272±0.016	0.960	0.42±0.02	0.56×10^{-2}	8.79×10^{-3}	Pseudo-Fickian
DC-GG-$Paam_{GA6.59}$	0.320±0.016	0.956	0.36±0.02	0.52×10^{-2}	8.42×10^{-3}	Pseudo-Fickian
Medium stimuli: Neutral (pH 7) buffer						
B-CD-g-(Paac-co-Paam)	0.285±0.008	0.997	0.65±0.02	4.16×10^{-4}	8.05×10^{-3}	Anomalous
Non-UVPTT based gel						
GG-g-Paam	0.417±0.012	0.974	0.36±0.02	2.70×10^{-2}	11.35×10^{-3}	Pseudo-Fickian
DC-GG-$Paam_{GA0.80}$	0.337±0.014	0.964	0.33±0.01	1.67×10^{-2}	11.19×10^{-3}	Pseudo-Fickian
DC-GG-$Paam_{GA1.60}$	0.287±0.013	0.972	0.39±0.02	1.33×10^{-2}	11.51×10^{-3}	Pseudo-Fickian
DC-GG-$Paam_{GA2.20}$	0.316±0.004	0.996	0.35±0.01	1.15×10^{-2}	10.97×10^{-3}	Pseudo-Fickian

Sample code	Diffusion rate constant, k_D (hr^{-1})	Adj. R-Square	Diffusion exponent, n	Diffusion co-efficient, D_S ($cm^2.hr^{-1}$)	Front velocity, u ($cm.hr^{-1}$)	Diffusion/solvent transport type
DC-GG-$Paam_{GA4.39}$	0.355±0.005	0.995	0.32±0.01	1.09×10^{-2}	10.81×10^{-3}	Pseudo-Fickian
DC-GG-$Paam_{GA6.59}$	0.295±0.008	0.989	0.38±0.01	0.75×10^{-2}	10.62×10^{-3}	Pseudo-Fickian
Medium stimuli: Alkaline (pH 9.2) buffer						
B-CD-g-(Paac-co-Paam)	0.348±0.015	0.990	0.56±0.03	7.93×10^{-4}	10.30×10^{-3}	Anomalous
Non-UVPTT based gel						
GG-g-Paam	0.501±0.010	0.977	0.35±0.01	3.21×10^{-2}	12.22×10^{-3}	Pseudo-Fickian
DC-GG-$Paam_{GA0.80}$	0.438±0.011	0.972	0.24±0.01	2.84×10^{-2}	12.82×10^{-3}	Pseudo-Fickian
DC-GG-$Paam_{GA1.60}$	0.396±0.009	0.979	0.27±0.01	2.26×10^{-2}	12.83×10^{-3}	Pseudo-Fickian
DC-GG-$Paam_{GA2.20}$	0.379±0.005	0.992	0.28±0.01	1.88×10^{-2}	12.84×10^{-3}	Pseudo-Fickian
DC-GG-$Paam_{GA4.39}$	0.278±0.004	0.997	0.38±0.01	1.19×10^{-2}	12.84×10^{-3}	Pseudo-Fickian
DC-GG-$Paam_{GA6.59}$	0.268±0.008	0.988	0.40±0.01	0.98×10^{-2}	12.85×10^{-3}	Pseudo-Fickian

Table 5.8(b): Measured values of Diffusion rate constant with Adj.R-square, diffusion co-efficient, diffusion exponent, front velocity and type of diffusion at temperature stimulated ES phenomenon

Sample code	Diffusion rate constant, k_D (hr^{-1})	Adj. R-Square	Diffusion exponent, n	Diffusion co-efficient, D_S ($cm^2.hr^{-1}$)	Front velocity, u ($cm.hr^{-1}$)	Diffusion/solvent transport type
Temperature stimuli: 10 °C						
UVPTT based gel						
B-CD-g-(Paac-co-Paam)	0.265±0.008	0.997	0.68±0.02	2.69×10^{-4}	6.29×10^{-3}	Anomalous
Non-UVPTT based gel						
GG-g-Paam	0.051±0.006	0.967	0.83±0.04	0.26×10^{-2}	0.99×10^{-2}	Anomalous
DC-GG-$Paam_{GA0.80}$	0.280±0.010	0.980	0.38±0.01	1.20×10^{-2}	1.04×10^{-2}	Pseudo-Fickian
DC-GG-$Paam_{GA1.60}$	0.222±0.006	0.992	0.45±0.01	0.83×10^{-2}	1.03×10^{-2}	Pseudo-Fickian
DC-GG-$Paam_{GA2.20}$	0.247±0.007	0.991	0.43±0.01	0.76×10^{-2}	1.00×10^{-2}	Pseudo-Fickian
DC-GG-$Paam_{GA4.39}$	0.321±0.008	0.986	0.34±0.01	0.83×10^{-2}	0.99×10^{-2}	Pseudo-Fickian
DC-GG-$Paam_{GA6.59}$	0.209±0.009	0.982	0.49±0.02	0.43×10^{-2}	0.95×10^{-2}	Pseudo-Fickian
Temperature stimuli: 40 °C						
UVPTT based gel						
B-CD-g-(Paac-co-Paam)	0.273±0.006	0.999	0.67±0.01	6.22×10^{-4}	10.34×10^{-3}	Anomalous
Non-UVPTT based gel						
GG-g-Paam	0.163±0.013	0.934	0.49±0.03	1.19×10^{-2}	1.21×10^{-2}	Pseudo-Fickian

Sample code	Diffusion rate constant, k_D (hr^{-1})	Adj. R-Square	Diffusion exponent, n	Diffusion co-efficient, D_S ($cm^2.hr^{-1}$)	Front velocity, u ($cm.hr^{-1}$)	Diffusion/solvent transport type
DC-GG-$Paam_{GA0.80}$	0.438±0.008	0.986	0.25±0.01	2.50×10^{-2}	1.20×10^{-2}	Pseudo-Fickian
DC-GG-$Paam_{GA1.60}$	0.397±0.009	0.981	0.29±0.01	1.97×10^{-2}	1.19×10^{-2}	Pseudo-Fickian
DC-GG-$Paam_{GA2.20}$	0.267±0.011	0.997	0.38±0.02	1.14×10^{-2}	1.19×10^{-2}	Pseudo-Fickian
DC-GG-$Paam_{GA4.39}$	0.337±0.010	0.979	0.32±0.01	1.24×10^{-2}	1.19×10^{-2}	Pseudo-Fickian
DC-GG-$Paam_{GA6.59}$	0.217±0.010	0.984	0.50±0.02	0.67×10^{-2}	1.74×10^{-2}	Fickian

Table 5.8(c): Measured values of Diffusion rate constant with Adj.R-square, diffusion co-efficient, diffusion exponent, front velocity and type of diffusion at visible light irradiated ES phenomenon

Sample code	Diffusion rate constant, k_D (hr^{-1})	Adj. R-Square	Diffusion exponent, n	Diffusion co-efficient, D_S ($cm^2.hr^{-1}$)	Front velocity, u ($cm.hr^{-1}$)	Diffusion/solvent transport type
Temperature stimuli: Laser light irradiation (532 nm, 500mW)						
UVPTT based gel						
B-CD-g-(Paac-co-Paam)-1	0.572±0.021	0.979	0.39±0.03	8.35×10^{-4}	1.19×10^{-2}	Pseudo-Fickian
B-CD-g-(Paac-co-Paam)-3	0.575±0.022	0.978	0.39±0.04	13.11×10^{-4}	1.82×10^{-2}	Pseudo-Fickian
Non-UVPTT based gel						
DC-GG-$Paam_{GA4.39}$-1	0.437±0.006	0.999	0.60±0.01	3.98×10^{-3}	3.61×10^{-2}	Anomalous
DC-GG-$Paam_{GA4.39}$-3	0.477±0.005	0.999	0.54±0.01	5.92×10^{-3}	4.26×10^{-2}	Anomalous
DC-GG-$Paam_{GA4.39}$-5	0.518±0.014	0.994	0.48±0.02	8.40×10^{-3}	4.90×10^{-2}	Pseudo-Fickian

5.9 Experimental Procedure: Stimuli Assisted Volume Switching of Polymer

From Section 5.3, the effect of medium (acidic to basic), external temperature and visible light stimuli on equilibrium swelling event was discussed and found all the formulated gel samples were showed positive responsive nature on all external stimuli. This section is focused on gel responsivity, how the gels are responded in volumetric/spatial changes with respect to the swing of the intensity of the external stimuli. The experimentation was done in four combinations of applied external stimuli, such as, Combination I: on solo medium pH as external stimuli, Combination II: on solo external temperature as stimuli, Combination III: dual responsivity with the help of combined stimuli of medium pH and external temperature and Combination IV: visible light stimuli responsiveness on AuNP composites. The volumetric alteration (switching) is studied by applying pulsatile external stimuli in all four combination cases. The volume switching of polymer is meant to be the swelling-deswelling of polymer by responding the applied stimuli. The experimental procedure was followed as discussed below.

Combination I: pH Effect on Spatial Alteration

The spatial alteration because of pH effect as external stimulus was accomplished in two manners: LOW(L)-HIGH(H)-LOW(L) method (LHL) and HIGH(H)-LOW(L)-HIGH(H) method (HLH). In the LHL approach, the ES of dry sample was done in 10 ml of 1% (w/v %) low pH buffer solution and followed by the pH of swelling medium was switched to high pH. Every sole hour the weight of the sample was measured by blotting excess surface adhered liquid. The extended swelling phase of the polymer was recorded for 12 h. The dimension and weight were measured of swelled polymer. The pH of swelling medium was altered to low pH again for understanding of the spatial change due to pH swing. The effect of reduced pH was observed on dynamic deswelling of the polymer at each lone hour by quantifying its weight and dimension for another 12 h. This complete approach i.e. initial LOW pH state to extended HIGH pH state to LOW pH state was termed as LHL approach. The pH aided percentage of memory loss ($ML_{pH}\%$) was calculated by Eq. (5.37) by measuring the volume change of the polymer. The memory loss was estimated by subtracting the volume of the deswelled polymer at final Low pH state from volume of ES polymer at initial low pH state. In second method i.e. in HLH approach, polymer sample was dipped into the high pH solution at (initial HIGH

state) for equilibrium swelling. After taking the dimension and weight of the swelled polymer, pH of the solvent was set at low pH to deswell of the sample. At every single hour, the polymer was taken out from solution, extra water was blotted out and weight was measured for 12 h. Thereafter, pH was switched to again final high pH to complete pH switching cycle. The spatial alteration was evaluated in similar manner as before in LHL approach w.r.t. the initial high pH state and final high pH state. Both methods were performed in for all of the formulations. Each switching experiment was executed for two cycles with five iterations each.

$$\%\ \text{of}\ ML_{pH}\ \text{in LHL, HLH} = \frac{|\ \text{Vol at initial ES pH} - \text{Vol at low/high pH}\ |}{\text{Vol at initial ES pH}} \times 100\ \% \qquad (5.37)$$

Combination II: Thermal Effect on Spatial Switching

The outcome of spatial change due to temperature effect as external stimulus was accomplished in two manners: forward approach (FWA) and reverse approach (REVA). In the first approach, the ES of dry sample done in 10 ml of 1% (w/v %) pH 7 solution at 10 °C and followed by the temperature of the environment was switched to 40 °C. The sample swelled further at 40 °C after ES at 10 °C. Every sole hour polymer sample was taken out of solution, excess surface adhered liquid was blotted and the weight of the sample was measured. The dynamic swelling phase of the polymer was recorded for 12 h. The dimension and weight were measured of swelled polymer and the temperature diminished at 10 °C to understand the spatial change due to temperature swing. The effect of reduced temperature was observed on dynamic deswelling of the polymer at each lone hour by quantifying its weight and dimension for another 12 h. This complete approach i.e. 10 °C (initial LOW state) to 40 °C (HIGH state) to 10 °C (final LOW state) was termed as forward approach (FWA). The temperature aided memory loss (ML) was calculated by measuring the volume change of the polymer. The memory loss was estimated by subtracting the volume of the deswelled polymer at final LOW state at 10 °C from volume of ES polymer at initial LOW state at 10 °C. In second method i.e. in reverse approach (REVA), polymer sample was dipped into the pH 7 solution at 40 °C (initial HIGH state) for equilibrium swelling. After taking the dimension and weight of the swelled polymer, temperature of the pH 7solution was set at 10 °C (LOW) to deswell of the sample. At every single hour, the polymer was taken out from solution, extra water was blotted out and weight was measured for 12 h. Thereafter, temperature switched to 40 °C (final HIGH state) to complete thermoresponsive switching cycle. The spatial

alteration was evaluated in similar manner as before in Forward approach w.r.t. the initial HIGH state at 40 °C and final HIGH state at 40 °C. Both methods were performed in neutral buffer medium for all of the formulations. The percentage of memory loss (ML_{Thermo} %) was calculated by Eq. (5.38). Each switching experiment was executed for two cycles with five iterations each.

$$ML_{Thermo}\ \%\ \text{in FWA, REVA} = \frac{|\text{Initial vol at LOW/HIGH} - \text{vol at final LOW/HIGH}|}{\text{Initial vol at LOW/ HIGH}} x100\ \%(5.38)$$

Combination III: Effect of Combined Stimuli on Spatial Changes: Dual Responsivity

In previous sections the solo pH responsivity was investigated in different pH mediums at room temperature whereas the effect of solo temperature as external stimuli was performed at 10 °C and 40 °C in neutral pH medium. Now the dual responsivity of all formulated gels were executed in three different methods with the combination of pH and temperature: Case I: ES done at 40 °C in pH 7 medium, then switched to pH 4 at 10 °C and pH 9.2 at 10 °C, Case II: ES done at 4 °C in pH 9.2 medium, then switched to pH 4 at 10 °C and pH 7 at 10 °C and Case III:. ES done at 40 °C in pH 4 medium, then switched to pH 7 at 10 °C and pH 9.2 at 10 °C. The effect of dual responsivity of the gels was investigated by measuring the alteration in mass of sample and volumetric changes in sample. The experimental procedure was followed the same as discussed in Combination I and II.

Combination IV: Effect of Visible Light Stimuli on Spatial Changes

The effect of visible light stimuli on both UVPTT and non-UVPTT based composite gels were explored by applying laser irradiation (530 nm, 500 mW) on the composites. The light was applied on pulsatile mode. Due to have the positive stimuli responsive nature of the composites on light stimuli, the laser irradiated (kept ON) for solvent loading and OFF the laser to release the solvent. As discussed in last three sections, the percentage of volumetric changes was calculated by Eq. (5.39). Each switching experiment was executed for two cycles with five iterations each.

$$ML_{Light}\ \% = \frac{|\text{Initial vol at LOW/HIGH} - \text{vol at final LOW/HIGH}|}{\text{Initial vol at LOW/ HIGH}} x100\ \% \qquad (5.38)$$

The LOW and HIGH states are denoting the state of stimuli when laser kept OFF and ON respectively.

5.10 Experimental Analysis: Stimuli Assisted Volume Switching of Polymer

This section is focused on the experimental investigations on volume switching of synthesized gels under different stimuli conditions.

PART A UVPTT Based Gel

The effects of stimuli on efficiency of reversible volume switching of β-CD modified UVPTT based gels are discussed here based on the experimental data.

5.10.1A Combination I: Effect of pH Switching on Volume Alteration

The volumetric changes with respect to the applied medium stimuli (in pulsatile mode) are investigated as described in last section. Two switching cycles were performed for each experiment. The pH switching effect on each ES sample was analyzed in three combinations – Case I: ES sample (in pH 4) is switched to pH 7 and again switched down to pH 4 , Case II: ES sample (in pH 4) is switched to pH 9.2 again switched down to pH 4 and Case III: ES sample (in pH 7) is switched to pH 9.2 again switched down to pH 7. The Fig. 5.35 (a)-(c) depict the effect of pH stimuli switching on synthesized IPN gel sample for Case I, Case II and Case III conditions respectively. The ability to solvent release was investigated by measuring (v/v) percentage of memory loss (ML%) after completion of each cycle using Eq. (5.37).

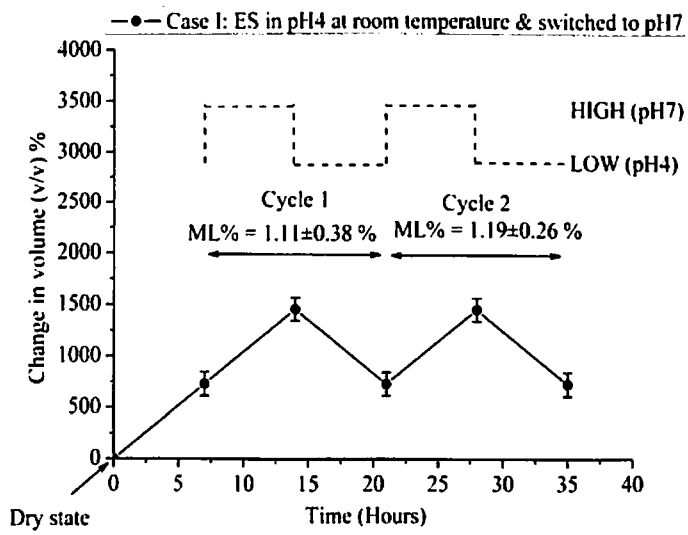

Fig. 5.35(a): Case I: Effect of pH switching (pH 4-pH 7-pH 4-pH 7-pH 4)

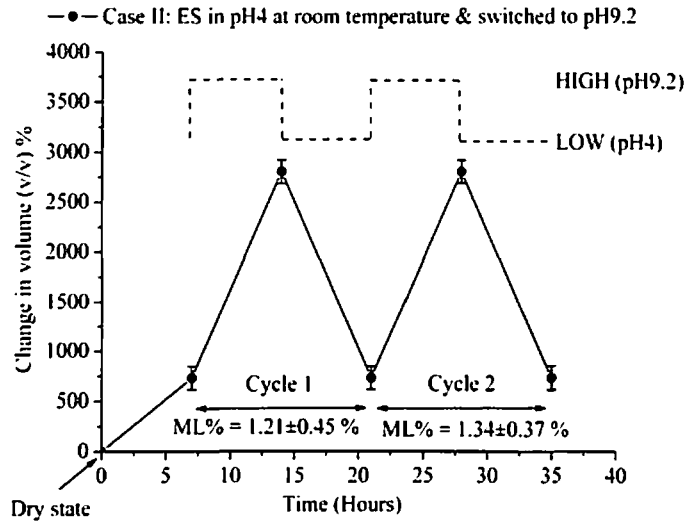

Fig. 5.35(b): Case II: Effect of pH switching (pH 4-pH 9.2-pH 4-pH 9.2-pH 4)

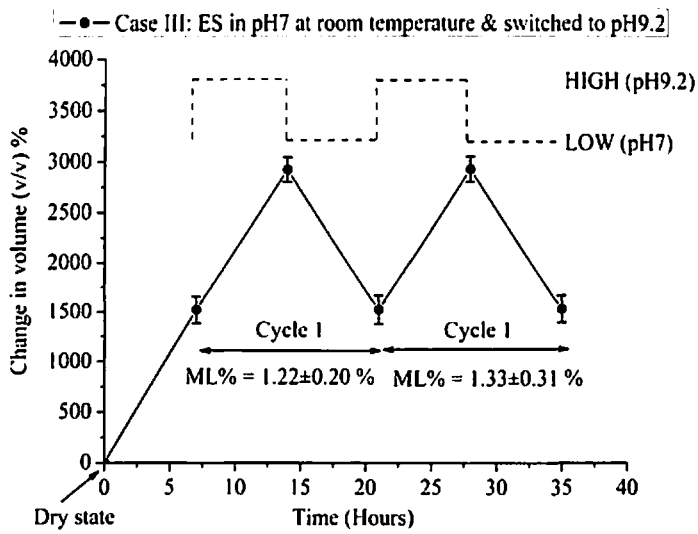

Fig. 5.35(c): Case III: Effect of pH switching (pH 7-pH 9.2-pH 7-pH 9.2-pH 7)

The higher change in volumetric expansion of gel sample performed in Case II and Case III switching than other, which indicates the greater ability to solvent intake by the gel network. The (v/v) ML% increased slightly in Cycle 2 in each Case. This signifies that the solvent release capability is decreased depending upon the number of cycles performed under same condition.

5.10.2A Combination II: Thermal Effect on Volume Switching

To demonstrate the effect of external stimuli on reversible volumetric change of the expanded polymer with the variation of temperature, two approaches were followed as discussed in previous section. Fig. 5.36(a)-(b) depict the dynamic profile on percentage of volume change of the sample with FWA and REVA approached temperature stimuli respectively. The sample volume was calculated from the measured dimensions of sample at each temperature swapping instances. The (v/v) percentages of memory losses (ML) for each cycle for both approaches were calculated from volume of polymer by using Eq. (5.38). The ML% signifies the ability of the gel sample to restore its initial ES volume after thermal switching from LOW-HIGH-LOW (FWA) or HIGH-LOW-HIGH (REVA), which implies the capability of solute/solvent release from swelled polymer network. Fig. 5.36(a)-(b) portrays that, the percentage of memory loss of 1.05±0.41% and 1.55±0.87% occurred in cycle 1 and cycle 2 of FWA respectively, whereas, 1.02±0.89% and 0.83±0.31% of memory losses were observed in cycle 1 and cycle 2 in REVA. This says that the synthesized IPN gel has greater ability to retain its previous volumetric shape through REVA switching after freeing the loaded solvent from its network under external stimuli.

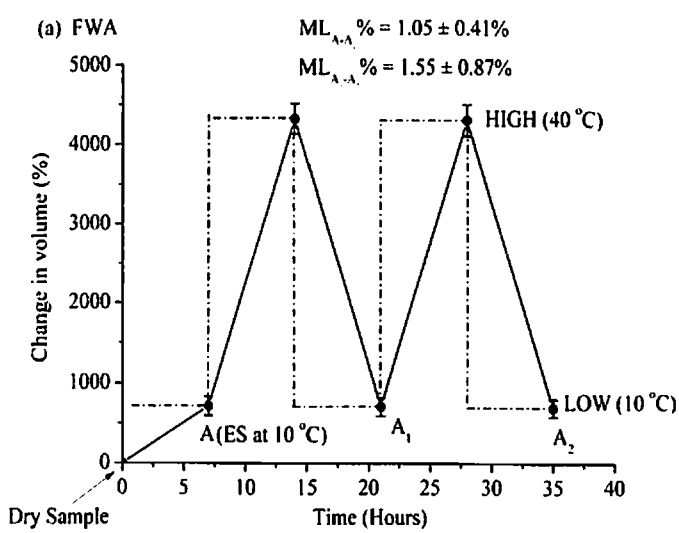

Fig. 5.36(a): Forward Approach (FWA), the effect of temperature on volume alteration

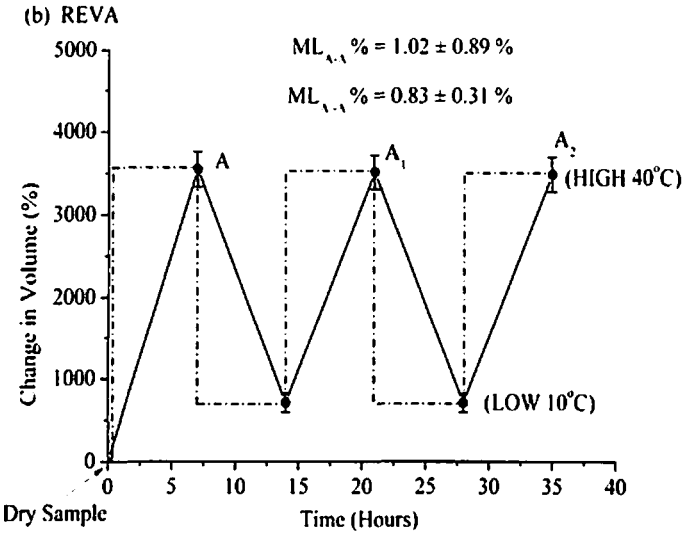

Fig. 5.36(b): Reverse Approach (REVA), the effect of temperature on volume alteration

The minimum memory loss reveals the lower quantity of solute/solvent retention inside the polymer network and hence higher capacity of solute/solvent comes out from the loaded polymer network. A little bit higher volumetric percentage of memory loss (ML) observed in FWA in each cycle than that in REVA, due to the swelling phase in FWA involved extended swelling at 40 °C (HIGH) followed by ES at 10 °C which lost the elasticity of gel to retain its desired volume of ES. During extended swelling phase in FWA, the enthalpy was enhanced by the work done in terms of extended volume expansion of polymer perhaps due to added heat energy into gel network. Hence, the network chain got more stretched and mesh size increased as well to hold more solvent/solute molecule. As a result, the extended swelling in FWA dominates the Deswell phenomenon and hence the FWA provides higher ML % than REVA. In this section, the extended swelling in FWA played vital role for deswelling phenomenon with optimal swelling properties to deliver poor performance on solvent/solute release from polymer network than REVA switching. Furthermore, equilibrium swelling at high temperature (40 °C) performed a significant role as switching activities for solvent/solute intake-release application by means of volume change as well spatial variation of gel sample. Therefore, REVA is a better option to release the solute/solvent from sample network than FWA.

5.10.3A Effect of Combined Stimuli: Dual Responsivity for Solvent Release

In last two sections, it was found that the pH and temperature has an immense effect on volume alterations on the sample. It was also noticeable that, the temperature stimuli based REVA approach was more significant way to release the solvent from polymer network by maintaining the lowest percentage of memory loss (ML%) than FWA. This section is aimed to evaluate the responsivity of the gel on dual external stimuli of pH and temperature in three different cases, as described in Combination IV in Section 5.8. The responsiveness of the gel was investigated by measuring the percentage of volume changes using experimental data. Fig. 5.37 depicts the behavioural nature through the volume changes (in percentage) of the UVPTT gel under applied dual stimuli for all cases. The ES sample is reduced its volume on dual stimuli conditions, which reveals that, the solvent are freed from the gel network and thus deswelled on stimuli.

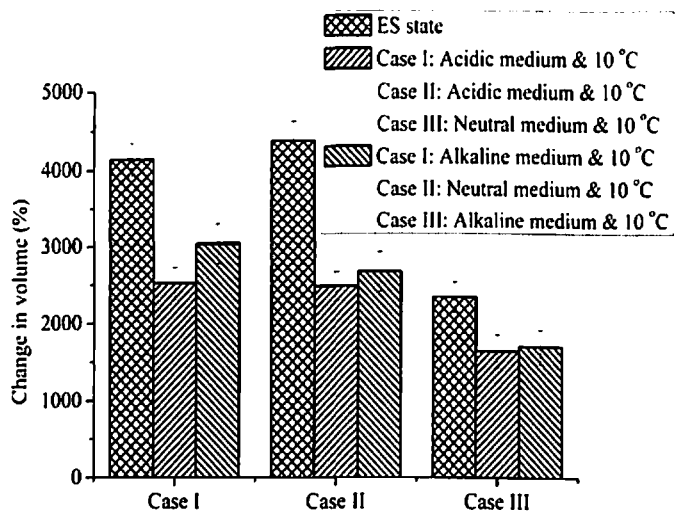

Fig. 5.37: Responsivity of UVPTT gel on dual stimuli

Additionally, in combination with pH, the temperature influenced more on to shrink the gel network once the medium switched from pH 4 to pH 9.2. In Section 5.9.1A, it was observed that the polymer shape expanded with the alteration of medium from pH 4 to pH 9.2 and pH 7 to pH 9.2, but reverse phenomenon occurred when for dual stimuli (combination of pH and temperature) is applied on gel samples. This proofs the impact of temperature as external stimuli over polymer network.

5.10.4A Combination III: Visible Light Effect on Volume Switching

Fig. 5.38 depicts the reversible volume changing events i.e change in volume (%) of the UVPTT composite gels under pulsatile visible light stimuli. The zero percentage of memory loss found for both the composites in both switching cycles. The zero ML% (assessed from Eq. (5.39)) signifies the ability of the composite sample to restore its initial ES volume after light switching, which implies that the equilibrium composites are 100% efficient to release loaded solvent after switching OFF the laser irradiation.

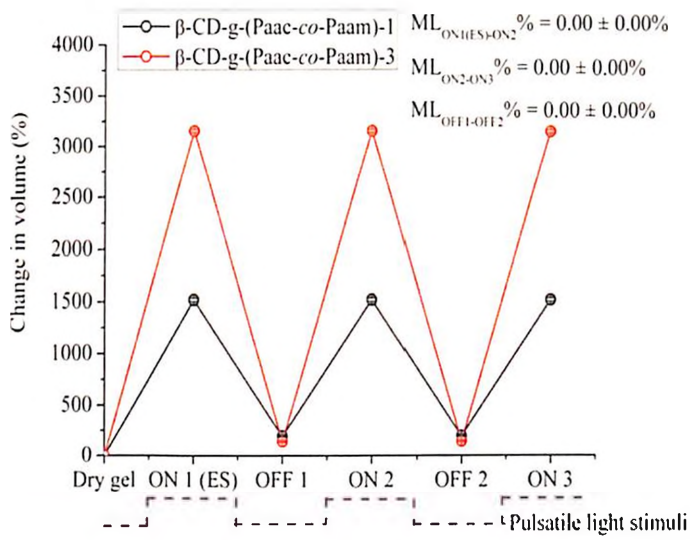

Fig. 5.38: Visible light switching effect on UVPTT composites

PART B: Non-UVPTT Based Gel

The effects of stimuli on efficiency of reversible volume switching of guar gum modified non-UVPTT based gels are discussed here based on the experimental data.

5.10.1B Combination I: Effect of Pulsatile Solo Medium pH

The dry samples were equilibrium swelled in pH 4, pH 7 and pH 9.2 in room temperature (25 °C) separately. Two switching cycles were performed for each experiment. The pH switching effect on each ES sample was analyzed in three combinations – Case I: ES sample (in pH 4) is switched to pH 7 and again switched down to pH 4 to complete a cycle, Case II: ES sample (in pH 4) is switched to pH 9.2 and switched down to pH 4 to complete a cycle. Case III: ES sample (in pH 7) is switched to pH 9.2 and switched down to pH 7 for completion of a cycle. Fig. 5.39(a)-(c) depict the effect of pH stimuli switching on all formulated gel samples for Case I, Case II and Case II conditions respectively. The percentage of memory loss (ML%) after

completion of each cycle was measured by Eq. (5.37). The (w/w) ML_{pH}% decreased in Cycle 2 for each gels in each Cases. The graft sample, GG-g-Paam performed higher (w/w) percentage of ML_{pH} in each cycle as well as all switching conditions.

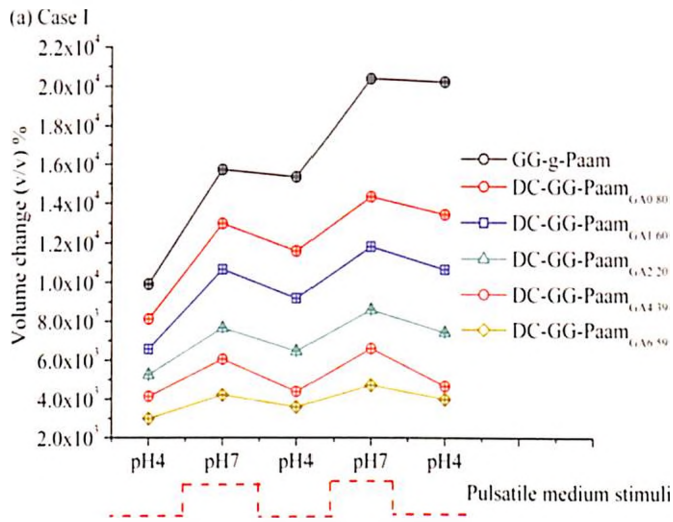

Fig. 5.39(a): Case I: Effect of pH switching on ES samples

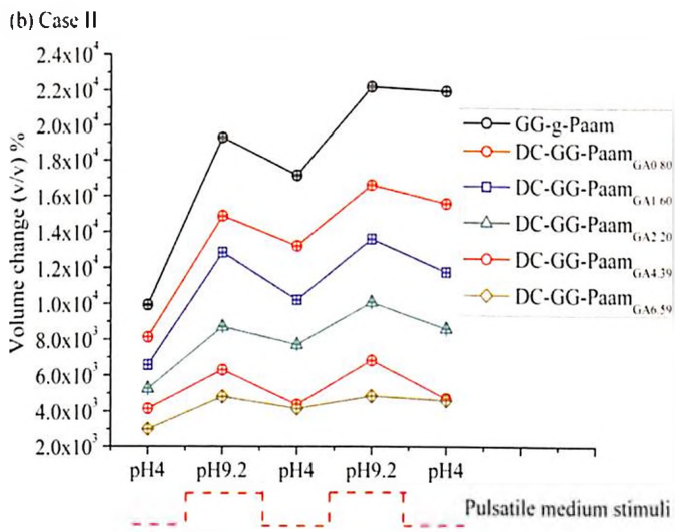

Fig. 5.39(b): Case II: Effect of pH switching on ES samples

This indicates that the graft gel has lesser ability to deswell when the medium is shifted from lower pH to higher one without altering the environmental temperature. Furthermore, (v/v) ML_{pH}% varied in both the cycles with varying of GA concentration in double cross linked gel samples. The sample DC-GG-$Paam_{GA4.39}$ provided lowest (v/v) ML_{pH}% in each cycle under all medium switching environments. This indicates that the concentration of GA present in DC-GG-$Paam_{GA4.39}$ improved the ability to deswell the gel network by performing optimum swelling activities, and thus lowest (v/v) ML_{pH}% performed in each cycle of all medium switching conditions among all other formulated gel samples.

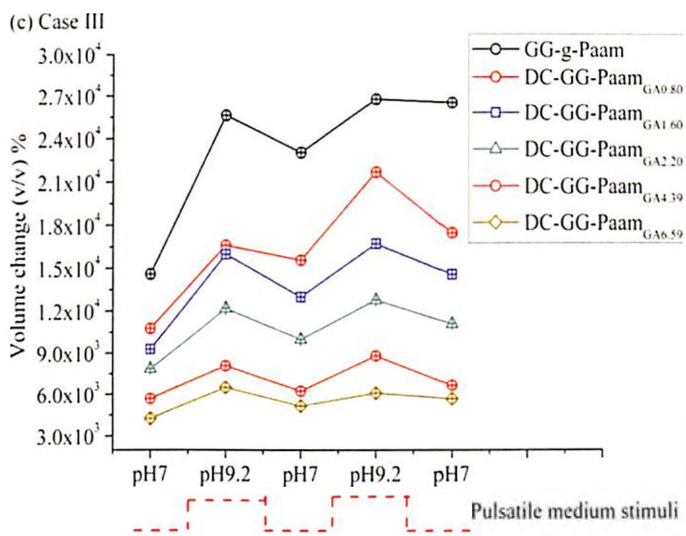

Fig. 5.39(c): Case III: Effect of pH switching on ES samples

5.10.2B Thermal Effect on Spatial Switching

To demonstrate the effect of reversible volumetric change of the swelled polymer with the variation of temperature, two approaches were followed: FWA and REVA. The experimentation was followed as described in last section. All the experiments were performed for two switching cycles. The percentages of memory losses ML_{Thermo}% for each cycle for both approaches were calculated from volume of polymer by using Eq. (5.38) as discussed in last section. For FWA, Fig. 5.40(a)-(b) portrays that, the percentage of volumetric changes (normalized by dry sample volume) dependencies on the applied stimuli for all samples. From both FWA and REVA, it is cleared that, the volume changes are increased with the increase of temperature stimuli and vise versa with the stimuli switches to lower one (10 °C), which means the gels are uptake the solvent at

higher temperature stimuli at 40 °C and released at 10 °C. This swelling-deswelling phenomenon proved the positive stimuli responsive of the gels on the applied temperature stimuli.

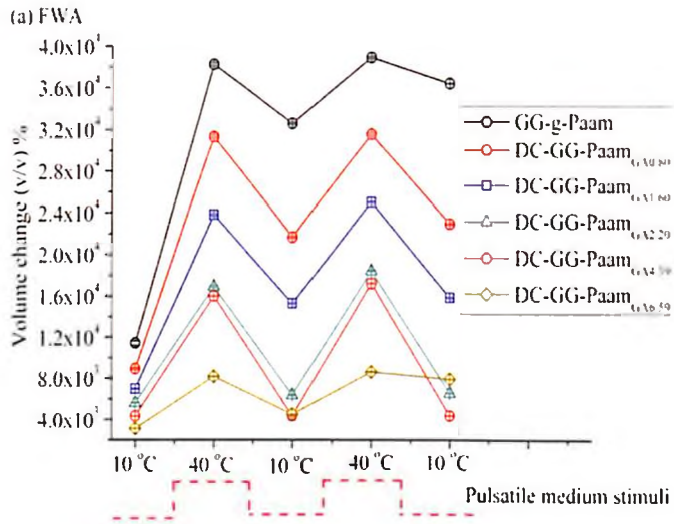

Fig. 5.40(a): Forward Approach (FWA), the effect of temperature on volume alteration

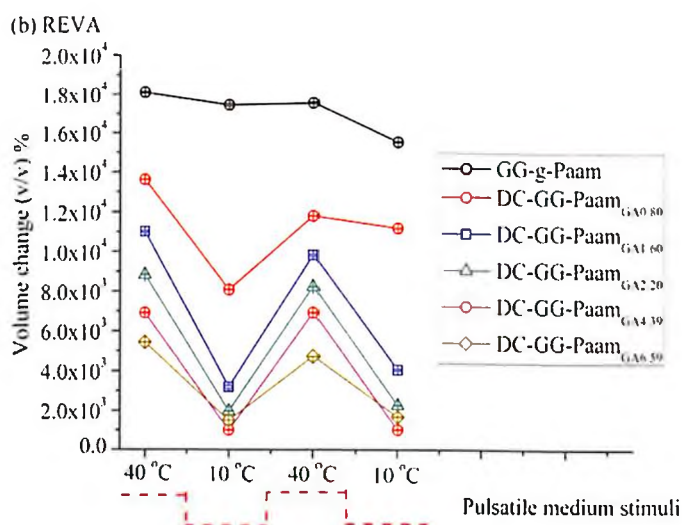

Fig. 5.40(b): Reverse Approach (REVA), the effect of temperature on volume alteration

The ML_{Thermo}% signifies the ability of the gel sample to restore its initial ES volume after thermal switching from LOW-HIGH-LOW (FWA) or HIGH-LOW-HIGH (REVA), which implies the capability of solute/solvent release from swelled polymer network. The minimum ML_{Thermo}% reveals the lower quantity of solute/solvent retention inside the polymer network and hence higher capacity of solute/solvent comes out from the loaded polymer network. Therefore, there is

an important role for double cross linked network rather than graft gel for optimum release of solute/solvent from sample network.

After completion of cycle 1 (in FWA), the maximum ML_{Thermo}% of 181.93±5.27% was found for graft sample and is decreased for formulated double cross linked polymer with enhancing the molar concentration of GA. The lowest percentage of ML_{Thermo} found for DC-GG-$Paam_{GA4.39}$ at both cycles in FWA. However, for REVA, the graft sample gave lower ML_{Thermo}% than FWA after cycle 1. The percentage of ML_{Thermo} was increased for graft and all other double cross linked samples (except DC-GG-$Paam_{GA4.39}$) after cycle 2 than previous state in cycle 1. This is happened due to the swelling phase in FWA involved extended swelling at 40 °C (HIGH) followed by ES at 10 °C which lost the elasticity of gel to retain its desired volume of ES. The ML_{Thermo}% found higher after cycle 1 of FWA than REVA, which is due to the extended stretching of polymer chain due to extended swelling of equilibrium swelled sample. But the sample, DC-G-$Paam_{GA4.39}$ performed lowest percentage of memory loss at each cycle for both FWA and REVA.

During extended swelling phase in FWA, the heat free energy (enthalpy) was elevated by the work done in terms of extended volume expansion of polymer perhaps due to added heat energy into gel network. Hence, the network chain got more stretched and mesh size increased as well to hold more solvent/solute molecule. Furthermore, in case of REVA, the percentages of memory loss, ML_{Thermo}% found slightly higher after cycle 2 than cycle 1, which indicates the loss of ability to retain the previous volumetric shape due to temperature effect and thus loss of chain elasticity. As a result, the extended swelling in FWA dominates the deswell phenomenon and hence the FWA provides higher ML_{Thermo}% than REVA. Therefore, GA played vital role for deswelling phenomenon with optimal swelling properties to deliver better performance on solvent/solute release from polymer network. Enhancement of cross linking density increased the entropic forces due to the tightened network with more disordered chain, led to limit the gel swelling. Introduction of increasing cross linker offered the polymer to exhibit the lower percentage of memory loss because of due to enhancement of chain elastic free energy, which facilitated to regain its previous state by hindering the further swelling and hence deswell happened. The

DC-GG-Paam$_{GA4.39}$ delivered minimum ML_{Thermo}% of 0.26% and 0.17% for FWA and REVA respectively, which confirmed DC-GG-Paam$_{GA4.39}$ has the best performance for solvent/solute release by its volume changes with respect to the temperature swing between 10 °C and 40 °C. Furthermore, the solo temperature performed a significant role as external stimuli for solvent/solute intake-release application by means of volume change as well spatial variation of gel sample.

5.10.3B Effect of Combined Stimuli: Dual Responsivity for Solvent Release

In last two sections, it was found that the pH and temperature has an immense effect on spatial changes on all the formulated gel samples. It was also noticeable that, the temperature stimuli based REVA approach was more significant way to release the solvent from polymer network by maintaining the lowest percentage of memory loss (ML%) than FWA. This section is aimed to scrutinize the responsivity of the polymers on dual external stimuli of pH and temperature in three different stimuli cases, as described in last section. The dual responsivity of all samples is shown in Fig. 5.41(a)-(c) for all cases.

From Fig. 5.41(a)-(c), greater impact on the volume change on the ES sample after applying the dual stimuli. All ES gels are shrank their volume on dual stimuli conditions, which reveals that, the solvent are freed from the gel network and thus deswelled on stimuli. Furthermore, the combined dual stimuli affects in better on switching application on deswelling activities of gel samples than switching by solo pH stimuli as well as solo temperature stimuli. Additionally, in combination with pH, the temperature influenced more on to shrink the gel network once the medium switched from pH 4 to pH 9.2.

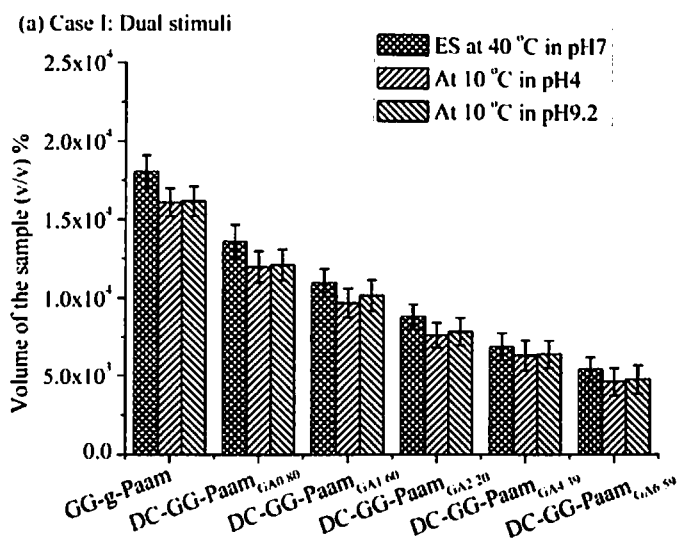

Fig. 5.41(a): Dual responsivity in Case I

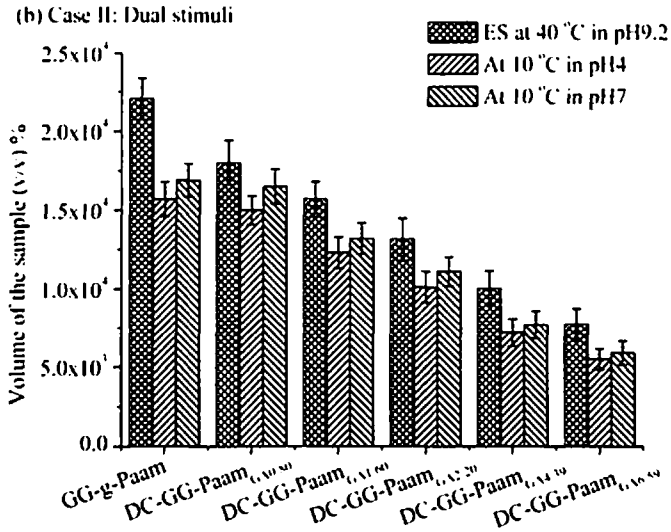

Fig. 5.41(b): Dual responsivity in Case II

In Section 5.9.1B, it was observed that the polymer shape expended (swelled) with the alteration of medium from pH 4 to pH 9.2 and pH 7 to pH 9.2, but reverse phenomenon occurred when for dual stimuli (combination of pH and temperature) is applied on gel samples. This corroborated that the impact of temperature as external stimuli over polymer network. Therefore, from the discussion on the effect of external stimuli e.g. solo pH, solo temperature, dual stimuli and visible light, it can be concluded that, DC-GG-Paam$_{GA4.39}$ is the best possible gel sample, having highest capability to solvent release with optimum capability of solvent intake among other formulated gels.

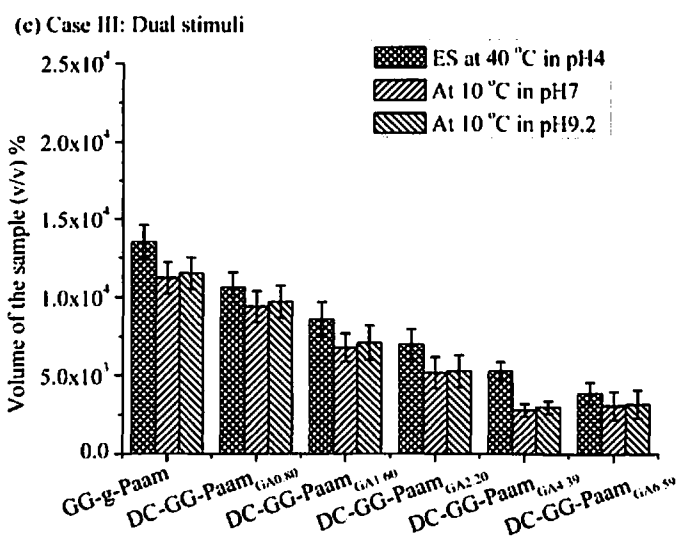

Fig. 5.41(c): Dual responsivity in Case III

5.10.4B Combination IV: Visible Light Effect on Volume Switching

Fig. 5.42 depicts the reversible volume changing phenomenon i.e change in volume (%) of the non-UVPTT composite gels under pulsatile visible light

stimuli. The zero percentage of memory loss found for all three composites in both switching cycles.

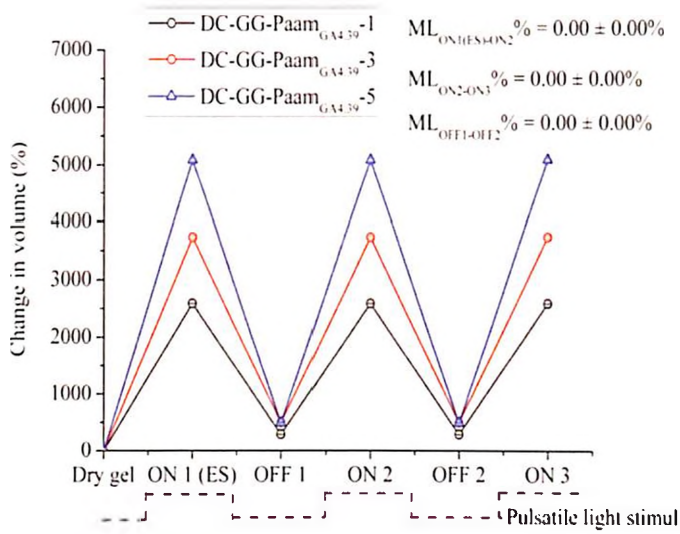

Fig. 5.42: Visible light stimuli effect on volume switching of non-UVPTT composites

The zero ML% signifies the ability of the composite sample to restore its initial ES volume after light switching, which implies that the equilibrium composites are 100% efficient to release the loaded solvent after switching OFF the laser irradiation. Further, higher percentage of volume changing in higher concentration of AuNP reinforced equilibrium solvent loaded gel (DC-GG-Paam$_{GA4.39}$-3) signify the higher capacity of solvent loading on applied light stimuli and thus have ability to release more solvent.

5.11 Swelling and De-Swelling: Role of Network Energy on Stimuli

From Section 5.3 on ES events, it was observed that the synthesized gels were responded as positive hydrogel, i.e. the higher volumetric expansion was found in higher intensified stimuli for all gels. All the gels were expanded their shape in alkaline medium than acidic and neutral medium, similar, phenomenon found in case of temperature stimuli, i.e more swelled occurred at 40 ^{o}C than 10 ^{o}C. Thus, both UVPTT and non-UVPTT based hydrogels were capable to intake more solvent on high intense external stimuli.

Subsequently, from Section 5.9, the solvent release from the loaded (swelled) hydrogels was demonstrated by changing the stimuli in pulsatile manner. As the gels have positive responsivity on the applied stimuli, thus the swelled gels were switched to the lower intense stimuli to deswell the gels via solvent release. In brief, for the pulsatile medium

stimuli swelling-deswelling activities, the gels were released the solvent when the samples were swelled in acidic medium (pH 4), followed by further swelling in either neutral (pH 7) or alkaline medium (pH 9.2) and then shifted to lower pH i.e in acidic (pH 4). Similarly, the neutral medium (pH 7) was used to get ES of gels, followed by the ES gel switched to alkaline medium (pH 9.2) for extended loading of solvent and then shifted to pH 7 for solvent release. In pulsatile medium switching application, the gels were intake the solvent at higher pH medium and released the solvent at lower pH medium.

For, pulsatile temperature stimuli, the FWA and REVA were applied for solvent loading-releasing events, which were demonstrated in Section 5.9.2A and 5.9.2B. The gels were released the solvent from its network at low temperature (10 °C) in REVA and FWA. But in dwell stimuli based switching application; the temperature plays a vital role with medium. It was found that the solvent release happened in Case III, when the gels were equilibrium swelled in acidic medium (pH 4) at 40 °C and switched to neutral medium (pH 7) at 10 °C, which shows the lower temperature effect the network chain and dominated over the medium during deswelling event in Case III.

Thus this section is intended to analyze the role of internal energy and the osmotic effect on the hydrogel chain network due to the applied pulsatile external stimuli for swelling and deswelling of the gels. From Table. ANX I.1, ANX I.2 and ANX I.3 (Annexure I), the behaviour (dependencies) of enthalpic heat energy for mixing (ΔH_{mix}), solvent entropy (ΔS_{mix}) and chain configurational entropy $\left(\Delta S_{mix\,Chain\,config}\right)$ for both β–CD modified UVPTT IPN and guar gum modified non-UVPTT gels on applied pulsatile stimuli is summerized in below Table 5.9. The reversible swelling-deswelling of UVPTT polymer involves breaking and establishment of inter or intra molecular hydrogen bonding of polymer in the aqueous medium. Above the VPTT, there is the dissociation of hydrogen bonding between amide and carboxylic groups of PAAm and PAAc respectively, which leads to polymer swelling by polymer-water interaction where as at below VPTT the formation of hydrogen bonding increases the polymer-polymer interaction, leading of polymer deswelling. During LOW to HIGH thermal switching in both approaches, the total heat content is increased, results in dissociation of hydrogen bonding in PAAc-PAAm molecules into gel network. So the enthalpy was enhanced at the HIGH state for dissociation of intermolecular hydrogen bond into gel network. So β-CD-g-(PAAc-*co*-PAAm) has enthalpy driven volume phase change.

Table. 5.9: Dependencies of enthalpy, solvent entropy and the chain configurational entropy energies on pulsatile stimuli for both UVPTT IPN and non-UVPTT gels

Stimuli environment	Approach/ Case	State of gel	ΔH_{mix}	ΔS_{mix}	$\Delta S_{mix\ Chain\ config}$
Medium pH switch	Case I	Swelling	Increase	Increase	Decrease
		Deswelling	Decrease	Decrease	Increase
	Case II	Swelling	Increase	Increase	Decrease
		Deswelling	Decrease	Decrease	Increase
	Case III	Swelling	Increase	Increase	Decrease
		Deswelling	Decrease	Decrease	Increase
Temperature switch	FWA	Swelling	Increase	Increase	Decrease
		Deswelling	Decrease	Decrease	Increase
	REVA	Swelling	Increase	Increase	Decrease
		Deswelling	Decrease	Decrease	Increase
Dual stimuli switch	Case I	Deswelling	Decrease	Decrease	Increase
	Case III	Deswelling	Decrease	Decrease	Increase

For swelling event on applied HIGH state of medium pH (in Case I, II and III in Section 5.9.1A and 5.9.1B) and the external temperature in FWA and REVA approaches (Section 5.9.2A and 5.92B), the heat free energy (enthalpy) was increased and supported by the work done in terms of the volume expansion of the gel. Hence, the network chain got more stretched and thus enlarged the mesh size as well to hold more solvent/solute molecule. The polymer chains connecting with the cross link points are elongated due to the volume expansion during swelling, thus the chain configurational entropy $\left(\Delta S_{mix\ Chain\ config}\right)$ is reduced due to the available less probability of configuration in the gel lattice. The lesser chain configurational entropy indicates the higher arrangement of the polymer chains at the expanded state of the gel. To oppose this configurational chain entropy, the entropy of mixing of solvent is increased, which favoured the gel to swell upon the switching the stimuli to HIGH.

On the other hand, the osmotic pressure has an effect on the UVPTT and non-UVPTT polymer chain network during stimuli applied. The elastic osmotic pressure due to chain elasticity (Π_{el}) was enhanced with the diminishes the mixing osmotic pressure (Π_{mix}). As a result, the lesser osmotic pressure inside the gel network was established than environment. The measured values of osmotic pressure parameters are listed in Table ANX I.4, I.5 and I.6 in Annexure I. Thus more solvent/solute molecules diffuse-in inside

the polymer. Therefore, the hydrogels were swelled by their volume expansion under HIGH state of applied stimuli (for pulsatile medium pH and temperature).

In contrast to, deswell state, when the HIGH state of stimuli switched to LOW state for both medium pH (in Case I, II and III in Section 5.9.1A and 5.9.1B) and the external temperature in FWA and REVA approaches (Section 5.9.2A and 5.92B), the enthalpy heat energy was lowered and supported by the work done in terms of the volume shrinkage of the gel. Hence, the network chain got relaxed and thus reduced the mesh size as well to free the solvent/solute molecule from its network chain. The entropy for solvent mixing energy is decreased, which confirmed that the availability of higher probable configuration into lattice and thus chain configurational entropy is increased. Thus deswelling phenomenon of the gel has taken place.

On the other, the osmotic pressure has an effect on the polymer chain network once the stimuli were switched to LOW sate. The chain elastic osmotic pressure (Π_{el}) was lowered with the increases of the mixing osmotic pressure (Π_{mix}). As a result, the pressure inside the gel network was increased than environment, which facilitated the outward flow of the solvent/solute from the network. Thus solvent/solute molecules diffuse-out from the polymer. Therefore, the hydrogels were shrinkage their volume under LOW state of applied stimuli (for pulsatile medium pH and temperature) and thus deswell event was happened.

In dual stimuli switching phenomenon (Section 5.9.3B), the ES samples were deswelled by shrinking their volume in all Cases (Case I, II and III). But with the switching stimuli combination of alkaline and 10 °C in Case I and III, the deswelling event of equilibrium swelled gels was quite contradictory with respect to the solo medium pH switching response. But the deswelling happened due to both the enthalpy heat energy and the entropic energy for solvent mixing were reduced with the increase of chain configurational entropy. As a result, the network chain got relaxed and thus the mesh size shrunk as well to free the solvent/solute molecule from its network chain. On the other, the chain elastic osmotic pressure (Π_{el}) was decreased with the increases of the mixing osmotic pressure (Π_{mix}). As a result, the pressure inside the gel network was increased than environment, which facilitated the outward flow of the solvent/solute from the network. Thus solvent/solute molecules diffuse-out from the polymer. Thus deswelling phenomenon has taken place. Thus, the external switching stimuli effect on

the developed energy inside the polymer chain and hence the solvent loading and releasing activities were performed via reversible volume change action of the gels.

5.12 Comparison Between UVPTT and Non-UVPTT on Stimuli Responsiveness

In previous sections, the responses of polymers are investigated at different stimuli. In Section 5.3, the guar gum modified non-UVPTT gels showed higher volumetric equilibrium swelling than β-CD modified UVPTT gel under all applied stimuli. This confirms the higher solvent holding capability of non-UVPTT gels than UVPTT polymer. In Section 5.9, the efficiency of both UVPTT and non-UVPTT based gels were analyzed through reversible volume alteration properties by applying pulsed stimuli with two complete cycles. The effects on the volume regain capacity (percentage of memory loss) for both UVPTT and non-UVPTT based gels on solo pH switching and solo temperature switching are summarized in Table. 5.10A-5.11A and Table 5.10B-11B respectively.

Table 5.10A: Effect of solo pH switching on percentage of Memory Loss (ML%) of β-CD modified UVPTT gel

Percentage of Memory Loss (ML) (v/v) %					
Case I		Case II		Case III	
Cycle 1	Cycle 2	Cycle 1	Cycle 2	Cycle 1	Cycle 2
1.11±0.38	1.19±0.26	1.21±0.45	1.34±0.37	1.22±0.20	1.33±0.31

Table 5.10B: Effect of solo pH switching on percentage of Memory Loss (ML%) of guar gum modified non-UVPTT gels

Sample Code	Percentage of Memory Loss (v/v) (ML_{pH}%)					
	Case I		Case II		Case III	
	Cycle 1	Cycle 2	Cycle 1	Cycle 2	Cycle 1	Cycle 2
GG-*g*-Paam	54.38±1.82	31.41±1.50	71.04±2.03	27.82±4.39	57.39±5.24	15.17±6.49
DC-GG-$Paam_{GA0.80}$	42.46±8.88	15.85±6.99	60.88±3.99	17.52±5.38	43.93±2.02	12.04±2.50
DC-GG-$Paam_{GA1.60}$	39.47±6.16	15.79±4.24	53.64±3.65	14.74±2.55	39.11±1.88	11.82±2.10
DC-GG-$Paam_{GA2.20}$	22.68±7.13	14.79±4.17	45.06±5.62	11.16±2.06	26.55±1.59	10.50±2.85
DC-GG-$Paam_{GA4.39}$	6.11±4.05	6.18±1.81	5.04±2.16	7.23±3.65	9.33±1.67	6.21±2.01
DC-GG-$Paam_{GA6.59}$	19.56±2.64	10.76±2.71	37.11±3.01	10.43±2.57	21.03±1.96	9.53±2.28

Table 5.11A: Effect of solo temperature switching on percentage of Memory Loss (ML%) of UVPTT gel

Percentage of Memory Loss (ML) (v/v) %			
FWA		REVA	
Cycle 1	Cycle 2	Cycle 1	Cycle 2
1.05±0.41	1.55±0.87	1.02±0.89	0.83±0.31

Table 5.11B: Effect of solo temperature switching on percentage of Memory Loss (ML%) of non-UVPTT gels

Sample Code	ML_{Thermo}% (v/v) at FWA		ML_{Thermo}% (v/v) at REVA	
	Cycle 1	Cycle 2	Cycle 1	Cycle 2
G-g-Paam	181.93±5.27	10.34±0.25	3.40±0.83	6.50±1.18
DC-GG-$Paam_{GA0.80}$	137.88±2.99	5.41±0.90	13.74±1.88	26.99±3.80
DC-GG-$Paam_{GA1.60}$	114.23±1.55	3.48±0.46	10.99±1.16	20.12±2.16
DC-GG-$Paam_{GA2.20}$	13.03±0.70	2.58±0.89	7.14±1.61	11.56±1.19
DC-GG-$Paam_{GA4.39}$	0.26±0.09	0.69±0.26	0.32±0.11	0.34±0.04
DC-GG-$Paam_{GA6.59}$	41.04±0.60	41.60±0.73	13.06±0.10	9.72±0.15

From the Table. 5.10A-B and Table 5.11A-B, the lowest memory loss found in UVPTT than non-UVPTT on both solo pH and solo temperature stimuli. In contrast with the GA effect on the non-UVPTT gels, the 4.39 mmol GA containing DC-GG-$Paam_{GA4.39}$ gel performed lowest memory loss than other guar gum modified graft and double cross linked non-UVPTT gels. This confirmed the maximum release efficiency of loaded solvent than other non-UVPTT based gels.

Further, among the AuNP reinforced composite gels (Section 5.3.3A and Section 5.3.3B), non-UVPTT composites gives higher equilibrium swelling ability than UVPTT IPN composite under identical laser irradiation, specifies the non-UVPTT composites have higher capability of solvent loading. On other hand, for visible light stimulated volume switching phenomenon, both β-CD modified UVPTT based IPN composite gels (β-CD-g-(Paac-co-Paam)-1 and β-CD-g-(Paac-co-Paam)-3) and guar gum modified non-UVPTT based composite gels (DC-GG-$Paam_{GA4.39}$-1, DC-GG-$Paam_{GA4.39}$-3 and DC-GG-$Paam_{GA4.39}$-5) achieved zero percentage of memory losses. Thus, the AuNP reinforced composites (both UVPTT and non-UVPTT) are the best performing hydrogels than bare UVPTT and non-UVPTT gels (having no reinforcement of AuNP into

network) and the pulsed visible light stimuli is the best alternative approach to maximize the composites more efficient to release the solvent.

5.13 Conclusion

This chapter demonstrated the different external stimuli effects on both UVPTT and non-UVPTT hydrogels for their efficiency on solvent loading or discharging capability. After applying the stimuli on both UVPTT and non-UVPTT polymers, they both have shown their positive responsivity with the stimuli intensities of medium pH, temperature, combination of pH and temperature and visible light which we were expecting from both of the polymers. But, the responsiveness to external stimuli of published hydrogels are mostly opposite in nature. The applied external stimuli based equilibrium swelling responses of all synthesized UVPTT and non-UVPTT gels and their composites are summarized in Table 5.12. The outcomes of swelling capabilities (based on external stimuli) of the synthesized hydrogels in this current research are more than 100 times than that of the reported gels, which are listed in Table 5.13.

The temperature stimulated hydrogels showed the equilibrium swelling in the range of 23-34% [31] at 25 °C, 178.0±5 to 957.8±28 (wt/wt)% [32] at 25 °C, equilibrium swelling ratio of 6.57-20.68 [33] at the temperature range of 20 °C–50 °C and swelling ratio of 5.14 at 37 °C [34]. Wang *et al.* [35] reported the 7-15 (wt/wt)% swelling ratio of polymer at 37 °C. Where, the current research observed 626.88±46.67 to 1167.16±66.69 (wt/wt)% for the UVPTT IPN and 382.62±2.45 to 1845.71±2.88 (wt/wt)% for non-UVPTT gels at temperature range of 10 °C–40 °C.

Further, in case of temperature stimulated solvent release, Taktak *et al.* [36] reported Water released at a temperature of 30 °C was 62%, while hydrogel lost 90% of water at 60 °C because of the LVPT nature of polymer. Sivaprakasam *et al.* [37] observed 70% water released at 40 °C from the copolymer of PNIPaam and Aac. 80-90% water was released from β-CD modified PNIPaam polymer, reported by Wang *et al.* [38]. Whereas, present research exhibited 0.83±0.31% to 1.55±0.87% memory loss in the pulsatile temperature range of 10 °C to 40 °C for UVPTT polymer and 0.26±0.09% to 0.69±0.26% for 4.39 mmol GA containing non-UVPTT polymer (DC-GG-Paam$_{GA4.39}$). The UVPTT polymer released 99.17% to 98.45 % solvent while the non-UVPTT polymer released 99.31% to 99.74% solvent.

Further, on application of medium stimuli (acidic, neutral and alkaline) the UVPTT gel performed equilibrium swelling of 594.77±36.27 to 750.43±39.87 (wt/wt)% and 362.76±5.22 to 1792.86±6.54 (wt/wt)% equilibrium swelling for non-UVPTT hydrogels, whereas 100-125 (wt/wt)% [39], 305.2±15 (wt/wt) % [32] of the (w/w) percentage of swelling found in acidic medium and 600-700% swelling (in water medium) reported by Nielsen *et al.* [40] and Nadia *et al.* [41] reported 5-70 swelling index in acidic and neutral medium.

In case of medium pH assisted solvent release, the synthesized UVPTT gel performed 1.11±0.38% to 1.34±0.37% of memory loss depending on applied pulsatile pH which indicates about 98.66% to 98.89% of solvent release from the gel network. Similarly 5.04±2.16% to 9.33±1.67% of memory loss showed in 4.39 mmol GA containing non-UVPTT polymer (DC-GG-Paam$_{(GA4.39)}$), indicating 90.67% to 94.96% release of solvent under identical pulsatile pH stimuli. While, Taktak *et al.* [36] reported 85% water release in alkaline medium from acidic pH. Angar *et al.* [42] showed 15%-55% water from PEG-Paam copolymer in acidic medium.

The visible light stimuli approach is unique over reported UV sensitive hydrogels [43], [44], [45]. The published research demonstrated the UV sensitive chromophore (azobenzene, spyrobenzopyran, Triphenylmethane-leuco etc.) based formulations for drug release. The incorporated chromophores are carcinogenic [46] and UV light is not safe for biological cells. Some of researches have been performed for visible and NIR light actuated drug release by vis-NIR sensitive chromophore salt like Riboflavin, Methylene blue, Cardio green etc. The research documented that these chromophores have been used for vis-NIR drug release. The negative hydrogels released the drugs by vis-NIR triggering [47]. Linsley *et al.* [47] released 80% encapsulated cargo for 4 days of NIR exposure. Viger *et al.* [48] released 70% encapsulated solvent from the PLGA polymer for 90 min NIR exposure. But these chromophores molecules produce reactive oxygen species such as singlet oxygen or free radicals upon light irradiation, they can be toxic to cells and lead to irreversible damage [49]. It was also seen that increasing concentration of riboflavin and generation of hydrogen peroxide by visible light exposure resulted in decreased cell viability [50]. The current research overcame these limitations by making visible light sensitive spherical AuNP reinforced polymers. Spherical AuNP induces the cell death of cancer cells *in-vivo* and *in-vitro* but there is no any toxicity found of Spherical AuNP with 5 to 10 nm size to healthy cells like HaCa, as well as cancer cell like MCF7 [51]. Another plus point of using spherical AuNP

reinforced polymers is that the current research is aimed for light triggered loading of solvent and released solvent without light exposure for which the gold nanoparticle could not able to toxicate the released solvent like chromophore as they are chemically stable to irradiated light. The reported visible light stimulated UCST polymer (Paac-Paam) showed the 18.3±3% equilibrium swelling [52] whereas the current research on β-CD modified UVPTT-AuNP composites showed 134.20±3.27% to 141.51±2.12% quilibrium swelling under visible light irradiation. Further more the guar gum modified non-UVPTT-AuNP composites showed 862.37±12.69% to 924.16±11.99% quilibrium swelling under identical condition. However, according to our best knowledge the guar gum/Paam based AuNP has not been yet investigated. The zero percentage of memory loss i.e 100% solvent release was found for pulsatile visible light stimulated solvent UVPTT and non-UVPTT gels in 2 h. Whereas, the higher memory losses were observed in pulsatile pH and temperature stimuli. The lowest memory loss indicates the lowest retention of solvent into gel network after release. Therefore, the synthesized UVPTT and non-UVPTT gels and their nanocomposites showed their efficient responses in all external stimuli like medium pH, temperature and visible light. Moreover, the nanocomposites of both gels have highest efficiency for solvent loading/releasing on light stimuli. In contrast between UVPTT, non-UVPTT gels and their AuNP reinforced composites, the UVPTT responded faster than non-UVPTT polymers. Further, the non-UVPTT hydrogels have higher out-of-plane expansion than β-CD IPNs, and thus have higher ability to load the solvent.

Furthermore, current research showed the swelling kinetics for all synthesized UVPTT and non-UVPTT gels and their nanocomposites by all applied stimuli like medium pH, temperature and visible light. Also, the increased rate constant with increase of stimuli intensity, proves the positive responsive nature with stimuli. Thus, the synthesized positive UVPTT and non-UVPTT gels have a great impact in current research for low temperature depended solvent release and would have great advantage over reported LCST based thermoresponsive hydrogels [53]- [66]. Therefore, in current research could have the advantageous impact on safe release of antibiotics at low temperature (below 30 °C) stimuli.

Finally, the synthesized β-CD modified UVPTT IPN and guar gum modified non-UVPTT gels are of positive type hydrogels. The non-UVPTT based double cross linked (by GA) gels have more solvent release capability than graft gel. The 4.39 mmol GA containing non-UVPTT gel has highest solvent release ability (with lowest solvent

retention into gel network) among other double cross linked non-UVPTT polymers. Further, the AuNP reinforced UVPTT and non-UVPTT composites exhibited visible light sensitivity to release the solvent with 100% solvent release. Therefore, the temperature, dual stimuli (combination of medium pH and temperature) and the visible light stimuli could be the best possible approach for drug release applications, which are investigated in next chapter.

Table 5.12: Stimuli responsiveness on Equilibrium swelling in current research

Gel formulation code	Equilibrium swelling (w/w,v/v) % based on External stimuli				
	Medium			Temperature	
	Acidic buffer (pH 4)	Neutral buffer (pH 7)	Alkaline buffer (pH 9.2)	10 °C	40 °C
Non-composite					
β-CD-g-(Paac-*co*-Paam)	594.77±36.27, 722.03±34.92	718.77±41.36, 1549.54±89.32	750.43±39.87, 2496.32±86.05	626.88±46.67, 737.81±58.45	1167.16±66.69, 2751.60±52.32
GG-g-Paam	1640.71±5.77, 9913.68±212.39	1715.60±8.50, 14189.30±308.07	1792.86±6.54, 18977.25±411.46	1498.33±4.48, 11460.80±205.98	1845.71±2.88, 17818.40±263.83
DC-GG-Paam$_{GA0.80}$	1414.52±7.11, 7934.85±209.96	1544.64±8.11, 10535.20±304.65	1590.50±7.11, 15657.21±409.66	1439.05±0.897, 8929.60±123.67	1633.10±5.70, 13250.40±344.83
DC-GG-Paam$_{GA1.60}$	1278.57±7.21, 6469.15±210.71	1437.79±7.77, 9158.42±212.49	1553.02±6.08, 12448.54±306.41	1327.14±6.96, 7118.40±84.69	1544.52±3.58, 10852.00±135.36
DC-GG-Paam$_{GA2.20}$	902.43±6.21, 5204.84±214.01	947.40±8.11, 7802.51±214.51	1052.81±7.74, 10319.72±313.67	929.05±3.88, 5649.60±99.33	1182.31±6.07, 8863.20±55.45
DC-GG-Paam$_{GA4.39}$	426.14±7.04, 4123.89±211.44	964.45±7.22, 5684.41±217.55	1045.12±6.69, 8039.72±208.22	919.76±1.93, 4470.40±23.13	1172.62±5.48, 6963.20±51.19
DC-GG-Paam$_{GA6.59}$	362.76±5.22, 2988.75±212.86	501.81±6.88, 4238.41±205.46	541.14±7.96, 6552.36±210.05	382.62±2.45, 3238.40±42.68	633.10±5.13, 5396.80±51.13
Composite gels					
	Equilibrium swelling (w/w,v/v) % based on Visible light as applied external stimuli				
β-CD-g-(Paac-*co*-Paam)-1	134.20±3.27, 1832.86±22.28				
β-CD-g-(Paac-*co*-Paam)-3	141.51±2.12, 3365.60±16.63				
DC-GG-Paam$_{GA4.39}$-1	862.37±12.69, 2594.00±10.39				
DC-GG-Paam$_{GA4.39}$-3	900.00±21.28, 3713.38±23.17				
DC-GG-Paam$_{GA4.39}$-5	924.16±11.99, 5093.60±16.63				

Table 5.13: Summarization of stimuli responsive swelling on reported hydrogel

Material	Applied stimuli for swelling	Swelling ratio	Ref #
Non imprinted hydrogels containing ethylene glycol dimethacrylate (EDGMA), 2-hydroxyethyl methacrylate (HEMA) and methacrylic acid (MAA)	Room temperature (25 °C)	23%-33% (w/w) depending on gel composition	[31]
Ciprofloxacine(CFX) -imprinted hydrogel containing EGDMA, HEMA, CFX and MAA	Room temperature (25 °C)	32%-34% (w/w) depending on gel composition	[31]
β-CD-cl-PNIPAm	pH 7.4, 37 °C	ESR: 178.0±5% to 236.9±7%	[32]
β-CD-cl-PMAc	pH 7.4, 37 °C	ESR: 661.7±19% to 957.8±28%	[32]
β-CD-cl-(PNIPAm-co-PMAc)	pH 1.2, 37 °C pH 7.4, 25 °C pH 7.4, 37 °C	ESR in pH 1.2, 37 °C: 305.2±15% ESR in pH 7.4, 25 °C: 885.2±26% ESR in pH 7.4, 37 °C: 568.8±17%	[32]
Thermoresponsive PniPAAm based poly(ε-caprolactone dimethacrylate) biohydrogel	Temperature (20 °C to 50 °C)	At 20 °C, equilibrium swelling: 6.57 to 20.68 depending on gel composition ESR decreased with increase the temperature	[33]
carbopol-*cl*-poly (2-hydroxyethylmethacrylate) hydrogel	Temperature pH	In pH 2.2: 100-125(w/w)%, In pH 7.4: 325 (w/w)% (approx), In simulated wound fluid (pH8): 429.23±33.23 (w/w)% At 27 °C and 37 °C: 200-225(w/w)% At 47 °C: 350-375(w/w)%	[39]
PVA/poly(acrylamide-co-diallyldimethyl ammonium chloride) semi-IPN	DI water at room temperature	ESR (w/w)%: 6500-14000%	[67]
Cellulose/TiO2/β-CD composite hydrogel	DI water, room temperature	ESR (w/w)%: 203.6% approx.	[68]
Ultrasonic hydrogel containing acrylamide and acrylic acid as monomer and cross linking with methylene bis-acrylamide	DI water at room temp. Temp. (5 °C to 45 °C) in DI water With pH medium (pH 2 to pH 10)	Equilibrium swelling (w/w): In DI water-898.90 Temp. varied swelling (w/w): max swelling of 898.90 at 5 °C and minimum swelling of 342.10 at 45 °C With pH variation: 116.42 (in pH 2) to 589.03 (in pH 10).	[69]

References

[1] D. Zhao, X. Shi, T. Liu, X. Lu, G. Qiu, and K. J. Shea, 'Synthesis of surfactant-free hydroxypropyl methylcellulose nanogels for controlled release of insulin &', *Carbohydr. Polym.*, vol. 151, pp. 1006–1011, 2016.

[2] Y. C. Chen, L. C. Liaoa, P. L. Lub, C. L. Loc, H. C. Tsaid, C. Y. Huange, K. C. Weie, T. C. Yenf, G. H. Hsiue 'The accumulation of dual pH and temperature responsive micelles in tumors', *Biomaterials*, vol. 33, no. 18, pp. 4576–4588, 2012.

[3] W. Hong, D. Chena, L. Jia, J. Gu, H. Hu, X. Zhao, M. Qiao 'Thermo- and pH-responsive copolymers based on PLGA-PEG-PLGA and poly(l-histidine): Synthesis and in vitro characterization of copolymer micelles', *Acta Biomater.*, vol. 10, no. 3, pp. 1259–1271, 2014.

[4] X. Hu, X. Hao, Y. Wu, J. Zhang, X. Zhang, P. C. Wang, G. Zou and X. J. Liang 'Multifunctional hybrid silica nanoparticles for controlled doxorubicin loading and release with thermal and pH dual response', *J. Mater. Chem. B*, vol. 1, no. 8, pp. 1109–1118, 2013.

[5] L. Wang, B. Li, F. Xu, Z. Xu, D. Wei, Y. Feng, Y. Wang, D. Jia, Y. Zhou 'UV-crosslinkable and thermo-responsive chitosan hybrid hydrogel for NIR-triggered localized on-demand drug delivery', *Carbohydr. Polym.*, vol. 174, no. July, pp. 904–914, 2017.

[6] S. Li, R. Vatanparast, and H. Lemmetyinen, 'Cross-linking kinetics and swelling behaviour of aliphatic polyurethane', *Polymer (Guildf).*, vol. 41, no. 15, pp. 5571–5576, 2000.

[7] I. Katime and E. Mendizábal, 'Swelling Properties of New Hydrogels Based on the Dimethyl Amino Ethyl Acrylate Methyl Chloride Quaternary Salt with Acrylic Acid and Monomers in Aqueous Solutions', *Mater. Sci. Appl.*, vol. 1, pp. 162–167, 2010.

[8] R. W. Korsmeyer, S. R. Lustig, and A. Nikolaos, 'Solute and Penetrant Diffusion in Swellable Polymers . I . Mathematical Modeling', *J. Polym. Sci. Part B Polym. Phys.*, vol. 24, pp. 395–408, 1986.

[9] H. Scholt, 'Kinetics of Swelling of Polymers and Their Gels', *J. Pharm. Sci.*, vol. 81, no. 5, pp. 467–470, 1992.

[10] G. W. R. Davidson III and N. A. Peppas, 'Solute and penetrant diffusion in swellable polymers v. relaxation-controlled transport in p(hema-co-mma) copolymers', *J. Control. Release*, vol. 3, pp. 243–258, 1986.

[11] W. Xue, S. Champ, and M. B. Huglin, 'Network and swelling parameters of chemically crosslinked thermoreversible hydrogels', *Polymers (Basel).*, vol. 42, pp. 1–5, 2001.

[12] P. J. Flory, *Principles of Polymer Chemistry*. Ithaca, New York: Cornell University Press, 1953.

[13] Z. Y. Ding, J. J. Aklonis, and R. Salovey, 'Model Filled Polymers. VI. Determination of the Crosslink Density of Polymeric Beads by Swelling', *J Polym Sci B Poly Phys*, vol. 29, no. 8, pp. 1035–1038, 1991.

[14] N. A. Peppas and E. W. Merrill, 'Poly(vinyl Alcohol) Hydrogels: Reinforcement of Radiation-Crosslinked Networks by Crystallization', *J. Polym. Sci. Polym. Chem. Ed.*, vol. 14, pp. 441–457, 1976.

[15] T. Canal and N. A. Peppas, 'Correlation between mesh size and equilibrium degree of swelling of polymeric networks', *J. Biomed. Mater. Res.*, vol. 23, pp. 1183–1193, 1989.

[16] S. Niamlang, T. Buranut, A. Niansiri, and A. Sirivat, 'Controlled aloin release from crosslinked polyacrylamide hydrogels: Effects of mesh size, electric field strength and a conductive polymer', *Materials (Basel).*, vol. 6, no. 10, pp. 4787–4800, 2013.

[17] L. Shen and Z. Chen, 'Critical review of the impact of tortuosity on diffusion', *Chem. Eng. Sci.*, vol. 62, no. 14, pp. 3748–3755, 2007.

[18] Z. Xia, M. Patchan, J. Maranchi, J. Elisseeff, and M. Trexler, 'Determination of Crosslinking Density of Hydrogels Prepared from Microcrystalline Cellulose', *Appl. Polym. Sci.*, vol. 127, pp. 4537–4541, 2013.

[19] L. Brannon-Peppas and N. A. Peppas, 'Equilibrium swelling behavior of pH-sensitive hydrogels', *Chem. Eng. Sci.*, vol. 46, no. 3, pp. 715–722, 1991.

[20] R. A. Orwoll and P. A. Arnold, 'Polymer – Solvent Interaction Parameter X', in *Physical Properties of Polymers Handbook*, J. E. Mark, Ed. AIP Press, 1996, pp. 177–196.

[21] S. Link and M. A. El-sayed, 'Shape and size dependence of radiative, non-radiative and photothermal properties of gold nanocrystals', *Int. Rev. Phys. Chem.*, vol. 19, no. 3, pp. 409–453, 2000.

[22] X. Huang and M. A. El-Sayed, 'Gold nanoparticles: Optical properties and implementations in cancer diagnosis and photothermal therapy', *J. Adv. Res.*, vol. 1, no. 1, pp. 13–28, 2010.

[23] O. A. Yeshchenko, N. V Kutsevol, and A. P. Naumenko, 'Light-Induced Heating of Gold Nanoparticles in Colloidal Solution: Dependence on Detuning from Surface Plasmon Resonance', *Plasmonics*, vol. 11, pp. 345–350, 2016.

[24] T. C. Voice and W. J. Weber, 'Sorbent Concentration Effects in Liquid/Solid Partitioning', *Environ. Sci. Technol.*, vol. 19, no. 9, pp. 789–796, 1985.

[25] G. Pan and P. S. Liss, 'Metastable-equilibrium adsorption theory. I. Theoretical', *J. Colloid Interface Sci.*, vol. 201, no. 1, pp. 71–76, 1998.

[26] D. M. Di Toro, J. D. Mahony, P. R. Kirchgraber, A. L. O'Byrne, L. R. Pasquale, and D. C. Piccirilli, 'Effects of Nonreversibility, Particle Concentration, and Ionic Strength on Heavy Metal Sorption', *Environ. Sci. Technol.*, vol. 20, no. 1, pp. 55–61, 1986.

[27] A. K. Helmy, E. A. Ferreiro, and S. G. De Bussetti, 'Effect of particle association on 2,2'-bipyridyl adsorption onto kaolinite', *J. Colloid Interface Sci.*, vol. 225, no. 2, pp. 398–402, 2000.

[28] T. W. Chang and M. K. Wang, 'Assessment of sorbent/water ratio effect on adsorption using dimensional analysis and batch experiments', *Chemosphere*, vol. 48, no. 4, pp. 419–426, 2002.

[29] X. F. Wu, Y. L. Hu, F. Zhao, Z. Z. Huang, and D. Lei, 'Ion adsorption components in liquid/solid systems', *J. Environ. Sci. (China)*, vol. 18, no. 6, pp. 1167–1175, 2006.

[30] L. X. Zhao, S. E. Song, N. Du, and W. G. Hou, 'A sorbent concentration-dependent Freundlich isotherm', *Colloid Polym. Sci.*, vol. 291, no. 3, pp. 541–550, 2013.

[31] S. Kioomars, S. Heidari, B. Malaekeh-Nikouei, M. Shayani Rad, B. Khameneh, and S. A. Mohajeri, 'Ciprofloxacin-imprinted hydrogels for drug sustained release in aqueous media', *Pharm. Dev. Technol.*, vol. 22, no. 1, pp. 122–129, 2017.

[32] J. Gan, X. X. Guan, J. Zheng, H. Guo, K. Wu, L. Liang and M. Lu 'Biodegradable, thermoresponsive PNIPAM-based hydrogel scaffolds for the sustained release of levofloxacin', *RSC Adv.*, vol. 6, no. 39, pp. 32967–32978, 2016.

[33] A. Roy, P. P. Maity, A. Bose, S. Dhara, and S. Pal, 'β-Cyclodextrin based pH and thermo-responsive biopolymeric hydrogel as a dual drug carrier', *Mater. Chem. Front.*, vol. 3, no. 3, pp. 385–393, 2019.

[34] B. B. Mandal, S. Kapoor, and S. C. Kundu, 'Biomaterials Silk fibroin / polyacrylamide semi-interpenetrating network hydrogels for controlled drug release', *Biomaterials*, vol. 30, no. 14, pp. 2826–2836, 2009.

[35] Q. Wang, R. Hou, Y. Cheng, and J. Fu, 'Super-tough double-network hydrogels reinforced by covalently compositing with silica-nanoparticles', *Soft Matter*, vol. 8, pp. 6048–6056, 2012.

[36] F. Taktak, 'Rapid Deswelling of PDMAEMA Hydrogel in Response to pH and Temperature Changes and Its Application in Controlled Drug Delivery', *Afyon Kocatepe Univ. J. Sci. Eng.*, vol. 16, no. 1, pp. 68–75, 2016.

[37] K.Sivaprakasam, P. Mawilmada, J.N. Schoess, L. Schaefer, Y.H. Lee, L. Ramakrishnan, M. Mandell 'Rapid Deswelling of Poly(N-Isopropyl Acrylamide-Co-Acrylic Acid) Hydrogels in Response to Temperature Changes', *World Res. J. Biomater. ISSN World Res. J. Biomater.*, vol. 1, no. 1, pp. 2278–7046, 2012.

[38] Y. Wang, N. Yang, D. Wang, Y. He, L. Chen, and Y. Zhao, 'Poly (MAH-β-cyclodextrin-co-NIPAAm) hydrogels with drug hosting and thermo/pH-sensitive for controlled drug release', *Polym. Degrad. Stab.*, vol. 147, no. November 2017, pp. 123–131, 2018.

[39] B. Singh, A. Sharma, A. Sharma, and A. Dhiman, 'Design of Antibiotic Drug Loaded Carbopol- Hydrogel for Wound Dressing Applications Abstract Materials used', *iMdePub Journals*, vol. 4, pp. 1–9, 2017.

[40] A. L. Nielsen, F. Madsen, and K. L. Larsen, 'Cyclodextrin modified hydrogels of PVP/PEG for sustained drug release', *Drug Deliv.*, vol. 16, no. 2, pp. 92–101, 2009.

[41] N. S. Malik, M. Ahmad, and M. U. Minhas, 'Cross-linked β-cyclodextrin and carboxymethyl cellulose hydrogels for controlled drug delivery of acyclovir', *PLoS One*, vol. 12, no. 2, pp. 1–17, 2017.

[42] N. E. Angar and D. Aliouche, 'Deswelling of hydrogels in aqueous and polyethylene glycol solutions. A new approach for drug delivery application', *Period. Polytech. Chem. Eng.*, vol. 62, no. 2, pp. 137–143, 2018.

[43] H. Y. Yoon, H. Koo, K. Y. Choi, I. C. Kwon, K. ChoiJae, H. Park, K. Kim, 'Photo-crosslinked hyaluronic acid nanoparticles with improved stability for in vivo tumor-targeted drug delivery', *Biomaterials*, vol. 34, pp. 5273–5280, 2013.

[44] C. Chiang and C. Chu, 'Synthesis of photoresponsive hybrid alginate hydrogel with photo-controlled release behavior', vol. 119, pp. 18–25, 2015.

[45] Y. Guan, H. B. Zhao, L. X. Yu, S. C. Chen, and Y. Z. Wang, 'Multi-stimuli sensitive supramolecular hydrogel formed by host-guest interaction between PNIPAM-Azo and cyclodextrin dimers', *RSC Adv.*, vol. 4, no. 10, pp. 4955–4959, 2014.

[46] R. Klajn, 'Spiropyran-based dynamic materials', *Chem. Soc. Rev.*, vol. 43, no. 1, pp. 148–184, 2014.

[47] C. S. Linsley, V. Y. Quach, G. Agrawal, E. Hartnett, and B. M. Wu, 'Visible light and near infrared-responsive chromophores for drug delivery-on-demand applications', *Clin. Res. Hepatol. Gastroenterol.*, vol. 39, no. 1, pp. 9–19, 2015.

[48] M. L. Viger, W. Sheng, K. Dore, A. H. Alhasan, C. J. Carling, J. Lux, C. de G. Lux, M. Grossman, R. Malinow, A. Almutairi 'Near-infrared-induced heating of confined water in polymeric particles for efficient payload release', *ACS Nano*, vol. 8, no. 5, pp. 4815–4826, 2014.

[49] R. Chen, X. Wang, X. Yao, X. Zheng, J. Wang, and X. Jiang, 'Near-IR-triggered photothermal/photodynamic dual-modality therapy system via chitosan hybrid nanospheres', *Biomaterials*, vol. 34, no. 33, pp. 8314–8322, 2013.

[50] J. Hu, Y. Hou, H. Park, B. Choi, S. Hou, A. Chung, M. Lee 'Visible light

crosslinkable chitosan hydrogels for tissue engineering', *Acta Biomater.*, vol. 8, no. 5, pp. 1730–1738, 2012.

[51] S. Vijayakumar and S. Ganesan, 'Size-dependent in vitro cytotoxicity assay of gold nanoparticles', *Toxicol. Environ. Chem.*, vol. 95, no. 2, pp. 277–287, 2013.

[52] Y. Xu, O. Ghag, M. Reimann, P. Sitterle, P. Chatterjee, E. Nofen, H. Yu, H. Jiang, L. L. Dai 'Development of visible-light responsive and mechanically enhanced "smart" UCST interpenetrating network hydrogels', *Soft Matter*, vol. 14, no. 1, pp. 151–160, 2018.

[53] R. S. Lee, C. H. Lin, I. A. Aljuffali, K. Y. Hu, and J. Y. Fang, 'Passive targeting of thermosensitive diblock copolymer micelles to the lungs: Synthesis and characterization of poly(N-isopropylacrylamide)-block-poly(ε-caprolactone)', *J. Nanobiotechnology*, vol. 13, no. 1, pp. 1–12, 2015.

[54] M. Gregoritza, V. Messmann, K. Abstiens, F. P. Brandl, and A. M. Goepferich, 'Controlled Antibody Release from Degradable Thermoresponsive Hydrogels Cross-Linked by Diels – Alder Chemistry', *Biomacromolecules*, vol. 18, pp. 2410–2418, 2017.

[55] E. Ahmad, Y. Feng, J. Qi, W. Fan, Y. Ma, and H. He, 'Evidence of nose-to-brain delivery of nanoemulsions : cargoes but not vehicles', *Nanoscale*, vol. 9, no. 3, pp. 1174–1183, 2017.

[56] Y. Wang, S. Jiang, H. Wang, and H. Bie, 'A mucoadhesive , thermoreversible in situ nasal gel of geniposide for neurodegenerative diseases', *PLoS One*, vol. 12, no. 12, pp. 1–17, 2017.

[57] M. K. Bain, B. Bhowmick, D.Maity, D. Mondal, Md. M. R. Mollick, B. K. Paul, M. Bhowmik, D. Rana, D. Chattopadhyay 'Effect of PVA on the gel temperature of MC and release kinetics of KT from MC based ophthalmic formulations', *Int. J. Biol. Macromol.*, vol. 50, no. 3, pp. 565–572, 2012.

[58] M. Bhowmik, G. Sarkar, D. Rana, I. Roy, N. R. Saha, S. Ghosh, M. Bhowmik, D. Chattopadhyay 'Effect of xanthan gum and guar gum on in situ gelling ophthalmic drug delivery system based on poloxamer-407', *Int. J. Biol. Macromol.*, vol. 62, pp. 117–123, 2013.

[59] S. Patil, A. Kadam, S. Bandgar, and S. Patil, 'Formulation and evaluation of an in situ gel for ocular drug delivery of anticonjunctival drug', *Cellul. Chem. Technol.*, vol. 49, no. 1, pp. 35–40, 2015.

[60] Z. Luo, L. Jin, L. Xu, Z. L. Zhang, J. Yu, S. Shi, X. Li, H. Chen 'Thermosensitive PEG – PCL – PEG (PECE) hydrogel as an in situ gelling system for ocular drug delivery of diclofenac sodium', vol. 7544, 2016.

[61] Z. Zhang, Z. He, R. Liang, Y. Ma, W. Huang, R. Jiang, S. Shi, H. Chen, X. Li 'Fabrication of a Micellar Supramolecular Hydrogel for Ocular Drug Delivery', *Biomacromolecules*, vol. 17, pp. 798–807, 2016.

[62] S. Deepthi and J. Jose, 'Novel hydrogel-based ocular drug delivery system for the treatment of conjunctivitis', *Int. Opthalmology*, pp. 1–12, 2018.

[63] W. Wang, E. Wat, P. C. L. Hui, B. Chan, F. S. F. Ng, C. W. Kan, X. Wang, H. Hu, E. C.W.Wong, C. B. S. Lau, P. C. Leung 'Dual-functional transdermal drug delivery system with controllable drug loading based on thermosensitive poloxamer hydrogel for atopic dermatitis treatment', *Sci. Rep.*, vol. 6, pp. 1–10, 2016.

[64] S. B. Turturro, M. J. Guthrie, A. A. Appel, P. W. Drapala, E. M. Brey, V. H. Pérez-Luna, W. F. Mieler, J. J. Kang-Mieler 'The effects of cross-linked thermo-responsive PNIPAAm-based hydrogel injection on retinal function', *Biomaterials*, vol. 32, no. 14, pp. 3620–3626, 2011.

[65] F. Din, R. Rashid, O. Mustapha, D. W. Kim, J. H. Park, S. K. Ku, Y. K. Oh, J. O. Kim, Y. S. Youn, C. S. Yong, H. G. Choi 'Development of a novel solid lipid nanoparticles loaded dual-reverse thermosensitive nanomicelle release and reduced toxicity', *RSC Adv.*, vol. 5, pp. 43687–43694, 2015.

[66] C. Casadidio, M. Eugenia, A. Trampuz, M. Di, R. Censi, and P. Di, 'Daptomycin-loaded biodegradable thermosensitive hydrogels enhance drug stability and foster bactericidal activity against Staphylococcus aureus', *Eur. J. Pharm. Biopharm.*, vol. 130, pp. 260–271, 2018.

[67] S. S. Sana and V. K. N. Boya, 'Poly (vinyl alcohol)/poly (acrylamide-codiallyldimethyl ammonium chloride) semi-IPN hydrogels for ciprofloxacin hydrochloride drug delivery', *IET Nanobiotechnology*, vol. 11, no. 1, pp. 52–56, 2015.

[68] H. Zhang, J. Zhu, Y. Hu, A. Chen, L. Zhou, H. Gao, Y. Liu, S. Liu ' Study on Photocatalytic Antibacterial and Sustained-Release Properties of Cellulose/TiO 2 / β -CD Composite Hydrogel ', *J. Nanomater.*, vol. 2019, pp. 1–12, 2019.

[69] R. Ebrahimi and M. Salavaty, 'Controlled drug delivery of ciprofloxacin from ultrasonic hydrogel', *E-Polymers*, vol. 18, no. 2, pp. 187–195, 2018.

Chapter 6

Polymer Application Studies

Chapter 5 described the responsivity, solvent loading-unloading efficiency of both β-CD based UVPTT and guar gum modified non-UVPTT polymer in terms of their reversible volume alterations by sensing different stimuli. This chapter is dedicated for the investigation of the effectiveness of stimuli triggered volume switching of both β-CD modified and guar gum modified positive hydrogels as drug dispensing vehicle. The biological activity of the released substance is proven by *in-vitro* bacterial proliferation.

6.1 Introduction

In the Chapter 5, the stimuli triggered behavioural properties of all synthesized formulated gel samples have been studied. The solo pH of swelling medium, solo environmental temperature, combination of duo pH-thermo and visible light were used as external stimuli and it was observed that, β-CD modified UVPTT based gel and guar gum modified non-UVPTT based double cross linked gel, DC-GG-Paam$_{GA4.39}$ exhibited highest efficiency for solvent release. So we have been preceded with β-CD-g-(Paac-*co*-Paam) and guar gum modified non-UVPTT based double cross linked gel, DC-GG-Paam$_{GA4.39}$ for drug release mechanism. Many researchers have used Paac-*co*-Paam and it's composite for many medicinal applications. Let's have a glance the reported drug release methods and efficiency using Paac-*co*-Paam. Liang *et al.* [1] observed the urea release mechanism from kaolin and Paac-*co*-Paam composite. No stimuli was used during urea loading and loaded hydrogel was immersed in buffer medium with varying stimuli like temperature and pH where the water absorbency and urea release rate was directly proportional with elevated stimuli intensity. Urea loading-release without stimuli was observed by Mahfoudhi *et al.* [2] and the percentage of released urea from loaded dry hydrogel was observed by water diffusion in and urea diffusion out. Chitosan modified Paac-*co*-Paam was used for releasing ascorbic acid by observing the diffusion mechanism of polymer in aqueous solution where drug was loaded during the synthesis [3]. The same composition of polymer was loaded with Bovine Serum Albumin (BSA) protein without any stimuli but released in different pH

medium like 1.2, 6.8 and 7.4 for swelling and protein release [4]. More swelling indicated more protein release. For oral administration, bacterial cellulose modified Paac-*co*-Paam was swelled more in simulated intestinal fluid (SIF, pH 7.4) and released more Theophylline than in simulated gastric fluid (SGF) with lesser released of Theophylline with the help of mechanical stirrer [5]. This result confirmed the suitability of hydrogels for oral controlled drug release in the lower gastrointestinal tract. In reported work it is seen that drug was loaded without stimuli, by which controlling of loading dose is a struggling point. In some cases drug was released without also stimuli for which drug release cannot be controlled by patient on demand basis as well as release time. To control these issues, this chapter is aimed to utilize the stimuli triggered volume switching of β-CD-g-(Paac-*co*-Paam) in loading as well as releasing the drug.

If we rewind the reported work on guar gum (GG) based Paam, only GG-g-Paam has been used for drug release application. 5-amino salicylic acid was released by pH stimulus (pH 2, 7.2 and 10) from polyacrylamide grafted guar gum (GG-g-Paam) by drug dissolution [6]. Shahid *et al.* [7] used the same polymeric materials to release Triamcinolone in colonic system (pH 7.2) and in gastro-enteric system (pH 1.2) by polymer swelling. Gowrav *et al.* [8], prepared pH-sensitive pellets of Polyacrylamide-grafted-guar gum (GG-g-Paam) to colon specific release of an anti-diabetic drug, Glimepiride. The drug release from the polymer has been assisted with the dissolution apparatus with a particular rpm. These limitations motivated the present research to utilized stimuli triggered volume transition of GG based graft gel as well as double crosslinked gel to reduce the probability for contamination of drug as well as to control the dose of encapsulated drug. Temperature is such kind of external stimuli which can be applied in the form of pulsatile mode to the drug delivery vehicle to encapsulate-release the drug without disturbing the self pH of the drug and without applying any external shaker/dissolution apparatus to deliver the drug in simplest and compact way. This guar gum based drug disperser (DD) with high glass transition temperature has been used to release the drug in low temperature (<25 °C) without changing any physicochemical assisted phase transition.

Furthermore, this chapter is aimed to investigate the following points:

(i) Effects of different external stimuli on both β-CD modified gel and the guar gum modified gel for antibiotic dispensing activities. For this application, ciprofloxacin hydrochloride (CFXH) is employed as model drug as its very

common antibiotic, which is applicable for a wide variety of medical treatments.

(ii) The scope of applicability of β-CD-g-(Paac-*co*-Paam) and guar gum modified gels and their AuNP reinforced composites are also discussed.

(iii) The *in-vitro* antimicrobial effect of released drug has been studied.

6.2 Ciprofloxacine Hydrochloride: A Model Drug

The Ciprofloxacine hydrochloride (1-cyclopropyl-6-fluoro-4-oxo-7-(piperazin-1-yl)-quinoline-3-carboxylic acid hydrochloride) (CFXH) is a class IV of the Biopharmaceutics Classification System drug [9]. It is fluoroquinolone antibacterial compound, contains a secondary alkylamine (piperazine ring), two tertiary acrylamines and a carboxylic acid (Fig. 6.1).

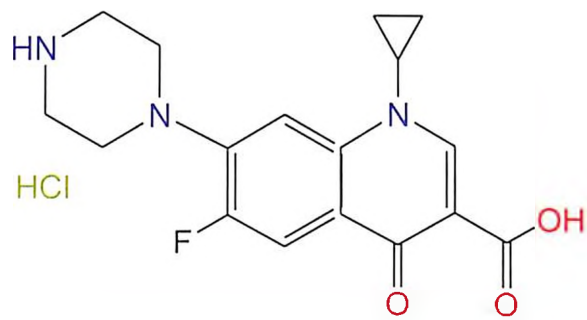

Fig. 6.1: Structure of Ciprofloxacine hydrochloride

CFXH is amphoteric in nature for which it can react with both acid and basic. Its aqueous solubility is pH dependent, due to the presence of the carboxylic and NH groups of piperazine, with the zwitterionic and un-ionized forms being dominant at neutral pH [10], having isoelectric point at 7.42 [11]. CFXH is predominantly absorbed in the proximal part of the gastrointestinal tract (GIT) [12] due to the ionization of NH group containing piperazine ring of CFXH at the pH 1.0-3.5 [13], whereas, carboxylic group ionized to form carboxylate ions in the medium containing pH 5.6-7.0.

➢ **Procedure of Calculation on Amount of CFX Solute in Experimental Solution:**

As a model drug we have used: CIPLOX Eye Drop, CIPLA, Mumbai, India in where 0.3% (w/v) total CFXH solute was present. 0.3% (w/v) CIPLOX drop means, 100 ml of CIPLOX eye drop contains 0.3 gm of CFXH solute. We selected 0.3% (v/v) and 0.7% (v/v) of drug concentration from stock solution where in the present of CFXH solute (wt) have been calculated below:

A. For 0.3% CFXH solution:

Aim: To prepare 10 ml of 0.3% concentrated CFXH solution

Therefore, the 100 ml of 0.3% CFXH stock solution contains 0.3 ml of CIPLOX eye drop.

As per CIPLOX eye drop, 0.3 ml of CIPLOX eye drop contains 0.0009 gm CFXH solute.

e.g., 100 ml of experimented stock solution contains 0.0009 gm of CFX solute.

Therefore, 10 ml of 0.3 (v/v) % CFXH solution contains 0.09 mg of CFXH solute.

B. For 0.7% CFX solution:

Aim: To prepare 10ml of 0.7% concentrated CFX stock solution

Therefore, the 100ml of 0.7% CFX stock solution contains 0.7 ml of CIPLOX eye drop.

As per CIPLOX eye drop, 0.7 ml of CIPLOX eye drop contains 0.0021 gm CFX solute.

e.g., 100 ml of experimented stock solution contains 0.0021 gm of CFX solute.

Therefore, 10 ml of 0.7 (v/v) % CFXH solution contains 0.21 mg of CFXH solute.

6.3 Experimental Procedure: Gel as Drug Dispenser

The drug "dispenser" defines as a system which has both encapsulation capability of therapeutic agent as well the ability to release the encapsulated cargo on demand basis. A good dispenser should have the tendency to release the higher amount of encapsulated cargo. To evaluate the efficiency of being a good dispenser, we performed stimuli based drug release study on both UVPTT and non-UVPTT gels. To investigate the efficacy of the drug entrapment into the sample network and discharge from loaded sample, stimuli triggered volume switching phenomenon was observed. In Chapter 5, the gel sensitivity on environmental temperature, medium pH stimuli, dual stimuli with medium pH and external temperature and the visible light was explored. It was also found that, the REVA temperature assisted swelling-deswelling phenomenon performed highest efficiency of the gels in terms of greater ability of the solvent release with minimum volumetric memory loss. Therefore, in drug entrapment-release experimentation, the external temperature stimulus was applied for temperature assisted loading and releasing activities. However, the solo medium pH and combination of medium pH and external temperature were also used as stimuli for release event for a specific application such as gastro retentive delivery. For this release event, the on demand variable drug loading capability is

key point to make the drug carrier system as patient compliance. Thus, temperature based FWA approach was used for loading to control the loading dose. This loading approach is termed as forward step approach (FSA). The visible light was used for drug encapsulation-discharge application. The drug dispensing activities involving entrapment and release categorized by applied stimuli events are concisely shown in flow Fig. 6.2.

From the Fig. 6.2, the drug entrapment and release experimentation is categorised into three different combinations; such as,

Combination I: Temperature assisted loading and temperature assisted release.
Combination II: Forward step approached temperature assisted loading and medium pH aided release.
Combination III: Forward step approached temperature assisted loading and dual stimuli based on medium pH and external temperature aided release.
Combination IV: visible light assisted loading and releasing.

All the four combinations are described in the successive sections. The drug dispensing experimentations were carried out for both β-CD modified UVPTT gel and guar gum modified non-UVPTT gels to standout the drug dispensing efficiency in all applied stimuli combinations. The experimental discussions we divided into two parts for two different types of gels. The initial dimensions and other parameters for all samples are considered as mentioned in Table 6.1 for experimentations.

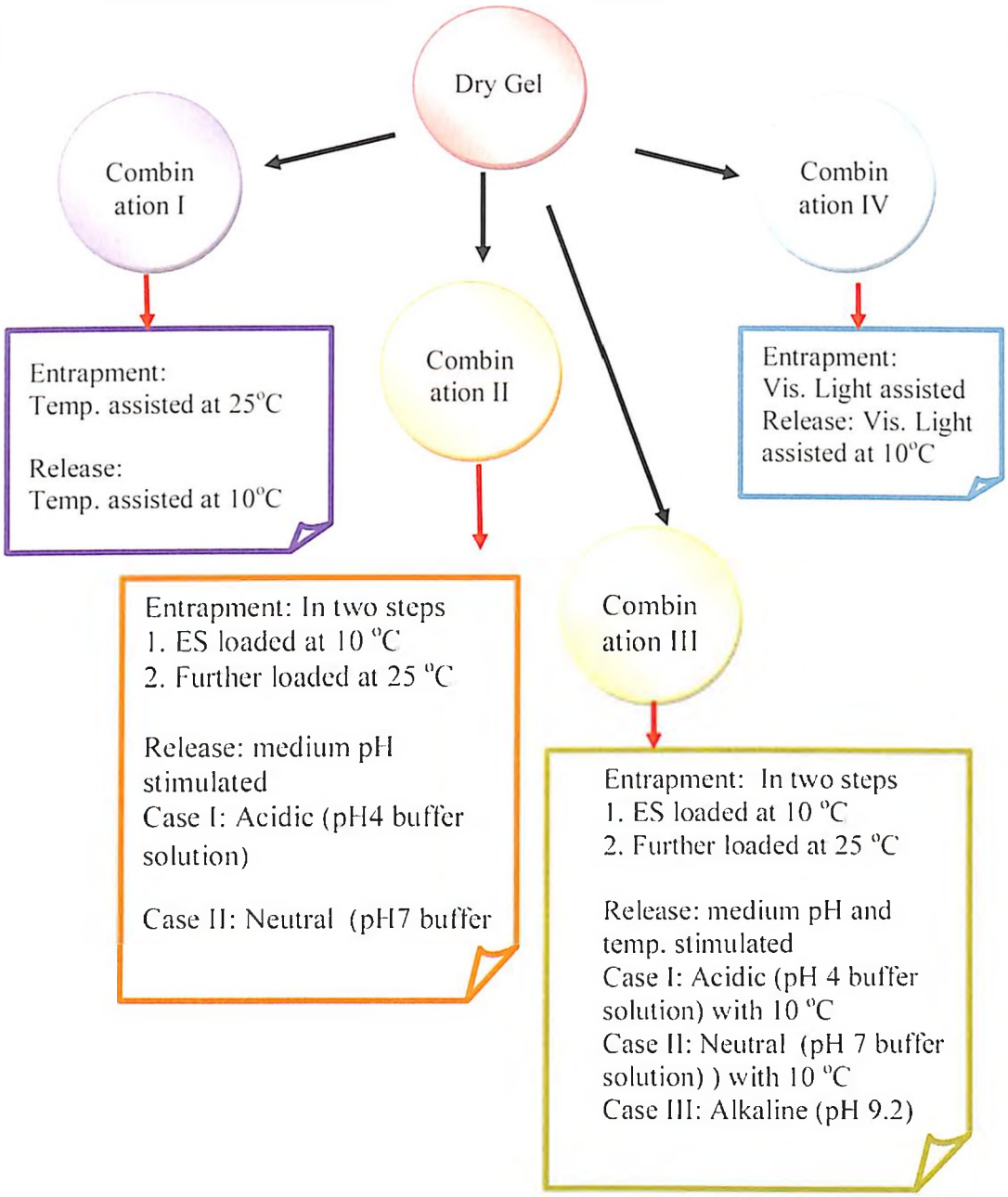

Fig. 6.2: Flow chart for drug dispensing activities in different combinations

6.3.1 Combination I

The CFXH entrapment and release experimentation through Combination I was performed by two distinct events, called CFXH entrapment into polymer network and release event of loaded drug. Thus, this event can be written into two sub modes:

Mode I: Temperature assisted drug loading

Mode II: Temperature assisted release

For CFXH entrapment event, 25 °C was used as external temperature stimuli and 10°C was applied to free the loaded CFXH from the gel. The detail procedure for both Mode I and Mode II events are described in below.

Mode I: Temperature Assisted Drug Loading

The dry gel sample was used to imbibe the prepared 0.3% (v/v) and 0.7% (v/v) CFXH drug solutions for 12 h. duration at 25 °C. The weight and dimension of drug loaded sample were noted by using an electronic weighing balance (Shimadzu AU Series) with the accuracy of 0.001 g. The weight of CFXH loaded gel sample recorded at fixed intervals (every single hour for β-CD modified gel and every 3 h interval for guar gum modified gel) by blotted out the sample surface adhere extra drug solution. The dynamic percentage of entrapped drug solute into the gel network is calculated by Eq. (6.1).

$$\text{Drug solute entrap.}_{\text{Comb.I}}\ (\text{mg.cc}^{-1})\% = \frac{Q_{entrap_t}}{V_{dry}} x100\ \% \qquad (6.1)$$

The percentage of entrapped CFXH solute is expressed as the amount of entrapped CFXH solute into gel sample network with respect to per volume of the dry gel.

The Q_{entrap_t} is the amount of loaded CFXH solute in mg at time "t"

The total quantity of CFXH solute entrapment, $Q_{Entrap\ Comb.\ I}$ (expressed in mg) into the gel after 12 h at 25 °C is assessed by Eq. (6.4).

$$Q_{Entrap\ Comb.\ I} = (W_{12} - W_{dry})\ x\ Q_{S_{0.3\ or\ 0.7}} \qquad (6.2)$$

where, W_{12} is the sample weight in gm after 12 h of temperature assisted loading.

$Q_{S_{0.3\ or\ 0.7}}$ is the quantity of CFXH solute present in per ml of 0.3 (v/v)% and 0.7 (v/v) % CFXH solution and it is expressed in mg.

For 0.3 (v/v) % CFXH solution, $Q_{S_{0.3}} = 0.009$ mg/gm of 0.3 (v/v)% CFXH solution. For 0.7 (v/v) % CFXH solution, $Q_{S_{0.7}} = 0.021$ mg/gm of 0.7 (v/v)% CFXH solution.

Mode II: Temperature Assisted Release

In this the mode of CFXH release, the REVA (as discussed in Chapter 5) temperature switching approach is applied. The low temperature, 10 °C was used as external environmental stimuli due to the gels have the positive responsivity on stimuli. Therefore, lower temperature (10 °C) than loading temperature was

applied for volume shrinking and thus the CFXH release happened. The temperature assisted (Mode I) CFXH loaded samples were used for Mode II release event. For drug release investigation, the CFXH loaded sample was kept in an empty air tight vial at 10 °C for 12 h. and hence the sample deswelled by releasing CFXH. The supernatant CFXH was collected in fixed time intervals (every single hour for β-CD modified gel and every 3 h. interval for guar gum modified gel) and quantity of collected released CFXH was measured by volumetric micro pipette and cumulative release was quantified as mass released at 12 h. over the total mass of the drug-filled polymer. The weight of sample also recorded. The dynamic CFXH solute release is measured by Eq. (6.3) and it is expressed in gm.

$$Q_{Comb.I\,t} = (W_{12} - W_{Rel_t}) \times Q_{S_{0.3\ or\ 0.7}} \qquad (6.3)$$

where, $Q_{Comb.I\,t}$ is the quantity of released CFXH solute at time "t" and is expressed in mg. $W_{Rel\,t}$ is the sample weight after released the CFXH at time t.

The (wt/wt)% of CFXH solute release was evaluated based on the amount of entrapped CFXH solute during Mode I loading into polymer sample after 12 h. and the cumulative release of CFXH was estimated by Eq. (6.4).

$$\text{CFXH solute release}_{Comb.I}\ (wt/wt)\% = \left(\frac{Q_{Comb.I\,t}}{Q_{Entrap\ Comb.I}}\right) \times 100\ \% \qquad (6.4)$$

where, $Q_{Entrap_{Comb.I}}$ is the quantity of the entrapped CFXH solute into gel at 25 °C through Mode I.

The percentage of CFHX solute retention $(R_{CFXH\ solute\ Comb.I}\ \%)$ into the gel network is calculated to figure out the efficacy of the polymer sample as drug carrier to deliver the drug solute with respect to its capability on the entrapment and release of drug. The $R_{CFXH\ solute_{Mode\ II}}\%$ is calculated by using Eq. (6.5).

$$R_{CFXH\ solute_{Comb.I}}\ \% = \frac{Q_{Entrap_{Comb.I}} - Q_{12\ Mode\ II}}{V_{dry}} \times 100\ \% \qquad (6.5)$$

where, $Q_{12\ Mode\ II}$ (in mg) is the quantity of released CFXH solute at 10 °C after 12 h. from loaded polymer during Mode II release event. The lower degree of $R_{CFXH\ solute_{Comb.I}}\ \%$ will be indicated the higher efficacy of the gel, due to its better capacity to release the CFXH solute from network.

6.3.2 Combination II

In the Combination II, forward step approached (FSA) temperature assisted loading was applied to facilitate the dosage of the loaded drug. This FSA involves two steps loading events – extended phase loading at 25 °C followed by equilibrium loading at 10 °C. On the other hand, the release done in medium stimulated by different pHs of the buffer solvent. Thus, this can be divided into two events:

Mode I: Forward step approached (FSA) temperature assisted loading

Mode II: Medium pH aided release

The detail procedure for both Mode I and Mode II events are described in below.

Mode I: Forward Step Approached (FSA) Temperature Assisted Drug Loading

The prepared drug solutions of 0.3 (v/v) % and 0.7 (v/v) % were entrapped by triggering of external temperature through forward step approach (FSA) manner. In this manner, the CFXH entrapped into gel in two steps – firstly, the dry gel samples were dipped into the capped vial containing the drug solution and the environmental temperature maintained at 10 °C until the equilibrium loaded state (ELS) of the gels, followed by the vial containing ELS samples with CFXH kept at 25 °C till 12 h. The CFXH drug containing ELS samples were further swelled by taking the CFXH solution once the environmental temperature switched from lower temperature (10 °C) to higher temperature (25 °C), due to the positive thermo-responsive nature of the polymer (discussed in Chapter 5). The state of the gels during the temperature UP switching (from 10 °C to 25 °C) is named as extended loaded state (ExtLS) of the sample. The weight of the sample was recorded. Further, the dimension of the ELS gels were recorded using slide calliper. The dynamic percentage of entrapped drug solute into the ExtLS gel network at each time instant is calculated by Eq. (6.6).

$$\text{Drug solute entrp}_{\text{Comb.II}}\,(\text{mg.cc}^{-1})\% = \frac{Q_{entrap_t}}{V_{dry}} \times 100\ \% \qquad (6.6)$$

where, Drug solute entrp $_{\text{Comb.II}}$ $(\text{mg.cc}^{-1})\%$ is the percentage of entrapped drug solute into the ExtLS gel. The Q_{entrap_t} (expressed in mg) is the quantity of loaded CFXH solute during drug loading at time "t" and is measured by Eq. (6.2).

The total quantity of CFXH solute entrapment in Mode I during Combination II, $Q_{Entrap\ Comb.\ II}$ (expressed in mg) into ExtLS gel after 12 h. at 25 °C is assessed by Eq. (6.7).

$$Q_{Entrap\ Comb.II} = (W_{ExtLS} - W_{dry}) \times Q_{S_{0.3\ or\ 0.7}} \qquad (6.7)$$

where, W_{ExtLS} is the weight of the ExtLS gel at 25 °C and is expressed in gm and $Q_{S_{0.3\ or\ 0.7}}$ holds identical significance as described in Combination I.

Mode II: Medium pH Aided Release

In Chapter 5, it was perceived that the synthesized gel samples have the responsivity on the pH of the medium. Thus, in Mode II, the variation of medium pH was utilized as triggered stimuli to release CFXH solute from the FSA temperature assisted CFXH loaded ExtLS gel network. To execute the drug release events from drug loaded ExtLS polymer, the 10 ml of medium pH (buffer solution of pH 4 / pH 7 / pH 9.2) was used. Based on the release medium, the CFXH release experimentation is divided into three cases, e.g. Case I: the CFXH loaded ExtLS sample kept into acidic buffer solution of pH 4 at room temperature, Case II: the CFXH loaded ExtLS sample kept into neutral buffer solution of pH 7 at room temperature and Case III: the CFXH loaded ExtLS sample kept into alkaline buffer solution of pH 9.2 at room temperature. The CFXH loaded ExtLS samples changes their weight and volume depended on applied medium pH stimuli. The weight of the sample was recorded. Further, the dimension of each sample noted once the sample reduced at constant weight by releasing the CFXH. The dynamic CFXH solute release is measured by Eq. (6.8) and it is expressed in gm.

$$Q_{Case\ I\ or\ II\ or\ III\ t} = Q_{Entrap\ Comb.II} - (W_{ExtLS} - W_{Mode\ II\ t}) \times Q_{S_{0.3\ or\ 0.7}} \qquad (6.8)$$

where, $Q_{Case\ I\ or\ II\ or\ III\ t}$ is the quantity of released CFXH solute at time "t" and is expressed in mg. The $Q_{Entrap\ Comb.II}$ is total amount of entrapped CFXH solute during Mode I of loading. W_{ExtLS} and $W_{Mode\ II\ t}$ are the weight in gm of the loaded ExtLS gel and the weight of the sample at time instant "t" during Mode II release event respectively. The total quantity of released CFXH solute in Mode II, $Q_{Case\ I\ or\ II\ or\ III}$ is quantified by Eq. (6.9).

$$Q_{Case\ I\ or\ II\ or\ III} = Q_{Entrap\ Comb.II} - (W_{ExtLS} - W_{Mode\ II}) \times Q_{S_{0.3\ or\ 0.7}} \qquad (6.9)$$

where, $W_{Mode\ II}$ is the final weight (in gm) of the sample after release in Mode II. The (wt/wt) percentage of CFXH solute release was evaluated based on the amount of CFXH solute entrapment through FSA based loading in Mode I into ExtLS sample and estimated by Eq. (6.10).

$$\text{CFXH solute release}_{\text{Comb. II Case I or II or III}}\ (\text{wt/wt})\ \% = \left(\frac{Q_{\text{Case I or II or III}_t}}{Q_{\text{Entrap Comb.III}}}\right) \times 100\ \% \qquad (6.10)$$

Where, $Q_{Entrap\ Comb.II}$ is the total quantity of the entrapped CFXH solute into ExtLS gel at 25 °C. The percentage of CFHX solute retention ($R_{CFXH\ solute_{Comb.\ II}}$ %) into the gel network is calculated to figure out the efficacy of the polymer as drug carrier to deliver the drug solute with respect to its capability on the entrapment and release of drug. The $R_{CFXH\ solute\ Comb.\ II}$ % is calculated by using Eq. (6.11).

$$R_{CFXH\ solute\ Comb.\ II}\ \% = \frac{Q_{Entrap\ Comb.II} - Q_{\text{Case I or II or III}}}{V_{dry}} \times 100\ \% \qquad (6.11)$$

where, $Q_{\text{Case I or II or III}}$ (in mg) is the total quantity of released CFXH solute at 10 °C during Mode II release event in Combination II.

6.3.3 Combination III

In Combination III, the CFXH was loaded in same manner with FSA as Mode I of Combination II experimentation. However, the dual stimulus with the blended of medium pH and the external temperature was applied during release event. Thus, the release event can be divided into two events:

Mode I: Forward step approached (FSA) temperature assisted loading.

Mode II: Dual stimulus blended of medium pH and temperature assisted release.

The Mode I loading procedure is already discussed in Section 6.3.1. The detail procedure for Mode II release event is described as below.

Mode II: Dual Stimulus Blended of pH and Temperature Assisted Drug Release

In this mode of release, both the thermo and pH responsive properties of polymers were utilized to investigate the drug release activities. The release activities performed in dual stimuli based environment in acidic, neutral and alkaline buffer mediums i.e. pH 4, pH 7 and pH 9.2 with the external temperature of 10 °C. The CFXH release experimentation is

divided in three cases based on the applied stimuli, such as Case I: The CFXH loaded ExtLS sample kept into acidic medium (pH 4 buffer solution) and 10 °C was applied as external temperature; Case II: The CFXH loaded ExtLS sample kept into neutral medium (pH7 buffer solution) and 10 °C was applied as external temperature and Case III: The CFXH loaded ExtLS sample kept into alkaline medium (pH 9.2 buffer solution) and 10 °C was applied as stimuli. The dynamic CFXH solute release is measured by Eq. (6.12) and it is expressed in mg.

$$Q_{\text{Case I or II or III}_t} = Q_{\text{Entrap}_{\text{Comb.III}}} - \left(W_{\text{ExtLS}} - W_{\text{Case I or II or III}_t}\right) \times Q_{S_{0.3 \text{ or } 0.7}} \quad (6.12)$$

where, $Q_{\text{Case I or II or III}_t}$ is the quantity of released CFXH solute at time "t" for Case I, Case II and Case II during release event and is expressed in mg. The $Q_{\text{Entrap}_{\text{Comb.III}}}$ is the total amount of entrapped CFXH solute during Combination III experimentation.

W_{ExtLS} and $W_{\text{Case I or II or III}}$ are the weights in gm of the loaded ExtLS gel and the weight of the sample at time instant "t" during Case I, Case II and Case II release events respectively.

The total quantity of released CFXH solute in Combination III, $\left(Q_{\text{Comb.III Case I or II or III}}\right)$ is quantified by Eq. (6.13).

$$Q_{\text{Comb.III Case I or II or III}} = Q_{\text{Entrap}_{\text{Comb.III}}} - \left(W_{\text{ExtLS}} - W_{\text{Case I or II or II}}\right) \times Q_{S_{0.3 \text{ or } 0.7}} \quad (6.13)$$

Where, $Q_{\text{Comb.III Case I or II or III}}$ is the total quantity of released CFXH solute and is expressed in mg.

The $W_{\text{Case I or II or III}}$ is the final weight (in gm) of the drug released gel.

The (wt/wt) % of CFXH solute release was evaluated based on the total amount of CFXH solute loaded into ExtLS gel sample and estimated by Eq. (6.14).

$$\text{CFXH solute release (wt/wt)}_{\text{Comb.III Case I or II or III}} \% = \left(\frac{Q_{\text{Comb. III}_t}}{Q_{\text{Entrap Comb. III}}}\right) \times 100\ \% \quad (6.14)$$

where, $Q_{\text{Comb. III}_t}$ is the quantity of released CFXH solute at time "t" with the external stimuli in Case I, II and III from gel and is expressed in mg. The percentage of CFHX solute retention $\left(R_{\text{CFXH solute}_{\text{Comb.III}}} \%\right)$ into the gel network is calculated to figure out the efficacy of the polymer as drug carrier to deliver the drug solute with respect to its capability on the entrapment and release of drug. The $R_{\text{CFXH solute Comb.III}}$ % is calculated by using Eq. (6.15).

$$R_{CFXH\ solute\ Comb.\ III}\ \% = \frac{Q_{Entrap\ Comb.III} - Q_{Comb.III\ Case\ I\ or\ II\ or\ III}}{V_{dry}} \times 100\ \% \quad (6.15)$$

The degree of $R_{CFXH\ solute\ Comb.\ II}$ % is indicated the efficacy of the gel.

6.3.4 Combination IV

In the Combination IV, the visible light was used as stimuli to entrap the CFXH solute inside the gel network. The 532 nm, 500 mW CW laser source was used as visible light spectra. The light source was used in pulsatile mode: the HIGH state depicts as laser ON phase and the LOW state signifies the laser OFF phase. The AuNP reinforced gel composites were used for Combination IV experimentation. As the positive responsivity on external light stimuli present in both the UVPTT and non-UVPTT gels, the gel network uptake the CFXH solute by laser irradiation e.g. in HIGH state and freed the loaded drug solute once the laser source withheld e.g. in LOW state of light stimuli. The sample code of AuNP reinforced gel composites are considered as mentioned in Chapter 5.

6.4 Results and Discussions: Gel as Drug Dispenser

This section is aimed to analyze the efficiency of the gels in all four combinations of applied stimuli (as described in Section 6.3) for drug entrapment and release based on the experimental data. The 0.3 (v/v) % and 0.7 (v/v) % CFXH drug solutions were used for all experimentation. The drug dispensing experimentations were carried out for both β-CD modified UVPTT gel and guar gum modified non-UVPTT gels to standout the drug dispensing efficiency in all applied stimuli combinations. The dimension and the average weight of the dry samples are considered as mentioned in Table 6.1.

Table. 6.1: Dry/initial sample parameters

Sample Code	Dimension, L x W x H (mm)	Avg. weight, W_{dry} (gm)*
PART A (UVPTT based)		
β-CD-g-(Paac-*co*-Paam)	5 × 5 × 0.25	0.021 ± 0.001
β-CD-g-(Paac-*co*-Paam)-1	5 × 5 × 0.25	0.041 ± 0.001
β-CD-g-(Paac-*co*-Paam)-3	5 × 5 × 0.25	0.045 ± 0.001
PART B (non-UVPTT based)		
GG-g-Paam	5 × 5 × 1	0.084 ± 0.003
DC-GG-$Paam_{GA4.39}$	5 × 5 × 1	0.083 ± 0.002
DC-GG-$Paam_{GA4.39}$-1	5 × 5 × 1	0.088 ± 0.002
DC-GG-$Paam_{GA4.39}$-3	5 × 5 × 1	0.094 ± 0.001
DC-GG-$Paam_{GA4.39}$-5	5 × 5 × 1	0.097 ± 0.001

* SD error (n=5)

PART A: β-CD Modified UVPTT Gel

This section is objected for exploring the usefulness of the stimuli on UVPTT based hydrogel for CFXH solute dispensing based on the experimental facts.

6.4.1A Combination I: Temperature Assisted Drug Loading-Releasing

The drug was loaded at 25 °C by following the Mode I as discussed in Section 6.3.1 and the release event done at 10 °C by following Mode II process. To investigate the efficiency of gel samples as CFXH carrier, the percentage of CFXH solute entrapment and the (wt/wt) percentage of CFXH solute release were calculated by using Eq. (6.1) and Eq. (6.4) respectively. The percentage of CFXH solute entrapped into polymer network and the percentage of CFXH solute released from polymer network for both 0.3 (v/v)% and 0.7 (v/v)% drug solutions is represented in Fig. 6.3 and Fig 6.4 respectively. For 0.3 (v/v) % CFXH solution, 22.44±0.16% CFXH solute entrapment found, whereas, in case of 0.7 (v/v)% CFXH solution 54.84±0.37% CFXH solute entrapment capability found. After applying the lower temperature stimuli, Fig. 6.4 depict that, the gel network freed 86.65±3.04% of solute from the 0.7 (v/v)% drug solution, but slightly lesser percentage, 85.50±3.00% release found from lower concentration of drug solution. As the hydrophilicity increased in 0.7 (v/v)% CFXH drug solution as compared to 0.3 (v/v)% drug solution, hence, capability for percentage of drug intake by the gel is higher in higher concentration of drug solution (0.7 (v/v)%) than lower one (0.3 (v/v)%).

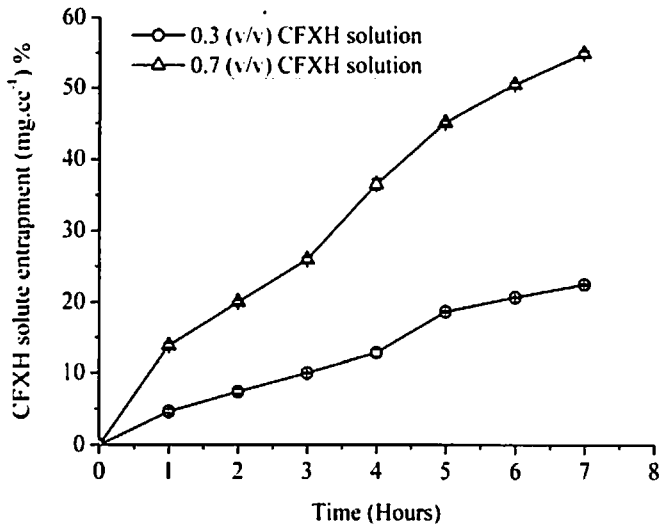

Fig. 6.3: Percentage of CFXH solute entrapment for 0.3 (v/v)% and 0.7 (v/v)% solutions

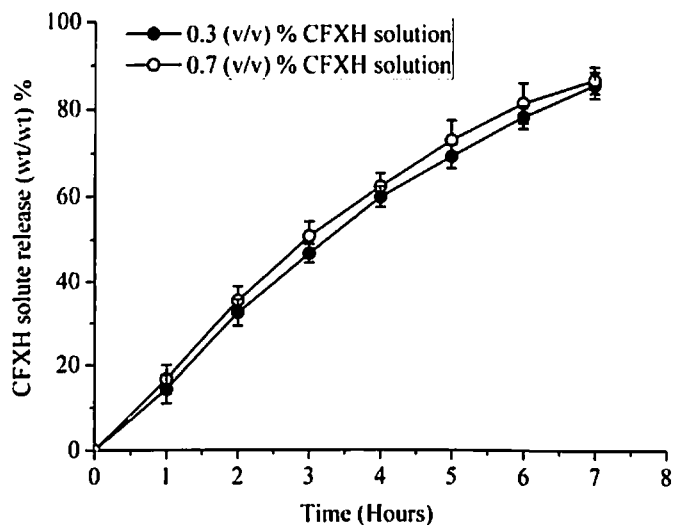

Fig. 6.4: Percentage of CFXH solute release for 0.3 (v/v)% and 0.7 (v/v)% solutions

The efficiency of gel was assessed by computing the percentage of CFXH solute retention $(R_{CFXH\ solute\ Comb.I}\ \%)$ into the polymer network by using Eq. (6.5). The Fig. 6.5 portrays that, the lowest percentage of CFXH solute retention per 100 cc of dry gel found for lower concentration of drug solution than higher one. The 3.25±0.69% and 7.32±1.7% solute retained for 0.3 (v/v)% and 0.7 (v/v)% CFXH solution respectively after identical release period of 12 h. The higher tendency to retain the CFXH solute observed for 0.7 (v/v)% solution in both the gels, due to the higher entrapment capability than lower concentrated drug solution.

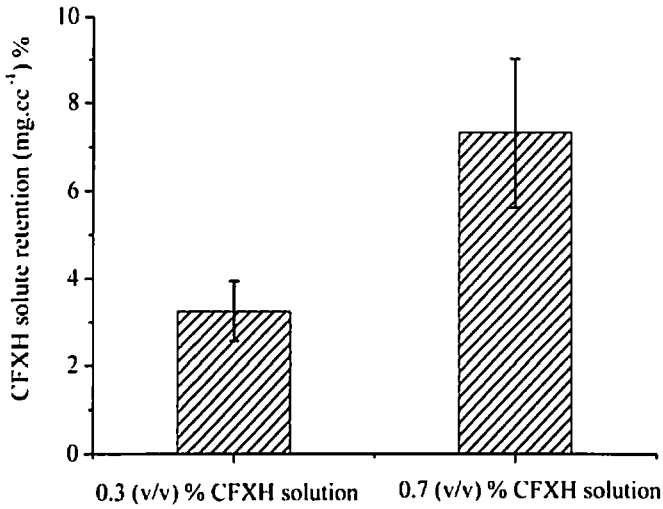

Fig. 6.5: CFXH solute retention ($mg.cc^{-1}$) % for both CFXH solutions

Therefore, it can be concluded that, for temperature assisted drug loading and releasing activities (Combination I), the gel showed a good dispensing efficacy in external temperature stimuli based loading and releasing events for both 0.3 (v/v)% and 0.7 (v/v)% CFXH solutions.

6.4.2ACombination II: Temperature Assisted Drug Loading and pH Aided Drug Release

In Combination II CFXH load-release event, the percentage of CFXH entrapment, Drug solute $entrp_{Comb.II}(mg.cc^{-1})\%$ into the polymer sample during extended loading state at 25 °C was computed from the temperature assisted experimental data by using Eq. (6.6). Fig. 6.6, depicts the CFXH solute entrapment percentage for both drug solutions. The ExtLS gel loaded 25.43±0.22% and 62.76±0.73% CFXH solute from 0.3 (v/v)% CFXH solution and 0.7 (v/v)% CFXH solution respectively after completion of ExtLS at 25 °C. The higher ability to entrap the CFXH solute from the 0.7 (v/v)% drug solution found due to higher hydrophilic nature of the drug solution. The sample gets equilibrium loading for 7 h. and then continues 3 h. dwell state at 10 °C to confirm no further intake the solvent/solute. Thereafter, the ExtLS performed at 25 °C for another 7 h. for extended loading of the drug.

The pH 4 buffer medium assisted percentage (wt/wt) of cumulative release of CFX solute $\left(\text{CFXH solute release}_{\text{Comb. II Case I}}\ (wt/wt)\ \%\right)$ for both 0.3% and 0.7% CFXH

solutions are computed by using Eq. (6.10) and the respective graphical presentation with respect to the time (hrs) instances are shown in Fig. 6.7.

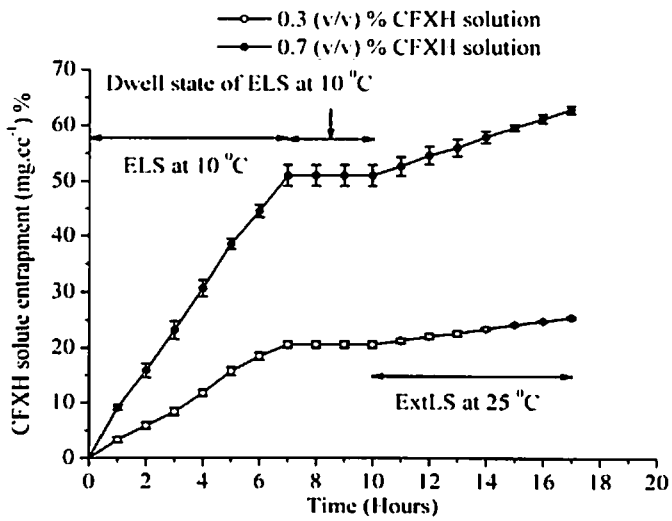

Fig. 6.6: Percentage of CFXH solute entrapment into β-CD modified ExtLS

The ExtLS sample released 65.01±0.56% and 69.16±1.00% of CFXH solute for 0.3 (v/v)% and 0.7 (v/v)% CFXH solutions respectively with the acidic medium (in pH 4 buffer solution) stimulus whereas, no significant response observed in Case II and Case III for neutral and alkaline medium stimuli. Due to positive pH stimuli responsiveness of the gel network, the ExtLS sample started to intake the drug solvent/solute once the ExtLS polymer kept into neutral buffer (pH 7) and alkaline (pH 9.2) medium.

The percentage of CFXH solute retention is quantified by Eq. (6.11) with the help of CFXH solute loading and pH 4 buffer medium assisted releasing experimental data and represented in Fig. 6.8. The gel performed better efficacy for 0.3 (v/v)% CFXH solution by lower tendency to retain the CFXH solute than that for 0.7 (v/v)% solution. The 16.53±0.06% and 43.41±1.02% solute retained for 0.3 (v/v)% and 0.7 (v/v)% CFXH solution respectively. The lower percentage of CFXH retention (for 0.3 (v/v)% CFXH solution) signifies that the gel is capable to release higher amount of drug solute per unit volume of the sample than concentrated drug solution (0.7 (v/v)% CFXH solution). Although, the elevated slope of percentage of CFXH solute entrapment in ExtLS phase (Fig. 6.6) for 0.7 (v/v)% CFXH solution signifies, higher ability to entrap the solute from 0.7 (v/v)% CFXH solution during ExtLS. Therefore, the acidic medium stimulus showed the best possible external stimuli over other mediums (neutral and alkaline) to make the better efficient dispensing carrier in case of Combination II stimulated drug dispensing phenomenon

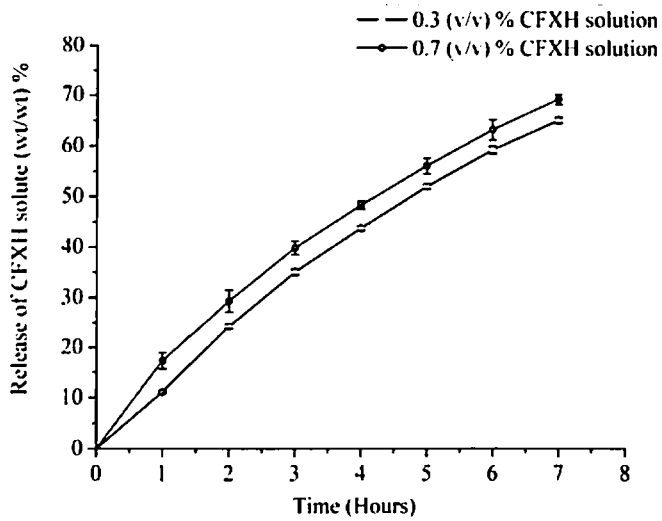

Fig. 6.7: Release of CFXH solute (wt/wt) % for 0.3 (v/v)% and 0.7 (v/v)% CFXH solutions

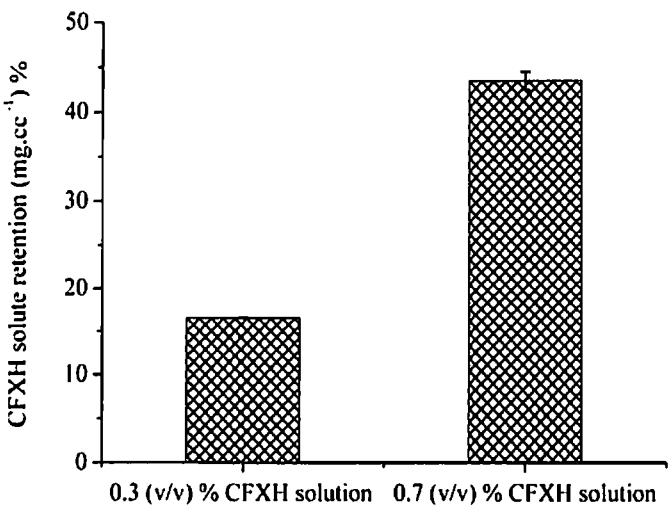

Fig. 6.8: CFXH solute retention ($mg.cc^{-1}$) % for 0.3 (v/v)% and 0.7 (v/v)% CFXH solutions

6.4.3A Combination III: Temperature Assisted Drug Loading and Dual Stimuli (Combination of Temperature and pH) Assisted Drug Discharge

The dual stimuli based on the combination of medium pH and the environmental temperature (10 °C) was applied in Combination III to understand the effect in CFXH solute release from the sample. The duo stimuli assisted percentage (wt/wt) of cumulative release of CFX solute for both 0.3% and 0.7% CFXH solutions are computed by using Eq. (6.14) and is represented in Fig. 6.9. As discussed in Section 6.4.2A, there were no substantial effects observed for Case II and Case III release event of Combination III. This was happened due to the positive pH sensitivity of the gel. But, in

Case I (Fig. 6.9), the 75.89±2.58% and 81.37±1.90% CFXH solute release observed for 0.3 (v/v)% and 0.7 (v/v)% CFXH solutions respectively from ExtLS sample.

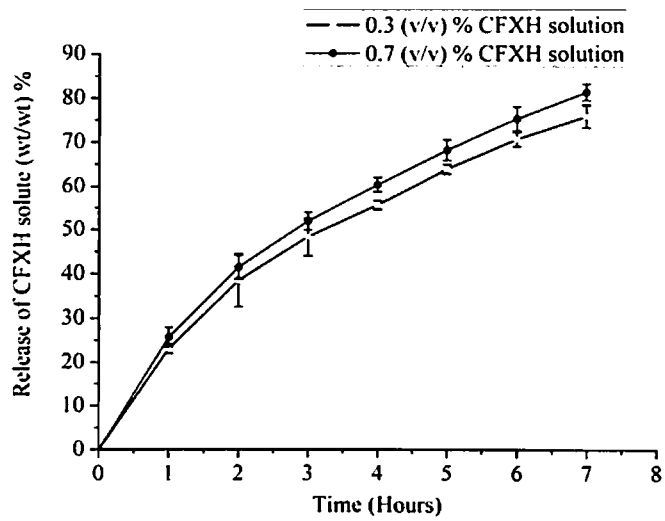

Fig. 6.9: Release of CFXH solute (wt/wt) % for 0.3 (v/v)% and 0.7 (v/v)% CFXH solution

The percentage of CFXH solute retention is quantified by Eq. (6.15) with the help of CFXH solute loading and dual stimuli assisted releasing experimental data and represented in Fig. 6.10.

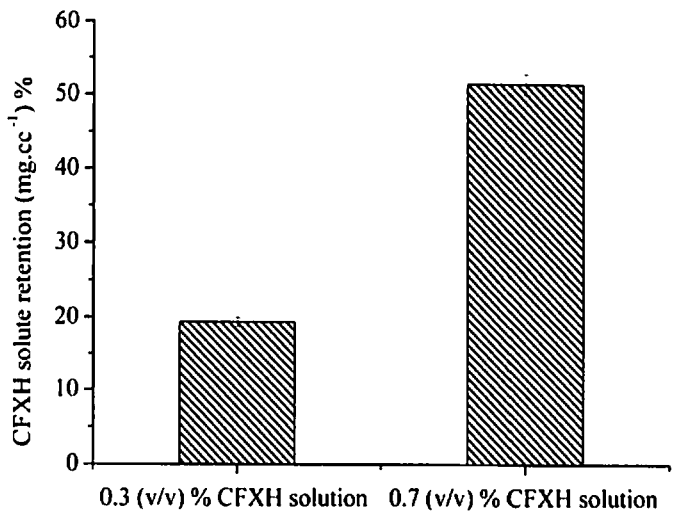

Fig. 6.10: CFXH solute retention (mg.cc-1) % for 0.3 (v/v)% and 0.7 (v/v)% CFXH solution

The Fig. 6.10 indicates that, the 19.30±0.60% and 51.08±1.41% of CFXH solute retention were observed for 0.3 (v/v)% and 0.7 (v/v)% CFXH solutions respectively. This reveals that the gel performed higher efficiency for lesser concentration the drug solute containing solution with a higher dispensing ability, retaining lesser amount of CFXH solute in per unit of dry gel volume. Therefore, the acidic medium stimulus with

combination of lower temperature stimuli showed the best possible external stimuli over other mediums (neutral and alkaline) to make the better efficient dispensing carrier in Combination III stimulated drug dispense.

6.4.4A Combination IV: Visible light Assisted Drug Loading and Discharge

The visible light stimuli was applied in pulsed mode (as described in Section 6.3) for Combination IV to investigate the CFXH solute release effectiveness from Au-NP reinforced β-CD-g-(Paac-*co*-Paam) IPN gel. The percentage of CFXH solute load-release profiles for both 0.3 (v/v)% and 0.7 (v/v)% CFXH solutions for all composite IPNs are showed in Fig. 6.11(a)-(d).

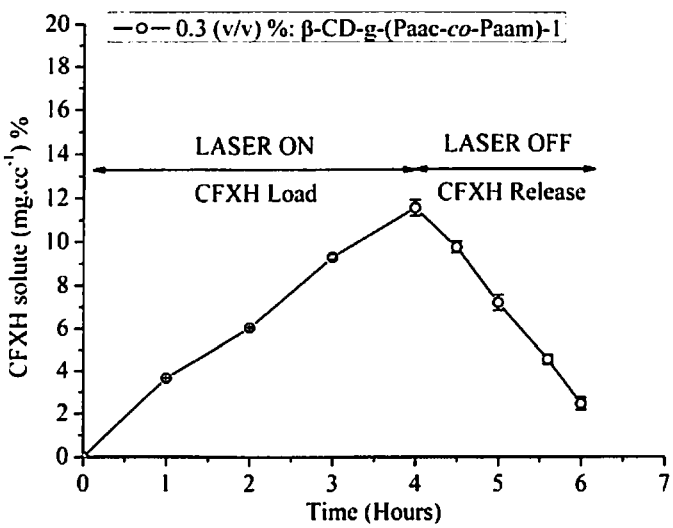

Fig. 6.11(a): CFXH solute entrapment and release profile for 0.3 (v/v)% CFXH solution for β-CD-g-(Paac-*co*-Paam)-1 composite gel

The β-CD-g-(Paac-*co*-Paam)-3 composite IPN gel loaded higher percentage of CFXH solutes (both from 0.3 (v/v)% and 0.7 (v/v)% CFXH solutions) per 100 cc of dry composite sample than β-CD-g-(Paac-*co*-Paam)-1 composite IPN gel, due to the presence of higher AuNP concentration and thus produced the higher amount of localize heat, which assists to expand the gel network to entrap more drug solvent/solute. The 15.18±0.24% and 40.16±0.54% CFXH solute entrapped by the ELS β-CD-g-(Paac-*co*-Paam)-3 composite gel from 0.3% and 0.7% CFXH solutions respectively, whereas, the β-CD-g-(Paac-*co*-Paam)-1 composite gel held only 11.55±0.36% and 36.32±2.25% of CFXH solutes under identical laser irradiation period of 4 h. to reach ELS state. Further, with the LOW state of laser irradiation (laser OFF

state), the composite gel samples released the CFXH solutes due to the positive opto stimuli responsivity. Irrespective of CFXH solution and identical time duration of 2 h. of LOW state of laser (OFF), the β-CD-g-(Paac-*co*-Paam)-3 composite liberated higher percentage of CFXH solute per 100 cc of dry gel (11.08±0.32% and 27.40±0.55% for 0.3 (v/v)% and 0.7 (v/v)% CFXH solutions respectively) than β-CD-g-(Paac-*co*-Paam)-1.

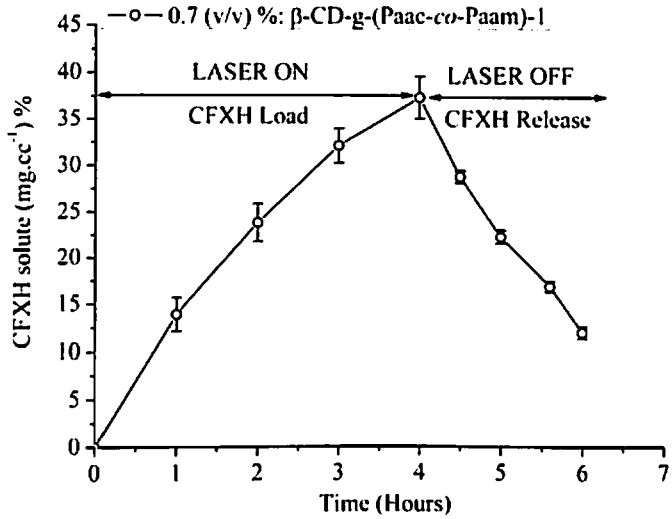

Fig. 6.11(b): CFXH solute entrapment and release profile for 0.7 (v/v)% CFXH solution in β-CD-g-(Paac-*co*-Paam)-1 composite

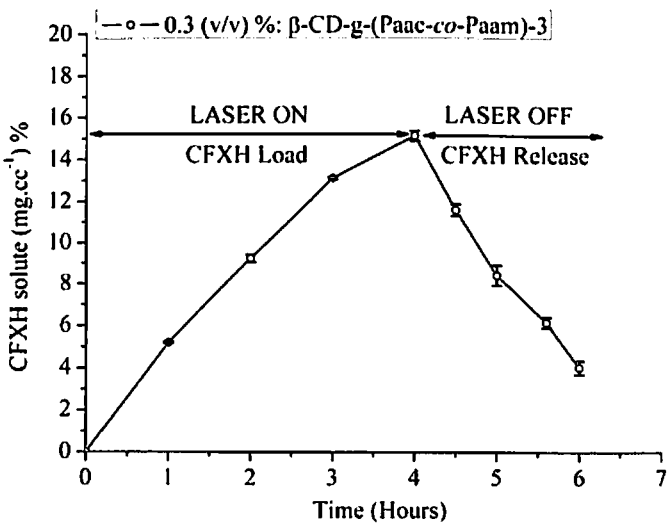

Fig. 6.11(c): CFXH solute entrapment and release profile for 0.3 (v/v)% CFXH solution in β-CD-g-(Paac-*co*-Paam)-3 composite

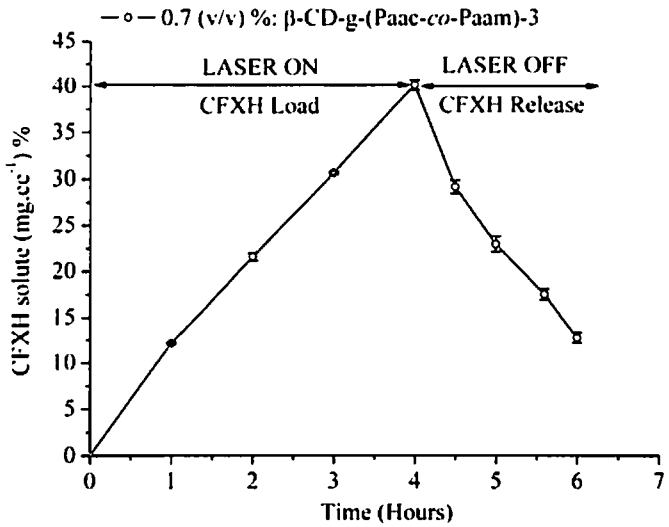

Fig. 6.11(d): CFXH solute entrapment and release profile for 0.7 (v/v)% CFXH solution in β-CD-g-(Paac-*co*-Paam)-3 composite

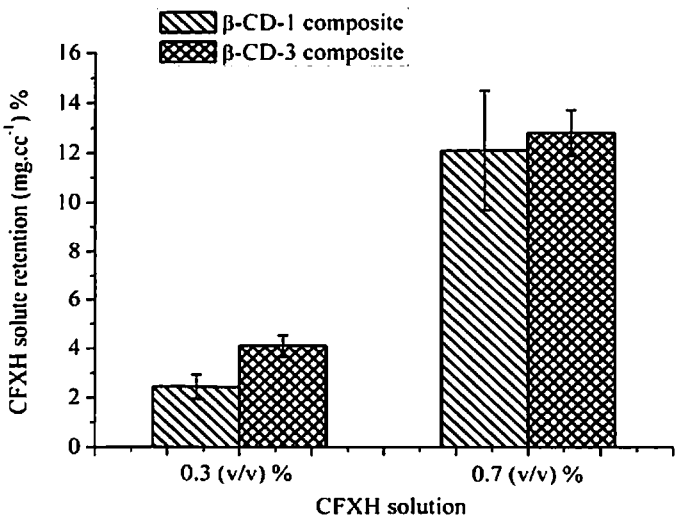

Fig. 6.12: Percentage of CFXH solute retention for 0.3(v/v)% and 0.7 (v/v)% CFXH solution in β-CD modified UVPTT based composites

The retained percentage of CFXH solute per 100 cc of dry composite IPNs (β-CD-g-(Paac-*co*-Paam)-1 and β-CD-g-(Paac-*co*-Paam)-3) after one shot of laser OFF state (with 2 hrs. duration) is depicted in Fig. 6.12. The higher percentage of CFXH solute retention found for 0.7 (v/v)% CFXH solution for both higher AuNP concentrated INPs than lower concentrated CFXH solution (0.3 (v/v)%).

PART B: Guar gum Modified Non-UVPTT Gel

This section is intended to investigate the efficacy of both non-UVPTT based hydrogels for CFXH solute dispensing through all stimuli combinations as discussed in the Section 6.3.

6.4.1 Combination I: Temperature Assisted Drug Loading Releasing

The drug was loaded at 25 °C by following the Mode I as discussed in Section 6.3.1 and the release event done at low external temperature following by Mode II process. To investigate the release efficiency of gel samples as CFXH carrier, the percentage of CFXH solute entrapment and the (wt/wt) percentage of CFXH solute release were calculated by using Eq. (6.1) and Eq. (6.4) respectively. The percentage of CFXH solute entrapped into polymer network and the percentage of CFXH solute released from polymer network for both 0.3 (v/v)% and 0.7 (v/v)% drug solutions are represented in Fig. 6.13(a)-(b) and Fig. 6.14(a)-(b) respectively. For 0.3 (v/v)% CFXH solution, 59.89±1.09% CFXH solute entrapment found in graft gel (GG-g-Paam) network, whereas, the 4.39 mmol GA containing double cross linked gel (DC-GG-PaamGA4.39) loaded 42.01±1.08% CFXH solute. However, in case of 0.7 (v/v)% CFXH solution, the GG-g-Paam and DC-GG-Paam$_{GA4.39}$ showed 153.08±4.36% and 105.86±4.88% CFXH solute entrapment capability respectively.

After temperature switched down to 10 °C, DC-GG-Paam$_{GA4.39}$ provided the highest 94.06±2.89% and 96.05±1.29% (w/w) of CFXH cumulative release from polymer network for both 0.3 (v/v)% and 0.7 (v/v)% solutions (Fig. 6.14(a)-(b)) respectively, whereas graft one (GG-g-Paam) endow with the lowest percentage of CFXH release of 30.19±0.92% and 32.50±2.73% for 0.3 (v/v)% and 0.7 (v/v)% drug solutions respectively. As the hydrophilicity increased in 0.7 (v/v)% CFXH drug solution as compared to 0.3 (v/v)% drug solution, hence, capability for percentage of drug intake by the samples are higher in higher concentration of drug solution (0.7 (v/v)%) than lower one (0.3 (v/v)%) and hence percentage of release is also increased. The efficiency of gel as drug dispenser was assessed by computing the percentage of CFXH solute retention ($R_{CFXH\ solute\ Comb.I}$ %) into the polymer network by using Eq. (6.5) and depicted in Fig. 6.15. The lowest percentage of CFXH solute retention per 100 cc of dry gel found in double cross linked gel, DC-GG-Paam$_{GA4.39}$ than graft one, GG-g-Paam for both the CFXH solutions.

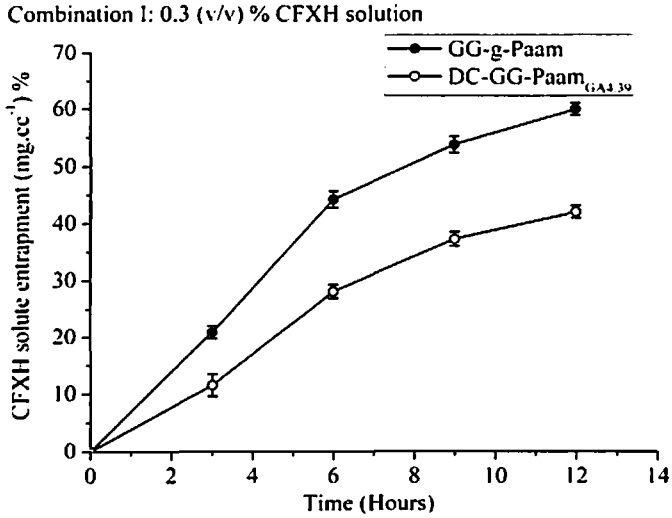

Fig. 6.13(a): Percentage of CFXH solute entrapment for 0.3 (v/v)% CFXH solution

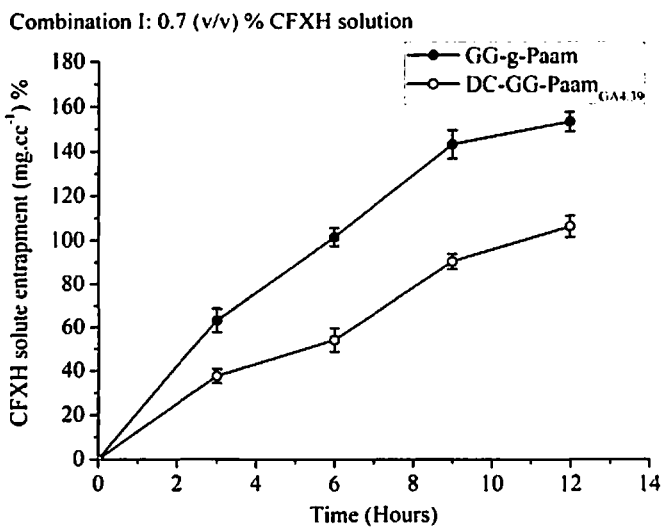

Fig. 6.13(b): Percentage of CFXH solute entrapment for 0.7 (v/v)% CFXH solution

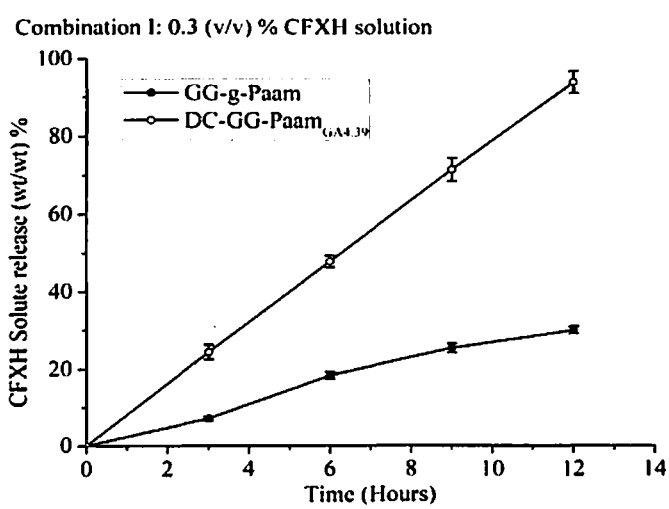

Fig. 6.14(a): Percentage of CFXH solute release for 0.3 (v/v)% CFXH solution

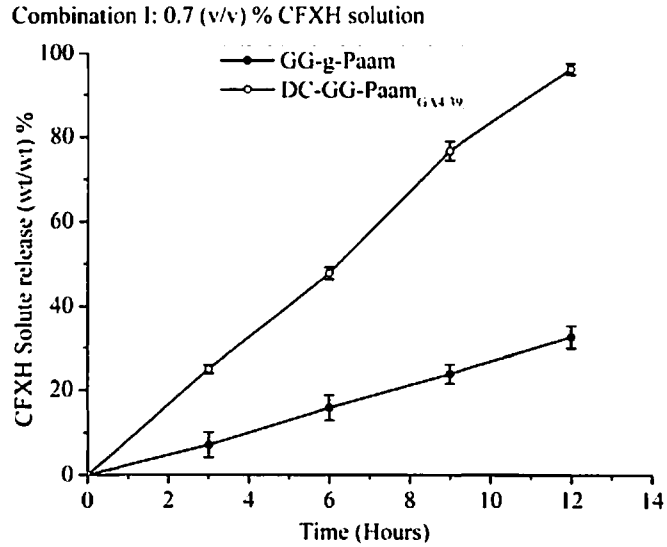

Fig. 6.14(b): Percentage of CFXH solute release for 0.7 (v/v)% CFXH solution

The DC-GG-Paam$_{GA4.39}$ retained 1.98±0.76% and 3.54±1.49% CFXH solute for 0.3 (v/v)% and 0.7 (v/v)% solutions respectively, whereas, graft sample retained 42.82±1.46% and 102.34±1.74% for same CFXH solutions respectively after identical release period of 12 hrs. Thus the DC-GG-Paam$_{GA4.39}$ network indicates the higher efficacy as drug carrier than graft gel. The DC-GG-Paam$_{GA4.39}$ has lowest capability of CFXH solute retention may due to presence of higher chain elasticity than that in graft gel. The crosslinking of GA in DC-GG-Paam$_{GA4.39}$ tightened the gel network by lowering the mesh size and thus chain elasticity is enhanced. Further, the higher tendency to retain the CFXH solute observed for 0.7 (v/v)% solution in both the gels, due to the higher entrapment capability than lower concentrated drug solution.

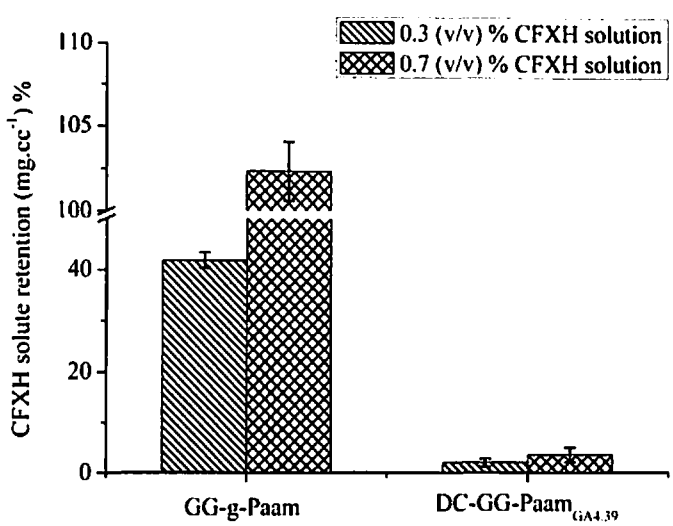

Fig. 6.15: CFXH solute retention (mg.cc^{-1})% for both CFXH solutions

Therefore, it can be concluded that, for temperature assisted drug loading and releasing activities (Combination I), the double cross linked polymer (DC-GG-Paam$_{GA4.39}$) is more efficient than graft gel (GG-g-Paam) due to the lowest drug solute retention capability for both 0.3 (v/v)% and 0.7 (v/v)% CFXH solutions.

6.4.2 Combination II: Temperature Assisted Drug Loading and pH Aided Drug Release

In Combination II CFXH load-release event, the percentage of CFXH entrapment, Drug solute entrp$_{Comb.II}$(gm.cc^{-1})% into the polymer sample during extended loading state at 25 °C was computed from the temperature assisted experimental data by using Eq.(6.6). Fig. 6.16(a)-(b), depicts the CFXH solute entrapment percentage for both graft (GG-g-paam) and double crosslinked (DC-GG-Paam$_{GA4.39}$) gel samples for both drug solutions. The ExtLS GG-g-Paam loaded 59.69±1.04% and 64.91±2.63% CFXH solute from 0.3 (v/v)% CFXH solution and 0.7 (v/v)% CFXH solution respectively, while the GA crosslinked DC-GG-Paam$_{GA4.39}$ entrapped 47.95±1.19% and 51.03±0.57% CFXH solute from 0.3 (v/v)% CFXH solution and 0.7 (v/v)% CFXH solution respectively. During CFXH solute loading, the graft gel, GG-g-Paam took 30 h. to reach ELS state for both the drug solutions, while the double cross linked gel, DC-GG-Paam$_{GA4.39}$ reached to its ELS state at 23 h.

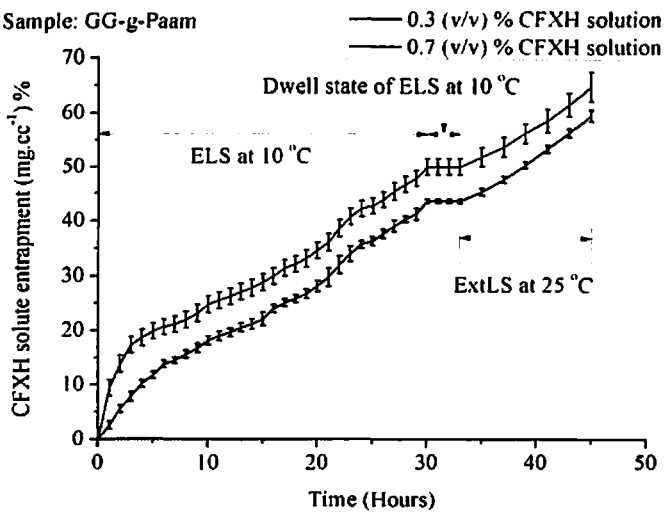

Fig. 6.16(a): Percentage of CFXH solute entrapment into GG-g-Paam ExtLS

As campared to the 0.3 (v/v)%, higher ability to entrap the CFXH solute from the 0.7 (v/v)% drug solution found in both graft and double cross linked gel samples due to

the stimuli effect on polymer network parameters such as mesh size, porosity and tortuosity, which are discussed in Section 6.7. Furthermore, irrespective of CFXH solution concentration, the tortuosity and porosity has immense effect on gel to further intake of CFXH solute at 25 °C during extended loading state. The role of network parameters of the ExtLS samples during loading of CFXH solute is briefly discussed in Section 6.7.

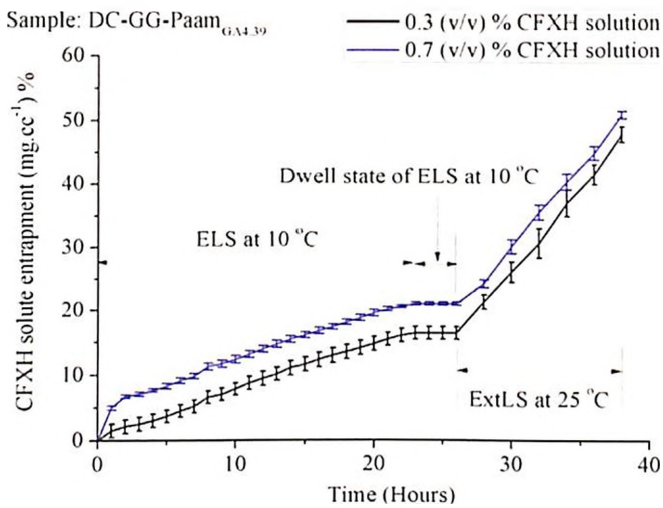

Fig. 6.16(b): Percentage of CFXH solute entrapment into DC-GG-Paam$_{GA4.39}$

The pH 4 buffer medium assisted percentage (wt/wt) of cumulative release of CFX solute $\left(\text{CFXH solute release}_{\text{Comb. II Case I or II or III}}\ (\text{wt/wt})\%\right)$ for both 0.3 (v/v)% and 0.7 (v/v)% CFXH solutions are computed by using Eq. (6.10) and the respective graphical presentation with respect to the time (hours) instances are shown in Fig. 6.17(a)-(b) respectively. The ExtLS DC-GG-Paam$_{GA4.39}$ sample released 33.80±0.94% and 47.21±1.19% of CFXH solute for 0.3 (v/v)% and 0.7 (v/v)% CFXH solutions respectively, whereas, graft gel, GG-g-Paam performed only 12.11±0.81% and 16.94±4.03% CFXH solute release respectively. The CFXH solute release carried on for ExtLS DC-GG-Paam$_{GA4.39}$ for time duration of 60 h., where a shorter release time of 30 hrs found in case of graft gel, GG-g-Paam for both the drug solutions. On the contrary, no significant drug solute release observed for pH 7 and pH 9.2 buffer medium assisted release phenomenon for both 0.3 (v/v)% and 0.7 (v/v)% CFXH solutions. During release event in pH 7 buffer medium, the CFXH loaded gel samples slashed down its weight till 9 h. and thereafter, the samples began to intake the medium solution by increasing its weight. Likewise, for the release medium of pH 9.2 buffer solution, the sample weight falls only in first 3 h. and afterwards, the sample starts to gain its weight

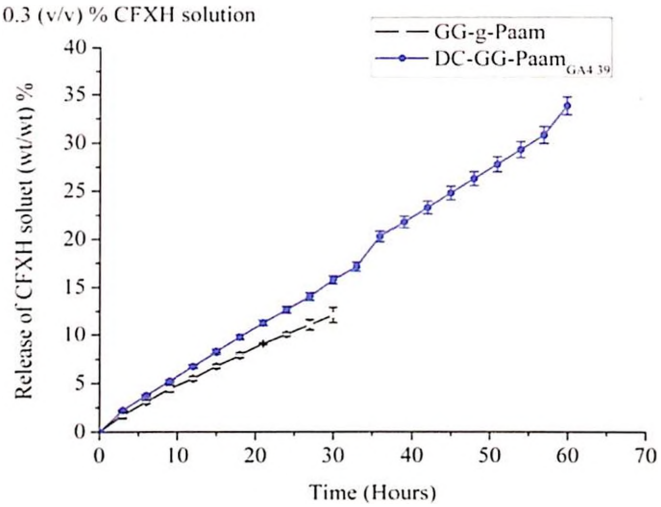

Fig. 6.17(a): Release of CFXH solute (wt/wt)% for 0.3 (v/v)% CFXH solution

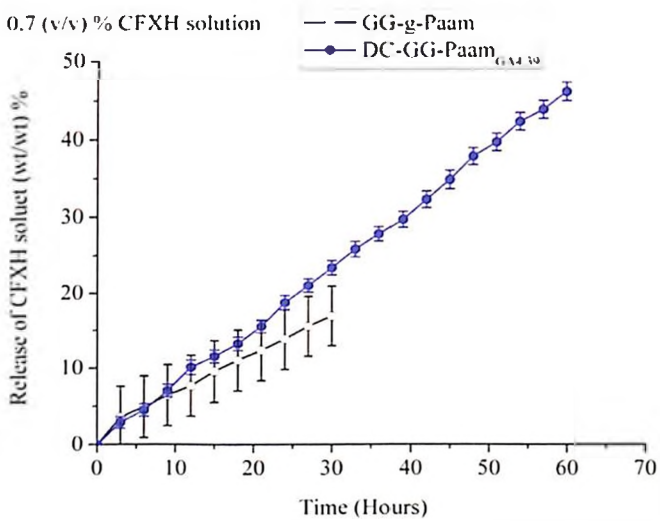

Fig. 6.17(b): Release of CFXH solute (wt/wt)% for 0.7 (v/v)% CFXH solution

due to higher pH of the medium. The increment of weight happened due to the positive responsive nature in pH medium as discussed in Section 5.9 in Chapter 5.

The percentage of change of weight of graft, GG-g-Paam and double cross linked gel, DC-GG-Paam$_{GA4.39}$ samples for both drug solutions in the release mediums of pH 7 and pH 9.2 buffer solutions are given in Fig. 6.18(a)-(d). The inset figure of Fig. 6.18(a)-(d) depicts the (wt/wt) percentage of CFXH solute release performed during the weight loss of the gel samples in the release medium of pH 7 and pH 9.2. The CFXH solute release of 1.45±0.31% and 2.05±0.15% found for graft gel, GG-g-Paam for 0.3 (v/v)% and 0.7 (v/v)% CFXH solution respectively in pH 7 release medium, while double cross

linked gel, DC-GG-Paam$_{GA4.39}$ performed 2.15±0.27% and 5.14±0.72% CFXH solute release for both CFXH solutions in same release medium.

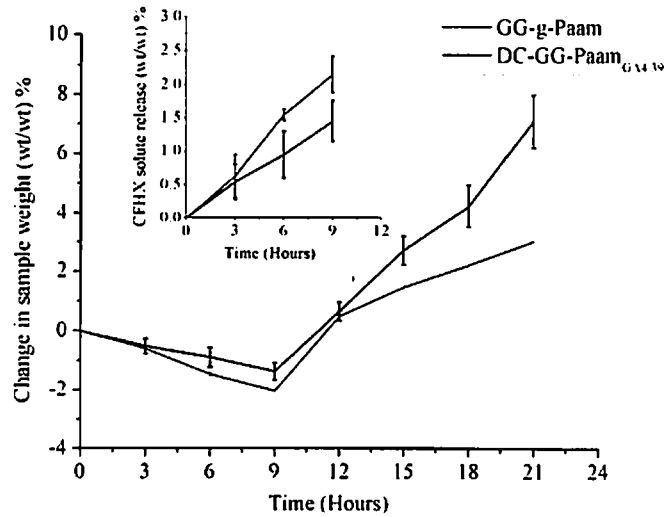

Fig. 6.18(a): Change of sample weight (%) for 0.3 (v/v)% CFXH solution in pH 7

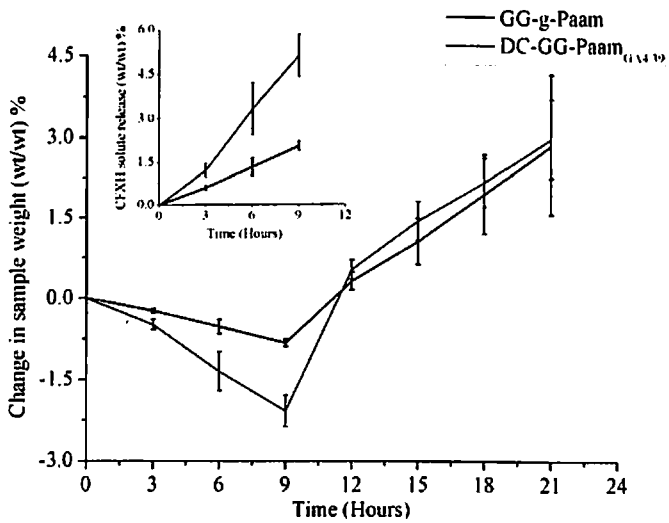

Fig. 6.18(b): Change of sample weight (%) for 0.7 (v/v)% CFXH solution in pH 7

For release medium of pH 9.2, the graft gel performed 0.98±0.40% and 1.02±0.47% CFXH solute release and double cross linked sample freed 0.67±0.24% and 2.17±0.39% release for both CFXH solutions.

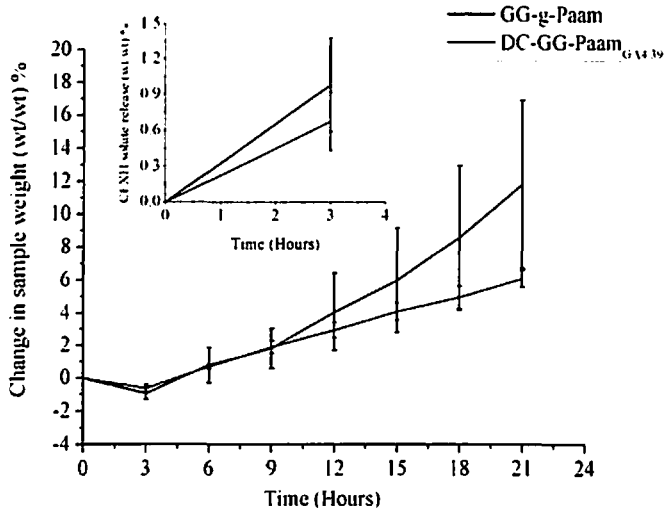

Fig. 6.18(c): Change of sample weight (%) for 0.3 (v/v)% CFXH solution in pH 9.2

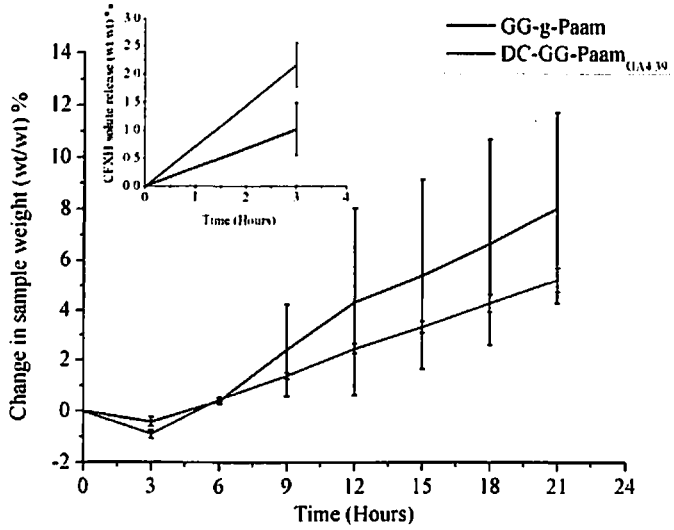

Fig. 6.18(d): Change of sample weight (%) for 0.7 (v/v)% CFXH solution in pH 9.2

Therefore, the release of CFXH solute in pH 7 and pH 9.2 is awfully negligible than that in acidic buffer medium (pH 4). Hence, the acidic release medium as the drug release event keeps consideration for further studies than neutral and alkaline release medium for Combination II. Thus, it can be concluded that, the CFXH release in Combination II is mostly suitable in acidic (pH 4) medium than neutral and alkaline medium.

The percentage of CFXH solute retention is quantified by Eq. (6.11) with the help of CFXH solute loading and pH 4 buffer medium assisted releasing experimental data and represented in Fig. 6.19.

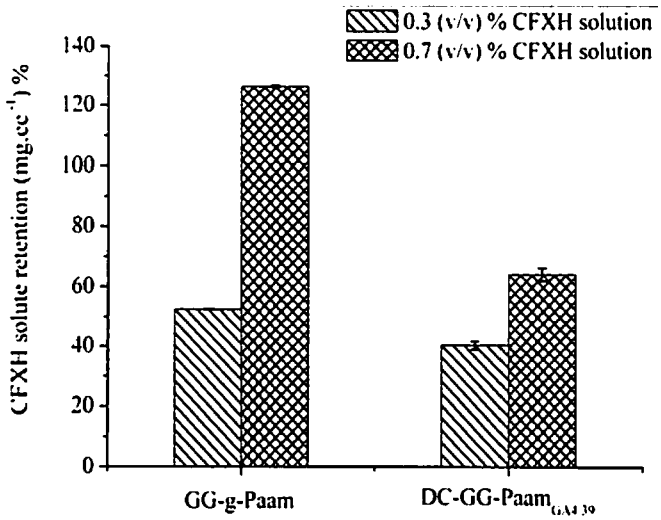

Fig. 6.19: CFXH solute retention (mg.cc-1) % for 0.3 (v/v)% and 0.7 (v/v)% CFXH

The 40.39±1.34% and 64.06±2.13% of CFXH solute retention were observed in DC-GG-Paam$_{GA4.39}$ for 0.3 (v/v)% and 0.7 (v/v)% CFXH solutions respectively, where, the graft gel, GG-g-Paam exhibited higher CFXH solute retention tendency of 52.47±0.06% and 126.25±0.28% for both of the CFXH solutions (Fig. 6.19), which is due to presence of more flexibility into DC-GG-Paam$_{GA4.39}$ gel network chain than graft one. Although, the graft sample, GG-g-Paam network has greater ability to uptake the CFXH solute than double cross linked DC-GG-Paam$_{GA4.39}$ in their ELS at 10 °C for both CFXH solutions, but lesser capability to absorb CFXH at their ExtLS at 25 °C (Fig. 6.16(a)-(b)), due to lower chain elasticity (role of elasticity is described in Section 6.7 in this chapter) than DC-GG-Paam$_{GA4.39}$. Hence, due to larger chain elasticity, GA cross linked DC-GG-Paam$_{GA4.39}$ has higher capability to entrap CFXH solute at ExtLS at 25 °C. Due to the same reason, the cumulative release of CFXH is higher in case of DC-GG-Paam$_{GA4.39}$. Therefore, the acidic medium stimulus is the best possible external stimuli over other mediums (neutral and alkaline) to make the better efficient dispensing carrier in case of Combination II stimulated drug dispensing phenomenon.

6.4.3 Combination III: Temperature Assisted Drug Loading and Dual Stimuli (combination of temperature and medium pH) Assisted Drug Discharge

The dual stimuli based on the combination of medium pH and the environmental temperature was applied in Combination III to understand the effect in CFXH solute release from the gel samples. The duo stimuli assisted percentage (wt/wt) of cumulative release of CFX solute for both 0.3 (v/v)% and 0.7 (v/v)% CFXH solutions are computed

by using Eq. (6.14) are shown in Fig. 6.20(a)-(f) for Case I, Case II and Case III. In Case I, (Fig. 6.20(a)-(b)), the 95.50±0.33% and 96.31±0.73% CFXH solute release was observed for 0.3 (v/v)% and 0.7 (v/v)% CFXH solutions respectively from ExtLS DC-G-Paam$_{GA4.39}$ sample, whereas, the graft gel, GG-g-Paam freed only 63.70±0.59% and 73.45±2.27% respectively. The CFXH solute release carried on for ExtLS DC-GG-Paam$_{GA4.39}$ for time duration of 39 h., where a shorter release time of 21 h. found in case of graft gel, GG-g-Paam for both the drug solutions.

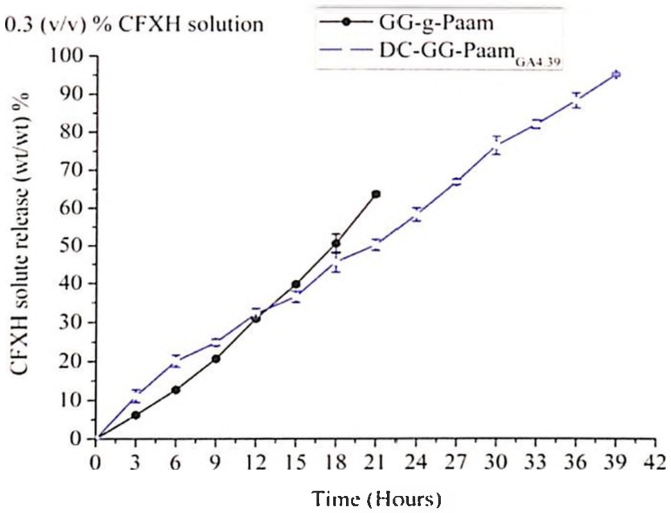

Fig. 6.20(a): Case I: Release of CFXH solute (wt/wt)% for 0.3 (v/v)% CFXH solution

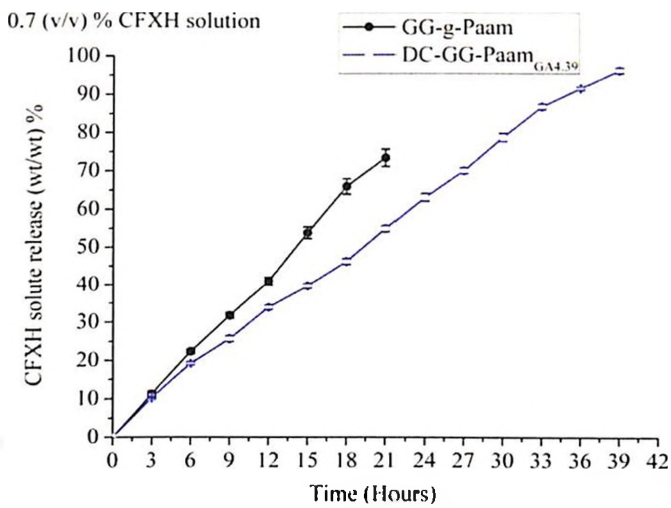

Fig. 6.20(b): Case I: Release of CFXH solute (wt/wt)% for 0.7 (v/v)% CFXH solution

On the other hand, no significant CFXH solute release observed for other release stimuli in Case II (pH 7 as medium and 10 °C) and Case III (pH 9.2 as medium and 10 °C) for both 0.3 (v/v)% and 0.7 (v/v)% CFXH solutions (Fig. 6.20(c)-(f)). The inset figure of Fig. 6.20(c)-(f) depicts the (wt/wt) percentage of CFXH solute release performed during the weight loss of the gel samples in Case II and Case III. During release event in Case II

(Fig. 6.20(c)-(d)), the CFXH loaded gel samples slashed down its weight till 9 h. and thereafter, the samples began to intake the medium solution by increasing its weight. But, for Case III (Fig. 6.20(e)-(f)), the sample weight falls only in first 3 h. and afterwards, the sample starts to gain its weight due to higher pH of the medium. The increment of weight happened due to the positive responsive nature in pH stimuli as discussed in Chapter 5. The inset figure of Fig. 6.20(c)-(f) depicts the (wt/wt) percentage of CFXH solute release performed during the weight loss of the gel samples in both Case II and Case III for both the CFXH solutions.

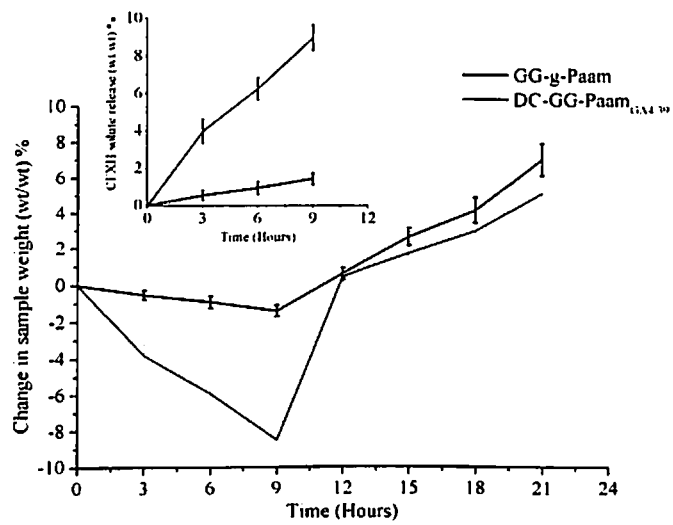

Fig. 6.20(c): Case II: Release of CFXH solute (wt/wt) % for 0.3 (v/v)% CFXH solution

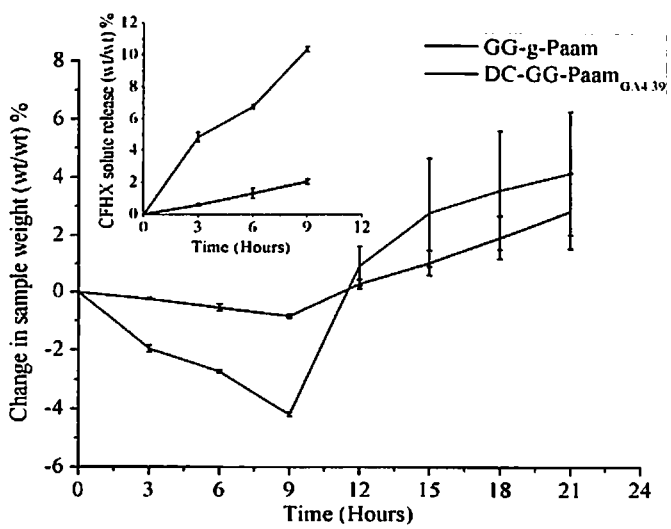

Fig. 6.20(d): Case II: Release of CFXH solute (wt/wt) % for 0.7 (v/v)% CFXH solution

The CFXH solute release of 1.45±0.31% and 2.05±0.15% found for graft gel, GG-g-Paam for 0.3% and 0.7% CFXH solution respectively in Case II, while double cross linked gel, DC-GG-Paam$_{GA4.39}$ performed 9.00±0.68% and 10.34±0.17% CFXH solute release for both CFXH solutions under same stimuli combination in Case II.

Whereas, in Case III stimuli condition, the graft gel performed 0.98±0.40% and 1.02±0.47% CFXH solute release and double cross linked sample freed 0.62±0.20% and 8.26±0.20% release for both CFXH solutions.

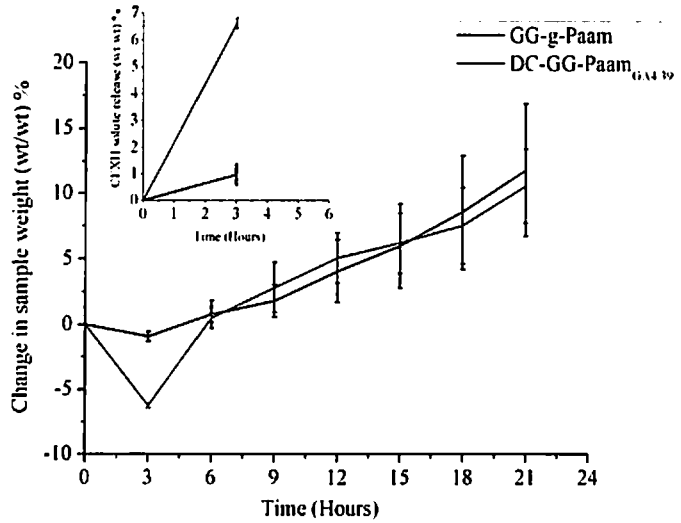

Fig. 6.20(e): Case III: Release of CFXH solute (wt/wt) % for 0.3 (v/v)% CFXH solution

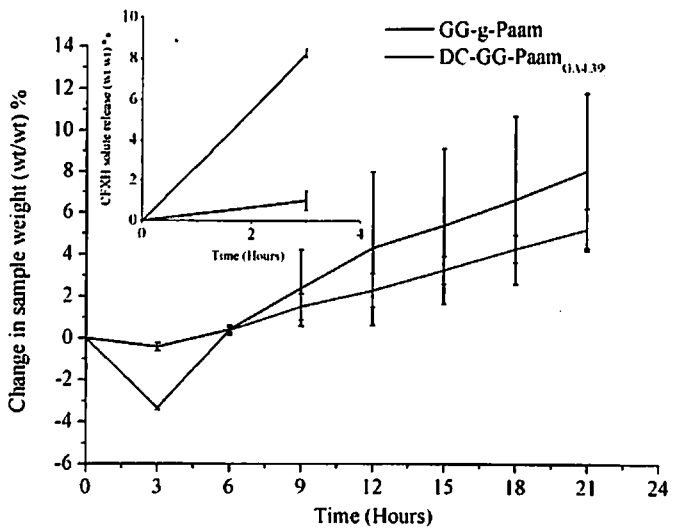

Fig. 6.20(f): Case III: Release of CFXH solute (wt/wt)% for 0.7 (v/v)% CFXH solution

Therefore, the release of CFXH solute in pH 7 and pH 9.2 is awfully insignificant than that in Case I stimuli condition. Thus, it can be concluded that, the CFXH release in Combination III is mostly suitable for Case I e.g. for the duo stimuli of acidic (pH 4) release medium with 10 °C environmental temperature

The percentage of CFXH solute retention is quantified by Eq. (6.15) with the help of CFXH solute loading and dual stimuli assisted releasing experimental data and represented in Fig. 6.21.

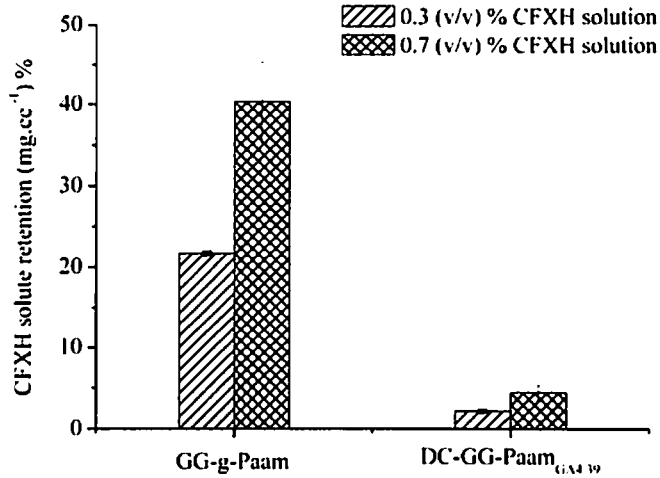

Fig. 6.21: CFXH solute retention (mg.cc^{-1})% for 0.3 (v/v)% and 0.7 (v/v)% CFXH solution

From Fig. 6.21, the 2.16±0.17% and 4.40±0.93% of CFXH solute retention were observed in DC-G-Paam$_{GA4.39}$ for 0.3 (v/v)% and 0.7 (v/v)% CFXH solutions respectively, where, the graft gel, GG-g-Paam exhibited higher CFXH solute retention tendency of 21.67±0.24% and 40.32±5.00% for both of the CFXH solutions, which is due to presence of more elastic free energy i.e lower absolute value of $\Pi_{Rel_{el}}$ (Table ANX II.4 in Annexure II) into DC-GG-Paam$_{GA4.39}$ gel network chain than graft one. Due to the same reason, the cumulative release of CFXH is higher in case of DC-GG-Paam$_{GA4.39}$.

6.4.4 Combination IV: Visible light assisted drug loading and discharge

The CFXH solute dispensing activities in Au-NP reinforced non-UVPTT based DC-GG-Paam$_{GA4.39}$-1, DC-GG-Paam$_{GA4.39}$-3 and DC-GG-Paam$_{GA4.39}$-5 composites performed by applying visible light (laser based) in pulsatile mode as per discussed in section 6.3. The percentage of CFXH solute load-release profiles for both 0.3 (v/v)% and 0.7 (v/v)% CFXH solutions for all three composites showed in Fig. 6.22(a)-(b).

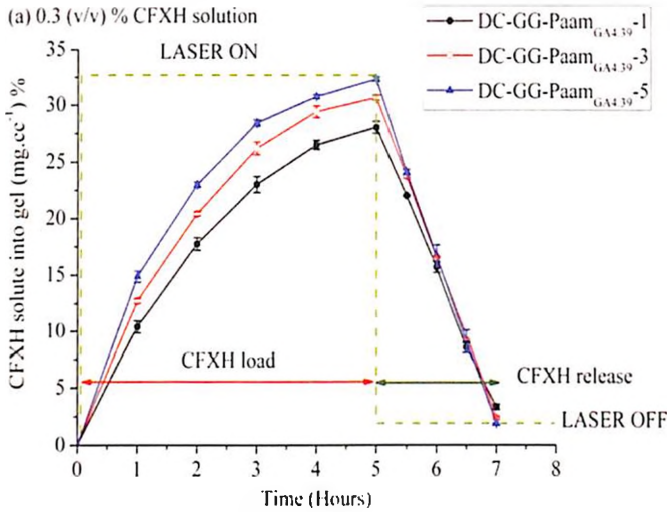

Fig. 6.22(a): CFXH solute entrapment and release profile for 0.3 (v/v)% CFXH solution in non-UVPTT based composite gels

The composite (DC-GG-Paam$_{GA4.39}$-5) containing higher concentration of NPs has shown higher CFXH entrapment capability (32.32±0.22% and 94.72±1.27% for 0.3(v/v)% and 0.7(v/v)% CFXH solutions respectively) than lower NP concentrated DC-GG-Paam$_{GA4.39}$-1 composite. This happened due to the development of higher amount of localize heat, and thus assists to expand the gel network to intake more drug solvent/solute.

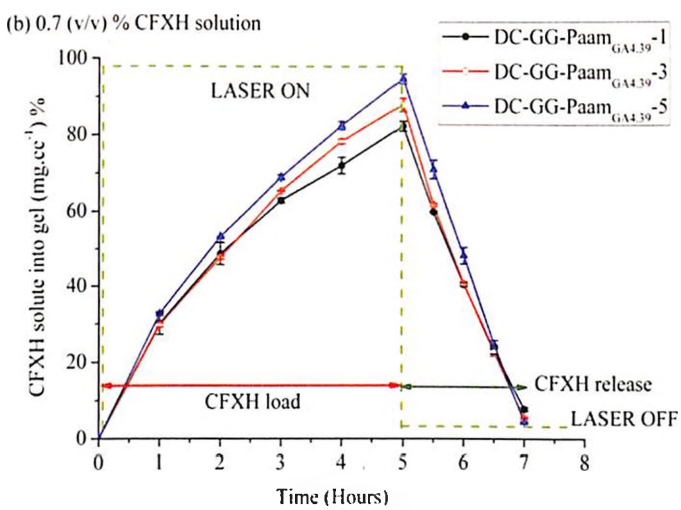

Fig. 6.22(b): CFXH solute entrapment and release profile for 0.7 (v/v)% CFXH solution in non-UVPTT based composite gels

Further, with the LOW state of laser irradiation (laser OFF state), the composite gel samples released the CFXH solutes due to the positive opto stimuli responsivity. Irrespective of CFXH solution and identical time duration of 2 h of

LOW state of laser (OFF), the higher AuNP concentrated composite (DC-GG-Paam$_{GA4.39}$-5) liberated more CFXH solute per 100 cc of dry gel (30.38±0.21% and 90.22±1.31% for 0.3 (v/v)% and 0.7 (v/v)% CFXH solutions respectively) than DC-GG-Paam$_{GA4.39}$-1 composite.

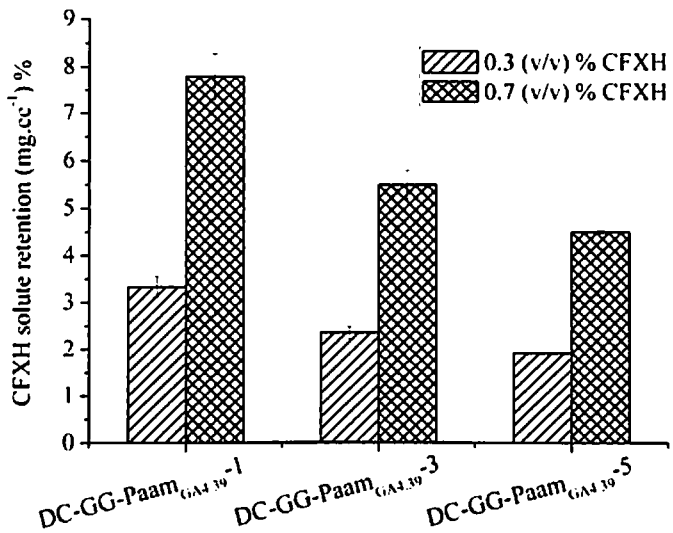

Fig. 6.23: Percentage of CFXH solute retention non-UVPTT based composite gels

The retained percentage of CFXH solute per 100 cc of dry composites after one shot of laser OFF state (with 2 hrs duration) is depicted in Fig. 6.23. The higher percentage of CFXH solute retention found for 0.7 (v/v)% CFXH solution for all three composites than lower concentrated CFXH solution (0.3 (v/v)%) due to higher tendency to entrap into network.

6.5 Comparison Study on Drug Release Efficacy of Both UVPTT and Non-UVPTT based Gels Under Different Stimuli Combinations

From the Section 6.4, the gel responsivity of UVPTT and non-UVPTT based gels and composites on drug carrier activities for each stimuli combination of drug entrapment-release events for both 0.3% and 0.7% CFXH solutions can be summarizes in Table6.2(a)-(b) and Table 6.3(a)-(b) respectively.

Table 6.2(a): The efficiency of UVPTT based gels and composites for 0.3 (v/v)% CFXH release

Stimuli applied	Sample Code	CFXH entrapment ($mg.cc^{-1}$)%	CFXH release (wt/wt)%	CFXH retention ($mg.cc^{-1}$)%
Combination I: Temperature assisted loading and temperature assisted releasing				
Load: 25 °C Release: 10 °C	β-CD-g-(Paac-*co*-Paam)	22.44 ± 0.16	85.50 ± 3.00	3.25 ± 0.69
Combination II: Forward step approached (FSA) temperature assisted drug loading and medium pH aided drug release				
Load: 10 °C in ES	β-CD-g-(Paac-*co*-Paam)	--	--	--
Load: 25 °C in ExtLS Release:pH 4 medium	β-CD-g-(Paac-*co*-Paam)	25.43 ± 0.22	65.01 ± 0.56	16.53 ± 0.06
Load: 25 °C in ExtLS Release:pH 7 medium	β-CD-g-(Paac-*co*-Paam)	25.43 ± 0.22	NIL	NIL
Load: 25 °C in ExtLS Release:pH 9.2 medium	β-CD-g-(Paac-*co*-Paam)	25.43 ± 0.22	NIL	NIL
Combination III: Forward step approached (FSA) temperature assisted drug loading and dual stimuli based on the combination of temperature and medium pH assisted drug release				
Load: 10 °C in ES	β-CD-g-(Paac-*co*-Paam)	--	--	--
Load: 25 °C in ExtLS Release: pH 4 medium and 10 °C	β-CD-g-(Paac-*co*-Paam)	25.43 ± 0.22	75.89 ± 2.58	19.30 ± 0.60
Load: 25 °C in ExtLS Release: pH 7 medium and 10 °C	β-CD-g-(Paac-*co*-Paam)	25.43 ± 0.22	NIL	NIL
Load: 25 °C in ExtLS Release:pH 9.2 medium and 10 °C	β-CD-g-(Paac-*co*-Paam)	25.43 ± 0.22	NIL	NIL
Combination IV: Laser irradiated drug loading and releasing				
Load: Laser ON Release: Laser OFF	β-CD-g-(Paac-*co*-Paam)-1	11.55 ± 0.36 ($mg.cc^{-1}$) %	9.11 ± 0.27 ($mg.cc^{-1}$) %	2.44 ± 0.22 ($mg.cc^{-1}$) %
	β-CD-g-(Paac-*co*-Paam)-3	15.18 ± 0.24 ($mg.cc^{-1}$) %	11.08 ± 0.32 ($mg.cc^{-1}$) %	4.10 ± 0.21 ($mg.cc^{-1}$) %

Table 6.2(b): The efficiency of UVPTT based gels and composites for 0.7 (v/v)% CFXH release

Stimuli applied	Sample Code	CFXH entrapment ($mg.cc^{-1}$)%	CFXH release (wt/wt)%	CFXH retention ($mg.cc^{-1}$)%
Combination I: Temperature assisted loading and temperature assisted releasing				
Load: 25 °C Release: 10 °C	β-CD-g-(Paac-*co*-Paam)	54.84 ± 0.37	86.65 ± 3.04	7.32 ± 1.70
Combination II: Forward step approached (FSA) temperature assisted drug loading and medium pH aided drug release				
Load: 10 °C in ES	β-CD-g-(Paac-*co*-Paam)	--	--	--
Load: 25 °C in ExtLS Release:pH 4medium	β-CD-g-(Paac-*co*-Paam)	62.76 ± 0.73	69.16 ± 1.00	43.41 ± 1.02
Load: 25 °C in ExtLS Release:pH 7medium	β-CD-g-(Paac-*co*-Paam)	62.76 ± 0.73	NIL	NIL
Load: 25 °C in ExtLS Release:pH 9.2 medium	β-CD-g-(Paac-*co*-Paam)	62.76 ± 0.73	NIL	NIL
Combination III: Forward step approached (FSA) temperature assisted drug loading and dual stimuli based on the combination of temperature and medium pH assisted drug release				
Load: 10 °C in ES	β-CD-g-(Paac-*co*-Paam)	--	--	--
Load: 25 °C in ExtLS Release: pH 4 buffer medium and 10 °C	β-CD-g-(Paac-*co*-Paam)	62.76 ± 0.73	81.37 ± 1.90	51.08 ± 1.41
Load: 25 °C in ExtLS Release: pH 7 buffer medium and 10 °C	β-CD-g-(Paac-*co*-Paam)	62.76 ± 0.73	NIL	NIL
Load: 25 °C in ExtLS Release: pH 9.2 buffer medium and 10 °C	β-CD-g-(Paac-*co*-Paam)	62.76 ± 0.73	NIL	NIL
Combination IV: Laser irradiated drug loading and releasing				
Load: Laser ON Release: Laser OFF	β-CD-g-(Paac-*co*-Paam)-1	37.32 ± 2.25 ($mg.cc^{-1}$) %	25.26 ± 0.72 ($mg.cc^{-1}$) %	12.06 ± 0.62 ($mg.cc^{-1}$) %
	β-CD-g-(Paac-*co*-Paam)-3	40.16 ± 0.54 ($mg.cc^{-1}$) %	27.40 ± 0.55 ($mg.cc^{-1}$) %	12.76 ± 0.44 ($mg.cc^{-1}$) %

Table 6.3(a): The efficiency of non-UVPTT based gels and composites for 0.3 (v/v)% CFXH release

Stimuli applied	Sample Code	CFXH entrapment ($mg.cc^{-1}$)%	CFXH release (wt/wt)%	CFXH retention ($mg.cc^{-1}$)%
Combination I: Temperature assisted loading and temperature assisted releasing				
Load: 25 °C Release: 10 °C	GG-g-Paam	59.89 ± 1.09	30.19 ± 0.92	41.82 ± 1.46
	DC-GG-$Paam_{GA4.39}$	42.01 ± 1.08	94.06 ± 2.89	1.98 ± 0.76
Combination II: Forward step approached (FSA) temperature assisted drug loading and medium pH aided drug release				
Load: 10 °C in ES	GG-g-Paam	43.62 ± 0.33	--	--
	DC-GG-$Paam_{GA4.39}$	16.52 ± 1.00	--	--
Load: 25 °C in ExtLS Release:pH 4 medium	GG-g-Paam	59.69 ± 1.04	12.11 ± 0.72	52.46 ± 0.06
	DC-GG-$Paam_{GA4.39}$	47.95 ± 1.19	33.80 ± 0.94	40.39 ± 1.34
Load: 25 °C in ExtLS Release: pH 7 medium	GG-g-Paam	59.69 ± 1.04	NIL	NIL
	DC-GG-$Paam_{GA4.39}$	47.95 ± 1.19	NIL	NIL
Load: 25 °C in ExtLS Release:pH 9.2 medium	GG-g-Paam	59.69 ± 1.04	NIL	NIL
	DC-GG-$Paam_{GA4.39}$	47.95 ± 1.19	NIL	NIL
Combination III: Forward step approached (FSA) temperature assisted drug loading and dual stimuli based on the combination of temperature and medium pH assisted drug release				
Load: 10 °C in ES	GG-g-Paam	43.62 ± 0.33	--	--
	DC-GG-$Paam_{GA4.39}$	16.52 ± 1.00	--	--
Load: 25 °C in ExtLS Release:pH 4 medium and 10 °C	GG-g-Paam	59.69 ± 1.04	63.70 ± 0.59	21.67 ± 0.24
	DC-GG-$Paam_{GA4.39}$	47.95 ± 1.19	95.50 ± 0.33	2.16 ± 0.17
Load: 25 °C in ExtLS Release:pH 7 medium and 10 °C	GG-g-Paam	59.69 ± 1.04	NIL	NIL
	DC-GG-$Paam_{GA4.39}$	47.95 ± 1.19	NIL	NIL
Load: 25 °C in ExtLS Release: pH 9.2 buffer medium and 10 °C	GG-g-Paam	59.69 ± 1.04	NIL	NIL
	DC-GG-$Paam_{GA4.39}$	47.95 ± 1.19	NIL	NIL
Combination IV: Laser irradiated drug loading and releasing				
Load: Laser ON Release: Laser OFF	DC-GG-$Paam_{GA4.39}$-1	28.03 ± 0.52	24.70 ± 0.31 ($mg.cc^{-1}$) %	3.33 ± 0.22 ($mg.cc^{-1}$) %
	DC-GG-$Paam_{GA4.39}$-3	30.62 ± 0.23	28.26 ± 0.36 ($mg.cc^{-1}$) %	2.36 ± 0.13 ($mg.cc^{-1}$) %
	DC-GG-$Paam_{GA4.39}$-5	32.32 ± 0.22	30.38 ± 0.20 ($mg.cc^{-1}$) %	1.93 ± 0.02 ($mg.cc^{-1}$) %

Table 6.3(b): The efficiency of non-UVPTT based gels and composites for 0.7 (v/v)% CFXH release

Stimuli applied	Sample Code	CFXH entrapment ($mg.cc^{-1}$)%	CFXH release (wt/wt)%	CFXH retention ($mg.cc^{-1}$)%
Combination I: Temperature assisted loading and temperature assisted releasing				
Load: 25 °C Release: 10 °C	GG-g-Paam	153.08 ± 4.36	32.50 ± 2.73	67.50 ± 2.73
	DC-GG-$Paam_{GA4.39}$	105.86 ± 4.88	96.05 ± 1.29	3.95 ± 1.29
Combination II: Forward step approached (FSA) temperature assisted drug loading and medium pH aided drug release				
Load: 10 °C in ES	GG-g-Paam	50.10 ± 1.50	NA	NA
	DC-GG-$Paam_{GA4.39}$	21.19 ± 0.28	NA	NA
Load: 25 °C in ExtLS Release:pH 4 medium	GG-g-Paam	64.91 ± 2.63	25.92 ± 1.04	48.11 ± 2.63
	DC-GG-$Paam_{GA4.39}$	51.03 ± 0.57	78.17 ± 0.21	12.24 ± 1.38
Load: 25 °C in ExtLS Release:pH 7 medium	GG-g-Paam	64.91 ± 2.63	NIL	--
	DC-GG-$Paam_{GA4.39}$	51.03 ± 0.57	NIL	--
Load: 25 °C in ExtLS Release:pH 9.2 medium	GG-g-Paam	64.91 ± 2.63	NIL	--
	DC-GG-$Paam_{GA4.39}$	51.03 ± 0.57	NIL	--
Combination III: Forward step approached (FSA) temperature assisted drug loading and dual stimuli based on the combination of temperature and medium pH assisted drug release				
Load: 10 °C in ES	GG-g-Paam	50.10 ± 1.50	NA	NA
	DC-GG-$Paam_{GA4.39}$	21.19 ± 0.28	NA	NA
Load: 25 °C in ExtLS Release: pH 4 buffer medium and 10 °C	GG-g-Paam	64.91 ± 2.63	80.67 ± 2.01	12.58 ± 1.68
	DC-GG-$Paam_{GA4.39}$	51.03 ± 0.57	96.80 ± 0.30	1.63 ± 0.16
Load: 25 °C in ExtLS Release:pH 7 medium and 10 °C	GG-g-Paam	64.91 ± 2.63	NIL	--
	DC-GG-$Paam_{GA4.39}$	51.03 ± 0.57	NIL	--
Load: 25 °C in ExtLS Release: pH 9.2 medium and 10 °C	GG-g-Paam	64.91 ± 2.63	NIL	--
	DC-GG-$Paam_{GA4.39}$	51.03 ± 0.57	NIL	--
Combination IV: Laser irradiated drug loading and releasing				
Load: Laser ON Release: Laser OFF	DC-GG-$Paam_{GA4.39}$-1	82.18 ± 1.26	74.38 ± 0.77 ($mg.cc^{-1}$) %	7.79 ± 0.49 ($mg.cc^{-1}$) %
	DC-GG-$Paam_{GA4.39}$-3	87.78 ± 1.78	82.28 ± 1.49 ($mg.cc^{-1}$) %	5.50 ± 0.30 ($mg.cc^{-1}$) %
	DC-GG-$Paam_{GA4.39}$-5	94.72 ± 1.28	90.22 ± 1.30 ($mg.cc^{-1}$) %	4.51 ± 0.03 ($mg.cc^{-1}$) %

From above Table 6.2(a)-(b) and Table 6.3(a)-(b), it is clearly noticeable that, all the gels performed efficiently on the applied stimuli Combination I, II and IV (depending on AuNP concentration) than Combination III. In case of glutaraldehyde cross linked non-UVPTT gel exhibits lesser drug solute retention, which is directing higher efficacy as drug carrier than graft gel. Further, the stimuli in Combination IV i.e. the light assisted loading and releasing phenomenon showed highest efficiency for types of UVPTT and non-UVPTT based composites.

6.6 Drug Entrapment-Release Kinetics: Theoretical Overview

In Chapter 5, the diffusion based osmotic driven solvent loading phenomenon observed for the synthesized gels. This section is aimed to understand the osmotic and diffusion effect inside the gel chain network during drug solute dispensing activities. The release kinetics is investigated through different well established release kinetics such as 0^{th} order, 1^{st} order, Higuchi and Korsmeyer-Peppas release kinetics under all three combinational dispensing events.

6.6.1 Theoretical aspect on drug entrapment kinetics: effect of osmotic pressure, diffusion and gel network parameters

During CFX entrapment into polymer network, introduction of CFX solute molecules into polymer network results the swelling of gel sample by stretching of network chains and thus less chain configurational entropy welcomes the retractive force to return the gel network to its original un-stretched state (as discussed in Chapter 5). The higher disorder of the polymer chain indicates more chain configurational entropy produced inside the chain network. Considering the ionic contribution of drug medium, the relation between the total chemical potential and the chemical potential contributions during CFXH solute intake can be expressed as the well established Eq. (6.19) [14].

$$\mu_1 - \mu_1^0 = (\Delta\mu_1)_{mix} + (\Delta\mu_1)_{el} + (\Delta\mu_1)_{ion} \qquad (6.19)$$

Where, μ_1 and μ_1^0 are the chemical potentials of the solution in the polymer-drug solution medium and the chemical potential of the pure solvent respectively. The 1^{st} term of Eq.(6.19) is due to the mixing contribution to the chemical potential for polymer-solvent interactions, 2^{nd} term is due to the elastic contribution to the potential energy of polymer chains and the 3^{rd} term is due to the ionic contribution from surrounding drug solution/medium and the polymer-drug solution interaction system. According to Peppas

et al.[14], the mixing contribution to the chemical potential energy $(\Delta\mu_1)_{mix}$ and the chain elasticity contributed chemical potential $(\Delta\mu_1)_{el}$ for crosslinked polymeric system and expressed as Eq. (6.20) and Eq. (6.21) respectively.

$$(\Delta\mu_1)_{mix} = RT\,[\ln(1-\phi) + \phi + \chi\phi^2] \tag{6.20}$$

$$(\Delta\mu_1)_{el} = RT\left(\frac{V_1}{\upsilon_{P_{CFXH}} M_C}\right)\left(1 - \frac{2M_C}{M_n}\right)\left(\phi^{1/3} - \frac{\phi}{2}\right) \tag{6.21}$$

Where, $\upsilon_{P_{CFXH}}$ represents the specific volume of the CFXH loaded gel sample and is calculated from the experimental data by using Eq. (6.22).

$$\upsilon_{P_{CFXH}} = \frac{1}{\rho_{P_{CFXH}}} \tag{6.22}$$

Where, $\rho_{P_{CFXH}}$ denotes the density of the CFXH loaded sample and is expressed in gm.cc^{-1}. The ionic contribution $(\Delta\mu_1)_{ion}$ can be measured from either Eq. (6.23A) or Eq. (6.23B) depending on the ionic concentration of CFXH solution/medium (C_m) and polymer network (C_p) [14].

$$(\Delta\mu_1^m)_{ion} - (\Delta\mu_1)_{ion} = \frac{RTV_1\rho^2_{P_{CFXH}} i^2\phi^2}{4I} \quad ; \text{for } C_m > C_P \tag{6.23A}$$

$$(\Delta\mu_1^m)_{ion} - (\Delta\mu_1)_{ion} = \frac{RTV_1\rho_{P_{CFXH}} i\phi}{z_-} \quad ; \text{for } C_m < C_P \tag{6.23B}$$

Where, R is the universal gas constant and its value taken as 8.314 J.mol^{-1}.K^{-1} and T is the absolute temperature (experimental).

V_1 and ϕ are the molar volume of the solvent and polymer volume fraction, which are defined already defined in Section 5.6 in Chapter 5.

The "I" represents the ionic strength (expressed in mol) of the CFXH solution, it was assessed by Eq. (6.24).

$$I = \frac{1}{2}\sum_{x=1}^{n} m_x Z_x^2 \tag{6.24}$$

Where, m_x is the molar concentration of the ion x, Z_x is the charge number of that ion x. The "i" denotes the ionization factor of the drug solution, was measured by Eq. (6.25) and z_- represents the number of negatively charged species. $(\Delta\mu_1^m)_{ion}$ is chemical potential of the surrounding medium and measured by Eq. (6.26A) and by Eq. (6.26B) for drug solution and pH4 medium respectively [14].

$$i = \frac{K_a}{10^{-pH} + K_a} \tag{6.25}$$

$$(\Delta\mu_1^m)_{ion} = RTX_{CFXH}\ln\Upsilon \tag{6.26A}$$

$$(\Delta\mu_1^m)_{ion} = -V_1 R T \sum_j C_j \qquad (6.26B)$$

Where, the equilibrium constant, K_a was calculated from the dissociation constants of used model drug (considering pKa = 6.09 for carboxylic acid group and pKa = 8.74 for nitrogen on piperazinyl ring). X_{CFXH} is the mole fraction of CFXH solute in the drug solutions 0.3 (v/v)% and 0.7 (v/v)% and Υ is the activity co-efficient of water solvent and this was assessed by well known Debye-Huckel Equation. The Debye-Huckel limiting law expression Eq. (6.27).

$$\ln(\Upsilon) = -A Z^2 \sqrt{I} \qquad (6.27)$$

The "A" is constant and is considered as 0.509 $mol^{-1/2} Kg^{1/2}$. The C_j represents the ion concentration of the release medium (pH 4/pH 7/pH 9.2).

As discussed the role of osmotic pressure parameters in Section 5.6 in Chapter 5, the equivalent osmotic pressure can be expressed as Eq. (6.28), considering the ionic contribution of the drug medium.

$$\Pi_{eq} = \Pi_{mix} + \Pi_{el} + \Pi_{ion} \qquad (6.28)$$

Furthermore, the equivalent osmotic pressure, π_{eq} with respect to the chemical potential is expressed as Eq. (6.29) [15].

$$\mu_1 - \mu_1^0 = -\Pi_{eq} V_1 \qquad (6.29)$$

Hence, the equivalent osmotic pressure, Π_{eq} can be determined by substituting the Eqs.(6.19), (6.20), (6.21) and (6.23A) or (6.23B) into Eq. (6.29) and can be expressed as Eq. (6.30A) and Eq. (6.30B) depending on the ionic concentration into the CFXH solution medium and the polymer network for entrapment and release state of polymer respectively.

$$\Pi_{Entrp_{eq}} = -\frac{RT}{V_1}\{\ln(1-\varphi) + \varphi + \chi\varphi^2\} - RT\left\{\left(\frac{\rho_{SP}}{M_C}\right)\left(1-\frac{2M_C}{M_n}\right)\left(\varphi^{1/3} - \frac{\varphi}{2}\right)\right\} - RT\left\{\frac{X_{CFX}\ln\Upsilon}{V_1} - \frac{i^2\rho_{SP}^2\varphi^2}{4I}\right\} \qquad (6.30A)$$

$$\Pi_{Rel_{eq}} = -\frac{RT}{V_1}\{\ln(1-\varphi) + \varphi + \chi\varphi^2\} - RT\left\{\left(\frac{\rho_{SP}}{M_C}\right)\left(1-\frac{2M_C}{M_n}\right)\left(\varphi^{1/3} - \frac{\varphi}{2}\right)\right\} + RT\left\{\sum_j C_j + \frac{i\varphi\rho_{SP}}{z_-}\right\} \qquad (6.30B)$$

The 1st term of both Eq. (6.30A) and Eq. (6.30B) is responsible for mixing osmotic pressure (Π_{mix}) and 2nd term is responsible for the elastic response (Π_{el}) of the gel network and 3rd one from ionic contribution (Π_{ion}) from gel network and the surrounding medium. The Π_{mix} and Π_{el} can be expressed as Eq.

(6.31) and Eq. (6.32) respectively. Further, the ion contributed osmotic pressure (Π_{ion}) can be expressed as Eqs. (6.33A) and (6.33B) respectively, depending on the ionic concentration of medium and polymer network.

$$\Pi_{mix} = -\frac{RT}{V_1}\{\ln(1-\varphi) + \varphi + \chi\varphi^2\} \quad (6.31)$$

$$\Pi_{el} = -RT\left\{\left(\frac{\rho_{SP}}{M_C}\right)\left(1-\frac{2M_C}{M_n}\right)\left(\varphi^{1/3}-\frac{\varphi}{2}\right)\right\} \quad (6.32)$$

$$\Pi_{ion} = -RT\left\{\frac{X_{CFX}\ln\Upsilon}{V_1} - \frac{i^2\rho_{SP}^2\varphi^2}{4I}\right\}; \text{for } C_m > C_P \quad (6.33A)$$

$$\Pi_{ion} = RT\left\{\sum_j C_j + \frac{i\varphi\rho_{SP}}{z_-}\right\}; \text{for } C_m < C_P \quad (6.33B)$$

Due to the chemical potential gradient, the chemical diffusion takes place and thus results in net transport of mass. To understand the diffusional effect on CFXH entrapment in all three drug dispensing combinations, the Fick's 2nd law of diffusion was applied. The diffusion rate constant (k_D) of drug solution was calculated from experimental swelling data by using well defined Eq. (6.34) [16].

$$\frac{W_t}{W_{Load}} = k_D . t^n \quad (6.34)$$

where, W_t and W_{Laod} are the weight of the gel sample at a time "t" and final weight of the sample at after CFXH loading during entrapment phenomenon respectively. The "n" denotes the type of diffusion occurred inside the polymer gel network.

The other important parameter called diffusion co-efficient, D_S ($cm^2.hr^{-1}$) of the solvent into polymer gel, indicative of the diffusion mobility was measured by Eq. (6.35)[17] sample during swelling.

$$D_S = \frac{k_D h^2}{\pi^2} \quad (6.35)$$

where, h represents the thickness of drug loaded polymer and π is the constant (3.14159). The occurred front velocity of solvent during entrapment interaction into polymer network, u ($cm.hr^{-1}$) is assessed by Eq. (6.36) [18].

$$u = \left(\frac{dv}{dt}\right)\frac{1}{2A} \quad (6.36)$$

where, $\left(\frac{dv}{dt}\right)$ is the change in volume of per unit time and A represents the surface area of swelled polymer sample and A is multiplied by 2, considering the opposite bi-directional solvent penetration at both sides of rectangular sample.

6.6.2 Theoretical Aspect on Drug Release Kinetics: Effect of Osmotic Pressure and Diffusion

The CFXH was released with the positive stimuli responsiveness of the polymers, hence, the ionic concentration of CFXH solution medium (C_m) is less than that of polymer network (C_p). Further, as medium pH was applied for Combination II and Combination III based dispensing release events, thus ion contributed osmotic pressure ($\Pi_{Rel\,ion}$) was considered. Therefore, based on the previously discussed osmotic pressure parameters in Section 6.6.1, the mixing osmotic pressure ($\Pi_{Rel\,mix}$), osmotic pressure due to chain elasticity ($\Pi_{Rel\,el}$) and ion contributed osmotic pressure ($\Pi_{Rel\,ion}$) for release events are expressed as Eq. (6.37), (6.38) and (6.39) respectively.

$$\Pi_{Rel\,mix} = -\frac{RT}{V_1}\{\ln(1-\varphi)+\varphi+\chi\varphi^2\} \tag{6.37}$$

$$\Pi_{Rel\,el} = -RT\left\{\left(\frac{\rho_{SP}}{M_C}\right)\left(1-\frac{2M_C}{M_n}\right)\left(\varphi^{1/3}-\frac{\varphi}{2}\right)\right\} \tag{6.38}$$

$$\Pi_{Rel\,ion} = RT\left\{\sum_j C_j + \frac{i\varphi\rho_{SP}}{z_-}\right\} \tag{6.39}$$

To investigate the release kinetics, the well known 0^{th} order, 1^{st} order, Higuchi and Korsmeyer-Peppas kinetics applied on the experimental release data. To determine the release rates, the empirical release equations of Eq. (6.40)-(6.42) for 0^{th} order, 1^{st} order and Higuchi release kinetics respectively are used. The non-liner curve fitting algorithms are applied through Origin 8 Pro software.

$$Q_t = Q_0 + K_0 t \tag{6.40}$$

$$\ln Q_t = \ln Q_0 + K_1 t \tag{6.41}$$

$$Q_t = K_h t^{1/2} \tag{6.42}$$

where Q_t is the amount of drug release at time "t", Q_0 is the initial amount of of loaded drug in the gel slab. K_0, K_1, and K_h are the respective release rate constants for 0^{th} order, 1^{st} order and Higuchi kinetics. To empathize the diffusional release mechanism, the experimental CFXH released data fitted to Korsmeyer-Peppas Eq.(6.43).

$$\frac{W_t}{W_{Rel}} = K_{D\,Rel}\cdot t^n \tag{6.43}$$

where, $\frac{W_t}{W_{Rel}}$ is the fraction of released drug at time t, W_t and W_{Rel} are the amounts of released drug at time "t" during release event and the final amount of released

drug. The $K_{D\,Rel}$ is the release rate constant and "n" is the release exponent. The assessed "n" value was used to appraise the release mechanism and the transport category for released drug.

As discussed the diffusional effect inside the polymer network, the diffusion co-efficient, $D_{S\,Rel}$ ($cm^2.hr^{-1}$) of the solvent into polymer gel was measured by Eq.(6.44).

$$D_{S\,Rel} = \frac{K_{D\,Rel}\, h^2}{\pi^2} \tag{6.44}$$

where, h represents the thickness of CFXH released gel. The occurred front velocity during solvent/solute release (u_{Rel}) was calculated by using the Eq. (6.45).

$$u_{Rel} = \left(\frac{dv}{dt}\right)_{Rel} \times \frac{1}{2\,A_{Rel}} \tag{6.45}$$

where, $\left(\frac{dv}{dt}\right)_{Rel}$ is the change in volume of gel sample during drug release per unit time and A_{Rel} represents the surface area of drug released gel sample and A is multiplied by 2, considering the opposite bi-directional solvent penetration at both side of rectangular sample.

6.7 Drug Entrapment-Release Kinetics: Investigational Analysis

The present section is analyzed the role of the osmotic and diffusion effect inside the gel chain network during entrapment and release of drug solute. The release kinetics is also evaluated through different well established release kinetics from the experimentally obtained data.

6.7.1 Analysis on Drug Entrapment Kinetics: Effect of Gel Parameters, Osmotic Pressure and Diffusion

Based on the CFXH loading phenomenon, discussed in Section 6.3.1, 6.3.2 and 6.3.3, the CFXH solute entrapment can be categorized as: Approach I: the CFXH solute was loaded at 25 °C and in Approach II: temperature assisted forward step approach (FSA) was followed during CFXH loading. In Approach II, the CFXH entrapped at 10 °C until ES state and followed by ExtLS was done at 25 °C. The Approach II is further classified as Approach II(A) and Approach II(B) dependent on the state of the sample during FSA. The Approach II(A) involves the CFXH loading during ESL at 10 °C and Approach II(B) for the CFXH loading into ExtLS state at 25 °C.

The developed equivalent osmotic pressure $\left(\Pi_{Entrp_{eq}}\right)$ inside the gel during CFXH entrapment is quantified from the experimental loading data by using Eq. (6.30A). The equivalent osmotic pressure involving mixing osmotic pressure (Π_{mix}), osmotic pressure due to chain elasticity (Π_{el}) and ion contributed osmotic pressure (Π_{ion}) are determined from the Eqs. (6.31), (6.32) and (6.33A) respectively. The parameters used in Eq. (6.30A), polymer volume fraction (ϕ), polymer-solvent interaction parameter (χ), molecular weight between two cross links (M_C), Mn are determined as described in Section 5.6 in Chapter 5 from the CFXH loading experimental data.

From the Table 6.2(a)-(b) and Table 6.3(a)-(b), it was found that the higher amount of CFXH solute entrapped into both the gel samples for 0.7 (v/v)% CFXH solution than 0.3 (v/v)% via temperature assisted Combination I loading event. Same observation found in case of FSA temperature assisted Combination II loading event in ESL loading state at 10 °C and ExtLS at 25 °C. This phenomenon takes place due to larger mesh size and lower mixing osmotic pressure (Π_{mix}) (see Table ANX II.1 in Annexure II) inside gel network, which results higher mixing ability between gel solute. indicating that the lesser tendency of resistive pressure inside gel network than environment and hence more CFXH solute diffuse-in into the polymer network. In addition, the higher tortuosity produced in case of 0.7 (v/v)% CFXH solution, which make easier to hold more CFXH solute into gel network during loading event at Approach I and Approach II. However, the porosity is decreased with the higher CFXH solute concentrated drug solution (0.7 (v/v)%).

Furthermore, irrespective of the CFXH solute concentration in FSA based Approach IIA and Approach IIB loading phenomenon during ELS and ExtLS loading events at 10 °C and ExtLS at 25 °C, the tortuosity increases with decrease of porosity inside the ExtLS samples at higher temperature (25 °C), and mesh size increased as well. The higher tortuosity with lesser porosity indicates the longer pathways for solvent/solute to come into the gel network. As a result, at higher temperature (in Approach IIB during ExtLS state), more CFXH solute entered into gel and trapped in due to the presence of larger mesh size of the network.

Apart from osmotic effect on CFXH loading event, the diffusion mechanism also have great impact on the gel network for solute loading. To understand the diffusion effect into the gel network, the diffusion rate constant (K_D), diffusion co-efficient (D_s) and front velocity of the solvent (u) are assessed by Eqs. (6.34), (6.35) and (6.36) respectively and are listed in Table ANX II.2 in ANNEXURE II. The Classical Freundlich Model through Origin Pro 8 was used to calculate the values of k_D and "n" from the experimental data. From Table ANX II.2, irrespective of the CFXH solution concentration, the diffusion rate constant and the diffusion co-efficient are directly proportional to the applied temperature stimuli to entrap the CFXH solute via FSA based Approach II A and Approach II B. Also, as the tortuosity increased with the increase of temperature stimuli in Approach IIB during extended CFXH loading, thus the diffusional front velocity (u) is also increased, which advances the diffusion rate constant (k_D) as well and thus diffusivity (diffusion co-efficient) speeds up during CFXH loading into ExtLS gel in Approach II B. The effect of tortuosity on the diffusion rate constant and diffusivity harmonize with *Shen et al.* [19]. Therefore, the CFXH solute penetrates more into polymer samples through wider tortuous path at higher temperature stimuli (in Approach IIB). Hence, the diffusional absorption of CFXH solvent/solute activities are performed during CFXH entrapment into the polymer network. The anomalous diffusion took place in case of temperature assisted CFXH loading at 25 °C in Approach I and CFXH loading in ES state at 10 °C in Approach IIA, whereas, pseudo-Fickian diffusion happened in ExtLS at 25 °C in Approach IIB. All the generated adj. R-square values are found greater than 0.9 during calculating the K_D values, all the fitted curve shown their best suitability with the experimental data.

Therefore, in conclusion, the osmotic pressure driven diffusional phenomenon happened inside the gel network during CFXH entrapment in both Approach I and Approach II stimuli approaches.

6.7.2 Analysis on Drug Release Kinetics: Effect of Gel Parameters, Osmotic Pressure and Diffusion

In the CFXH dispensing procedure discussed in Section 6.3 and experimental release events as discussed in Section 6.4, the applied stimuli for release events of dispensing combination can be categorized as:

Pattern I: Temperature assisted release event at 10 °C.

Pattern II: Acidic buffer medium (pH 4) assisted release.

Pattern III: Dual stimuli (pH 4 buffer medium with 10 °C as external temperature) assisted release.

Patter IV: Visible light stimulated release.

To analyze the release kinetics, the rate constantsK_0, K_1, K_h and $K_{D\,Rel}$ are assessed by using Eq. (6.40)-(6.42) respectively, through non-linear curve fitting algorithm by Origin 8. The obtained Adj.-R-square values from the fitted curve for each rate constants are noted and listed in Table ANX II.3 in ANNEXURE II. It was observed that the values of Adj.-R-square for zero order and Korsmeyer-Peppas rate constants, K_0 and $K_{D\,Rel}$ are higher and near to unity as compared to 1^{st} order and Higuchi release rate constants, K_1 and K_h in all combination of release patterns. Thus, it confirmed that, the CFXH solute release followed 0^{th} order and Korsmeyer-Peppas release mechanisms. Further, due to maintaining the 0^{th} order release kinetics, all the gel samples are suitable for controlled drug release applications, which imply that the rate of drug release is constant through the release period. The constant and uniform slop at each release instant (Fig. 6.4, 6.7, 6.9, 6.11(a)-(d), 6.14(a)-(b), 6.17(a)-(b), 6.20(a)-(b) and 6.22(a)-(b)) were encouraged the controlled release manner of the gel at each pattern. In addition, the release exponent, "n" acquired from the fitted curve, found in the range of 0.78±0.03 to 1.29±0.03 depending on the stimuli applied during release pattern, which indicates the anomalous diffusion based CFXH solute release is performed. The calculated values of all the release rate constants K_0, K_1, K_h and $K_{D\,Rel}$ with their corresponding Adj.-R-square values, the release exponent, n and the type of transport phenomenon for each release pattern event are given in the Table ANX II.3.

The developed equivalent osmotic pressure $\left(\Pi_{Rel_{eq}}\right)$ inside the gel during CFXH release is quantified from the experimental release data by using Eq. (6.30B). The equivalent osmotic pressure combining of three osmotic parameters such as mixing osmotic pressure$\left(\Pi_{Rel_{mix}}\right)$, osmotic pressure due to chain elasticity $\left(\Pi_{Rel_{el}}\right)$ and ionic contributed osmotic pressure $\left(\Pi_{Rel_{ion}}\right)$ are determined from the Eqs. (6.37), (6.38) and (6.39) respectively. The parameters used in Eq. (6.30B), polymer volume fraction (ϕ), polymer-solvent interaction parameter (χ), molecular weight between two cross links (M_C), Mn are determined as described

in Section 5.6 in Chapter 5 from the CFXH release experimental data. The $\Pi_{Rel\,mix}$, $\Pi_{Rel\,el}$, $\Pi_{Rel\,eq}$ and ϕ are given in Table II.4.

For the temperature assisted Pattern I release event, the double crosslinked gel (DC-GG-Paam$_{GA4.39}$) network formed higher crosslink density (CLD) with lower mesh size (ζ) and molecular weight between two cross links (M_C) than graft gel (GG-g-Paam) for both the CFXH solutions, which creates gel network more dense and tighten and thus porosity increases. Hence, the longer tortuous path is formed and thus the loaded CFXH solute has the higher scope to come out from the network under low temperature stimuli. Moreover, the higher mixing osmotic pressure ($\Pi_{Rel\,mix}$) developed inside DC-GG-Paam$_{GA4.39}$ than GG-g-Paam for both CFXH solutions indicate the drug solvent/solute came out from the gel network and thus more release performed. The negative values of the elastic osmotic pressure ($\Pi_{Rel\,el}$) specify that the outward flow of CFXH solvent/solute from the gel network to the environment. Furthermore, the positive equivalent (total) osmotic pressure ($\Pi_{Rel\,eq}$) is produced inside the graft gel network, whereas, the DC-GG-Paam$_{GA4.39}$ built a negative $\Pi_{Rel\,eq}$, this proofs that the elastic osmotic pressure ($\Pi_{Rel\,el}$) dominated in double cross linked gel for CFXH solute release. Thus larger amount of CFXH solute release performed by GA cross linked gel (DC-GG-Paam$_{GA4.39}$) under identical stimuli in Pattern I release. There is no effect of ionic osmotic pressure on total osmotic pressure due to absence of ionic contribution from external medium.

Further, from Table ANX II.5, for 0.7 (v/v)% CFXH solution, the diffusivity and the front velocity increased in both the guar gum modified graft and double cross linked gels during release event in Pattern I release than 0.3 (v/v)% CFXH solution. The higher diffusivity and the higher front velocity within an identical release duration of 12 h enhances the higher release rate ($K_{D\,Rel}$) and thus have the higher capability to release more quantity of CFXH solute per 100 cc of the dry gel.

In case of Pattern II and III release, the ionic concentration of the release medium affects on the polymer volume fraction and thus the mixing osmotic pressures inside the gel network got affected. Due to the lower volume fraction in DC-GG-Paam$_{GA4.39}$ than graft, the mixing osmotic pressure ($\Pi_{Rel\,mix}$) developed inside the DC-GG-Paam$_{GA4.39}$ is

less than that inside the graft gel, whereas, higher elastic osmotic pressure ($\Pi_{Rel\ el}$) grown inside DC-GG-Paam$_{GA4.39}$ than graft gel. Thus, the ionic contribution from medium stimuli plays a great role on the effective chain elasticity to develop higher $\Pi_{Rel\ el}$ than graft sample. Therefore, the GA containing double cross linked gel (DC-GG-Paam$_{GA4.39}$) freed higher percentage of CFXH solute by retaining lower percentage of loaded CFXH solute per 100 cc of dry gel than graft sample.

The anomalous diffusion based transport happened in medium stimulated Pattern II and duo stimuli based Pattern III release events. The diffusivity and the front velocity also played a linear relationship (see Table ANX II.5) with the applied stimuli and the solute concentration into the experimental drug solutions for both gel samples.

Therefore, the osmotic pressure driven anomalous diffusion mechanism performed the shrinkage of CFXH loaded polymer network to release CFXH solute under applied stimuli in all Pattern I, II and II release events.

6.8 Confirmation on CFXH release

The released solvent from the polymer were confirmed by UV-Visible spectrum, whether the released solvent contained ciprofloxacin or not. The chemical activity of the released drug can be investigated by detecting the UV spectra of 0.3 (v/v)% CFXH at wavelength of 270 nm for and 272 nm for 0.7 (v/v)% CFXH as exhibited in Fig. 6.24(a)-(b). The respective spectra appear to be virtually identical proposing that there was no significant change in chemical and bioactivity of the drug during its loading and prolong release.

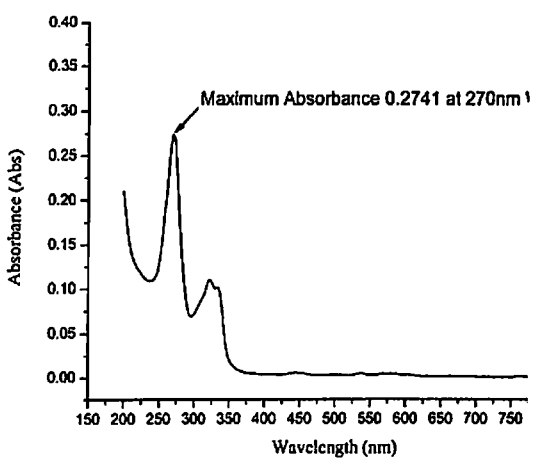

Fig: 6.24 (a): UV-Spectra of 0.3% CFX release

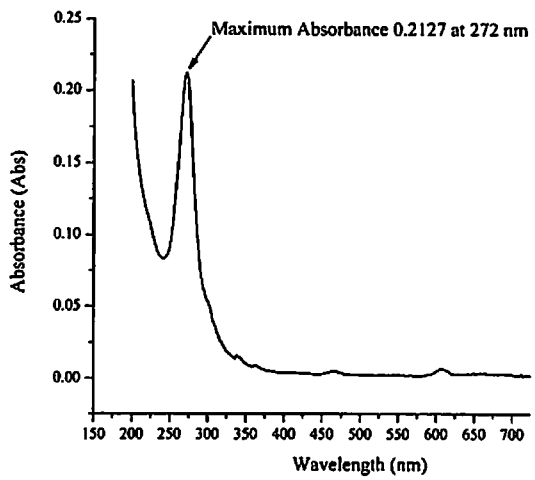

Fig: 6.24 (b): UV-Spectra of 0.7% CFX release

CFXH, has antibacterial property against both gram negative and gram positive bacteria. The inhibitory effects of released solvent or CFXH on the bacterial growth were estimated by means of turbidity measurement. 2 x 12 well plates were used for both gram- negative bacteria *E. coli* K12 as well as gram-positive bacteria *Bacillus* growth experiments. For *E. coli* K12 growth, 100 ml Nutrients Broth (NB) was prepared by dissolving 13 $mg.ml^{-1}$ NB in 100 ml Milli-Q water. The Broth was autoclaved at 120 °C for 1hr. In each well 3 ml NB was obtained where the released CFXH was added with the varying concentration of 200 µl to 2000 µl. In the plate, triplicate wells were used for NB, controlled cell culture and drug aided cell culture. In Fig. 6.25, I1, I2, I3 indicates the iteration 1, iteration 2, iteration 3 respectively. After that 30 µl *E. coli* K12 cell culture was added into each well from the 10 ml of revived E. coli culture with the optical density (OD) of ~1. Controlled wells were contained no CFXH. The plates were subjected to incubation at 37 °C 12 h. to allow the bacteria to grow. Optical density (OD) readings were taken after growth experiments using UV-Vis spectrophotometer at a wavelength of 600 nm. All readings were taken in clear, polystyrene 96-shallow-well, flat-bottom plates. Prior to the reading of each plate, the microplate reader was "blanked" with a plate containing 1 $ml.well^{-1}$ of NB media. After that controlled grown cell culture and polymer aided cultures with 1 $ml.well^{-1}$ were subjected for taking OD readings. The same experimental procedure was followed for effect of released CFXH on *Bacillus Subtilis*. The optical density (OD) of revived growth of *Bacillus* was 0.4. The pH of media was maintained at 7.0. The bacterial inhibition percentage was determined by Eq. (6.46).

$$\% \text{ bacterial inhibition} = \frac{I_C - I_S}{I_C} \times 100\ \% \qquad (6.46)$$

where I_C is the absorbance value of the control bacterial suspension and I_S is the absorbance value of the bacterial suspension containing different samples each time. the calculated percentage of bacterial inhibition with the corresponding CFXH dose are given in below Table 6.4. The growth of *E. coli* and *Bacillus* were measured by turbidity at 600 nm. The bacteriological media has high absorbance in UV light (400 nm) but very low absorbance in visible light (600 nm).

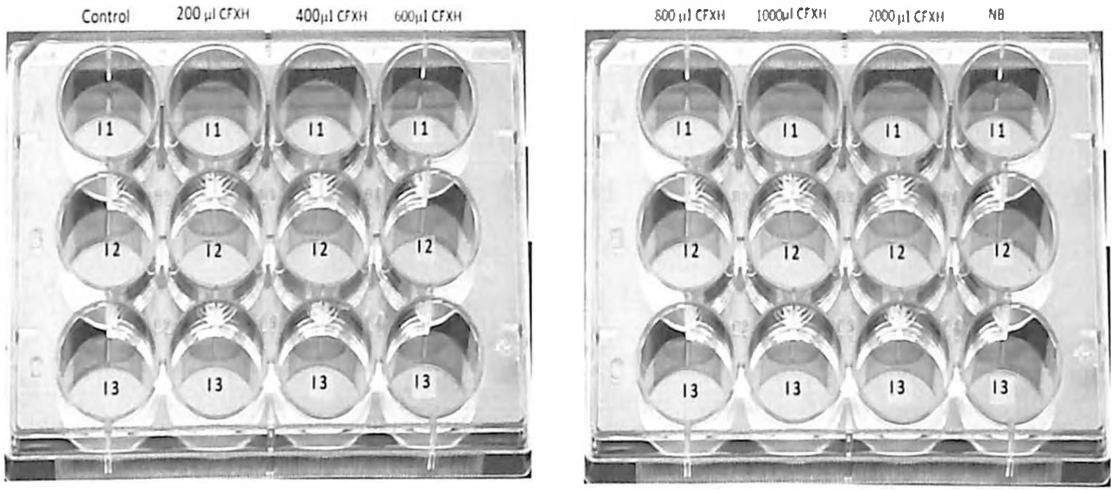

Fig. 6.25: 12 Well cell culture plate

The growth of bacteria or measuring the turbidity of growth media at 600nm is preferable because at this wavelength, the cells will not be killed as they would under too much UV light. The turbidity readings with the polymer addition were then carried out after 12 h. incubation. When the drug was not added into growth media, that media was termed as control and the OD 0.987± 0.015 was noted for *E. coli* and OD 0.397±0.003 was for *Bacillus Subtilis*. But when the drug with increasing concentrations of 200 µl to 2000 µl were mixed with the referential broth, the growth rate was affected, causing an apparent linear reduction on the maximum light scattering or OD.

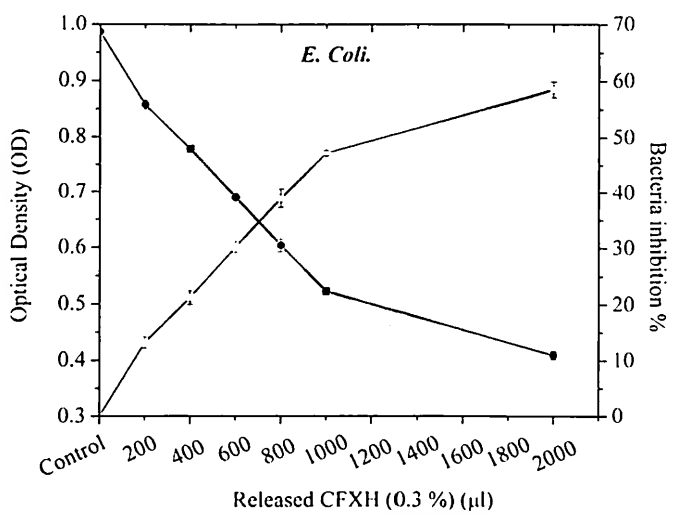

Fig. 6.26 (a): Effect of 0.3 (v/v)% CFXH on *E. coli* proliferation

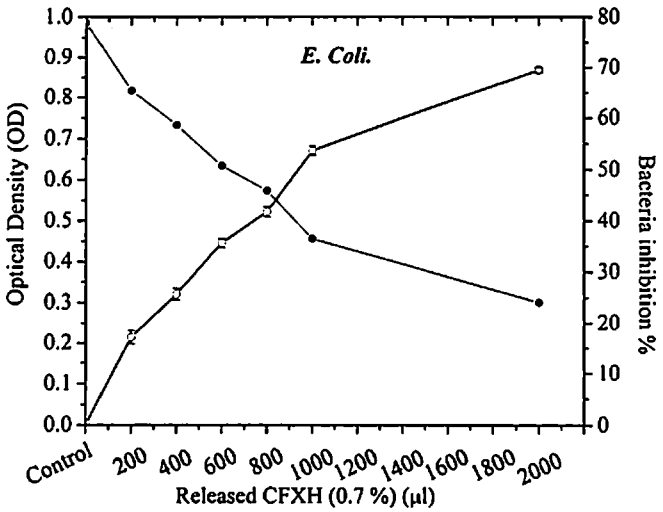

Fig. 6.26 (b): Effect of 0.7 (v/v)% CFXH on *E. coli* proliferation

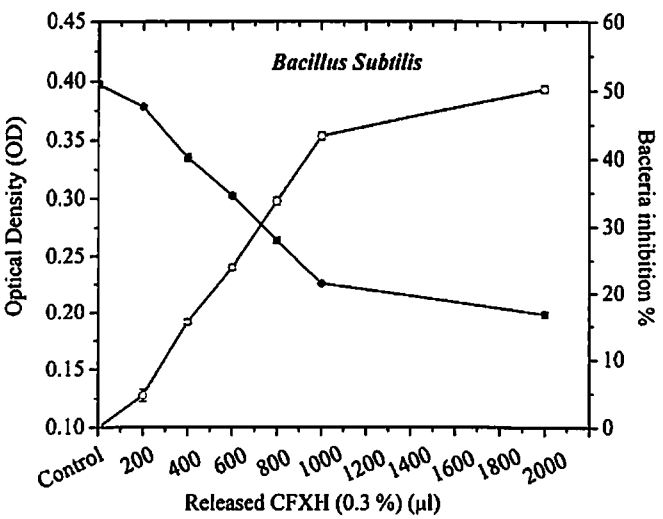

Fig. 6.26 (c): Effect of 0.3% CFXH on *Bacillus* proliferation

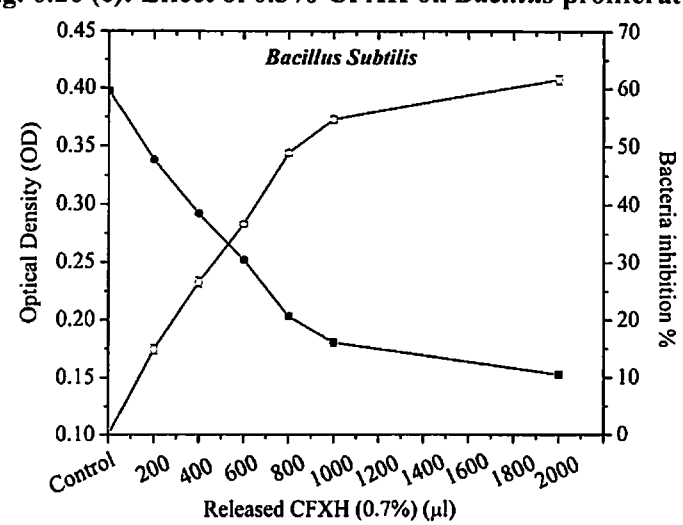

Fig. 6.26 (d): Effect of 0.7 (v/v)% CFXH on *Bacillus* proliferation

In Fig 6.26(a), the *E. Coli* proliferation has been hindered after applying the 0.3 (v/v)% CFXH from 200 µl (OD-0.857±0.009) to 2000 µl (OD-0.409±0.008) where in the bacteria population decreased from 13.099±1.4% (200 µl) to 58.500±1.4% (2000 µl). The OD was recorded less when 0.7 (v/v)% drug was applied due to hindrance of *E. Coli* (Fig. 6.26(b)) population and less scattering than in case of 0.3 (v/v)% CFXH. For 200 µl 0.7 (v/v)% CFXH OD was 0.817±0.001 and it was decreased at 2000 µl with OD-0.301±0.001. The 0.7 (v/v)% drug had more antibacterial property than 0.3 (v/v)% for which the viable bacteria was inhibited from 17.182±1.36% (200 µl) to 69.487±0.575% (2000 µl). The primary mechanism of action of CFXH involves inhibition of the intracellular enzymes DNA gyrase or topoisomerase II and topoisomerase IV [2]. To start the antibacterial effect, antibiotics compounds enter bacterial cells to inhibition of the enzymes topoisomerase II (DNA gyrase) and topoisomerase IV, which are required for bacterial DNA replication, transcription, repair, strand and recombination[1]. This process was executed very fast for *E.coli* than bacillus for that reason bacillus got scope to protect their topoisomerase II (DNA gyrase) and topoisomerase IV to be inhibited from CFXH leading to less cell inhibition than *Ecoli*. The bacterial inhabitation by Ciprofloxacine is given Table 6.4.

Table 6.4: Antibacterial effect on *E. Coli.* and *Bacillus Subtilis*

CFXH dose (µl)	Optical density (OD)	Bacteria inhibition %
Bacteria: *E.Coli.* CFXH solution: 0.3 (v/v)%		
200	0.857±0.009	13.10±1.04
400	0.778±0.006	21.14±1.18
600	0.690±0.001	30.06±1.02
800	0.603±0.012	38.84±1.65
1000	0.522±0.006	47.06±0.44
1200	0.409±0.008	58.50±1.39
Bacteria: *E.Coli.* CFXH solution: 0.7 (v/v)%		
200	0.817±0.001	17.18±1.36
400	0.733±0.001	25.70±1.13
600	0.635±0.002	35.67±0.93
800	0.574±0.001	41.81±0.98
1000	0.457±0.002	53.71±0.91

[1] https://www.drugbank.ca/drugs/DB00537

CFXH dose (µl)	Optical density (OD)	Bacteria inhibition %
1200	0.301±0.001	69.49±0.57
Bacteria: *Bacillus Subtilis* CFXH solution: 0.3 (v/v)%		
200	0.378±0.001	4.78±0.88
400	0.335±0.004	15.69±0.38
600	0.302±0.002	23.99±0.44
800	0.263±0.003	33.81±0.61
1000	0.225±0.001	43.37±0.55
1200	0.198±0.003	50.25±0.55
Bacteria: *Bacillus Subtilis* CFXH solution: 0.7 (v/v)%		
200	0.338±0.001	14.85±0.81
400	0.292±0.002	26.51±0.86
600	0.252±0.002	36.58±0.42
800	0.203±0.003	48.83±0.47
1000	0.180±0.003	54.62±0.58
1200	0.153±0.003	61.57±0.82

The anti-bacterial effect of CFXH was followed the same trend in the case of *Bacillus Subtilis* (Fig. 6.26(c)-(d)). In case of 0.3% CFXH *Bacillus* population hindered from 4.778±0.875% (200 µl) to 50.252±0.549% (2000 µl) whereas in case of 0.7 (v/v)% CFXH viable *Bacillus* decreased from 14.845±0.813 to 61.574± 0.816%.

The result of antibacterial action of CFXH was positively reflected even after prolonged released time. It is concluded that the synthesized polymer is a successful antibiotic dispenser.

6.9 Conclusion

The Ciprofloxacin loading-releasing activities are demonstrated in this chapter with different stimuli combinations, such as temperature assisted loading and releasing (Combination I), temperature assisted loading and medium pH aided release (Combination II), temperature assisted loading and dual stimuli assisted release (Combination III) and visible light (532 nm, 500 mW) assisted loading and releasing (Combination IV).

Both UVPTT and non-UVPTT gels are exhibited proficient responsiveness in temperature stimulated loading in both Combination I and II. The extended loading of

CFXH into equilibrium loaded gel network via Combination II, showed the ability to load the CFXH further into equilibrium loaded gel. These substantiate the suitability of on-demand CFXH loading into both UVPTT and non-UVPTT gels.

In reported researches, drugs were encapsulated within the polymeric formulations during synthesis[20]-[34] etc. which were limited for on-demand drug loading with controllable dose. But in present research both UVPTT and non-UVPTT gels were loaded with drugs for on-demand and dose controlling purpose.

At a glance, in reported researches it has been seen that 21.3% of Insulin was loaded in HPMC hybrid nanogel [23], 25.9–28.5% of US597 was loaded into PLGA-PEG-PLGA carrier micelle [35], 81.6% Methotrexate (MTX) was loaded into poly-L-lactide (PLLA) microspheres [36], 75% to 98% Indomethacin was encapsulated into poly-caprolactone (PCL) porous microsphere [37], N-trimethyl chitosan chloride (TMC) based PEG encapsulated 70% insulin [38], 93% Alprozolam was encapsulated chitosan-poly vinyl alcohol (PVA) hydrogel matrix for transdermal drug delivery [39], 63.27% Piroxicam was entrapped in β-CD modified lipid transfersome [40].

If we look back the encapsulation of antibiotic, the PEG-g-PHCs encapsulated 30(w/w)% CFXH [41], Levofloxacin (LV) were loaded into microparticles [27], 64.77±0.37% to 77.38±0.29% Norfloxacin was loaded into copolymer of chitosan with sodium tripolyphosphate [42], Silicon hydrogel contact lens encapsulated 66.64±15.53 to 79.42±15.32 $\mu g.mg^{-1}$ [43], 34.5% Curcumin was loaded in to Konjacglucoman based polymer [44]. Where as in current research the UVPTT gel loaded 22.44±0.16–62.76±0.73 $(mg.cc^{-1})$% depending on CFXH volume concentration by temperature triggering. In case of guar modified non-UVPTT gels entrapped 16.52±0.1–153.08±4.36 $(mg.cc^{-1})$% CFXH depending on CFXH volume concentration by temperature triggering. On the other hand the UVPTT composites loaded 11.55±0.36 $(mg.cc^{-1})$% to 40.16±0.54 $(mg.cc^{-1})$% by visible laser irradiation while non-UVPTT composites loaded 28.03±0.52 $(mg.cc^{-1})$% to 94.72±1.28 $(mg.cc^{-1})$% upon visible laser irradiation.

In published researches, HPMC hybrid gels showed pH responsive release of insulin was 8% at pH 1.2 and 49% at pH 7 in incubate shaker at 37 °C but 30% to 75% temperature sensitive release at different temperatures of 27 °C, 32 °C, 37 °C and 42 °C at pH 7 [23]. 90% of US597 was released from PLGA-PEG-PLGA carrier micelle [35]. 38.0% of the Methotrexate (MTX) was released from PLLA matrix [36]. 35% cumulative release of the drug was observed from poly-caprolactone (PCL) microsphere [37]. 45% drug

release was observed from N-trimethyl chitosan chloride (TMC) based PEG [38]. 54% Alprozolam was release was released from chitosan-poly vinyl alcohol (PVA) hydrogel matrix [39]. In reported CFXH release phenomenon, 45% *in-vitro* and 80% *in-vivo* CFXH was released from PEG-g-PHCs [41]. 30–50% Levofloxacin (LV) was released from microparticles [27]. Copolymer of chitosan with sodium tripolyphosphate released 82.61%–95.74% Norfloxacin [42]. Photo-cleavable ciprofloxacin (PC–CIP) azide group containing hydrogel released 14.1±3.4% after 2 mints UV irradiation,9.4±0.08% after 3 mints UV irradiation and 23.4±5.2% after 5 mints UV irradiation. Curcumin was released 83.9% in pH5,55.9% at pH 7 from Konjacglucoman based polymer [44]. The more reported researches on CFXH release are listed in Table 6.5. In current research, 0.3(v/v)% CFXH solution, the 85.50±3.00 (wt/wt)% of CFXH release was performed by UVPTT IPN gel with respect to temperature stimuli, whereas, 65.01±0.56 (wt/wt)%, 75.89±2.58 (wt/wt)% of CFXH release were observed in medium pH and combination of medium pH and temperature assisted stimuli respectively. In contrast with the 0.7 (v/v)% CFXH solution, 86.65±3.04 (wt/wt)%, 69.16±1.00 (wt/wt)% and 81.37±1.90 (wt/wt)% of CFXH were freed from gel network in temperature, medium pH and combination of medium pH and temperature stimuli respectively. The CFXH deliver efficiency varied 3.25±0.69 ($mg.cc^{-1}$)% to 51.08±1.41 ($mg.cc^{-1}$)% (in terms of CFXH retention into the gel network) w.r.t the applied stimuli and the CFXH solute concentration. On the other hand, the UVPTT gels released 9.11±0.27 ($mg.cc^{-1}$)% to 27.40±0.55 ($mg.cc^{-1}$)% of CFXH under visible light irradiation, showing the CFXH deliver efficiency of 2.44±0.22 ($mg.cc^{-1}$)% to 12.76±0.44 ($mg.cc^{-1}$)% depending of CFXH solute concentration.

For guar modified non-UVPTT gels, the double cross linked GG-DC-$Paam_{GA4.39}$ gel exhibited more efficient release than graft gel. The GG-DC-$Paam_{GA4.39}$ gel released 33.80±0.94 (wt/wt)% to 96.80±0.30 (wt/wt)% depending on the applied stimuli (temperature, medium pH and combination of medium pH and temperature) and the CFXH solute concentration. Under such stimuli conditions, the GG-DC-$Paam_{GA4.39}$ gel showed release efficiency of 1.98±0.76 ($mg.cc^{-1}$)% to 40.39±1.34 ($mg.cc^{-1}$)% based on the applied release stimuli of temperature, medium pH and combination of medium pH and temperature. Whereas, the non-UVPTT composite showed higher efficiency of 1.93±0.02 ($mg.cc^{-1}$)% to 7.79±0.49 ($mg.cc^{-1}$)% by lesser retaining of CFXH inside the gel network. The negative hydrogels released the drugs by vis-NIR triggering [45].

Linsley *et al.* [45] released 80% encapsulated cargo for 4 days of NIR exposure. Viger *et al.* [46] released 70% encapsulated solvent from the PLGA polymer for 90min NIR exposure.

Table 6.5: Drug Encapsulation/Release on reported research

Material	Drug	Intake	Release	Release Stimuli	Release kinetic	Ref
Carbomer hydrogel	Ciprofloxacine	No data available	Upto 10% (approx) in DI water at 37 °C till 6 hrs Upto 70% (approx) in 0.9% NaCl at 37 °C till 6 hrs 60% released at 24 hrs in 0.9% NaCl at 37 °C	0.9% NaCl and DI water	Zero order kinetics	[47]
poly(2-hydroxyethyl methacrylate) (pHEMA)	Ciprofloxacine-HCl	No data available	0.30mg (approx) in 24 hrs 0.35 mg (approx) in 48 hrs 0.328+/-0.013 mg in 144 hrs	Water bath shaker at 100 rpm	Not reported	[48]
pHEMA + HA 35 kDa	Ciprofloxacine-HCl	No data available	0.30mg (approx) in 24 hrs 0.30-0.35 mg in 48 hrs 0.337+/-0.033 mg in 144 hrs	Water bath shaker at 100 rpm	Not reported	[48]
pHEMA + HA 132kDa	Ciprofloxacine-HCl	No data available	0.30-0.35 mg in 24 hrs 0.35-0.40 mg in 48 hrs 0.361+/-0.005 mg in 144 hrs	Water bath shaker at 100 rpm	Not reported	[48]
poly(2-hydroxyethylmethacrylate) tris(trimethylsiloxy)silylpropyl methacrylate (pHEMA TRIS)	Ciprofloxacine-HCl	No data available	0.07-0.08 mg in 24 hrs 0.09-0.10 mg in 24 hrs 0.099+/-0.012 mg in 144 hrs	Water bath shaker at 100 rpm	Not reported	[48]
pHEMA TRIS + HA 35 kDa	Ciprofloxacine-HCl	No data available	0.07-0.08 mg in 24 hrs 0.09-0.10 mg in 24 hrs 0.085+/-0.004 mg in 144 hrs	Water bath shaker at 100 rpm	Not reported	[48]
pHEMA TRIS + HA 132 kDa	Ciprofloxacine-HCl	No data available	0.07-0.08 mg in 24 hrs 0.09-0.10 mg in 24 hrs 0.133+/-0.022 mg in 144 hrs	Water bath shaker at 100 rpm	Not reported	[48]
N,N-dimethylacrylamide tris(trimethylsiloxy)silylpropyl methacrylate (DMAA TRIS)	Ciprofloxacine-HCl	No data available	0.05-0.06 mg in 24 hrs 0.05 mg (approx) in 48 hrs 0.048+/-0.003 mg in 144 hrs	Water bath shaker at 100 rpm	Not reported	[48]

Material	Drug	Intake	Release	Release Stimuli	Release kinetic	Ref
DMAA TRIS + HA 35 kDa	Ciprofloxacine-HCl	No data available	0.05-0.06 mg in 24 hrs 0.06 mg (approx) in 48 hrs 0.068+/-0.005 mg in 144 hrs	Water bath shaker at 100 rpm	Not reported	[48]
DMAA TRIS + HA 132 kDa	Ciprofloxacine-HCl	No data available	0.06-0.07 mg in 24 hrs 0.08-0.09 mg in 48 hrs 0.086+/-0.022 mg in 144 hrs	Water bath shaker at 100 rpm	Not reported	[48]
Non imprinted hydrogels containing ethylene glycol dimethacrylate (EDGMA), 2-hydroxyethyl methacrylate (HEMA) and methacrylic acid (MAA)	Ciprofloxacine	0.5-4.5 µg/mg dry gel depending on gel composition and CFX concentration	In 0.9% NaCl solution (depending on gel composition): Upto 100% within 10 hrs In tear medium (depending on gel composition): Upto 70% (approx) within 10 hrs 90% released at 24 hrs and 100% released at 48 hrs	0.9% NaCl solution and artificial tear at 37 °C	Fickian diffusion with Korsmeyer-Peppas release kinetics followed.	[49]
Ciprofloxacine(CFX) - imprinted hydrogel containing EGDMA, HEMA, CFX and MAA	Ciprofloxacine	Upto 8.0 µg/mg dry gel depending on gel composition and CFX concentration	In 0.9% NaCl solution (depending on gel composition): 70-75% release within 10 hrs 60-80% release found at 24 hrs and 48 hrs In tear medium (depending on gel composition): 60-70% release found at 24 hrs and 48 hrs	0.9% NaCl solution at 37 °C	Fickian diffusion with Korsmeyer-Peppas release kinetics followed.	[49]
Chitosan with sodium tripolyphosphate (TPP)	Norfloxacin (antibiotic)	64.77±0.37%-77.38±0.29% depending on gel formulation	32.34%-46.35% in 1st one hour (burst phase) 82.61%-95.74% in next 12 hrs (sustained release phase)	Vertical diffusion celss, with an arrangement of magnetic stirrer, temperature maintained at 37 °C	Higuchi kinetic model followed. Sustained release profile maintained.	[42]

Material	Drug	Intake	Release	Release Stimuli	Release kinetic	Ref
Silicon hydrogel contact lens	Ciprofloxacine HCl	66.64±15.53 to 79.42±15.32 μg/mg of dry polymer depending on gel formulation	In 24 hrs: 5.5mg/gm dry polymer In 48 hrs: 0.3mg/gm dry polymer In 72 hrs: 0.02-0.04 mg/gm of dry gel	Phosphate buffered saline medium	Not reported	[43]
Photo-cleavable ciprofloxacin (PC-CIP) azide group containing hydrogel	Ciprofloxacine	No data available	14.1±3.4% released after 2 mints UV irradiation 9.4±0.08% released after 3 mints UV irradiation 23.4±5.2% released after 5 mints UV irradiation	On-demand release by UV irradiation	Not reported	[50]
Thermoresponsive PniPAAm based poly(ε-caprolactone dimethacrylate) biohydrogel	Livofloxacine	No data available	In burst release period of 1st 9 hours: 7-12% After that, 15-28% Release improved upto 80-90% in GSH containing 0.1M, pH 7.4 medium	0.1M, pH 7.4 at above LCST (37 °C) Glutathione (GSH) with medium 0.1M, pH 7.4	Not reported	[51]
β-cyclodextrin based (β -CD-cl-(PNIPAm-co-PMAc)) pH and thermoresponsive biopolymer	Metronidazole and ofloxacine (in combination)	No data available	75-80% in pH7.4 at 25 °C 50-65% in pH7.4 at 37 °C	In drug dissolution apparatus with 60 rpm at 25 °C and 37 °C in pH1.2 and pH7.4 medium	Zero order and Korsmeyer-Peppas release kinetics followed. Anomalous non-Fickian diffusion followed.	[52]
PVA/poly(acrylamide-co-diallyldimethyl ammonium chloride) semi-IPN	Ciprofloxacine hydrochloride	No data available	70-90% , total release time 12 hrs	In drug dissolution apparatus with 100 rpm at 37 °C in pH7.4 medium	Non-Fickian diffusion	[53]

Material	Drug	Intake	Release	Release Stimuli	Release kinetic	Ref
Cellulose/TiO2/β-CD composite hydrogel	Curcumin	20.71%-24.22%	23 (w/w)%-33(w/w)% after 10 hrs	pH7.4 at 37 °C, centrifuged	Suitable for sustained release activities	[54]
Ultrasonic hydrogel containing acrylamide and acrylic acid as monomer and cross linking with methylene bis-acrylamide	Ciprofloxacine	No data available	Max released at 5 °C and minimum released at 45 °C Maximum released in pH 8 (intestine or colon) Minimum released in pH 2 (stomach)	Temp. (5 °C, 20 °C, 37 °C and 45 °C) pH (2,8 and 10)	Controlled delivery Temp. assisted release duration: 60 mints. pH medium assisted release duration: 90 mints	[55]
Fibrin hydrogel containing sodium alginate	Ciprofloxacine hydrochloride USP	No data available	Initial burst effect in 24 hrs with 60% cumulative release. Upto 90% (approx) cumulative release in 48 hrs. Upto 95% (approx) cumulative release in 168 hrs.	Incubation, Tri buffered saline solution (pH7.6), 37 °C	Not reported	[56]
carbopol-*cl*-poly (2-hydroxyethylmethacrylate) hydrogel	Moxifloxacine	No data available	Upto 9 mg/gm of gel in 24 hrs	Simulated wound fluid (pH8) at 37 °C	Non-Fickian diffusion Hixson-Crowell kinetics suited perfectly	[57]
PEG-g-PHCs	Ciprofloxacine	30(w/w)%	45% (approx) *in-vitro* and 80% *in-vivo*		Not reported	[41]
Na-algenate, Algenate lyase	DNase, Levofloxacine	67% DNase 40% levofloxacine	30-50%		Not reported	[27]
Carbopol-940, HPMC	Norfloxacine	98.30%-99.97%	70-90%	Temperature	Not reported	[58]

Material	Drug	Intake	Release	Release Stimuli	Release kinetic	Ref
Konjacglucoman	Curcumin	34.5%	83.9% in pH 5, 55.9% at pH 7.4	pH	Not reported	[44]
Chitosam grafted glycidyl methacrylate	Amoxicillin	In pH1.2: 98% In pH7.4: 76%	In pH1.2: 12.03mg drug/gm polymer In pH7.4: 6.48 mg drug/gm polymer	pH, shaker	Not reported	[59]
Guar gum grafted Pnipaam, Sodium alginate (NaAlg)	Isoniazid (INZ)	No data available	In pH7 at 25 ^{O}C: 60% In pH7 at 37 ^{O}C: 40%	pH (pH7) and temperature (25 ^{O}C, 37 ^{O}C), shaker	Not reported	[60]
Guar gum grafted Pnipaam	Sinomenine hydrochloride	No data available	< 40% at 40 ^{O}C in pH 6.8	Temperature (35 ^{O}C, 40 ^{O}C), shaker	Not reported	[61], [62]
Chitosan, Paam grafted guar gum,	Ciprofloxacine	No data available	pH7.4: 90%	pH (pH1.2, pH7.4), shaker	Not reported	[63]
Paam grafted guar gum	Triamcinolone	No data available	pH1.2: 12% pH7.4: 54%	pH (pH1.2, pH7.4), shaker	Not reported	[7]
Guaran grafted Paam,	VRP, NFD	No data available	60%-80% of NFD(by soaking) 40%-90% of NFD (during synthesis)	Not available, shaker	Not reported	[64]

In release events, the gels are responded in a controlled manner under both temperature and acidic buffer medium. However, no significant release response observed in neutral and alkaline mediums, due to elevated swelling nature present in higher pH. Furthermore, the release via medium pH stimuli (in Combination II) is suitable for gastro retentive applications. Thus, the pH stimuli can be a good gastro retentive antibiotic dispenser for prolonged (30-60 h. for GG-g-Paam and DC-GG-Paam$_{GA4.39}$) as well as short duration (7 h. for β-CD IPN gel). Due to dimensional constraints of β-CD modified IPN gel, offers lesser ability to drug solute loading and release, which diminishes the efficiency than guar gum modified gel.

Furthermore, the temperature assisted and visible light irradiated CFXH loading and releasing via Combination I and IV could be suitable in transdermal patch applications. The positive thermo responsivity of UVPTT and non-UVPTT gels, having potentiality of on-demand loading and releasing. Further, intensity of these stimuli can be controlled easily, which make the system more compliance to the patient. The nanocomposites can be applicable for light controlled transdermal delivery applications, which can be an alternative approach to solve the uncontrolled drug release of reported hydrogel based transdermal patch having no stimuli with continuous release. This could be advantageous over reported transdermal drug delivery patches [25], [39], [65].

Last but not least, the synthesized UVPTT and non-UVPTT gels and their composites in this research showed positive stimuli responsive efficient carrier for *in-vitro* noninvasive antibiotic release without involving any external mechanical shaker or dissociation unit over reported noninvasive drug vehicles [6]- [8], [32], [36], [37], [66]-[69].

The increasing percentage of inhibition for both *E. Coli.* and *Bacillus Subtilis* bacteria in release drug solvent medium confirmed the trace of ciprofloxacine in the released media.

References:

[1] R. Liang and M. Liu, 'Preparation of Poly (acrylic acid- co -acrylamide)/ Kaolin and Release Kinetics of Urea from It', *J. Appl. Polym. Sci.*, vol. 106, pp. 3007–3017, 2007.

[2] N. Mahfoudhi and S. Boufi, 'Poly (acrylic acid-co-acrylamide)/ cellulose nanofibrils nanocomposite hydrogels: effects of CNFs content on the hydrogel properties', *Cellulose*, vol. 23, no. 6, pp. 3691–3701, 2016.

[3] F. Becerra-bracamontes, J. C. Sa´nchez-Di´az, E. Michel-valdivia, P. Ortega-gudin, and A. Marti´nez-Ruvalcaba, 'Design of a Drug Delivery System Based on Poly (acrylamide- co -acrylic acid)/ Chitosan Nanostructured Hydrogels', *J. Appl. Polym. Sci.*, vol. 106, pp. 3939–3944, 2007.

[4] M. B. Povea, W. A. Monal, J. V. C. Rodríguez, A. M. Pat, N. B. Rivero, and C. P. Covas, 'Interpenetrated Chitosan-Poly (Acrylic Acid-Co-Acrylamide) Hydrogels. Synthesis, Characterization and Sustained Protein Release Studies', *Mater. Sci. Appl.*, vol. 2, no. 6, pp. 509–520, 2011.

[5] M. C. I. Amin, N. Ahmad, M. Pandey, and C. J. Xin, 'Stimuli-responsive bacterial cellulose-g-poly (acrylic acid-co-acrylamide) hydrogels for oral controlled release drug delivery', vol. 9045, no. 2003, pp. 1–10, 2013.

[6] G. Sen, S. Mishra, U. Jha, and S. Pal, 'Microwave initiated synthesis of polyacrylamide grafted guar gum (GG-g-PAM)— Characterizations and application as matrix for controlled release of 5-amino salicylic acid', *Int. J. Biol. Macromol.*, vol. 47, no. 2, pp. 164–170, 2010.

[7] M. Shahid, S. A. Bukhari, Y. Gul, H. Munir, F. Anjum, M. Zuber, T. Jamil, K. M. Zia, 'Graft polymerization of guar gum with acryl amide irradiated by microwaves for colonic drug delivery', *Int. J. Biol. Macromol.*, vol. 62, pp. 172–179, 2013.

[8] M. P. Gowrav, U. Hani, H. G. Shivakumar, R. A. M. Osmani, and A. Srivastava, 'Polyacrylamide grafted guar gum based glimepiride loaded pH sensitive pellets for colon specific drug delivery: Fabrication and characterization', *RSC Adv.*, vol. 5, no. 97, pp. 80005–80013, 2015.

[9] S. A. Breda, A. F. Jimenez-kairuz, R. H. Manzo, and M. E. Olivera, 'Solubility behavior and biopharmaceutical classification of novel high-solubility ciprofloxacin and norfloxacin pharmaceutical derivatives', *Int. J. Pharm.*, vol. 371, no. 1–2, pp. 106–113, 2009.

[10] C. Cordeiro, D. J. Wiseman, P. Lutwyche, M. Uh, J. C. Evans, B. B. Finlay, M. S. Webb, 'Antibacterial Efficacy of Gentamicin Encapsulated in pH-Sensitive Liposomes against an In Vivo Salmonella enterica Serovar Typhimurium Intracellular Infection Model', *Antimicrob. Agents Chemother.*, vol. 44, no. 3, pp. 533–539, 2000.

[11] A. Dalhoff, S. Schubert, and A. Vente, 'Pharmacodynamics of Finafloxacin, Ciprofloxacin, and Levofloxacin in Serum and Urine against TEM- and SHV-Type

Extended-Spectrum-' -Lactamase- Producing Enterobacteriaceae Isolates from Patients with Urinary Tract Infections', *Antimicrob. Agents Chemother.*, vol. 61, no. 5, pp. 1–10, 2017.

[12] S. Harder, U. Fuhr, D. Beermann, and A. H. Staib, 'Ciprofloxacin absorption in different regions of the human gastrointestinal tract . Investigations with the hf-capsule', *Br. J. Clin. Pharmacol.*, vol. 30, no. 1, pp. 35–39, 1990.

[13] T. L. Lemke, D. A. Williams, V. F. Roche, and S. W. Zito, *Foye's Principles of Medical Chemistry*, 7th ed. Lippincott Williams & Wilkins, a Wolters Kluwer business., 2013.

[14] L. Brannon-Peppas and N. A. Peppas, 'Equilibrium swelling behavior of pH-sensitive hydrogels', *Chem. Eng. Sci.*, vol. 46, no. 3, pp. 715–722, 1991.

[15] R. A. Orwoll and P. A. Arnold, 'Polymer – Solvent Interaction Parameter X', in *Physical Properties of Polymers Handbook*, J. E. Mark, Ed. AIP Press, 1996, pp. 177–196.

[16] R. W. Korsmeyer, S. R. Lustig, and A. Nikolaos, 'Solute and Penetrant Diffusion in Swellable Polymers . I . Mathematical Modeling', *J. Polym. Sci. Part B Polym. Phys.*, vol. 24, pp. 395–408, 1986.

[17] H. Scholt, 'Kinetics of Swelling of Polymers and Their Gels', *J. Pharm. Sci.*, vol. 81, no. 5, pp. 467–470, 1992.

[18] G. W. R. Davidson III and N. A. Peppas, 'Solute and penetrant diffusion in swellable polymers v. relaxation-controlled transport in p(hema-co-mma) copolymers', *J. Control. Release*, vol. 3, pp. 243–258, 1986.

[19] L. Shen and Z. Chen, 'Critical review of the impact of tortuosity on diffusion', *Chem. Eng. Sci.*, vol. 62, no. 14, pp. 3748–3755, 2007.

[20] T. Jiang, T. Wang, T. Li, S. Shen, B. He, and R. Mo, 'Cite This: ACS Nano 2018, 12, 9693−9701 www.acsnano.org Enhanced Transdermal Drug Delivery by Transfersome-Embedded Oligopeptide Hydrogel for Topical Chemotherapy of Melanoma', *ACS Nano*, vol. 12, no. 10, pp. 9693–9701, 2018.

[21] E. Chuang, K-J Lin, F-Y Su, F-L. Mi, B. Maiti, C-T. Chen, S-P. Wey, T-C. Yen, J-H. Juang, H-W. Sung, 'Noninvasive imaging oral absorption of insulin delivered by nanoparticles and its stimulated glucose utilization in controlling postprandial hyperglycemia during OGTT in diabetic rats', *J. Control. Release*, vol. 172, no. 2, pp. 513–522, 2013.

[22] L. Mei, F. He, R-Q. Zhou, C-D. Wu, R. Liang, R. Xie, X-J. Ju, W. Wang, L.-Y. Chu, 'Novel Intestinal-Targeted Ca-Alginate-Based Carrier for pH- Responsive Protection and Release of Lactic Acid Bacteria', *ACS Appl. Mater. Interfaces*, vol. 6, pp. 5962–5970, 2014.

[23] D. Zhao, X. Shi, T. Liu, X. Lu, G. Qiu, and K. J. Shea, 'Synthesis of surfactant-free hydroxypropyl methylcellulose nanogels for controlled release of insulin &',

Carbohydr. Polym., vol. 151, pp. 1006–1011, 2016.

[24] D. Lee, S. Cho, H. S. Park, and I. Kwon, 'Ocular Drug Delivery through pHEMA-Hydrogel Contact Lenses Co-Loaded with Lipophilic Vitamins', *Nat. Publ. Gr.*, vol. 6, no. July, pp. 1–8, 2016.

[25] G. Sarkar, J. T. Orasugh, N. R. Saha, I. Roy, A. Bhattacharyya, A. K. Chattopadhyay, D. Ranad, D. Chattopadhyay, 'Cellulose nanofibrils/chitosan based transdermal drug delivery vehicle for controlled release of ketorolac tromethamine Gunjan', *New J. Chem.*, vol. 41, no. 24, pp. 15312–15319, 2017.

[26] X. Zhou, Y. Zhao, S. Chen, S. Han, X. Xu, J. Guo, M. Liu, L. Che, X. Li, J. Zhang, 'Self-Assembly of pH-Responsive Microspheres for Intestinal Delivery of Diverse Lipophilic Therapeutics', 2016.

[27] G. A. Islan, M. E. Ruiz, J. F. Morales, M. L. Sbaraglini, A. V. Enrique, G. Burton, A. Talevi, L. E. Bruno-Blanchc, G. R. Castro, 'Hybrid inhalable microparticles for dual controlled release of levofloxacin and DNase : physicochemical characterization and in vivo targeted delivery to the lungs', *J. Mater. Chamistry B*, vol. 5, pp. 3132–3144, 2017.

[28] G. Kim, C. Piao, J. Oh, and M. Lee, 'Self-assembled polymeric micelles for combined delivery of anti-inflammatory gene and drug to the lungs by inhalation', *Nanoscale*, vol. 10, no. 4, pp. 8503–8514, 2018.

[29] C. Cheng, X. Zhang, J. Xiang, Y. Wang, C. Zheng, Z. Lu and C. Li, 'Development of novel self-assembled poly(3-acrylamidophenylboronic acid)/ poly(2-lactobionamidoethyl methacrylate) hybrid nanoparticles for improving nasal adsorption of insulin', *Soft Matter*, vol. 8, no. 3, pp. 765–773, 2012.

[30] P. C. Bhatt, P. Srivastava, P. Pandey, W. Khan, and B. P. Panda, 'Nose to brain delivery of astaxanthin-loaded solid lipid nanoparticles: fabrication, radio labeling, optimization and biological studies', *RSC Adv.*, vol. 6, no. 12, pp. 10001–10010, 2016.

[31] J. M. Knipe, L. E. Strong, and N. A. Peppas, 'Enzyme- and pH-Responsive Microencapsulated Nanogels for Oral Delivery of siRNA to Induce TNF - α Knockdown in the Intestine', 2016.

[32] J. Huarte, S. Espuelas, Y. Lai, B. He, J. Tang, and J. M. Irache, 'Oral delivery of camptothecin using cyclodextrin / poly (anhydride) nanoparticles', *Int. J. Pharm.*, vol. 506, pp. 116–128, 2016.

[33] R. Boppana, R. V Kulkarni, G. K. Mohan, S. Mutalik, and T. M. Aminabhavi, 'RSC Advances In vitro and in vivo assessment of novel pH- sensitive interpenetrating polymer networks of a graft copolymer for gastro-protective delivery of', *RSC Adv.*, vol. 6, pp. 64344–64356, 2016.

[34] A. J. Sami, M. Khalid, T. Jamil, S. Aftab, S. A. Mangat, A.R. Shakoori, S. Iqbal, 'Formulation of novel chitosan guargum based hydrogels for sustained drug release of

paracetamol', *Int. J. Biol. Macromol.*, vol. 108, pp. 324–332, 2018.

[35] X. Chen, J. Chen, B Li, X. Y, R. Zeng, Y. Liu, T. Li, R. J.Y. Ho, J. Shao, 'PLGA-PEG-PLGA triblock copolymeric micelles as oral drug delivery system : In vitro drug release and in vivo pharmacokinetics assessment', *J. Colloid Interface Sci.*, vol. 490, pp. 542–552, 2017.

[36] A. Chen, C. Zhao, S. Wang, Y. Liu, and D. Lin, 'Generation of porous poly-L-lactide microspheres by emulsion-combined precipitation with a compressed CO2 antisolvent process', *J. Mater. Chem. B*, vol. 1, pp. 2967–2975, 2013.

[37] Y. Gao, M. Chang, Z. Ahmad, and J. Li, 'Magnetic-responsive microparticles with customized porosity for drug delivery', *RSC Adv.*, vol. 6, no. 9, pp. 88157–88167, 2016.

[38] H. Nazar, P. Caliceti, B. Carpenter, A. I. El-Mallah, D. G. Fatouros, M. Roldo, S. M. van der Merwea and J. Tsibouklisa, 'A once-a-day dosage form for the delivery of insulin through the nasal route: in vitro assessment and in vivo evaluation', *Biomater. Sci.*, vol. 1, no. 3, pp. 306–314, 2013.

[39] P. Maji, A. Gandhi, S. Jana, and N. Maji, 'Preparation and Characterization of Maleic Anhydride Cross-Linked Chitosan-Polyvinyl Alcohol Hydrogel Matrix Transdermal Patch', *J. PharmaSciTech*, vol. 2, no. 2, pp. 62–67, 2013.

[40] H. Ferreira, A. Ribeiro, and R. Silva, 'Deformable Liposomes for the Transdermal Delivery of Piroxicam', *J. Pharm. Drug Deliv. Res.*, vol. 4, no. 4, pp. 1–6, 2015.

[41] J. Du, I. M. El-sherbiny, and H. D. Smyth, 'Swellable Ciprofloxacin-Loaded Nano-in-Micro Hydrogel Particles for Local Lung Drug Delivery', *AAPS PharmSciTech*, vol. 15, no. 6, pp. 1535–1544, 2014.

[42] P. Upadhayay, M. Kumar, and K. Pathak, 'Norfloxacin loaded pH triggered nanoparticulate in-situ gel for extraocular bacterial infections: Optimization, ocular irritancy and corneal toxicity', *Iran. J. Pharm. Res.*, vol. 15, no. 1, pp. 3–22, 2016.

[43] A. Hui, M. Willcox, and L. Jones, 'In vitro and in vivo evaluation of novel ciprofloxacin-releasing silicone hydrogel contact lenses', *Investig. Ophthalmol. Vis. Sci.*, vol. 55, no. 8, pp. 4896–4904, 2014.

[44] J. Luan, K. Wu, C. Li, J. Liu, X. Ni, M. Xiao, Y. Xu, Y. Kuang, F. Jiang 'pH-Sensitive drug delivery system based on hydrophobic modified konjac glucomannan', *Carbohydr. Polym.*, vol. 171, pp. 9–17, 2017.

[45] C. S. Linsley, V. Y. Quach, G. Agrawal, E. Hartnett, and B. M. Wu, 'Visible light and near infrared-responsive chromophores for drug delivery-on-demand applications', *Clin. Res. Hepatol. Gastroenterol.*, vol. 39, no. 1, pp. 9–19, 2015.

[46] M. L. Viger, W. Sheng, K. Dore, A. H. Alhasan, C. J. Carling, J. Lux, C. de G. Lux, M. Grossman, R. Malinow 'Near-infrared-induced heating of confined water in polymeric particles for efficient payload release', *ACS Nano*, vol. 8, no. 5, pp. 4815–4826, 2014.

[47] M. F. Sanchez, S. A. Breda, E. A. Soria, L. I. Tártara, R. H. Manzo, and M. E. Olivera, 'Ciprofloxacin-lidocaine-based hydrogel: development, characterization, and in vivo evaluation in a second-degree burn model', *Drug Deliv. Transl. Res.*, vol. 8, no. 5, pp. 1000–1013, 2018.

[48] D. Nguyen, A. Hui, A. Weeks, M. Heynen, E. Joyce, H. Sheardown, L. Jones 'Release of Ciprofloxacin-HCl and Dexamethasone Phosphate by Hyaluronic Acid Containing Silicone Polymers', *Materials (Basel).*, vol. 5, no. 12, pp. 684–698, 2012.

[49] S. Kioomars, S. Heidari, B. Malaekeh-Nikouei, M. Shayani Rad, B. Khameneh, and S. A. Mohajeri, 'Ciprofloxacin-imprinted hydrogels for drug sustained release in aqueous media', *Pharm. Dev. Technol.*, vol. 22, no. 1, pp. 122–129, 2017.

[50] Y. Shi, V. X. Truong, K. Kulkarni, Y. Qu, G. P. Simon, R. L. Boyd, P. Perlmutter, T. Lithgow and J. S. Forsythe 'Light-triggered release of ciprofloxacin from an in situ forming click hydrogel for antibacterial wound dressings', *J. Mater. Chem. B*, vol. 3, no. 45, pp. 8771–8774, 2015.

[51] J. Gan, X. X. Guan, J. Zheng, H. Guo, K. Wu, L. Liang and M. Lu 'Biodegradable, thermoresponsive PNIPAM-based hydrogel scaffolds for the sustained release of levofloxacin', *RSC Adv.*, vol. 6, no. 39, pp. 32967–32978, 2016.

[52] A. Roy, P. P. Maity, A. Bose, S. Dhara, and S. Pal, 'β-Cyclodextrin based pH and thermo-responsive biopolymeric hydrogel as a dual drug carrier', *Mater. Chem. Front.*, vol. 3, no. 3, pp. 385–393, 2019.

[53] S. S. Sana and V. K. N. Boya, 'Poly (vinyl alcohol)/poly (acrylamide-codiallyldimethyl ammonium chloride) semi-IPN hydrogels for ciprofloxacin hydrochloride drug delivery', *IET Nanobiotechnology*, vol. 11, no. 1, pp. 52–56, 2015.

[54] H. Zhang, J. Zhu, Y. Hu, A. Chen, L. Zhou, H. Gao, Y. Liu, and S. Liu ' Study on Photocatalytic Antibacterial and Sustained-Release Properties of Cellulose/TiO 2 / β - CD Composite Hydrogel ', *J. Nanomater.*, vol. 2019, pp. 1–12, 2019.

[55] R. Ebrahimi and M. Salavaty, 'Controlled drug delivery of ciprofloxacin from ultrasonic hydrogel', *E-Polymers*, vol. 18, no. 2, pp. 187–195, 2018.

[56] J. Chotitumnavee, T. Parakaw, R. Laovanitch, S. Chareerat, P. Salintorn , P. Chanya, T. Teeraporn, A. Natthaya, T. Natthawadee, N. Ruangsawasdi 'In vitro evaluation of local antibiotic delivery via fibrin hydrogel', J. Dent. Sci., vol. 14, no. 1, pp. 7–14, 2019.

[57] B. Singh, A. Sharma, A. Sharma, and A. Dhiman, 'Design of Antibiotic Drug Loaded Carbopol- Hydrogel for Wound Dressing Applications Abstract Materials used', *iMdePub Journals*, vol. 4, pp. 1–9, 2017.

[58] S. Patil, A. Kadam, S. Bandgar, and S. Patil, 'Formulation and evaluation of an in situ gel for ocular drug delivery of anticonjunctival drug', *Cellul. Chem. Technol.*, vol. 49, no. 1, pp. 35–40, 2015.

[59] D. Aycan and N. Alemdar, 'Development of pH-responsive chitosan-based hydrogel modified with bone ash for controlled release of amoxicillin', *Carbohydr. Polym.*, vol. 184, no. October 2017, pp. 401–407, 2018.

[60] P. B. Kajjari, L. S. Manjeshwar, and T. M. Aminabhavi, 'Novel pH- and Temperature-Responsive Blend Hydrogel Microspheres of Sodium Alginate and PNIPAAm- g -GG for Controlled Release of Isoniazid', *AAPS PharmSciTech*, vol. 13, no. 4, pp. 1147–1157, 2012.

[61] Y. Y. Lang, S. M. Li, W. S. Pan, and L. Y. Zheng, 'Thermo- and pH-sensitive drug delivery from hydrogels constructed using block copolymers of poly(N-isopropylacrylamide) and Guar gum', *J. Drug Deliv. Sci. Technol.*, vol. 16, no. 1, pp. 65–69, 2006.

[62] Y. Lang, T. Jiang, S. Li, and L. Zheng, 'Study on Physicochemical Properties of Thermosensitive Hydrogels Constructed Using Graft-Copolymers of Poly (N - isopropylacrylamide) and Guar Gum', *J. Appl. Polym. Sci.*, vol. 108, pp. 3473–3479, 2008.

[63] P. B. Kajjari, L. S. Manjeshwar, and T. M. Aminabhavi, 'Novel interpenetrating polymer network hydrogel microspheres of chitosan and poly(acrylamide)- grafted - guar gum for controlled release of ciprofloxacin', *Ind. Eng. Chem. Res.*, vol. 50, no. 23, pp. 13280–13287, 2011.

[64] K. S. Soppirnath and T. M. Aminabhavi, 'Water transport and drug release study from cross-linked polyacrylamide grafted guar gum hydrogel microspheres for the controlled release application q', vol. 53, pp. 87–98, 2002.

[65] Z. Gu and J. Wu, 'Poly(ester amide)-based hybrid hydrogels for efficient transdermal insulin delivery', *J. Mater. Chamistry B*, vol. 6, no. 42, pp. 6723–6730, 2018.

[66] M. Agüeros, L. Ruiz-Gatóna, C. Vauthier, K. Bouchemal, S. Espuelas, G. Ponchel, J.M. Irache 'Combined hydroxypropyl- ' -cyclodextrin and poly (anhydride) nanoparticles improve the oral permeability of paclitaxel', *Eur. J. Pharm. Sci.*, vol. 38, pp. 405–413, 2009.

[67] Z. Zhang, Z. He, R. Liang, Y. Ma, W. Huang, R. Jiang, S. Shi, H. Chen, X. Li 'Fabrication of a Micellar Supramolecular Hydrogel for Ocular Drug Delivery', *Biomacromolecules*, vol. 17, pp. 798–807, 2016.

[68] D. Zhao, X. Shi, T. Liu, X. Lu, G. Qiu, and K. J. Shea, 'Synthesis of surfactant-free hydroxypropyl methylcellulose nanogels for controlled release of insulin &', *Carbohydr. Polym.*, vol. 151, pp. 1006–1011, 2016.

[69] V. Pokharkar, V. Patil, and L. Mandpe, 'Engineering of polymer – surfactant nanoparticles of doxycycline hydrochloride for ocular drug delivery Engineering of polymer – surfactant nanoparticles of doxycycline hydrochloride for ocular drug delivery', *Drug Deliv.*, vol. 22, no. 4, pp. 955–968, 2015.

Chapter 7

Biocompatibility Analysis, Conclusion and Future Scope

Chapter 6 depicted the efficiency of both UVPTT and non-UVPTT hydrogels for stimuli triggered drug dispensing application. But it is important to check the presence of toxic agent inside the gel network, which can toxicate the encapsulated drug. So, this Chapter is dedicated to analyze the biocompatibility.

7.1 Introduction

The biocompatibility of polymer in drug delivery mechanism involves the study of effect of the polymer and its relation in biological environment. The material has to be nontoxic, non-allergic and non-carcinogenic. In drug delivery biocompatibility study is important especially of drug delivery vehicle so that the presence of toxic agent cannot transport to targeted area through drug. The evaluation of polymer's biocompatibility study can be progressed through *in-vitro* and *in-vivo* methods. *In-vivo* method is important for investigating the biocompatibility which involves the invasive way of animal testing where the material or released drug need to implant into animal body cavity. But in this method, the material perhaps does not create any tissue damage but can kill the animals by released drug or from some unforeseen problem such as intravascular coagulation, embolic events, chelation of ions vital to homeostasis, [1] etc. To avoid the cruelty, hazardous act on animals and large number of animals *in-vitro* findings are become the matter of interest. This method involves the mammalian cell based models to check the *cytotoxicity* of material [2]. In this testing, cell viability is observed in the presence of material or released drug.

The microorganisms can also play a severe role on polymeric drug dispenser. Contamination of drug dispensing polymeric vehicle by microorganism is a serious issue. The attack of bacteria into polymer can transport the impurities to the drug. As both of the polymers have prolonged utilization during drug loading-releasing, so antimicrobial property of polymers should have. The antimicrobial property of polymer offers the enhancing use of antibiotic material in place of antibiotic agent [3]. The drug can be safe from microbial contamination and the post administered infection can be

prevented by the antimicrobial polymer. The successful biocompatibility and antibacterial testing decides the polymer to be biomaterial.

7.2 Cytotoxicity Analysis

The cytotoxicity investigation procedure was followed on both UVPTT and non-UVPTT polymer. Cell viability was conducted on MCF-7 cells. MCF-7 is breast cancer cell was extracted in 1970 from a woman with cancerous breast and MCF is termed according to Michigan Cancer Foundation-7 [4]. Cytocompatibility assay was conducted using XTT dye. XTT Cell Viability Assay dye helps to determine live cell numbers using standard photometric microplate readers. The live cell numbers are used to assess the rate of cell proliferation and to screen cytotoxic agents. MCF-7 cells were cultured in Dulbecco's modified Eagle's medium (DMEM) supplemented with 1.2% glutamine 1% antimycotic solution at 37 °C in a humidified incubator (5% CO_2, 95% air). A stock solution of the 10 $mg.mL^{-1}$ of the polymer was prepared in DMEM. Meanwhile, L929 cells (2×10^3 $cells.well^{-1}$) were seeded in 96-well plates and incubated at 37 °C in a humidified incubator (5% CO_2, 95% air) for 24 h. for attachment. L929 cells type of connecting tissue which was extracted from mouse body and is a type of MCF-7 cell line. These MCF-7 cells were then treated individually with the different concentrations of the polymer. Untreated cells were used as a control. After 72 h. of treatment, viability was assayed by the XTT assay. Briefly, a 1 $mg.ml^{-1}$ solution of XTT reagent and 1.53 $mg.mL^{-1}$ solution of phenazine methylsulfate in water were prepared, and 5µL of phenazine methylsulfate was added to each mL of the XTT solution. 25 µL of the mixture was added to each well, the culture plate was incubated for 2 h. at 37 °C, and the absorbance of each well at 480 nm was then measured. Wells treated with media represented 100% viable cells, and wells containing no cells represented background signal.

Cytotoxicity of both UVPTT and non-UVPTT polymer was analyzed using XTT assay with MCF-7 cell line. Cells were treated for 72 h. and after that, viability of the cells were analyzed by XTT assay. From the cytotoxicity study, it was established that the polymer was highly biocompatible with very low direct cytotoxic activity. β-CD modified IPN offered 85.33% viable cell (Fig. 7.1). From Fig. 7.2, 79.84% cell viability was observed at very high dose of 1000 $\mu g.ml^{-1}$ for the DC-GG-$Paam_{GA4.39}$ where as GG-g-Paam showed; the viability of 72.84% (Fig.7.3) with 1000 $\mu g.ml^{-1}$ dose may be

due to presence of GA in DC-GG-Paam$_{GA4.39}$ which suppressed the acrylamide monomer effect. These data confirms that this polymer can be safely used for drug delivery application.

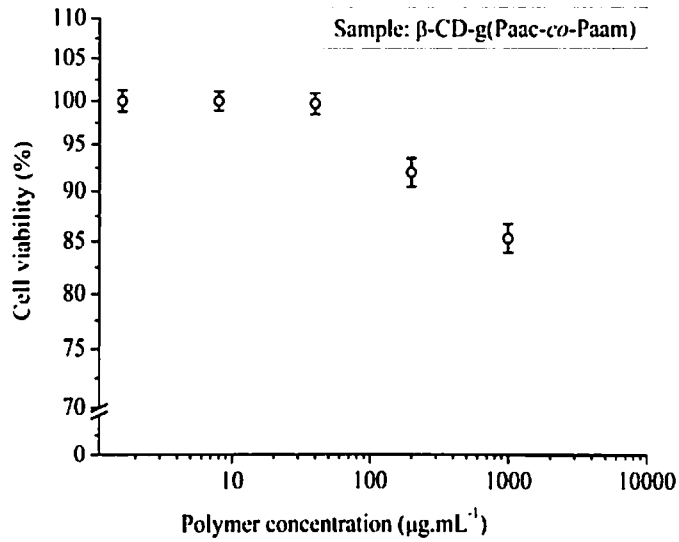

Fig.. 7.1: Cell viability of L929 cell with variable concentration of β-CD-g-(Paac-*co*-Paam)

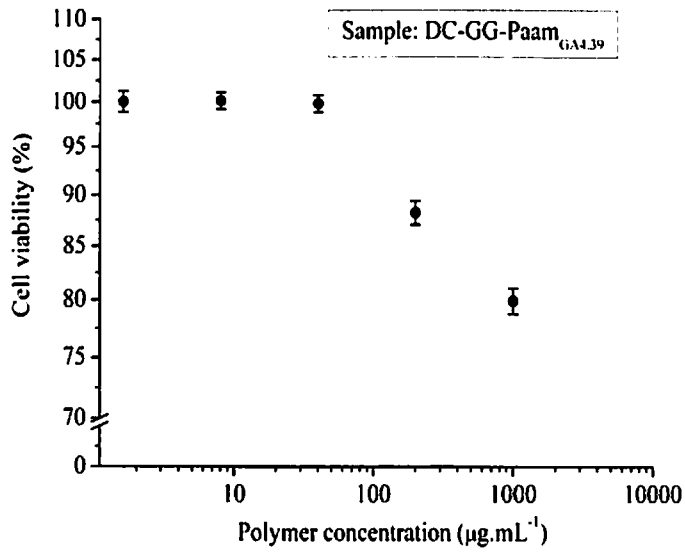

Fig. 7.2: Cell viability of L929 cell with variable concentration of DC-GG-Paam$_{GA4.39}$

The composite materials were proceeded for cytocompatibility and the process was followed same as bare polymers. The L929 mouse fibroblast cells were cultured in controlled condition without polymer composite and with the increasing concentration of polymer nanocomposite. The concentration of polymer was varied from 10 to 140 μg.mL^{-1}.

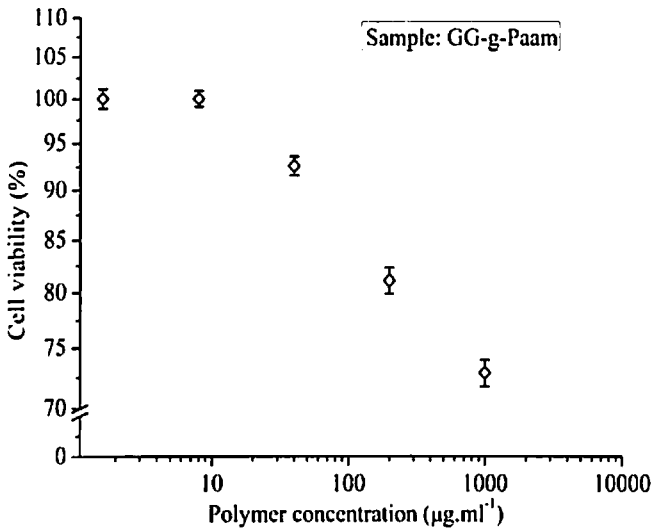

Fig. 7.3: Cell viability of L929 cell with variable concentration of GG-g-Paam

According to the reported researches [5]-[8] the AuNPs are toxic to many cell lines like AGS (human gastric adenocarcinoma cells), A549 (human lung adenocarcinoma epithelial), NIH3T3 (mouse embryonic fibroblast), PK-15 (porcine kidney), and Vero (African green monkey kidney) etc. at 24 h. Keeping these points in mind we have also performed the investigation on the cytotoxicity of both UVPTT and non-UVPTT composites for 24 h. For maintaining impartiality MCF-7 cell line was used for investigation. It was seen that in Fig. 7.4, 92.67±1.15% and 90.76±0.58% viable cells were observed in β-CD-g(Paac-*co*-Paam)-1 and β-CD-g(Paac-*co*-Paam)-3 respectively. Similarly 93.83±0.76%, 90.42±1.0.58% and 86.09±1.00% viable cells were observed for DC-GG-Paam$_{GA4.39}$-1, DC-GG-Paam$_{GA4.39}$-3 and DC-GG-Paam$_{GA4.39}$-5 respectively (Fig. 7.5). Reported researches showed that no cell toxicity found of spherical AuNP with 5 to 17 nm size to healthy cells like HaCa, as well as cancer cell like MCF7 [9]. But in the current research, the diameter of nanoparticles was in the range of 2 nm to 20 nm. For that reason very low concentrated polymer nanocomposite was used as dose and the composites were proven to be nontoxic. In the supporting of nontoxicity of developed polymer nanocomposite, the literature says that saccharide or saccharide modified polymer capped AuNPs [10], [11] are nontoxic. In current research as the nanoparticles were *in-situ* synthesized and reinforced so apparently the nanoparticles were capped by polymers and as a result polymer nanocomposites were nontoxic.

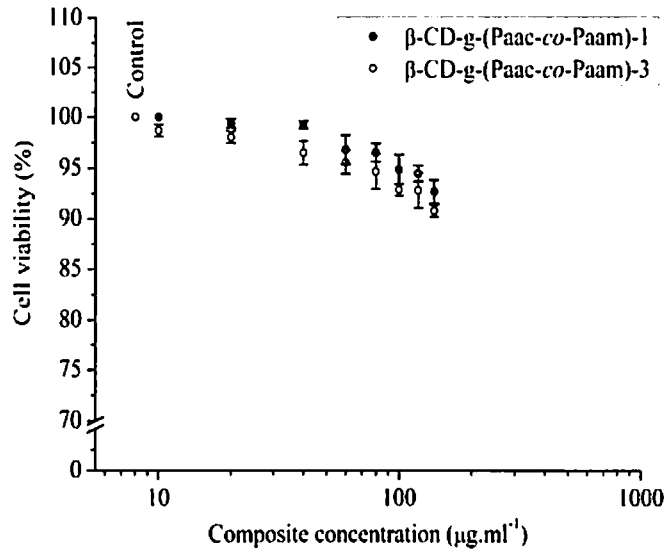

Fig. 7.4: Cell viability of L929 cell with variable concentration of β-CD-g-(Paac-*co*-Paam) nanocomposite

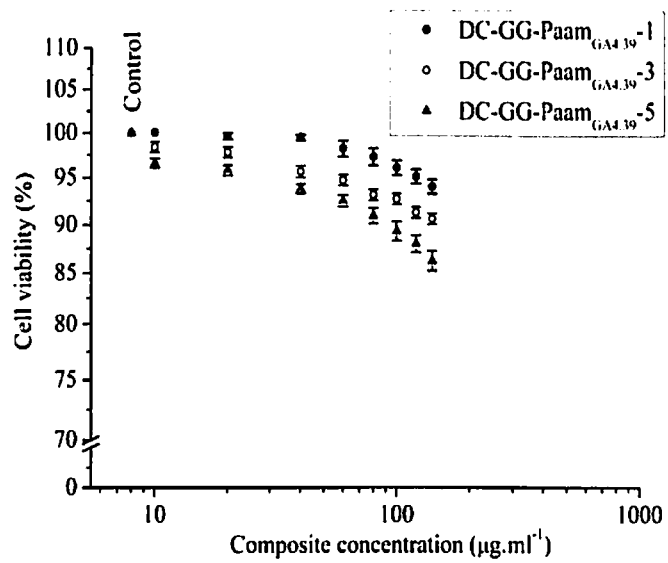

Fig. 7.5: Cell viability of L929 cell with variable concentration of GG-g-Paam composites

7.3 Antibacterial Analysis

The inhibitory effects of UVPTT and non-UVPTT polymer on the bacterial growth were estimated by means of turbidity measurement. 2 × 12 well plates were used for gram negative bacteria *E. coli* K12 growth and gram positive bacteria *Bacillus Subtilis* growth experiments. The detailed experimental procedure is discussed in Chapter 6, Section 6.8. 100 ml Nutrients Broth (NB) was prepared by dissolving 13 $mg.ml^{-1}$ NB in 100 ml Milli-Q water. The Broth was autoclaved at 120 °C for 1 h. In each well 3 ml NB was dropped where the polymer was added with the varying concentration of 200 $\mu g.ml^{-1}$ to

4000 $\mu g.ml^{-1}$. After that 30 µl *E. coli* K12 cell culture was added from the 10 ml of revived *E. coli* culture with the optical density (OD) of 1.0. Triplicate wells were used from the plate for NB, controlled cell culture and polymer aided cell culture. Controlled wells were contained no polymer. The same experimental procedure was followed for effect of released CFXH on *Bacillus Subtilis*. The optical density (OD) of revived growth of *Bacillus* was 0.4. The plates were subjected to incubation at 37 °C 12 h. to allow the bacteria to grow. Optical density (OD) readings were taken after growth experiments using UV-Vis spectrophotometer at a wavelength of 600 nm. All readings were taken in clear, polystyrene 96-shallow-well, flat-bottom plates. Prior to the reading of each plate, the microplate reader was "blanked" with a plate containing 1 $ml.well^{-1}$ of NB media. After that controlled grown cell culture and polymer aided cultures with 1 $ml.well^{-1}$ were subjected for taking OD readings. The pH of media was maintained at 7.0. The percentage of bacteria inhibition was determined by the following equation:

$$\% \text{ bacterial inhibition} = \frac{I_C - I_S}{I_C} \times 100\ \% \qquad (7.1)$$

Where, I_C is the absorbance value of the control bacterial suspension and I_S is the absorbance value of the bacterial suspension containing different samples each time.

The growth of *E. coli* and *Bacillus Subtilis* were measured by turbidity at 600 nm. The turbidity readings with the polymer addition were then carried out after 12 h incubation. When the polymeric medium was not added into growth media, that media was termed as control and the OD was noted as 1.0 and 0.4 for *E. coli* and *Bacillus Subtilis*. In the control growth there is a zero inhibition and 100% cell were present. But when the polymer with increasing concentrations was mixed with the referential broth, the growth rate was temporarily affected, causing a reduction on the maximum absorbance which indicates that the polymer act positively in reducing bacteria proliferation. The UVPTT polymer (β-CD-g-(Paac-*co*-Paam)) performed 88.00±5.02% and 60.00±4.67% cell inhibition on *E. Coli* and *Bacillus Subtilis* microbes respectively (Fig. 7.6). Whereas GG-g-Paam gel offered 72.00±4.67% and 50.00±4.76% cell inhibition on *E. Coli* and *Bacillus Subtilis* microbes

respectively (Fig. 7.7). DC-GG-Paam$_{GA4.39}$ reduced *E. Coli* and *Bacillus Subtilis* proliferation of 82.00±4.45% and 58.75±4.23% respectively (Fig. 7.8). The reducing percentage of viable bacterial cell is more in DC-GG-Paam$_{GA4.39}$ than GG-g-Paam due to presence of glutaraldehyde which has an antimicrobial effect [12]. The apparent linear tendency in increasing percentage of cell inhibition proven that the increasing amount of polymer had tendency to reduce bacterial population.

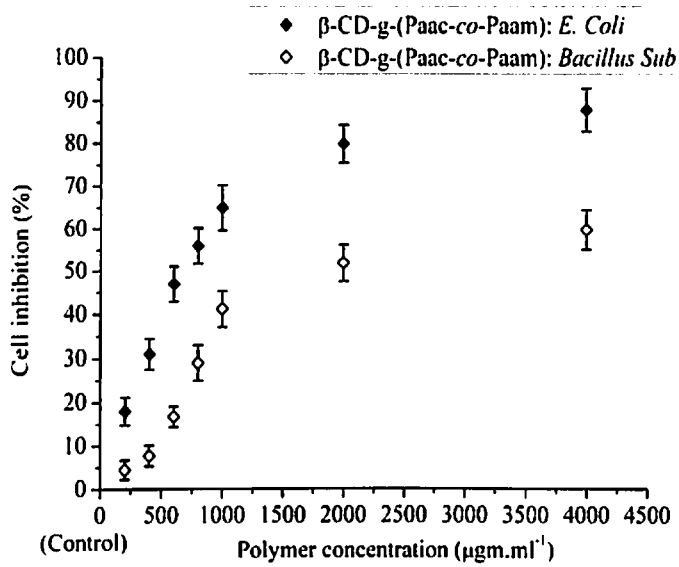

Fig. 7.6: Bacterial inhibition effect of β-CD-g-(Paac-*co*-Paam)

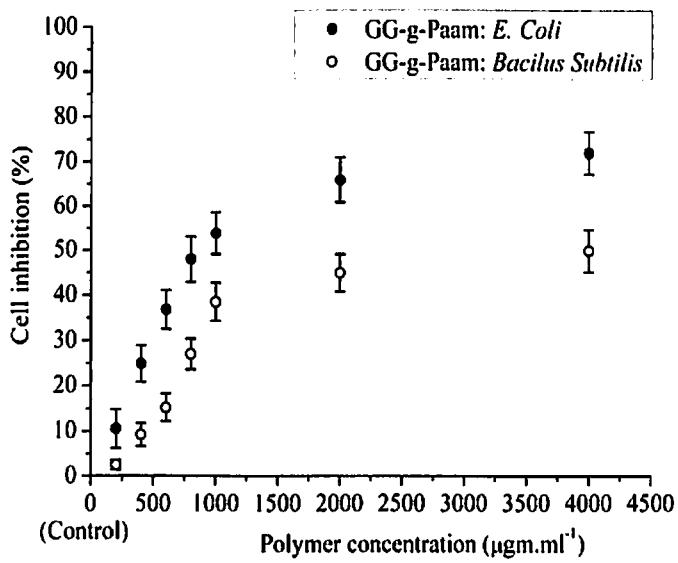

Fig. 7.7: Bacterial inhibition effect of GG-g-Paam

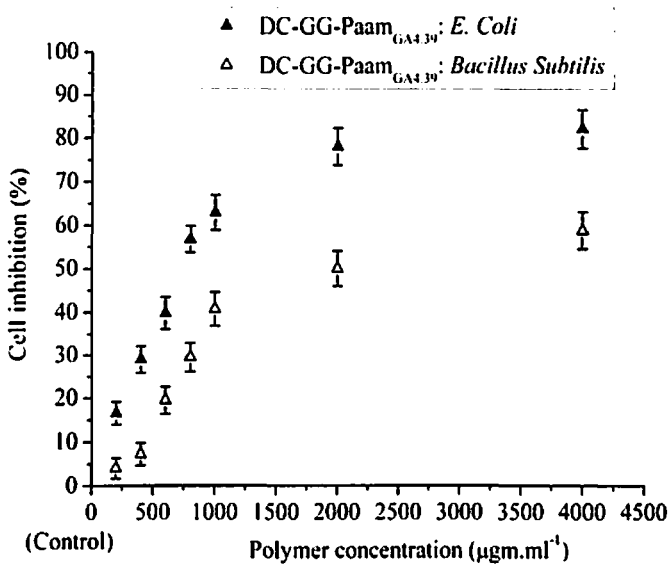

Fig. 7.8: Bacterial inhibition effect of DC-GG-Paam$_{GA4.39}$

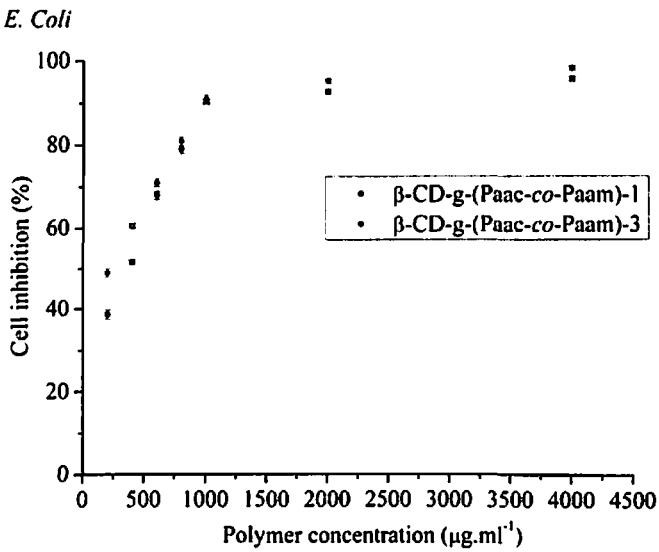

Fig. 7.9(a): Bacterial inhibition effect of β-CD IPN composites on *E. Coli*

The composites of both UVPTT and non-UVPTT gels were experimented for investigation of antimicrobial activity by maintaining same procedures and polymer concentrations (200 μg.ml^{-1} to 4000 μg.ml^{-1}). The β-CD-g-(Paac-*co*-Paam)-1 composite provided 95.67±0.58% *E. Coli* (Fig. 7.9(a)) and 90±0.75% *B. Subtilis* inhibition (Fig. 7.9(b)). Whereas the β-CD-g-(Paac-*co*-Paam)-3 provided 98.33±0.58% *E. Coli.* (Fig. 7.9(a)) and 92.50±0.44% *B. Subtilis* (Fig. 7.9(b)) inhibition. On the other hand non-UVPTT composites inhibited 95.67±0.58% to 100.00±0.61% *E. Coli* (Fig. 7.10(a)) and 95.00±0.81% to 100.00±0.31% *B. Subtilis* (Fig. 7.10(b)).

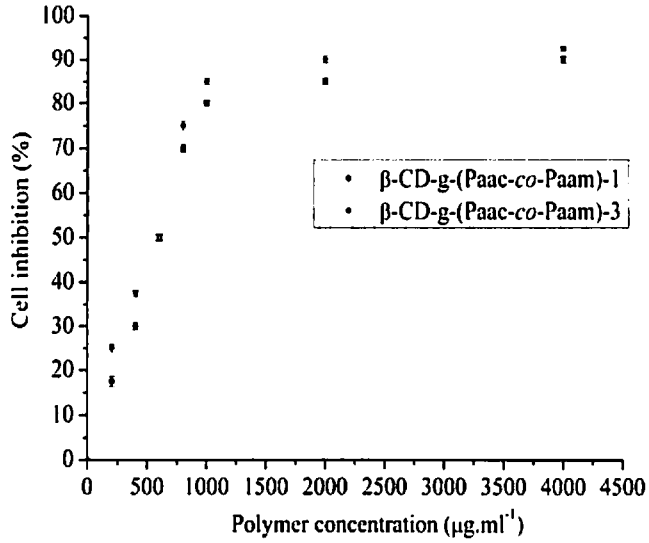

Fig. 7.9(b): Bacterial inhibition effect of β-CD IPN composites on *B. Subtilis*

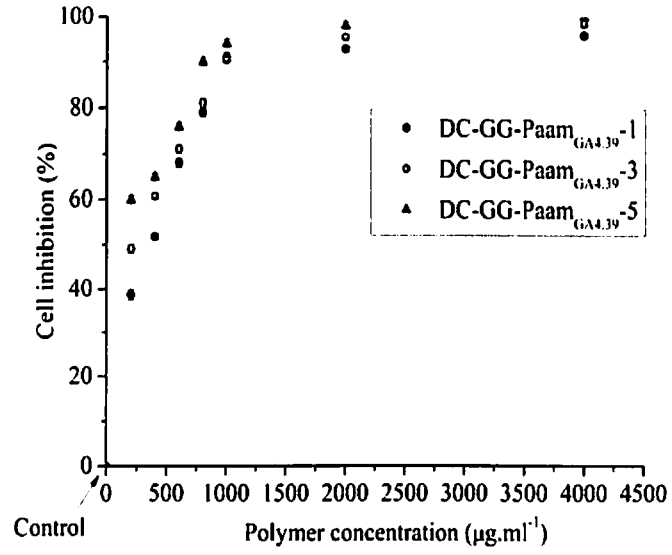

Fig. 7.10(a): Bacterial inhibition effect of non-UVPTT composites on *E. Coli*

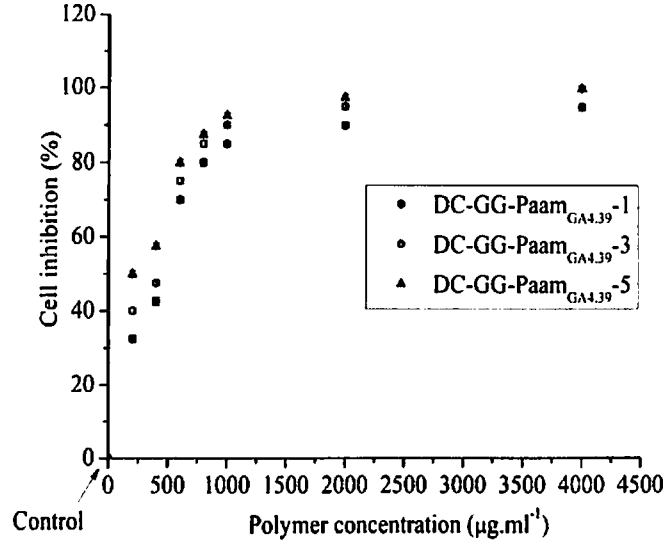

Fig. 7.10(b): Bacterial inhibition effect of non-UVPTT composites on *Bacillus. Subtilis*

Therefore, from cytotoxic and antimicrobial analysis it can be concluded that both of the polymers are a successful "Biopolymer".

7.4 Overall Conclusions

- This thesis demonstrated thermal assisted free radical bulk polymerization for synthesis of both β-CD modified hybrid UVPTT hydrogel and guar gum modified non- UVPTT hydrogel. The bulk reaction improved the yield of graft gel than reported work upto 101.59±8.46% for UVPTT based IPN and 107.48±1.53% for non-UVPTT hydrogel.
- The use of aqueous media in bulk polymerization has avoided the used of carcinogenic organic solvents and the possible presence of reactants related impurities were successfully removed by condensation refluxing method. The absences of such impurities have been confirmed in Chapter 4.
- The acid hydrolysis of both polymers has supported the acid stability, which can protect the polymer and encapsulated drug from the enzymatic degradation and first pass metabolism. The proof of acid stability is described in Chapter 4 and the acid stabled slow drug released demonstrated a successful oral administered drug release in Chapter 6.
- In order to avoid the antibiotic released above their thermal stability temperature by negative hydrogel. This research work has been successfully developed the positive thermoresponsive hydrogel where drug was loaded at 25 °C and released at 10 °C.
- Developed both the gels are multi stimuli responsive such as temperature, pH and light. The pulsatile stimuli approach has shown a good response on solvent/ solute release through reversible volume changing phenomena. FSA approach has been successfully demonstrated for the extended loading of the solvent which could be the possibility to titrate the dose of drug.
- Temperature assisted on-demand drug loading- releasing hopefully resolved the thermal assisted challenges of transdermal patch. Due to the positive thermosensitivity of gels, drug release event was possible when the low temperature is applied which is the solution for uncontrolled drug released for transdermal delivery. The stimuli responsive analysis is described in Chapter 5 and 6.
- The gold nanoparticle (AuNP) reinforced polymer nanocomposite has made the polymer visible light sensitive, hence the usage of chromophores and UV light can be

avoided in its application. Chapter 5 and Chapter 6 have been demonstrated the visible light triggered solute and/or drug loading and release.

- This research showed the higher percentage of drug release performance of UVPTT and non-UVPTT gels by applying external stimuli without application of any external mechanical shaker or paddle rotator with, which is beneficial over reported such paddle arranged drug release vehicles. The simultaneous application of pH and temperature has been released more solvent/ drug than solo stimuli without help of mechanical shaker.
- The light and thermosensitivity of both polymers can be used as non-invasive transdermal drug delivery whereas pH assisted drug release can be used as prolonged drug dispenser for oral administration.
- Cytotoxicity and antimicrobial analysis in Chapter 7 have confirmed that both the gels can be termed as "Biopolymer".

It is concluded that, the developed positive stimuli responsive biopolymer and their noninvasive bioactivity of release drug by performing *in-vitro* testing on bacteria and mouse breast cancer cell has been demonstrated successfully by fulfilling the challenges in the existing research.

7.5 Future Scope of Works

- Analysis of mechanical properties of polymer is important for polymer based drug release device. In application platform, how the polymer reacts to stimuli and how hard or soft it is, can be studied by its mechanical characterization. The stress-strain generation during polymer swelling-deswelling or its reversible volume gain can be possibly evaluated by mechanical study.
- The polymerization parameter and their variable concentration like monomer concentration, initiator concentration, reaction temperature; have major role play in the swelling- deswelling of synthesized product. In the UVPTT polymer, the extensive study in varying concentration of β-CD, Paac, Paam can be done to study the changes in stimuli triggered swelling- deswelling of polymer. If we see guar gum based polymer, further investigations are required by varying the concentration of guar gum, Paam, MBA.

- The pore size and density were uncontrollable during synthesis which can be overcome by using porogen during its synthesis. In emulsion polymerization, use of porogen is essential to create the porous nanoparticulate system. The porogen is a pore forming agent which provides the equal pore size and density as well as uniform distribution of pores which are important parameters for any porous material for their loading-releasing properties.
- Incorporation of porogen material makes the polymer fast responsive. It encourages extensive research to make the polymers fast responsive and enhance its stimuli triggered smartness.
- Uniform distribution of nanoparticle is another future research topic which needs to be explored in case of other stimuli sensitivity of polymer like photoconductivity.
- The stimuli triggered delivery of anticancer therapeutic agent can be investigated by both UVPTT and non-UVPTT polymers because the anticancer drugs are stable in high temperature region (~200 ^{o}C) and that drug can be delivered at the Tg of the both polymer.
- Mucoadhesive property of polymer is needed to study in future especially when the polymer is acts as gastroprotective drug dispenser, which will confirm the adhesive strength of polymer on the wall of GI track during prolonged drug release.
- Biodegradation is the important property of polymer for gastroretentive delivery so that it degrades inside the body to facilitate its own excretion from body. So the both synthesized polymers are need to be further studied for their chemical modification to be biodegradable.
- Last but not least, there are possibilities to do wide range of research on these gels for polymeric device micro-fabrication for non-invasive drug dispensers through transdermal patch. The gels can be used as drug reservoir and dispenser, triggered by temperature and light.

References:

[1] D. S. Kohane and R. Langer, 'Biocompatibility and drug delivery systems', *Chem. Sci.*, vol. 1, no. 4, pp. 441–446, 2010.

[2] S. O. Rogero, S. M. Malmonge, A. B. Lugão, T. I. Ikeda, L. Miyamaru, and Á. S. Cruz, 'Biocompatibility Study of Polymeric Biomaterials', *Artif. Organs*, vol. 27, no. 5, pp. 424–427, 2003.

[3] T. Chemistry and S. Review, 'The Chemistry and Applications of Antimicrobial Polymers: A State-of-the-Art Review', *Biomacromolecules*, vol. 8, no. 5, pp. 1359–1384, 2007.

[4] A. V Lee, S. Oesterreich, and N. E. Davidson, 'MCF-7 Cells — Changing the Course of Breast Cancer Research and Care for 45 Years', *JNCI J Natl Cancer Inst*, vol. 107, no. 7, pp. 1–4, 2015.

[5] S. M. Chuang *et al.*, 'Extensive evaluations of the cytotoxic effects of gold nanoparticles', *Biochim. Biophys. Acta - Gen. Subj.*, vol. 1830, no. 10, pp. 4960–4973, 2013.

[6] H. K. Kiranda, R. Mahmud, D. Abubakar, and Z. A. Zakaria, 'Fabrication, Characterization and Cytotoxicity of Spherical-Shaped Conjugated Gold-Cockle Shell Derived Calcium Carbonate Nanoparticles for Biomedical Applications', *Nanoscale Res. Lett.*, vol. 13, no. 1, pp. 1–10, 2018.

[7] Y. J. Lee, E. Y. Ahn, and Y. Park, 'Shape-dependent cytotoxicity and cellular uptake of gold nanoparticles synthesized using green tea extract', *Nanoscale Res. Lett.*, vol. 14, pp. 1–14, 2019.

[8] I. Fratoddi, I. Venditti, C. Cametti, and M. V. Russo, 'How toxic are gold nanoparticles? The state-of-the-art', *Nano Res.*, vol. 8, no. 6, pp. 1771–1799, 2015.

[9] S. Vijayakumar and S. Ganesan, 'Size-dependent in vitro cytotoxicity assay of gold nanoparticles', *Toxicol. Environ. Chem.*, vol. 95, no. 2, pp. 277–287, 2013.

[10] H. Kaur *et al.*, 'Study of in vitro toxicity of glucose capped gold nanoparticles in malignant and normal cell lines', *Adv. Mater. Lett.*, vol. 4, no. 12, pp. 888–894, 2013.

[11] M. Türk, U. Tamer, E. Alver, H. Çiftçi, A. U. Metin, and S. Karahan, 'Fabrication and characterization of gold-nanoparticles/chitosan film: A scaffold for L929-fibroblasts', *Artif. Cells, Nanomedicine Biotechnol.*, vol. 41, no. 6, pp. 395–401, 2013.

[12] S. . P. . GORMAN and E. M. . SCOTT, 'A Review Antimicrobial Activity. Uses and Mechanism of Action of Glutaraldehyde', *J. Appl. Bacteriol.*, vol. 48, pp. 161–190, 1980.

[13] A. Hui, M. Willcox, and L. Jones, 'In vitro and in vivo evaluation of novel ciprofloxacin-releasing silicone hydrogel contact lenses', *Investig. Ophthalmol. Vis. Sci.*, vol. 55, no. 8, pp. 4896–4904, 2014.

[14] Y. Shi *et al.*, 'Light-triggered release of ciprofloxacin from an in situ forming click hydrogel for antibacterial wound dressings', *J. Mater. Chem. B*, vol. 3, no. 45, pp. 8771–8774, 2015.

[15] P. Upadhayay, M. Kumar, and K. Pathak, 'Norfloxacin loaded pH triggered nanoparticulate in-situ gel for extraocular bacterial infections: Optimization, ocular irritancy and corneal toxicity', *Iran. J. Pharm. Res.*, vol. 15, no. 1, pp. 3–22, 2016.

[16] S. Kioomars, S. Heidari, B. Malaekeh-Nikouei, M. Shayani Rad, B. Khameneh, and S. A. Mohajeri, 'Ciprofloxacin-imprinted hydrogels for drug sustained release in aqueous media', *Pharm. Dev. Technol.*, vol. 22, no. 1, pp. 122–129, 2017.

[17] R. Ebrahimi and M. Salavaty, 'Controlled drug delivery of ciprofloxacin from ultrasonic hydrogel', *E-Polymers*, vol. 18, no. 2, pp. 187–195, 2018.

[18] B. Singh, A. Sharma, A. Sharma, and A. Dhiman, 'Design of Antibiotic Drug Loaded Carbopol- Hydrogel for Wound Dressing Applications Abstract Materials used', *iMdePub Journals*, vol. 4, pp. 1–9, 2017.

[19] H. Zhang *et al.*, ' Study on Photocatalytic Antibacterial and Sustained-Release Properties of Cellulose/TiO 2 / β -CD Composite Hydrogel ', *J. Nanomater.*, vol. 2019, pp. 1–12, 2019.

[20] R. S. Lee, C. H. Lin, I. A. Aljuffali, K. Y. Hu, and J. Y. Fang, 'Passive targeting of thermosensitive diblock copolymer micelles to the lungs: Synthesis and characterization of poly(N-isopropylacrylamide)-block-poly(ε-caprolactone)', *J. Nanobiotechnology*, vol. 13, no. 1, pp. 1–12, 2015.

[21] M. Gregoritza, V. Messmann, K. Abstiens, F. P. Brandl, and A. M. Goepferich, 'Controlled Antibody Release from Degradable Thermoresponsive Hydrogels Cross-Linked by Diels – Alder Chemistry', *Biomacromolecules*, vol. 18, pp. 2410–2418, 2017.

[22] E. Ahmad, Y. Feng, J. Qi, W. Fan, Y. Ma, and H. He, 'Evidence of nose-to-brain delivery of nanoemulsions : cargoes but not vehicles', *Nanoscale*, vol. 9, no. 3, pp. 1174–1183, 2017.

[23] Y. Wang, S. Jiang, H. Wang, and H. Bie, 'A mucoadhesive , thermoreversible in situ nasal gel of geniposide for neurodegenerative diseases', *PLoS One*, vol. 12, no. 12, pp. 1–17, 2017.

[24] M. K. Bain *et al.*, 'Effect of PVA on the gel temperature of MC and release kinetics of KT from MC based ophthalmic formulations', *Int. J. Biol. Macromol.*, vol. 50, no. 3, pp. 565–572, 2012.

[25] M. Bhowmik *et al.*, 'Effect of xanthan gum and guar gum on in situ gelling ophthalmic drug delivery system based on poloxamer-407', *Int. J. Biol. Macromol.*, vol. 62, pp. 117–123, 2013.

[26] S. Patil, A. Kadam, S. Bandgar, and S. Patil, 'Formulation and evaluation of an in situ gel for ocular drug delivery of anticonjunctival drug', *Cellul. Chem. Technol.*, vol. 49, no. 1, pp. 35–40, 2015.

[27] Z. Luo *et al.*, 'Thermosensitive PEG – PCL – PEG (PECE) hydrogel as an in situ gelling system for ocular drug delivery of diclofenac sodium', vol. 7544, 2016.

[28] Z. Zhang *et al.*, 'Fabrication of a Micellar Supramolecular Hydrogel for Ocular Drug Delivery', *Biomacromolecules*, vol. 17, pp. 798–807, 2016.

[29] S. Deepthi and J. Jose, 'Novel hydrogel-based ocular drug delivery system for the treatment of conjunctivitis', *Int. Opthalmology*, pp. 1–12, 2018.

[30] W. Wang *et al.*, 'Dual-functional transdermal drug delivery system with controllable drug loading based on thermosensitive poloxamer hydrogel for atopic dermatitis treatment', *Sci. Rep.*, vol. 6, pp. 1–10, 2016.

[31] S. B. Turturro *et al.*, 'The effects of cross-linked thermo-responsive PNIPAAm-based hydrogel injection on retinal function', *Biomaterials*, vol. 32, no. 14, pp. 3620–3626, 2011.

[32] F. Din *et al.*, 'Development of a novel solid lipid nanoparticles loaded dual-reverse thermosensitive nanomicelle release and reduced toxicity', *RSC Adv.*, vol. 5, pp. 43687–43694, 2015.

[33] C. Casadidio, M. Eugenia, A. Trampuz, M. Di, R. Censi, and P. Di, 'Daptomycin-loaded biodegradable thermosensitive hydrogels enhance drug stability and foster bactericidal activity against Staphylococcus aureus', *Eur. J. Pharm. Biopharm.*, vol. 130, pp. 260–271, 2018.

[34] H. Yeol *et al.*, 'Photo-crosslinked hyaluronic acid nanoparticles with improved stability for in vivo tumor-targeted drug delivery', *Biomaterials*, vol. 34, pp. 5273–5280, 2013.

[35] C. Chiang and C. Chu, 'Synthesis of photoresponsive hybrid alginate hydrogel with photo-controlled release behavior', vol. 119, pp. 18–25, 2015.

[36] P. Maji, A. Gandhi, S. Jana, and N. Maji, 'Preparation and Characterization of Maleic Anhydride Cross-Linked Chitosan-Polyvinyl Alcohol Hydrogel Matrix Transdermal Patch', *J. PharmaSciTech*, vol. 2, no. 2, pp. 62–67, 2013.

[37] G. Sarkar *et al.*, 'Cellulose nanofibrils/chitosan based transdermal drug delivery vehicle for controlled release of ketorolac tromethamine Gunjan', *New J. Chem.*, vol. 41, no. 24, pp. 15312–15319, 2017.

[38] Z. Gu and J. Wu, 'Poly(ester amide)-based hybrid hydrogels for efficient transdermal insulin delivery', *J. Mater. Chamistry B*, vol. 6, no. 42, pp. 6723–

6730, 2018.

[39] M. Agüeros *et al.*, 'Combined hydroxypropyl- ' -cyclodextrin and poly (anhydride) nanoparticles improve the oral permeability of paclitaxel', *Eur. J. Pharm. Sci.*, vol. 38, pp. 405–413, 2009.

[40] M. P. Gowrav, U. Hani, H. G. Shivakumar, R. A. M. Osmani, and A. Srivastava, 'Polyacrylamide grafted guar gum based glimepiride loaded pH sensitive pellets for colon specific drug delivery: Fabrication and characterization', *RSC Adv.*, vol. 5, no. 97, pp. 80005–80013, 2015.

[41] G. Sen, S. Mishra, U. Jha, and S. Pal, 'Microwave initiated synthesis of polyacrylamide grafted guar gum (GG-g-PAM)— Characterizations and application as matrix for controlled release of 5-amino salicylic acid', *Int. J. Biol. Macromol.*, vol. 47, no. 2, pp. 164–170, 2010.

[42] M. Shahid *et al.*, 'Graft polymerization of guar gum with acryl amide irradiated by microwaves for colonic drug delivery', *Int. J. Biol. Macromol.*, vol. 62, pp. 172–179, 2013.

[43] D. Zhao, X. Shi, T. Liu, X. Lu, G. Qiu, and K. J. Shea, 'Synthesis of surfactant-free hydroxypropyl methylcellulose nanogels for controlled release of insulin &', *Carbohydr. Polym.*, vol. 151, pp. 1006–1011, 2016.

[44] J. Huarte, S. Espuelas, Y. Lai, B. He, J. Tang, and J. M. Irache, 'Oral delivery of camptothecin using cyclodextrin / poly (anhydride) nanoparticles', *Int. J. Pharm.*, vol. 506, pp. 116–128, 2016.

[45] V. Pokharkar, V. Patil, and L. Mandpe, 'Engineering of polymer – surfactant nanoparticles of doxycycline hydrochloride for ocular drug delivery Engineering of polymer – surfactant nanoparticles of doxycycline hydrochloride for ocular drug delivery', *Drug Deliv.*, vol. 22, no. 4, pp. 955–968, 2015.

[46] A. Chen, C. Zhao, S. Wang, Y. Liu, and D. Lin, 'Generation of porous poly-L-lactide microspheres by emulsion-combined precipitation with a compressed CO2 antisolvent process', *J. Mater. Chem. B*, vol. 1, pp. 2967–2975, 2013.

[47] Y. Gao, M. Chang, Z. Ahmad, and J. Li, 'Magnetic-responsive microparticles with customized porosity for drug delivery', *RSC Adv.*, vol. 6, no. 9, pp. 88157–88167, 2016.

[48] A. Roy, P. P. Maity, A. Bose, S. Dhara, and S. Pal, 'β-Cyclodextrin based pH and thermo-responsive biopolymeric hydrogel as a dual drug carrier', *Mater. Chem. Front.*, vol. 3, no. 3, pp. 385–393, 2019.

[49] J. Gan *et al.*, 'Biodegradable, thermoresponsive PNIPAM-based hydrogel scaffolds for the sustained release of levofloxacin', *RSC Adv.*, vol. 6, no. 39, pp. 32967–32978, 2016.

[50] S. S. Sana and V. K. N. Boya, 'Poly (vinyl alcohol)/poly (acrylamide-

codiallyldimethyl ammonium chloride) semi-IPN hydrogels for ciprofloxacin hydrochloride drug delivery', *IET Nanobiotechnology*, vol. 11, no. 1, pp. 52–56, 2015.

[51] M. F. Sanchez, S. A. Breda, E. A. Soria, L. I. Tártara, R. H. Manzo, and M. E. Olivera, 'Ciprofloxacin-lidocaine-based hydrogel: development, characterization, and in vivo evaluation in a second-degree burn model', *Drug Deliv. Transl. Res.*, vol. 8, no. 5, pp. 1000–1013, 2018.

[52] D. Nguyen *et al.*, 'Release of Ciprofloxacin-HCl and Dexamethasone Phosphate by Hyaluronic Acid Containing Silicone Polymers', *Materials (Basel).*, vol. 5, no. 12, pp. 684–698, 2012.

[53] J. Chotitumnavee *et al.*, 'In vitro evaluation of local antibiotic delivery via fibrin hydrogel', *J. Dent. Sci.*, vol. 14, no. 1, pp. 7–14, 2019.

[54] J. Du, I. M. El-sherbiny, and H. D. Smyth, 'Swellable Ciprofloxacin-Loaded Nano-in-Micro Hydrogel Particles for Local Lung Drug Delivery', *AAPS PharmSciTech*, vol. 15, no. 6, pp. 1535–1544, 2014.

[55] G. A. Islan *et al.*, 'Hybrid inhalable microparticles for dual controlled release of levofloxacin and DNase : physicochemical characterization and in vivo targeted delivery to the lungs', *J. Mater. Chamistry B*, vol. 5, pp. 3132–3144, 2017.

[56] J. Luan *et al.*, 'pH-Sensitive drug delivery system based on hydrophobic modified konjac glucomannan', *Carbohydr. Polym.*, vol. 171, pp. 9–17, 2017.

[57] D. Aycan and N. Alemdar, 'Development of pH-responsive chitosan-based hydrogel modified with bone ash for controlled release of amoxicillin', *Carbohydr. Polym.*, vol. 184, no. October 2017, pp. 401–407, 2018.

[58] P. B. Kajjari, L. S. Manjeshwar, and T. M. Aminabhavi, 'Novel pH- and Temperature-Responsive Blend Hydrogel Microspheres of Sodium Alginate and PNIPAAm- g -GG for Controlled Release of Isoniazid', *AAPS PharmSciTech*, vol. 13, no. 4, pp. 1147–1157, 2012.

[59] Y. Y. Lang, S. M. Li, W. S. Pan, and L. Y. Zheng, 'Thermo- and pH-sensitive drug delivery from hydrogels constructed using block copolymers of poly(N-isopropylacrylamide) and Guar gum', *J. Drug Deliv. Sci. Technol.*, vol. 16, no. 1, pp. 65–69, 2006.

[60] Y. Lang, T. Jiang, S. Li, and L. Zheng, 'Study on Physicochemical Properties of Thermosensitive Hydrogels Constructed Using Graft-Copolymers of Poly (N - isopropylacrylamide) and Guar Gum', *J. Appl. Polym. Sci.*, vol. 108, pp. 3473–3479, 2008.

[61] P. B. Kajjari, L. S. Manjeshwar, and T. M. Aminabhavi, 'Novel interpenetrating polymer network hydrogel microspheres of chitosan and poly(acrylamide)-grafted -guar gum for controlled release of ciprofloxacin', *Ind. Eng. Chem. Res.*, vol. 50, no. 23, pp. 13280–13287, 2011.

[62] K. S. Soppirnath and T. M. Aminabhavi, 'Water transport and drug release study from cross-linked polyacrylamide grafted guar gum hydrogel microspheres for the controlled release application q', vol. 53, pp. 87–98, 2002.

Table ANX I.1: Combination I: Calculated values of energy parameters and mesh size on different stimuli switching combinations

Sample code	Stimuli	Total heat energy (Enthalpy), ΔH_{mix} ($\times 10^{-25}$) (J)	Solvent entropy, ΔS_{mix} ($\times 10^{-27}$) ($J.K^{-1}$)	Chain configurational entropy, $\Delta S_{mix\ Chain\ config}$ ($\times 10^{-3}$) ($J.K^{-1}$)	Mesh size, $\zeta(\times 10^{2})$ (Å)
Combination I: pH stimuli switch (Case I)					
β-CD-g-(Paac-*co*-Paam)	pH4	6.78	4.66	9.55	0.49
	pH7	7.01	4.68	6.70	3.89
	pH4	6.97	4.64	12.60	1.96
GG-g-Paam	pH4	27.96	18.93	1.32	2.41
	pH7	28.36	19.00	0.51	58.70
	pH4	28.34	18.98	0.54	55.72
DC-GG-$Paam_{GA0.80}$	pH4	27.88	18.90	1.77	1.87
	pH7	28.30	18.95	1.11	24.90
	pH4	28.29	18.94	1.26	21.91
DC-GG-$Paam_{GA1.60}$	pH4	27.82	18.88	2.16	1.58
	pH7	28.29	18.93	1.36	20.20
	pH4	28.10	18.76	5.46	4.45
DC-GG-$Paam_{GA2.20}$	pH4	27.56	18.80	4.27	0.89
	pH7	28.21	18.86	2.69	9.57
	pH4	28.18	18.83	3.35	7.55
DC-GG-$Paam_{GA4.39}$	pH4	26.61	18.47	18.28	0.26
	pH7	28.02	18.69	7.79	3.03
	pH4	27.82	18.48	17.72	2.09
DC-GG-$Paam_{GA6.59}$	pH4	26.31	18.36	24.83	0.20
	pH7	27.93	18.61	10.97	2.09
	pH4	27.68	18.40	22.71	0.95

Sample code	Stimuli	Total heat energy (Enthalpy), ΔH_{mix} ($\times 10^{-25}$) (J)	Solvent entropy, ΔS_{mix} ($\times 10^{-27}$) ($J.K^{-1}$)	Chain configurational entropy, $\Delta S_{mix\ Chain\ config}$ ($\times 10^{-3}$) ($J.K^{-1}$)	Mesh size, $\zeta(\times 10^{2})$ (Å)
Combination I: pH stimuli switch (Case II)					
β-CD-g-(Paac-*co*-Paam)	pH4	6.78	4.66	9.12	0.49
	pH9.2	7.01	4.68	6.06	4.34
	pH4	6.97	4.66	9.82	1.77
GG-g-Paam	pH4	27.96	18.93	1.32	2.41
	pH9.2	28.37	19.01	0.37	83.90
	pH4	28.34	18.98	0.65	45.20
DC-GG-Paam$_{GA0.80}$	pH4	27.88	18.90	1.77	1.87
	pH9.2	28.33	18.97	0.78	36.90
	pH4	28.31	18.96	0.97	29.00
DC-GG-Paam$_{GA1.60}$	pH4	27.82	18.88	2.16	1.58
	pH9.2	28.31	18.95	1.04	27.10
	pH4	28.18	18.83	3.28	7.75
DC-GG-Paam$_{GA2.20}$	pH4	27.56	18.80	4.27	0.89
	pH9.2	28.24	18.88	2.22	11.80
	pH4	28.18	18.83	3.35	7.55
DC-GG-Paam$_{GA4.39}$	pH4	26.61	18.47	18.28	0.26
	pH9.2	28.09	18.75	5.65	4.29
	pH4	27.95	18.63	10.26	2.25
DC-GG-Paam$_{GA6.59}$	pH4	26.31	18.36	24.83	0.20
	pH9.2	28.02	18.69	7.80	3.03
	pH4	27.81	18.50	16.37	1.35

Sample code	Stimuli	Total heat energy (Enthalpy), ΔH_{mix} ($\times 10^{-25}$) (J)	Solvent entropy, ΔS_{mix} ($\times 10^{-27}$) ($J.K^{-1}$)	Chain configurational entropy, $\Delta S_{mix\ Chain\ config}$ ($\times 10^{-3}$) ($J.K^{-1}$)	Mesh size, $\zeta(\times 10^{2})$ (Å)
Combination I: pH stimuli switch (Case III)					
β-CD-g-(Paac-*co*-Paam)	pH7	6.83	4.68	6.61	0.67
	pH9.2	7.03	4.69	5.38	4.94
	pH7	7.00	4.67	7.77	3.31
GG-g-Paam	pH7	27.98	18.94	1.21	2.60
	pH9.2	28.34	18.98	0.67	44.20
	pH7	28.33	18.97	0.75	38.60
DC-GG-Paam$_{GA0.80}$	pH7	27.93	18.92	1.49	2.16
	pH9.2	28.32	18.96	0.94	30.00
	pH7	28.31	18.95	1.01	27.70
DC-GG-Paam$_{GA1.60}$	pH7	27.89	18.91	1.71	1.92
	pH9.2	28.31	18.96	0.98	28.70
	pH7	28.29	18.94	1.24	22.30
DC-GG-Paam$_{GA2.20}$	pH7	27.60	18.81	3.89	0.97
	pH9.2	28.24	18.89	2.08	12.70
	pH7	28.21	18.85	2.79	9.21
DC-GG-Paam$_{GA4.39}$	pH7	27.61	18.81	3.76	0.99
	pH9.2	28.23	18.87	2.36	11.10
	pH7	28.18	18.83	3.36	7.56
DC-GG-Paam$_{GA6.59}$	pH7	26.87	18.56	13.38	0.34
	pH9.2	28.11	18.76	5.25	4.66
	pH7	27.99	18.66	8.75	2.67

Table ANX I.2: Combination II: Calculated values of energy parameters and mesh size on different stimuli switching combinations

Sample code	Stimuli	Total heat energy (Enthalpy), $\Delta H_{mix}(\times 10^{-25})$ (J)	Solvent entropy, ΔS_{mix} $(\times 10^{-27})$ $(J.K^{-1})$	Chain configurational entropy, $\Delta S_{mix\ Chain\ config}$ $(\times 10^{-3})$ $(J.K^{-1})$	Mesh size, ζ $(\times 10^{3})$ (Å)
Combination II: Temperature switch (FWA)					
β-CD-g-(Paac-*co*-Paam)	10°C	6.47	4.68	8.79	0.053
	40°C	7.38	4.70	1.97	1.48
	10°C	6.66	4.68	8.97	0.28
GG-g-Paam	10°C	26.48	18.93	2.24	0.16
	40°C	29.71	18.97	0.08	46.10
	10°C	26.92	18.95	1.50	1.83
DC-GG-Paam$_{GA0.80}$	10°C	26.42	18.91	2.66	0.13
	40°C	29.69	18.95	0.15	22.10
	10°C	26.88	18.93	2.27	1.15
DC-GG-Paam$_{GA1.60}$	10°C	26.37	18.89	3.11	0.12
	40°C	29.68	18.95	0.19	17.20
	10°C	26.86	18.91	2.69	0.96
DC-GG-Paam$_{GA2.20}$	10°C	26.26	18.85	4.07	0.09
	40°C	29.65	18.91	0.42	7.13
	10°C	26.84	18.89	3.13	0.81
DC-GG-Paam$_{GA4.39}$	10°C	25.97	18.75	7.42	0.05
	40°C	29.66	18.92	0.33	9.30
	10°C	26.71	18.76	6.84	0.35
DC-GG-Paam$_{GA6.59}$	10°C	25.14	18.44	22.66	0.02
	40°C	29.48	18.76	2.89	0.90
	10°C	26.62	18.68	10.25	0.23
Combination II: Temperature switch (REVA)					
β-CD-g-(Paac-*co*-Paam)	40°C	7.28	4.70	1.91	0.19
	10°C	6.09	4.24	219.60	0.009
	40°C	7.37	4.69	2.60	1.09

Sample code	Stimuli	Total heat energy (Enthalpy), $\Delta H_{mix}(\times 10^{-25})$ (J)	Solvent entropy, ΔS_{mix} $(\times 10^{-27})$ $(J.K^{-1})$	Chain configurational entropy, $\Delta S_{mix\ Chain\ config}$ $(\times 10^{-3})$ $(J.K^{-1})$	Mesh size, ζ $(\times 10^{3})$ (Å)
GG-g-Paam	40°C	29.57	28.95	0.15	1.52
	10°C	26.85	18.90	2.97	0.87
	40°C	29.65	18.92	0.41	7.59
DC-GG-$Paam_{GA0.80}$	40°C	29.48	18.92	0.35	0.72
	10°C	26.73	18.78	6.21	0.39
	40°C	29.63	18.89	0.63	4.65
DC-GG-$Paam_{GA1.60}$	40°C	29.42	18.90	0.52	0.52
	10°C	26.60	18.66	10.90	0.21
	40°C	29.62	18.88	0.72	4.02
DC-GG-$Paam_{GA2.20}$	40°C	29.29	18.86	0.98	0.31
	10°C	26.56	18.62	12.85	0.18
	40°C	29.57	18.85	1.24	2.22
DC-GG-$Paam_{GA4.39}$	40°C	29.02	18.77	2.54	0.14
	10°C	26.18	18.29	33.40	0.06
	40°C	29.49	18.77	2.56	1.02
DC-GG-$Paam_{GA6.59}$	40°C	28.42	18.58	8.48	0.05
	10°C	25.68	17.89	71.80	0.02
	40°C	29.18	18.51	11.67	0.20

Table ANX I.3: Combination III: Calculated values of energy parameters and mesh size on different stimuli switching combinations

Sample code	Stimuli	Total heat energy (Enthalpy), ΔH_{mix} ($\times 10^{-25}$) (J)	Solvent entropy, ΔS_{mix} ($\times 10^{-27}$) ($J.K^{-1}$)	Chain configurational entropy, $\Delta S_{mix\ Chain\ config}$ ($\times 10^{-4}$) ($J.K^{-1}$)	Mesh size, $\zeta(\times 10^{2})$ (Å)
Combination III: Dual stimuli switch (Case I)					
β-CD-g-(Paac-*co*-Paam)	ES at 40°C in pH7	7.25	4.69	25.61	1.51
	At 10°C in pH4	6.58	4.60	234.86	0.99
	At 10°C in pH9.2	6.59	4.61	229.31	1.02
GG-g-Paam	ES at 40°C in pH7	29.28	18.86	10.42	2.96
	At 10°C in pH4	26.54	18.61	133.79	1.69
	At 10°C in pH9.2	26.57	18.63	123.49	1.85
DC-GG-Paam$_{GA0.80}$	ES at 40°C in pH7	29.23	18.84	13.06	2.42
	At 10°C in pH4	26.46	18.54	171.13	1.28
	At 10°C in pH9.2	26.51	18.58	150.38	1.47
DC-GG-Paam$_{GA1.60}$	ES at 40°C in pH7	29.19	18.83	14.79	2.19
	At 10°C in pH4	26.44	18.52	183.74	1.19
	At 10°C in pH9.2	26.51	18.58	150.09	1.48
DC-GG-Paam$_{GA2.20}$	ES at 40°C in pH7	29.03	18.78	25.06	1.41
	At 10°C in pH4	26.24	18.35	295.59	0.71

Sample code	Stimuli	Total heat energy (Enthalpy), ΔH_{mix} ($\times 10^{-25}$) (J)	Solvent entropy, ΔS_{mix} ($\times 10^{-27}$) ($J.K^{-1}$)	Chain configurational entropy, $\Delta S_{mix\ Chain\ config}$ ($\times 10^{-4}$) ($J.K^{-1}$)	Mesh size, $\zeta(\times 10^{2})$ (Å)
	At 10°C in pH9.2	26.32	18.42	245.23	0.87
DC-GG-Paam$_{GA4.39}$	ES at 40°C in pH7	29.02	18.77	25.49	1.39
	At 10°C in pH4	26.30	18.39	262.03	0.81
	At 10°C in pH9.2	26.33	18.42	243.13	0.88
DC-GG-Paam$_{GA6.59}$	ES at 40°C in pH7	28.42	18.58	85.13	0.51
	At 10°C in pH4	25.75	17.95	661.70	0.30
	At 10°C in pH9.2	25.79	17.98	623.32	0.32
Combination III: Dual stimuli switch (Case III)					
β-CD-g-(Paac-*co*-Paam)	ES at 40°C in pH4	7.10	4.64	87.31	0.54
	At 10°C in pH7	6.46	4.50	597.82	0.36
	At 10°C in pH9.2	6.47	4.51	554.39	0.39
GG-g-Paam	ES at 40°C in pH4	29.43	18.91	4.78	5.68
	At 10°C in pH7	26.70	18.75	73.95	3.23
	At 10°C in pH9.2	26.71	18.76	69.20	3.47
DC-GG-Paam$_{GA0.80}$	ES at 40°C in pH4	29.36	18.89	7.13	4.02
	At 10°C in pH7	26.64	18.69	95.45	2.41

Sample code	Stimuli	Total heat energy (Enthalpy), ΔH_{mix} ($\times 10^{-25}$) (J)	Solvent entropy, ΔS_{mix} ($\times 10^{-27}$) ($J.K^{-1}$)	Chain configurational entropy, $\Delta S_{mix\ Chain\ config}$ ($\times 10^{-4}$) ($J.K^{-1}$)	Mesh size, $\zeta(\times 10^{2})$ (Å)
	At 10°C in pH9.2	26.65	18.70	93.65	2.46
DC-GG-Paam$_{GA1.60}$	ES at 40°C in pH4	29.29	18.86	10.14	3.00
	At 10°C in pH7	26.57	18.63	121.68	1.86
	At 10°C in pH9.2	26.58	18.65	116.58	1.95
DC-GG-Paam$_{GA2.20}$	ES at 40 C in pH4	29.40	18.90	5.83	4.78
	At 10°C in pH7	26.65	18.71	90.56	2.57
	At 10°C in pH9.2	26.67	18.73	82.07	2.86
DC-GG-Paam$_{GA4.39}$	ES at 40°C in pH4	29.14	18.81	17.62	1.89
	At 10°C in pH7	26.39	18.48	206.25	1.05
	At 10°C in pH9.2	26.44	18.52	180.94	1.21
DC-GG-Paam$_{GA6.59}$	ES at 40°C in pH4	29.04	18.78	24.24	1.45
	At 10°C in pH7	26.27	18.37	276.96	0.76
	At 10°C in pH9.2	26.29	18.39	263.03	0.81

Table ANX I.4: Combination I: Calculated values osmotic parameters on different stimuli switching combinations

Sample code	Stimuli	Mixing osmotic pressure, Π_{mix} (Pa)	Elastic osmotic pressure, Π_{el} ($\times 10^3$) (Pa)	Equivalent osmotic pressure, Π_{eq} (Pa)
Combination I: pH stimuli switch (Case I)				
β-CD-g-(Paac-*co*-Paam)	pH4	5.19×10^3	60.37	6.56×10^4
	pH7	87.35	61.48	6.16×10^4
	pH4	3.06×10^2	60.20	6.05×10^4
GG-g-Paam	pH4	2.60×10^2	8.53	8.79×10^3
	pH7	0.52	8.98	8.98×10^3
	pH4	0.57	7.45	7.45×10^5
DC-GG-Paam$_{GA0.80}$	pH4	4.01×10^2	9.40	9.81×10^3
	pH7	2.44	9.57	9.57×10^3
	pH4	3.11	8.99	8.99×10^3
DC-GG-Paam$_{GA1.60}$	pH4	5.41×10^2	10.80	1.14×10^4
	pH7	3.62	13.40	1.34×10^4
	pH4	57.90	12.50	1.26×10^4
DC-GG-Paam$_{GA2.20}$	pH4	15.00×10^2	10.71	1.22×10^4
	pH7	14.20	11.60	1.16×10^4
	pH4	21.90	10.50	1.06×10^4
DC-GG-Paam$_{GA4.39}$	pH4	1.32×10^4	7.22	2.04×10^4
	pH7	1.18×10^2	9.03	0.91×10^4
	pH4	6.01×10^2	8.85	0.94×10^4
DC-GG-Paam$_{GA6.59}$	pH4	2.10×10^4	7.95	2.89×10^4
	pH7	2.32×10^2	10.10	1.02×10^4
	pH4	9.84×10^2	9.82	1.08×10^4

Sample code	Stimuli	Mixing osmotic pressure, Π_{mix} (Pa)	Elastic osmotic pressure, Π_{el} ($\times 10^3$) (Pa)	Equivalent osmotic pressure, Π_{eq} (Pa)
Combination I: pH stimuli switch (Case II)				
β-CD-g-(Paac-*co*-Paam)	pH4	5.19×10^3	60.37	6.56×10^4
	pH9.2	71.51	60.40	6.05×10^4
	pH4	3.67×10^2	58.70	5.91×10^4
GG-g-Paam	pH4	2.60×10^2	8.53	8.79×10^3
	pH9.2	0.27	9.24	9.24×10^3
	pH4	0.84	8.24	8.24×10^3
DC-GG-Paam$_{GA0.80}$	pH4	4.01×10^2	9.40	9.81×10^3
	pH9.2	1.19	9.58	9.58×10^3
	pH4	1.85	9.18	9.18×10^3
DC-GG-Paam$_{GA1.60}$	pH4	5.41×10^2	10.80	1.14×10^4
	pH9.2	2.11	11.20	1.12×10^4
	pH4	21.00	7.95	0.80×10^4
DC-GG-Paam$_{GA2.20}$	pH4	15.00×10^2	10.70	1.22×10^4
	pH9.2	9.64	11.30	1.13×10^4
	pH4	21.90	10.10	1.01×10^4
DC-GG-Paam$_{GA4.39}$	pH4	1.32×10^4	7.22	2.04×10^4
	pH9.2	62.20	10.30	1.04×10^4
	pH4	2.03×10^2	10.10	1.03×10^4
DC-GG-Paam$_{GA6.59}$	pH4	2.10×10^4	7.95	2.89×10^4
	pH9.2	1.18×10^2	9.79	0.99×10^4
	pH4	5.14×10^2	9.38	0.99×10^4

Sample code	Stimuli	Mixing osmotic pressure, Π_{mix} (Pa)	Elastic osmotic pressure, Π_{el} ($\times 10^3$) (Pa)	Equivalent osmotic pressure, Π_{eq} (Pa)
Combination I: pH stimuli switch (Case III)				
β-CD-g-(Paac-*co*-Paam)	pH7	2.93×10^3	37.21	4.01×10^4
	pH9.2	56.43	37.82	3.79×10^4
	pH7	1.17×10^2	37.00	3.71×10^4
GG-g-Paam	pH7	2.28×10^2	5.99	6.22×10^3
	pH9.2	0.87	6.24	6.24×10^3
	pH7	1.12	5.59	5.59×10^3
DC-GG-Paam$_{GA0.80}$	pH7	3.09×10^2	7.53	7.84×10^3
	pH9.2	1.73	7.74	7.74×10^3
	pH7	2.02	7.14	7.14×10^3
DC-GG-Paam$_{GA1.60}$	pH7	3.82×10^2	8.29	8.67×10^3
	pH9.2	1.89	8.45	8.45×10^3
	pH7	3.01	7.94	7.94×10^3
DC-GG-Paam$_{GA2.20}$	pH7	1.30×10^3	7.39	8.70×10^3
	pH9.2	8.46	7.44	7.44×10^3
	pH7	15.20	7.20	7.21×10^3
DC-GG-Paam$_{GA4.39}$	pH7	1.24×10^3	10.20	1.15×10^4
	pH9.2	10.90	11.00	1.10×10^4
	pH7	22.00	10.30	1.03×10^4
DC-GG-Paam$_{GA6.59}$	pH7	8.29×10^3	8.29	1.66×10^4
	pH9.2	53.70	8.78	0.88×10^4
	pH7	1.48×10^2	8.56	0.90×10^4

Table ANX I.5: Combination II: Calculated values osmotic parameters on different stimuli switching combinations

Sample code	Stimuli	Mixing osmotic pressure, Π_{mix}(Pa)	Elastic osmotic pressure, Π_{el} ($\times 10^3$) (Pa)	Equivalent osmotic pressure, Π_{eq} (Pa)
Combination II: Temperature stimuli switch (FWA)				
β-CD-g-(Paac-*co*-Paam)	10°C	4.25×10^3	21.77	2.60×10^4
	40°C	7.93	22.90	2.29×10^4
	10°C	0.15×10^3	21.08	2.12×10^4
GG-g-Paam	10°C	5.43×10^2	5.88	6.42×10^3
	40°C	0.01	6.09	6.09×10^3
	10°C	4.18	5.97	5.98×10^3
DC-GG-Paam$_{GA0.80}$	10°C	7.01×10^2	6.99	7.69×10^3
	40°C	0.05	7.06	7.06×10^3
	10°C	9.57	5.89	5.90×10^3
DC-GG-Paam$_{GA1.60}$	10°C	8.87×10^2	8.38	9.26×10^3
	40°C	0.07	8.46	8.46×10^3
	10°C	13.50	7.38	7.40×10^3
DC-GG-Paam$_{GA2.20}$	10°C	1.33×10^3	9.36	10.69×10^3
	40°C	0.37	10.80	10.76×10^3
	10°C	18.30	9.22	9.24×10^3
DC-GG-Paam$_{GA4.39}$	10°C	3.28×10^3	9.71	12.99×10^3
	40°C	0.23	11.40	11.45×10^3
	10°C	86.60	10.50	10.59×10^3
DC-GG-Paam$_{GA6.59}$	10°C	1.74×10^4	7.48	24.88×10^3
	40°C	17.00	8.61	8.63×10^3

Sample code	Stimuli	Mixing osmotic pressure, Π_{mix}(Pa)	Elastic osmotic pressure, Π_{el} ($\times 10^3$) (Pa)	Equivalent osmotic pressure, Π_{eq} (Pa)
	10°C	1.93×10^2	8.21	8.40×10^3
Combination II: Temperature stimuli switch (REVA)				
β-CD-g-(Paac-*co*-Paam)	40°C	3.30×10^4	13.74	4.67×10^4
	10°C	8.21×10^4	9.05	9.12×10^4
	40°C	13.87	13.87	1.39×10^4
GG-g-Paam	40°C	10.10	10.20	1.02×10^4
	10°C	16.40	4.36	0.44×10^4
	40°C	0.34	7.53	0.75×10^4
DC-GG-Paam$_{GA0.80}$	40°C	37.40	10.00	1.01×10^4
	10°C	71.40	6.09	0.62×10^4
	40°C	0.81	9.63	0.96×10^4
DC-GG-Paam$_{GA1.60}$	40°C	66.90	10.90	1.09×10^4
	10°C	219.00	9.92	1.01×10^4
	40°C	1.07	11.00	1.10×10^4
DC-GG-Paam$_{GA2.20}$	40°C	174.00	10.90	1.10×10^4
	10°C	303.00	10.20	1.05×10^4
	40°C	3.18	10.90	1.09×10^4
DC-GG-Paam$_{GA4.39}$	40°C	721.00	10.20	1.09×10^4
	10°C	2.01×10^3	8.70	1.07×10^4
	40°C	13.50	10.30	1.03×10^4
DC-GG-Paam$_{GA6.59}$	40°C	4.38×10^3	8.33	1.27×10^4
	10°C	9.09×10^3	6.73	1.58×10^4

Sample code	Stimuli	Mixing osmotic pressure, Π_{mix}(Pa)	Elastic osmotic pressure, Π_{el} ($\times 10^3$) (Pa)	Equivalent osmotic pressure, Π_{eq} (Pa)
	40°C	0.28×10^3	9.28	0.96×10^4

Table ANX I.6: Combination I: Calculated values osmotic parameters on different stimuli switching combinations

Sample code	Stimuli	Mixing osmotic pressure, $\Pi_{mix}(\times 10^2)$ (Pa)	Elastic osmotic pressure, Π_{el} $(\times 10^3)$ (Pa)	Equivalent osmotic pressure, $\Pi_{eq}(\times 10^4)$ (Pa)
Combination III: Dual stimuli switch (Case I)				
β-CD-g-(Paac-*co*-Paam)	ES at 40°C in pH7	7.26	19.90	2.06
	At 10°C in pH4	10.00	14.90	1.59
	At 10°C in pH9.2	9.54	12.60	1.35
GG-g-Paam	ES at 40°C in pH7	1.89	5.33	0.55
	At 10°C in pH4	3.28	2.44	0.28
	At 10°C in pH9.2	2.80	2.49	0.28
DC-GG-$Paam_{GA0.80}$	ES at 40°C in pH7	2.65	6.52	0.68
	At 10°C in pH4	5.34	3.01	0.35
	At 10°C in pH9.2	4.14	3.10	0.35
DC-GG-$Paam_{GA1.60}$	ES at 40°C in pH7	3.19	7.71	0.80
	At 10°C in pH4	6.15	3.62	0.42
	At 10°C in pH9.2	4.12	3.68	0.41
DC-GG-$Paam_{GA2.20}$	ES at 40°C in pH7	7.03	8.02	0.87
	At 10°C in pH4	15.80	3.96	0.55
	At 10°C in pH9.2	10.90	4.07	0.52
DC-GG-$Paam_{GA4.39}$	ES at 40°C in pH7	7.21	10.10	1.08
	At 10°C in pH4	12.40	4.92	0.62
	At 10°C in pH9.2	10.70	4.98	0.60
DC-GG-$Paam_{GA6.59}$	ES at 40°C in pH7	43.80	8.28	1.27
	At 10°C in pH4	77.30	4.77	1.25
	At 10°C in pH9.2	68.70	4.76	1.16

Sample code	Stimuli	Mixing osmotic pressure, $\Pi_{mix}(\times 10^2)$ (Pa)	Elastic osmotic pressure, Π_{el} $(\times 10^3)$ (Pa)	Equivalent osmotic pressure, $\Pi_{eq}(\times 10^4)$ (Pa)
Combination III: Dual stimuli switch (Case III)				
β-CD-g-(Paac-*co*-Paam)	ES at 40°C in pH4	45.50	22.70	2.72
	At 10°C in pH7	63.30	16.60	2.29
	At 10°C in pH9.2	54.60	16.50	2.20
GG-g-Paam	ES at 40°C in pH4	0.59	9.88	0.99
	At 10°C in pH7	1.01	4.40	0.45
	At 10°C in pH9.2	0.89	4.16	0.42
DC-GG-Paam$_{GA0.80}$	ES at 40°C in pH4	1.07	10.20	1.03
	At 10°C in pH7	1.68	4.91	0.51
	At 10°C in pH9.2	1.62	4.48	0.46
DC-GG-Paam$_{GA1.60}$	ES at 40°C in pH4	1.81	11.80	1.19
	At 10°C in pH7	2.72	6.23	0.65
	At 10°C in pH9.2	2.50	5.52	0.58
DC-GG-Paam$_{GA2.20}$	ES at 40°C in pH4	0.79	13.80	1.38
	At 10°C in pH7	1.51	7.16	0.73
	At 10°C in pH9.2	1.24	6.82	0.69
DC-GG-Paam$_{GA4.39}$	ES at 40°C in pH4	4.15	15.00	1.54
	At 10°C in pH7	7.74	7.75	0.85
	At 10°C in pH9.2	5.97	7.32	0.79
DC-GG-Paam$_{GA6.59}$	ES at 40°C in pH4	6.69	16.60	1.72
	At 10°C in pH7	13.90	7.98	0.94
	At 10°C in pH9.2	12.50	7.97	0.92

Table ANX II.1: Calculated values of Π_{mix}, Π_{el} and $\Pi_{Entrp\ eq}$ from drug entrapment experimental data

Sample Code	Π_{mix} (Pa) (0.3% CFXH soln./0.7% CFXH soln.)	Π_{el} (x 10^3) (Pa) (0.3% CFXH soln./0.7% CFXH soln.)	$\Pi_{Entrp\ eq}$ (x 10^9) (Pa) (0.3% CFXH soln./0.7% CFXH soln.)
Approach I: Loading at 25°C (0.3% CFXH soln./0.7% CFXH soln.)			
GG-g-Paam	1.65 / 1.15	6.57 / 6.43	1.70 / 0.27
DC-GG-Paam$_{GA4.39}$	6.67 / 4.93	9.65 / 9.67	6.09 / 1.03
Approach IIA: Loading at 10°C via ELS (0.3% CFXH soln./0.7% CFXH soln.)			
GG-g-Paam	5.53 / 3.20	6.88 / 6.75	3.03 / 0.45
DC-GG-Paam$_{GA4.39}$	242.05 / 92.61	10.70 / 11.50	28.33 / 4.30
Approach IIB: Loading at 25°C via ExtLS (0.3% CFXH soln./0.7% CFXH soln.)			
GG-g-Paam	1.67 / 1.20	6.14 / 6.03	1.49 / 0.24
DC-GG-Paam$_{GA4.39}$	3.96 / 3.10	6.98 / 6.44	2.66 / 0.39

Table ANX II.2: Calculated values of diffusion rate constant (K_D), Adj.R-Square, loading exponent (n), diffusivity (D_S) and front velocity (u) during drug entrapment from experimental data

Sample Code	K_D (hr^{-1}) (0.3% CFXH soln. / 0.7% CFXH soln.)	Adj.R-Square (0.3% CFXH soln./0.7% CFXH soln.)	Loading exponent (n) (0.3% CFXH soln. / 0.7% CFXH soln.)	Diffusivity (x 10^{-2}) (D_S) (0.3% CFXH soln. / 0.7% CFXH soln.)	Front vel. (x 10^{-2}) (u) (0.3% CFXH soln. / 0.7% CFXH soln.)
Approach I: Loading at 25°C					
GG-g-Paam	0.227±0.060 / 0.238±0.043	0.921 / 0.958	0.61±0.12 / 0.59±0.09	1.85 / 2.19	1.48 / 1.58
DC-GG-$Paam_{GA4.39}$	0.176±0.050 / 0.196±0.022	0.938 / 0.955	0.72±0.13 / 0.74±0.11	1.29 / 1.55	1.40 / 1.83
Approach IIA: Loading at 10°C via ELS					
GG-g-Paam	0.094±0.007 / 0.178±0.014	0.979 / 0.946	0.68±0.02 / 0.48±0.03	0.35 / 0.76	0.99 / 1.08
DC-GG-$Paam_{GA4.39}$	0.128±0.008 / 0.242±0.013	0.986 / 0.971	0.65±0.02 / 0.44±0.02	0.21 / 0.41	0.85 / 0.87
Approach IIB: Loading at 25°C via ExtLS					
GG-g-Paam	0.672±0.028 / 0.723±0.027	0.911 / 0.985	0.15±0.02 / 0.12±0.02	3.36 / 4.13	4.69 / 5.16
DC-GG-$Paam_{GA4.39}$	0.319±0.030 / 0.364±0.022	0.960 / 0.977	0.44±0.04 / 0.39±0.03	0.81 / 1.06	2.36 / 2.65

Table ANX II.3: Calculated values of release rate constants (K_0, K_1, K_h and $K_{D\,Rel}$) with their corresponding Adj. R-Square and release exponent (n) from the release experimental data

Sample Code	K_0 / Adj. R-Square	K_1 / Adj. R-Square	K_h / Adj. R-Square	$K_{D\,Rel}$ / Adj. R-Square	n	Type of transport
Pattern I: Temperature assisted release event at 10°C (for 0.3 (v/v) % CFXH solution)						
GG-g-Paam	2.622 ± 0.205 / 0.976	0.141 ± 0.042 / 0.827	7.938 ± 0.782 / 0.818	0.114 ± 0.036 / 0.956	0.89 ± 0.14	Anomalous
DC-GG-Paam$_{GA4.39}$	7.843 ± 0.059 / 0.999	0.151 ± 0.033 / 0.898	23.326 ± 2.407 / 0.807	0.089 ± 0.001 / 0.999	0.97 ± 0.01	Anomalous
Pattern II: Acidic medium (pH4) assisted release event (for 0.3 (v/v) % CFXH solution)						
GG-g-Paam	0.395 ± 0.009 / 0.995	0.055 ± 0.007 / 0.905	1.921 ± 0.093 / 0.881	0.057 ± 0.001 / 0.999	0.84 ± 0.01	Anomalous
DC-GG-Paam$_{GA4.39}$	0.546 ± 0.006 / 0.998	0.031 ± 0.002 / 0.943	3.433 ± 0.163 / 0.823	0.015 ± 0.001 / 0.997	1.01 ± 0.02	
Pattern III: Dual stimuli (Acidic medium and 10°C) assisted release event (for 0.3 (v/v) % CFXH solution)						
GG-g-Paam	3.013 ± 0.144 / 0.984	0.103 ± 0.011 / 0.957	10.377 ± 1.210 / 0.714	0.019 ± 0.002 / 0.998	1.29 ± 0.03	
DC-GG-Paam$_{GA4.39}$	2.388 ± 0.040 / 0.996	0.045 ± 0.004 / 0.937	12.737 ± 0.655 / 0.845	0.032 ± 0.003 / 0.995	0.93 ± 0.03	Anomalous
Pattern I: Temperature assisted release event at 10°C (for 0.7 (v/v) % CFXH solution)						
GG-g-Paam	2.715 ± 0.151 / 0.988	0.137 ± 0.035 / 0.862	8.623 ± 0.592 / 0.884	0.136 ± 0.006 / 0.999	0.80 ± 0.02	Anomalous
DC-GG-Paam$_{GA4.39}$	8.030 ± 0.263 / 0.996	0.145 ± 0.034 / 0.882	24.423 ± 2.247 / 0.831	0.105 ± 0.011 / 0.995	0.91 ± 0.05	Anomalous
Pattern II: Acidic medium (pH4) assisted release event (for 0.7 (v/v) % CFXH solution)						
GG-g-Paam	0.513 ± 0.018 / 0.988	0.053 ± 0.006 / 0.916	2.634 ± 0.107 / 0.902	0.070 ± 0.008 / 0.989	0.78 ± 0.03	Anomalous
DC-GG-Paam$_{GA4.39}$	0.773 ± 0.005 / 0.999	0.031 ± 0.001 / 0.936	4.867 ± 0.226 / 0.828	0.017 ± 0.001 / 0.999	0.99 ± 0.01	Anomalous
Pattern III: Dual stimuli (Acidic medium and 10°C) assisted release event (for 0.7 (v/v) % CFXH solution)						
GG-g-Paam	1.539 ± 0.067 / 0.998	0.087 ± 0.012 / 0.919	13.533 ± 1.078 / 0.814	0.050 ± 0.005 / 0.996	0.99 ± 0.03	Anomalous
DC-GG-Paam$_{GA4.39}$	2.484 ± 0.005 /0.999	0.044 ± 0.004 /0.922	13.259 ± 0.662 /0.854	0.036 ± 0.002 /0.997	0.92 ± 0.02	Anomalous

Table ANX II.4: Calculated values of polymer volume fraction (ϕ), $\Pi_{Rel\ mix}$, $\Pi_{Rel\ el}$ and $\Pi_{Rel\ eq}$ from release experimental data

Sample Code	Polymer volume fraction (ϕ),	$\Pi_{Rel\ mix}$ (x 10^7) (Pa)	$\Pi_{Rel\ el}$ (x 10^7) (Pa)	$\Pi_{Rel\ eq}$ (x 10^7) (Pa)
Pattern I: Temperature assisted release event at 10°C (for 0.3 (v/v) % CFXH solution)				
GG-g-Paam	0.88	8.16	- 7.62	0.55
DC-GG-Paam$_{GA4.39}$	0.91	11.21	- 12.82	- 1.61
Pattern II: Acidic medium (pH4) assisted release event (for 0.3 (v/v) % CFXH solution)				
GG-g-Paam	0.95	18.25	- 18.24	2.48 x 10^6
DC-GG-Paam$_{GA4.39}$	0.87	7.72	- 11.61	2.48 x 10^6
Pattern III: Dual stimuli (Acidic medium and 10°C) assisted release event (for 0.3 (v/v) % CFXH solution)				
GG-g-Paam	0.78	3.80	- 4.15	2.35 x 10^6
DC-GG-Paam$_{GA4.39}$	0.70	1.89	- 1.89	2.35 x 10^6
Pattern I: Temperature assisted release event at 10°C (for 0.7 (v/v) % CFXH solution)				
GG-g-Paam	0.87	7.38	- 6.94	0.43
DC-GG-Paam$_{GA4.39}$	0.92	11.49	- 15.35	- 3.86
Pattern II: Acidic medium (pH4) assisted release event (for 0.7 (v/v) % CFXH solution)				
GG-g-Paam	0.93	14.68	- 14.68	2.48 x 10^6
DC-GG-Paam$_{GA4.39}$	0.84	5.87	- 5.87	2.48 x 10^6
Pattern III: Dual stimuli (Acidic medium and 10°C) assisted release event (for 0.7 (v/v) % CFXH solution)				
GG-g-Paam	0.74	2.77	- 1.72	2.35 x 10^6
DC-GG-Paam$_{GA4.39}$	0.71	2.05	- 1.05	2.35 x 10^6

Table ANX II.5: Calculated values of diffusivity (Ds) and front velocity (u) during drug release from experimental data

Sample Code	**Diffusivity (Ds) (x 10^{-3}) ($cm^2.hr^{-1}$) (0.3% CFXH soln. / 0.7% CFXH soln.)**	**Front velocity (u) (x 10^{-3}) ($cm.hr^{-1}$) (0.3% CFXH soln. / 0.7% CFXH soln.)**
Pattern I: Temperature assisted release event at 10°C		
GG-g-Paam	5.69 / 7.05	9.08 / 11.27
DC-GG-$Paam_{GA4.39}$	2.71 / 3.59	9.25 / 13.48
Pattern II: Acidic medium (pH4) assisted release event		
GG-g-Paam	2.23 / 3.20	1.34 / 2.18
DC-GG-$Paam_{GA4.39}$	0.08 / 0.23	2.36 / 2.38
Pattern III: Dual stimuli (Acidic medium and 10°C)		
GG-g-Paam	0.15 / 1.30	11.89 / 18.12
DC-GG-$Paam_{GA4.39}$	0.01 / 0.12	20.07 / 23.49

Table ANX III.1: Equilibrium swelling (wt/wt)% data of β-CD modified UVPTT and guar gum modified non-UVPTT based gel

Sample formulation code	Swelling (wt/wt) % based on medium pH stimuli*			Swelling (wt/wt) % based on temperature stimuli*	
	Acidic (pH4 medium)	Neutral (pH7 medium)	Alkaline (pH9.2 medium)	10 °C	40 °C
β-CD-g-(Paac-co-Paam)	594.77±36.27	718.77±41.36	750.43±39.87	626.88±46.67	1167.16±66.69
GG-g-Paam	1640.71±5.77	1715.60±8.50	1792.86±6.54	1498.33±7.48	1845.71±2.88
DC-GG-Paam$_{GA0.80}$	1414.52±7.11	1544.64±8.11	1590.50±7.11	1439.05±0.89	1633.10±5.70
DC-GG-Paam$_{GA1.60}$	1278.57±7.21	1437.79±7.77	1553.02±6.08	1327.14±6.96	1544.52±3.58
DC-GG-Paam$_{GA2.20}$	902.43±6.21	947.40±8.11	1052.81±7.74	929.05±3.88	1182.31±6.07
DC-GG-Paam$_{GA4.39}$	426.14±7.04	964.45±7.22	1045.12±6.69	919.76±1.93	1172.62±5.48
DC-GG-Paam$_{GA6.59}$	362.76±5.22	501.81±6.88	541.14±7.96	382.62±2.45	633.10±5.13

* SD error (n=5)

Table ANX III.2: Equilibrium swelling (v/v)% data of β-CD modified UVPTT and guar gum modified non-UVPTT based gel

Sample formulation code	Swelling (v/v) % based on medium pH stimuli*			Swelling (v/v) % based on temperature stimuli*	
	Acidic (pH4 medium)	Neutral (pH7 medium)	Alkaline (pH9.2 medium)	10 °C	40 °C
β-CD-g-(Paac-co-Paam)	722.03±34.92	1549.54±89.32	2496.32±86.05	737.81±58.45	2751.60±52.32
GG-g-Paam	9913.68±212.39	14189.30±308.07	18977.25±411.46	11460.80±205.98	17818.40±263.43
DC-GG-Paam$_{GA0.80}$	7934.85±209.96	10535.20±304.65	15657.21±409.66	8929.60±123.67	13250.40±344.83
DC-GG-Paam$_{GA1.60}$	6469.15±210.71	9158.42±212.49	12448.54±306.41	7118.40±84.69	10852.00±135.36
DC-GG-Paam$_{GA2.20}$	5204.84±214.01	7802.51±214.51	10319.10±313.67	5649.60±99.33	8863.20±55.45
DC-GG-Paam$_{GA4.39}$	4123.89±211.44	5684.41±217.55	8039.72±208.22	4470.40±23.13	6963.20±51.19
DC-GG-Paam$_{GA6.59}$	2988.75±212.86	4238.41±205.46	6552.36±210.5	3238.40±42.68	5396.80±51.13

* SD error (n=5)

Table ANX III.3: Equilibrium swelling (wt/wt)% and (v/v)% data of β-CD modified UVPTT and guar gum modified non-UVPTT based composites

Sample formulation code	Swelling (wt/wt) % based on visible light stimuli*	Swelling (v/v) % based on visible light stimuli*
β-CD-g-(Paac-co-Paam)-1	134.19±3.27	1832.86±22.28
β-CD-g-(Paac-co-Paam)-3	141.51±2.12	3365.60±16.63
DC-GG-Paam$_{GA4.39}$-1	862.37±12.69	2594.00±10.39
DC-GG-Paam$_{GA4.39}$-3	900.00±21.28	3713.38±23.17
DC-GG-Paam$_{GA4.39}$-5	924.16±11.99	5093.60±16.63

* SD error (n=5)

Table ANX III.4: Measured parameters of Equilibrium swelled β-CD modified UVPTT and guar gum modified non-UVPTT based gels under ES stimuli

Sample formulation code	Parameters					
	Polymer volume fraction, ϕ	Mol. Wt. between two cross links, M_C ($gm.mol^{-1}$) $\times 10^6$	Cross link density, ρ_C ($mol.cc^{-1}$) $\times 10^{-6}$	Mesh size, ζ (Å)	Porosity (P)	Tortuosity (τ)
ES Stimuli: Acidic (pH4 Medium)						
β-CD-g-(Paac-co-Paam)	0.0474±0.003	0.58±0.15	5.89±0.11	50.17±5.37	0.94±0.02	1.06±0.03
GG-g-Paam	0.0178±0.003	8.08±0.50	0.42±0.50	241.00±7.22	0.55±0.03	1.48±0.04
DC-GG-$Paam_{GA0.80}$	0.0205±0.007	5.34±0.45	0.61±0.60	187.00±11.30	0.58±0.02	1.44±0.05
DC-GG-$Paam_{GA1.60}$	0.0227±0.005	4.11±0.42	0.80±0.70	158.00±12.23	0.65±0.02	1.37±0.04
DC-GG-$Paam_{GA2.20}$	0.0318±0.005	1.65±0.35	2.02±0.80	89.40±10.44	0.67±0.02	1.34±0.05
DC-GG-$Paam_{GA4.39}$	0.0330±0.006	0.23±0.20	14.40±0.60	26.40±8.88	0.69±0.03	1.32±0.04
DC-GG-$Paam_{GA6.59}$	0.0756±0.004	0.15±0.01	21.97±0.80	20.30±9.11	0.70±0.03	1.30±0.05
ES Stimuli: Neutral (pH7 Medium)						
β-CD-g-(Paac-co-Paam)	0.0391±0.002	0.96±0.22	3.50±0.13	69.31±6.51	0.84±0.02	1.16±0.02
GG-g-Paam	0.0170±0.006	9.09±0.50	0.37±0.30	260.00±9.23	0.39±0.02	1.69±0.04
DC-GG-$Paam_{GA0.80}$	0.0188±0.008	6.75±0.60	0.49±0.40	216.00±10.11	0.48±0.02	1.57±0.05

Sample formulation code	Parameters					
	Polymer volume fraction, ϕ	Mol. Wt. between two cross links, M_C ($gm.mol^{-1}$) $\times 10^6$	Cross link density, ρ_C ($mol.cc^{-1}$) $\times 10^{-6}$	Mesh size, ζ (Å)	Porosity (P)	Tortuosity (τ)
DC-GG-Paam$_{GA1.60}$	0.0202±0.005	5.62±0.50	0.59±0.30	192.00±8.66	0.52±0.03	1.52±0.04
DC-GG-Paam$_{GA2.20}$	0.0303±0.006	1.87±0.40	1.78±0.50	96.90±9.23	0.53±0.02	1.50±0.05
DC-GG-Paam$_{GA4.39}$	0.0298±0.008	1.47±0.50	3.95±0.40	79.60±7.33	0.59±0.02	1.43±0.05
DC-GG-Paam$_{GA6.59}$	0.0558±0.003	0.36±0.30	9.45±0.40	34.30±6.21	0.62±0.03	1.40±0.04
ES Stimuli: Alkaline (pH9.2 Medium)						
β-CD-g-(Paac-co-Paam)	0.0379±0.003	1.05±0.17	3.20±0.10	73.29±7.56	0.64±0.02	1.38±0.02
GG-g-Paam	0.0163±0.004	10.23±0.60	0.33±0.20	279.00±10.22	0.31±0.02	1.83±0.05
DC-GG-Paam$_{GA0.80}$	0.0182±0.006	7.33±0.70	0.45±0.30	228.00±11.76	0.33±0.03	1.79±0.04
DC-GG-Paam$_{GA1.60}$	0.0187±0.005	6.89±0.50	0.48±0.30	218.00±10.82	0.41±0.02	1.67±0.06
DC-GG-Paam$_{GA2.20}$	0.0274±0.008	2.47±0.60	1.35±0.40	115.00±10.50	0.44±0.03	1.63±0.05
DC-GG-Paam$_{GA4.39}$	0.0276±0.006	2.14±0.40	3.37±0.30	104.00±11.24	0.45±0.02	1.61±0.04
DC-GG-Paam$_{GA6.59}$	0.0520±0.004	0.43±0.30	7.76±0.30	38.80±12.26	0.47±0.03	1.58±0.04
ES Stimuli: 10 °C						
β-CD-g-(Paac-co-Paam)	0.0462±0.002	0.61±0.12	5.52±0.17	52.27±7.11	0.91±0.03	1.09±0.02

Sample formulation code	Parameters					
	Polymer volume fraction, ϕ	Mol. Wt. between two cross links, M_C ($gm.mol^{-1}$) $\times 10^6$	Cross link density, ρ_C ($mol.cc^{-1}$) $\times 10^{-6}$	Mesh size, ζ (Å)	Porosity (P)	Tortuosity (τ)
GG-g-Paam	0.0231±0.003	3.98±0.16	0.85±0.45	155.00±6.10	0.44±0.02	1.63±0.03
DC-GG-$Paam_{GA0.80}$	0.0251±0.004	3.09±0.19	1.06±0.43	133.00±7.06	0.54±0.02	1.49±0.04
DC-GG-$Paam_{GA1.60}$	0.0271±0.003	2.52±0.16	1.31±0.44	117.00±7.21	0.62±0.01	1.39±0.03
DC-GG-$Paam_{GA2.20}$	0.0310±0.003	1.76±0.18	1.89±0.42	93.20±7.11	0.63±0.02	1.39±0.04
DC-GG-$Paam_{GA4.39}$	0.0418±0.004	0.78±0.13	4.27±0.46	56.20±5.70	0.68±0.015	1.33±0.03
DC-GG-$Paam_{GA6.59}$	0.0723±0.003	0.17±0.13	19.43±0.44	22.00±7.50	0.72±0.02	1.29±0.02
ES Stimuli: 40 oC						
β-CD-g-(Paac-co-Paam)	0.0247±0.003	3.35±0.21	1.00±0.13	150.88±8.20	0.88±0.02	1.12±0.02
GG-g-Paam	0.0059±0.003	7.34±0.37	0.02±0.01	252.00±11.12	0.35±0.015	1.76±0.02
DC-GG-$Paam_{GA0.80}$	0.0092±0.004	5.52±0.31	0.07±0.03	213.00±9.32	0.41±0.02	1.66±0.03
DC-GG-$Paam_{GA1.60}$	0.0112±0.003	3.79±0.36	0.12±0.09	163.00±8.54	0.48±0.013	1.57±0.03
DC-GG-$Paam_{GA2.20}$	0.0153±0.004	2.47±0.35	0.28±0.14	118.00±8.33	0.52±0.018	1.52±0.03
DC-GG-$Paam_{GA4.39}$	0.0246±0.003	1.36±0.26	0.99±0.16	85.00±6.23	0.56±0.02	1.47±0.02
DC-GG-$Paam_{GA6.59}$	0.0446±0.004	0.67±0.31	5.06±0.15	50.50±7.18	0.61±0.015	1.41±0.03

* SD error (n=5)

List of Publications

1. **Tamalika Bhakat,** Ajay Agarwal, N.N. Sharma "Smart Polymer for in-vivo application in Glaucoma treatment", , Miami Winter Symposium: Nanotechnology in Biomedicine, Nature Publishing Group, Miami Florida, USA, 26-29 Feb. **2012.**
2. **Tamalika Bhakat,** Ajay Agarwal, N.N. Sharma"Mechanical Behavior of Thermoresponsive Hydrogel Embedded with Gold Nanoshell", J. BioNanoScience, Springer, Vol. 3(4) , pp.348-355, December **2013**
3. **Tamlika Bhakat,** Suman, Madhusree Sarkar, Ajay Agarwal, NN Sharma "Study on swelling of stimuli responsive positive hydrogel", , 1st Int. Symposium on Nanoparticles /Nanomaterials Advances (ISN2A-2014), Caparica, Portugal, 134-135, 19-22 Jan. **2014.**
4. **Tamalika Bhakat,** Ajay Agarwal, Madhushree Sarkar, Niti Nipun Sharma "Swelling-Deswelling Behavior of Hydrogel for Microfluidic Application", , Indo-UK Workshop, Micro and Nano Fluidics for Health and Diagnostics, Fluidics HD, 27-28 August **2015.**
5. **Tamalika Bhakat,** Ajay Agarwal, N.N. Sharma "Gold Nanoshell Reinforced Positive Hydrogel For Glaucoma Monitoring", 9th IEEE International Conference on Nano/Molecular Medicine & Engineering (NANOMED 2015), Honolulu, Hawaii, USA , 15-18 November **2015.**
6. **Tamalika Bhakat,** Madhushree Sarkar, Ajay Agarwal, Niti Nipun Sharma and Sachin U. Belgamwar, Role of Thermodynamic Energies on Temperature Stimulated Volume Switching of Upper Volume Phase Transition Temperature (UVPTT) based hydrogel, Advances in Polymer Science and Rubber Technology, IIT Kharagpur, India, September 24-27, **2019,**
7. **Tamalika Bhakat,** Aniruddha Roy, Ajay Agarwal, Niti Nipun Sharma and Sachin U. Belgamwar, Bio-Hydrogel for Prolonged Controlled Gastro-Retentive Drug Dispenser, IEEE India Council International Conference , Rajkot, India, December 13-16, **2019**

Biography of Candidate

Tamalika Bhakat received her Bachelor of Technology (Electronics and Telecommunication Engineering) from West Bengal University of Technology, West Bengal, India in 2007 followed by Master of Technology in Mechatronics from Indian Institute of Engineering Science and Technology (IIEST), Shibpur, Howrah, West Bengal, India in 2009. After completion of M.Tech, she joined in Birla Institute of Technology and Science (BITS-Pilani) and started in interdisciplinary filed as research scholar. Her area of research interest are multi functional Biopolymer, drug delivery. She has 7 years of teaching experience from 2011 to 2017. Presently she is serving as a reviewer of Springer-Nature from 2018.

Biography of Supervisor

Dr. Sachin Ulhasrao Belgamwar received his B.E. degree in Mechanical Engineering from Anuradha Engineering College, Chikhli, Amaravati University, India in 1999 and the M.E. and Ph.D Degree in Mechanical Engineering from Birla Institute of Technology and Science, Pilani, India, in 2001 and 2014 respectively. His PhD research was on "Investigations on Multiwalled Carbon Nanotube Reinforced Copper". After working for six years in different engineering colleges, he joined the Mechanical Engineering Department, Birla Institute of Technology and Science, BITS-Pilani, Pilani Campus, Pilani, India in January 2007 as a Lecturer. Currently he is working as Assistant Professor in Mechanical Engineering Department and he also holds the position of Faculty-in-Charge, First Degree (FD) Admission at Birla Institute of Technology and Science, Pilani Campus, India. His area of research is on

- Electrochemical synthesis of carbon nanotube reinforced metal-matrix composites.
- Quantification of carbon nanotube distribution in composites, and microstructure-property correlations.
- Thermo-physical properties and characterization of the nanocomposite.
- MEMS

He has 12+ years teaching expertise on MEMS, Thermodynamics, Power Plant Engineering, Transport Phenomena, Mechanics of Solid, Fluid Mechanics, Computer Aided Design and Kinematics & dynamics of Machines. He has supervised several Ph.D., masters and undergraduate students for thesis and project work. Dr. Belgamwar has been served as Principal Investigator and co-Principal Investigator in many projects based on CNT Reinforced Metal Matrix, Electrical and Thermal characterization of nano-composite, Dynamic Modelling and Experimental Analysis of Double Row Deep Groove Ball Bearing with Multiple Localized Defect funded by BITS-Pilani Seed Grant, Research Initiation Grant and Aeronautics R&D Board respectively. Currently he is Principal Investigator of an on-going project based on "Power assistive hybrid e-trike (PAH e-trike) for disabled person in rural and urban regions of India". He has more than 20 national and international publications and one granted patent on "Method of producing uniform mixture of copper and carbon nanotube in bulk for copper metal nanocomposite".

Biography of Co-Supervisor

Prof. Niti Nipun Sharma completed his B.E. (Mechanical) from REC, Srinagar (now NIT, Srinagar) and M.E. (Mechanical) and Ph.D. both from BITS, Pilani. Prof. Sharma served as visiting professor in EPFL, Switzerland during May-August 2014. He is first recipient of Kris Ramachandran best faculty award in 2010 at BITS, Pilani. Prof. Sharma specialized in Robotics and was a part of team which developed 'ACYUT', the humanoid from BITS. Currently he is Professor and Pro-President at Manipal University Jaipur. He is also Associate Dean at Faculty of Engineering.

Prof. Sharma has three patents, over 100 technical papers and peer reviewed National and International conferences, several invited/keynote talks in India and abroad. He served as principal investigator and co-principal investigator in several funded projects from nodal agencies like DBT, UGC, CSIR-CEERI, NPMASS and Industries. Currently Prof. Sharma is working in Interdisciplinary areas of MEMS and Nanotechnology.

He is Guest Editor, Journal of Bionanoscience (Springer), Associate Editor of International Journal of Smart Sensors and Intelligent Systems, has reviewed many articles for IEEE Tr. Systems, Man and Cybernetics, IEEE Tr. Education, and has been on-board of many Technical Committees of reputed National and International Conference. He was co-chair for Int. Conf. on Emerging Technologies (ETMN-2013), International Conference on Emerging Mechanical Technology Macro to Nano (EMTM2N-2007), co-organizer of 2nd ISSS-MEMS-2007 conference with CSIR-CEERI, Pilani and organized Northern Region NPMASS MEMS Software Training Program from 19-24 Feb. 2011.

Biography of Co-Supervisor

Dr. Ajay Agarwal is Sr. Principal Scientist, Coordinator, Smart Sensors Area, & Head of Nano Biosensors Group at CSIR-Central Electronics Engineering Research Institute, Pilani; involved in the development of Nanotechnologies MEMS, microfluidics and Micro-sensors. He is also Professor at Academy of Scientific and Innovative Research (AcSIR), New Delhi. Earlier as Member of Technical Staff, he served Institute of Microelectronics, Singapore for over 9 years. He received B.Eng. from NIT, Rourkela followed by M.S. and Ph.D. from BITS, Pilani. His engagement with semiconductor industries and research institutes is for over 26 years. He has about 230 research publications in peer-reviewed journals or international conferences, over 35 invited/ plenary/ keynote talks and over 25 patents (granted or filled). He is associated with professional societies like Senior member of IEEE, USA; Life Fellow of MSI (India), The Institution of Engineers (India) and IETE (India), and member MRS, Singapore [till 2009], etc. He is bestowed with various awards including 2008 National Technology Award, Singapore; 2009 Excellence Award, IME Singapore; "Collaboration Development Award" British High Commission, Singapore for the year 2005 and 2006, Super Kaizen (4 times) and Best Kaizen (7 times) at USHA (India) Ltd., etc.

Development of Micro-, Nano-technologies, MEMS and semiconductor processes for various applications are his main research interests. He has been instrumental in numerous collaborative projects with industries/ universities like Sony, Japan; Opaldia, UK; SiMEMS, Singapore; BioChip Innovations, Australia; Silver Brook, Ireland and Australia; ST Kinetics, Singapore; Panasonic, Japan; Intelligent Chip Connections, Singapore; NUS, NTU, Univ. of London, etc. Some of his achievements include the development of silicon nanowire-based devices including electronic biochemical sensor system integrated with fluidics and read-out electronics; development of biochips like lateral patch-clamp arrays, micro-fluidics on transparent substrates, Cell sorter cum counter, Micro-viscometer, etc.; silicon-based nanostructured substrates for Surface Enhanced Raman Spectroscopy (SERS), gas sensors, etc. He has also contributed significantly to the development of silicon micro-mirror arrays; polysilicon interconnects for 3D-stacking, implantable neural probes, etc.